JOURNAL OF BIOLOGICAL REGULATORS & HOMEOSTATIC AGENTS
Volume 32, No. 5, September - October, 2018

CONTENTS

EDITORIAL

ROLE OF MACROPHAGES IN THE PATHOGENESIS OF ATHEROSCLEROSIS AND AORTOCORONARY GRAFT DISEASE

B. PEREK[1], K. KOWALSKA[2], B. KEMPISTY[2,3,4], A. NOWICKI[5], M. DYSZKIEWICZ-KONWIŃSKA[3], M. NOWICKI[2], M. JANKOWSKI[3], M.J. NAWROCKI[3] and A. MALIŃSKA[2,6]

[1]Department of Cardiac Surgery and Transplantology, Poznan University of Medical Sciences, Poznan, Poland; [2]Department of Histology and Embryology, Poznan University of Medical Sciences, Poznan, Poland; [3]Department of Anatomy, Poznan University of Medical Sciences, Poznan, Poland; [4]Department of Obstetrics and Gynaecology, University Hospital and Masaryk University, Brno, Czech Republic; [5]Department of Toxicology, Poznan University of Medical Sciences, Poznan, Poland; [6]Department of Anatomy and Histology, University of Zielona Gora, Zielona Gora, Poland

Received March 27, 2018 – Accepted June 22, 2018

Atherosclerosis and disease of graft implanted to bypass occluded coronary or peripheral arteries are similar processes. Patency of implanted grafts is of paramount importance in respect to long-term outcomes. Although few cell types participate in atherosclerotic plaque formation, macrophages play a crucial role. In this article we review the fate of monocytes that infiltrate vessel wall following endothelium damage, and then undergo transformation to macrophages (identified as CD68 positive cells) and eventually lead to severe stenosis of vessel. Opposing biological activity of two subpopulations of macrophages and their impact on plaque instability and its calcification is also presented. At the end of this paper, a possible clinical significance of pre-existing, CD68 positive cell infiltration of vessel wall, applied as aortocoronary grafts, is discussed.

Coronary artery bypass grafting (CABG) as a method of choice in treatment of diffuse coronary artery disease (CAD) was proved to be sufficient to relieve angina and reduce the risk of death from acute coronary syndromes (1). During these procedures, surgeons harvest veins [usually saphenous vein, (SV)] or other arteries [usually internal thoracic (ITA) and/or, radial (RA)] to bridge over severely stenotic or occluded coronary arteries. The late outcome of CABG is determined by the fate of implanted aortocoronary bypasses as well as progression of atherosclerosis in the native coronary arteries. It is estimated that 10 years after primary surgery, the majority of arterial grafts are patent while as many as 50% of venous bypasses are occluded (2).

Changes in their walls are a consequence of damage to the wall of the vessel that initiates repair mechanisms in which the active involvement is attributed to platelets (in early stages), smooth muscle cells (SMCs), perivascular fibroblasts and macrophages. In the current work we focused on the importance of macrophages in the pathogenesis of aortocoronary bypass disease.

Key words: macrophages, atherosclerosis, plaque instability, graft disease

Mailing address:
Bartosz Kempisty, PhD,
Department of Histology and Embryology,
Department of Anatomy,
Poznań University of Medical Sciences,
6 Święcickiego St., 60-781 Poznań, Poland
Tel./Fax: +48 61 8546418 / +48 61 8546440,
e-mail: bkempisty@ump.edu.pl

0393-974X (2018)

Macrophages

Tissue macrophages are derived from circulating monocytes. The ultrastructural equipment of macrophages, such as well developed Golgi apparatus and lysosome, as well as folded cell membrane forming a net of caveolae, is an example of their adaptation to the functions – high phagocytic activity and the ability for movement and migration. The main function of macrophages is to maintain tissue haemostasis. In response to the activation of their surface and cytoplasmic receptors, macrophages exhibit the ability for phenotypic polarity, both pro-inflammatory (M1) and anti-inflammatory (M2) (3).

The differentiation of macrophages towards M1 subpopulation is carried out through typical activation of these cells due to bacterial or viral infections, as well as in response to tissue damage associated with increased production of active forms of nitric oxide (NO). The polarization of macrophages in the M1 direction is associated with their cytotoxic properties and the ability to secrete proinflammatory cytokines such as tumour necrosis factor α (TNFα), interleukin (IL)-1, IL-6, IL-8, IL-12 and chemokines (4). M1 macrophages can also present antigens and activate the responses involving Th1 and Th17 lymphocytes.

Macrophages exhibiting M2 phenotype are activated through an alternative pathway and usually exhibit the anti-inflammatory characteristics observed in regeneration, atherosclerosis, cancer or tissue fibrosis. M2 macrophages secrete immunosuppressive cytokines such as IL-10, IL-4, IL-13, transforming β growth factor (TGF β) as well as fibrosis promoting factors, including fibronectin.

Macrophages in atherosclerosis

Atherosclerosis and aortocoronary bypass disease are similar biological processes that ultimately lead to a reduction in blood flow and organ ischemia. In the case of heart, clinically, these disseases manifest through the onset and/or progression of CAD, the major form of which is acute coronary syndrome (ACS) (5).

Atherosclerosis is a dynamic disease process that often lasts for many years, beginning as a defensive response of the walls of the vessel to damage caused by mechanical factors (high blood pressure shearing forces), oxidative stress associated with the excessive formation of free radicals, and some infections or oxidized forms of low density lipoprotein (LDL). Endothelial injury initiates the processes of the immune response. Macrophages present in the inner wall of the vessel are a constant source of numerous chemokines, cytokines, growth factors and proteolytic enzymes (6). They also activate other cells, including T lymphocytes. This activation eventually results in expression of E selectin, adhesion molecules (VCAM, vascular cell adhesion molecule), cell adhesion molecules (ICAM, intracellular adhesion molecule) that promote adhesion of circulating monocytes to the surface of endothelial cells (7).

During transmigration through cell junctions of endothelial cells and further through the basal membrane, monocytes are converted into macrophages. The most important role is played by MCP-1 (monocyte chemotactic protein-1) along with its receptor, CCR2 (C-C chemokine receptor type 2) (8).

The differentiation of monocytes into macrophages is associated with the emergence of scavenger receptors (SRs) on their surface that allow the uptake of modified LDL (mLDL) (9). Initially, this is a beneficial phenomenon, as it reduces the harmful effects of mLDL on endothelial cells and smooth muscle. However, it eventually leads to unlimited lipid absorption by macrophages. Inside the cell, mLDL release free cholesterol, which then undergoes esterification. Clumping of cholesterol esters, in the form of lipid droplets within the macrophage cells occurs, giving them a morphological form of so-called foam cells, which, after disintegration, are a source of extracellular deposits of cholesterol (10).

The active macrophages secrete also numerous chemotactic factors and stimulate cellular response involving Th1 lymphocytes. In addition, the high concentration of platelet-derived growth factor (PDGF) and insulin-like growth factor (IGF), secreted by macrophages, stimulates the SMC migration from the middle membrane to the inner membrane where they proliferate and transform from contractile to synthetic phenotype (11). The synthesis of extracellular matrix (ECM) proteins, i.e. collagen

and proteoglycans, leads to the plaque increases. Foam cells undergo apoptosis and their content creates a necrotic or lipid core of the atherosclerotic plaque, surrounded by compact fibrous cover.

Macrophage subpopulation and atherosclerosis plate morphology

Both subpopulations of macrophages (M1 and M2) are observed in the process of atherosclerotic plaque formation (12). M1 macrophages, with pro-inflammatory properties, together with T lymphocytes are usually identified within unstable plaque, in which a relatively large lipid nucleus is covered by a thin fibrous layer. Metalloproteinases, the proteolytic enzymes produced by macrophages M1, notably MMP2 and MMP9, accelerate degradation of the connective tissue covering atherosclerotic plaque. Rupture of the plaque activates the clotting process, including the aggregation of platelets at the site of damage, deposition of fibrin and formation of a clot, that may lead to obstruction of the arteries and ischemic events (13). The M2 phenotype macrophages have anti-inflammatory properties and their presence was demonstrated in stable plaques with a relatively thick fibrous cover.

The antagonistic role of two macrophage subpopulations is also disclosed in the plaque mineralization that in the past was considered as a passive process. However, in recent years it has been shown that it is a dynamic, regulated and highly structured phenomenon, with the macrophages actively involved (14). The increasing concentration of extracellular calcium is a potent chemotactic factor that promotes the migration of macrophages into the wall of the vessel. Although both subpopulations possess calcium binding receptors on their surface (CaR, calcium-sensing receptor), calcium ions activate antagonistic response. In the case of macrophages M1, calcium dependent activation results in the production and release of IL-6, TNF-α and bone morphogenetic protein-2 (BMP-2), which contribute to the inflammation and promotion of the calcification process (15). In contrast, the M2 macrophages produce osteopontin, contributing to the inhibition of the calcification and, in addition, to the removal of hydroxyapatite deposits from the vessel wall (16). Thus, the process of plaque mineralization is another example where the plasticity of the macrophage population is observed under the influence of the changing conditions of the microenvironment. This could be used in daily clinical practice. Vitamin D receptor activator (VDRA), which has the ability to initiate a change of the phenotype of the macrophages from M1 to M2 under conditions of high concentration of calcium ions, is a ligand that is especially promising as a target of clinical research. (17).

Macrophages and graft failure

Maintenance of patency of vascular bypass is a key indicator of sustainable therapeutic success in cardiac and vascular surgery. Therefore, identification and recognition of the role of cells, whose activity can determine the proper structure and function of the bypass is extremely important. The main reason for the limitation of transplant patency is the hyperplasia of its inner and central membranes that is a prerequisite for the development of the atherosclerotic process, which is the final cause of obstruction (18). At the root of all the aforementioned dysfunctions of the vessel lies a chronic inflammation ongoing in its wall and macrophages are the main 'players' in regulating the course of inflammation (19). It has been shown that changes in the inner and central membranes leading to obstructive vascular occlusion are accompanied by intensive migration of macrophages into the wall of the vessel. The involvement of macrophages in the above process appears to be analogous to the role of these cells in the process of plaque formation. However, studies on the analysis of the effects of macrophages on the dynamics of change in the transplant wall showed, that not only the mere presence of these cells in the wall of the vessel is important, but also their location in the individual layers. It has been shown that the presence of these cells in the inner membrane of the saphenous vein can be treated as an indicator of early transplant obstruction forecast (20).

Macrophages in carcinogenesis

Chronic inflammation is intimately associated with carcinogenesis. Macrophages, the most common

non-tumor cell type in tumor microenvironments, play central roles in inflammation and participate in tumor development. Macrophages seem capable of producing the growth factors needed by at least some cancer cells, and this can explain not only the preferential growth of metastases in wounds, but the promotion of carcinogenesis by wounding. While pro-inflammatory M1 macrophages may be cytotoxic to tumor cells, the anti-inflammatory M2 macrophages are also involved in tumor progression by fostering invasion, extracellular matrix remodeling, angiogenesis, metastasis and suppression of anti-tumor immune responses. Tumor-associated macrophages, polarized toward the phenotype M2 by several cytokines present in the tumor microenvironment, activate the angiogenesis process through the production of VEGF.

CONCLUSIONS

The process of atherosclerosis, like aortocoronary bypass disease, is highly complex, involving a number of cell lines and biologically-released active substances. Some of the most important cells in the process are macrophages. Although their emergence in the early stages involves repairing the damaged vessel wall, it further leads to uncontrollable thickening and may cause the onset of clinical complications of atherosclerosis, such as a myocardial infarction, stroke or limb ischemia. However, not all lesions on the site of atherosclerotic plaques can be evaluated negatively. There is increasing scientific evidence that the some of the effects, such as anti-inflammatory activities and atherosclerotic plaque stabilizing action of the M2 macrophage subpopulation, are positive.

ACKNOWLEDGEMENTS

This publication is part of the project : 1) "WroVasc – Integrated Cardiovascular Centre", co-financed by the European Regional Development Fund, within Innovative Economy Operational Program, 2007-2013 realized in Regional Specialized Hospital, Research and Development Center in Wroclaw and 2) State Committee for Scientific Research - Grant No. 5958/B//P01/2010/38.

REFERENCES

1. Head SJ, Mack MJ, Holmes DR, Mohr FW, Morice M-C, Serruys PW, Kappetein AP. Incidence, predictors and outcomes of incomplete revascularization after percutaneous coronary intervention and coronary artery bypass grafting: a subgroup analysis of 3-year SYNTAX data. Eur J Cardio-Thoracic Surg 2012; 41(3):535-41.
2. Gansera B, Schmidtler F, Angelis I, Kiask T, Kemkes B, Botzenhardt F. Patency of internal thoracic artery compared to vein grafts - postoperative angiographic findings in 1189 symptomatic patients in 12 years. Thorac Cardiovasc Surg 2007; 55(7):412-17.
3. Alvarez MM, Liu JC, Trujillo-de Santiago G, Cha B-H, Vishwakarma A, Ghaemmaghami AM, Khademhosseini A. Delivery strategies to control inflammatory response: Modulating M1–M2 polarization in tissue engineering applications. J Control Release 2016; 240:349-63.
4. Liu Y-C, Zou X-B, Chai Y-F, Yao Y-M. Macrophage polarization in inflammatory diseases. Int J Biol Sci 2014; 10(5):520-29.
5. Bundhoo SS, Kalla M, Anantharaman R, et al. Outcomes following PCI in patients with previous CABG. Catheter Cardiovasc Interv 2011; 78(2):169-76.
6. Brown RA, Shantsila E, Varma C, Lip GYH. Current understanding of atherogenesis. Am J Med 2017; 130(3):268-82.
7. Ley K, Huo Y. VCAM-1 is critical in atherosclerosis. J Clin Invest 2001; 107(10):1209-10.
8. Robbins CS, Hilgendorf I, Weber GF, et al. Local proliferation dominates lesional macrophage accumulation in atherosclerosis. Nat Med 2013; 19(9):1166-72.
9. Moore KJ, Freeman MW. Scavenger receptors in atherosclerosis: beyond lipid uptake. Arterioscler Thromb Vasc Biol 2006; 26(8):1702-11.
10. Hilgendorf I, Swirski FK, Robbins CS. Monocyte fate in atherosclerosis. Arterioscler Thromb Vasc Biol 2015; 35(2):272-79.
11. Tang R, Cui X-B, Wang J-N, Chen S-Y. CTP Synthase 1, a Smooth muscle-sensitive therapeutic target for effective vascular repair. Arterioscler Thromb Vasc Biol 2013; 33(10):2336-44.

12. Roma-Lavisse C, Tagzirt M, Zawadzki C, et al. M1 and M2 macrophage proteolytic and angiogenic profile analysis in atherosclerotic patients reveals a distinctive profile in type 2 diabetes. Diabetes Vasc Dis Res 2015; 12(4):279-89.
13. Fuster V, Moreno PR, Fayad ZA, Corti R, Badimon JJ. Atherothrombosis and High-risk plaque. J Am Coll Cardiol 2005; 46(6):937-54.
14. Ikeda K, Souma Y, Akakabe Y, et al. Macrophages play a unique role in the plaque calcification by enhancing the osteogenic signals exerted by vascular smooth muscle cells. Biochem Biophys Res Commun 2012; 425(1):39-44.
15. Dube PR, Birnbaumer L, Vazquez G. Evidence for constitutive bone morphogenetic protein-2 secretion by M1 macrophages: Constitutive auto/paracrine osteogenic signaling by BMP-2 in M1 macrophages. Biochem Biophys Res Commun 2017; 491(1):154-58.
16. Ge Q, Ruan C-C, Ma Y, et alJ. Osteopontin regulates macrophage activation and osteoclast formation in hypertensive patients with vascular calcification. Sci Rep 2017; 7:40253.
17. Li X, Speer MY, Yang H, Bergen J, Giachelli CM. Vitamin D receptor activators induce an anticalcific paracrine program in macrophages: requirement of osteopontin. Arterioscler Thromb Vasc Biol 2010; 30(2):321-26.
18. Muto A, Model L, Ziegler K, Eghbalieh SDD, Dardik A. Mechanisms of vein graft adaptation to the arterial circulation: insights into the neointimal algorithm and management strategies. Circ J 2010; 74(8):1501-12.
19. Tabas I, Bornfeldt KE. Macrophage phenotype and function in different stages of atherosclerosis. Circ Res 2016; 118(4):653-67.
20. Malinska A, Perek B, Buczkowski P, Kowalska K, Ostalska-Nowicka D, Witkiewicz W, Nowicki M. CD68 expression in aortocoronary saphenous vein bypass grafts. Histochem Cell Biol 2013; 140(2):183-88.

EDITORIAL

IL-33 MEDIATES ALLERGY THROUGH MAST CELL ACTIVATION: POTENTIAL INHIBITORY EFFECT OF CERTAIN CYTOKINES

L. TETTAMANTI[1], S.K. KRITAS[2], C.E. GALLENGA[2], C. D'OVIDIO[4], F. MASTRANGELO[5], G. RONCONI[6], Al. CARAFFA[7], E. TONIATO[8] and P. CONTI[9]

[1]Department of Medical and Morphological Science, University of Insubria, Varese, Italy; [2]Department of Microbiology and Infectious Diseases, Aristotle University of Thessaloniki, Macedonia, Greece; [3]Department of Biomedical Sciences and Specialist Surgery, Section of Ophthalmology, University of Ferrara, Italy; [4]Section of Legal Medicine, Department of Medicine and Aging Sciences, "G. d'Annunzio" University of Chieti–Pescara, Italy; [5]Department of Medical Science and Biotechnology, University of Foggia, Foggia, Italy; [6]UOS Clinica dei Pazienti del Territorio, Policlinico Gemelli, Rome, Italy; [7]School of Pharmacy, University of Camerino, Camerino, Italy; [8]Department of Medical, Oral and Biotechnological Sciences, University "G. d'Annunzio" of Chieti-Pescara, Chieti, Italy; [9]Immunology Division, Postgraduate Medical School, University of Chieti-Pescara, Chieti, Italy

Received August 27, 2018 - Accepted October 3, 2018

Mast cells (MCs) are hematopoietic immune cells commonly found in adjacent to blood vessels in the lamina propria of airway mucosa. They are important in allergic reactions since the cross-linking of their surface high affinity receptor FcεRI induces activation of these cells, and provokes the synthesis, degranulation and release of inflammatory mediators including arachidonic acid-derived eicosanoids (de novo synthesized), stored enzyme mediators, and inflammatory TH1 and TH2 cytokines, and chemokines. Interleukin (IL)-33 participates in innate and adaptive immunity and inflammation and, acting on CD34+ cells, causes MC differentiation and maturation. IL-33 is generated by activated immune cells, and activates MCs which degranulate and release pro-inflammatory mediators. IL-33 is very important in mediating allergic inflammation and can be induced by IL-1 beta. It is also called "alarmin" and is an inflammatory cytokine IL-1 family member, expressed from mocytes and MCs, which binds its receptor ST2, provoking its release after cell damage. MC-derived allergic compounds in response to IL-33 is critical to innate type 2 immunity. IL-37 is expressed by immune and non-immune cells after pro-inflammatory stimulus. IL-37, an anti-inflammatory cytokine, binds IL-18Rα and suppresses pro-inflammatory IL-1 beta released by activated immune cells such as macrophages. Here, we hypothesize that pro-inflammatory IL-1 family member cytokines released by activated MCs, mediating inflammatory allergic phenomenon, can be suppressed by IL-37.

Cytokines are proteins produced by different cells which mediate the communication of immune cells and inflammatory responses, including allergy. Interleukin (IL)-33 (formerly IL-1F11) is one of the latest IL-1 subfamily members, mainly expressed by immune cells including innate lymphoid cell 2

Key words: allergy, mast cells, IL-33, IL-37, cytokines

Mailing address:
Prof. Pio Conti,
Postgraduate Medical School,
University of Chieti,
Viale Unità d'Italia 73, Chieti, Italy
Tel./Fax: +39 0871 574136
e-mail: pconti@unich.it

0393-974X (2018)

(ILC2), and Th2 cells, and its involved in innate and adaptive immunity and inflammation (1).

IL-33 is a 30 kDa cytokine which binds its specific receptor ST2 derived from TLR/IL-1R super family. ST2 receptor forms heterodimer with IL-1 receptor accessory protein (IL-1RAcP) which both bind IL-33. IL-33 is the ligand for the former orphan receptor ST2, also called IL-1R4, and is mainly associated with the TH2 immune response. The immature precursor of IL-33 is cleaved from caspase-1 that produces mature and active IL-33 released after cell damage (2). Therefore, after cell injury or necrosis, NF-kB, p38 and JNK are activated with released IL-33 which is called "alarmin".

IL-33 induces M2 macrophage polarization and favors the production of cytokines/chemokines in these and other cells. It is also a driver of type 2 immune cells in several inflammatory disorders. IL-33 activates dendritic cells and also induces polarization of Th2 cells, playing a role in type 2 diseases. In addition, it regulates innate immune cells through the activation of monocytes and tissue mast cells (MCs) (3).

IL-33 acts on $CD34^+$ cells participating in MC differentiation and maturation. This cytokine is stored in the nucleus and is mainly produced by mononuclear cells, but also several other cells can generate it, including MCs (Table I). In inflammatory diseases, such as asthma and allergy, IL-33 drives nucleus secretion, TH2 polarization, eosinophil recruitment and provokes hyperplasia (4).

Moreover, IL-33 is involved in many different pathological conditions, such as cardiovascular diseases, arthritis, infections, sepsis, atherosclerosis, neurological diseases, cancer and allergy. MC-released IL-33 plays a protective role versus parasites, bacteria and virus infections. However, for unclear reason, IL-1 release suppresses IL-33 (5).

Therefore, MCs express IL-33 ST2 receptor and generate this cytokine which can activate MCs to generate several cytokines such as IL-1, IL-2, IL-4, IL-5, IL-6, and TNF, and also chemokines including CXCL8, CCL1, CCL2, and CCL17, and probably more (6). On the other hand, MCs are involved in the maturation of IL-33 from the immature form. It is interesting that chymase, an MC stored enzyme, can degrade IL-33 into inactive form, as if it were a defensive response to the inflammatory insult.

Parasite infections mediate by MCs strongly induces IL-33 mRNA expression in epithelial cells, demonstrating a significant correlation between MCs and IL-33. The main cells that IL-33 can activate are: MCs, macrophages, NK cells, granulocytes and TH2 cells (7).

MAST CELLS

MCs are immune cells originating from human cord blood $CD34^+$ cells which differentiate and grow into MCs in the presence of stem cell factor (SCF) and IL-6 (8). MCs are ubiquitous in the body and represent one of the most important defensive

Table I. *IL-33 expression.*

a) Cells that express IL-33 mRNA*:* macrophages, mast cells, epithelial cells, dendritic cells

b) Cells that express IL-33 protein: hematopoietic cells, macrophages, dendritic cells, fibroblasts, adipocytes, smooth muscle cells, endothelial cells, bronchial cells, osteoblasts, epithelial cells, hepatocytes

c) IL-33 organ expression: stomach, skin, brain, lung, colon, liver, synovial tissue

systems of our organism, in response to numerous different antigens (9). MCs participate in innate and adaptive immunity, and after activation they release pro-inflammatory compounds including chemical mediators, cytokines/chemokines and arachidonic acid products (10). They can clearly respond to allergens and therefore are involved in allergic reaction and inflammation.

MCs express on their surface *c-kit* receptor, and the high affinity receptor ($K_{d=}$ 10^{-10} M) FcεRI for immunoglobulin E (IgE). The stimulation of FcεRI receptor leads to cascade activation of a mitogen-activated protein (MAP) kinase cascade and a phophatidylinositol-specific phospholipase C (PI-PLCγ) (11). The stimulation of mitogen-activated protein (MAP) kinase family members, ERK, JNK and p38, activates many transcription factors including NF-kB, leading MCs to generate and release inflammatory cytokines and chemokines, PGD2, and leukotrienes LTC4, D4 and E4.

Allergy is characterized by the presence of inflammation due to immune cells, where MCs react with TH2 cells and are important elements to the allergenic response (12). Therefore, inflammation in allergic reaction is mediated by both innate and acquired immune cells. Hence, IL-33 induces MCs to secrete Th2 type-cytokines such as IL-4 which promotes TH2 differentiation.

At the intra-cellular level, IL-33 induces MyD88 which plays a critical role in TLR signaling and its deficiency completely abolishes NF-kB and MAP kinase bacterial activation. In addition, MyD88-deficient mice are totally defective in IL-1 and IL-18 cytokine production. Moreover, TLR4-mediated response to LPS involves also MyD88 pathways activating MAP kinases and NF-kB and, consequently, inflammatory cytokine release (Fig. 1).

Toll interleukin-1 receptor (TIR) domain starts with the MyD88 signal, IL-1 receptor-activated kinases (IRAKs), and NFκB (13). When MyD88 becomes phosphorylated, along with IRAKs, it generates a pro-inflammatory signal to the nucleus.

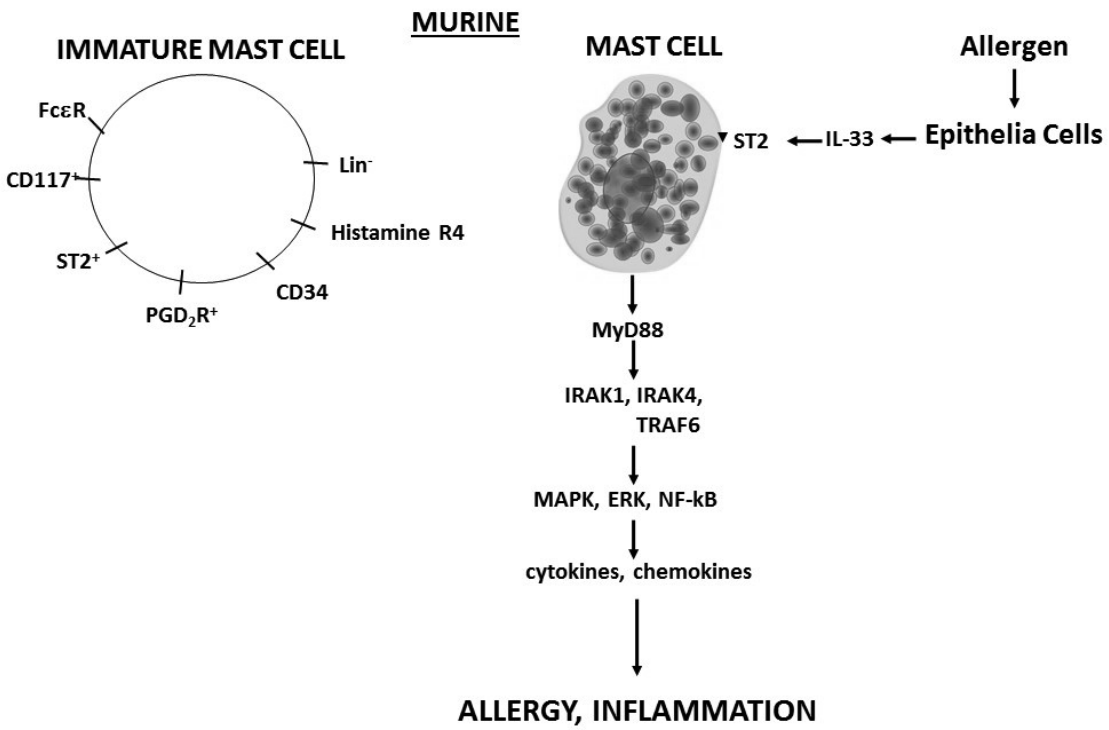

Fig. 1. *Murine mast cells derived from immature mast cells can be activated by ST_2 receptor through IL-33 generated by epithelial cells stimulated by allergen. This effect leads to the production of MyD88 and the release of cytokines/chemokine mediating allergic inflammation. MyD88 can be inhibited by IL-37 released from activated macrophages.*

Hence, MyD88 binds to the TIR domain and begins the cascade of kinases leading to the activation of NFkB and inflammatory cytokine production.

Stimulation of MCs with IL-33 induces also cytokines IL-13 and IL-5, while activating cells with anti-IgE results in a hyperproduction of IL-13. Furthermore, there is a drastic up-regulation of the chemokine CCR7 mRNA receptors after stimulation of MCs with IL-33 or anti-IgE.

MCs express and produce IL-33 which drives allergic diseases, causes inflammation and induces gamma IFN in viral infections. Moreover, IL-33 plays a role in skin inflammation and atopic dermatitis (14). In this disease, the allergens stimulate the epidermis that releases IL-33 which activates both the MCs and the 2 innate lymphoid cells (ILC2) which respectively produce IL-2 with activation of Treg cells, and production of IL-5 and IL-13 which stimulate allergic eosinophils. On this occasion, the Treg lymphocytes go into clonal duplication and produce IL-10 which inhibits the production of IL-5 and IL-13 (15).

IL-33 knock-out mice fail to express allergic inflammatory reaction, showing that this cytokine is decisive for the expression of atopic dermatitis (1).

After cell injury or necrosis there is the activation of NF-kB, p38 and JNK with release of IL-33 which exacerbates inflammation. Therefore, cytokine IL-33 plays an important role in several inflammatory diseases including allergy, asthma, autoimmune diseases, rheumatoid arthritis, sepsis and atherosclerosis (1).

IL-37

Previously, other cytokines, such as IL-10 and TGF-β, were found to be anti-inflammatory. In addition, IL-1 receptor antagonist (IL-1RA), acting on IL-1 receptor down-regulates inflammation (16).

IL-37 is an important new inhibitor of innate immunity and inflammatory IL-1 family members, including IL-1β, IL-18 and IL-33. IL-37 is also decisive in acquired immunity since it has an effect on T cells (17). IL-37 level increases in inflammatory conditions, and is expressed and mainly generated by immune cells, including circulating monocytes, tissue macrophages, dendritic cells, tonsillar B cells, and plasma cells (18).

Caspase-1 is a fundamental intracellular processing enzyme responsible for the maturation of IL-1β, IL-18 and IL-37 (19). Caspase-1 inhibitors partially down-regulate IL-1, demonstrating that it is not the only one responsible for the processing of IL-37. IL-37 inhibits allergic inflammation induced by TLR and its *in vivo* suppression leads to an increase in inflammatory cytokines such as IL-1 (20). Mice *in vivo* treatments with IL-37 effectively reduce the infiltration of immune cells and inflammation induced by IL-1, IL-6, and TNF (17, 21).

Allergic reactions are mediated by several cytokines including IL-1, TNF and MC-released IL-33. In these inflammatory reactions IL-37 has an important potential inhibitory effect (22).

Dinarello et al. report that transgenic mice (IL-37tg) expressing the human gene of IL-37 are less likely to encounter inflammatory diseases (17). Therefore, as the allergy mediated by cytokines is an inflammatory disease, it is possible that IL-37 plays a therapeutic inhibitory role (23).

However, more studies are needed to understand the specific effect of IL-37 and its likely side effects.

REFERENCES

1. Dinarello CA. An IL-1 family member requires caspase-1 processing and signals through the ST2 receptor. Immunity 2005; 23(5):461-62.
2. Dinarello CA, Simon A, van der Meer JW. Treating inflammation by blocking interleukin-1 in a broad spectrum of diseases. Nat Rev Drug Discov 2012;11(8):633-52.
3. Caraffa A, Conti C, D Ovidio C, et al. New concepts in neuroinflammation: mast cells pro-inflammatory and anti-inflammatory cytokine mediators. J Biol Regul Homeost Agents 2018; 32(3):449-54.
4. Mukai K, Tsai M, Saito H, Galli SJ. Mast cells as sources of cytokines, chemokines, and growth factors. Immunol Rev 2018; 282(1):121-50.
5. Pan D, Buchheit KM, Samuchiwal SK, Liu T, Cirka H, Raff H, Boyce JA. Cyclooxygenase 1 mediates IL-33-induced extracellular signal regulated kinase activation in mast cells; Implications for aspirin

sensitivity. J Allergy Clin Immunol 2018; doi: 10.1016/j.jaci.2018.06. [Epub ahead of print].
6. Ogasawara N, Klingler AI, Tan BK, et al. Epithelial activators of type 2 inflammation: Elevation of thymic stromal lymphopoietin, but not IL-25 or IL-33, in chronic rhinosinusitis with nasal polyps in Chicago, Illinois. Allergy 2018; doi: 10.1111/all.13552.
7. Conti P, Caraffa A, Ronconi G, et al. Mast cells participate in allograft rejection: can IL-37 play an inhibitory role? Inflamm Res 2018 doi: 10.1007/s00011-018-1166-3.
8. Galli SJ. The mast cell-IgE paradox: from homeostasis to anaphylaxis. Am J Pathol 2016; 186(2):212-24.
9. Taracanova A, Alevizos M, Karagkouni A, et al. SP and IL-33 together markedly enhance TNF synthesis and secretion from human mast cell mediated by the interaction of their receptors. Proc Natl Acad Sci U S A 2017; 114(20):E4002-E4009. doi: 10.1073/pnas.1524845114.
10. Theoharides TC, Zhang B, Kempuraj D, et al. IL-33 augments substance P-induced VEGF secretion from human mast cells and is increased in psoriatic skin. Proc Natl Acad Sci U S A 2010; 107(9):4448-53.
11. Galli SJ, Kalesnikoff J, Grimbaldeston MA, Piliponsky AM, Williams CM, Tsai M. Mast cells as "tunable" effector and immunoregulatory cells: recent advances. Annu Rev Immunol 2005; 23:749-86.
12. Conti P, Tettamanti L, Mastrangelo F, et al. Impact of fungi on immune responses. Clin Ther 2018; 40(6):885-88.
13. Dinarello CA. Overview of the IL-1 family in innate inflammation and acquired immunity. Immunol Rev 2018; 281(1):8-27.
14. Petra AI, Tsilioni I, Taracanova A, Katsarou-Katsari A, Theoharides TC. Interleukin 33 and interleukin 4 regulate interleukin 31 gene expression and secretion from human laboratory of allergic diseases 2 mast cells stimulated by substance P and/or immunoglobulin E. Allergy Asthma Proc 2018; 39(2):153-60.
15. Conti P, Kempuraj D, Kandere K, et al. IL-10, an inflammatory/inhibitory cytokine, but not always. Immunol Lett 2003; 86(2):123-29.
16. Lewis EC, Mizrahi M, Toledano M, et al. alpha1-Antitrypsin monotherapy induces immune tolerance during islet allograft transplantation in mice. Proc Natl Acad Sci U S A 2008; 105(42):16236-41.
17. Cavalli G, Dinarello CA. Suppression of inflammation and acquired immunity by IL-37. Immunol Rev 2018; 281(1):179-90.
18. Conti P, Caraffa A, Mastrangelo F, et al. Critical role of inflammatory mast cell in fibrosis: Potential therapeutic effect of IL-37. Cell Prolif 2018; e12475. doi: 10.1111/cpr.12475. [Epub ahead of print]
19. Kritas SK, Gallenga CE, D Ovidio C, et al. Impact of mold on mast cell-cytokine immune response. J Biol Regul Homeost Agents 2018; 32(4):763-68.
20. Conti P, Caraffa A, Ronconi G, et al. Impact of mast cells in depression disorder: inhibitory effect of IL-37 (new frontiers). Immunol Res 2018 doi: 10.1007/s12026-018-9004-9. [Epub ahead of print] Review.
21. Conti P, Ronconi G, Kritas SK, Caraffa A, Theoharides TC. Activated mast cells mediate low-grade inflammation in type 2 diabetes: interleukin-37 could be beneficial. Can J Diabetes 2018; doi: 10.1016/j.jcjd.2018.01.008.
22. Conti P, Caraffa A, Ronconi G, Kritas SK, Mastrangelo F, Tettamanti L, Theoharides TC. Impact of mast cells in mucosal immunity of intestinal inflammation: Inhibitory effect of IL-37. Eur J Pharmacol 2018; 818:294-99.
23. Conti P, Carinci F, Caraffa A, Ronconi G, Lessiani G, Theoharides TC. Link between mast cells and bacteria: Antimicrobial defense, function and regulation by cytokines. Med Hypotheses 2017; 106:10-14.

BALANCE BETWEEN EPITHELIAL AND STROMAL MARKER EXPRESSION AND DISTRIBUTION IN PRIMARY CULTURE MODEL OF PORCINE ENDOMETRIUM DURING REAL-TIME CELL PROLIFERATION

K. WOJTANOWICZ-MARKIEWICZ[1], M.J. NAWROCKI[2], M. BRĄZERT[3], K. OŻEGOWSKA[3], M. JANKOWSKI[2], M. ROJEWSKA[2], I. KOCHEROVA[2], M. KULUS[1], M. JESETA[4], A. BRYJA[2], L. POROWSKI[5], D. BUKOWSKA[1], M.T. SKOWROŃSKI[6], A. BRĘBOROWICZ[7], M. BRUSKA[2], M. ZABEL[5,8], M. NOWICKI[9], B. KEMPISTY[2,4,9] and P. ANTOSIK[1]

[1]Veterinary Center, Nicolaus Copernicus University in Torun, Torun, Poland; [2]Department of Anatomy, Poznan University of Medical Sciences, Poznan, Poland; [3]Department of Infertility and Reproductive Endocrinology, Poznan University of Medical Sciences, Poznan, Poland; [4]Department of Obstetrics and Gynecology, University Hospital and Masaryk University, Brno, Czech Republic; [5]Division of Anatomy and Histology, University of Zielona Góra, Zielona Góra, Poland; [6]Faculty of Biology and Biotechnology, University of Warmia and Mazury in Olsztyn, Olsztyn, Poland; [7]Department of Pathophysiology, Poznan University of Medical Sciences, Poznan, Poland; [8]Department of Histology and Embryology, Wroclaw Medical University, Wroclaw, Poland; [9]Department of Histology and Embryology, Poznan University of Medical Sciences, Poznan, Poland

Received April 19, 2018 – Accepted July 2, 2018

The similarity between humans and pigs, when it comes to tissue morphology, makes *Sus scrofa* not only a good research model, but also a potential source of cells for tissue engineering. Cell samples obtained from the pig donor, could be influenced *in vitro,* in order to become a source of tissue material for xenotransplantation, reconstructive and regenerative medicine. Significant amounts of data point to especially major similarities in pig and human reproductive systems. Because of that, particular scientific focus is centered on research concerning porcine COCs, theca and granulosa cells in primary cultures. One of the aspects of the reproductive process, that is still largely undiscovered, is the interaction between preimplantation blastocyst and maternal uterine tissues. In this study, we used molecular analysis techniques, such as RT-qPCR and immunocytochemistry, to analyze the expression and distribution of cytokeratin 18 and panCytokeratins 8, 18 and 19 and vimentin in porcine luminal endometrial epithelial cells, coupled with analysis of their behavior in RTCA. The results have confirmed the presence of epithelial, as well as stromal cell markers in the cells, varying in levels at different stages of culture. They have also given insight into the modes of proliferation and differentiation of studied cells in *in vitro* culture, as well as providing additional proof for the possible mesenchymal transdifferentiation of epithelial cells.

The phylogenetic similarity between humans and pigs (*sus scrofa domestica*) has led to substantial use of this species as model in biomedical research. In most of the cases the research is concentrated on the possibility of xenotransplantation and/or finding a source of tissue products applicable in cardiac

Key words: pig, uterus cells, cytokeratin, vimentin, real-time proliferation

Mailing address:
Bartosz Kempisty, PhD
Department of Anatomy,
Poznan University of Medical Sciences,
6 Swiecickiego St., 60-781 Poznan, Poland
Tel.: +48 61 854 64 18 - Fax: +48 61 854 64 40
e-mail: bkempisty@ump.edu.pl

0393-974X (2018)

surgery or orthopedics (1). Much of the existing data suggests several similarities in human and pig reproduction concerning the structures involved, cellular morphology and/or associated processes and their regulations. Therefore, the research that involves pig reproductive cells (oocytes), or embryos may be a potential model for studying physiology and pathophysiology of human reproduction (2, 3).

The primary culture of cumulus-oocytes complexes (COCs), theca cells (TC) or granulosa cells (GC) are frequently used as a model for research of ovum maturation and development, as well as the proliferation and differentiation of surrounding somatic cells that build the structure of mammalian antral follicle (4, 5). In our study, it was found that GC real-time proliferation and differentiation is associated with differential expression and distribution of selected genes and proteins, such as connexins and gonadotropin receptors (6). Moreover, we used the porcine endometrial epithelial cell model for studying expression and distribution of progesterone receptors (classic nuclear and membrane form, PGR, PGRMC1), during luminal epithelial cell real-time proliferation. Recently, we have shown that the value of proliferation index for luminal epithelial cells differs significantly from GC proliferation index, since luminal cells reach the log phase after only 120-144 hours of *in-vitro* cultivation (IVC) (7).

Uterine endometrial tissue is composed of luminal, glandular and stromal epithelium. It was found that vimentin is a marker of stromal epithelium, while cytokeratin 8 (Cyt8) and 18 (Cyt18) belong to luminal epithelium markers (8, 9). The expression of cytokeratins has often been found in reproductive tissues, such as the trophoblast and endometrial glands (10). Therefore, it has been suggested that they may display a significant role during physiological function of uterus, such as proper endometrial embryo recognition, implantation, placentation and fetus development. Since it was found that cytokeratins belong to the large family of intermediate filaments that build the intracytoplasmic skeleton in epithelial tissues, it is suggested that they might form the structure and morphology of cells, and may be involved in the processes of cell division and its regulation, cell differentiation and movement (11, 12).

The interaction between growing embryo (preimplantation blastocyst) and maternal endometrium, on molecular level, is still an enigmatic issue of mammalian reproduction. The movement, as well as founding of implantation locations, significantly determines proper fetus growth. Since the cytokeratins may regulate the processes of cell signaling and movement, it has been suggested that they may be also involved in regulation of embryo-maternal interactions in the endometrial tissue of the uterus. The aim of this study was to analyze the expression and distribution of cytokeratin Cyt18, pan cytokeratin (PanCyt) 8, 18, 19 and vimentin (Vim), in porcine luminal epithelial cells in primary cultivation model.

MATERIALS AND METHODS

Animals

In this study, crossbred Landrace gilts (n=45) at the age of about nine months, which displayed two regular estrous cycles, were collected from a commercial herd. All the animals were checked daily for estrus behavior and were slaughtered after reaching the anestrus phase of the estrus cycle. The uteri were then transported at 38°C to the laboratory within 30 min.

Endometrial cells (ECs) selection and culture

After slaughter, the uterine horns were washed twice with PBS (137 mM NaCl, 27 mM KCl, 10 mM Na_2HPO_4, 2 mM KH_2PO_4, pH 7.4) and immediately cut into small pieces (25-35 mg). Surface uterine epithelial cells were surgically removed using sterile surgical blades. The cell suspension obtained from this digestion was filtered through a mesh to remove non-dissociated fragments of tissue and then incubated with 0.05% collagenase I (Sigma Aldrich, Madison, USA) for 25 min at 38°C in a shaking water bath. Isolated cells were washed three times by centrifugation (10 min at 200 g) with Dulbecco's modified Eagle's medium (DMEM; Sigma Aldrich, Madison, USA) supplemented with gentamicin (20µg/mL) and 0.1% BSA. The resulting luminal epithelial cells were filtered and washed three times by centrifugation (10 min at 200 g) with supplemented DMEM. The final pellet

of luminal epithelial cells was resuspended in DMEM supplemented with 10% fetal calf serum (FCS; Sigma Aldrich, Madison, USA) and 10,000 U mL^{-1} penicillin G, 10 mg mL^{-1} streptomycin and 25 µg mL^{-1} amphotericin B (antibiotic antimycotic solution; Sigma Aldrich, Madison, USA). The viability of the cells was 90 to 95%, as judged by trypan blue staining (Sigma Aldrich, Madison, USA). The cells were cultured at 38°C in a humidified atmosphere of 5% CO_2. The culture medium was changed every 3 days.

In vitro endometrial cell cultivation using a real-time cell analyzer

The recovered endometrial cells were transferred into an E-Plate 16 of a real-time cell analyzer (RTCA), (Roche-Applied Science, GmbH, Penzberg, Germany), which consisted of an RTCA, an RTCA SP station, and RTCA software. The cells were then cultured in 200 µl of standard porcine culture medium that consisted of Dulbecco's Modified Eagle's Medium (DMEM, Sigma-Aldrich, USA) as mentioned above. The cells were cultured for 0-168 h at 38.5°C under 5% CO_2 in air. The cultivation medium was replaced every three days. After each period of cultivation, the cells were treated with trypsin (0.25% trypsin in a balanced salt solution, Sigma-Aldrich, St. Louis, MO, USA), and the collected pool of proliferating cells was used for RT-qPCR analysis. After each cultivation period, the cell index (CI) was used to evaluate the relative and quantitative changes in electrical cell impedance. The cell status was determined using RTCA software.

Confocal microscopy analysis of Cytokeratin 18, panCytokeratin (8, 18, 19) and Vimentin expression and distribution in porcine luminal epithelial cells

The luminal epithelial cells were transferred into an X-well Lumox (94. 6150. 401, 4-well lumox Detachable, Sarstedt AG & Co. KG). The cells were then cultured in 1 ml of standard porcine culture medium that consisted of Dulbecco's Modified Eagle's Medium (DMEM, Sigma-Aldrich, USA) as mentioned above. The cells were cultured for 0-168 h at 38.5°C under 5% CO2 in air. The cultivation medium was replaced every three days. The cells ware fixed using acetone-methanol (1:1) for 10 min at -20°C and washed three times in PBS/PVP (0.2%). To block nonspecific binding, samples were incubated in 3% BSA in PBS with 0.1% Tween 20 for 30 min at RT. The luminal epithelial cells were incubated for 1 h at room temperature (RT) with mouse monoclonal anti-cytokeratin 18 antibody (DC10), with mouse monoclonal anti-cytokeratin 8, 18, 19 antibody (ab 41825) and with mouse monoclonal vimentin antibody (ab 20346), (purchased from Dako and Abcam, respectively) diluted 1:500 in PBS/1.5% BSA/0.1% Tween 20. After several washes with PBS/0.1% Tween 20, samples with the primary antibodies mentioned above were incubated for 1 h at RT with fluorescein isothiocyanate (FITC)-conjugated goat anti-rabbit IgG Ab and diluted 1:500 in PBS/0.1% Tween20. Following washing in PBS/0.1% Tween20, the luminal epithelial cells were stained with 0.1 µg/ml 4,6-diamino-2-phenylindole (DAPI; Santa Cruz Biotechnology, Santa Cruz, CA, USA) in mineral oil, mounted on glass slides in an antifade solution drop and examined under an LSN 510 confocal system in a Fluoview 10i microscope (Olympus). FITC was excited at 488 nm with an argon laser, and emissions were imaged through a 505-530 nm filter. All confocal microscopic images were analyzed using Imaris 7.2 software (BitPlane, Zurich, Switzerland).

RNA extraction from porcine luminal epithelial cells

Total ribonucleic acid (RNA) was extracted from samples using TRI Reagent (Sigma, St Louis, MO, USA) and RNeasy MinElute cleanup Kit (Qiagen, Hilden, Germany). The amount of total messenger RNA (mRNA) was determined from the optical density at 260 nm, and the RNA purity was estimated using the 260/280 nm absorption ratio (higher than 1.8) (Nano Drop spectrophotometer, Thermo Scientific, ALAB, Poland). The RNA integrity and quality were checked on a Bioanalyzer 2100 (Agilent Technologies, Inc., Santa Clara, CA, USA). The resulting RNA integrity numbers (RINs) were between 8.5 and 10 with an average of 9.2 (Agilent Technologies, Inc., Santa Clara, CA, USA). The RNA in each sample was diluted to a concentration of 100 ng/µl with an OD260/OD280 ratio of 1.8/2.0. From each RNA sample, 500 ng of RNA was taken. The remaining amount of isolated RNA was used for the RT-qPCR study.

Real-time quantitative polymerase chain reaction analysis

Total RNA was isolated from luminal epithelial cells on each of the seven days of culture. The RNA samples

were re-suspended in 20 µl of RNase-free water and stored in liquid nitrogen. RNA samples were treated with DNase I and reverse-transcribed (RT) into cDNA. Real-time quantitative polymerase chain reaction (RT-qPCR) was conducted in a Light Cycler real-time PCR detection system (Roche Diagnostics GmbH, Mannheim, Germany) using SYBR® Green I as a detection dye, with target cDNA quantified using the relative quantification method. The relative abundance of CHRDL1, FST, TGFβR3, SMAD4, and ID1 transcripts in each sample was standardized to the internal standards. For amplification, 2 µl of cDNA solution was added to 18 µl of QuantiTect® SYBR® Green PCR (Master Mix Qiagen GmbH, Hilden, Germany) and primers (Table I). One RNA sample of each preparation was processed without the RT-reaction to provide a negative control for subsequent PCR.

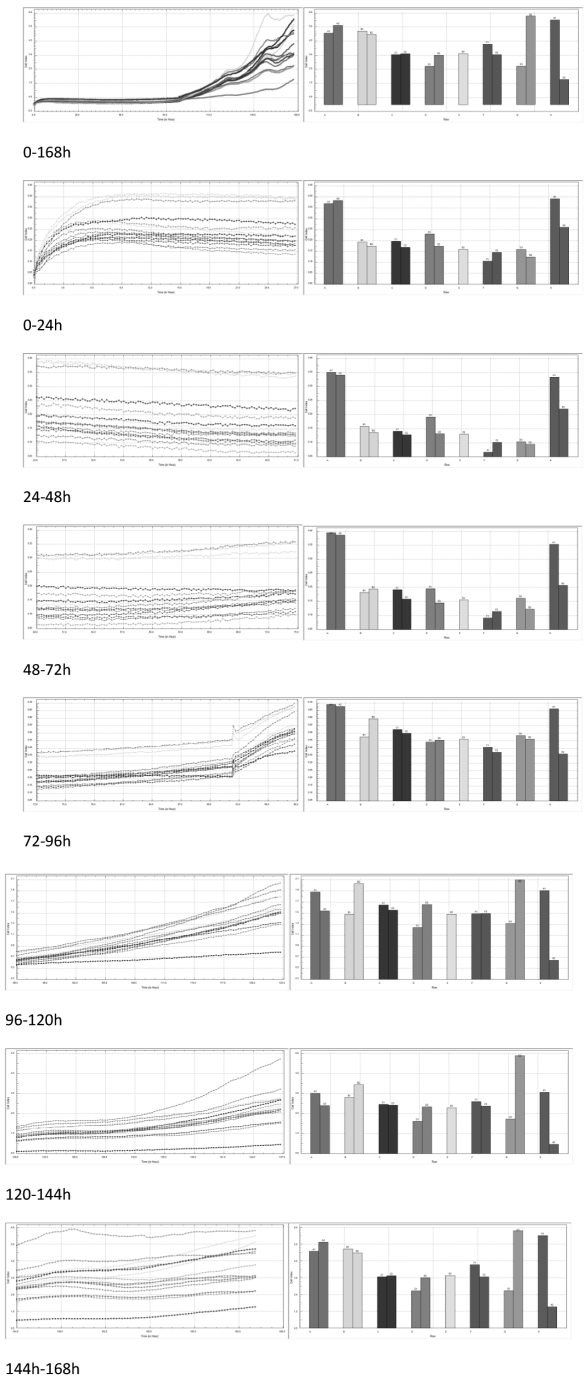

Fig. 1. *Real time cell analysis (RTCA) results, in different time periods of primary culture, presented in form of a line graph, with starting and ending cell index plotted on a corresponding bar graphs. Each sample is drawn using a different color on both of the graphs.*

Statistical analysis

One-way ANOVA followed by the Tukey post-test was used to compare the RTCA quantification results. The experiments were carried out with at least four replicates. The differences were considered to be significant at $*P < 0.05$, $**P < 0.01$ and $***P < 0.001$. The statistical calculations were applied to compare the results in each investigated group to the highest normalized proliferation index at each time point. GraphPad Prism version 4.0 software (GraphPad Software, San Diego, CA, USA) was used for all statistical calculations.

RESULTS

RTC analysis showed a specific pattern of cell proliferation, based on cell index analysis. The cell index was almost unchanged for the first 90 hours. Then, around hour 93, it started to rapidly increase. The total increase in cell index varied between the cell samples. However, every population's index rose. The results of specific time periods are presented in Fig. 1.

Cells analyzed during RTCA, were subjected to immunofluorescent staining, using specific antibodies for CK18, pCK and Vimentin, with DAPI serving as positive control. The results were analyzed using confocal microscopy and are presented in Fig. 2.

As can be seen, intense, intracellular, extranuclear luminosity can be observed in all of the tests and time periods apart from 24th hour of culture when detecting Vim. While in that case the fluorescence is not observable easily, it is present, as confirmed

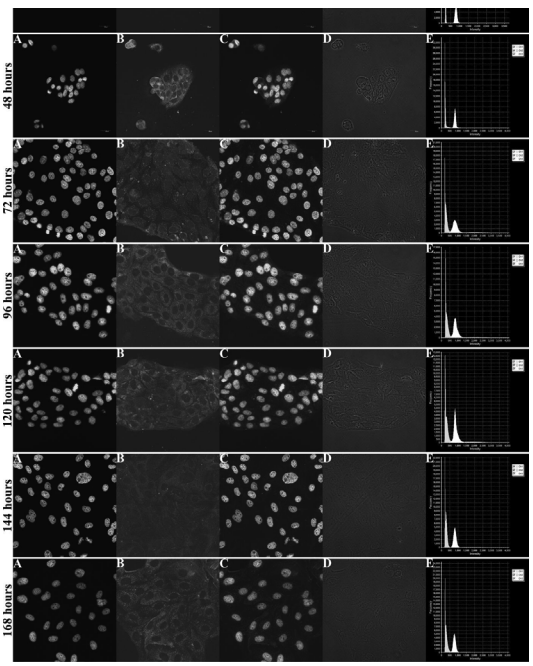

A

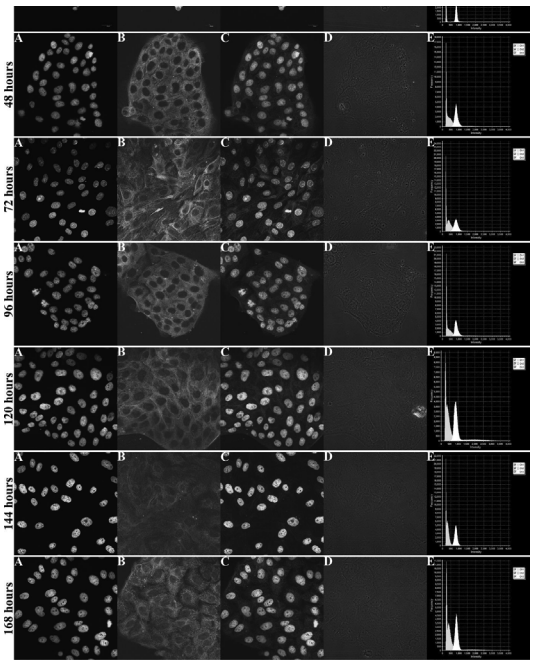

B

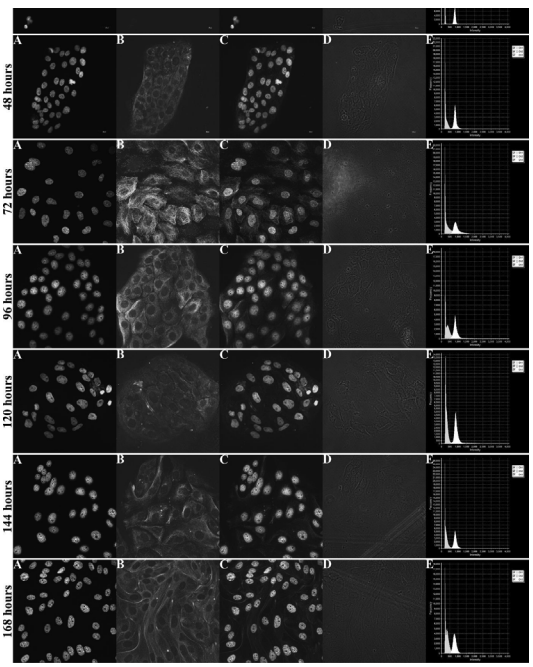

C

Fig. 2. ***A)*** *Immunofluorescence test results, with the primary antibody designed to detect CK18. A-positive control using DAPI; B-Results of CK18 detection using FitC; C-positive control using DAPI, presented together with CK18 detection using FitC; D-negative control without the use of cytochrome; E-levels of fluorescence presented on a graph.* ***B)*** *Immunofluorescence test results, with the primary antibody designed to detect pCK. A-positive control using DAPI; B-Results of pCK detection using FitC; C-positive control using DAPI, presented together with pCK detection using FitC; D-negative control without the use of cytochrome; E-levels of fluorescence presented on a graph.* ***C)*** *Immunofluorescence test results, with the primary antibody designed to detect Vim. A-positive control using DAPI; B-Results of Vim detection using FitC; C-positive control using DAPI, presented together with Vim detection using FitC; D-negative control without the use of cytochrome; E-levels of fluorescence presented on a graph.*

by the fluorescence graph. These results confirm the presence of all of the cellular antigens analyzed throughout the culture period.

Additionally, the region of interest intensity of fluorescence of specific antibodies was compared at different time periods of primary culture. The results are presented in the form of bar graphs in Fig. 3.

As can be seen on the graphs, most of the markers present distinct patterns of fluorescence intensity. CK18 is the most intense at hour 48, later stabilizing at around half of the highest value, until the end of observation. pCK was most fluorescent at hour 24, with luminosity decreasing over 2.5-fold at hour 48, rising 50% at hour 72 and then stabilizing till the end of observation. With regard to Vimentin, initial fluorescence is very low, rising slightly at hour 48 and reaching its peak value, more than 5-fold higher than initially, at hour 72. After the peak, the intensity of fluorescence gradually decreases, stabilizing at around 60% of the peak at the end of observation.

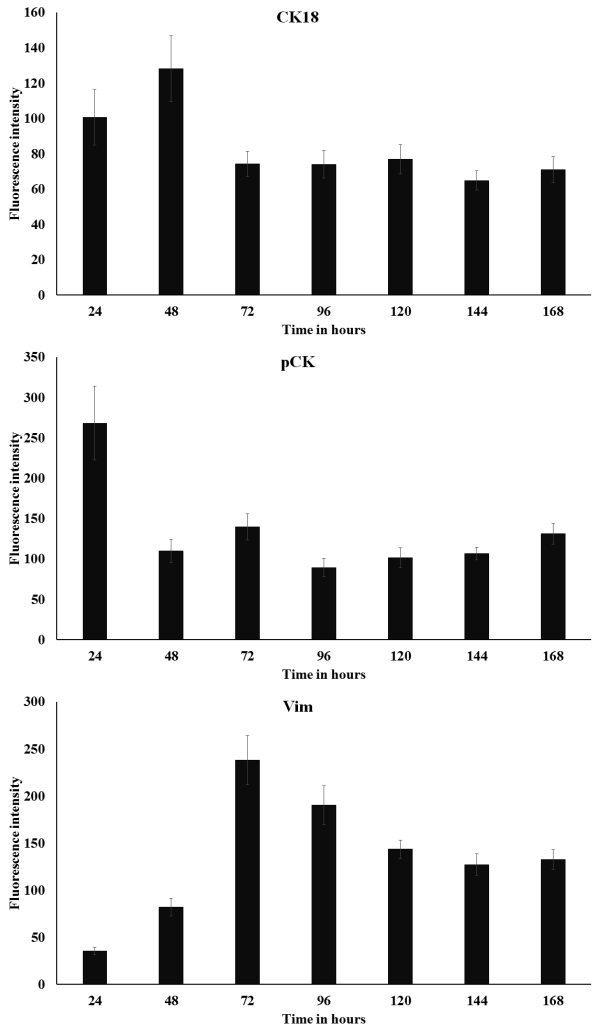

Fig. 3. *Region of interest (ROI) fluorescence intensity measurement results, presented as a bar graph for different stages of primary culture.*

Finally, the levels of the studied markers were analyzed using the RT-qPCR method. The results are shown in Fig. 4.

As can be seen, at hour 48 the expression of all of the markers fell, except from Vimentin, which rose significantly. The levels of expression stabilized at hour 72, with CK19 exhibiting a major rise this time. At hour 96, most of the genes retain their level of expression, except for CK19 which presents a major fall. Throughout the rest of the culture time, all of the genes exhibited no major changes, apart from a small but steady increase in expression.

DISCUSSION

The mammalian endometrium is composed of several layers, which differ significantly in the matter of tissue morphology. However, the physiological properties of cells, isolated form distinct layers and cultured *in vitro*, are not yet fully recognized. It is suggested that cells cultured *in vitro*, characterized by different morphology, have distinct biochemical and metabolomic status. Moreover, isolating and collecting the selected layers of endometrium, such as luminal, glandular and stromal epithelium, still brings difficulties. However, since the epithelial and stromal endometrial markers are well defined, a possibility exists to differentiate between cell types, and/or tissue specimens cultured *in vitro,* after immunohistochemical assays. Recently, we investigated the gene expression and protein cellular distribution of cytokeratins and vimentin, which brings new possibilities to distinguish epithelial and stromal origin of porcine buccal pouch mucosal cells, cultured *in vitro,* during short-term, real-time proliferation. Therefore, we may suggest that the expression of cytokeratins, and/or vimentin, in epithelial/stromal cells *in vitro,* is a good primary culture model for recognition of cell origin, as well

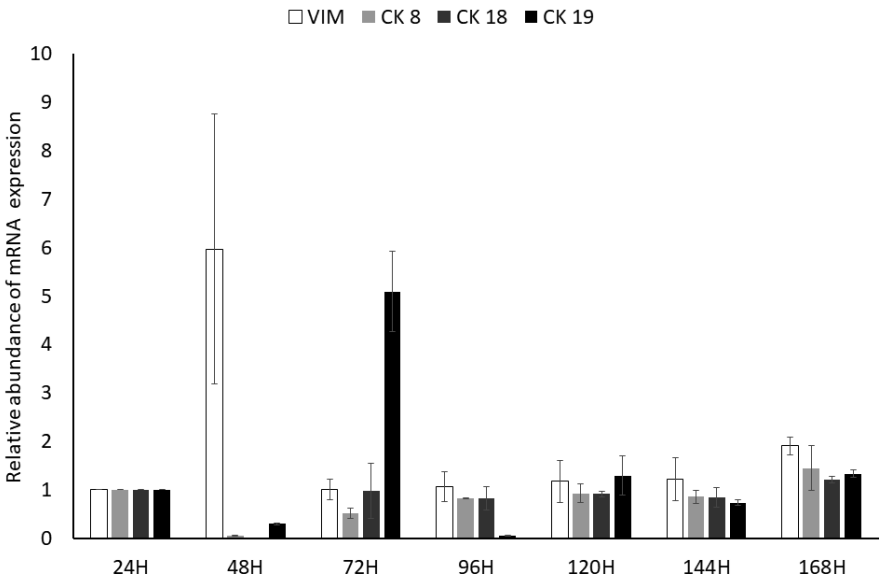

Fig. 4. *Results of RT-qPCR analysis of relative levels of gene expression, with 24 h of culture serving as reference level, in different periods of culture. VIM-Vimentin, CK 8-Cytokeratin 8, CK 18-Cytokeratin 18, CK 19-Cytokeratin 19.*

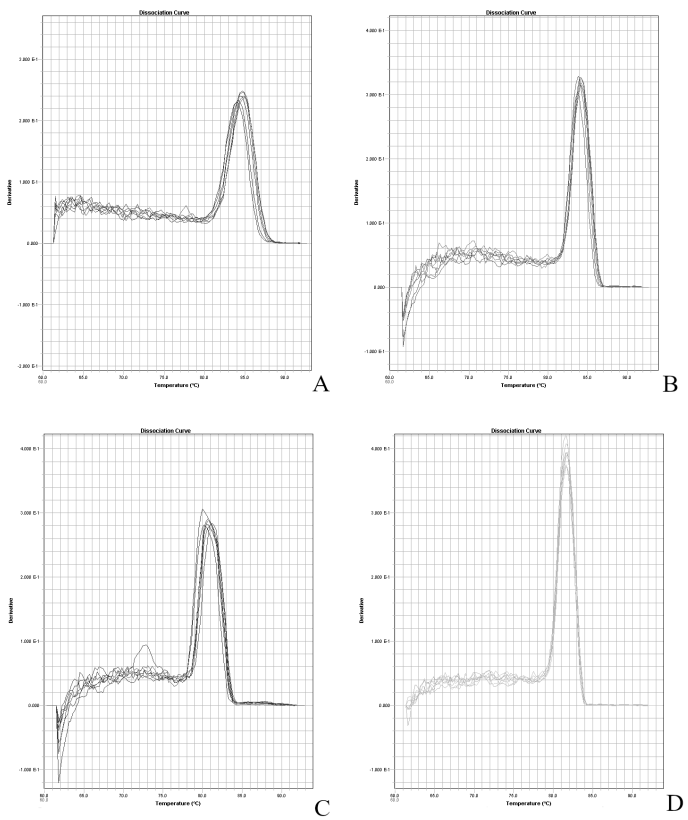

Fig. 5. *Dissociation curves that confirm the specificity of the amplification products obtained in the RT-qPCR analysis. A- Cytokeratin 8, B- Cytokeratin 18, C- Cytokeratin 19, D- Vimentin.*

as for distinguishing the subtle morphological and biochemical properties of isolated cells.

A large number of luminal epithelial cells can be obtained from porcine uterine horns during isolation, which makes them a good source of those cells. The most obvious *in vitro* challenge is to characterize the epithelial cells and the layer from which the cell population originates (13). For this purpose, immunofluorescence studies, analysing expression of vimentin and cytokeratin in epithelial luminal cells, were performed. Primary cultured epithelial cells were observed to show positive signals for cytokeratin, while expression for vimentin in cells increased with rut duration. Although the cells morphologically retained endometrial traits during 7 days of culture, as well as after many passages, they were positive for both the epithelial marker, cytokeratin, and stromal marker, vimentin. It has been repeatedly reported that epithelial cells containing cytokeratin acquire vimentin during *in vitro* culturing periods (14). Co-expression of both epithelial and mesenchymal markers *in vitro* has been explained as transformation of epithelial cells into mesenchymal cells (15). It was also thought that this transition correlates with a loss of contact between cells that results from disaggregation of cells during the epithelial cell preparation period (16). In previous studies on endometrial cells, there were reports of vimentin expression in *in vitro* cultures, while trophoblasts maintained epithelial character (17). However, this was on the side of the trophoblast, not the epithelium of the uterus (18). With increasing frequency transformational plasticity of epithelial and endothelial cells is brought to light, which may explain the increase in expression of vimentin during subsequent days of cell culture (15).

In addition to these observations, a previous study (19) also indicated that the development of endometrial cells requires biochemical communication, as well as interactions between cells if pregnancy is to occur, suggesting that communication between the uterine epithelial cells should be studied not only by co-culture systems, but also in flexible and dynamic cell environments.

Studies conducted on primary prostate epithelial cell cultures have shown that primary luminal cells have the ability to differentiate into luminal cells. Molecular studies proved that distinct transcriptomes of basal and luminal cells are also found in the epithelial cell types, as well as in the epithelial compartment and the underlying stroma. Understanding such crosstalk could be instrumental for understanding the normal development and tumorigenesis of prostate (20).

Other reports expressed the need for communication between epithelial and primary luminal cells. The basal cells sense luminal factors, creating a narrow body projection that can intersect tight epithelial junctions. Studies on the structural plasticity of basal cells in rat epididymis and vas deferens during postnatal development, and their modulation by androgens in adulthood by using immunofluorescence techniques for cytokeratin 5, showed that the primary cells are absent at birth, which supports the theory that basal epithelium is undifferentiated at birth (21). Moreover, sources indicate that these basic cell extensions towards lumen can intersect tight junction connections (TJCs) to scan the lumen environment and pass their findings on to neighbouring cells. This provides evidence for the presence of communication between basal and luminal cells (21).

As a part of the epithelial cytoskeleton, keratin is important for the mechanical stability and integrity of epithelial cells and tissues. It was found that keratin is not simply statically present in intracellular skeletal structures, but is highly dynamic. In addition, some keratins also have regulatory functions and are involved in intracellular signalling pathways, e.g. stress protection, wound healing and apoptosis. Furthermore, cytokeratin 8, 18 and 19 are major factors in the protection of placental barrier and trophoblast functions (11, 22). Cytokeratin 8 and 17 protect cells against apoptosis (12, 23), and play a role in the regulation of protein synthesis and cell size during wound healing involving intracellular signalling pathways. Keratins, unsurprisingly, have very different signalling functions outside of their mechanical roles (9). Our studies show an increase in the activity of cytokeratin 18 in the first 48 hours and panCytokeratins (6, 8, 19, 20) in the first 72 hours of primary culture, which indicates strong

cell proliferation, increasing their number and size necessary to form a suitable cellular layer. However, expression of vimentin increases during the first 72 hours which, in turn, suggests the beginning of cell differentiation and formation of mesenchymal cells.

The balance between epithelial and stromal markers is very important in the diagnosis of cancer. Vimentin is strongly positive in the mesenchymal component, and intense staining of CK14, CK19 and pan-CK may be detected in the epithelium (10, 24). Detailed knowledge on these biomarkers may help in the detection and treatment of many diseases, not only cancer.

Each cell is subject to a molecular time measurement mechanism, controlled by a biological clock that operates by means of a negative feedback mechanism, based on levels of transcriptional actuators and repressors, thus controlling behavior, physiology and gene expression according to the time of day. This results in a set of highly cyclic transcriptional activities that peak at various phases throughout the day, driving the rhythmic expression of many other genes. Mechanisms that operate at the post-transcriptional level affecting the daily RNA matrix (mRNA) and protein kinetics are additional factors contributing to the generation of differences between cells (25). Our research shows high vimentin gene expression at 48 h in the rtPCR study, with the protein at its highest at 72 h, showing that differences in organ-to-body translation efficiency can correct the time of protein production from rhythmic mRNA, and levels of core protein production, in accordance with tissue specificity. In addition, the divergence of gene expression is largely programmed at the level of transcript abundance. The widespread differences in translational efficiency between organs serve to achieve greater consistency in the production of protein between tissues. It is conceivable that such translational compensation reflects selective pressure to maintain exact protein levels instead of mRNA levels (25).

On the other hand, the cell culture is exposed to a number of stressful stimuli that disturb cell homeostasis, and an important part of the coordinated cellular reaction that occurs is the control of protein synthesis. After restriction of nutrients or environmental stress conditions, mTOR signalling, the main regulator of protein synthesis, is inhibited, while the eIF2α (eukaryotic initiator 2α) kinase and GCN2 (general control nonderepressible 2) are activated. Although they use separate mechanisms, both are able to initiate a general closure of protein synthesis, which is accompanied by specific mRNA translations. This translational control induces an adaptive response that allows cells to survive by conserving energy and selectively inducing stress-resistant proteins (26–28). In addition, the global reduction of mRNA translation may also preserve protein homeostasis (or proteostasis), preventing the production of excessive amounts of proteins, some of which may be undesirable for normal cellular function. It has been shown that not only the internal tendencies of aggregation proteins, but also their high cellular levels can drive their aggregation into non-functional and sometimes cytotoxic structures. Although the cells have evolved, an extensive network of proteolytic systems protects the integrity of the proteome and provides proteostasis. The functionality of these systems is triggered by stress, aging or pathologies, which cause widespread aggregation of the proteome that occurs under these conditions (26, 29).

ACKNOWLEDGEMENTS

This study was funded by grant number UMO-2016/21/B/NZ9/03535 from the Polish National Centre of Science and by grant number 502-01-02227367-08414 from Poznan University of Medical Sciences

REFERENCES

1. Febrero B, Ríos A, López-Navas A, et al. Teenagers and their future role in transplantation: an analysis of their attitudes toward solid organ xenotransplantation. Transplant Proc 2018; 50(2):526-29.
2. Budna J, Celichowski P, Bryja A, et al. Significant down-regulation of "biological adhesion" genes in porcine oocytes after IVM. Int J Mol Sci 2017; 18(12):2685.
3. Kranc W, Jankowski M, Budna J, et al. Amino acids

metabolism and degradation is regulated during porcine oviductal epithelial cells (OECs) primary culture in vitro – a signaling pathways activation approach. Med J Cell Biol 2018; 6(1):18-26.
4. Kranc W, Budna J, Chachuła A, et al. "Cell migration" is the ontology group differentially expressed in porcine oocytes before and after in vitro maturation: a microarray approach. DNA Cell Biol 2017; 36(4):273-82.
5. Jankowski M, Dyszkiewicz-Konwińska M, Budna J, et al. Does migrative and proliferative capability of epithelial cells reflect cellular developmental competence? Med J Cell Biol 2018; 6(1):1-7.
6. Kempisty B, Ziółkowska A, Piotrowska H, et al. Short-term cultivation of porcine cumulus cells influences the cyclin-dependent kinase 4 (Cdk4) and connexin 43 (Cx43) protein expression--a real-time cell proliferation approach. J Reprod Dev 2013; 59(4):339-45.
7. Kempisty B, Wojtanowicz-Markiewicz K, Ziółkowska A et al. Association between progesterone and estradiol-17beta treatment and protein expression of pgr and PGRMC1 in porcine luminal epithelial cells: a real-time cell proliferation approach. J Biol Regul Homeost Agents 29(1):39-50.
8. Skowronski MT. Distribution and quantitative changes in amounts of aquaporin 1, 5 and 9 in the pig uterus during the estrous cycle and early pregnancy. Reprod Biol Endocrinol 2010; 8(1):109.
9. Moll R, Divo M, Langbein L. The human keratins: biology and pathology. Histochem Cell Biol 2008; 129(6):705-33.
10. Niu H, Liu J, Chen Y, Geng N. Ameloblastic fibro-odontosarcoma of the mandible with active epithelial proliferation: A rare case report. Mol Clin Oncol 2017; 7(6):971-75.
11. Hesse M, Berg T, Wiedenmann B, Spengler U, Woitas RP, Magin TM. A frequent keratin 8 p.L227L polymorphism, but no point mutations in keratin 8 and 18 genes, in patients with various liver disorders. J Med Genet 2004; 41.
12. Tong X, Coulombe PA. Keratin 17 modulates hair follicle cycling in a TNFalpha-dependent fashion. Genes Dev 2006; 20(10):1353-64.
13. Guseva N V, Knight ST, Whittimore JD, Wyrick PB. Primary cultures of female swine genital epithelial cells in vitro: a new approach for the study of hormonal modulation of Chlamydia infection. Infect Immun 2003; 71(8):4700-10.
14. Li X, Li Z, Hou D, Zhao Y, Wang C, Li X. The bovine endometrial epithelial cells promote the differentiation of trophoblast stem-like cells to binucleate trophoblast cells. Cytotechnology 2016; 68(6):2687-98.
15. Hernández EÁ, Kahl S, Seelig A. et al. Acute dietary fat intake initiates alterations in energy metabolism and insulin resistance. J Clin Invest 2017; 127(2):695-708.
16. Zeiler M, Leiser R, Johnson GA, Tinneberg H-R, Pfarrer C. Development of an in vitro model for bovine placentation: a comparison of the in vivo and in vitro expression of integrins and components of extracellular matrix in bovine placental cells. Cells Tissues Organs 2007; 186(4):229-42.
17. Yamakoshi S, Bai R, Chaen T, et al. Expression of mesenchymal-related genes by the bovine trophectoderm following conceptus attachment to the endometrial epithelium. Reproduction 2012; 143(3):377-87.
18. Donker RB, Mouillet JF, Chu T, Hubel CA, Stolz DB, Morelli AE, Sadovsky Y. The expression profile of C19MC microRNAs in primary human trophoblast cells and exosomes. Mol Hum Reprod 2012; 18(8):417-24.
19. Krishnaswamy S, Kanteti R, Duke-Cohan J,S et al. Ethnic differences and functional analysis of MET mutations in lung cancer. Clin Cancer Res 2009; 15(18):5714-23.
20. Zhang D, Park D, Zhong Y, et al. Stem cell and neurogenic gene-expression profiles link prostate basal cells to aggressive prostate cancer. Nat Commun 2016; 7:10798.
21. Shum WWC, Da Silva N, McKee M, Smith PJS, Brown D, Breton S. Transepithelial projections from basal cells are luminal sensors in pseudostratified epithelia. Cell 2008; 135(6):1108-17.
22. Hesse M, Franz T, Tamai Y, Taketo MM, Magin TM. Targeted deletion of keratins 18 and 19 leads to trophoblast fragility and early embryonic lethality. EMBO J 2000; 19(19):5060-70.
23. Caulín C, Salvesen GS, Oshima RG. Caspase cleavage of keratin 18 and reorganization of intermediate

filaments during epithelial cell apoptosis. J Cell Biol 1997; 138(6):1379-94.
24. Choi W, Czerniak B, Ochoa A, Su X, Siefker-Radtke A, Dinney C, McConkey DJ. Intrinsic basal and luminal subtypes of muscle-invasive bladder cancer. Nat Rev Urol 2014; 11(7):400-10.
25. Castelo-Szekely V, Arpat AB, Janich P, Gatfield D. Translational contributions to tissue specificity in rhythmic and constitutive gene expression. Genome Biol 2017; 18(1):116.
26. Arnsburg K, Kirstein-Miles J. Interrelation Between Protein Synthesis, Proteostasis and Life Span. Curr Genomics 2014; 15(1):66-75.
27. Borbolis F, Syntichaki P. Cytoplasmic mRNA turnover and ageing. Mech Ageing Dev 2015; 152:32-42.
28. Spriggs KA, Bushell M, Willis AE. Translational regulation of gene expression during conditions of cell stress. Mol Cell 2010; 40(2):228-37.
29. Díaz-Villanueva J, Díaz-Molina R, García-González V. Protein folding and mechanisms of proteostasis. Int J Mol Sci 2015; 16(12):17193-230.

AZITHROMYCIN INFLUENCES AIRWAY REMODELING IN ASTHMA VIA THE PI3K/Akt/mTOR/HIF-1α/VEGF PATHWAY

X. ZHAO[1,2], FQ. YU[2], XJ. HUANG[1], BY. XU[1], YL. LI[1], XY. ZHAO[2], HF. GUO[2] and B. LUAN[1]

[1]Department of Pediatrics, Third Affiliated Hospital, Zhengzhou University, Zhengzhou, China; [2]Maternal and Child health hospital of Zhengzhou City, Zhengzhou, China

Received February 6, 2018 – Accepted July 30, 2018

Asthma is a respiratory disease that affects people of all walks of life, and is a hotspot of continuous research, with significant manpower and resources invested in its study. Airway remodeling is an important associated pathological change, and a mark of the irreversible damage produced by asthma. It involves compositional and functional changes in the cells of the airway walls, leading to reversible structural changes, and complicating treatment. Airway remodeling is mediated by different inflammatory pathways which have been targeted for treatment, with good results. However, given its complexity, systematic study of the pathogenesis of airway remodeling is still needed, and additional targeted therapies are necessary. Macrolide drugs, such as erythromycin, azithromycin, and clarithromycin, have antibacterial effects and also influence the cytokine secretion of macrophages and T-lymphocytes. They have direct effects on a variety of cytokines, inhibiting inflammation and reducing airway reactivity. In this study, we investigated the protective effect of azithromycin on airway remodeling through the phosphoinositol-3 kinase/Akt/mechanistic target of rapamycin kinase/hypoxia-inducible factor 1α (HIF-1α)/vascular endothelial growth factor (VEGF) pathway. We observed that a long course of azithromycin could significantly reduce airway reactivity and ovalbulmin-induced pathological alterations in asthmatic mice. Gene expression analysis confirmed that HIF-1α and VEGF were significantly down-regulated following a long course of azithromycin administration.

Bronchial asthma is manifested by repeated reversible episodic airway obstruction with ongoing inflammation (1). Its pathogenesis is complex, involving airway hyperresponsiveness (AHR), inflammation, and remodeling, and remains incompletely understood (2). Asthma prevalence has increased over the last 20 years (3). Approximately 300 million people suffer from asthma worldwide, and this number is predicted to rise to over 400 million in the next 10–15 years (4).

Airway remodeling is a pathological change that marks the irreversible damage that asthma can cause (5). The pathological changes result in limited airflow, cause AHR, and increase the frequency of acute attacks. At present, asthma treatments mainly inhibit inflammation, limiting remodeling, but there can be stark individual differences in treatment effects. Therefore, research examining the mechanisms of different treatments in particular types of asthma is important for future individualized treatment.

Macrolide drugs can be used as immune regulators in diffuse generic bronchitis, bronchial asthma, cough

Key words: asthma, mice, airway remodeling, inflammation, hypoxia-inducible factor 1α, vascular endothelial growth factor

Mailing address:
Dr Bin Luan,
Department of Pediatrics,
Third Affiliated Hospital,
Zhengzhou University, Zhengzhou, 450000, China
Tel.: +371 66903341 - Fax: +371 66992000
e-mail: xiuxiali2015@163.com

0393-974X (2018)

variant asthma, and chronic obstructive pulmonary disease (6). In this study, we examined the effects of azithromycin as it displays good gastrointestinal tolerability, better tissue penetration, and a longer half-life than other large macrolides, suggesting higher compliance and effectiveness (7).

Phosphoinositide-3-kinase (PI3K) is a key signal transduction enzyme involved in cell transformation. PI3K activation is related to cell survival, migration, cytoskeletal reorganization, and metabolism (8). The overall effect of PI3K inhibition *in vivo* is determined by opposing actions in different lymphocyte subsets (9). PI3K and Akt activate mechanistic target of rapamycin kinase (mTOR), a 289 kDa serine/threonine kinase that regulates the synthesis of protein involved in cell cycle progression and mitosis (10) through a phosphorylation cascade involving ribosomal protein S6 kinase and eukaryotic translation initiation factor 4E binding protein 1 (11). Hasaneenet et al. (12) found that applying mechanical pressure to airway smooth muscle induces hypoxia-inducible factor 1α (HIF-1α)-dependent vascular endothelial growth factor (VEGF) expression through the mTORpathway. Cheng (13) found that inhibitors of PI3K/Akt/mTOR signaling, such as wortmannin, and rapamycin, can markedly decrease HIF-1α. Through high expression and regulation of its target genes, HIF-1α influences energy metabolism and vascular tension (14). VEGF is a main HIF-1α target molecule in anoxic environments and by influencing VEGF expression, HIF-1α is directly involved in angiogenesis (15). In this study, we aimed to verify the effects of the PI3K/Akt/mTOR/ HIF-1α/VEGF pathway on airway remodeling and examine the effects of azithromycin treatment.

MATERIALS AND METHODS

Study animals

Male BALB/c mice were purchased from the Laboratory Animal Center, at Zhengzhou University, and housed under standard conditions (ambient temperature, (22±1°C); humidity, (60±10%); with a 12-h light/dark cycle) throughout the study. All mice were bred and housed under pathogen-free conditions and maintained according to the recommendations of the National Institutes of Health Guide for Care and Use of Laboratory Animals (Publication NO. 86-23, revised 1985).

Study groups

Fifty mice (6–8 weeks old) were randomly divided into five groups (n=10 each): control group containing non-sensitized animals, an asthma group (sensitized with OVA), a short-course azithromycin (AZM) group (OVA sensitization plus short-course AZM treatment), a long-course azithromycin (AZM) group (OVA sensitization plus long-course AZM treatment), and a positive control group (OVA sensitization plus budesonide treatment).

Chemicals, drugs, and reagent kits

OVA (grade III) and aluminum hydroxide ($Al(OH)_3$) were obtained from Sigma-Aldrich Chemical Co., USA. Azithromycin and budesonide were obtained from Pfizer Pharmaceuticals Ltd. and AstraZeneca Pharmaceuticals Ltd., respectively. Test reagent kits included an IgE enzyme-linked immunosorbent assay (ELISA) kit (Express Biotech, USA). All other chemicals and reagents used were of analytical grade.

Study design

On days one, eight, and fifteen, mice were intraperitoneally injected with 0.2 mL of a mixture containing 20 μg OVA and 1 mg Al(OH)3 for sensitization.

Starting on day 22, the mice were subjected to 2% OVA saline inhalation for 30 min every other day. The control group was intraperitoneally injected with normal saline, and administered saline atomization starting on day 22.

The short-course azithromycin group received 0.09 mg/g azithromycin by gavage, 30 min before each OVA atomization, for 14 days; the long-course azithromycin group was treated for 28 days. The positive control group was treated with budesonide 2 min before each OVA atomizing inhalation for 14 days

The lungs of the mice were harvested 24 h after experimental completion. The mice were anesthesized with ether and half of them were subjected to rapid thoracotomy of the left lung. The tissue was frozen in liquid nitrogen for reverse transcription-quantitative polymerase chain reaction (RT-qPCR) and Western blot analysis. The left atrium, and right ventricle were opened for pulmonary artery catheterization to the right, and

the middle lobe was quickly rinsed with physiological saline, before 24 h fixation in 4% formaldehyde, graded ethanol dehydration, and paraffin embedding. Sections (5 μm) were subjected to hematoxylin and eosin (HE) and immunohistochemical staining.

For the other half of the mice, the skin of the neck was cut, exposing the trachea. After intubation, lavage was performed three times, with 0.6 mL PBS, and the lavage fluid was analyzed by cell counting and ELISA.

After HE staining, lung sections from the five groups were compared by Masson and PAS staining by measuring the thickness of the airway wall of smooth muscle layer and submucosa as well as the collagen in the goblet cells of phase-contrast.

AHR measurements

AHR to acetylcholine chloride (ACH; Sigma, St. Louis, MO, USA) was measured by whole-body and invasive plethysmography (Buxco Electronics Inc., NY, USA). Twenty-four hours after the last OVA challenge, mice were anesthetized with ether, and a tracheal tube was inserted via a tracheotomy. The mice were then placed in a whole-body phethysmography chamber and the tracheal tube was connected to the ventilator for mechanical ventilation with a tidal volume of 0.2 mL and a frequency of 140 breaths/min. After 3 min of equilibration on the ventilator, PBS containing increasing doses of ACH (0, 3.125, 6.25, 12.5, and 25 mg/mL) was administered through the ventilator with an ultra-sonic nebulizer. Lung resistance (RL) was measured to express the change in AHR (16) .

Real-time polymerase chain reaction

Total RNA was isolated from lung tissue using the QiagenRNeasyPlus Mini kit (Qiagen, USA) according to the manufacturer's protocol. RNA concentration and purity were determined on a P 300 NanoPhotometer (Implen, USA) and RNA integrity was examined by formaldehyde agarose gel electrophoresis. RNA samples (100 ng) were processed with a Qiagen RT-qPCR kit (Qiagen, USA) according to the manufacturer's protocol.

Total RNA was extracted with TRIzol, and the TaKaRa reverse transcription kit was used to generate cDNA, with a 10 μL reaction volume. The cDNAs were combined with SYBR, Master Mix, and upstream and downstream primers for RT-q PCR. All primers were synthesized by TaKaRa Biotechnology (Dalian) Service Co. Ltd., and were designed based on the rat genes, as follows: HIF-1α: 5′/-AGCCGGGAACGTATCTGGA3′, 5′-TGGAAACTCACACGCCAGAAG3′; Vegf: 5′-TGATGTGCAAATTTCCGTTCC3′, 5′-CGAGACCACCTTATACCAGCGTTA3′; glyceraldehyde-3-phosphate dehydrogenase (Gapdh): 5′-ATGGTGGTGAAGACGCCAGT-3′, 5′-GCACCGTCAAGGCTGAGAAC3′. A Rotor Gene 2000 RT-qPCR system was used for amplification. Each sample was assayed in triplicate. The reaction conditions included a denaturation step at 95°C for 30 s, then 40 cycles of 95°C for 5 s, and 60°C for 20 s. The standard solubility curve was analyzed, and the CT value of the linear exponential multiplication phase was used to calculate the initial copy number of the cDNA template. In each sample, HIF-1α and VEGF expression was measured along with that of the housekeeping protein GAPDH. The CT values of the OVA and treatment groups were compared to the CT values of the control group, and relative multiples were obtained .

Preparation of tissue samples and histopathology

The left lungs of all animals were dissected immediately after sacrifice, washed with ice cold saline, blotted with filter paper, and fixed in 10% formalin in saline for 72 h. Paraffin sections, (5-μm thick) were prepared by conventional methods, and stained with HE as described previously (17). Each slice was counted by light microscopy at 400× magnification on an IDA-2000 high definition digital microscopic image analysis system, with high expression of three horizons. The average optical density of positive responses from the perspective of each value was measured, using the average optical density of three visual values to represent the relative VEGF and HIF-1α expression in bronchopulmonary tissue.

Statistical analysis

For histopathological study, perivascular and peribronchiolar inflammation scores were analyzed using *Chi*-squared tests. Differences were considered significant when < 0.05.

RESULTS

Establishment of a murine model of asthma

OVA mice had obvious activity, shortness of

breath, and abdominal muscle spasms during the modeling process, as well as incontinence, raised fur, and slow, sluggish performance in some mice. The AHR of the OVA group was significantly higher than that of the control group ($P<0.05$). In addition, the airways of OVA mice were infiltrated by a large number of inflammatory cells, while mice in the control group showed increased alveolar wall integrity, thick airway epithelia, and no obvious inflammatory cell infiltration.

Effects of azithromycin on airway inflammation in asthmatic mice

Inflammatory cell infiltration was significantly lower after azithromycin administration than in the OVA group (Fig. 2).

Effects of azithromycin on AHR to acetylcholine chloride

Lung resistance (RL) was used to estimate the effect of azithromycin on AHR to increasing concentrations of ACH using whole-body invasive plethysmography. As illustrated in Fig. 3, there was no significant difference in the baseline RL values of the different groups. RL increased dose-dependently with ACH administration in all groups except the control group, in which there was only a slight increase. RL was increased in the OVA group compared with the control group ($P<0.05$); this increase was reversed by both budesonide and azithromycin ($P<0.05$ *vs* the OVA group). There was no significant difference between the budesonide and short-course azithromycin groups, but long-course azithromycin significantly reduced the RL compared with budesonide or short-course azithromycin ($P<0.05$, Fig. 3)

Total serum IgE levels

The serum total IgE level in the OVA group was significantly increased compared to the control group ($P<0.05$; Fig. 4). However, significant reductions in serum total IgE were observed in mice treated with budesonide and azithromycin. No significant difference was observed between the budesonide and short-course azithromycin groups, but long-course azithromycin significantly reduced the total serum IgE compared with budesonide or short-course azithromycin ($P<0.05$).

Determination of HIF-1α and VEGF expression in lung tissue by RT-qPCR

Both HIF-1α and VEGF expression were increased in the OVA group compared to the control. These increases were almost completely inhibited by treatment with budesonide and azithromycin (Fig. 5).

Determination of VEGF concentration in lung tissue by ELISA

As shown in Fig. 6, the VEGF concentration increased with OVA stimulation, but was decreased by administration of budesonide and azithromycin. Long-course azithromycin significantly reduced the concentration of VEGF compared with budesonide or short-course azithromycin ($P<0.05$).

PI3K, Akt, mTOR, and HIF-1α were detected in mouse lung tissues by Western blot. Each protein displayed significantly higher expression in the OVA group compared to the control group (Fig. 7).

DISCUSSION

Airway remodeling involves subepithelial fibrosis with collagen deposition, smooth muscle hyperplasia and hypertrophy, increased mucus production, submucosal gland and airway wall thickening, goblet cell metaplasia, and neovascularization (18, 19).

Several researchers have studied the effects of different targets and compounds on airway remodeling. The suppression of eosinophil-ASM interactions via RGD-binding integrins attenuates eosinophil-induced ASM remodeling in asthma (20). House dust mite inhalation markedly increases airway goblet cell numbers and epithelium and subepithelial smooth muscle layer thickness. House dust mite-induced airway inflammation, remodeling, and Th2/Th17-type cell accumulation involves signal transducer and activator of transcription 3 activation, which can be prevented by C188-9 treatment (21).

In addition, an increasing number of studies indicate that some older medicines may have promising new functions as asthma treatments. Nuria et al. (22) found that glycomacropeptide (GMP)

Table I. *HIF-1a and VEGFmRNA expression in lung tissues of mice in each group.*

	control group	Model group	Azithromycin short course	Azithromycin long course	budesonide
HIF-1a	1	3.36±0.41	2.38±0.34	1.58±0.17	2.13±0.43
VEGF	1	2.01±0.18	1.91±0.17	1.39±0.14	1.72±0.21

Table II. *Comparison of VEGF content in BALF of mice in each group.*

ng/ml	control group	Model group	Azithromycin short course	Azithromycin long course	budesonide
VEGF	98.00±8	257.67±43.28	191.00±19.23	124.00±14.63	201.83±21.84

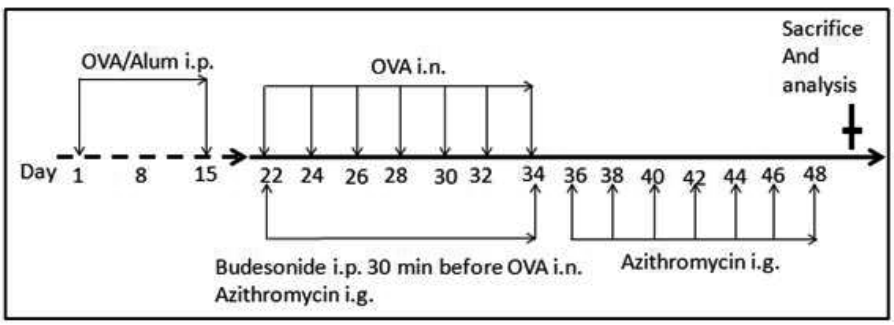

Fig. 1. *Experimental protocol for asthma murine model. OVA: ovalbumin; Alum: aluminum hydroxide; i,p.: intraperitoneal.*

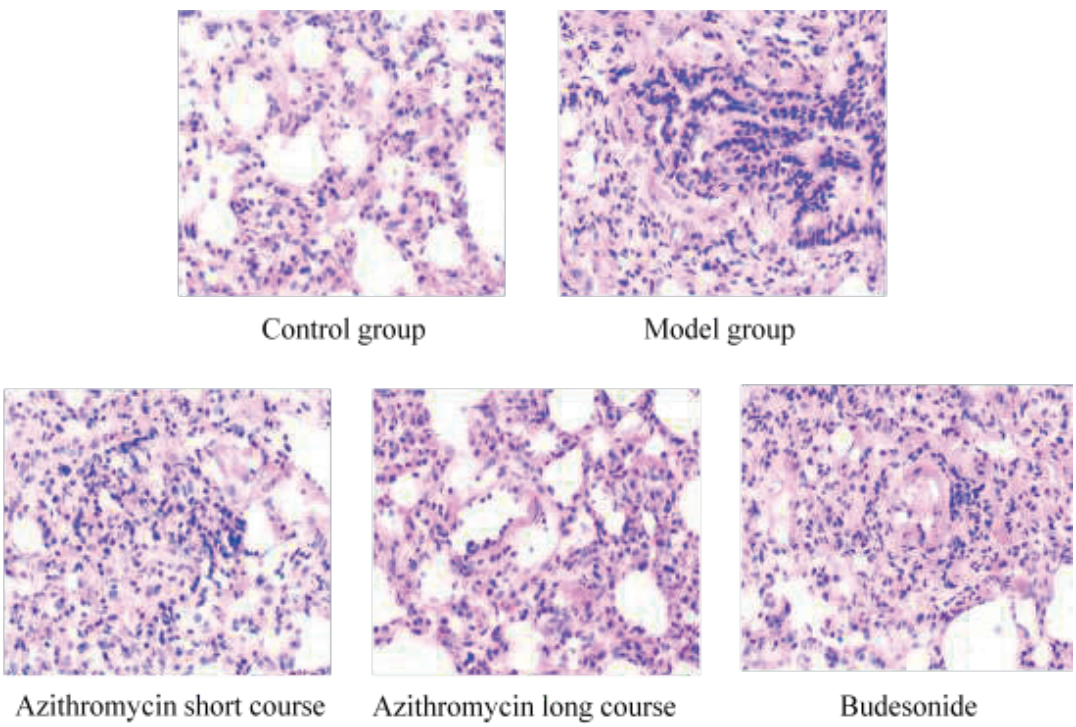

Fig. 2. *Comparison of inflammatory cell infiltration in lung tissue of mice,* x *400*

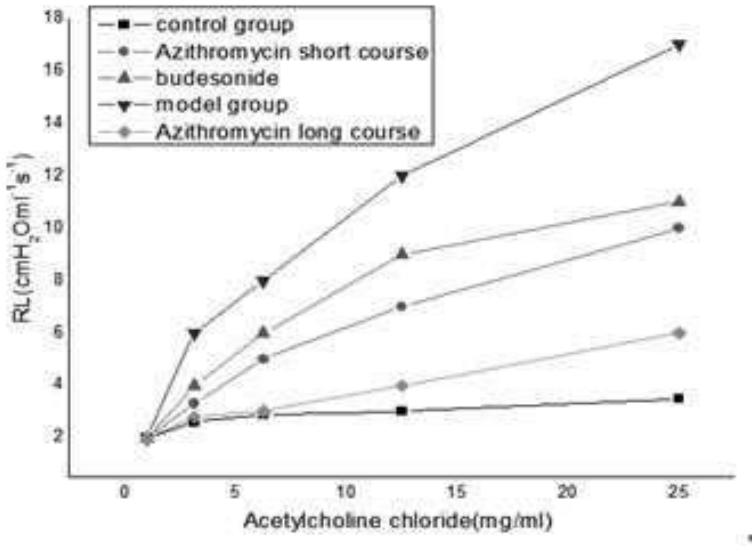

Fig. 3. *Comparison of airway reactivity between model group and control group.*

possesses prophylactic effects in the development of allergic asthma. Histological studies demonstrated that GMP markedly inhibits eosinophil infiltration, goblet cell hyperplasia, and collagen deposition in lung tissue. Intranasal administration of rosiglitazone can prevent not only airway inflammation but also airway remodeling associated with chronic allergen challenge. This beneficial effect is mediated by inhibiting the toll-like receptor 4 and nuclear factor κB (NF-κB) pathways (23). Chronic treatment with a combination of low-dose tiotropium and ciclesonide inhibited airway inflammation and remodeling in a guinea pig model of chronic asthma, suggesting that combined treatment with anticholinergics and corticosteroids may have anti-inflammatory and anti-remodeling activities in allergic airway diseases (24).

There are also many studies on plants and animals extracts. For example, Yu et al. (25) demonstrated that tHGA is an orally active compound that prevents airway remodeling in a murine model of chronic allergic asthma. The oral administration of resveratrol effectively suppressed allergic airway inflammation and remodeling in lung tissues. These effects were mediated by suppressing TGF-β1 expression and downstream Smad activation in lung tissues, as well as the epithelial-to-mesenchymal transition in bronchial epithelial cells (26).

In conclusion, airway remodeling is a complex process with many pathological characteristics, and the aforementioned studies demonstrate that remodeling is mediated by a number of different inflammatory pathways, resulting in many treatment options with good results. However, systematic study of its pathogenesis is still needed and additional targeted therapies are necessary.

Previous studies have demonstrated that azithromycin treatment reduces airway epithelial apoptosis by decreasing the Bax/Bcl-2 ratio and caspase-3 level, thus ameliorating airway epithelial injury, and decreasing airway remodeling (27). The targeting of inflammatory pathways for airway remodeling by azithromycin remains an active area of study. Choi et al. reported that protein kinase Cδ inhibition attenuated allergic airway inflammation by suppressing the PI3K/Akt/mTOR/ HIF-1α/VEGF pathway (28). However, this pathway had not been investigated in airway remodeling, and the present study aimed to investigate the possible protective effects of azithromycin on airway remodeling through this pathway.

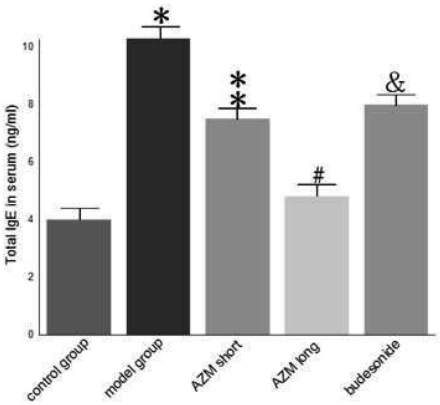

Fig. 4. *Level of serum total IgE each group.*

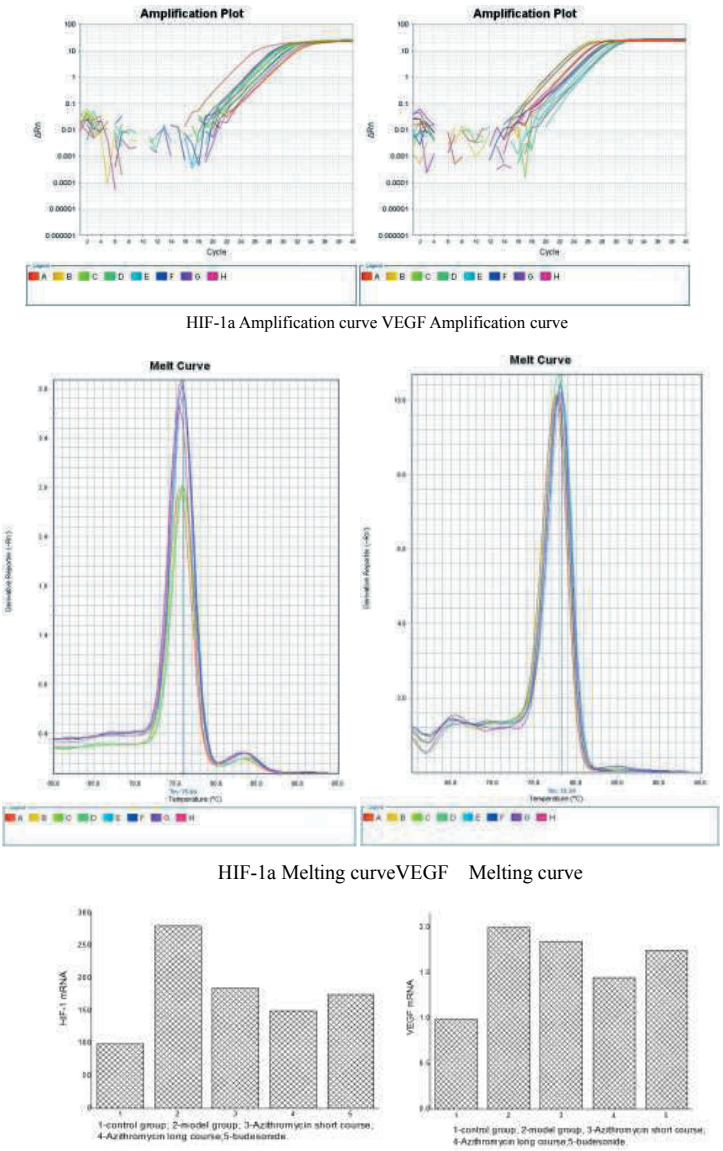

Fig. 5. *mRNA of HIF 1a and VEGF were determined by RT-PCR.*

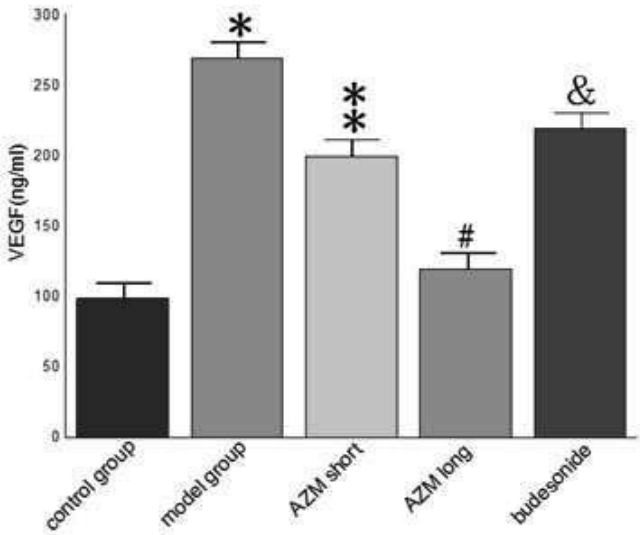

Fig. 6. *The content of VEGF protein in lung tissue of each group was measured by ELISA.*

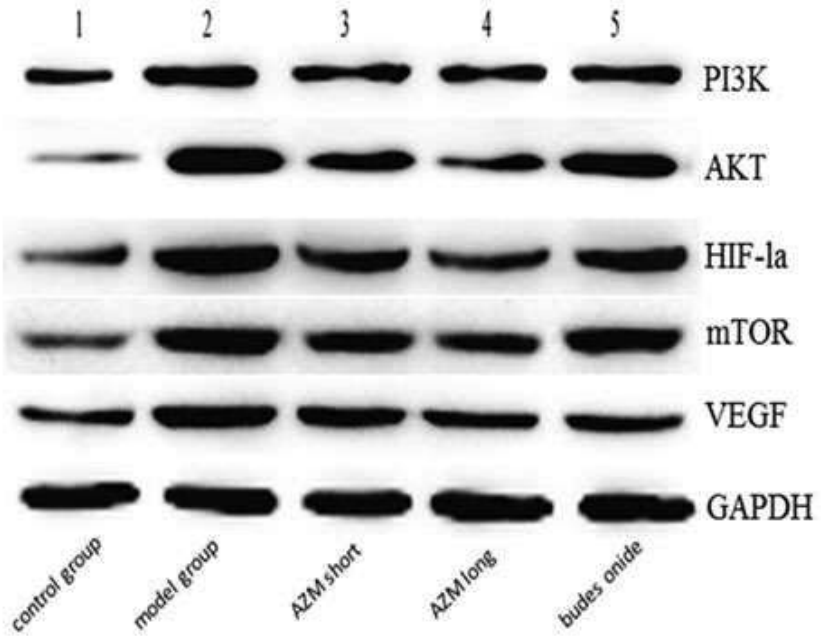

Fig. 7. *Protein content of PI3K, Akt, mTOR, HIF-1α and VEGF in each group is shown by Western blot.*

We successfully established a murine model of asthma, and observed the effects of azithromycin on airway inflammation AHR to acetylcholine chloride, and RL and total serum total IgE levels. The effects of azithromycin on PI3K, Akt, mTOR, HIF-1, and VEGF expression were also analyzed, and long-course azithromycin significantly reduced their expression. The results demonstrate the effects of azithromycin in reducing the bronchial inflammation in OVA- sensitized mice consistent with previous studies (29).

Although azithromycin is effective in animal

experiments, it can cause adverse reactions, such as gastrointestinal distress and rashes, as well as abnormal liver enzyme levels in some patients. The antibacterial effects of azithromycin and its optimal dosages are well established, but its role in regulating immunity requires further study, as does the proper course of treatment.

In summary, the PI3K/Akt /mTOR /HIF-1 alpha / VEGF signal pathway is involved in the occurrence and development of asthma in the OVA-sensitized mice. Both azithromycin and budesonide can reduce airway inflammation and improve airway remodeling via inhibition of the PI3K/Akt/mTOR/HIF-1 alpha/ VEGF signaling pathway in the lung. Azithromycin has the same efficacy as budesonide in the treatment of asthma, and the airway inflammation and airway remodeling may be better inhibited by appropriately prolonging the therapeutic period of azithromycin.

ACKNOWLEDGEMENTS

We thank Haixia Li for help and manuscript preparation. This study was supported by the Department of Health Henan province of China (122102310627) and Henan Province Education Department of China (2007320054).

REFERENCES

1. Nadeem A, Siddiqui N, Alharbi NO, Alharbi MM. Airway and systemic oxidant-antioxidant dysregulation in asthma: a possible scenario of oxidants spill over from lung into blood. Pulm Pharmacol Ther 2014; 29:31-40.
2. Bosnjak B, Tilp C, Tomsic C, Dekan G, Pieper MP, Erb KJ, Epstein MM. Tiotropium bromide inhibits relapsing allergic asthma in BALB/c mice. Pulm Pharmacol Ther 2014; 27:44-51.
3. Belice PJ, Becker EA. Effective education parameters for trigger remediation in underserved children with asthma: a systematic review. J Asthma http://dx.doi.org/10.1080/02770903. 2016; 1198374.
4. Hall S, Agrawal DK. Key mediators in the immunopathogenesis of allergic asthma. Int Immunol 2014; 23:316-29.
5. Malmstrom K, Pelkonen AS, Makela MJ. Inflammation and airway responsiveness in early childhood asthma. Curr Opin Allergy Cl 2013; 13:203-10.
6. Crosbie PA, Woodhead MA. Long-term macrolide therapy in chronic inflammatory airway diseases. Eur Respir J 2009; 33:171-81.
7. Ran XM, Zhao Y, Huang Y, Wang CZ, Cheng XM, Jiang YF. Azithromycin can improve the asthmatic inflammation in mice by inhibiting the functional activity of Th17 cells. J Third Mil Med Univ 2013; 35:421-25.
8. Ma HJ, Zhu WY, Wang DG, Yue XZ, Li CR. Endothelin-1 combined with extracellular matrix proteins promotes the adhesion and chemotaxis of amelanotic melanocytes from human hair follicles in vitro. Cell Biol Int 2006; 30:999-1006.
9. Fruman DA, Chiu H, Hopkins BD, Bagrodia S, Cantley LC, Abraham RT. The PI3K pathway in human disease. Cell 2017; 170:605-35.
10. Liao MJ, Chen HF. Targeted therapy on PI3K/Akt/mTOR signaling pathway in breast cancer. Chin J Cancer Res 2012; 19:230-34.
11. Miao G, Liu B, Guo X, Zhang X, Liu GJ. Reduction behavior induced by HL010183, a metformin derivative against the growth of cutaneous squamous cell carcinoma. Int J Clin Exp Pathol 2015; 8:287-97.
12. Hasaneen NA, Zucker S, Lin RZ, Vaday GG, Panettieri RA, Foda HD. Angiogenesis is induced by airway smooth muscle strain. Am J Physiol-Lung 2007; 293:1059-68.
13. Cheng F, Zhang XQ, Song ML, Tang J. PI3K/Akt/mTOR signaling pathway is involved in the regulation of hypoxia inducible factor -1 alpha expression in rats with acute pancreatitis. Chin J Emerg Med 2010; 30:330-34.
14. Kim EJ, Yoo YG, Yang WK, Lim YS, Na TY, Lee IK, Lee MO. Transcriptional activation of HIF-1 by RORalpha and its role in hypoxia signaling. Arterioscler Thromb Vasc Biol 2008; 28:1796-802.
15. Tanaka T, Wakamatsu T, Daijo H, Hirota K. Persisting mild hypothermia suppersses hypoxia-inducible factor-1 alpha protein synthesis and hypoxia-inducible factor-1-mediated gene expression. Am J Physiol-Reg I 2010; 298:661-71.
16. Yao J, Jiang M Z, Zhang YS, Liu X, Du Q, Feng GZ. Chrysin alleviates allergic inflammation and airway remodeling in a murine model of chronic asthma. Int

Immunol 2016; 32:24-31.
17. Mizutani N, Nabe T, Yoshino S. Semaphorin 7A plays a critical role in IgE-mediated airway inflammation in mice. Eur J Pharmacol 2015; 764:149-156.
18. Kang JY. Jo MR, Kang HH, et al. Long-term azithromycin ameliorates not only airway inflammation but also remodeling in a murine model of chronic asthma. Pulm Pharmacol Ther 2016; 36:37-45.
19. EI-Sherbeeny NA, Hassan ZA, Ateyya H. Tiron ameliorates oxidative stress and inflammation in a murine model of airway remodeling. Int Immunol 2016; 39:172-80.
20. Januskevicius A, Gosens R, Sakalauskas R, et al. Suppression of eosinophil integrins prevents remodeling of airway smooth muscle in asthma. Front Physiol 2017; 7:680-98.
21. Gavino AC, Nahmod K, Bharadwaj U, Makedonas G, Tweardy DJ. STAT3 inhibition prevents lung inflammation ,remodeling, and accumulation of Th2 and Th17 cells in a murine asthma model. Allergy 2016; 71:1684-92.
22. Roldán NR, Jiménez M, Cervantes-García D, Marín E, Salinas E. Glycomacropeptide administration attenuates airway inflammation and remodeling associated to allergic asthma in rat. Inflamm Res 2016; 65:273-83.
23. Hwa YL, Chin KR, Ji YK, et al. Effect of intranasal rosiglitazone on airway inflammation and remodeling in a murine model of chronic asthma. Korean J Intern Med 2016; 31:89-97.
24. Kistemaker LE, Bos IS, Menzen MH, Maarsingh H, Meurs H, Gosens R. Combination therapy of tiotropium and ciclesonide attenuates airway inflammation and remodeling in a guinea pig model of chronic asthma. Resp Res 2016; 17:13-23.
25. Yu ZL, Khozirah S, Manraj SC, Chau LT, Mohd RS, Daud AI. An orally active geranylacetophenone attenuates airway remodeling in a murine model of chronic asthma. Eur J Pharmacol 2017; 797:53-64.
26. Hwa YL, In KK, Hyoung KY, Soon SK, Chin KR, Sook YL. Inhibitory effects of resveratrol on airway remodeling by transforming growth factor-β/Smad signaling pathway in chronic asthma model. Allergy Asthma Immu 2017; 9:25-34.
27. Liu YQ, Pu Y, Li D, Zhou L, Wan L. Azithromycin ameliorates airway remodeling via inhibiting airway epithelium apoptosis. Iife Sci 2017; 170:1-8.
28. Choi YH, Jin GY, Li LC, Yan G H. Inhibition of Protein Kinase C Delta attenuate allergic airway inflammation through suppression of PI3K/Akt/mTOR/HIF-1 Alpha/VEGF Pathway. Plos One 2013; 8:1-16.
29. Youngkang J, Renjo M, Huikang H, et al. Long-term azithromycin ameliorates not only airway inflammation but also remodeling in a murine model of chronic asthma. Pulm Pharmacol Ther 2016; 36:37-45.

ENZYME LINKED RECEPTOR PROTEIN SIGNALING PATHWAY IS ONE OF THE ONTOLOGY GROUPS THAT ARE HIGHLY UP-REGULATED IN PORCINE OOCYTES BEFORE *IN VITRO* MATURATION

S. BORYS[1], M. BRĄZERT[2], M. JANKOWSKI[1], I. KOCHEROVA[1], K. OŻEGOWSKA[2], P. CELICHOWSKI[3], M.J. NAWROCKI[1], W. KRANC[1], A. BRYJA[1], M. KULUS[4], M. JESETA[5], W. PIEŃKOWSKI[6], A. BRĘBOROWICZ[7], D. BUKOWSKA[4], P. ANTOSIK[4], L. PAWELCZYK[2], M.T. SKOWROŃSKI[4], K.P. BRÜSSOW[4], M. BRUSKA[1], M. ZABEL[8,9], M. NOWICKI[3] and B. KEMPISTY[1,3,5]

[1]Department of Anatomy, Poznan University of Medical Sciences, Poznan, Poland; [2]Department of Infertility and Reproductive Endocrinology, Poznan University of Medical Sciences, Poznan, Poland; [3]Department of Histology and Embryology, Poznan University of Medical Sciences, Poznan, Poland; [4]Veterinary Center, Nicolaus Copernicus University in Toruń, Torun, Poland; [5]Department of Obstetrics and Gynecology, University Hospital and Masaryk University, Brno, Czech Republic; [6]Division of Perinatology and Women's Diseases, Poznan University of Medical Sciences, Poznan, Poland; [7]Department of Pathophysiology, Poznań University of Medical Sciences, Poznan, Poland; [8]Department of Human Morphology and Embryology, Wroclaw University of Medical Sciences, Wroclaw, Poland; [9]Division of Anatomy and Histology, University of Zielona Góra, Zieloga Góra, Poland

Received May 25, 2018 – Accepted July 19, 2018

Before being able to fully participate in the processes associated with its function as a female gamete, the oocyte needs to undergo a range of changes to achieve its mature form. These morphological, biochemical and metabolomic processes are induced by the somatic tissues surrounding the oocyte, through the expression of specific transcription and growth factors. The maturation of the oocyte is highly important for the proceedings that lead to successful fertilization, early embryonic development and implantation. Domestic pigs were used as models for our study, with the cumulus-oocyte complexes obtained from the ovaries that were recovered at slaughter. After shedding of the cumulus, oocytes were assessed with BCB test, with the viable ones chosen to undergo *in vitro* maturation. With the use of expression microarrays, we analyzed gene expression before and after IVM and detected major changes in both genes that were proven to be associated with oocyte maturation before (*FOS, VEGFA, CHRDL1, TGFBR3, FST, INSR, ID1, TXNIP, SMAD4, MAP3K1, EIF2AK3* and *KIT*) and genes not previously linked with reproduction associated processes (*MYO1E, PHIP, KLF10* and *SHOC2)*. All the genes were briefly described, with consideration of possible involvement of the newly discovered elements of the transcriptome in the process of oocyte maturation.

Key words: pig, oocytes, microarray assays, in vitro maturation (IVM)

Mailing address:
Bartosz Kempisty PhD,
Department of Histology and Embryology,
Department of Anatomy, Poznań University of Medical Sciences,
6 Święcickiego St., 60-781 Poznań, Poland
Tel.: +48 61 8546418 - Fax: +48 61 8546440
e-mail: bkempisty@ump.edu.pl

0393-974X (2018)

Before ovulation and subsequent successful monospermic fertilization, mammalian cumulus–oocyte complexes (COCs) undergo several morphological, biochemical and metabolomic changes. The main modification in morphology, within the COCs, involves cumulus oophorus expansion, which is recognized as the most important marker of oocyte successful maturation, both *in vivo* and *in vitro* (IVM) (4). Additionally, during COC maturation, the molecular changes encompass significant chromosomal reorganization and/or storage of RNA templates for subsequent protein biosynthesis. Hence, the proper COC maturation is substantially accompanied by induction of mechanisms and activation of specific metabolic pathways that build the whole orchestrated cellular and subcellular "biochemical machinery". As shown in our previous experiments, the activation of this machinery in mammalian oocytes is accompanied by induction of signaling pathways, which are associated with up-regulation of growth factor expression, mostly included in transforming growth factor beta superfamily (TGFB), such as; bone morphogenic proteins (BMPs) and growth differentiation factors (GDFs) (2, 3, 18)there exist many differences that promote these processes in vivo and in vitro. Therefore, this study aimed to investigate the differences in RNA expression profiles between porcine oocytes before and after IVM using microarray and real-time quantitative polymerase chain reaction (RT-qPCR. However, maturation of the oocytes, both nuclear and cytoplasmic, together with their growth and development, which belong to processes determining cell survival, are mostly regulated on the metabolomic level by activation of enzymes crucial for cell life (19).

The COC metabolic activity is substantially regulated by maintenance of oocyte–cumulus "dialogue" and bi-directional transport of small substances between these cells. The gap junction connections (GJC), which are formed between cumulus cells and oocyte, are involved in this process as the main regulators of cell-to-cell inter-transport. Furthermore, it was demonstrated by our experiments that proteins belonging to connexins (CXs), which build the GJC in mammalian COCs, are also involved in subcellular nuclear-cytoplasmic shuttling, which is one of the proofs for metabolite trafficking between the cells and cellular metabolic status (25). It was previously observed that ATP-ases and GTP-ases, as well as enzymes involved in lipids and glucose metabolisms, belong to the main regulators of maintenance of oocytes metabolic, energetic and oxidative status (23). Despite the fact that cell survival is maintained by metabolic status, the regulation of cell maturation, growth, development and/or surrounding somatic cell differentiation are significantly stimulated by induction of the enzymes involved in signaling pathways. This unique process involves mechanisms regulated by activation of several molecules, such as G protein, cAMP, protein kinases, phospholipases and IP3. It was found in several mammalian models that stimulation of activity of these molecules belongs to the main mechanisms of cell proliferation, growth and differentiation both *in vivo* and *in vitro*. Moreover, activation of enzymes important for cell survival belongs to the group of specific "checkpoints" that control the maintenance of proper cellular metabolic status. Although the enzymes involved in mammalian oocyte metabolisms are mostly determined, it still remains unclear whether and which of them are involved in regulation of oocyte maturation capability. Therefore, in this study we used porcine oocytes as the model to better understand the mechanisms of metabolic pathway induction and determination of transcriptomic profile of these enzymes in relation to oocyte maturational status.

MATERIALS AND METHODS

Animals

A total of 45 pubertal crossbred Landrace gilts, bred on a local commercial farm, were used in this study. They had a mean age of 155 days (range 140–170 days) and a mean weight of 100 kg (95-120 kg). All the animals were housed under identical conditions and fed the same forage (depending on age and reproductive status). The experiments were approved by the Local Ethics Committee.

Collection of porcine ovaries and cumulus-oocyte-complexes (COCs)

Ovaries and reproductive tracts were recovered at slaughter and transported to the laboratory at 38°C in 0.9% NaCl within 40 min. To provide optimal conditions for subsequent oocyte maturation and fertilization *in vitro*, the ovaries of each animal were placed in 5% fetal bovine serum solution (FBS; Sigma-Aldrich Co., St. Louis, MO, USA) in PBS. Single large follicles (>5 mm) were then opened by puncturing with a 5-ml syringe and 20-G needle in a sterile Petri dish, and COCs were recovered. The COCs were washed three times in modified PBS supplemented with 36µg/ml pyruvate, 50µg/ml gentamycin, and 0.5mg/ml BSA (Sigma-Aldrich, St. Louis, MO, USA). COCs were selected under an inverted Zeiss, Axiovert 35 microscope (Lübeck, Germany), counted, and morphologically evaluated using the scale suggested by Jackowska et al. (16). Only COCs of grade I with homogeneous ooplasm and uniform, compact cumulus cells were considered for the following steps of the experiment, resulting 300 grade I oocytes (3 x n=50 before IVM, 3 x n=50 after IVM).

Assessment of oocyte developmental competence by BCB test

To perform the BCB staining test, oocytes were washed twice in modified Dulbecco PBS (DPBS; Sigma-Aldrich, St. Louis, MO) supplemented with 50IU/ml penicillin, 50µg/ml streptomycin (Sigma-Aldrich, St. Louis, MO, USA), 0.4% BSA [w/v], 0.34 mM pyruvate, and 5.5 mM glucose (DPBSm). Thereafter, they were treated with 13 µM BCB (Sigma-Aldrich, St. Louis, MO) diluted in DPBSm at 38.5°C and 5% CO2 for 90 min. After treatment, the oocytes were transferred to DPBSm and washed twice. During the washing procedure, the oocytes were examined under an inverted microscope and classified as either stained blue (BCB+) or remained colorless (BCB–). Immature oocytes have compact cumulus cell layers that required removal for further oocyte evaluation. Next, the BCB+ COCs were first incubated with bovine testicular hyaluronidase (Sigma-Aldrich, St. Louis, MO, USA) for 2 min at 38°C to separate cumulus and granulosa cells. Cells were then removed by vortexing the BCB+ oocytes in 1% sodium citrate buffer followed by mechanical displacement using a small-diameter glass micropipette. Only the granulosa cell-free BCB+ oocytes were used for subsequent IVM and microarray analysis.

In vitro maturation of porcine COCs

After the first BCB test, the COCs which remained colorless (BCB-) were cultured in Nunclon™Δ 4-well dishes in 500 µl of standard porcine IVM culture medium TCM-199 (tissue culture medium) with Earle's salts and *L*-glutamine, (Gibco BRL Life Technologies, Grand Island, NY, USA) supplemented with 2.2mg/ml sodium bicarbonate (NacalaiTesque, Inc., Kyoto, Japan), 0.1mg/ml sodium pyruvate (Sigma-Aldrich, St. Louis, MO, USA), 10 mg/ml BSA (bovine serum albumin), (Sigma-Aldrich, St. Louis, MO, USA), 0.1 mg/ml cysteine (Sigma-Aldrich, St. Louis, MO, USA), 10% filtered porcine follicular fluid (v/v), and gonadotropin supplements at final concentrations of 2.5IU/ml hCG (Ayerst Laboratories, Inc., Philadelphia, PA, USA) and 2.5IU/ml eCG (Intervet, Whitby, ON, Canada). Wells were covered with a mineral oil overlay and cultured for 44 h at 38°C under 5% CO2. After cultivation, the BCB staining test was performed again, and BCB+ oocytes were used for further experiments.

RNA extraction from porcine oocytes

Oocytes investigated before and after *in vitro* maturation were pooled into three independent samples (50 oocytes per sample) for each experimental group. Total RNA was extracted from samples using TRI Reagent (Sigma, St Louis, MO, USA) and RNeasy MinElute cleanup Kit (Qiagen, Hilden, Germany). The amount of total mRNA was determined from the optical density at 260 nm, and the RNA purity was estimated using the 260/280 nm absorption ratio (higher than 1.8) (NanoDrop spectrophotometer, Thermo Scientific, ALAB, Poland). The RNA integrity and quality were checked on a Bioanalyzer 2100 (Agilent Technologies, Inc., Santa Clara, CA, USA). The resulting RNA integrity numbers (RINs) were between 8.5 and 10 with an average of 9.2 (Agilent Technologies, Inc.,

Santa Clara, CA, USA). The RNA in each sample was diluted to a concentration of 100ng/µl with an OD260/OD280 ratio of 1.8/2.0. From each RNA sample, 500 ng of RNA were taken for microarray analysis. The remaining amount of isolated RNA was used for the RT-qPCR study.

Microarray expression analysis and statistics

The Affymetrix procedure was previously described by Trejter et al. (29)the adrenal weight and the average volume of zona fasciculata cells of females are larger and secrete greater amounts of corticosterone than those of males. The molecular bases of these sex-related differences are poorly understood. In this study, to explore the molecular background of these differences, we defined zone- and sex-specific transcripts in adult male and female (estrous cycle phase. Total RNA (100 ng) from each pooled sample was subjected to two-round, sense cDNA amplification (Ambion® WT Expression Kit). The obtained cDNA was used for biotin labeling and fragmentation by AffymetrixGeneChip® WT Terminal Labeling and Hybridization (Affymetrix). Biotin-labeled fragments of cDNA (5.5 µg) were hybridized to the Affymetrix® Porcine Gene 1.1 ST Array Strip (48°C/20 h). Then, microarrays were washed and stained according to the technical protocol using the AffymetrixGeneAtlas Fluidics Station. The array strips were scanned employing Imaging Station of the GeneAtlas System. The preliminary analysis of the scanned chips was performed using AffymetrixGeneAtlasTM Operating Software. The quality of gene expression data was confirmed according to the quality control criteria provided by the software. The obtained CEL files were imported into downstream data analysis software.

All of the presented analyses and graphs were performed using Bioconductor and R programming languages. Each CEL file was merged with a description file. In order to correct background, normalize, and summarize results, we used the Robust Multiarray Averaging (RMA) algorithm (10). To determine the statistical significance of the analyzed genes, moderated t-statistics from the empirical Bayes method were performed. The obtained p-value was corrected for multiple comparisons using Benjamini and Hochberg's false discovery rate. The selection of significantly altered genes was based on a p-value under 0.05 and expression higher than two-fold.

Differentially expressed genes were subjected to the selection based on their involvement in morphogenesis and cellular differentiation. The differentially expressed gene list (separated for up- and down-regulated genes) was uploaded to DAVID software (Database for Annotation, Visualization and Integrated Discovery), where genes belonging to "enzyme linked receptor protein signaling pathway" GO term were obtained (7)Visualization, and Integrated Discovery (DAVID; http://www.david.niaid.nih.gov. The term "enzyme linked receptor protein signaling pathway" (GO:0007167) is defined as "Any series of molecular signals initiated by the binding of an extracellular ligand to a receptor on the surface of the target cell, where the receptor possesses catalytic activity or is closely associated with an enzyme such as a protein kinase, and ending with regulation of a downstream cellular process, e.g. transcription". It consists of 24,146 genes of which 1,239 are annotated to Sus scrofa organism.

Expression data of these genes were subjected to a hierarchical clusterization procedure, and their expression values were presented as a heat map. Besides predicting interactions, DAVID software also allowed to perform functional enrichment of GO terms based on previously uploaded gene sets from the "enzyme linked receptor protein signaling pathway" GO BP term. The top five GO terms that contained genes also belonging to "enzyme linked receptor protein signaling pathway" GO BP are shown in Table I. The relationship between genes that belongs to other GO terms were further investigated by GeneAnswers and GOplot R packages (15, 30).

Interactions between differentially expressed genes/proteins belonging to "enzyme linked receptor protein signaling pathway" ontology group were investigated by STRING10 software (Search Tool for the Retrieval of Interacting Genes). The list of gene names was used as query for interaction prediction. The search criteria were based on co-occurrences of genes/proteins in scientific texts (text mining), co-expression, and experimentally

observed interactions. The results of such analysis generated a gene/protein interaction network where the intensity of the edges reflected the strength of the interaction score.

Furthermore, we investigated the interactions between SMAD4 and FOS genes, as well as between KIT, VEGFA and INSR genes. These genes were subjected to Reactome database by Cytoscape 3.6.0 software (13,27). Reactome is the open-source, open access, manually curated and peer-reviewed pathway database, with the goal to provide intuitive bioinformatics tools for the visualization, interpretation and analysis of pathway knowledge to support basic and clinical research, genome analysis, modeling, systems biology and education. Cytoscape is an open source software platform for visualizing complex networks and integrating these with any type of attribute data. The analysis showed all genes that interact with chosen genes. Subsequently, we did Reactome Functional Interaction (FI) network for all genes from "enzyme linked receptor protein signaling pathway". To achieve that objective we used Reactome FI Cytoscape Plugin, designed to find protein network patterns. This plugin accesses the Reactome Functional Interaction (FI) network, a highly reliable, manually curated pathway-based protein functional interaction network covering close to 50% of human proteins, and allows to construct a FI sub-network based on a set of genes, query the FI data source for the underlying evidence for the interaction, build and analyze network modules of highly-interacting groups of genes, perform functional enrichment analysis to annotate the modules, expand the network by finding genes related to the experimental data set, display pathway diagrams, and overlay with a variety of information sources such as cancer gene index annotations.

Real-time quantitative polymerase chain reaction (RT-qPCR) analysis

Total RNA was isolated from GCs, before and after IVC, using an RNeasy mini column from Qiagen GmbH (Hilden, Germany). The RNA samples were resuspended in 20 µl of RNase-free water and stored in liquid nitrogen. RNA samples were treated with DNase I and reverse-transcribed (RT) into cDNA. RT-qPCR was conducted in a LightCycler real-time PCR detection system (Roche Diagnostics GmbH, Mannheim, Germany) using SYBR® Green I as a detection dye, and target cDNA was quantified using the relative quantification method. The relative abundance of PTX3, COX2, HAS2 and TSG6 transcripts in each sample was standardized to the internal standard glyceraldehyde-3-phosphate dehydrogenase (GAPDH). For amplification, 2 µl of cDNA solution was added to 18 µl of QuantiTect® SYBR® Green PCR (Master Mix Qiagen GmbH, Hilden, Germany) and primers (Table II). One RNA sample of each preparation was processed without the RT-reaction to provide a negative control for subsequent PCR.

To quantify the specific genes expressed in the GCs, the expression levels of specific oocyte mRNAs in each sample were calculated relative to PBGD and ACTB. To ensure the integrity of these results, the additional housekeeping gene, 18S, was used as an internal standard to demonstrate that PBGD and ACTB mRNAs were not differentially regulated in GC groups. The gene for 18S rRNA expression has been identified as an appropriate housekeeping gene for use in quantitative PCR studies. Expression of PBGD, ACTB, and 18S mRNA was measured in cDNA samples from isolated GCs.

RESULTS

To investigate oocyte transcriptome changes after *in vitro* maturation in relation to transcriptome profile of freshly isolated oocyte, before *in vitro* procedure, we performed whole gene expression analysis by Affymetrix® Porcine Gene 1.1 ST Array. Assay expression of more than 12,258 porcine transcripts was examined. The genes for which the fold change was higher than the cut-off value (fold>|2|) and corrected p value (adj $p<0.05$), were considered as differentially expressed. From the whole transcript that consisted of 419 different genes, 379 genes were down-regulated, and 40 genes were up-regulated in relation to the oocyte transcriptome before *in vitro* procedure.

Among these genes, those belonging to "enzyme linked receptor protein signaling pathway" gene

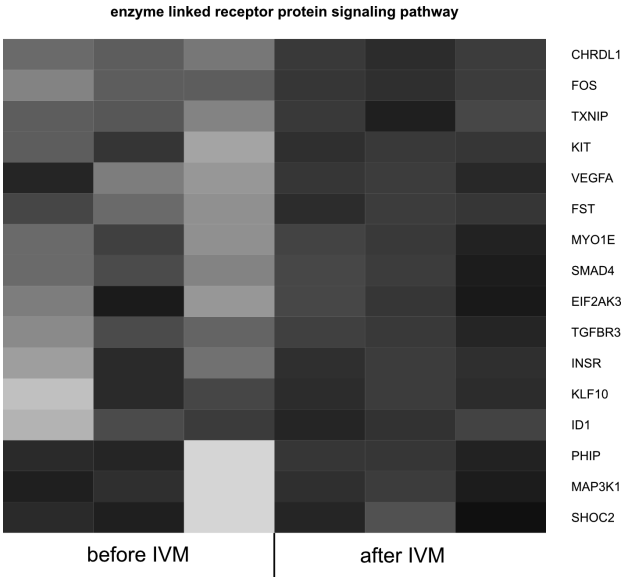

Fig. 1. *Heat map representation of differentially expressed genes belonging to the category "enzyme linked receptor protein signaling pathway" from GO.BP database. log2 signal intensity values were resized to Row Z-Score scale for any single genes (from -2, the lowest expression to +2, the highest expression).*

ontology biological process term were extracted by DAVID (Database for Annotation, Visualization and Integrated Discovery) software. Up- and down-regulated gene sets were subjected to DAVID searching separately and only gene sets, where adj. p values were lower than 0.05 were selected (Table III). This set of genes was subjected to hierarchical clusterization procedure and presented as a heatmap (Fig. 1.).

Genes from one particular GO group will belong also to other different GO term categories. By this reasoning we performed functional enrichments of GO terms based on previously uploaded gene set from "enzyme linked receptor protein signaling pathway" GO BP term. Top five GO terms that contain genes, that also belong to "enzyme linked receptor protein signaling pathway" gene ontology, are presented as a table, where its category, term, number of genes that it shares with "enzyme linked receptor protein signaling pathway", p-value and Benjamini – Hochberg's false discovery rate are shown (Table I). The mutual relationships between those terms are presented in Figs. 2 and 3.

STRING-generated interaction network was generated among differentially expressed genes belonging to the "enzyme linked receptor protein signaling pathway" term. Applied prediction methods used textmining, co-expression, experimentally observed interactions (Fig. 4).

The subsequent Reactome database analysis showed all genes that shared interactions between *KIT, INSR* and *VEGFA*. We also checked the interactions between *SMAD4* and *FOS* genes. The results showed that *SMAD4* and *FOS* also interacts with 48 other genes (Fig. 5) and *VEGFA, KIT* and *INSR* also interacts with 44 other genes (Fig. 6).

The Reactome Functional Interaction analysis only identified the *ID1, SMAD4, FOS, VEGFA*, *INSR* and *KIT* genes in reactome database. The analysis showed that FOS can indirectly stimulate the activity of other mention genes (Fig. 7).

Additionally, RT-qPCR validation was performed to confirm the results obtained through microarray analysis. The data obtained was compared and plotted as a bar graph (Fig. 8).

As can be seen, the direction of changes was confirmed in all examples. However, there is some variation in the difference between observed levels of gene expression. While in the case of most of the genes, the values are relatively comparable, some examples, such as *EIF2AK3, MYO1E, FOS, VEGFA*

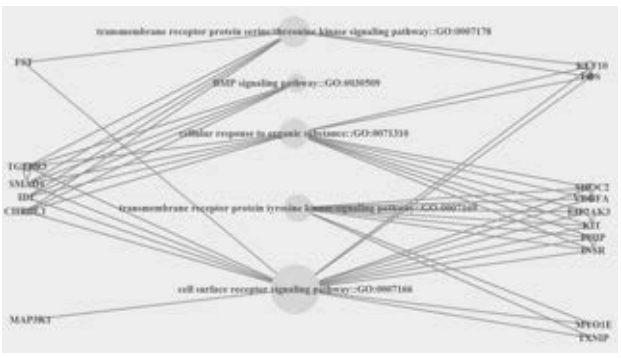

Fig. 2. *Concept-gene network showing differently expressed genes from enzyme linked receptor protein signalling pathway" and top five GO terms that shared genes with studied GO term.. The genes that belong to the same GO terms are sorted next to each other. The intensity of the dots represents the fold change.*

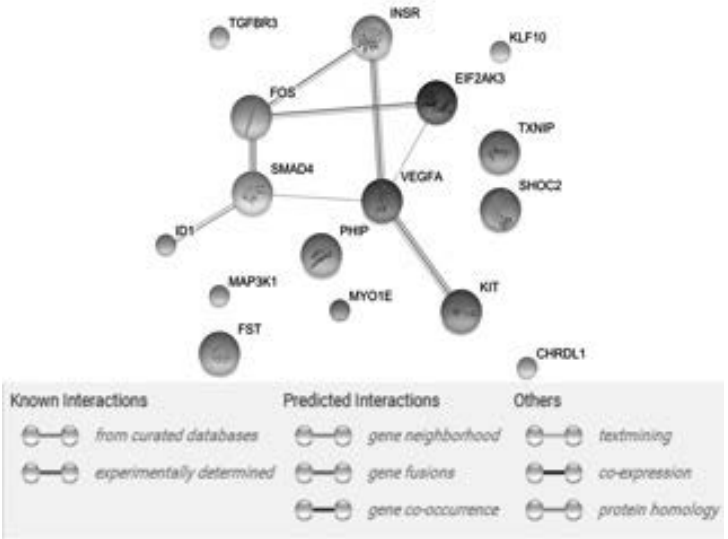

Fig. 3. *Representation of the mutual relationship between "enzyme linked receptor protein signalling pathway" and top five GO terms that shared genes with studied GO term. The ribbons indicate which gene belongs to which categories. The genes were sorted by fold change, from most to least changed gene.*

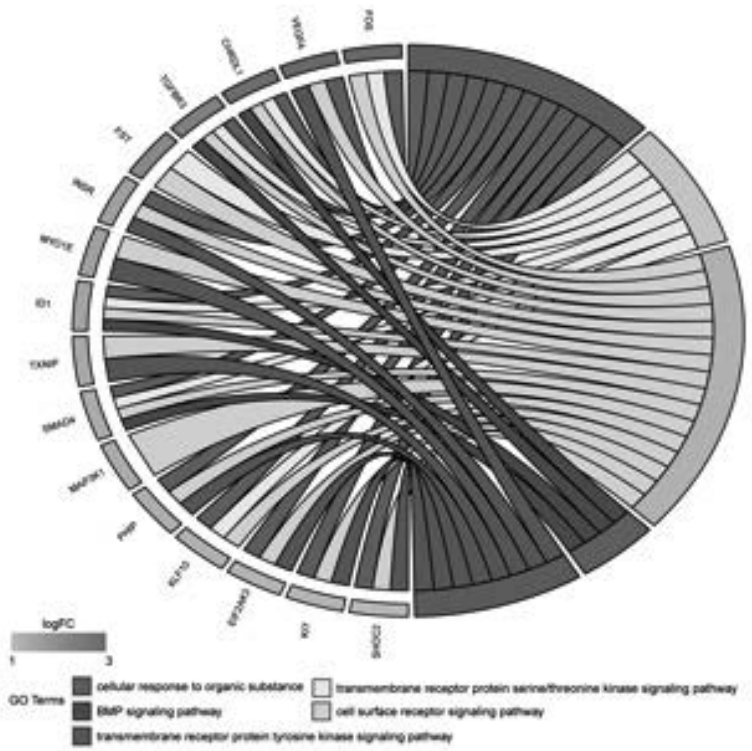

Fig. 4. *STRING-generated interaction network among differentially expressed genes belonging to the "enzyme linked receptor protein signalling pathway" ontology group. Applied prediction methods: text mining, co-expression, experimentally observed interactions.*

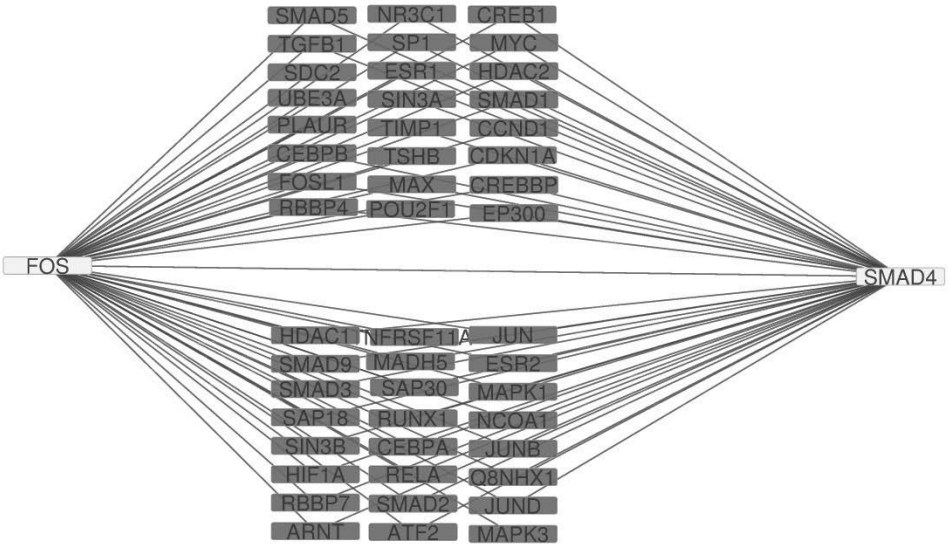

Fig. 5. *Visualization of genes interacting with SMAD4 and FOS genes. The nodes show other genes that interacts with SMAD4 and FOS genes.*

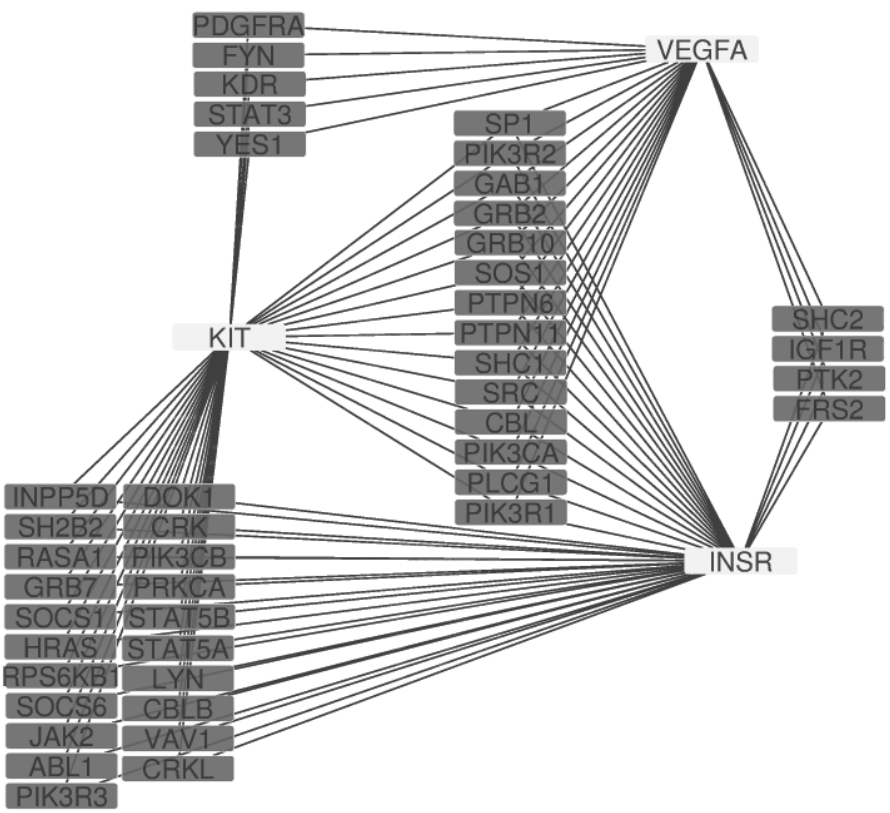

Fig. 6. *Visualization of genes interacting with VEGFA, KIT and INSR genes. The nodes show other genes that interact with VEGFA, KIT and INSR genes.*

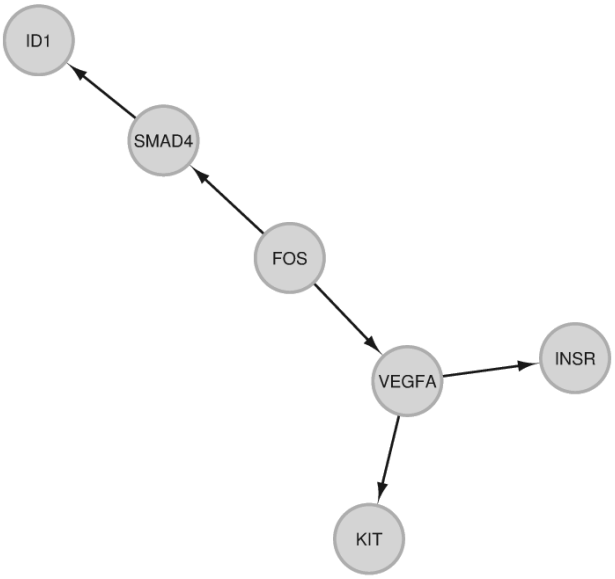

Fig. 7. *The Reactome Functional Interaction analysis of genes detected in the study. The arrow indicates stimulation of one protein by another.*

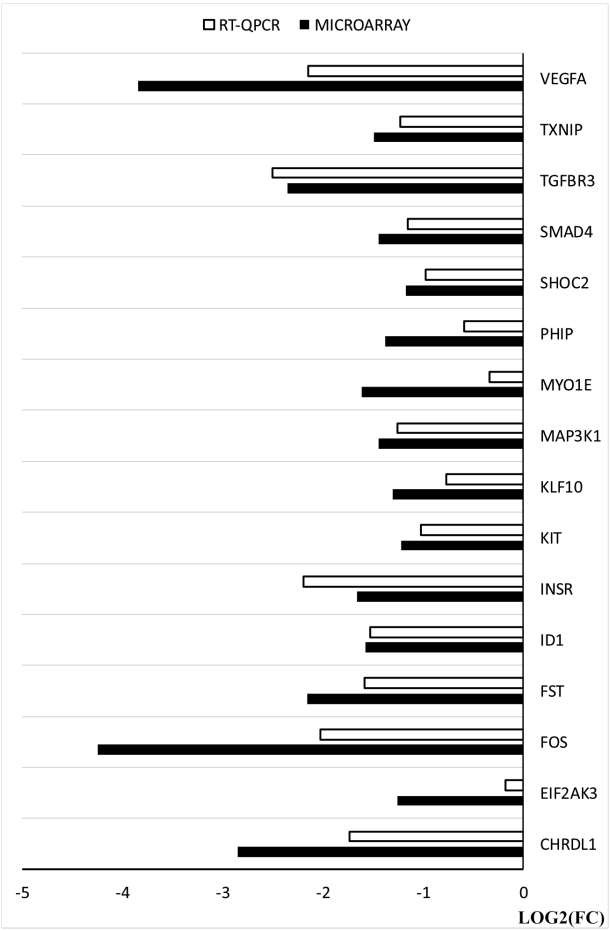

Fig. 8. *The comparison between microarray and RT-qPCR analysis.*

Table I. *Top five GO categories formed by genes differentially expressed belonging to the "enzyme linked receptor protein signalling pathway" ontology group.*

Category	Term	Count	%	P Value	Benjamini
GOTERM_BP_FAT	cell surface receptor signaling pathway	11	68.8	4.5E−7	2.1E−4
GOTERM_BP_FAT	transmembrane receptor protein tyrosine kinase signaling pathway	6	37.5	1.8E−5	5.7E−3
GOTERM_BP_FAT	transmembrane receptor protein serine/threonine kinase signaling pathway	5	31.2	6.8E−5	1.6E−2
GOTERM_BP_FAT	cellular response to organic substance	8	50.0	1.4E−4	2.6E−2
GOTERM_BP_FAT	BMP signaling pathway	4	25.0	1.9E−4	2.9E−2

Table II. *Sequences of primers used for RT-qPCR analysis.*

Gene	Accession Number	Primer Sequence (5'-3')	Length (bp)
CHRDL1	HGNC:29861	AGGGGATGGAGAATTGTCGT ACTTCTGGCTCCGGGAAAG	154
EIF2AK3	HGNC:3255	AACAGCGTTTACTTGGGAATG AAGGGTTTCCATTTGATTGTTG	152
FOS	NP_001116585	ATGATGTTCTCCGGCTTCAA CAGATCGGTGCAGAAGTCCT	159
FST	NP_001003662	CGACGAGGAGGACGTAAATG CGGGGTTTGTTCTTCTTGTT	150
ID1	NP_001231629	TTGGAGCTGAACTCGGAATC GGAACACATGCTGTCTCTGC	122
INSR	HGNC:6091	CACTTCTTCCGACATGTGGT GTCGGTGACTCTCTCTGGAC	160
KIT	NP_001037990	CGCCTGGGATTTTCTCTTCG ACAGCCTAATCTCATCGCCA	152
KLF10	NP_001127816	CCTGCTCCAGGGTTTTCC CTCCTGTATGTGTTCTCATGTGG	151
MAP3K1	HGNC:6848	TTCAGAAAACAGTATAAAAGATGAAGA CTACATTCTTCTGCCCAGATTG	150
MYO1E	HGNC:7599	CGAAAACAAAGTTAACCCTCCT TGGTTCCAGCTGTTGAAATG	150
PHIP	HGNC:15673	CCTGATGGGTCATGAAGATG	160
SHOC2	HGNC:15454	CCTGAGGAAATTGGTACACTGG ATGTCCTTGGCCTTCAATCA	160
SMAD4	Q9GKQ9	AACCACAAATGGAGCTCACC TGTTTTAATTCATTTTTGTGAAGATCA	150
TGFBR3	NP_999437	ATTGTGTGGTTGCCCTGTTT GGTGAAGCTCTCCATCAAGG	131
TXNIP	Q2HY40	GCCTCTGGGAACATCTTTCA CACAGGTGCCATTAAATCAGG	157
VEGFA	NP_999249	CTCTCTTGGGTGCATTGGAG TCTCGATTGGACGGCAGTAG	154

Table III. *Fold changes adjusted p values and Entrez Gene ID of differentially expressed genes belonging to the "enzyme linked receptor protein signalling pathway" functional category from David Geoterm BP database.*

Gene	Fold Change	Adj.P.Value	Database Accesion Number
CHRDL1	0.139365	4.74E-05	ENSSSCT00000027812
EIF2AK3	0.41889	0.008422	ENSSSCT00000008989
FOS	0.052794	4.74E-05	ENSSSCT00000002650
FST	0.224697	0.000365	ENSSSCT00000023776
ID1	0.335473	0.003974	NM_001244700
INSR	0.316016	0.001913	ENSSSCT00000014815
KIT	0.430444	0.002556	ENSSSCT00000009679
KLF10	0.405439	0.006845	NM_001134344
MAP3K1	0.368765	0.024748	AJ585088
MYO1E	0.326887	0.001132	AK236366
PHIP	0.385682	0.021116	ENSSSCT00000004941
SHOC2	0.442895	0.040665	AK231028
SMAD4	0.367802	0.001239	NM_214072
TGFBR3	0.196522	0.000406	NM_214272
TXNIP	0.355539	0.000781	ENSSSCT00000007319
VEGFA	0.069689	0.001913	AF041084

Symbols and names of the selected genes are shown.

and *PHIP,* present larger discrepancy between the two methods applied.

DISCUSSION

The data showed substantial up-regulation of several genes in oocytes before IVM as compared to after IVM. Before IVM genetic transcripts of genes *FOS, VEGFA, CHRDL1, TGFBR3, FST, INSR, MYO1E, ID1, TXNIP, SMAD4, MAP3K1, PHIP, KLF10, EIF2AK3, KIT* and *SHOC2* were expressed. However, after IVM these genes were down-regulated. This suggests that genes recruited in 'enzyme linked receptor protein signaling pathway' in porcine oocyte *in vitro,* may have a higher level of expression before the oocyte's mature. It shows that the process of oocyte maturation and developmental capacity is most probably orchestrated by genes whose transcripts belong to the group 'enzyme linked receptor protein signaling pathway'.

KIT is a proto-oncogene gene encoding a receptor tyrosine kinase, which plays an important role in the regulation of cell survival and proliferation, stem cell maintenance and gametogenesis. Recently, Saatcioglu et al. presented evidence that the receptor tyrosine kinase Kit controls reawakening of the oocytes (26). The next gene, eukaryotic translation initiation factor 2-alpha kinase (*EIF2AK3*), otherwise known as *PERK*,

is phosphorylated in response to environmental stress. It has been shown that *EIF2A3K* plays an important role in the ability of the endoplasmic reticulum ER for adaptation to stress in mammalian cells *in vitro* (12). The upregulation of *EIF2AK3* in porcine oocytes before IVM can be a substantial indicator of ER stress during *in vitro* maturation of the gametes.

Mitogen-activated Protein Kinases 3 and 1 (*MAP3K1*) also known as Extracellular Signal-Regulated Kinases 1 and 2 (ERK ½) are the intrafollicular mediators which stimulate the cumulus cell-oocyte complex (COC) growth and also oocyte maturation (8). In this investigation, we first present the expression profile of *MAP3K1* in porcine oocytes before and after IVM in relation to the regulation of "enzyme linked receptor protein signalling pathway". Cao at al. demonstrated that deletion or silencing of *MAP3K1* leads to cell cycle arrest or cell death. In their recent study they showed that knockout of *MAP3K1* triggered GCs apoptosis. They concluded that *MAP3K1* might be required for porcine GC survival (5).

The results of our study demonstrated up-regulation of *TGFBR3*, *FST* and *Smad4* (three members of TGF family) in porcine oocytes after IVM, compared to those analyzed in their immature form. Transforming growth factor-beta (TGF-**β**) is an important protein participating in several aspects of cell and tissue life, as well as apoptosis and survival. TGF-**β** is also responsible for regulation of somatic cell proliferation and differentiation *in vitro* and *in vivo*. Piotrowska et al. concluded that TGF-**β** and the TGF superfamily members control essential stages of folliculogenesis, oogenesis and embryogenesis in mammals (24). TGF-**β**3 (*TGFBR3*) is able to inhibit TGF-**β** signaling pathways, because of its ability to capture TGF-**β**. *TGFBR3* plays a role in suppression of cancer progression and metastasis (11). In the results of our work, we observed up-regulated expression of this gene in porcine COCs after IVM compared to before IVM.

Smad Family Member 4 (*SMAD4*) protein is a downstream signaling molecule of the TGF-**β** -superfamily. Research by Xing at al. indicated a substantial role of SMAD4 in oocyte maturation and other reproduction–related processes, as this protein can be found in porcine oocyte, granulosa and thecal cells (32).

Follistatin (*FST*) is a protein expressed in oocytes and granulosa cells in cattle. Follistatin can bind and regulate activity of TGF-beta superfamily members. FST binding blocks interactions with serine threonine kinase receptors, which inhibits ligand-induced Smad signaling. High levels of *FST* transcript correlated with good ovarian function and good-quality of the oocytes. Recently, Wang et al. reported that *FST* can play various roles in oocyte and granulosa cells during the formation of primordial follicles (31). *TXNIP*, coding for thioredoxin interacting protein was also highly up-regulated by IVM. *TXNIP* expression in porcine CCs was observed for first time. *TXNIP* is responsible for regulation of oxidative stress response and also may inhibit glucose and lactate production. Su-Yeon at al. during his research noted that *TXNIP* is an essential regulator of glucose metabolism, cytoplasmic streaming and meiotic maturation of the mouse oocytes (20). The inhibitor of DNA binding (*ID1*) belongs to a family of four proteins regulating inhibiting activity of transcription factors, by controlling their possibility to bind DNA. The members of ID family have two main functions: to maintain proliferation and to inhibit differentiation. Blaha et al. explored the effect of epiregulin, amphiregulin and follicle stimulating hormone (FSH) on gene expression in porcine CCs. The results of their microarray experiments showed that FSH administration led to down-regulated expression of genes such as *FOS* and *ID1/3* (1). On the contrary, results of our microarray experiment demonstrated up-regulation of *ID1* and *FOS* after *in-vitro* maturation. Further studies are indispensable to determine how significant the *ID1* is for the regulation of folliculogenesis and to discover its physiological meaning for fertility and reproductive diseases.

Another test gene in our study is the insulin receptor (*INSR*). *INSR* was first identified in the granulose cells of antral human follicles. Recent study showed that *INSR* is widely distributed in all ovarian tissues, in the granulosa and theca cells in bovine species. Insulin is a peptide hormone, the actions of which are mediated through *INSR*. This hormone plays a very important role in the ovary, as a mediator of follicular development and oocyte maturation. Roberta at al.

found that supplementation of the medium with the insulin and FSH causes an increase in *INSR* mRNA levels. Insulin works through its own receptor to inflict the reply of granulose cells to gonadotropins (6). The defects in the *INSR* gene manifest through impaired ovulation and defects in oocyte maturation. Furthermore, our findings also show that *INSR* may be an important factor in the development of oocytes.

The results of our study have also shown increased expression of chordin-like 1 (*CHRDL1*), also known as neurogenesin-1 (*NRLN1*) in porcine oocytes after IVM as compared to those analyzed before IVM. *NRLN-1* acts a mediator of BMP signaling pathways. This pathway plays a crucial role in the regulation of cell growth, development and differentiation, as well as their survival and apoptosis. The role of *CHRDL1* in oocyte maturation is not yet known. Budna at al. suggested that transcript of *CHRDL1* and *BMP1* could reflect embryonic development (3)there exist many differences that promote these processes in vivo and in vitro. Therefore, this study aimed to investigate the differences in RNA expression profiles between porcine oocytes before and after IVM using microarray and real-time quantitative polymerase chain reaction (RT-qPCR. Vascular endothelial growth factor A (VEGFA) causes proliferation and migration of vascular endothelial cells, being crucial for physiological and pathological angiogenesis. VEGF may inhibit apoptosis of ovarian follicular cells in cattle, sheep, and rats. VEGF showed that it has the potential to amend the quality of mature porcine oocytes. Kere at al., in their study, added exogenous VEGF to culture media to estimate its result on porcine oocyte maturation. Their results suggest that VEGFA supplementation in maturation medium improved oocyte maturation. VEGF ameliorated quality and promoted development of porcine parthenotes (17) although 5, 50, or 500\u00a0ng/mL did not significantly affect nuclear maturation of oocytes. Parthenotes from oocytes cultured either in in\u00a0vitro maturation or in\u00a0vitro culture medium supplemented with 5 or 50\u00a0ng/mL VEGFA had an improved blastocyst rate and increased total numbers of cells ($P < 0.05$. In our study, we observed high up-regulation of VEGFA-related gene in mature oocytes, compared to immature oocytes. We postulated that VEGFs play a crucial role in further development of mature porcine oocytes.

Another tested gene is the FOS Proto-Oncogene (*FOS*), a member of the immediate response family of transcription factor. *FOS* transcription is generally activated in reply to exogenous ligands. The expression of *FOS* has been indicated as a marker of germ cell development. Hess and al. showed that *FOS* plays an important role in regulation of proliferation, differentiation and cell survival. The expression of *FOS* and *BCL2* genes is present within the preimplantation embryo. The protein products of this gene showed marked staining from the two-cell to the blastocyst stage (14).

The secondary group of genes could not be assigned to any specific system or mechanism of function related to the reproductive process. All exert a broad spectrum of actions but have never been associated with the oocyte or folliculogenesis. Kruppel Like Factor 10 (*KLF10*), a zinc finger transcription factor, is a protein which rapidly induces *TGFB1,2* and *3*, epidermal growth factor, as well as bone morphogenetic protein-2. Generally, *KLF10* is related to cell differentiation and it is the target gene for the various signaling pathways. Recent findings by Subramaniam et al. showed that *KLF10* can support TGF-β inhibition of cell proliferation and inflammation, or can activate apoptosis (28) KLF10, a member of the Kr\u00fcppel-like family of transcription factors, there have been multiple publications regarding its functions and its immediate family members, in numerous cell types. KLF10 has been shown to be rapidly induced by TGFbeta1, 2, 3, E(2. *KLF10*'s functions have not been linked to the reproduction-associated processes but can activate or inhibit transcription of many genes.

The next gene, *SHOC-2,* encodes leucine rich, scaffold protein. *SHOC-2* (*SUR-8*) can up-regulate Ras-MAP kinase signaling in cells and is able to form a complex with Ras and Raf that increases the activation of endoplasmic reticulum. The study by Li at al. showed that *SHOC-2* can selectively change the signal strength of Ras and RTK but not to other effectors, for example PI3K (21). The Pleckstrin Homology Domain Interacting Protein (*PHIP*) gene encodes a protein that binds to the insulin receptor substrate 1 protein. Moreover, *PHIP* has the ability

to regulate glucose transport and translocation in skeletal muscle cells. Recent data show that the encoded protein can also regulate growth and survival of pancreatic beta cells. Increasing expression of PHIP can promote melanoma in humans (9)gene expression, and glucose transport. The N terminus of IRS-1 contains a pleckstrin homology (PH. *MYO1E*, a gene encoding myosin 1E, was the last of the detected genes. Podocytes play crucial roles as constituents of the glomerular filtration barrier. Mao et al. in their study results showed that MYO1E is crucial component contributing to the functional integrity of podocytes. Down-regulation of MYO1E expression may cause alternation of podocyte shape and cause their drop-out from the glomerular basement membrane. The effect of these defects may lead to handicap of glomerular filtration barrier and proteinuria (22). As a result of our research, we suggest, that these factors are also potentially involved in the *in vitro* maturation of oocytes.

ACKNOWLEDGEMENTS

Publication of this article was made possible by grant number UMO-2016/21/B/NZ9/03535 from the Polish National Centre of Science and 502-01-02227367-08414 from Poznan University of Medical Sciences.

REFERENCES

1. Blaha M, Nemcova L, Kepkova KV, Vodicka P, Prochazka R. Gene expression analysis of pig cumulus-oocyte complexes stimulated *in vitro* with follicle stimulating hormone or epidermal growth factor-like peptides. Reprod Biol Endocrinol 2015; 13(1):113.
2. Budna J, Bryja A, Celichowski P, et al. Genes of cellular components of morphogenesis in porcine oocytes before and after IVM. Reproduction 2017; 154(4):535-45.
3. Budna J, Bryja A, Celichowski P, et al. "Bone development" is an ontology group upregulated in porcine oocytes before *in vitro* maturation: a microarray approach. DNA Cell Biol 2017; 36(8):638-46.
4. Budna J, Celichowski P, Karimi P, et al. Does porcine oocytes maturation *in vitro* is regulated by genes involved in transforming growth factor beta receptor signaling pathway? Adv Cell Biol 2017; 5(1):1-14.
5. Cao R, Wu W, Zhou X, et al.. Let-7g induces granulosa cell apoptosis by targeting MAP3K1 in the porcine ovary. Int J Biochem Cell Biol 2015; 68:148-57.
6. Chaves RN, Duarte ABG, Rodrigues GQ, et al. The effects of insulin and follicle-simulating hormone (FSH) during *in vitro* development of ovarian goat preantral follicles and the relative mRNA expression for insulin and FSH receptors and cytochrome p450 aromatase in cultured follicles. Biol Reprod 2012; 87(3):69.
7. Dennis G, Sherman BT, Hosack DA, Yang J, Gao W, Lane HC, Lempicki RA. DAVID: database for annotation, visualization, and integrated discovery. Genome Biol 2003; 4(5):P3.
8. Fan H-Y, Liu Z, Shimada M, Sterneck E, Johnson PF, Hedrick SM, Richards JS. MAPK3/1 (ERK1/2) in ovarian granulosa cells are essential for female fertility. Science 2009; 324(5929):938-41.
9. Farhang-Fallah J, Yin X, Trentin G, Cheng AM, Rozakis-Adcock M. Cloning and characterization of PHIP, a novel insulin receptor substrate-1 pleckstrin homology domain interacting protein. J Biol Chem 2000; 275(51):40492-97.
10. Gautier L, Cope L, Bolstad BM, Irizarry RA. affy--analysis of Affymetrix GeneChip data at the probe level. Bioinformatics 2004; 20(3):307-15.
11. Hanks BA, Holtzhausen A, Evans KS, et al. Type III TGF-β receptor downregulation generates an immunotolerant tumor microenvironment. J Clin Invest 2013; 123(9):3925-40.
12. Harding HP, Zhang Y, Bertolotti A, Zeng H, Ron D. Perk is essential for translational regulation and cell survival during the unfolded protein response. Mol Cell 2000; 5(5):897-904.
13. Haw R, Stein L. Using the reactome database. Curr Protoc Bioinforma 2012; Chapter 8:Unit 8.7.
14. Hess J, Angel P, Schorpp-Kistner M. AP-1 subunits: quarrel and harmony among siblings. J Cell Sci 2004; 117(25):5965-73.
15. Huang L, Feng G, Du P, et al. GeneAnswers: integrated interpretation of genes. R package version

2.22.0. 2014.
16. Jackowska M, Kempisty B, Antosik P, et al. The morphology of porcine oocytes is associated with zona pellucida glycoprotein transcript contents. Reprod Biol 2009; 9(1):79-85.
17. Kere M, Siriboon C, Liao JW, et al. Vascular endothelial growth factor A improves quality of matured porcine oocytes and developing parthenotes. Domest Anim Endocrinol 2014; 49:60-69.
18. Kranc W, Budna J, Chachuła A, et al. "Cell migration" is the ontology group differentially expressed in porcine oocytes before and after *in vitro* maturation: a microarray approach. DNA Cell Biol 2017; 36(4):273-82.
19. Kranc W, Celichowski P, Budna J, et al. Positive regulation of macromolecule metabolic process belongs to the main mechanisms crucial for porcine oocytes maturation. Adv Cell Biol 2017; 5(1):15-31.
20. Lee S-Y, Lee H-S, Kim E-Y, Ko J-J, Yoon TK, Lee W-S, Lee K-A. Thioredoxin-interacting protein regulates glucose metabolism and affects cytoplasmic streaming in mouse oocytes. PLoS One 2013; 8(8):e70708.
21. Li W, Han M, Guan KL. The leucine-rich repeat protein SUR-8 enhances MAP kinase activation and forms a complex with Ras and Raf. Genes Dev 2000; 14(8):895-900.
22. Mao J, Wang D, Mataleena P, et al. Myo1e impairment results in actin reorganization, podocyte dysfunction, and proteinuria in zebrafish and cultured podocytes. PLoS One 2013; 8(8):e72750.
23. Nawrocki MJ, Celichowski P, Budna J, et al. The blood vessels development, morphogenesis and blood circulation are three ontologic groups highly up-regulated in porcine oocytes before *in vitro* maturation. Adv Cell Biol 2017; 5(2):135-42.
24. Piotrowska H, Kempisty B, Sosinska P et al. The role of TGF superfamily gene expression in the regulation of folliculogenesis and oogenesis in mammals: a review. Vet Med (Praha) 2013; 58(10):505-15.
25. Rybska M, Knap S, Jankowski M et al. Cytoplasmic and nuclear maturation of oocytes in mammals – living in the shadow of cells developmental capability. Med J Cell Biol 2018; 6(1):13-17.
26. Saatcioglu HD, Cuevas I, Castrillon DH. Control of oocyte reawakening by Kit. PLOS Genet 2016; 12(8):e1006215.
27. Shannon P, Markiel A, Ozier O et al. Cytoscape: a software environment for integrated models of biomolecular interaction networks. Genome Res 2003; 13(11):2498-504.
28. Subramaniam M, Hawse JR, Rajamannan NM, Ingle JN, Spelsberg TC. Functional role of KLF10 in multiple disease processes. BioFactors 2010; 36(1):NA-NA.
29. Trejter M, Hochol A, Tyczewska M, et al. Sex-related gene expression profiles in the adrenal cortex in the mature rat: microarray analysis with emphasis on genes involved in steroidogenesis. Int J Mol Med 2015; 35(3):702-14.
30. Walter W, Sánchez-Cabo F, Ricote M. GOplot: an R package for visually combining expression data with functional analysis: Fig. 1. Bioinformatics 2015; 31(17):2912-14.
31. Wang Z, Niu W, Wang Y, Teng Z, Wen J, Xia G, Wang C. Follistatin288 regulates germ cell cyst breakdown and primordial follicle assembly in the mouse ovary. PLoS One 2015; 10(6):e0129643.
32. Xing N, Liang Y, Gao Z, He J, He X, Li H, Dong C. Expression and localization of Smad2 and Smad4 proteins in the porcine ovary. Acta Histochem 2014; 116(8):1301-6.

EXPRESSION OF IL-17A, E, AND F AND THEIR RECEPTORS IN NON-SMALL-CELL LUNG CANCER

Q. HUANG[1*], XC. MA[2*], X. YANG[3], W. WANG[1], Y. LI[1], Z. LV[1], C.J. CORRIGAN[4], Y. CHEN[1] and S. YING[1]

[1]Department of Immunology, School of Basic Medical Sciences, Capital Medical University, You An Men, Beijing, P. R. China; [2]Department of Chest Surgery, Beijing Anzhen Hospital, Capital Medical University, Beijing, P. R. China; [3]Department of Respiratory Medicine, Beijing Tongren Hospital, Capital Medical University, P. R. China; [4]King's College London, MRC and Asthma UK Centre in Allergic Mechanisms of Asthma, Division of Asthma, Allergy and Lung Biology, London, UK

Received May 31, 2018 – Accepted August 2, 2018

[*]These Authors contributed equally to this work

Lung cancer is the leading cause of cancer-related morbidity and mortality worldwide. Interaction of nascent or established lung tumour cells with various cytokines and infiltrating immune cells has been implicated in lung cancer pathogenesis. In this study, we systematically analysed immunoreactivity for IL-17A, IL-17E and IL-17F and their relevant receptors in the lung sections from non-small cell lung cancer (NSCLC) and normal control. Immunoreactivity for IL-17A, IL-17F, IL-17RA and IL-17RC, but not IL-17RB was significantly elevated in NSCLC compared with controls, while IL-17E was reduced. The median numbers of infiltrating lymphocytes and neutrophils and global macrophage (CD68) immunoreactivity of phagocytes were also elevated in NSCLC compared with control tissue sections. Furthermore, correlation between the expression of IL-17A and its receptors IL-17RA and IL-17RC varied according to NSCLC histopathological type. These data suggest that IL-17A, E, F and their receptors IL-17RA, RB, RC may be involved in the pathogenesis of NSCLC. Further understanding of the relationship between the IL-17/IL-17R axis and the tumour inflammatory microenvironment may reveal new therapeutic targets.

Lung cancer accounts for the highest cancer-related morbidity and is the most common cause of cancer death (1, 2). Although many factors have been implicated in the pathogenesis of lung cancer, local chronic inflammation associated with dysregulation of inflammatory cytokine expression is the best known aetiological factor in inflammation-related cancers (3, 4); indeed, it is reported that approximately 15% of all human cancers arise in the context of infection and chronic inflammation (5). Long-term inflammation promotes secretion of cytokines and chemokines which may lead to tumour initiation. Members of the IL-17 family of cytokines have been demonstrated to be central to the pathogenesis of a range of chronic inflammatory diseases, including those of the human airways (6), compatible with the hypothesis that chronic inflammation accompanied by changes in expression of these cytokines in the airways is an aetiological factor in lung carcinogenesis.

Key words: IL-17 cytokine family, IL-17 receptor, non-small cell lung cancer, inflammatory cell

Mailing address:
Dr Yan Chen,
Department of Immunology,
School of Basic Medical Sciences, Capital Medical University,
No. 10 Xitoutiao, You An Men,
Beijing 100069, P. R. China
Tel.: +86 01083911825, - Fax: +86 01083911743
e-mail: chenchen@ccmu.edu.cn

0393-974X (2018)

The IL-17 cytokine family comprises of IL-17A, IL-17B, IL-17C, IL-17D, IL-17E (also named IL-25) and IL-17F. Its members share 15~50% homology at the amino acid level and all play important roles in a variety of immune responses (7). In particular, it is reported IL-17A plays important roles in host defence against infection, chronic inflammatory diseases and autoimmune disorders (8, 9). The biological functions of IL-17F closely resemble those of IL-17A (10), partly because its gene is located in the same chromosomal region as that of IL-17A (6p12) and it shares the highest amino acid homology with IL-17A (11, 12). In contrast, IL-17E has the lowest homology with IL-17A and differs functionally from the other members of the IL-17 cytokine family in stimulating the production of Th2 cytokines and regulating allergic responses (13, 14). IL-17 cytokines form homodimer or heterodimer ligands which bind to various IL-17 receptors (IL-17R) complexes. The IL-17R family has five subunits named IL-17RA to IL-17RE. IL-17A and IL-17F homo- or hetero-dimers utilize the same receptor complexes consisting of IL-17RA and IL-17RC, while IL-17E binds to the heterodimer IL-17RA/IL-17RB (6).

IL-17A expression in peripheral blood has been reported to be elevated in NSCLC patients and has been implicated in lung cancer progression by a variety of mechanisms (15, 16). In contrast, Tania Benatar et al. reported that IL-17E has anti-tumour activity in a variety of human tumour xenograft models, including lung cancers (17). Despite these observations, however, very little is known about the expression and location of IL-17 cytokine family members and their receptors in NSCLC. NSCLC accounts for approximately 85% of all cases of lung cancer (18), squamous cell carcinoma (SCC) and adenocarcinoma (ADC) being the most common histopathological types. In this study we address the hypothesis that IL-17 family cytokines play a role in determining the phenotype and progression of human NSCLC, either directly or by modifying the environmental immune response. Consequently, we set out to assess normal or tumour lung tissue expression of IL-17A, IL-17E, IL-17F and their receptors in NSCLC as well as the nature of any associated inflammatory cellular infiltration in this context. Finally, we looked for correlations of expression of IL-17 family cytokine members with clinical parameters including disease progression and histopathological type.

MATERIALS AND METHODS

Human tissue specimens

Human specimens from resected lung tissue were obtained at the Beijing Anzhen Hospital, People's Republic of China, from January 2013 to December 2016. In accordance with Ethical Principles and an approval from Capital Medical University Ethics Committee, written informed consent was obtained from all patients to collect tumour tissue from 59 cases of lung cancer diagnosed by conventional means as ADC or SCC and 10 specimens of normal lung tissue. None of the patients had received any preoperative chemotherapy or radiotherapy prior to surgery.

Immunohistochemistry

The formalin-fixed, paraffin-embedded tissue samples were cut into 4-μm serial sections, mounted on slides then deparaffinised by baking the slides at 60°C for 2 h and finally washed with PBS 3 times. Antigen retrieval was then performed by immersing the slides in boiling citrate buffer for 20 min then cooling to room temperature, after which the sections were washed 3 times for 5 min each in PBS. Endogenous peroxidase was blocked with 3% H_2O_2 for 1 h, after which the sections were washed again 3 times for 5 min each in PBS then incubated with 3% BSA with 0.3% Triton X-100 in PBS for 1 h at room temperature. Primary antibodies against human IL-17/IL-17A (NBP1-42746), IL-17E/IL-25 (NB100-56541), IL-17F (NBP2-21684), IL-17RA (ab133416, Abcam), IL-17RB (AF1207, R&D), and IL-17RC (NBP1-83112) were purchased from Novus Biologicals (USA), Abcam (Hong Kong, China) and R&D systems (USA), respectively. In addition, antibodies against human pan T lymphocytes (anti-CD3: ab699, Abcam), macrophages (anti-CD68: 3F103: sc-70761, Santa Cruz) and neutrophils (anti-neutrophil elastase: ab21595, Abcam) were also used to identify infiltrating inflammatory cells in lung tissues. Optimal titrations of the various antibodies were determined prior to the formal experiments.

Immunohistochemistry was performed according

to our previously described technique (19, 20). Briefly, sections were then incubated with each primary antibody overnight at 4°C, washed and then incubated with secondary antibody (211-005-109, mouse anti-rabbit or 115-005-003, goat anti-mouse) and peroxidase-conjugated third antibody (715-035-150, donkey anti-mouse or 705-035-003, donkey anti-goat, Jackson Immuno- Research (USA)) for 1h at room temperature, respectively. As a negative control, PBS was substituted for the primary, antigen-specific antibodies. The immunoreactivity was visualized after developing with DAB (3, 3'-diaminobenzidine). The sections were counterstained with haematoxylin for 3.5 min, rinsed with water, dehydrated and then cover slipped.

Images were taken with a Digital DS-Ri2 camera (Nikon). Global expression of immunoreactivity for the IL-17 cytokine family members and their receptors and macrophages was quantified as the percentage staining of the total stainable area of the sections as defined by the haematoxylin counterstaining, while the numbers of the other inflammatory cells were expressed as the numbers of stained positive cells per unit area.

Real-time PCR

To further explore RNA expression of IL-17A, total RNA was extracted by Trizol and reverse transcripted into cDNA using PrimeScript RT reagent Kit according to the manufacture's instruction. Primers were designed to the sequences as follows: for IL-17A, sense: 5'-TCCCACGAAATCCAGGATGC-3' and anti-sense: 5'-GGAT GTTCAGGTTGACCATCAC-3'; for GAPDH, sense: 5'-GGAGCGAGATCCCT CCAAAATGAPDH-3' andanti-sense:5'-GGCTGTTGTCATACTTCTCATGG-3'; RT-PCR amplification reactions were prepared with the SYBR Green PCR kit (Bio-rad, USA) and performed using the 7500 Real-Time PCR system (Applied Biosystems, USA). GAPDH was the reference gene and the relative expression levels of mRNA was counted with the threshold cycle (CT) method-fold change(2-ΔΔCT).

Table I. *Patient characteristics.*

Status	Age	Gender (F/M)	Sources	Stage Classification	
Control	37~70	5/5	resection specimens		
n=10					
Squamous	32~82	2/27	resection specimens	stage 1	n=16
n=29				stage 2	n=8
				stage 3	n=3
				stage 4	n=2
Adenocarcinoma	33~75	20/10	resection specimens	stage 1	n=24

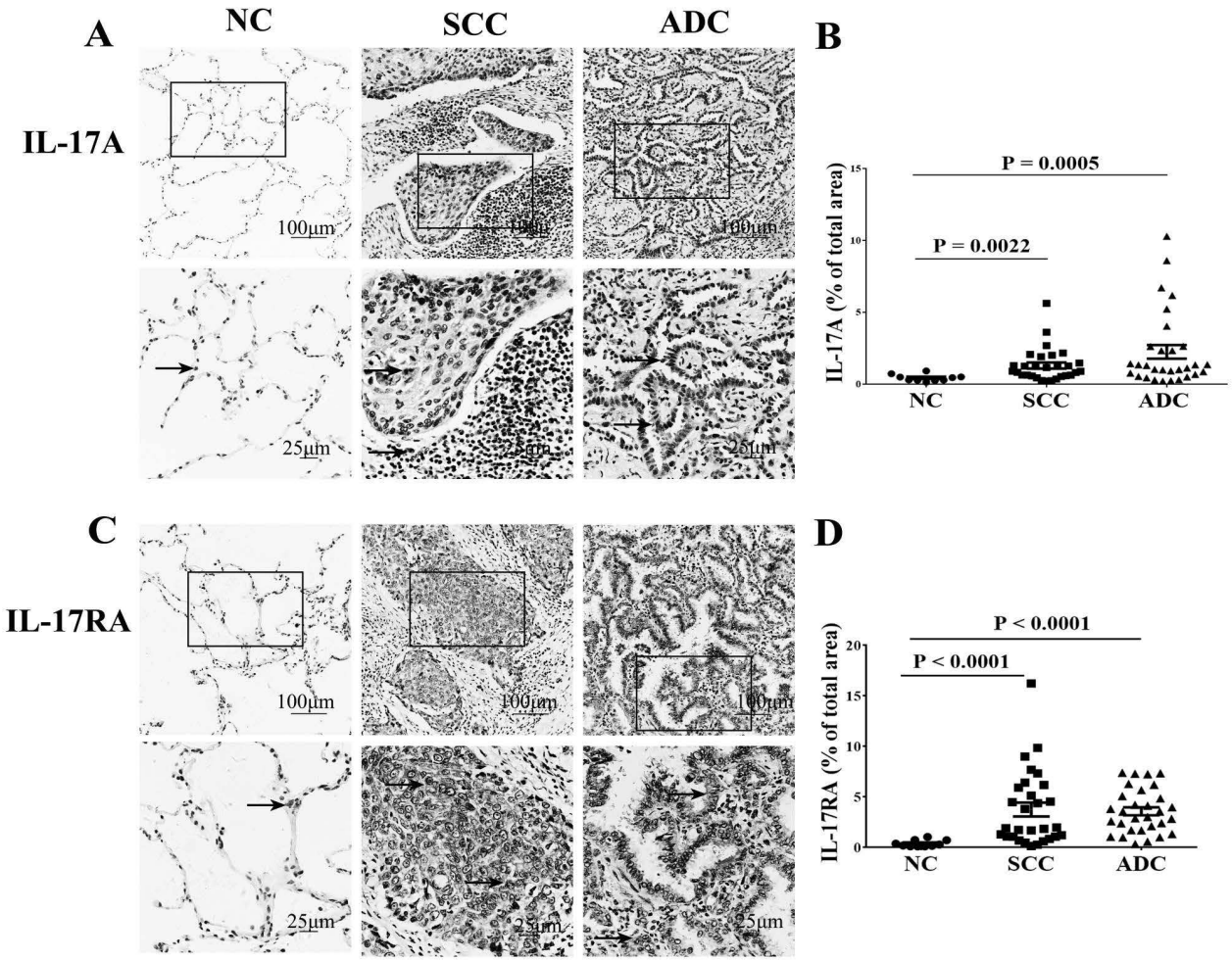

Fig. 1. *Immunoreactivity for IL-17A and IL-17RA in NC, SCC and ADC tissues. Representative photomicrographs of IL-17A (**A**) and IL-17RA (**C**) expression in lung tissue sections from subjects with NC (n = 10), SCC (n = 29) and ADC (n = 30) (original magnification × 10 and 40). Expression of IL-17A (**B**) and IL-17RA (**D**) immunoreactivity expressed as a percentage of the entire area of the section as defined by haematoxylin staining. Arrows show examples of positively stained cells.*

Statistical analysis

Statistical significance was determined by Kruskal-Wallis analysis of variance, followed by the Mann-Whitney U-test where appropriate, using GraphPad Prism software version 6.1 (GraphPad Software, La Jolla, CA, USA). A P-value of 0.05 or less was considered statistically significant.

RESULTS

Characteristics of the subjects

Demographic characteristics of the patients with NSCLC and the non-diseased control subjects are summarised in Table I. The median age of the patients with NSCLC was 64 years (range 32-82 years) and comprised of 37 males and 22 females. The median age of the control subjects was 59 years (range, 37-70 years) and comprised of 5 males and 5 females. In patients with NSCLC there were 50 patients with stage 1 or 2 and 9 with stage 3 or 4.

IL-17A and IL-17RA immunoreactivity and localisation

Immunohistochemical staining revealed that the median expression of global IL-17A immunoreactivity was significantly elevated in the NSCLC tissue compared with the control, normal lung tissue (Fig. 1, A and B, $p < 0.05$), although there was no significant difference in the extent of this between SCC and ADC. IL-17A immunoreactivity was observed in macrophages, alveolar epithelial

cells and some malignant cells in the sections from the NSCLC patients. Similarly to IL-17A, the median global IL-17RA immunoreactivity was also significantly elevated in the NSCLC tissue compared with the control tissue (Fig. 1, C and D, $p < 0.05$), with no difference in the extent of this between SCC and ADC. Again similarly to IL-17A, IL-17RA immunoreactivity was located predominantly in epithelial cells and macrophages.

IL-17F and IL-17RC immunoreactivity and localisation

The median global immunoreactivity for IL-17F was significantly elevated in the NSCLC tissue compared with the control tissue (Fig. 2, A and B, $p < 0.05$), and again there was no significant difference in the extent of this between SCC and ADC. IL-17F immunoreactivity was expressed principally in macrophages as well as epithelial cells and some malignant cells. A similar picture was evident with the median global expression of immunoreactivity for IL-17RC, which was elevated in the NSCLC tissue as compared to the control tissue, again with no difference in the extent of this between SCC and ADC (Fig. 2, C and D, $p < 0.05$). Again similarly to IL-17F, immunoreactivity was located predominantly in macrophages but was also evident in some malignant cells.

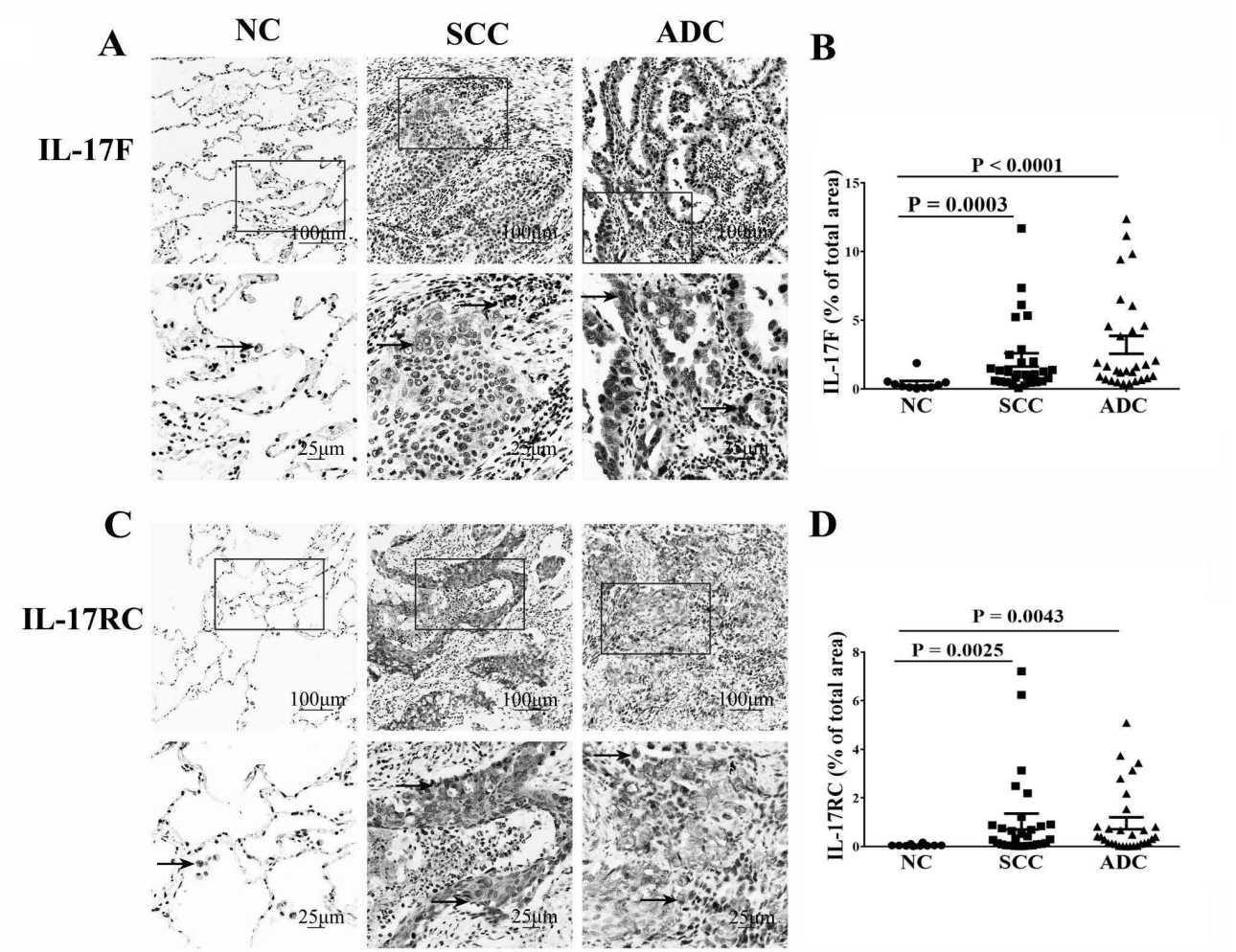

Fig. 2. *Immunoreactivity for IL-17F and IL-17RC in NC, SCC and ADC tissues. Representative photomicrographs of IL-17F (**A**) and IL-17RC (**C**) expression in lung tissue sections from subjects with NC (n = 10), SCC (n = 29) and ADC (n = 30) (original magnification × 10 and 40). Expression of IL-17F (**B**) and IL-17RC (**D**) immunoreactivity expressed as a percentage of the entire area of the section as defined by haematoxylin staining. Arrows show examples of positively stained cells.*

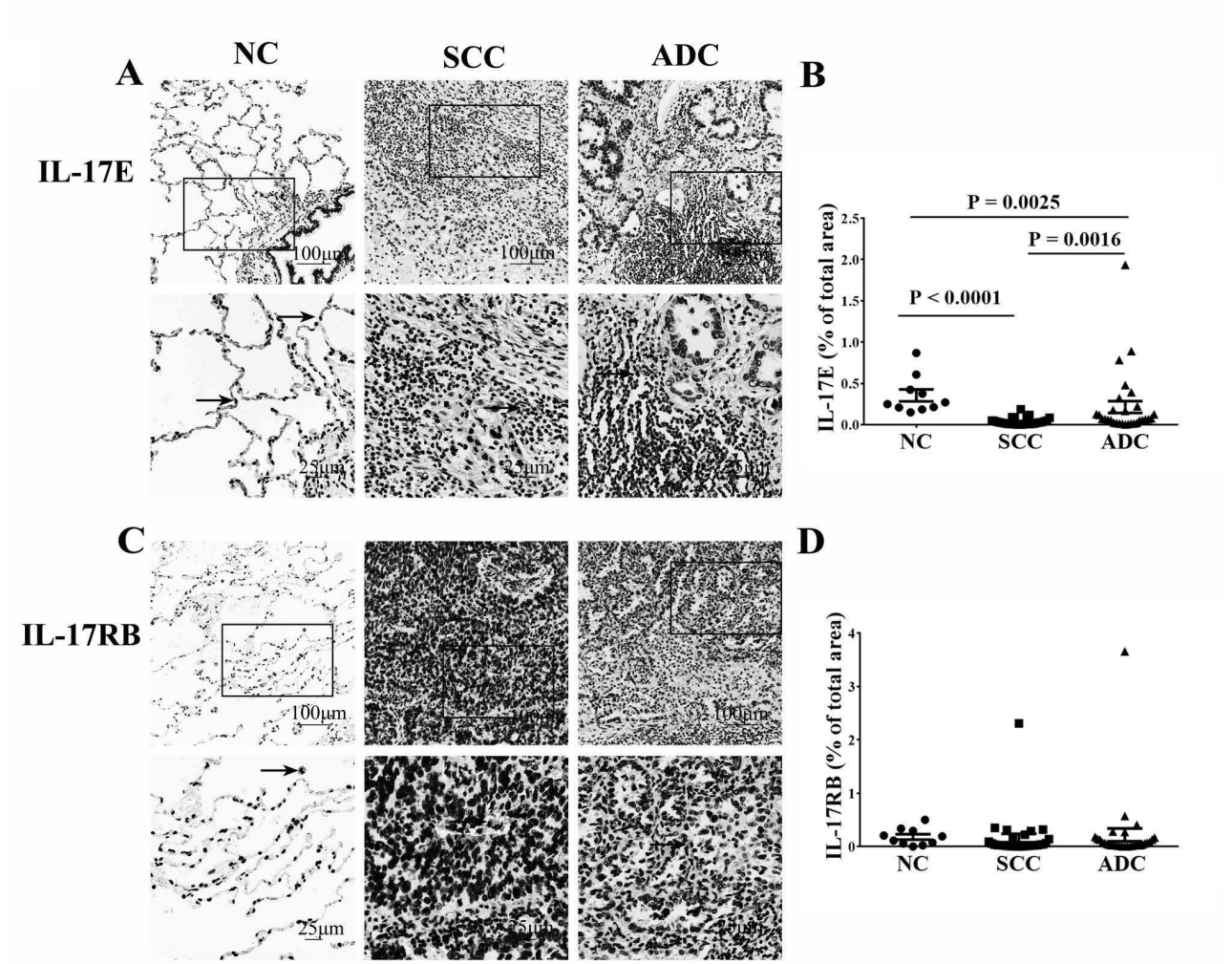

Fig. 3. *Immunoreactivity for IL-17E and IL-17RB in NC, SCC and ADC tissues. Representative photomicrographs of IL-17E (**A**) and IL-17RB (**C**) expression in lung tissue sections from subjects with NC (n = 10), SCC (n = 29) and ADC (n = 30) (original magnification × 10 and 40). Expression of IL-17E (**B**) and IL-17RB (**D**) immunoreactivity expressed as a percentage of the entire area of the section as defined by haematoxylin staining. Arrows show examples of positively stained cells.*

IL-17E and IL-17RB immunoreactivity and localisation

Compared with the normal control tissue, the median global expression of IL-17E immunoreactivity was significantly reduced in NSCLC, particularly in SCC in which its median global expression was also significantly reduced compared with ADC (Fig. 3, A and B, $p < 0.05$). IL-17E immunoreactivity was observed in macrophages and epithelial cells. In contrast, the median expression of IL-17RB immunoreactivity was low and did not significantly differ in normal control, SCC and ADC tissue (Fig. 3, C and D). IL-17RB immunoreactivity was observed in macrophages, epithelial cells and some malignant cells.

Infiltration with lymphocytes, macrophages and neutrophils

Infiltration of T lymphocytes into the lung tissue was quantified by immunohistochemical analysis using anti-CD3 antibody. We observed a significantly elevated median number of $CD3^+$ T cells in the tissue sections from the NSCLC patients compared with those of the normal controls (Fig. 4, A and B, $p < 0.05$). Macrophage infiltration was assessed based on the global expression of CD68 immunoreactivity. Again, we observed significantly elevated median global CD68 immunoreactivity in the tissue sections from the NSCLC patients compared with those from the controls (Fig. 4, C and D, $p < 0.05$). Finally, we

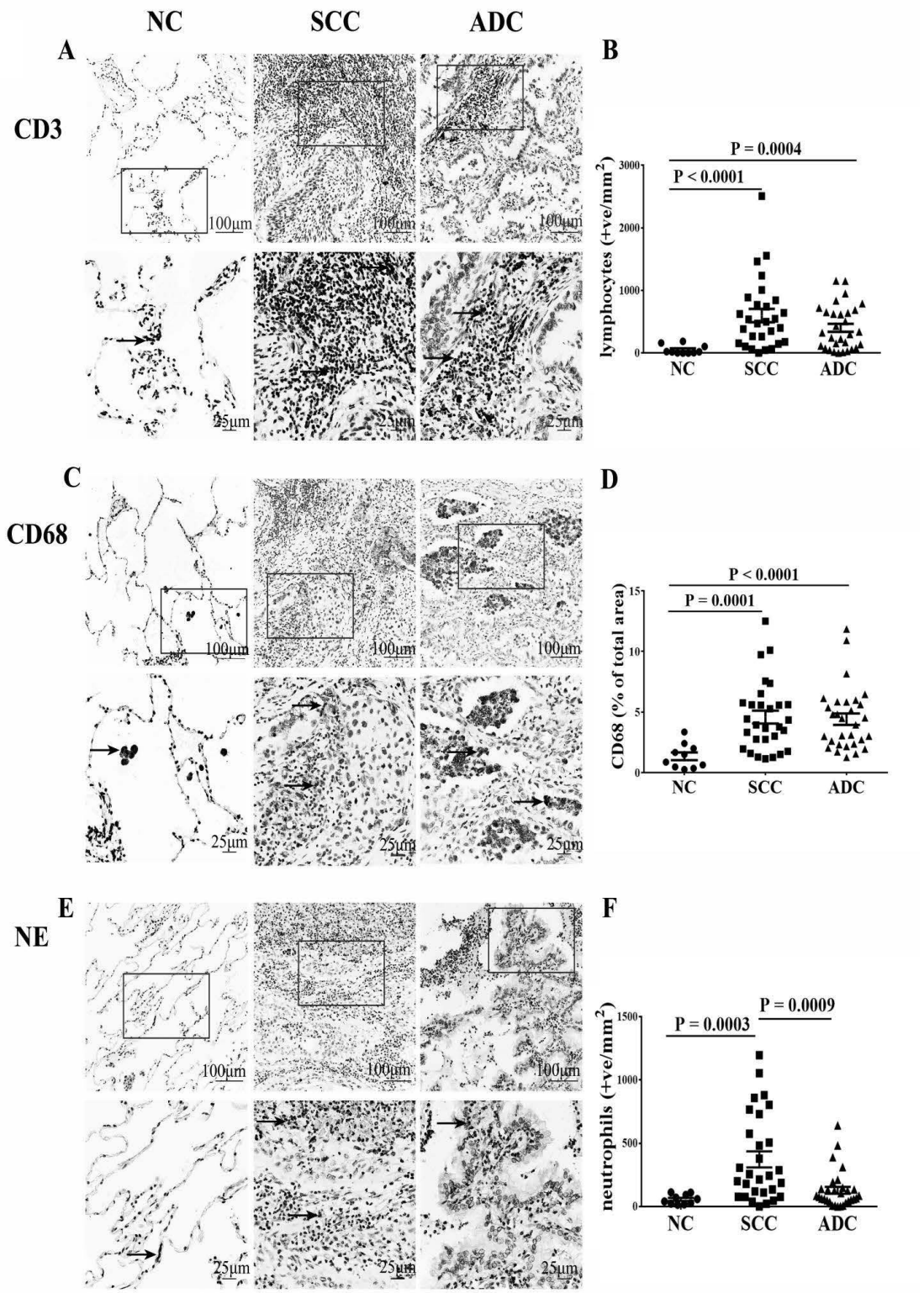

Fig. 4. *Infiltration T cells, macrophages and neutrophils into NC, SCC and ADC tissues. Representative photomicrographs of CD3⁺ T cells (**A**), CD68⁺ macrophages (**C**) and neutrophil elastase (NE)⁺ neutrophils (**E**) in lung tissue sections from subjects with NC (n = 10), SCC (n = 29) and ADC (n = 30) (original magnification × 10 and 40). Quantitative analysis of numbers of CD3⁺ T cells (**B**) and elastase⁺ neutrophils (**F**) per unit area of lung sections. Quantitative analysis of CD68⁺ macrophage immunoreactivity (**D**) expressed as a percentage of the entire area of the section as defined by haematoxylin staining. Arrows show examples of positively stained cells.*

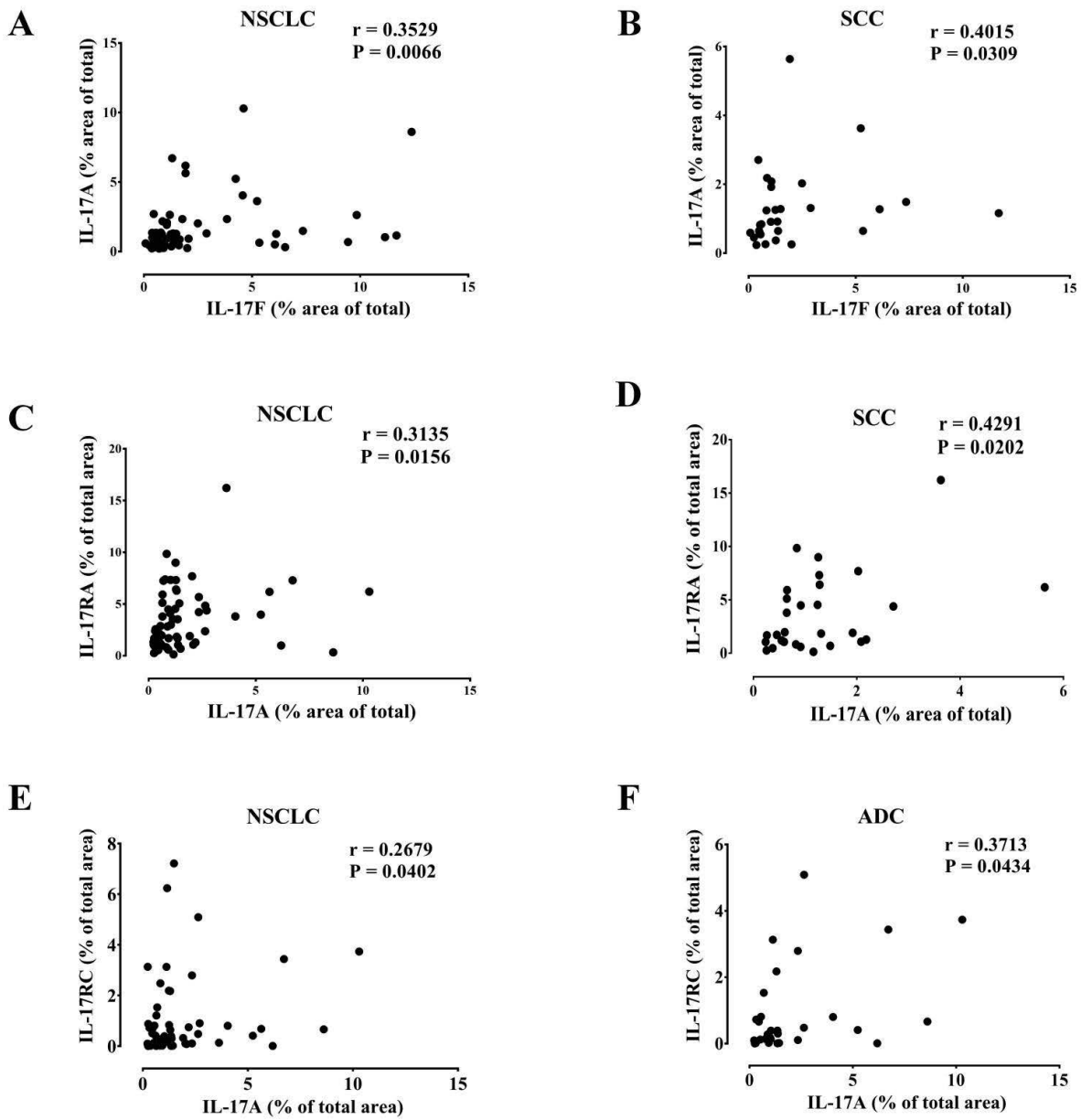

Fig. 5. *Relationships between expression of IL-17 family ligands and their receptors in lung tissue sections from patients with NSCLC and subgroups of the patients with SCC and ADC.* ***A, B****) Positive correlation between IL-17A and IL-17F.* ***C, D****) Positive correlation between IL-17A and IL-17RA.* ***E, F****) Positive correlation between IL-17A and IL-17RC.*

enumerated elastase$^+$ neutrophils in all tissue sections and found that the median number of neutrophils was elevated in the tissue sections from the patients with SCC compared to those from both the patients with ADC and the normal controls (Fig. 4, E and F, $p < 0.05$), with no significant difference between the numbers in the sections from the ADC patients and the normal controls.

Correlation of expression of IL-17 cytokine family members and their receptors with infiltration of inflammatory cells in NSCLC

Considering the tissue sections from all of the patients with NSCLC, we found that the median global immunoreactivity for IL-17A significantly and positively correlated with that of IL-17F and both of its receptors IL-17RA and IL-17RC (Fig.

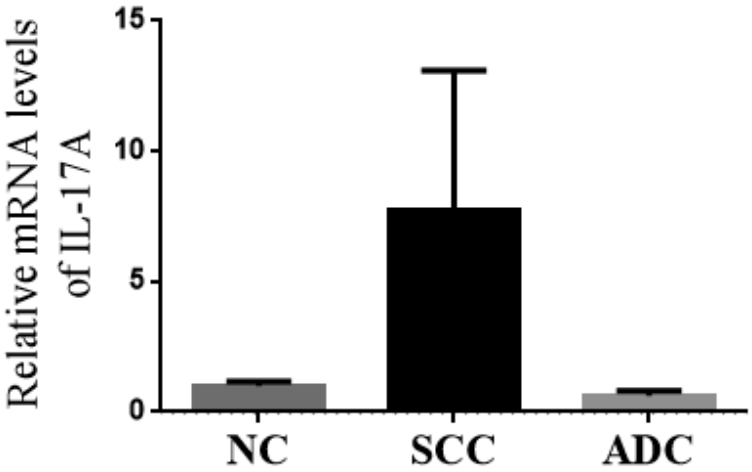

Fig. 6. *Comparison of IL-17A mRNA levels in lung tissue of NC, SCC and ADC using Real-time-PCR.*

5). The correlations between expression of IL-17A and IL-17F and its receptor IL-17RA were retained when considering SCC alone, whereas in the tissue sections from the ADC patients these correlations were lost and only the correlation between IL-17A and its receptor IL-17RC was retained. In addition, the numbers of $CD3^+$ lymphocytes significantly and positively correlated with median global IL-17A immunoreactivity considering all the patients with NSCLC, while global CD68 immunoreactivity significantly and positively correlated with that for IL-17RA (data not shown). We were unable, however, to establish any correlation in the present study between expression of the IL-17 group cytokines and tumour progression in the clinic.

mRNA Levels of IL-17A

Real-time PCR showed that the relative expression of IL-17A had a trend increase in SCC compared with control and ADC; however, there was no significant difference between groups (Fig. 6).

DISCUSSION

In this study we present what we believe is the first systematic comparison of the expression of the IL-17 group of cytokines and their receptors in human NSCLC directly *ex vivo*. Our data clearly support the hypothesis that IL-17A and the homologous IL-17F acting on their receptors IL-17RA and IL-17RC play a role in the pathogenesis of NSCLC, a concept which is gaining increasing inertia in the scientific literature (21, 22). In contrast, our data are compatible with a possible protective role for IL-17E, the functionally distinct member of the group.

While our study has not systematically addressed the possible sources of the IL-17 immunoreactivity in the tissue sections from the patients with NSCLC, it is reasonable to hypothesise that at least some of the local IL-17 production arises from infiltrating inflammatory cells, particularly T cells, macrophages and neutrophils, which are all established sources of IL-17 (5). Indeed, in our study global IL-17A immunoreactivity correlated with infiltrating $CD3^+$ T cell numbers in the tissue sections from all of the patients with NSCLC (although subjective analysis of the distribution of the IL-17 immunoreactivity in our sections also suggests airways epithelial cells and possibly the tumour cells themselves as additional sources). It is further possible to speculate that activation of these inflammatory cells by the tumour cells contributes to a positive feedback loop, reinforcing IL-17 production which further sustains tumorigenesis.

The significance of our findings is reinforced by other recent *in vitro* and animal studies suggesting that IL-17A has possible roles in the initiation, progression and metastasis of lung cancer (15, 16). Furthermore, further studies have linked elevated

serum concentrations of IL-17 with a poor prognosis in patients with various types of cancer, including lung cancer in humans (23, 24), whereas inhibition of the IL-17 axis has been shown in animal models to inhibit tumour invasion and propagation (25). Most of these studies have focussed on IL-17A, whereas our present findings also implicate the functionally similar molecule IL-17F. Indeed, IL-17F polymorphisms have been associated with the risk of lung cancer in a Chinese population (26). We were unable to establish any correlation in the present study between expression of the IL-17 group cytokines and tumour progression in the clinic, but this is scarecly surprising because there were relatively few patients with advanced disease, reducing the power of the study to detect such changes.

While IL-17A and IL-17F have similar biological activities, IL-17E has unique functions and is best characterised for its promotion of Th2-type immunity. IL-17E is produced by activated Th2 cells and mast cells, and its effects mediated through its specific receptor IL-17RB (even though IL-17RA is functionally required for IL-17E activity). In the present study we observed reduced global expression of IL-17E immunoreactivity in the tissue sections from patients with NSCLC compared with the controls. In contrast, expression of IL-17RB immunoreactivity was low but unaltered in the tumour tissue. The hypothesis suggested by our data that IL-17E exerts anti-tumour activity is supported by *in vivo* data using human lung tumour xenograft and colon cancer models in mice (17). Our study does not permit definition of the mechanism of this reduced expression of IL-17E, but this will first involve precise definition of its cells of origin in this situation.

We have referred previously in this discussion to the possible functional relationships between tumour and infiltrating inflammatory cells in NSCLC, particularly the possible feedback loop between inflammation promoting tumorigenesis which in turn induces further inflammation. Our data are compatible with the hypothesis that NSCLC contributes to IL-17 production *in vivo*, thus propagating the immune response and the drive for tumorigenesis. Macrophages are an important component of the tumour inflammatory microenvironment and appear to play a key role in the progression of lung cancer (27). It has been reported that lung cancer cells might recruit and polarise alveolar macrophages resulting in differential effects on tumour progression (28, 29). Future studies should address the subtypes of macrophages present in the microenvironment of lung tumours and their capacity to produce IL-17 group cytokines.

Neutrophils, another key component of inflammatory cellular infiltration have also recently received increased attention as a new type of tumour-infiltrating immune cell that may influence tumour growth and metastasis (30, 31). It has been reported that both IL-17A and IL-17F have the ability to promote neutrophil recruitment, since IL-17RA signalling up-regulates production of chemokines promoting neutrophil immigration (32). In the present study we observed a greater degree of neutrophilic inflammation in tissue sections from patients with SCC compared with ADC, suggesting that the propensity of tumour cells to attract neutrophils may vary with their phenotype.

Finally, our data also suggest the possibility that IL-17A may interact with distinct receptors in lung cancer cells according to their phenotype. It is worth to note that real-time PCR just showed the trend increase in the relative expression of IL-17A in SCC compared with other two groups, which were not consistent with their protein expression. This suggests that certain protein expression can not only regulated at transcription level but also at translation level and turn over level, as well as maintainnece of the stability of protein through changing tumour microenvironment (33, 34).

Obviously our study has some limitations. Because of the relative paucity of patients with very advanced disease, it is difficult to extrapolate our data to patients with a wider range of disease severity. Our data remain largely observational and must be reinforced with further functional studies of the effects of IL-17 on tumour formation and metastasis and its interaction with the inflammatory microenvironment in lung cancer, so that cogent new therapeutic targets may be identified.

ACKNOWLEDGEMENTS

We acknowledge financial support from the Basic Clinical Program of Capital Medical University (15JL14). We thank Associate Professor Shan Cheng, Department of Biochemistry and Molecular Biology, School of Basic Medical Sciences, Capital Medical University, for technical support.

REFERENCES

1. Chen W, Zheng R, Baade PD, et al. Cancer statistics in China, 2015. CA Cancer J Clin 2016; 66:115-32.
2. Siegel RL, Miller KD, Jemal A. Cancer Statistics, 2017. CA Cancer J Clin 2017; 67:7-30.
3. Moore MM, Chua W, Charles KA, Clarke SJ. Inflammation and cancer: causes and consequences. Clin Pharmacol Ther 2010; 87:504-8.
4. Conway EM, Pikor LA, Kung SH, Hamilton MJ, Lam S, Lam WL, Bennewith KL. Macrophages, inflammation, and lung cancer. Am J Respir Crit Care Med 2016; 193:116-30.
5. Nakamura K, Smyth MJ. Targeting cancer-related inflammation in the era of immunotherapy. Immunol Cell Biol 2017; 95:325-32.
6. Gu C, Wu L, Li X. IL-17 family: cytokines, receptors and signaling. Cytokine 2013; 64:477-85.
7. Iwakura Y, Ishigame H, Saijo S, Nakae S. Functional specialization of interleukin-17 family members. Immunity 2011; 34:149-62.
8. Eyerich K, Dimartino V, Cavani A. IL-17 and IL-22 in immunity: driving protection and pathology. Eur J Immunol 2017; 47:607-14.
9. Kuwabara T, Ishikawa F, Kondo M, Kakiuchi T. The Role of IL-17 and related cytokines in inflammatory autoimmune diseases. Mediators Inflamm 2017; 2017:3908061.
10. Xu S, Cao X. Interleukin-17 and its expanding biological functions. Cell Mol Immunol 2010; 7:164-74.
11. Moseley TA, Haudenschild DR, Rose L, Reddi AH. Interleukin-17 family and IL-17 receptors. Cytokine Growth Factor Rev 2003; 14:55-74.
12. Kolls JK, Linden A. Interleukin-17 family members and inflammation. Immunity 2004; 21:467-76.
13. Barlow JL, Mckenzie AN. IL-25: a key requirement for the regulation of type-2 immunity. Biofactors 2009; 35:178-82.
14. Corrigan CJ, Wang W, Meng Q, et al. Allergen-induced expression of IL-25 and IL-25 receptor in atopic asthmatic airways and late-phase cutaneous responses. J Allergy Clin Immunol 2011; 128:116-24.
15. Numasaki M, Watanabe M, Suzuki T, et al. IL-17 enhances the net angiogenic activity and in vivo growth of human non-small cell lung cancer in SCID mice through promoting CXCR-2-dependent angiogenesis. J Immunol 2005; 175:6177-89.
16. Li Q, Han Y, Fei G, Guo Z, Ren T, Liu Z. IL-17 promoted metastasis of non-small-cell lung cancer cells. Immunol Lett 2012; 148:144-50.
17. Benatar T, Cao MY, Lee Y, et al. IL-17E, a proinflammatory cytokine, has antitumor efficacy against several tumor types *in vivo*. Cancer Immunol Immunother 2010; 59:805-17.
18. Molina JR, Yang P, Cassivi SD, Schild SE, Adjei AA. Non-small cell lung cancer: epidemiology, risk factors, treatment, and survivorship. Mayo Clin Proc 2008; 83:584-94.
19. Corrigan CJ, Wang W, Meng Q, et al. T-helper cell type 2 (Th2) memory T cell-potentiating cytokine IL-25 has the potential to promote angiogenesis in asthma. Proc Natl Acad Sci U S A 2011; 108:1579-84.
20. Yao XJ, Huang KW, Li Y, et al. Direct comparison of the dynamics of IL-25- and 'allergen'-induced airways inflammation, remodelling and hypersensitivity in a murine asthma model. Clin Exp Allergy 2014; 44:765-77.
21. Fabre J, Giustiniani J, Garbar C, et al. Targeting the tumor microenvironment: the protumor effects of IL-17 related to cancer type. Int J Mol Sci 2016; 17:1433.
22. Verstockt B, Van Assche G, Vermeire S, Ferrante M. Biological therapy targeting the IL-23/IL-17 axis in inflammatory bowel disease. Expert Opin Biol Ther 2017; 17:31-47.
23. Punt S, Langenhoff JM, Putter H, Fleuren GJ, Gorter A, Jordanova ES. The correlations between IL-17 vs. Th17 cells and cancer patient survival: a systematic review. Oncoimmunology 2015; 4:e984547.
24. Pan B, Che D, Cao J, et al. Interleukin-17 levels

correlate with poor prognosis and vascular endothelial growth factor concentration in the serum of patients with non-small cell lung cancer. Biomarkers 2015; 20:232-39.
25. Zhang Q, Liu S, Ge D, et al. Targeting Th17-IL-17 Pathway in prevention of micro-invasive prostate cancer in a mouse model. Prostate 2017; 77:888-99.
26. He Y, Du Y, Wei S, et al. IL-17A and IL-17F single nucleotide polymorphisms associated with lung cancer in Chinese population. Clin Respir J 2017; 11:230-42.
27. Mei J, Xiao Z, Guo C, et al. Prognostic impact of tumor-associated macrophage infiltration in non-small cell lung cancer: A systemic review and meta-analysis. Oncotarget 2016; 7:34217-28.
28. Wu P, Wu D, Zhao L, et al. Inverse role of distinct subsets and distribution of macrophage in lung cancer prognosis: a meta-analysis. Oncotarget 2016; 7:40451-60.
29. Dehne N, Mora J, Namgaladze D, Weigert A, Brune B. Cancer cell and macrophage cross-talk in the tumor microenvironment. Curr Opin Pharmacol 2017; 35:12-19.
30. Moroy G, Alix AJ, Sapi J, Hornebeck W, Bourguet E. Neutrophil elastase as a target in lung cancer. Anticancer Agents Med Chem 2012; 12:565-79.
31. Bar-Ad V, Palmer J, Li L, et al. Neutrophil to lymphocyte ratio associated with prognosis of lung cancer. Clin Transl Oncol 2017; 19:711-17.
32. Pappu R, Ramirez-Carrozzi V, Ota N, Ouyang W, Hu Y. The IL-17 family cytokines in immunity and disease. J Clin Immunol 2010; 30:185-95.
33. Schwanhausser B, Busse D, Li N, et al. Global quantification of mammalian gene expression control. Nature 2011; 473:337-42.
34. Liu Y, Beyer A, Aebersold R. On the Dependency of Cellular Protein Levels on mRNA Abundance. Cell 2016; 165:535-50.

CROSS-TALK BETWEEN APELIN AND VASOPRESSIN IN RESPONSE TO DIFFERENT OSMOTIC STIMULI IN TYPE 2 DIABETIC RATS

A.F. DAWOOD[1,2*], M.M. SABRY[1*], S.A. ESTAPHAN[1], E.A. MOHAMED[3], S.F. YOUNES[2,4], L.A. RASHED[5] and A.W. ELZAINY[3]

[1]Physiology Department, Faculty of Medicine, Cairo University, Egypt; [2]Department of Basic Medical Sciences, College of Medicine, Princess Nourah Bint Abdulrahman University, Kingdom of Saudi Arabia; [3]Anatomy Department, Faculty of Medicine, Cairo University, Egypt; [4]Department of Pathology, Faculty of Medicine, Menoufia University, Egypt; [5]Biochemistry department, Faculty of Medicine, Cairo University, Egypt

Received May 28, 2018 – Accepted August 3, 2018

[*]These Authors contributed equally to this manuscript

Apelin, a peptide hormone that has been linked to insulin resistance, obesity and glucose metabolism, coexists with arginine vasopressin (AVP) in hypothalamic magnocellular neurons that control body fluid homeostasis. The significant correlation between serum glucose and serum osmolarity in uncontrolled DM indicates the need for adequate compensation, but how apelin and AVP contribute to this is still unsettled. This study aims to investigate the interaction between apelin and AVP in osmotic regulation in type 2 diabetes mellitus (T2DM), and to explore the underlying mechanism. Forty-eight adult male albino rats were divided into six groups: control (isotonic, ip 0.9% NaCl; hypotonic, ip distilled water; hypertonic, ip 2% NaCl) groups and T2DM (isotonic, hypotonic, hypertonic) groups. Serum levels of AVP, apelin, Na, glucose, serum and urine osmolarity were measured; kidney samples were taken for Aquaporin 2 channels (AQP2) and epithelial sodium channel gamma subunit (ENaCγ) gene expression. Hypothalamic tissue sections were used for immunohistochemical staining of apelin and AVP. Both in control and diabetic groups serum apelin, showed a significant negative correlation with serum AVP (r=-0.533, p≤ 0.001). Serum apelin and AVP were inversely proportional to their hypothalamic protein expression. Serum apelin and AVP were significantly higher in diabetic rats (P= 0.001) yet their percentage change in response to hypo and hyper-osmotic stimuli (1.5±0.7, -0.34±0.15 and -0.38±0.13, 1.95±0.36, respectively) was less pronounced when compared to control rats (3.28±0.52, -0.59±0.12 and -0.45±0.13, 2.58±0.93, respectively). Na and ENaCγ levels significantly increased in hypertonic rats, while AQP2 gene expression significantly increased in hypotonic rats. Both apelin and AVP reacted to osmotic stimuli in T2DM but with less sensitivity than in control rats. In spite of its abnormal increased levels in diabetic rats, apelin maintained its role through counteracting AVP action.

Diabetic patients frequently face acute osmotic challenges that are life-threatening such as diabetic ketoacidosis (1-5% mortality rate) (1) and non-ketotic diabetic coma (5-20% mortality rate) (2). This makes the study of physiological mechanisms to counteract acute osmotic stress in diabetes mellitus

Key words: apelin, vasopressin, aquaporin, epithelial sodium channel, diabetes mellitus

Mailing address:
Dr Suzanne Estaphan,
Kasr Al Ainy St.,
Post Code: 11562,
Cairo, Egypt
Tel.: +201223980336
e-mail: sestaphan@kasralainy.edu.eg

0393-974X (2018)

(DM) of great importance.

DM is linked to both hypo- and hyper-natremia reflecting the coexistence of hyperglycemia-related osmotic effects. Fasting blood glucose is known to be statistically correlated with the serum sodium concentration as well as serum osmolality (3).

Arginine vasopressin (AVP), is known to be released from the neurosecretory magnocellular neurons into the fenestrated capillaries of the posterior pituitary in response to variations in serum osmolality and plasma volume or under action of different neurohormones including angiotensin (Ang) II or III and natriuretic peptides (4).

An endogenous peptide, apelin, initially isolated from extracts of bovine stomach, was also identified in rat hypothalamic extracts. It is believed that apelin plays a role in neuroendocrine control of processes such as regulation of blood pressure, drinking, and food intake (5). Double immunofluorescence staining showed the colocalization of apelin with AVP in magnocellular supraoptic (SON) and the paraventricular (PVN) hypothalamic neurons, which raises the possibility that apelin and AVP are both involved in body fluid homeostasis in response to osmotic or volemic stimuli (6). In water homeostasis, it has been hypothesized that, in addition to the feedback control exerted by AVP on its own release, apelin may regulate AVP release (6). There is evidence that apelin acts to counteract AVP actions through regulation of AVP neuronal activity and AVP secretion (7, 8). Apelin has also been suggested to have an intrarenal effect being expressed in the rat and human kidney collecting ducts (9). Apelin receptor mRNA expression in the rat kidney has been detected along the vasa recta of the outer medulla (10).

Several pathologic disorders, including hyponatremia and polyuria-polydipsia syndrome, were found to significantly alter apelin and AVP secretion, probably in an effort of the apelin/AVP system to restore the water balance mediated by the two hormones (11). However, to our knowledge, the apelin/AVP interaction in cases of DM has not yet been explored, although it is an area of interest, being a chronic osmotic challenge altering both apelin and AVP secretion.

In addition to its role in urine concentration and body water homeostasis, AVP has also been suggested to play a part in glucose homeostasis (12). Apelin is also detected in adipose tissue, and is observed to have glucose-lowering effects both in fasting conditions and during glucose tolerance test (13). Although the role of apelin in glucose homeostasis was confirmed by the phenotype of apelin null (apelin$^{-/-}$) mice exhibiting hyperinsulinemia and insulin resistance (14), it is not understood whether it maintains its role in body fluid homeostasis together with AVP in such conditions or not.

The current study aims to investigate the interaction between apelin and AVP in response to acute osmotic stimuli in type 2 diabetic rats and to explore the underlying mechanisms.

MATERIALS AND METHODS

Experimental animals

A total of 48 adult male albino rats (150–200 g) were used in this study. The experimental protocol and procedures were approved by the Committee of the Ethics of Animal Experiments of the Faculty of Medicine, Cairo University. Rats were provided with veterinary care by the Laboratory Animal House Unit and were housed in wire mesh cages at a comfortable temperature of 23±1°C on an alternating 12:12 h light-dark cycle and had free access to rat chow and water. All animal procedures were performed in the Physiology and Biochemistry Departments, Faculty of Medicine, Cairo University, Egypt.

Experimental protocol

The rats were randomly divided into the following groups (n= 8 rats in each group). Group 1: control isotonic group, which received intraperitoneal (ip) isotonic 0.9% NaCl, 2ml/100g Body weight (BW). Group 2: control hypotonic group, which received ip distilled water, 2ml/100g BW. Group 3: control hypertonic group, which received ip 2% NaCl, 2ml/100g BW. Rats of the remaining groups received high fat diet (HFD) (20 kcal% protein, 20 kcal% carbohydrate, and 60 kcal% fat) for 14 days then were given a low dose streptozotocin (STZ) injection 30 mg/kg for induction of T2DM and were kept on HFD till day 20 (15). Group 4: type 2 diabetic isotonic group, rats received ip isotonic 0.9% NaCl, 2ml/100g BW. Group 5: type 2 diabetic hypotonic group, rats received ip

distilled water, 2ml/100g BW. Group 6: type 2 diabetic hypertonic group, rats received ip 2% NaCl, 2ml/100g BW. On day 20, when the experiment was carried out, in the HFD + STZ rats (group 4, 5 and 6), T2DM was confirmed by measuring fasting serum glucose, fasting insulin levels and homeostasis model assessment insulin resistance index (HOMA-IR) was calculated.

Thirty minutes after acute osmotic challenge, urine samples were collected separately for each rat, using special cages (16) for measurement of urine osmolarity. Rats were anaesthetized using intraperitoneal ketamine (90 mg/kg) and xylazine (15 mg/kg), blood samples were obtained by retro-orbital route, to measure serum levels of AVP, apelin, Na^+ and glucose.

The rats were then sacrificed by decapitation, the left kidneys were removed to measure aquaporin 2 (AQP2) channels and epithelial sodium channel gamma subunit (ENaCγ) gene expression.

Hypothalamic tissue sections were collected for immunohistochemical staining of apelin and AVP. The hypothalamic tissue was recognized by its anatomical relation to the pituitary gland and optic chiasma.

Detection of AQP2 and ENaCγ gene expression by real time PCR

Total RNA extraction

Total RNA was extracted from tissue homogenate using SV Total RNA Isolation System (Promega, Madison, WI, USA) according to manufacturer's instructions. The RNA concentrations and purity were measured with an ultraviolet spectrophotometer.

Complementary DNA (cDNA) synthesis

The cDNA was synthesized from 1 µg RNA using SuperScript III First-Strand Synthesis System as described in the manufacturer's protocol (#K1621, Fermentas, Waltham, MA, USA). In brief, 1 µg of total RNA was mixed with 50 µMoligo (dT) 20, 50 ng/µL random primers, and 10 mMdNTP mix in a total volume of 10 µL. The mixture was incubated at 56°C for 5 min, and then placed on ice for 3 min. The reverse transcriptase master mix containing 2 µL of 10× RT buffer, 4 µL of 25 mM MgCl2, 2 µL of 0.1 M DTT, and 1 µL of SuperScript® III RT (200 U/µL) was added to the mixture and was incubated at 25°C for 10 min followed by 50 min at 50°C.

Real-time quantitative PCR

Real-time PCR amplification and analysis were performed using an Applied Biosystem with software version 3.1 (StepOne™, USA). The reaction contained SYBR Green Master Mix (Applied Biosystems), gene-specific primer pairs (Table I) and were designed with Gene Runner Software (Hasting Software, Inc., Hasting, NY, USA) from RNA sequences from the gene bank. All primer sets had a calculated annealing temperature of 60°C. Quantitative RT-PCR was performed in a 25-µl reaction volume consisting of 2X SYBR Green PCR Master Mix (Applied Biosystems), 900 nM of each primer and 2 µl of cDNA. Amplification conditions were: 2 min at 50°C, 10 min at 95°C and 40 cycles of denaturation for 15 s and annealing/extension at 60°C for 10 min. Data from real-time assays were calculated using the v1·7 sequence detection software from PE Biosystems (Foster City, CA, USA). Relative expression of studied gene mRNA was calculated using the comparative Ct method. All values were normalized to beta actin which was used as the control housekeeping gene and reported as fold change over background levels detected in the diseased groups.

AVP and apelin were determined by enzyme linked immunosorbent assay kits, which were supplied by MyBiosource, USA according to the manufacturer's instructions (17).

Osmolarity of urine samples was determined on a cryoscopicosmometer (Fisk, Mark3 Osmometer, and Norwood, MA, USA) by freezing point depression.

Na^+ was measured by routine laboratory investigation (16).

Concise immunohistopathological staining of AVP and apelin in hypothalamic tissue

Representative sections of hypothalamus from each rat were obtained and preserved in 10% neutral buffered formalin for histopathological evaluation. Tissues were embedded in paraffin blocks, and 3-4 µm-thick sections were sliced from the prepared paraffin block. One was stained with Hematoxylin & Eosin to detect scattered astrocytic nuclei in the neuropil background of hypothalamus. The other 2 sections were mounted on positive charged slides. The slides were manually stained immunohistochemically with antibodies to AVP and apelin. Staining was carried out according to the manufacturer's instructions for each marker. All primary

antibodies, clones, and dilutions are listed in Table II. Positive and negative controls were applied for each run of staining. AVP positive control is hypothalamic tissue where staining showed noticeable heterogeneity. Cerebellar tissue was used as positive control for apelin.

Immunohistochemical evaluation of the staining was done semiquantitatively using H-score which combines both intensity and percentage of positive cells in each section. The staining for both AVP and apelin was primarily localized in cell bodies and processes. The intensity of immunostaining was assessed as follows: 1 – mild, 2 – moderate, and 3 – strong. H-score was calculated according to the formula Σ [intensity of staining X percentage of stained area] (18). Scoring was independently carried out blinded to the treatment groups of animals. A consensus agreement was made for mismatched scores.

Statistical analysis

Data were collected, tabulated and statistically analyzed using SPSS software statistical computer package version (IBM SPSS Statistics for Windows, Version 22.0. IBM Corp., Armonk, NY, USA). Data were tested for normality of distribution, with calculation of the mean and standard deviation for all parameters. *t*-test was used to compare between different variables among diabetic and non-diabetic rats. The one-way ANOVA (Analysis of variance) test with Bonferroni's multiple comparison with selected pairs Post-Hoc test was used to compare different variables among different tonicity groups. Significance level was adopted at $P \leq 0.05$.

Pearson Correlation was conducted to study the relationship between apelin, vasopressin, AQP2 and ENaCγ among the studied groups, scores $P \leq 0.05$ were considered statistically significant.

RESULTS

Insulin resistance and T2DM were confirmed in

Table I. *Primer sequence of the studied gene.*

	Primer sequence
ENaCγ	Forward primer :5'- GGAGCGTCTCCAGACTGTAC -3 Reverse primer 5′- ACGCACCACGCCCTGTGGCT - -3'
AQP2	Forward primer :5'- CACTTAGAGGCGGTGGGGTAAG -3 Reverse primer 5′-TTGAGTCCAGACGCCTTTGA -3
Beta actin	Forward primer :5'-GGTCGGTGTGAACGGATTTGG -3 Reverse primer:5′- ATGTAGGCCATGAGGTCCACC-3

Specific primer sequence of ENaCγ (epithelial sodium channel gamma subunit), AQP2: aquaporin 2 channels and b-actin (used as housekeeping gene)

Table II. *Reagent and conditions used for immunhistologic studies.*

Antibody	**Clone**	**Dilution**	**Cellular location**	**Manufacturer**
Vasopressin	Ab 68669	1/100	secreted	Abcam
Apelin	Ab 59469	1/500	secreted	Abcam

Primary antibodies, clones, and dilutions for immunostaining

HFD + STZ rats through the results of body weight (gm), fasting serum glucose(mmol/L), fasting insulin (uIU/ml) and (HOMA-IR) calculation at day 20 of the experiment (301.87±16.24, 12.14±1.4, 17.56±2.4, 9.5±2.03, respectively) compared to day 1 of the experiment (170.62±16.78, 4.65±0.5, 10.55±0.48, 2.14±0.22 respectively) ($P < 0.0001$).

Comparative study between the effects of change in osmolarity of body fluid in the control non-diabetic rats revealed a significant increase in the mean values of serum level of AVP (pg/ml), Na (meq/l), gene expression of ENaCγ, serum tonicity (mosm/kg), urine tonicity (mosm/kg) and H-score of apelin in the control hypertonic group as compared to corresponding values in control isotonic group (Table III and Fig. 1). However, there was a significant decrease in the mean value of serum level of apelin (ng/ml) and H-score of AVP in the control hypertonic group as compared to the control isotonic group. While the mean value AQP2 gene expression showed no significant difference between the control hypertonic group and control isotonic group.

On the other hand, there was a significant decrease in the mean values of serum level of AVP (pg/ml), Na (meq/l), serum tonicity (mosm/kg), urine tonicity (mosm/kg) and apelin H-score in the control hypotonic group as compared to corresponding values in control isotonic group. Moreover, there was a significant increase in the mean values of serum level of apelin (ng/ml), AQP2 gene expression and AVP H-score in the control hypotonic group as compared to control isotonic group. While the mean value ENaCγ gene expression showed no significant difference between the control hypotonic group and control isotonic group

Induction of DM by combining HFD and low-dose STZ resulted in a significant increase (p-value <0.05) in the mean values of serum level of AVP (pg/ml), Apelin (ng/ml), Na (meq/l) and serum tonicity (mosm/kg) in diabetic isotonic group compared to their corresponding values in the control isotonic group. However, there was no significant difference between the mean values of AQP2, ENaCγ gene expression and urine tonicity (mosm/kg) between the two studied groups. Immunohistochemical expression of apelin and AVP in hypothalamic tissue showed that H-score of apelin was significantly increased in diabetic rats as compared to control rats in the state of isotonicity, while AVP expression showed no statistically significant difference among both groups (Table III and Fig. 1).

Comparative study between the effects of change in osmolarity of body fluid on different studied parameters in the diabetic rats revealed a significant increase in the mean values of serum level of AVP (pg/ml), Na (meq/l), ENaCγ gene expression and serum tonicity (mosm/kg) and apelin H-score in the diabetic hypertonic group as compared to corresponding values in the diabetic isotonic group (Table III and Fig. 1). However, there was a significant decrease in the mean values of serum level of apelin (ng/ml) while the mean values of AQP2 gene expression and urine tonicity (mosm/kg) and AVP H-score in diabetic hypertonic group showed no statistical significance as compared to diabetic isotonic group (Fig. 2).

On the other hand, there was a significant decrease in the mean values of serum level of AVP (pg/ml), Na (meq/l), serum tonicity (mosm/kg) and urine tonicity (mosm/kg) and apelin H-score in the diabetic hypotonic group as compared to corresponding values in the diabetic isotonic group while the mean value of ENaCγ gene expression in the diabetic hypotonic group showed no statistical significance as compared to the diabetic isotonic group. Moreover, there was a significant increase in the mean values of serum level of apelin (ng/ml) and gene expression of AQP2 and AVP H-score in the control hypotonic group as compared to the control isotonic group (Fig. 2).

Percentage increase of serum levels of apelin (1.5±0.7) and percentage decrease of serum levels of AVP (- 0.38±0.13) in response to hypotonicity in the diabetic groups were less pronounced than their percentage change in the corresponding control groups (3.28±0.52; -0.45±0.13, respectively).

In addition, percentage decreases of serum levels of apelin (- 0.34±0.15) and percentage increase of serum levels of AVP (1.95±036) in response to hypertonicity in diabetic groups were less pronounced than their percentage change in the corresponding control groups (- 0.59±0.12; 2.58±0.93, respectively).

The correlations between apelin, vasopressin, AQP2 and ENaCγ among the studied groups

Among all the studied groups, there was a significant negative correlation between serum apelin and vasopressin levels. Moreover, AQP expression significantly negatively correlated with plasma AVP levels while significantly positively correlated with plasma apelin levels, and ENaC expression significantly positively correlated with plasma AVP levels while significantly negatively correlated with plasma apelin levels (Fig. 3).

DISCUSSION

The coexistance of apelin and AVP in magnocellular neurons, tied with the fact that they have contradictory biological effects and regulation mechanisms, confirm their interrelated roles maintaining body fluid homeostasis. There is no evidence yet whether this role is maintained in diabetic patients highly exposed to a number of osmotic crises such as diabetic ketoacidosis and hyperosmolar hyperglycemic state.

The present study attempted to compare the response of these two peptides to acute osmotic stimuli both in control and diabetic rats. We chose to collect our samples 30 minutes after the osmotic stimuli as previous studies showed that AVP secretion reaches a peak at this timing (8).

In our control rats, a significant negative

Table III. *Serum tonicity, Na, AVP, apelin , urine tonicity and hypothalamic AVP and apelin immunoreactivity among the studied groups.*

	Control isotonic	Control hypotonic	Control hypertonic	Diabetic isotonic	Diabetic hypotonic	Diabetic hypertonic
AVP (pg/ml)	4.1± 0.9	2.14± 0.14*	14.02± 1.18*	6.26± 0.64 *	3.84± 0.83@	18.35± 1.44@
Apelin (ng/ml)	14.35± 1.69	61.04± 6.62*	5.8± 1.82*	41.8± 9.21 *	99.89± 11.85@	26.54± 3.59 @
Na (meq/l)	130.79 ± 4.66	105.76± 2.77*	190.62± 2.58*	164.26± 7.46*	127.89± 4.13@	217.25± 30.26@
Serum tonicity (mosm/kg)	289.47 ± 4.54	274.25± 2.55*	321.55± 4.08*	306.44± 1.82 *	295.61± 4.5@	333.84± 5.92@
Urine tonicity (mosm/kg)	1402.5 ±178.5	1075± 51.69 *	1417.5± 23.75	1374.37 ± 175.8	950± 56.3 @	1463.7±2 04.23
AVP immunostain ing H score	140 ±52.6	197.5± 66.06*	81.25± 20.3*	152.5± 26	223.75± 51.25@	98.7± 26.95 @
Apelin immunostain ing H score	83.75± 16.8	52.5± 15.8*	142.5± 72.06 *	148.75± 23.56*	68.75± 28.4@	186.25± 56.25@

*Values are represented as mean± SD; *: Statistically significant compared to corresponding value in control isotonic group (P<0.05), @: Statistically significant compared to corresponding value in diabetic isotonic group (P<0.05). Isotonic groups received (ip) isotonic 0.9% NaCl, 2ml/100g BW, hypotonic groups received ip distilled water, 2ml/100g BW , hypertonic groups received ip 2% NaCl, 2ml/100g BW 30 minutes before samples collection. (AVP, arginine vasopressin; Na, serum sodium)*

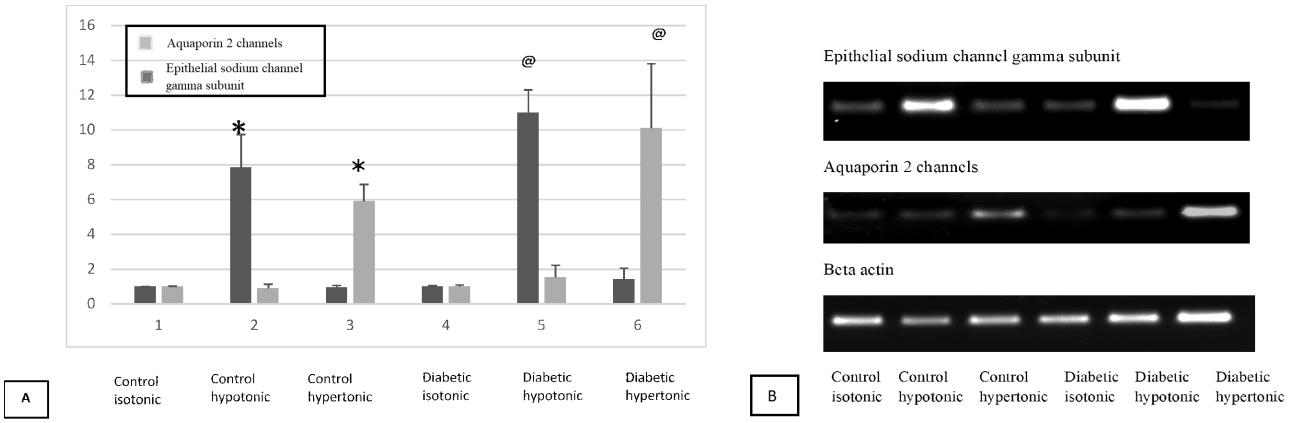

Fig. 1. *AQP2 and ENaCγ whole kidney gene expression chart (**A**) where values are represented as mean± SD; *: Statistically significant compared to corresponding value in control isotonic group (P<0.05), @: Statistically significant compared to corresponding value in diabetic isotonic group (P<0.05) and RT-qPCR relative blot (**B**).*

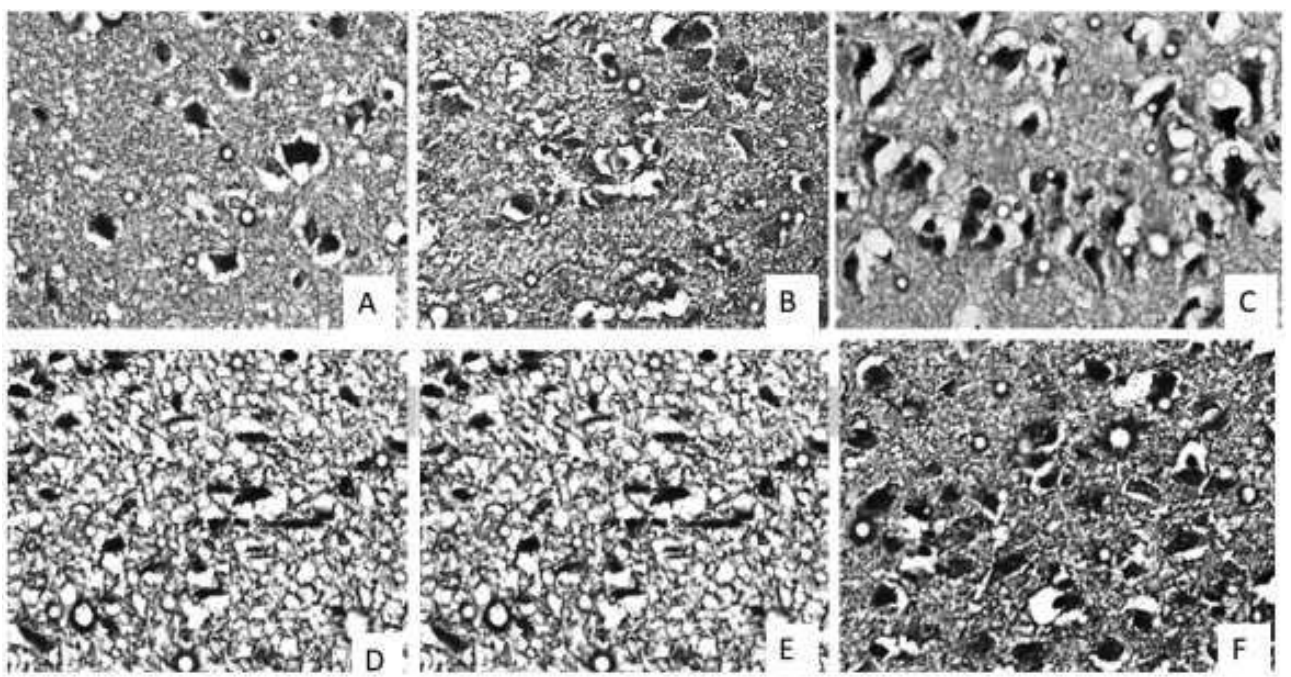

Fig. 2. *Sections from hypothalamic tissue stained with AVP immunohistochemistry showed moderate staining in diabetic isotonic rats (**A**), strong staining in diabetic hypotonic rats (**B**) and mild cytoplasmic staining of AVP in diabetic hypertonic rats (**C**). Sections stained with apelin show moderate staining in diabetic isotonic rats (**D**), mild cytoplasmic staining of apelin in diabetic hypotonic rats (**E**), and strong staining in diabetic hypertonic rats (**F**). Original magnification is X100. Immunohistochemical evaluation of the staining was done semiquantitatively using H-score which combines both intensity and percentage of positive cells in each section.*

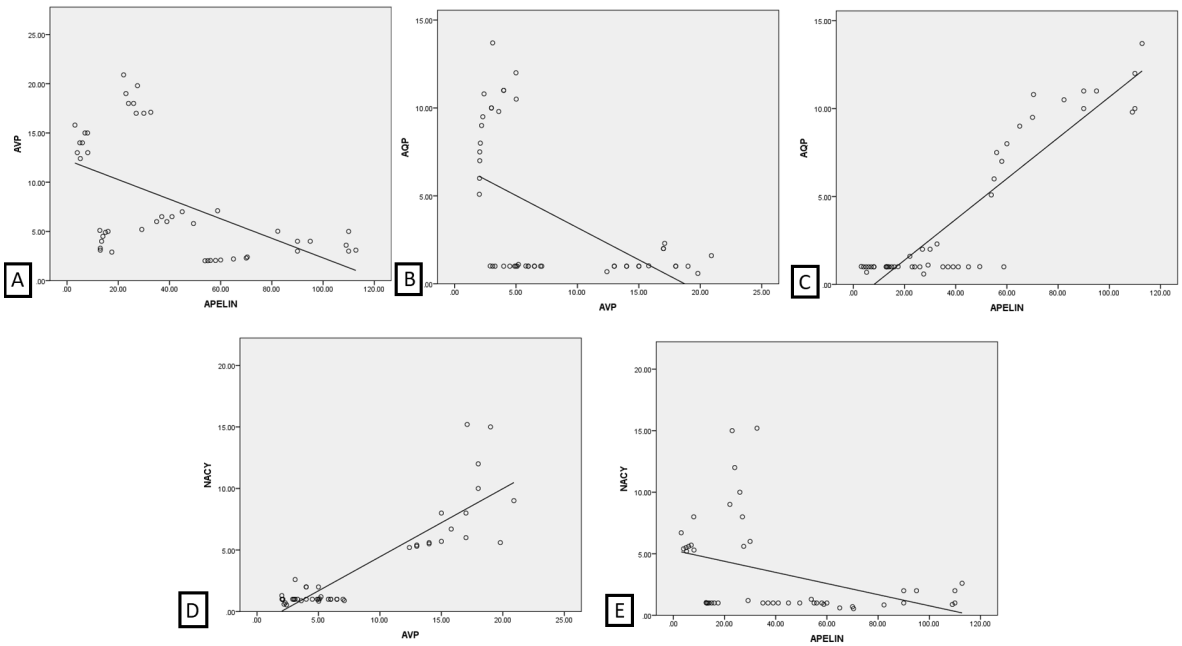

Fig. 3. *The correlations between serum level of apelin, vasopressin and whole kidney gene expression of AQP2 and ENaCγ among the studied groups. Among all the studied groups, there was a significant negative correlation between serum apelin and AVP levels (r=-0.533, p≤0.001) (**A**), AQP expression showed significant negative correlation with serum AVP level (r=-0.533, p≤0.001) (**B**), and showed significant positive correlation with serum apelin level (r=0.908, p≤0.001) (**C**), ENaCγ gene expression was significantly positively correlated with serum AVP level (r=0.882, p≤0.001) (**D**) while significantly negatively correlated with serum apelin level (r=-0.387, p=0.007) (**E**).*

correlation between serum apelin concentration and serum AVP concentration was observed 30 minutes after the acute osmotic challenge. Immunostaining of hypothalamic tissue for both apelin and AVP showed an inverse relation between their hypothalamic IR in comparison to their serum concentration.

Taken together, our data support previous studies indicating that AVP and apelin are regulated in opposition to maintain osmotic homeostasis (7). Dehydration stimulates the release of AVP from the magnocellular neurons into the bloodstream, and promotes apelin accumulation in these neurons rather than being released into the blood stream (19). In the current study, induction of T2DM and the resulting hypertonicity were accompanied by a parallel significantly higher serum level of AVP and apelin in diabetic groups as compared to their corresponding values in the control groups. Intriguingly, hypothalamic apelin and AVP IR in diabetic rats were also significantly higher as compared to control rats in the state of isotonicity.

Accumulating experimental and clinical evidence has shown that both plasma apelin (20, 21) and AVP (22) concentration are upregulated in T1DM and T2DM. It is also noteworthy that the SON and PVN nuclei were found to be hypertrophied in diabetic rats (23).

The increase in serum levels of AVP in diabetic rats is explained as an effort to conserve water in the face of an overwhelming solute diuresis resulting from glycosuria, which may lead to diabetes-associated hypovolemia (22). Also, there is resetting of the osmoreceptor for AVP secretion in such a way that higher plasma AVP levels are observed at comparable levels of plasma Na^+ (24).

The increased level of serum apelin detected in diabetic rats in the current study goes along with previously published clinical and experimental studies (21, 25).

Earlier studies demonstrated that although basal plasma AVP values were significantly higher in hyperglycemic patients compared to controls, the sensitivity of the AVP response to osmotic stimuli was significantly decreased. This decreased

sensitivity is likely attributable to several factors such as diabetic-induced hyperosmolarity and / or hypovolemia, exhaustion of AVP pool and resetting of osmotic threshold for AVP release from magnocellular neurons (26).

However, to our knowledge, no such study was conducted to investigate the response of apelin to osmotic stimuli and its relation to AVP in such conditions. Thus, one of the important aims of the current study was to highlight the impact of T2DM, as a chronic osmotic challenge, on apelin/AVP interaction in response to different acute osmotic stimuli, despite their altered levels in this diabetic milieu.

Our study shows that the reciprocal relationship between serum AVP and serum apelin in response to acute osmotic stimuli in diabetic groups was maintained, despite their significantly higher levels, compared to their corresponding values in the control groups. More importantly, the percentage change of both peptides in response to osmotic stimuli was less pronounced. The inverse relationship between the above-mentioned serum levels of both apelin and AVP and their hypothalamic protein expression was also maintained.

These results provide evidence that both apelin and AVP probably maintain their role in osmoregulation in T2DM but with elevated threshold.

For an organism to maintain its water balance, the kidneys should prevent additional water loss through the antagonistic regulation of apelin and AVP (6). Collecting ducts (CD) are considered responsible for the fine tuning of salt and water excretion, relying on ENaCy and AQP2 expressed at the apical surface of principal cells (27).

In our control rats, after 30 minutes, acute hypertonic stimulus caused a significant increase in mean values of ENaCγ but without changing the mean values of AQP2 expression. On the other hand, acute hypotonic stimulus caused a significant increase in the mean values of AQP2 expression but without changing the mean values of the ENaCγ.

Although our findings are unexpected in view of the current knowledge on effects of plasma osmolarity on AQP2 expression, the increased gene expression of AQP2 in hypotonic rats in this study could possibly be considered as an initial protective behavior by the cells in response to hypotonic stimulus that would most probably be reversed by time. In our data, despite increase in the mean value of gene expression of AQP2 in hypotonic control group, the mean values of urine tonicity decreased. These results suggest that this early increase in gene expression may not be associated with an overall net increase in AQP2 translocation to the apical membrane. This hypothesis and the underlying mechanism should be investigated at the cellular level.

This suggested dual effect of osmotic stimuli on AQP2 gene expression was also addressed by Hasler et al., who observed that NaCL-induced increase in osmolarity caused an initial downregulation of AQP2 gene expression which was followed 24 hours later by its upregulation. It has been shown that this transient AQP2 downregulation may be attributed to cellular water depletion, demanding osmolyte intracellular accumulation, an adaptive process required for renal epithelial cell survival. (28). Upon completion of osmolyte accumulation, this inhibitory effect is released with subsequent increase in the AQP2 expression and regaining transcellular water flux (29). In the long-term, AVP and hypertonicity increased AQP2 expression in a synergistic way (28).

Additionally, in our results, there was positive correlation between AVP level and ENaCγ expression in the hypertonic group. AVP improves urine concentration through stimulating sodium reabsorption that occurs at the level of the collecting ducts, and promotes additional iso-osmotic water reabsorption. This effect is thought to involve the activation of the ENaC (30). Besides the acute impact of AVP on ENaC-dependent sodium transport (31), it has some influence on the expression of ENaC subunits by activating the vasopressin type 2 receptor (32).

Also, regarding apelin, together with its central effect of apelin on AVP neurons, several studies suggest that the aquaretic outcome of apelin involves also a direct renal effect. In a subpopulation of cortical glomerular cells, apelin receptor mRNA has been detected along the vasa recta of the outer medulla, a region of the kidney believed to be critical

in controlling water and sodium balance (10).

It was demonstrated that apelin counteracted the AVP-induced cAMP production and [Ca^{+2}] immobilization via vasopressin receptor 2 (V2R), an effect that was studied on microdissected CD and thought to be responsible for AQP2 trafficking to the apical membrane and enhancing the physiological antagonist effect of vasopressin receptor 1a (V1a-R) on V2R (9).

To our knowledge, our study could be the first evidence demonstrating a significant correlation between the level of apelin and ENaCγ expression after 30 minutes of hypertonic osmotic challenge. The effect of the osmotic challenge on AQP2 and ENaCγ channel expression in our diabetic rats was similar to its effect in our control rats.

In conclusion, both apelin and AVP reacted to osmotic stimuli in T2DM but with less sensitivity than in normal control rats. In spite of its increased levels in diabetic rats, apelin maintained its role in osmoregulation through counteracting AVP actions on ENaCγ and AQP2 channels.

It would be of interest to investigate serum apelin and AVP levels in parallel with AQPs and ENaCγ channels at different time intervals and in various other pathologic states of hypo or hyperosmolarity.

The probable unsafe exposure of diabetic patients to acute osmotic stimulus without medical intervention to study the innate Apelin/AVP interaction in DM, could be considered the limitation of our study that necessitated the use of experimental animals in which the response may be not identical to humans.

REFERENCES

1. Kitabchi AE, Umpierrez GE, Miles JM, Fisher JN. Hyperglycemic crises in adult patients with diabetes. Diabetes Care 2009; 32(7):1335-43.
2. Das L, Pal R, Dutta P, Bhansali A. Diabetic striatopathy and ketoacidosis: Report of two cases and review of literature. Diabetes Res Clin Pract 2017; 128:1-5.
3. Rao G. Serum electrolytes and osmolality in diabetes mellitus. Indian J Med Sci 1992; 46(10):301-3.
4. Ludwig M. Dendritic release of vasopressin and oxytocin. J Neuroendocrinol 1998; 10(12):881-96.
5. Reaux A, Gallatz K, Palkovits M, Llorens-Cortes C. Distribution of apelin-synthesizing neurons in the adult rat brain. Neuroscience 2002; 113(3):653-62.
6. Galanth C, Hus-Citharel A, Li B, Llorens-Cortes C. Apelin in the control of body fluid homeostasis and cardiovascular functions. Curr Pharm Des 2012; 18(6):789-98.
7. De Mota N, Reaux-Le Goazigo A, El Messari S, et al. Apelin, a potent diuretic neuropeptide counteracting vasopressin actions through inhibition of vasopressin neuron activity and vasopressin release. Proc Natl Acad Sci USA 2004; 101(28):10464-69.
8. Azizi M, Iturrioz X, Blanchard A, et al. Reciprocal regulation of plasma apelin and vasopressin by osmotic stimuli. J Am Soc Nephrol 2008; 19(5):1015-24.
9. Hus-Citharel A, Bodineau L, Frugière A, Joubert F, Bouby N, Llorens-Cortes C. Apelin counteracts vasopressin-induced water reabsorption via cross talk between apelin and vasopressin receptor signaling pathways in the rat collecting duct. Endocrinology 2014; 155(11):4483-93.
10. O'Carroll A-M, Selby TL, Palkovits M, Lolait SJ. Distribution of mRNA encoding B78/apj, the rat homologue of the human APJ receptor, and its endogenous ligand apelin in brain and peripheral tissues. Biochim Biophys Acta 2000; 1492(1):72-80.
11. Flahault A, Couvineau P, Alvear-Perez R, Iturrioz X, Llorens-Cortes C. Role of the vasopressin/apelin balance and potential use of metabolically stable apelin analogs in water metabolism disorders. Front Endocrinol (Lausanne) 2017; 8:120.
12. Roussel R, El Boustany R, Bouby N, et al. Plasma copeptin, AVP gene variants, and incidence of type 2 diabetes in a cohort from the community. J Clin Endocrinol Metab 2016; 101(6):2432-39.
13. Dray C, Knauf C, Daviaud D, et al. Apelin stimulates glucose utilization in normal and obese insulin-resistant mice. Cell Metab 2008; 8(5):437-45.
14. Yue P, Jin H, Xu S, et al. Apelin decreases lipolysis via Gq, Gi, and AMPK-dependent mechanisms. Endocrinology 2011; 152(1):59-68.
15. Zhang F, Ye C, Li G, et al. The rat model of type 2 diabetic mellitus and its glycometabolism characters. Exp Anim 2003, 52(5):401-7.
16. Estaphan S, Eissa H, Elattar S, Rashed L, Farouk M.

A study on the effect of cimetidine and l-carnitine on myoglobinuric acute kidney injury in male rats. Injury 2015; 46(7):1223-30.
17. Miao X, Li Z, Hui Z, Liu F, Zhang X. Assessment of obestatin and arginine vasopressin (AVP) levels in acute renal failure and acute heart failure. Eur Rev Med Pharmacol Sci 2017; 21:3277-81.
18. John T, Liu G, Tsao M. Overview of molecular testing in non-small-cell lung cancer: mutational analysis, gene copy number, protein expression and other biomarkers of EGFR for the prediction of response to tyrosine kinase inhibitors. Oncogene 2009; 28(S1):S14.
19. Gouzènes L, Desarménien MG, Hussy N, Richard P, Moos FC. Vasopressin regularizes the phasic firing pattern of rat hypothalamic magnocellular vasopressin neurons. J Neurosci 1998; 18(5):1879-85.
20. Bertrand C, Valet P, Castan-Laurell I. Apelin and energy metabolism. Front Physiol 2015; 6(115).
21. Dray C, Debard C, Jager J, et al. Apelin and APJ regulation in adipose tissue and skeletal muscle of type 2 diabetic mice and humans. Am J Physiol Endocrinol Metab 2010; 298(6):E1161-69.
22. Zerbe RL, Vinicor F, Robertson GL. Plasma vasopressin in uncontrolled diabetes mellitus. Diabetes 1979; 28(5):503-8.
23. Dheen S, Tay S, Wong W. Arginine vasopressin- and oxytocin-like immunoreactive neurons in the hypothalamic paraventricular and supraoptic nuclei of streptozotocin-induced diabetic rats. Arch Histol Cytol 1994; 57(5):461-72.
24. Zerbe RL, Vinicor F, Robertson GL. Regulation of plasma vasopressin in insulin-dependent diabetes mellitus. Am J Physiol Endocrinol Metab 1985; 249(3):E317-25.
25. Boucher J, Masri B, Daviaud Dl, et al. Apelin, a newly identified adipokine up-regulated by insulin and obesity. Endocrinology 2005; 146(4):1764-71.
26. Iwasaki Y, Kondo K, Murase T, Hasegawa H, Oiso Y. Osmoregulation of plasma vasopressin in diabetes mellitus with sustained hyperglycemia. J Neuroendocrinol 1996; 8(10):755-60.
27. Nielsen S, DiGiovanni SR, Christensen EI, Knepper MA, Harris HW. Cellular and subcellular immunolocalization of vasopressin-regulated water channel in rat kidney. Proc Natl Acad Sci U S A 1993; 90(24):11663-67.
28. Hasler U, Vinciguerra M, Vandewalle A, Martin P-Y, Féraille E. Dual effects of hypertonicity on aquaporin-2 expression in cultured renal collecting duct principal cells. J Am Soc Nephrol 2005; 16(6):1571-82.
29. Miyakawa H, Woo SK, Dahl SC, Handler JS, Kwon HM. Tonicity-responsive enhancer binding protein, a rel-like protein that stimulates transcription in response to hypertonicity. Proc Natl Acad Sci U S A 1999; 96(5):2538-42.
30. Bouby N, Fernandes S. Mild dehydration, vasopressin and the kidney: animal and human studies. Eur J Clin Nutr 2003; 57(S2):S39.
31. Djelidi S, Fay M, Cluzeaud F, et al. Transcriptional regulation of sodium transport by vasopressin in renal cells. J Biol Chem 1997; 272(52):32919-24.
32. Nicco C, Wittner M, DiStefano A, Jounier S, Bankir L, Bouby N. Chronic exposure to vasopressin upregulates ENaC and sodium transport in the rat renal collecting duct and lung. Hypertension 2001; 38(5):1143-49.

GENES INVOLVED IN REGULATION OF CELLULAR METABOLIC PROCESSES, SIGNALING AND ADHESION ARE THE MARKERS OF PORCINE BUCCAL POUCH MUCOSAL CELLS LONG-TERM PRIMARY CULTURED *IN VITRO*

A. BRYJA[1], M. DYSZKIEWICZ-KONWIŃSKA[1,2], Y. HUANG[3,4], P. CELICHOWSKI[5], M.J. NAWROCKI[1], M. JANKOWSKI[1], K. BŁOCHOWIAK[6], K. MEHR[7], P. RAMLAU[8,9], A. NOWICKI[8], D. BUKOWSKA[10], P. ANTOSIK[10], K. OSMOLA[9], M. BRUSKA[1], M. ZABEL[11,12], M. NOWICKI[5] and B. KEMPISTY[1,5,13]

[1]Department of Anatomy, Poznan University of Medical Science, Poznań, Poland; [2]Department of Biomaterials and Experimental Dentistry, Poznan University of Medical Sciences, Poznań, Poland; [3]OMFS IMPATH Research Group, Department of Imaging and Pathology, Faculty of Medicine, University of Leuven and Oral and Maxillofacial Surgery, University Hospitals Leuven, Leuven, Belgium; [4]State Key Laboratory of Oral Diseases, West China College of Stomatology, Sichuan University, Chengdu, China; [5]Department of Histology and Embryology, Poznan University of Medical Science, Poznań, Poland; [6]Department of Oral Surgery, Poznan University of Medical Science, Poznań, Poland; [7]Department of Oral Rehabilitation, Poznań University of Medical Sciences, Poznań, Poland; [8]Department of Toxicology, Poznan University of Medical Sciences, Poznan, Poland; [9]Department of Maxillofacial Surgery, Poznan University of Medical Sciences, Poznan, Poland; [10]Veterinary Center, Nicolaus Copernicus University in Torun, Torun, Poland; [11]Division of Histology and Embryology, Department of Human Morphology and Embryology, Wroclaw Medical University, Wroclaw, Poland; [12]Division of Anatomy and Histology, University of Zielona Góra, Zielona Góra, Poland; [13]Department of Obstetrics and Gynecology, University Hospital and Masaryk University, Czech Republic

Received July 4, 2018 – Accepted August 29, 2018

Extraordinary abilities for continuous proliferation and differentiation, associated with constant renewal triggered by stimulation from the mastication process, together with the relative lack of aesthetic complications associated with post-surgery healing, have highlighted buccal pouch mucosa as a potential source of explants that could be used in transplantation and tissue engineering. Additionally, this tissue plays a major role in the oral drug delivery process, which brings special interest to its molecular properties in the context of new drug development. There is therefore a need to analyse the exact mechanisms of oral mucosa functioning, especially when it comes to the processes that are associated with the potential clinical applications. In this study we analysed a complete transcriptome of long-term *in vitro* cultures of porcine buccal pouch oral mucosa cells. Using a microarray approach, we focused on genes associated with cellular metabolic processes, signalling and adhesion, from 4 gene ontology groups: "Positive regulation of cellular component movement", "Positive regulation of cellular process", "Positive regulation of intracellular signal transduction" and "Single organism cell adhesion". Nineteen genes (CCL8, CXCL2, PLK2, DUSP5, PTGS2, LIF, CCL2, ATP1B1, REL, ITGB3, SCARB1,

Mailing address:
Bartosz Kempisty PhD,
Department of Histology and Embryology,
Department of Anatomy, Poznan University of Medical Sciences,
6 Święcickiego St., 60-781 Poznań, Poland
Tel./Fax: +48 61 8546418/+48 61 8546440,
e-mail: bkempisty@ump.edu.pl

0393-974X (2018)

UGCG, PDPN, LYN, ETS1, FCER1G, TGFB1, RFC4, LMO2) with fold changes higher than |2| and p value <0.05 were identified, described in context and analysed. While the study needs much further validation to become applicable in a clinical environment, it yields valuable information about the transcriptomic basis of oral mucosal cell functioning *in vitro*, that might serve as a reference for further research, aiming to apply this knowledge in clinical situations.

Key words: oral mucosa, microarrays, cell culture

The oral mucosal tissue is an extraordinary example of cellular balance, functioning to maintain integrity and content homeostasis. Consisting of large numbers of keratinocytes and fibroblasts, with their mutual proportion proprietary to its location and function, an enormous amount of regulation is required to maintain its structure (1). The tissue also exhibits significant regenerative potential, as forces of mastication cause continuous damage, that needs constant repair. It is therefore considered one of the top tissues that could be adopted for wide use in regenerative and reconstructive medicine (2). It is also the focus of scientists, as it exhibits one of the most prominent targets in drug delivery (3). However, while sampling of oral mucosa for autologous grafts presents better aesthetic outcomes than in other tissues, and with its epithelial origin and large plasticity facilitating transplant into many desired physiological regions, the amount of tissue that can be taken for these purposes is still limited. It is also the case when collecting samples for research purposes, as the material must be sources from deceased specimen or animal models for ethical reasons. All these limitations can be overcome with the use of bioengineered tissue, grown *in vitro* from small tissue explants. This approach would eliminate the need for large scale excisions being made to match the graft size, as well as allowing for a potentially unlimited source of research material (4). However, nowadays while the physiology and anatomy of most of the human tissues is relatively well known, the exact molecular mechanisms underlying their functioning are far from being discovered. Consequently, there is extensive basic research to be carried out to lay foundations for future *in vivo* and clinical studies that would allow for further advancements of many aspects of science and medicine associated with oral mucosa.

Hence, in this study we employ novel microarray technology to screen the transcriptome of primary oral mucosal cell culture and analyse the specific gene groups, associated with processes occurring while the cells are grown and maintained *in vitro*. Through that, we hope to gain insight into the impact that the *ex vivo* environment has on the oral mucosa, while identifying new markers of the processes occurring during the long-term culture. This should allow to create points of reference for future studies, aiming to apply the knowledge in various clinical situations.

MATERIALS AND METHODS

Animals

For this study, a total of 35 pubertal crossbred Polish Landrace gilts (young female pigs), bred on a commercial local farm were used. The animals had a mean age of 155 days (range 140–170 days) and the mean weight was 100 kg (95–120 kg). All of the animals were housed under identical conditions and fed the same forage (depending on age and reproductive status). All experiments were approved by Local Ethics Committee of the Poznan University of Life Sciences, Poland (permission no. 32/2012, 30.06.2012).

Cell isolation and culture

After slaughter, samples of buccal pouch mucosa were obtained within 40 min and transported to the laboratory. The excised tissue was washed twice in Dulbecco's phosphate buffered saline (D-PBS) (137 mM NaCl, 27 mM KCl, 10 mM Na_2HPO_4, 2 mM KH_2PO_4, pH 7.4). The surface of the buccal pouch was surgically removed using sterile surgical blades. The tissue fragments were incubated with 0.05% collagenase I (Sigma Aldrich,

Madison, WI, USA) for 2 hours at 37°C in a shaking water bath and then were treated witch 0.5% Trypsin/EDTA (Cascade Biologics, Portland, OR, USA) for 10 min. The cell suspension obtained from this digestion was filtered through mesh to remove non-dissociated tissue fragments. Isolated cells were washed three times by centrifugation (10 min at 200× g) with Dulbecco's modified Eagle's medium (DMEM; Sigma Aldrich, Madison, WI, USA) supplemented with gentamicin (20 µg/mL) and 0.1% BSA. The final cell pellet was resuspended in DMEM supplemented with 10% fetal calf serum (FCS; Sigma Aldrich, Madison, WI, USA) and 10 U/mL penicillin G, 10 mg/mL streptomycin, and 25 µg/mL amphotericin B. Cell viability was 90 to 95% as determined by trypan blue staining (Sigma Aldrich, Madison, WI, USA). The cells were cultured at 37°C in a humidified atmosphere of 5% CO_2. Once the oral mucosal cell cultures attained 70–80% confluency, they were passaged by washing with PBS, digested with 0.025% Trypsin/EDTA (Cascade Biologics, Portland, OR, USA), neutralized by a 0.0125% trypsin inhibitor (Cascade Biologics, Portland, OR, USA), centrifuged, and resuspended at a seeding density of 2 × 104 cells/cm^2. The culture medium was changed every three days. Before the collection of cells for the analysed samples, photos of the culture were taken to monitor the possible changes of morphology (Fig. 1). The reference sample photos (24 h) are not shown in the figure because of the difficulties in obtaining clear photograph of a primary culture in such early stages, due to visual contaminants proprietary to such culture.

Microarray expression analysis and statistics

Total RNA (100 ng) from each pooled sample [the isolation method has been previously described (5)] was subjected to two rounds of sense cDNA amplification (Ambion® WT Expression Kit). The obtained cDNA was used for biotin labeling and fragmentation by Affymetrix GeneChip® WT Terminal Labeling and Hybridization (Affymetrix). Biotin-labeled fragments of cDNA (5.5 µg) were hybridized to the Affymetrix® Porcine Gene 1.1 ST Array Strip (48°C/20 h). Microarrays were then washed and stained according to the technical protocol using the Affymetrix GeneAtlas Fluidics Station. The array strips were scanned employing Imaging Station of the GeneAtlas System. Preliminary analysis of the scanned chips was performed using Affymetrix GeneAtlasTM Operating Software. The quality of gene expression data was confirmed according to the quality control criteria provided by the software. The obtained CEL files were imported into downstream data analysis software, as previously described.

All the presented analyses and graphs were performed using Bioconductor and R programming languages. Each CEL file was merged with a description file. To correct background, normalize, and summarize results, we used the Robust Multiarray Averaging (RMA) algorithm. To determine the statistical significance of the analysed genes, moderated *t*-statistics from the empirical Bayes method were performed. The obtained p-value was corrected for multiple comparisons using Benjamini and Hochberg's false discovery rate. The selection of significantly altered genes was based on a p-value lower than 0.05 and expression higher than two-fold.

The differentially expressed gene list was uploaded to DAVID software (Database for Annotation, Visualization and Integrated Discovery) by bioconductor package "RDAVIDwebservice". From significantly enriched Gene Ontology terms extracted by DAVID software we selected those that contain more than 5 genes and Benjamini test p value lower than 0.05.

Subsequently, we analysed the relationship between the genes belonging to chosen GO terms with GOplot package. The GoPlot package had calculated the z-score: the number of up- regulated genes minus the number of down- regulated genes divided by the square root of the count. This information allowed to estimate the change course of each gene-ontology term.

Moreover, interactions between differentially expressed genes/proteins belonging to the chosen GO terms were investigated by STRING10 software (Search Tool for the Retrieval of Interacting Genes). The list of gene names was used as a query for an interaction prediction. The search criteria were based on co-occurrences of genes/proteins in scientific texts (text mining), co-expression, and experimentally observed interactions. The results of such analyses generated a gene/protein interaction network where the intensity of the edges reflected the strength of the interaction score.

Finally, the functional interaction between genes that belongs to the chosen GO BP terms were investigated by REACTOME FIViz application to the Cytoscape 3.6.0 software. The ReactomeFIViz app is designed to

find pathways and network patterns related to cancer and other types of diseases. This app accesses the pathways stored in the Reactome database, allowing to do pathway enrichment analysis for a set of genes, visualize hit pathways using manually laid-out pathway diagrams directly in Cytoscape, and investigate functional relationships among genes in hit pathways. The app can also access the Reactome Functional Interaction (FI) network, a highly reliable, manually curated pathway-based protein functional interaction network covering over 60% of human proteins.

Real time q-PCR analysis

The RT-qPCR method was used for four selected genes (*ATP1B1, CXCL2, PDPN, UGCG*) to confirm the results obtained in the analysis of expression microarrays. Tests were performed in three replicates. The RNA samples were resuspended in 20 µl of RNase-free water and stored in liquid nitrogen. RNA samples were treated with DNase I and reverse-transcribed into cDNA. RT-qPCR was conducted in a LightCycler real-time PCR detection system (Roche Diagnostics GmbH, Mannheim, Germany) using SYBR® Green I as a detection dye, and target cDNA was quantified using the relative quantification method. The relative abundance of *ATP1B1, CXCL2, PDPN* and *UGCG* transcripts in each sample was standardized to the internal standards *ACTB* and *HPRT*. For amplification, 2 µL of cDNA solution was added to 18 µL of QuantiTect® SYBR® Green PCR (Master Mix Qiagen GmbH, Hilden, Germany) and primers. One RNA sample of each preparation was processed without the RT-reaction to provide a negative control for subsequent PCR.

RESULTS

Whole transcriptome profiling by affymetrix microarray allow as analysing gene expression changes between 7, 15 and 30 days of buccal pouch mucosa cells culture. Using Affymetrix® Porcine Gene 1.1 ST Array Strip, we examined expression of 12257 transcripts. Genes with fold change higher than abs (2) and with corrected p value lower than 0.05 were considered as differentially expressed. This set of genes consists of 130 different transcripts. This study is the first detailed analysis, based on GO BP identification of differentially expressed genes belonging to the significantly enrichment GO BP terms.

DAVID (Database for Annotation, Visualization and Integrated Discovery) software was used for extraction of the gene ontology biological process term (GO BP) that contains differently expressed transcripts. Up- and down-regulated gene sets were subjected to DAVID searching separately and only gene sets where adj. p value were lower than 0.05 were selected. The DAVID software analysis showed that differently expressed genes belong to 56 Gene ontology groups. In this paper we focused on "positive regulation of cellular component movement", "positive regulation of cellular process", "positive regulation of intracellular signal transduction" and "single organism cell adhesion" GO BP terms. These sets of genes were subjected to hierarchical clusterization procedure and presented as heatmaps (Fig. 2). The gene symbols, fold changes in expression, Entrez gene IDs and corrected p values of those genes are shown in Table I. The enrichment of each GO BP term was calculated and is shown on the circle diagram (Fig. 3).

Moreover, in Gene Ontology, database genes that formed one particular GO group can also belong to other different GO term categories. For this reason we explored the gene intersections between selected GO BP terms. The relationship between those GO BP terms is presented as a circle plot (Fig. 4).

STRING interaction network was generated among differentially expressed genes belonging to each of the selected GO BP terms. Using such prediction method provided us with a molecular interaction network formed between protein products of the studied genes (Fig. 5). Finally, we investigated the functional interactions between the chosen genes with REACTOME FIViz app to Cytoscape 3.6.0 software. The results are shown in Fig. 6.

RT-qPCR analysis was performed in order to quantitatively validate the microarray analysis. The results are shown in Fig. 7. For *ATP1B1, CXCL2, PDPN* and *UGCG* genes, the directions of changes have been confirmed. The difference between the level of expression of the analysed genes between days 15 and 30 for both microarray and RT-qPCR methods is similar except for the PDPN gene. This

gene had a comparable level of expression between days 15 and 30 in the RT-qPCR method (Fig. 7).

DISCUSSION

The genes analysed in this study were selected according to GO Databases, to select potential markers of oral mucosal cells' metabolism, mutual adhesion and signalling *in vitro*. The microarray screening showed that these genes, belonging to "Positive regulation of cellular component movement", "Single organism cell adhesion", "Positive regulation of cellular process" and "Positive regulation of intracellular signal transduction", exhibited three expression patterns. They were all upregulated on day 7 of culture, with their respective levels falling on day 15. From then on, the transcriptomes presented different values, with some genes being upregulated on day 30, some expressing large downregulation and the final group showing a small fall, or no change in transcript levels. However, the results of this microarray have been validated by RT-qPCR analysis in other works by our team, both published (3) and unpublished. The outcomes of those validations show us, that while the patterns of expression are represented by the microarray analysis with high fidelity, the exact fold changes are rarely reflected in the heatmaps. Because of this fact, we decided to divide the genes in the analysed gene ontologies into two expression patterns, those that were only upregulated on day 7 of primary cultures and those showing an additional period of upregulation towards the end of the 30-day culture period. Additionally, the GO databases show a wide array of genes that are associated with the searched term, which are, in different ways, involved in the processes analysed. Consequently, while describing all the genes detected, we primarily focused on those that are directly associated with the topics of the manuscript, discussing their possible involvement in the *in vitro* associated processes.

The first group contains genes associated with cell proliferation, adhesion, migration and communication. The first gene of this group, *TGFB1,* encodes ligand of transforming growth factor beta family of proteins. These ligands take part in regulation of gene expression through receptors present on the cell surface that, in response to these specific signals, initiate activation of downstream SMAD family of transcription factors. Many types of cells express *TGFB1*, as well as its receptors. This gene has been proven to be associated with rapid cell proliferation and differentiation, through various interactions with different growth factors (7). Most notably, it plays an important role in osteoblastic bone formation, reproductive processes, as well as being detected at the sites of various tumours (8). In the context of oral mucosa, it has been attributed a role in submucous fibrosis formation, which might indicate heightened fibroblast activity in culture (9). The next gene *ITGB3*, encodes Integrin Subunit Beta cell surface receptor, therefore it participates in cell adhesion, as well as cell-surface involving signalling pathways. It is a major player in the process of wound closing, as it is a receptor for fibrinogen, plasminogen, prothrombin and thrombospondin (10). As it is involved in MAPK signalling, it was shown to be involved in oncogenesis associated with abnormalities in this signalling path (11). It has not been specifically associated with buccal pouch processes, so it most probably is a marker of increased proliferation and cell interactions in the culture.

Another gene that is associated with the cellular processes occurring during cell proliferation is *PLK2 (Polo Like Kinase 2).* Again, it has not been previously directly associated with the specific, buccal pouch-associated processes. However, it has been proven multiple times that it presents a crucial role in centriole duplication, which deems it essential for G1/S phase transition (12). Because of this fact, it is yet another marker of increased proliferation of the analysed cells *in vitro*.

All the transcripts above exhibit up-regulation on days 7 and 30 of culture, with downregulation on day 15. There is one more gene that shows this expression pattern in our analysis. *CCL2* encodes a C-C motif chemokine 2, responsible for attracting monocytes and basophils, but not eosinophils and neutrophils (13). Hence, despite sharing the pattern with the genes that have been specifically associated with cell proliferation, this gene fits more into

Table I. *Gene symbols, fold changes in expression, Entrez gene IDs and corrected p values of studied genes.*

OFFICIAL GENE SYMBOL	Fold Change D15/D7	Fold Change D30/D7	Fold Change D30/D15	adjusted p.value D15/D7	adjusted p.value D30/D7	adjusted p.value D30/D15	GENE ID
CCL8	0.1098374	0.1015572	0.9246133	0.0099092	0.002855	0.8648287	100302703
CXCL2	0.1585988	0.3618252	2.2813865	0.0282106	0.1000607	0.3277437	414904
PLK2	0.1660002	0.6091754	3.6697255	0.0282106	0.3101504	0.1884621	397251
DUSP5	0.1720052	0.3392398	1.9722648	0.0407438	0.1216767	0.4625691	100157144
PTGS2	0.176579	0.3277974	1.8563786	0.0332722	0.0861828	0.447703	397590
LIF	0.252965	0.3537276	1.398326	0.0127508	0.0230194	0.3296551	399503
CCL2	0.2544943	0.6892844	2.7084476	0.0407438	0.4043909	0.2350893	397422
ATP1B1	0.2671037	0.4974017	1.8622043	0.0311185	0.1230303	0.3265278	396898
REL	0.33281	0.5087624	1.5286872	0.0234279	0.0563739	0.3173859	100525104
ITGB3	0.3427885	0.7627618	2.2251672	0.038898	0.4213886	0.2350893	397063
SCARB1	0.3812346	0.5946187	1.5597186	0.0346365	0.1343271	0.3639803	397018
UGCG	0.3838483	0.584988	1.5240083	0.0237712	0.0709872	0.283766	100152737
PDPN	0.3878982	0.5660051	1.459159	0.0342294	0.1033121	0.4206462	100738269
LYN	0.3967411	0.4074091	1.0268892	0.0346365	0.0423341	0.980695	100152890
ETS1	0.3978662	0.4650034	1.1687432	0.0311185	0.0474721	0.7511418	100302363
FCER1G	0.4253226	0.4158716	0.9777794	0.0268357	0.0235654	0.9761984	397406
TGFB1	0.443799	0.8154499	1.8374307	0.0150164	0.2166007	0.0719885	397078
RFC4	0.4463921	0.4260966	0.9545343	0.0346365	0.0362881	0.9445628	100157731
LMO2	0.4833797	0.5386858	1.1144154	0.0268357	0.0348947	0.744229	100512825

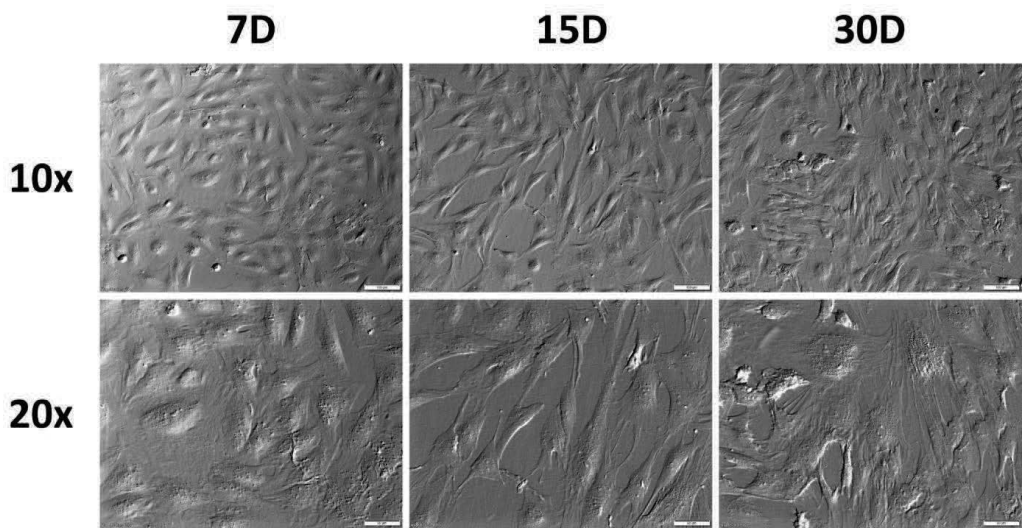

Fig. 1. *Photos of cell cultures prior to the material collection taken under an inverted microscope using relief contrast.*

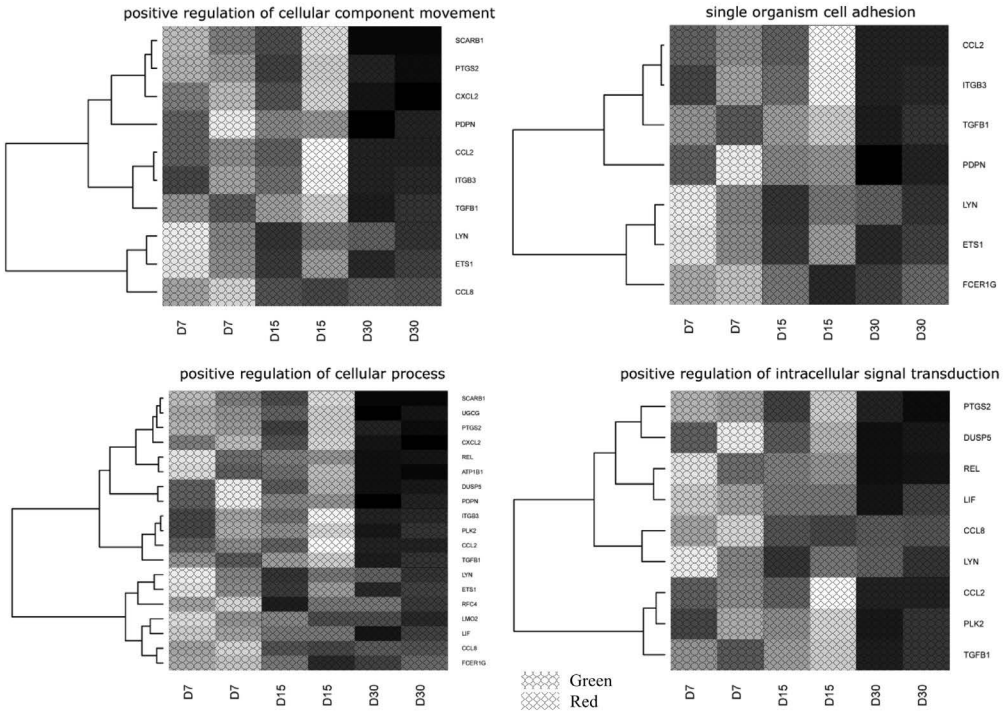

Fig. 2. *Heat map representation of differentially expressed genes belonging to the "positive regulation of cellular component movement", "positive regulation of cellular process", "positive regulation of intracellular signal transduction" and "single organism cell adhesion" GO BP terms. Log2 signal intensity values for any single gene were resized to Row Z-Score scale (from -2, the lowest expression to +2, the highest expression for single gene).*

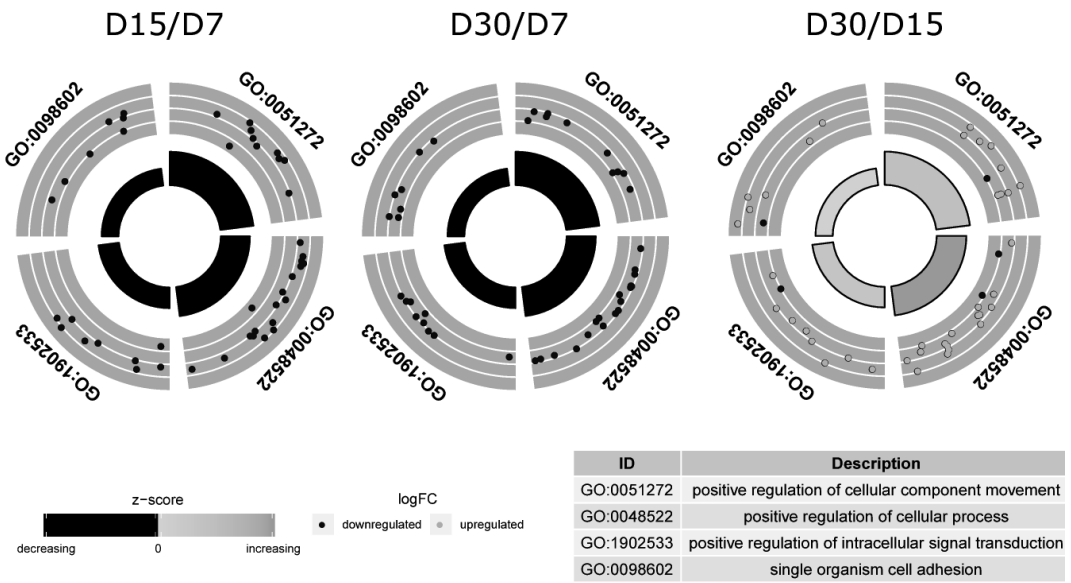

ID	Description
GO:0051272	positive regulation of cellular component movement
GO:0048522	positive regulation of cellular process
GO:1902533	positive regulation of intracellular signal transduction
GO:0098602	single organism cell adhesion

Fig. 3. *The circle plot showing the differently expressed genes and z-score of „positive regulation of cellular component movement", "positive regulation of cellular process", "positive regulation of intracellular signal transduction" and "single organism cell adhesion" GO BP terms. The outer circle shows a scatter plot for each term of the fold change of the assigned genes. The inner circle shows the z-score of each GO BP term. The width of each bar corresponds to the number of genes within GO BP term and the colour corresponds to the z-score.*

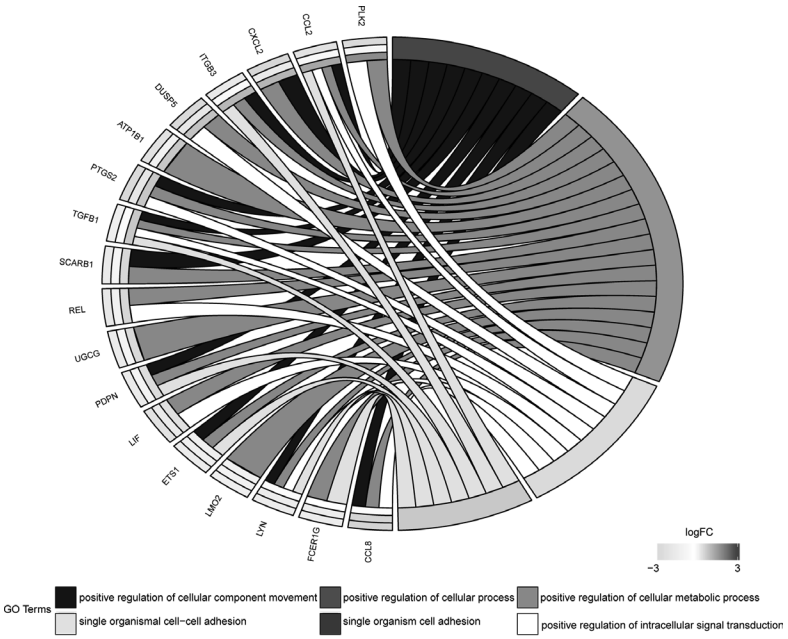

Fig. 4. *The representation of the mutual relationship between "positive regulation of cellular component movement", "positive regulation of cellular process", "positive regulation of intracellular signal transduction" and "single organism cell adhesion" GO BP terms. The ribbons indicate which gene belongs to which categories. The genes were sorted by logFC from most to least changed gene. The bars represent the logFC value of corresponding genes between D15/D7, D30/D7 and D30/D15.*

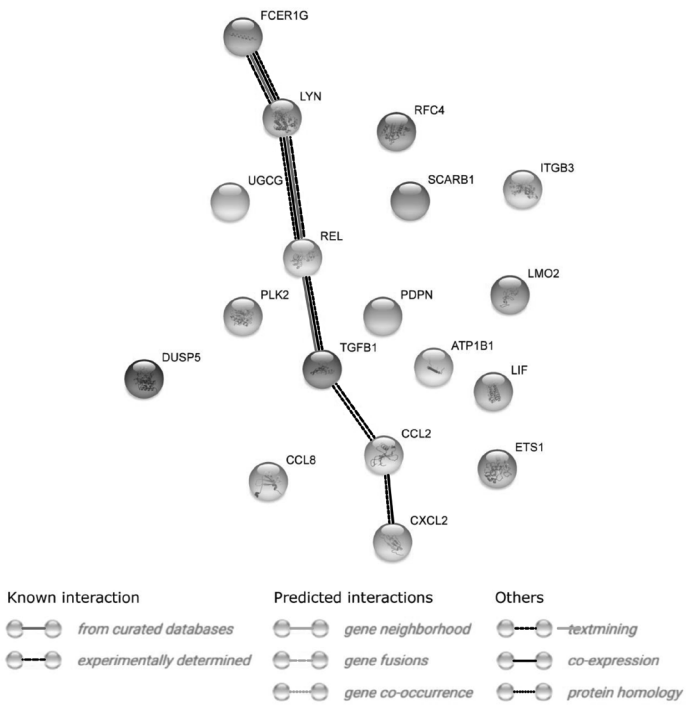

Fig. 5. *STRING-generated interaction network among differentially expressed genes belonging to the "positive regulation of cellular component movement", "positive regulation of cellular process", "positive regulation of intracellular signal transduction" and "single organism cell adhesion" GO BP terms. The intensity of the edges reflects the strength of interaction score.*

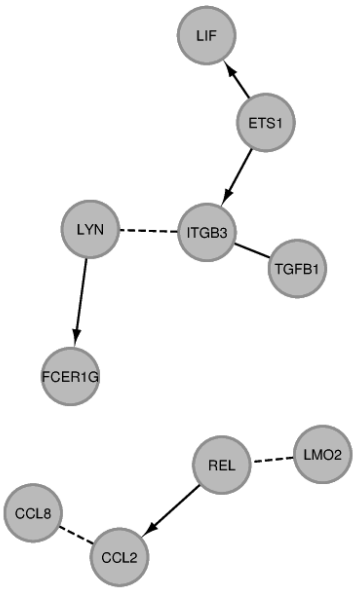

Fig. 6. *Functional interaction (FI) between differentially expressed genes belonging to the "positive regulation of cellular component movement", "positive regulation of cellular process", "positive regulation of intracellular signal transduction" and "single organism cell adhesion" GO BP terms. In this figure "->" stands for activating/catalysing, "-|" for inhibition, "-" for FIs extracted from complexes or inputs, and "---" for predicted FIs.*

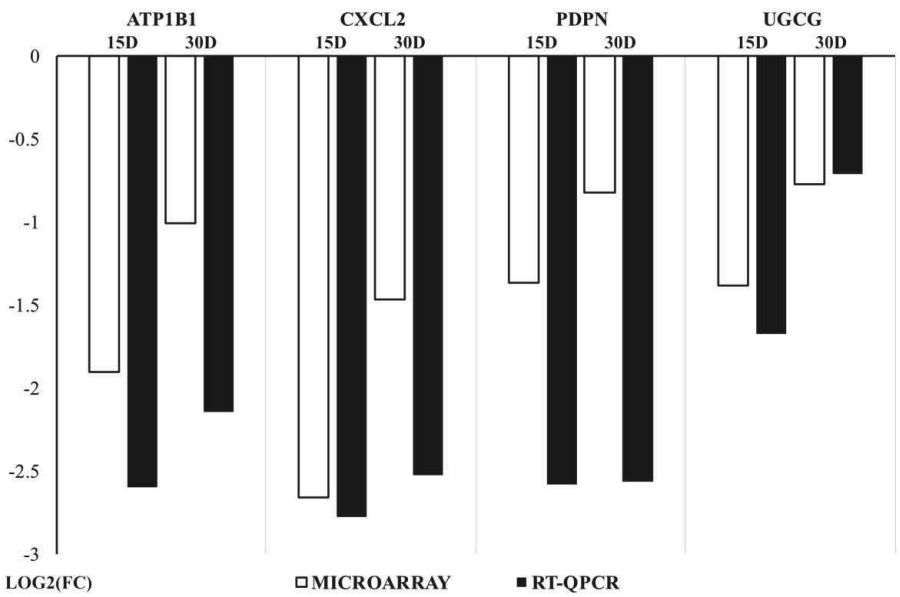

Fig. 7. *The results of RT-qPCR validation of ATP1B1, CXCL2, PDPN and UGCG genes. All the log2 of fold changes were described in relation to the transcript levels in 7 days of primary culture.*

the group of genes associated with inflammatory processes.

RFC4 and *PDPN* are two further genes that are functionally associated with the first described functional group. The first one, *Replication factor C subunit 4 4*, encodes a protein that is responsible for elongation DNA fragments that have been previously primed by DNA polymerase. It works together with an accessory protein required for its function-PCNA. While it possesses ATP-binding domains, it are not employed in ATP binding, but is essential for DNA recognition and clamp loading (14). Elevation of *RFC4* transcript levels can indicate increased DNA replication, being markers of upregulated proliferative activity of *in vitro* culture. PDPN, otherwise called *Podoplanin* encodes a protein that has a significant role in mediation of cell migration and adhesion (15). Interacting with various partner proteins, it can influence a range of different cells, causing a variety of effects from platelet aggregation, through tumour epithelial migration, to epithelial-mesenchymal transition (16). It has been proven to be associated with increased proliferative capabilities of cancerous keratinocytes, which indicates it could be a prominent marker of this oral mucosa component's *in vitro* propagation (17).

PTGS2, also known as *COX2*, is an enzyme essential for prostaglandin biosynthesis. It has been proven to be upregulated in many physiological conditions, as well as in malignancies, such as cancer. It has been proven to be associated with increased cell adhesion, differentiation, angiogenesis in tumour and apoptosis resistance (18). It has not been specifically attributed to oral mucosal cells, with its functions indicating that it might be a potential marker of their properties *in vitro*.

The last gene in the first described functional group is *DUSP5 (Dual Specificity Phosphatase 5)* which encodes a protein that, through phosphorylation of phosphoserine/threonine and phosphotyrosine residues, downregulates the MAP kinase superfamily. Being upregulated on day 7 of primary culture, this gene is a surprising observation, as it is associated with proliferation/differentiation inhibition rather than promotion (19).

The second functional group of genes described in this work is associated with the cellular function of the cultured cells. It contains genes associated with response to lipids and their metabolism, as well as other properties of oral mucosal cell functioning. *SCARB1* is the first member of this group. Scavenger Receptor Class B Member 1 Protein, encoded by this gene, is a receptor for a range of ligands, such as phospholipids, HDL, lipoproteins and other lipid soluble molecules. It is also responsible for mediating cholesterol transfer to and from HDL. However, it has also been suspected to take part in phagocytosis of apoptotic cells (20). *UGCG* (*UDP-Glucose Ceramide Glucosyltransferase*) encodes and enzyme that catalyses the first step in glycosphingolipid biosynthesis. It is essential for the production of these membrane-bound molecules that facilitate a range of cellular functions (21). *ATP1B* is a gene encoding a non-catalytic subunit of an ATPase enzyme. This specific component is responsible for Na^+/K^+ balance across the cellular membrane, playing an important role in osmoregulation (22). The aforementioned genes are an unsurprising find, as they are proprietary to the functioning of almost any cell, *in vivo* and *in vitro.* However, there are several other genes that are more likely to be considered markers of specific *in vitro* properties of oral mucosa derived cells. *LMO2* is the first of those genes. It encodes an LIM-domain protein, that serves its function predominantly in early embryonic yolk sac erythropoiesis, with some studies also noting its involvement in adult haematopoiesis (23). This gene has not been previously associated with any of the oral mucosal cell types. However it is a recognized oncogene, inducing stem-like properties in leukemic mice (24). Thus, it might be an indicator of added or retained plasticity of oral mucosal cell in *in vitro* culture. *LIF* (*Leukaemia Inhibitory* Factor) encodes a cytokine, that expresses multiple different roles in both the healthy organism and malignancies. Most prominently, it plays a major role in leukaemia, inducing hematopoietic differentiation in its cells (25). It has also been proven to be involved in reproductive processes, such as embryo implantation (26), as well as in inflammatory processes. Its presence in culture can indicate either the differentiation of oral mucosal cells, or be a

result of its secondary, proinflammatory function. This group is closed by three proto-oncogenes. *ETS1* encodes a transcription factor, belonging to ETS family (27). It is hard to determine its specific role in culture, as ETS TFs are known to function as both activators or inhibitors, depending on their acting location (28). However, as the gene is involved in tumorigenesis, especially development of stem-like properties (29), it could further indicate the stemness of oral mucosal cells on *in vitro* cultures. *LYN* encodes a non-receptor tyrosine-protein, facilitating signal transmission from cell surface receptors (30). Exhibiting numerous roles, from response to cytokines, through DNA damage mitigation and haematopoiesis, to various interactions with other proteins that alter its function depending on context (31), the effects of this gene are too unspecific to determine its role in the context of *in vitro* culture. The last protooncogene and the last gene in this group is *REL*, which encodes a transcription factor protein, regulating genes involved in apoptosis, oncogenic process, differentiation. However, it also exhibits a function in inflammation and immune response (32). This fact prevents us from determining whether the early upregulation of this gene is caused by *in vivo*/ *in vitro* properties of oral mucosa, differentiation of cells in culture, or by its function in cell immune response.

This brings us to the last functional group of genes that will be described briefly, as it does not directly link with the topic of the manuscript. There are three genes that exhibit their main function in response to pathogens and inflammation. *CCL8* is an antimicrobial gene, also involved in the immunoregulatory and inflammatory process, which encodes a chemokine that attracts monocytes, lymphocytes, basophils and eosinophils (33). *CXCL2* also presents antimicrobial function, encoding a chemokine that is expressed at inflammation sites. It has also been proven to be able to supress the proliferation of hematopoietic progenitor cells (34). Finally, *FCER1G* encodes a fragment of high affinity IgE receptor. It is most prominently involved in allergic reactions (35). All these genes are most probably elements of oral mucosal cell response to *ex vivo* conditions, being upregulated in early culture periods and downregulated on days 15 and 30.

Overall, the detected genes allowed us to presume certain patterns in the culture of oral mucosal cells. Most of the genes responsible for rapid proliferation and differentiation are upregulated on days 7 and 30, indicating that these are the periods in which the majority of culture growth occurs. It is unclear why the transcript levels are downregulated on day 15, however, it could be assumed that, after reaching the initial plateau of cell number, one of the constituents of the culture enters a stagnation period, then entering the growth phase again after the end of the *in vitro* viability of the other cell type. The elevated levels of genes attributed to cell function on day 7 might indicate that this period is crucial to the loss of initial oral mucosal identity and gain of mucosal-like state, proprietary for long-term cultures. Increased expression of antimicrobial/immune response / inflammatory genes at day 7 is explainable by the fact that the culture might still be carrying a mark of the initial culture periods in which the cells are still adapting to the new *ex vivo* conditions, while being exposed to potential pathogens that are later eliminated with medium changes and culture plate washing. There are several genes that have been detected in this type of culture for the first time and might serve as potential markers of *in vitro* associated processes in oral mucosal cells. However, it must be noted that this research is a transcriptomic study which, to gain validation needed for applying the knowledge in *in vivo* and clinical situations, would need to be confirmed by proteomic analyses. Concluding, this research allowed us to gain new insight into transcriptomic basis of oral mucosal cell functioning *in vitro*, which might later serve as a reference for further studies that would allow to apply this knowledge in a clinical environment.

REFERENCES

1. Bryja A, Dyszkiewicz-Konwińska M, Budna J, et al. Carcinogenesis in mammalian oral mucosa from the perspective of biomedical research. Med Weter 2017; 73(2):82-87.
2. Bryja A, Dyszkiewicz-Konwińska M, Budna J, et al. The biomedical aspects of oral mucosal epithelial

cell culture in mammals. J Biol Regul Homeost Agents 2017; 31(1):81-85.
3. Dyszkiewicz-Konwińska M, Nawrocki M, Huang Y, et al. New gene markers for metabolic processes and homeostasis in porcine buccal pouch mucosa during cells long term-cultivation—a primary culture approach. Int J Mol Sci 2018; 19(4):1027.
4. Mangera A, Chapple CR. Tissue engineering in urethral reconstruction--an update. Asian J Androl 2013; 15(1):89-92.
5. Kranc W, Jankowski M, Budna J, et al. Amino acids metabolism and degradation is regulated during porcine oviductal epithelial cells (OECs) primary culture in vitro – a signaling pathways activation approach. Med J Cell Biol 2018; 6(1):18-26.
6. Nawrocki MJ, Celichowski P, Budna J, et al. The blood vessels development, morphogenesis and blood circulation are three ontologic groups highly up-regulated in porcine oocytes before in vitro maturation. Adv Cell Biol 2017; 5(2):135-42.
7. Kingsley DM. The TGF-beta superfamily: new members, new receptors, and new genetic tests of function in different organisms. Genes Dev 1994; 8(2):133-46.
8. Cirillo N, Hassona Y, Celentano A, Lim KP, Manchella S, Parkinson EK, Prime SS. Cancer-associated fibroblasts regulate keratinocyte cell–cell adhesion via TGF-β-dependent pathways in genotype-specific oral cancer. Carcinogenesis 2017; 38(1):76-85.
9. Maria S, Kamath V, Satelur K, Rajkumar K. Evaluation of transforming growth factor beta1 gene in oral submucous fibrosis induced in Sprague-Dawley rats by injections of areca nut and pan masala (commercial areca nut product) extracts. J Cancer Res Ther 2016; 12(1):379.
10. Nurden AT, Fiore M, Nurden P, Pillois X. Glanzmann thrombasthenia: a review of ITGA2B and ITGB3 defects with emphasis on variants, phenotypic variability, and mouse models. Blood 2011; 118(23):5996-6005.
11. Huveneers S, Truong H, Danen EHJ. Integrins: Signaling, disease, and therapy. Int J Radiat Biol 2007; 83(11-12):743-51.
12. Chang J, Cizmecioglu O, Hoffmann I, Rhee K. PLK2 phosphorylation is critical for CPAP function in procentriole formation during the centrosome cycle. EMBO J 2010; 29(14):2395-406.
13. Dewald O, Zymek P, Winkelmann K, et al. CCL2/ Monocyte Chemoattractant Protein-1 Regulates Inflammatory Responses Critical to Healing Myocardial Infarcts. Circ Res 2005; 96(8):881-89.
14. Schmidt SL, Gomes XV, Burgers PM. ATP utilization by yeast replication factor C. III. The ATP-binding domains of Rfc2, Rfc3, and Rfc4 are essential for DNA recognition and clamp loading. J Biol Chem 2001; 276(37):34784-91.
15. Kaneko MK, Kato Y, Kameyama A, et al. Functional glycosylation of human podoplanin: Glycan structure of platelet aggregation-inducing factor. FEBS Lett 2007; 581(2):331-36.
16. Martin-Villar E, Megias D, Castel S, Yurrita MM, Vilaro S, Quintanilla M. Podoplanin binds ERM proteins to activate RhoA and promote epithelial-mesenchymal transition. J Cell Sci 2006; 119(21):4541-53.
17. Martín-Villar E, Scholl FG, Gamallo C, Yurrita MM, Muñoz-Guerra M, Cruces J, Quintanilla M. Characterization of human PA2.26 antigen (T1α-2, podoplanin), a small membrane mucin induced in oral squamous cell carcinomas. Int J Cancer 2005; 113(6):899-910.
18. Kosaka T, Miyata A, Ihara H, et al. Characterization of the human gene (PTGS2) encoding prostaglandin-endoperoxide synthase 2. Eur J Biochem 1994; 221(3):889-97.
19. Mandl M, Slack DN, Keyse SM. Specific inactivation and nuclear anchoring of extracellular signal-regulated kinase 2 by the inducible dual-specificity protein phosphatase DUSP5. Mol Cell Biol 2005; 25(5):1830-45.
20. Kawasaki Y, Nakagawa A, Nagaosa K, Shiratsuchi A, Nakanishi Y. Phosphatidylserine binding of class B scavenger receptor type I, a phagocytosis receptor of testicular sertoli cells. J Biol Chem 2002; 277(30):27559-66.
21. Proia RL. Glycosphingolipid functions: insights from engineered mouse models. Philos Trans R Soc Lond B Biol Sci 2003; 358(1433):879-83.
22. Bab-Dinitz E, Albeck S, Peleg Y, Brumfeld V, Gottschalk KE, Karlish SJD. A C-Terminal lobe of the β subunit of Na,K-ATPase and H,K-ATPase

resembles cell adhesion molecules. Biochemistry 2009; 48(36):8684-91.
23. Yamada Y, Warren AJ, Dobson C, Forster A, Pannell R, Rabbitts TH. The T cell leukemia LIM protein Lmo2 is necessary for adult mouse hematopoiesis. Proc Natl Acad Sci U S A 1998; 95(7):3890-95.
24. McCormack MP, Young LF, Vasudevan S, et al. The Lmo2 oncogene initiates leukemia in mice by inducing thymocyte self-renewal. Science (80-) 2010; 327(5967):879-83.
25. Garland JM, Quesenberry PJ, Hilton DJ (Douglas J. Colony-stimulating factors : molecular and cellular biology. [Internet]. M. Dekker ed 1997.
26. Cullinan EB, Abbondanzo SJ, Anderson PS, Pollard JW, Lessey BA, Stewart CL. Leukemia inhibitory factor (LIF) and LIF receptor expression in human endometrium suggests a potential autocrine/paracrine function in regulating embryo implantation. Proc Natl Acad Sci U S A 1996; 93(7):3115-20.
27. Garrett-Sinha LA. Review of Ets1 structure, function, and roles in immunity. Cell Mol Life Sci 2013; 70(18):3375-90.
28. Yordy JS, Li R, Sementchenko VI, Pei H, Muise-Helmericks RC, Watson DK. SP100 expression modulates ETS1 transcriptional activity and inhibits cell invasion. Oncogene 2004; 23(39):6654-65.
29. Yamaguchi E, Nakayama T, Nanashima A, Matsumoto K, Yasutake T, Sekine I, Nagayasu T. Ets-1 proto-oncogene as a potential predictor for poor prognosis of lung adenocarcinoma. Tohoku J Exp Med 2007; 213(1):41-50.
30. Ingley E. Functions of the Lyn tyrosine kinase in health and disease. Cell Commun Signal 2012; 10(1):21.
31. Malik M, Chen Y-Y, Kienzle MF, Tomkowicz BE, Collman RG, Ptasznik A. Monocyte migration and LFA-1-mediated attachment to brain microvascular endothelia is regulated by SDF-1 alpha through Lyn kinase. J Immunol 2008; 181(7):4632-37.
32. Köntgen F, Grumont RJ, Strasser A, Metcalf D, Li R, Tarlinton D, Gerondakis S. Mice lacking the c-rel proto-oncogene exhibit defects in lymphocyte proliferation, humoral immunity, and interleukin-2 expression. Genes Dev 1995; 9(16):1965-77.
33. Hori T, Naishiro Y, Sohma H, et al. CCL8 is a potential molecular candidate for the diagnosis of graft-versus-host disease. Blood 2008; 111(8):4403-12.
34. De Filippo K, Dudeck A, Hasenberg M, et al. Mast cell and macrophage chemokines CXCL1/CXCL2 control the early stage of neutrophil recruitment during tissue inflammation. Blood 2013; 121(24):4930-37.
35. van Vugt MJ, Heijnen IA, Capel PJ, et al. FcR gamma-chain is essential for both surface expression and function of human Fc gamma RI (CD64) in vivo. Blood 1996; 87(9):3593-99.

LETTER TO THE EDITOR

XUEBIJING ENHANCES NEUROPROTECTIVE EFFECTS OF ULINASTATIN ON TRANSIENT CEREBRAL ISCHEMIA VIA Nrf2-ARE SIGNAL PATHWAYS IN THE HIPPOCAMPUS

H-X. HU[1], M-Q. ZHU[2], Y-C. SUN[1], C. MA[3], X. WANG[2] and X-L. LIU[1]

[1]Department of Emergency Medicine, The First Hospital of Jilin University, Changchun, Jilin, China; [2]Department of Neurology and Neuroscience Center, The First Hospital of Jilin University, Changchun, Jilin, China; [3]Department of Brain Tumor Surgery, The First Hospital of Jilin University, Changchun, Jilin, China

Received March 28, 2018 – Accepted May 17, 2018

Prior studies have demonstrated that ulinastatin (UTI) plays a beneficial role in regulating cerebral ischemic injury evoked by cardiac arrest (CA). It is noteworthy to find interventions that can enhance effects of this drug and thereby increase its clinical application. Xuebijing (XBJ) is comprised of extracts from Chinese herbs and has been widely used in China as an anti-endotoxicity drug for the treatment of sepsis and ischemic disorders associated with multiple organ dysfunction syndrome. Thus, in this study we examined the effects of a combination of UTI and XBJ to improve neural injury in the process of neurological functions after transient cerebral ischemia. Our results show that CA impaired Nrf2-antioxidant response element (Nrf2-ARE) and superoxide dismutase (SOD) in the hippocampus CA1 region. This process further amplified products of oxidative stress, namely 8-isoprostaglandin F2α (8-iso PGF2α) and 8-hydroxy-2'-deoxyguanosine (8-OHdG). A lower dose of UTI failed to restore Nrf2-ARE and attenuate 8-iso PGF2α and 8-OHdG SOD following CA; however, systemic administration of XBJ amplified the effects of this dose of UTI on antioxidative signal pathway of the hippocampus. Overall, the results of this study have implications for the enhanced neuroprotective role played by a combination of XBJ and UTI in improving neural injury observed in transient cerebral ischemia; and Nrf2-ARE signal is a part of key mechanisms that are involved in neuroprotective effects of XBJ and UTI.

To the Editor,

Ulinastatin, urinary trypsin inhibitor (UTI), is a glycoprotein acting as a trypsin inhibitor (1). It can be derived from urine or synthetically produced and conventionally effective to treat pancreatitis, toxic shock and sepsis, etc. (1-3). The genes and proteins regulated by UTI are implicated in the inflammatory process (4). Previous studies indicate the protective effects of UTI against ischemia/reperfusion injury in numerous diseases (1). Our recent study further showed that UTI can attenuate amplification of central pro-inflammatory cytokine (PIC) and products of oxidative stress in rats with transient cerebral ischemia induced by cardiac arrest (CA) (5); whereas it improves CA impaired Nrf2-antioxidant response element (Nrf2-ARE) and superoxide dismutases (SOD). Through this process, UTI thereby leads to improvement of neurological functions, brain tissue edema and survival (5).

Xuebijing injection (XBJ), a Chinese medicine

Key words: Xuebijing, ulinastatin, oxidative stress, cardiopulmonary resuscitation, cardiac arrest, cerebral ischemia

Mailing address:
Dr Xu Wang,
Department of Neurology and Neuroscience Center,
Department of Emergency Medicine,
The First Hospital of Jilin University,
71 Xinmin Street, Changchun, Jilin 130021, China
Tel.: +86 431 88782593
e-mail: wangxxu2016@163.com

0393-974X (2018)

formula containing five herbs, is used as an addition to conventional therapy to sepsis and septic shock in China (6, 7). Combination of XBJ and standard treatment yielded better clinical outcome than standard treatment alone (6, 7). XBJ has been also reported to alleviate sepsis and ischemic disorders associated multiple organ dysfunction syndrome via mechanisms of anti-inflammation and anti-oxidative stress (8, 9).

When blood flow and oxygen delivery are halted it leads to systemic ischemic injury in various organs including brain during CA (10). Although cardiopulmonary resuscitation (CPR) is applied, inadequate blood flow and tissue oxygen delivery still persist due to myocardial dysfunction, hemodynamic instability and microvascular dysfunction. Thus, it is important to find drugs having better neuroprotective effects during neural injuries in cerebral ischemia. To further determine signal pathways by which drugs/biological agents that attenuate damage evoked by cerebral ischemia, would provide a rationale for clinical application of those drugs.

In this study we examined the effects of a combination of UTI and XBJ on neural injuries evoked by CA. We hypothesized that systemic administration of XBJ amplifies neuroprotective outcomes of UTI. We further hypothesized that the effects of XBJ are via improvement of Nrf2 and Nrf2-regulated NADPH quinone oxidoreductase-1 (NQO1) and SOD in hippocampus CA1 of ischemic animals. As a result, XBJ attenuates oxidative production 8-isoprostaglandin F2α (8-iso PGF2α, a product of oxidative stress); and 8-hydroxy-2'-deoxyguanosine (8-OHdG, a key biomarker of protein oxidation).

MATERIALS AND METHODS

All the animal procedures were approved by the Institutional Animal Care & Use Committee of Jilin University, which are in compliance with the Guideline for the Care and Use of laboratory Animals of the U.S. NIH. Male Sprague–Dawley rats (200–300g) were used in this study.

Induction of cerebral ischemia

The ischemia was produced in the CA model induced by asphyxia. Briefly, rats were anesthetized with an isoflurane-oxygen mixture (2-5% isoflurane in 100% oxygen). An endotracheal tube was first inserted and attached to a ventilator. The ventral tail artery was cannulated to monitor systemic arterial pressure. The right jugular vein was cannulated for a continuous infusion of saline (at a rate of 0.1 ml/hour) to maintain baseline blood pressure and fluid balance. Body temperature was continuously monitored and maintained at 37°C with a heating pad and external heating lamps. Asphyxia was induced by stopping mechanical ventilation and clamping the tracheal tubes at the end of expiration. Resuscitation efforts began 6 min following inducement of CA. For this purpose, rats were orotracheally intubated for mechanical ventilation accompanied by chest compression delivered by a mechanical compressor at a rate of 200/min for 5 min. Once spontaneous heartbeat returned, epinephrine (2 μg) was administered to achieve a mean arterial blood pressure of >80 mmHg. Ventilation was adjusted for animals to regain spontaneous respiration and achieve normoxia. In the sham operated animals, the same surgical procedures were performed without cardiac arrest and resuscitation.

Administration of drugs and experimental groups

The rats were divided randomly. Group 1 (n=10): the rats received the same surgical procedures and endotracheal intubation was performed with no asphyxia or CPR. Group 2 (n=15): CA and CPR were performed and 0.5 ml of saline was given (i.p., every 12 h for 7 days). Group 3 (n=28): CA and CPR were carried out and 2, 4, 6 ml/kg of XBJ was injected (i.p., once/day for 7 days). Group 4 (n=12): CA and CPR were carried out and 5000 units/kg of UTI (i.p., every 12 hours for 7 days). Group 5 (n=20): CA and CPR were carried out and 5000 units/kg of UTI (i.p., every 12 h for 7 days) and 2 ml/kg of XBJ were injected (i.p., once/day for 7 days). At the end of each experiment, the rats were sacrificed and then the hippocampus was removed for biochemical measurements. XBJ containing extracts of five herbs was purchased from Tianjin Chase Sun Pharmaceutical Co. Ltd (Tianjin, China).

ELISA measurement

The tissues from each rat were sampled for the analysis. In brief, the hippocampus CA1 region of the rats was removed under an anatomical microscopy. Total protein was extracted by homogenizing the hippocampus

sample in ice-cold immunoprecipitation assay buffer with protease inhibitor cocktail kit. The lysates were centrifuged and the supernatants were collected for measurements of protein concentrations using a bicinchoninic acid assay reagent kit.

The levels of 8-iso PGF2α and 8-OHdG were examined using ELISA kits (obtained from Promega Co. and Abcam Co.) according to the provided description and modification. Briefly, polystyrene 96-well microtitel immunoplates were coated with affinity-purified rabbit primary antibodies. Parallel wells were coated with purified rabbit IgG for evaluation of nonspecific signal. After overnight incubation, plates were washed. Then, the diluted samples and 8-iso PGF2α/8-OHdG standard solutions were distributed in each plate. The plates were washed and incubated with anti-8-iso PGF2α/8-OHdG galactosidase. Then, the plates were washed and incubated with substrate solution. After incubation, the optical density was measured using an ELISA reader with a wavelength of 575 nm.

Western blot analysis

After being denatured by heating at 95°C in an SDS sample buffer, the supernatant samples were loaded onto Mini-Protean TGX Precast gels and electrically transferred to a polyvinylidene fluoride membrane. The membrane was then incubated overnight with primary antibodies: rabbit anti-Nrf2, anti-NQO1 and anti-SOD. After being fully washed, the membrane was incubated with horseradish peroxidase-linked anti-rabbit secondary antibody and visualized for immunoreactivity. All antibodies were obtained from the Abcam Co. and Santa Cruz Biotech. The membrane was stripped and incubated with mouse anti-β-actin to show equal loading of the protein. The bands recognized by the primary antibody were visualized by exposure of the membrane onto an X-ray film. Then, the film was scanned and the optical densities of primary antibodies and β-actin bands were determined using the Scion Software (NIH, US). Values for densities of immunoreactive bands/β-actin band from the same lane were determined. Each of the values was then normalized to a control sample.

Neurological Severity Score (mNSS)

Seven days after the rats received all the treatments, the modified method of Neurological Severity Score (mNSS) was used to examine neurological functions, as described previously (5). Note that mNSS was generally used to assess a combination of motor, sensory, and balance functions. Neurological function was graded on a scale of 0–18 (normal score, 0; maximal deficit score, 18). An mNSS score of > 0 before CA indicated that the rats were abnormal and they were excluded from the experiment. The experiments were performed in a blind manner.

Statistical analysis

Experimental data were analyzed using one-way repeated measures analysis of variance (ANOVA). As appropriate, Tukey's *post hoc* tests were used. All values were presented as mean ± standard deviation. For all analyses, differences were considered significant at $P < 0.05$. All statistical analyses were performed using SPSS for Windows version 20.0 (SPSS Inc., Chicago, US).

RESULTS

Effects of XBJ and UTI on oxidative stress production

In this experiment, we first examined the effects of three doses of XBJ (2, 4, 6 ml/kg) on products of oxidative stress, namely 8-iso PGF 2*α* and 8-OHdG in CA rats. Fig. 1A shows that the levels of 8-iso PGF 2*α* and 8-OHdG were increased in the hippocampus of CA rats (P <0.05 *vs* control rats; n=10 in control and n=15 in CA rats). It is noted that increases of 8-iso PGF2*α* and 8-OHdG were significantly attenuated in CA rats with administration of 6 ml/kg of XBJ (n=10; P <0.05 *vs* CA rats without treatment/ n=15 and CA rats with lower doses of XBJ; n=12 with 2 ml/kg of XBJ and n=6 with 4 ml/kg of XBJ). There were no significant differences observed in the levels of 8-iso PGF2*α* and 8-OHdG between CA rats with no treatment and CA rats with 2 ml/kg of XBJ (P >0.05).

Next, we examined the enhancing effects of XBJ on UTI in modulating 8-iso PGF 2*α* and 8-OHdG. Fig. 1B demonstrates that a lower dose of UTI failed to alter the amplified levels of 8-iso PGF 2*α* and 8-OHdG in the hippocampus of CA rats (P >0.05, CA rats without treatment *vs* CA rats with a lower dose of UTI; n=12). As 2 ml/kg of XBJ and a lower dose of UTI were given, the levels of 8-iso PGF 2*α* and 8-OHdG were significantly decreased in CA rats

(n=20; P <0.05 *vs* CA rats with no treatment and CA rats with a lower UTI). There were no significant differences observed in the levels of 8-iso PGF2α and 8-OHdG between the control group and CA group with a combination of UTI and XBJ (P >0.05).

Effects of XBJ and UTI on antioxidant signal pathways

Fig. 2, A-C, shows that the protein expression levels of Nrf2 and Nrf2-regulated NQO1 and SOD were decreased in the hippocampus of CA rats and a lower dose of UTI failed to restore impaired Nrf2 signal expression and SOD (P>0.05, CA rats *vs* CA rats with no treatment; n=6-10). These figures further shows that downregulation of Nrf2/NQO1 and SOD in CA rats was improved after a combination of XBJ and UTI was applied (P<0.05, CA rats with UTI and XBJ *vs* CA rats with no treatment and CA rats with a lower dose of UTI alone; n=6-10).

Effects of XBJ and UTI on neurological functions

Fig. 2D shows that CA increased the mNSS in rats (P<0.05, control rats *vs* CA rats; n=10 in control and n=15 in CA group). This figure further demonstrates that a lower dose of UTI failed to attenuate the impaired mNSS in animals following

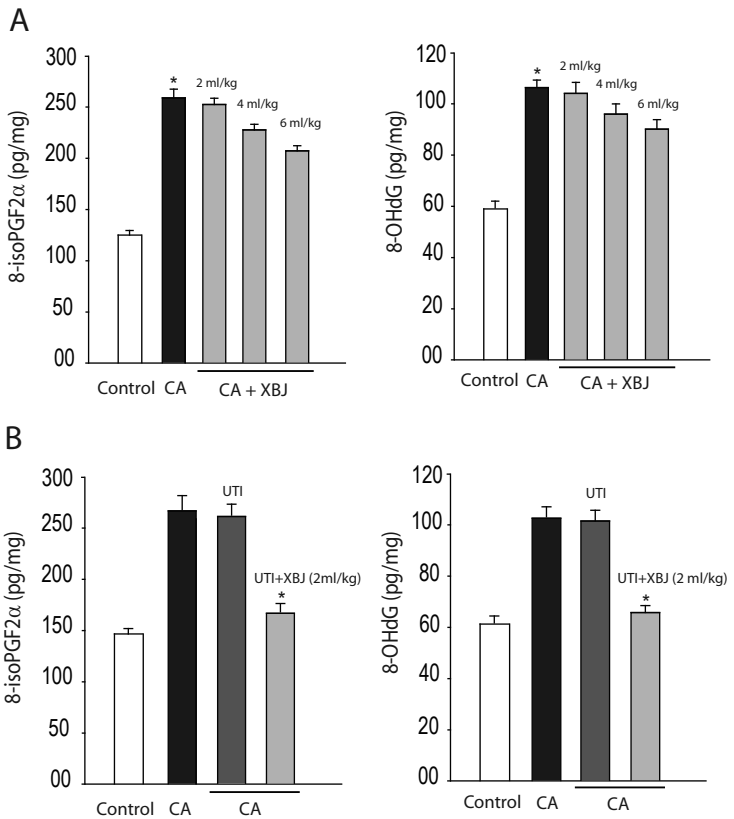

Fig. 1. *Effects of UTI and XBJ on products of oxidative stress.* ***A)*** *Induction of CA amplified the levels of oxidative product 8-iso PGF2α and 8-OHdG in the hippocampus CA1 region. Systemic administration of XBJ (6 ml/kg) attenuated increases of 8-iso PGF2α and 8-OHdG in CA rats. *P < 0.05 vs control rats and CA rats injected with 6 ml/kg of XBJ. n=10 in control; =15 in CA group; =12 in CA group with 2 ml/kg of XBJ, =6 in CA group with 4 ml/kg of XBJ; and =10 in CA group with 6 ml/kg of XBJ.* ***B)*** *Systemic administration of a lower dose of UTI (5000 units/kg; n=12) failed to attenuate increases of 8-iso PGF2α and 8-OHdG in CA rats. P > 0.05 vs CA rats without treatment (n=15). Note that a lower dose of XBJ (n=20) enhanced the effects of UTI on attenuating 8-iso PGF2α and 8-OHdG in CA rats. *P < 0.05 vs CA rats with no treatment and CA rats with a lower UTI. There were no significant differences observed in the levels of 8-iso PGF2α and 8-OHdG between control group and CA group with a combination of UTI and XBJ (P >0.05).*

CA (n=12; $P>0.05$ *vs* CA rats with no treatment), but a combination of UTI and XBJ significantly attenuated the impaired mNSS in CA animals (n=20; $P<0.05$ *vs* CA rats with UTI and CA rats with no treatment).

DISCUSSION

Nrf2 is a transcription factor and as a basic leucine zipper protein it regulates the expression of antioxidant proteins protecting against oxidative

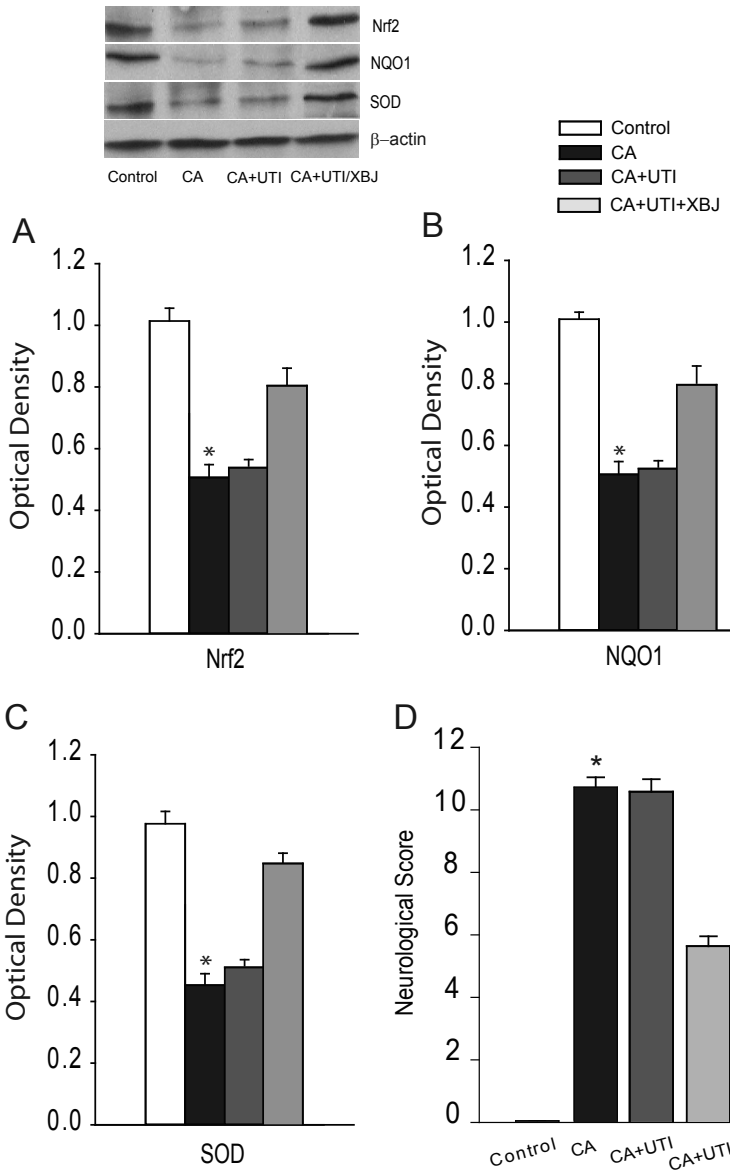

Fig. 2. *Effects of UTI and XBJ on antioxidant signal pathways and neurological functions.* ***A-C****) Protein expression levels of Nrf2-ARE and SOD were decreased in the hippocampus CA1 of CA rats. A lower dose of UTI (5000 units/kg) failed to restore impaired Nrf2/NQO1 and downregulated SOD. When XBJ (2 ml/kg) was given with a lower dose of UTI, Nrf2/NQO1 and SOD were increased. Top panel panels are representative bands. *P<0.05, CA rats vs control rats and CA rats injected with a combination of UTI and XBJ. N=6-10 in each group.* ***D****) Showing that the mnss was increased in rats after CA and it was significantly improved by systemic administration of UTI and XBJ. *P<0.05 vs control rats and CA rats injected with UTI and XBJ. The number of rats=10 in control; =15 in CA group; 12 in CA group with UTI; and =20 in CA group with UTI and XBJ.*

damage triggered by injury and inflammation (11). Numerous drugs that stimulate the Nrf2 pathway were used for treatment of diseases caused by oxidative stress (12). Under normal or unstressed conditions, Nrf2 is kept in the cytoplasm by a cluster of proteins that degrade it quickly (13-15). Under oxidative stress, Nrf2 is not degraded, but travels to the nucleus where Nrf2 binds to a DNA promoter and initiates transcription of anti-oxidative genes and their proteins (13-15). In the nucleus, Nrf2 combines (forms a heterodimer) with a small Maf protein and binds to the ARE in the upstream promoter region of many anti-oxidative genes, and initiates their transcription (15). Our data show that CA impairs the protein expression levels of Nrf2-ARE pathway in the hippocampus. We also observed that downregulation of Nrf2 and NQO1 were accompanied with decreases of SOD. Moreover, we observed that products of oxidative stress 8-iso PGF2α and 8-OHdG were increased in the hippocampus of CA rats.

In our previous work, we found that UTI can significantly recover impairment of Nrf2-ARE and SOD following CA. UTI can also attenuate amplification of 8-iso PGF2α and 8-OHdG in the hippocampus of CA rats. In order to determine the effects of XBJ on UTI, in the present study we injected a lower dose of UTI and observed that it did not alter the levels of 8-iso PGF2α and 8-OHdG and expression of Nrf2-ARE and SOD after induction of CA. Interestingly, a combination of this dose of UTI wuth XBJ restored impaired Nrf2-ARE and SOD and attenuated upregulated 8-iso PGF2α and 8-OHdG induced by CA. Consistent with this result, UTI and XBJ decreased the mNSS, indicating improvement of neurological functions. Thus, it is implicated as beneficial to ischemic brain diseases via activation of Nrf2-ARE with a combination of UTI and XBJ.

It should be noted that one source of reactive oxygen species production is the enzyme family of NADPH oxidase (NOX). NOX subunit NOX4 was shown highly expressed under ischemic conditions in the central nervous system. Vitamin C also plays a role in improving ischemic conditions as an antioxidant. Thus, supplement of vitamin C and/or drugs inhibiting NOX signal may also be considered with application of UTI and XBJ.

In conclusion, transient global ischemia induced by CA impairs the protein levels of Nrf2-ARE signal and SOD in the hippocampus, thereby leading to increase of products of oxidative stress. Systemic administration of UTI and XBJ has enhancing effects in improving deficiency of Nrf2-ARE and SOD in ischemic animals. As a result, a combination of UTI and XBJ improves neurological Severity Score in CA rats to a greater degree as compared with the respective usage of these drugs. Our data indicate the beneficial role played by a combination of UTI and XBJ in alleviating cerebral ischemia reperfusion injury via antioxidative mechanisms.

ACKNOWLEDGEMENTS

This study was supported by grants from the First Hospital of Jilin University (JDYY52015016), Norman Bethune Program of Jilin University (No.2015335), Science and Technology Development Program of Jilin Province (20160520160JH), as well as from the National Natural Science Foundation of China (No.81471830).

REFERENCES

1. Inoue K, Takano H. Urinary trypsin inhibitor as a therapeutic option for endotoxin-related inflammatory disorders. Expert Opin Investig Drugs 2010; 19:513-20.
2. Karnad DR, Bhadade R, Verma PK, Moulick ND, Daga MK, Chafekar ND, Iyer S. Intravenous administration of ulinastatin (human urinary trypsin inhibitor) in severe sepsis: a multicenter randomized controlled study. Intensive Care Med 2014; 40:830-38.
3. Wang G, Wen J, Wilbur RR, Wen P, Zhou SF, Xiao X. The effect of somatostatin, ulinastatin and Salvia miltiorrhiza on severe acute pancreatitis treatment. Am J Med Sci 2013; 346:371-76.
4. Inoue K, Takano H, Yanagisawa R, Yoshikawa T. Protective effects of urinary trypsin inhibitor on systemic inflammatory response induced by lipopolysaccharide. J Clin Biochem Nutr 2008; 43:139-42.
5. Jiang XM, Hu JH, Wang LL, Ma C, Wang X, Liu XL.

Effects of ulinastatin on global ischemia via brain pro-inflammation signal. Translational Neurosci 2016; 7:158-63.
6. Shi H, Hong Y, Qian J, Cai X, Chen S. Xuebijing in the treatment of patients with sepsis. Am J Emerg Med 2017; 35:285-91.
7. Zheng J, Xiang X, Xiao B, Li H, Gong X, Yao S, Yuan T. Xuebijing combined with ulinastaton benefits patients with sepsis: a meta-analysis. Am J Emerg Med 2018; 36(3):480-87.
8. Chen X, Feng Y, Shen X, Pan G, Fan G, Gao X, Han J, Zhu Y. Anti-sepsis protection of Xuebijing injection is mediated by differential regulation of pro- and anti-inflammatory Th17 and T regulatory cells in a murine model of polymicrobial sepsis. J Ethnopharmacol 2018; 211:358-65.
9. Chen Y, Tong H, Pan Z, et al. Xuebijing injection attenuates pulmonary injury by reducing oxidative stress and proinflammatory damage in rats with heat stroke. Exp Ther Med 2017; 13:3408-16.
10. Nolan JP, Neumar RW, Adrie C, et al. Post-cardiac arrest syndrome: Epidemiology, pathophysiology, treatment, and prognostication: A scientific statement from the International Liaison Committee on Resuscitation; the American Heart Association Emergency Cardiovascular Care Committee; the Council on Cardiovascular Surgery and Anesthesia; the Council on Cardiopulmonary, Perioperative, and Critical Care; the Council on Clinical Cardiology; the Council on Stroke. Resuscitation 2008; 79:350-79.
11. Moi P, Chan K, Asunis I, Cao A, Kan YW. Isolation of NF-E2-related factor 2 (Nrf2), a NF-E2-like basic leucine zipper transcriptional activator that binds to the tandem NF-E2/AP1 repeat of the beta-globin locus control region. Proc Natl Acad Sci U S A 1994; 91:9926-30.
12. Gold R, Kappos L, Arnold DL, et al. Placebo-controlled phase 3 study of oral BG-12 for relapsing multiple sclerosis. N Engl J Med 2012; 367:1098-107.
13. Itoh K, Chiba T, Takahashi S, et al. An Nrf2/small Maf heterodimer mediates the induction of phase II detoxifying enzyme genes through antioxidant response elements. Biochem Biophys Res Commun 1997; 236:313-22.
14. Sekhar KR, Rachakonda G, Freeman ML. Cysteine-based regulation of the CUL3 adaptor protein Keap1. Toxicol Appl Pharmacol 2010; 244:21-26.
15. Yamamoto T, Suzuki T, Kobayashi A, Wakabayashi J, Maher J, Motohashi H, Yamamoto M. Physiological significance of reactive cysteine residues of Keap1 in determining Nrf2 activity. Mol Cell Biol 2008; 28:2758-70.

LETTER TO THE EDITOR

PATIENT-REPORTED QUALITY OF LIFE AFTER ENDOSCOPIC SURGERY FOR PITUITARY LESIONS: A META-ANALYSIS

C-H. WANG[1] and N. ZHU[2]

[1]Department of Neurology, Beijing Tian Tan Hospital, Capital Medical University, Beijing, China; [2]National Institute for Viral Disease Control and Prevention, China Center for Disease Control and Prevention, Beijing, China

Received May 2, 2018 – Accepted June 12, 2018

Patient-reported outcomes are now considered as an important part of overall outcome assessment of a surgical intervention. The objective of the current study was to evaluate the patient-reported quality of life (QoL) of the subjects of endoscopic pituitary surgery. A literature search was carried out in several electronic databases and study selection was based on pre-determined eligibility criteria. Meta-analyses of standardized mean difference (SMD) were conducted to observe significance of difference between preoperative and postoperative scores of important tools. Sixteen studies were included [931 patients; 51.16 years (95% CI 49.13, 53.19) age; 48.41 % (43.74, 53.08) males]. Generally, there was no significant differences between postoperative and preoperative health-related QoL after postoperative month 1 or after fourth postoperative month. QoL after endoscopic pituitary surgery remains unchanged predominantly but may deteriorate in regard to physical role and sinonasal outcome transiently.

To the Editor,

Patient-reported QoL measures, such as sense of well-being, emotions, pain, functional status, and social interactions, are increasingly used to assess the outcome of a medical or surgical intervention (1). The QoL assessments may have several advantages such as improved preoperative counseling of patient, better anticipation of surgery, acceptance of surgical procedure and enhanced patient recovery. Furthermore, the QoL should also be used as an indicator of the success of surgical intervention (2).

Advancement in surgical techniques has made it possible to remove complex skull base tumors. Endoscopic surgery for skull base lesions is still evolving. Transnasal approaches utilize the nasal passage and paranasal sinuses to operate the skull base. Therefore, nasal trauma remains the source of many rhinological complications including sinusitis, epistaxis, synechiae, hyposmia, and anosmia (3). Among the intracranial neoplasms, pituitary adenomas have a prevalence of 16.7% (14.4% in autopsy studies and 22.5% in radiological cases) (4). Several pituitary tumors remain small in size and are either asymptomatic or with nonspecific symptoms. Consequently, it is very difficult to accurately measure the prevalence of pituitary adenomas in the general population.

Endoscopic surgical techniques utilized for the resection of pituitary adenomas are usually site-specific and are associated with general complications which necessitate evaluating the patient-reported QoL before and after surgery. Many studies have reported QoL assessments using various instruments for pituitary endoscopic surgery with

Key words: quality of life, QoL, endoscopic surgery, pituitary, tumor, adenoma

Mailing address:
Dr. Na Zhu,
National Institute for Viral Disease Control and Prevention,
China Center for Disease Control and Prevention,
Beijing, 102206, China
e-mail: beijing_nz@yahoo.com

0393-974X (2018)

transnasal route, but the outcomes are not always similar. Hence, we carried out a literature search to identify relevant studies to conduct a meta-analysis of general health-related QoL and sinonasal indices in order to have refined evidence regarding the effect of surgery on patient-reported QoL.

We followed the Cochrane Collaboration guidelines for conducting systematic reviews and meta-analyses for the present study. Inclusion criteria were: a) prospective or retrospective study reporting the outcomes of patient-reported QoL assessment performed by using a validated instrument ion patients who had undergone endoscopic transnasal or transseptal surgery; b) study reporting the evaluations of general health-related and/or rhinological QoL scores; c) study reporting preoperative as well as postoperative and/or later measurements. Electronic databases (Pubmed, Embase, Ovid and Google Scholar) were searched by using relevant keywords and medical subject headings. The primary phrase (Pituitary tumor – endoscopic surgery – quality of life) was used in combination with one or two of the following keywords: QoL, adenoma, macroadenoma, microadenoma, trans-nasal, trans-septal, trans-sphenoidal, skull base, questionnaire, inventory, Anterior Skull Base Nasal Inventory (ASK Nasal), Anterior Skull Base Questionnaire (ASBQ), Sinonasal Outcome Test (SNOT)-20/22, SNOT-20/22, prospective, and retrospective. The search encompassed research articles published in English language before April 2018.

Data regarding the demographic characteristics of the subjects and outcomes were extracted from each of the selected studies by using a standardized procedure and were organized in specialized datasheets. For the assessment of the changes in QoL scores at postoperative month 1, and at postoperative month 4 or beyond, meta-analyses of standardized

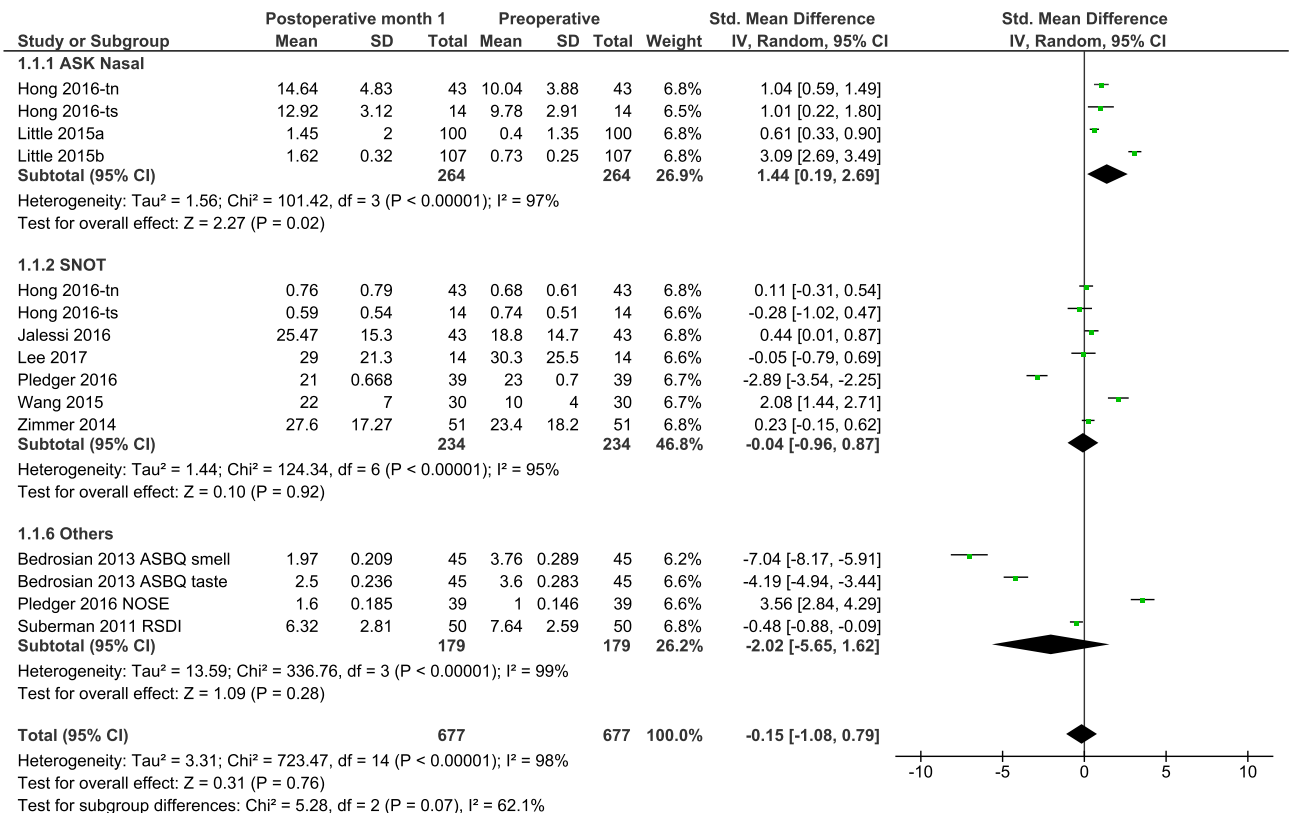

Fig. 1. *Forest graph of meta-analysis evaluating the changes in sinonasal QoL assessment tools at first postoperative month. In study identities, Hong 2016 tn and ts denotes transnasal and transseptal, respectively. Hong 2016 used SNOT-20 whereas the rest of the studies used SNOT-22 instrument.*

mean differences (SMD) were performed by using RevMan software (version 5.3.1; Cochrane Collaboration) to have inverse variance weighted effect sizes. Subgroup analyses were performed with regard to instruments. Between-study inconsistency was tested by I^2 index. For the assessment of publication bias, Begg's funnel plot symmetry and Egger`s precision tests were performed. All data are presented as weighted effect sizes with 95% confidence interval (CI).

Sixteen studies (5-19) fulfilled the eligibility criteria and therefore included in meta-analysis. In these studies, 931 patients with pituitary tumor underwent endoscopic surgery. There was no significant publication bias as indicated by the Begg's test (adjusted Kendall's Score = −8±20.18; p=0.692) or the Egger's test (bias coefficient = 0.302 [−9.94, 10.55]; p=0.950). Important characteristics of the included studies are presented in Table I. Mean age of these patients was 51.16 years [95% CI 49.13, 53.19] and 48.41% [43.74, 53.08] were male. QoL appraising instruments used in these studies included Anterior Skull Base Questionnaire (ASBQ), Anterior Skull Base Nasal Inventory (ASK Nasal), Rhinosinusitis Disability Index (RSDI), Sinonasal Outcome Test 20/22 (SNOT-20/22), and Vision-related QoL (VFQ).

Generally, there was no significant differences found between preoperative and postoperative scores at month 1 (SMD −0.15 [−1.08, 0.79]; p=0.76) or after 4 months (SMD −0.14 [−0.31, 0.03]; p=0.11). However, at postoperative month 1, assessment with ASK Nasal was associated with a significant change (SMD 1.44 [0.19, 2.69]; p=0.02) but SNOT scores were not significantly different before and after surgery (Fig. 1). At postoperative month 4, SNOT scores reduced significantly (SMD −0.38 [−0.55, −0.22]; p<0.00001) but scores of other

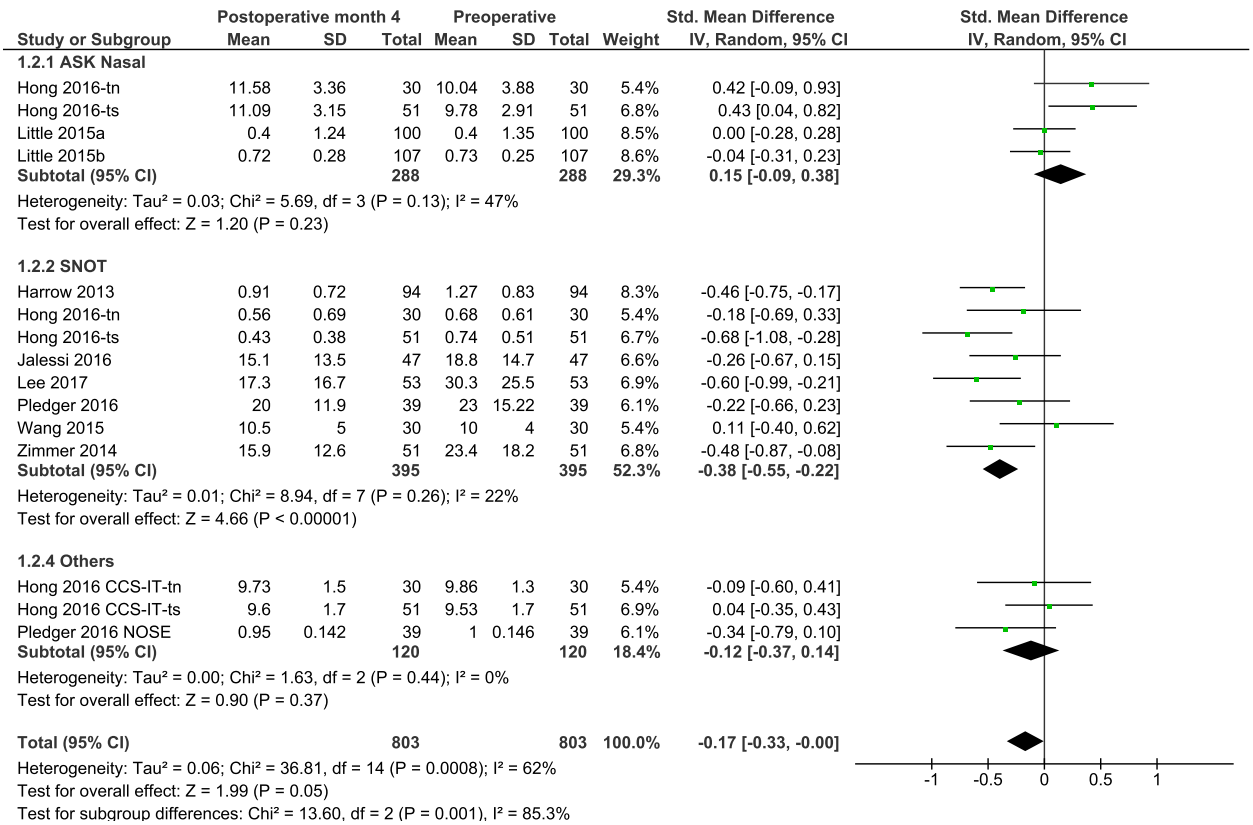

Fig. 2. *Forest graph of meta-analysis evaluating the changes in sinonasal QoL assessment tools at fourth postoperative month. In study identities, Hong 2016 tn and ts denotes transnasal and transseptal, respectively. Hong 2016 used SNOT-20 whereas the rest of the studies used SNOT-22 instrument.*

Table I. *Important characteristics of the included studies.*

Study	n	Age (years)	Males (%)	Design	QoL assessment tool	Pituitary tumor type	Surgery
Bedrosian 2013	45	51.1±11.6	48	Prospective non-RCT	ASBQ	Adenoma	Transsellar / transplanum / transtuberculum
Hong 2016	30	49.7±13.3	37	Retrospective	CCS-IT, ASBNI, SNOT-20	Non-functioning macro- / secretory adenoma	Transseptal / Transnasal transsphenoidal
Jalessi 2016	43	38.2±14.2	44	Prospective non-RCT	SNOT-22	Adenoma	Transsphenoidal
Lee 2017	14	56±11.3	33	Retrospective	SNOT-22	Adenoma	Septplasty / Inferior turbinoplasty
Little 2015a	100	51.7±15.5	44	Prospective non-RCT	ASK Nasal-12	Non-functioning adenoma	Transsphenoidal
Little 2015b	107	52.1±15.4	46	Prospective non-RCT	ASK Nasal-12, SF8, EQ-5D-5L	Non-functioning adenoma	Transsphenoidal
McCoul 2015	81	53.1±16.9	44	Prospective non-RCT	ASBQ, SNOT-22	Adenoma	Transsphenoidal / transethmoid / Transnasal / transmaxillary
Okamoto 2010	74	48.2±13.9	45	Prospective non-RCT	VFQ-25	Adenoma	Transsphenoidal
Pledger 2016	47	52±12	49	Prospective non-RCT	SNOT-22, NOSE,	Non-functioning adenoma	Transsphenoidal
Rioja 2016	38	48.9±3.5	36	Prospective non-RCT	BAST-24, SF36	Functional / non-functional adenoma	Transnasal transsphenoidal
Suberman 2011	50	53±12	71	Retrospective	RSDI	Functional / non-functional adenoma	Transnasal transsphenoidal
Tanemura 2012	30	53.5±14.6	57	Retrospective	GHQ30, SF36	Non-functioning macrodenoma	Transsphenoidal
Wang 2015	53	44.8±13.6	38	Prospective non-RCT	SNOT-22, SF36	Adenoma	Transsphenoidal
Wolf 2016	79	55.6±14.3	54	Prospective non-RCT	SF36	Micro- / macro-adenoma	Transsphenoidal
Wolf 2017	50	56.8±13.5	56	Prospective non-RCT	SF36	Adenoma	Transsphenoidal
Zimmer 2014	39	48	54	Prospective non-RCT	SNOT-22	Non-functional macroadenoma	Transnasal transsphenoidal

Abbreviations: ASBQ, Anterior Skull Base Questionnaire; ASK Nasal, Anterior Skull Base Nasal Inventory, BAST, Barcelona Smell Test; CCS-IT, Cross-Cultural Smell Identification Test; EQ-5D-5L, EuroQoL-5 dimensions-5 levels; GHQ, General Health Questionnaire; HRQoL, Health-related Quality of Life; NOSE, Nasal Obstruction Symptom Evaluation; QoL, quality of life; RCT, randomized controlled trial; RSDI, Rhinosinusitis Disability Index; SF, Short Form; SNOT, Sinonasal Outcome Test; VFQ, Vision-related Quality of Life

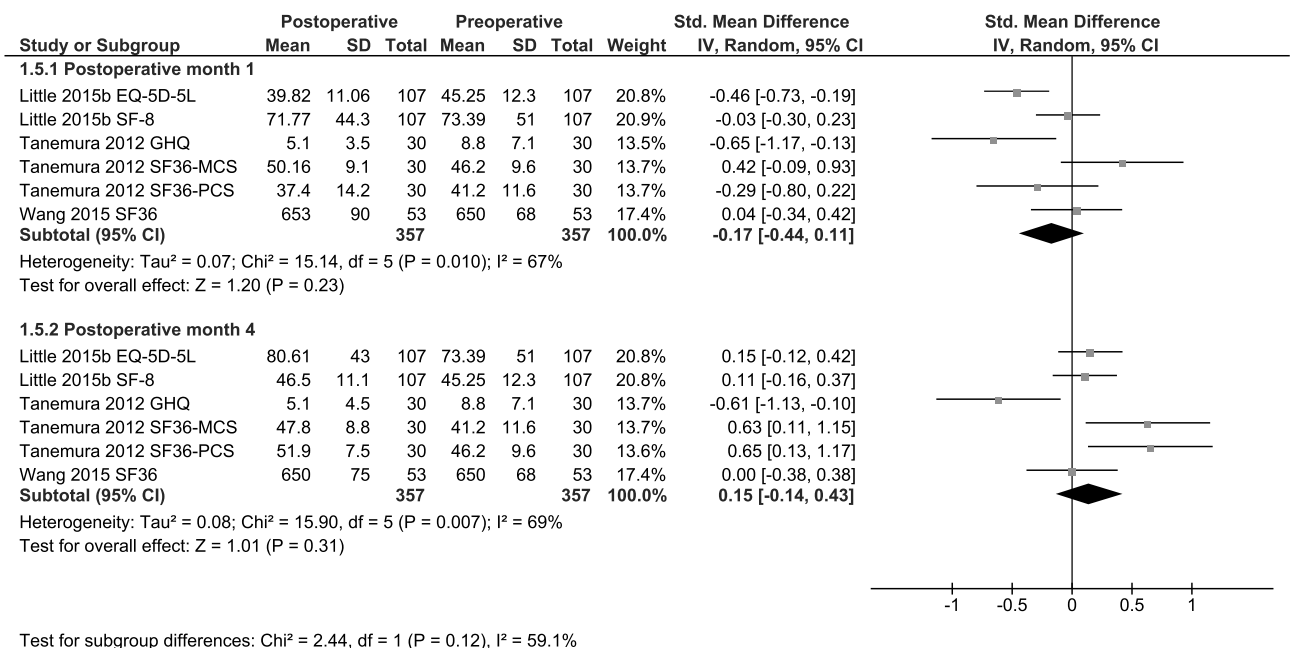

Fig. 3. *Forest graph of meta-analysis evaluating the changes in general health-related QoL one month and 4 months after surgery.*

instruments remained statistically indifferent (Fig. 2). Overall, there was no significant difference between preoperative and postoperative general health-related QoL at postoperative month 1 (SMD −0.17 [−0.44, 0.11]; p=0.23) or after fourth postoperative month (SMD 0.15 [−0.14, 0.43]; p=0.31) (Fig. 3).

Results of this meta-analysis show that endoscopic surgery for pituitary tumor is not associated with change in QoL as measured at postoperative months 1 or 4 or beyond with validated patient-reported tools, including general health-related QoL measuring tools and sinonasal tools especially the SNOT and ASK Nasal. In the present study, we observed that only the measurement with ASK Nasal was associated with significant difference between preoperative and 1-month postoperative scores but at the 4th month this difference vanished. We have detected that while SNOT scores were not significantly different from preoperative scores at postoperative month 1, SNOT scores reduced significantly at postoperative month 4. It is proposed that in patients with other medical conditions, SNOT-22 may over-rate the assessment which may be overcome by simultaneously using additional validated tools such as the ASBQ and/or NOSE.

The aim of endoscopic transsphenoidal surgery is to minimize the possibility of complications. Before surgery, it is therefore important that an otolaryngologist examines the nasal cavity for issues such as nasal polyposis, integrity of the posterior septal artery, septal perforations/deviations, turbinate obstruction etc. which may involve endoscopy and computed tomography. This allows for a better access through the nasal corridor to the Sella turcica for an efficient operation and is extremely important for maintaining a good postoperative QoL (7). Some limitations of the present study need to be considered while interpreting these QoL outcomes. Firstly, because of the reporting of QoL under a variety of instruments, especially in sinonasal assessments, the number of studies contributing data for the assessment of each tool's performance was limited. Only SNOT-based assessments had reasonable strength. Secondly, statistical heterogeneity was high for the majority of the analyses which demands the availability of more data from future studies for the refinement of the outcomes achieved in the present study.

Endoscopic pituitary surgery is not found to be associated with improved QoL. However, the surgery itself does not affect QoL except for postoperative month 1, which may also vary depending on the assessment tool. SNOT was not been found to be associated with any change in QoL at postoperative month 1 but may be associated with improvement in QoL after some months. ASK Nasal was found to reduce QoL at the first postoperative month which decreased by postoperative month 4. Thus, future studies may clarify the effects of these QoL tools.

REFERENCES

1. Little AS, Kelly D, Milligan J, et al. Prospective validation of a patient-reported nasal quality-of-life tool for endonasal skull base surgery: The Anterior Skull Base Nasal Inventory-12. J Neurosurg 2013; 119:1068-74.
2. McCoul ED, Anand VK, Bedrosian JC, Schwartz TH. Endoscopic skull base surgery and its impact on sinonasal-related quality of life. Int Forum Allergy Rhinol 2012 ; 2:174-81.
3. Berker M, Hazer DB, Yücel T, Gürlek A, Cila A, Aldur M, Onerci M. Complications of endoscopic surgery of the pituitary adenomas: analysis of 570 patients and review of the literature. Pituitary 2012; 15:288-300.
4. Ezzat S, Asa SL, Couldwell WT, Barr CE, Dodge WE, Vance ML, McCutcheon IE. The prevalence of pituitary adenomas: a systematic review. Cancer 2004; 101:613-19.
5. Cappabianca P, Cavallo LM, Esposito F, De Divitiis O, Messina A, De Divitiis E. Extended endoscopic endonasal approach to the midline skull base: the evolving role of transsphenoidal surgery. Adv Tech Stand Neurosurg 2008; 33:151-99.
6. Cusimano MD, Kan P, Nassiri F, et al. Outcomes of surgically treated giant pituitary tumours. Can J Neurol Sci 2012; 39:446-57.
7. Bedrosian JC1, McCoul ED, Raithatha R, Akselrod OA, Anand VK, Schwartz TH. A prospective study of postoperative symptoms in sinonasal quality-of-life following endoscopic skull-base surgery: dissociations based on specific symptoms. Int Forum

Allergy Rhinol 2013; 3:664-69.
8. Hong SD, Nam DH, Kong DS, Kim HY, Chung SK, Dhong HJ. Endoscopic modified transseptal transsphenoidal approach for maximal preservation of sinonasal quality of life and olfaction. World Neurosurg 2016; 87:162-69.
9. Jalessi M, Farhadi M, Asghari A, Hosseini M, Amini E, Pousti SB. Impact of endoscopic endonasal pituitary surgery on nasal airway patency. Med J Islam Repub Iran 2016; 30:379-86.
10. Lee DD, Peris-Celda M, Butrymowicz A, Kenning T, Pinheiro-Neto CD. Quality of life changes following concurrent septoplasty and/or inferior turbinoplasty during endoscopic pituitary surgery. World Neurosurg 2017; 98:303-7.
11. Little AS, Kelly D, Milligan J, et al. Predictors of sinonasal quality of life and nasal morbidity after fully endoscopic transsphenoidal surgery. J Neurosurg 2015; 122:1458-65.
12. Little AS, Kelly DF, Milligan J, et al. Comparison of sinonasal quality of life and health status in patients undergoing microscopic and endoscopic transsphenoidal surgery for pituitary lesions: a prospective cohort study. J Neurosurg 2015; 123:799-807.
13. McCoul ED, Bedrosian JC, Akselrod O, Anand VK, Schwartz TH. Preservation of multidimensional quality of life after endoscopic pituitary adenoma resection. J Neurosurg 2015; 123:813-20.
14. Okamoto Y, Okamoto F, Yamada S, Honda M, Hiraoka T, Oshika T. Vision-related quality of life after transsphenoidal surgery for pituitary adenoma. Invest Ophthalmol Vis Sci 2010; 51:3405-10.
15. Pledger CL, Elzoghby MA, Oldfield EH, Payne SC, Jane JA Jr. Prospective comparison of sinonasal outcomes after microscopic sublabial or endoscopic endonasal transsphenoidal surgery for nonfunctioning pituitary adenomas. J Neurosurg 2016; 125:323-33.
16. Rioja E, Bernal-Sprekelsen M, Enriquez K, et al. Long-term outcomes of endoscopic endonasal approach for skull base surgery: a prospective study. Eur Arch Otorhinolaryngol 2016; 273:1809-17.
17. Suberman TA, Zanation AM, Ewend MG, Senior BA, Ebert CS Jr. Sinonasal quality-of-life before and aer endoscopic, endonasal minimally invasive pituitary surgery. Int Forum Allergy Rhinol 2011; 1:161-66.
18. Tanemura E, Nagatani T, Aimi Y, Kishida Y, Takeuchi K, Wakabayashi T. Quality of life in nonfunctioning pituitary macroadenoma patients before and after surgical treatment. Acta Neurochir (Wien) 2012; 154:1895-902.
19. Wang S, Chen Y, Li J, Wei L, Wang R. Olfactory function and quality of life following microscopic endonasal transsphenoidal pituitary surgery. Medicine (Baltimore) 2015; 94(4):e465.

JOURNAL OF BIOLOGICAL REGULATORS & HOMEOSTATIC AGENTS Vol. 32, no. 5, 1157-1163 (2018)

LETTER TO THE EDITOR

EFFECTS OF FEMALE SEX HORMONES ON CHEMOTHERAPEUTIC PACLITAXEL-INDUCED NEUROPATHIC PAIN AND INVOLVEMENT OF INFLAMMATORY SIGNAL

YC. WANG[1*], N. LI[2*], Y. ZHAO[1] and LJ. ZHANG[1]

[1]Department of Thoracic Surgery, The First Hospital of Jilin University, Changchun, Jilin, China;
[2]Department of Neonatology, The First Hospital of Jilin University
Changchun, Jilin, China

Received May 21, 2018 Accepted June 15, 2018

*These Authors contributed equally to this work

Paclitaxel is used for the treatment of several types of cancers. However, one of its significant limiting complications is painful peripheral neuropathy during therapy. Gender is considered to play a role in modifying pain intensity. The present study examined the effects of female sex hormones on paclitaxel-induced neuropathic pain and the engagement of inflammatory signal of sensory nerves. Ovariectomies were performed on rats and subsequent hormone replacement with the combination of 17β-estradiol and progesterone was given. ELISA was used to determine the levels of proinflammatory cytokines (PICs) such as IL-1β, IL-6 and TNF-α in the dorsal root ganglion (DRG) of rats with different conditions of female sex hormones; moreover, Western blot analysis was used to examine expression of PIC receptors. The results of our study demonstrated that the increases of IL-1β, IL-6 and TNF-α; and expression of their respective receptors induced by paclitaxel were less in the DRG of ovariectomized rats with lack of female sex hormones. Thresholds of pain responses to mechanical and thermal stimuli appeared to be greater in ovariectomized rats with lack of female sex hormones. Overall, the findings indicate that circulating 17β-estradiol and progesterone contribute to the modulation of neuropathic pain response after administration of paclitaxel, likely via PIC signal in the sensory nerves, which is implicated to consider sex difference for pain management with application of chemotherapeutic paclitaxel.

To the Editor,

One of the most common and distressing symptoms suffered by patients with progression of cancer is pain (1). Cancer pain mainly arises from a tumor compressing or infiltrating tissue; from nerve and other changes caused by a hormone imbalance or immune response; and/or from treatments and diagnostic procedures (1, 2). It should be noted that cancer treatments (i.e., chemotherapy and radiotherapy) produce painful conditions that often persist after the treatment has ended (1, 2). Thus, improving the management of symptoms related to cancer therapies is of great clinical importance.

Paclitaxel is a widely prescribed chemotherapeutic agent for the treatment of breast, lung and other cancers, but is associated with a variety of serious side effects, including peripheral neuropathy, leukopenia, joint or muscle pain, vomiting and alopecia (3). Chemotherapy-induced peripheral neuropathy causes severe sensory disturbances that range from mild tingling to spontaneous painful burning paresthesia affecting the sensory nerves

Key words: 17β-estradiol, progesterone, cytokine, sensory nerve, chemotherapy, neuropathic pain

Mailing address:
Dr Lian-Jie Zhang,
Department of Thoracic Surgery,
The First Hospital of Jilin University, 71 Xinmin Street,
Changchun, Jilin 130021, China
e-mail: lianjie.zhang@aol.com

0393-974X (2018)

in the hands and feet and can persist long after cessation of chemotherapy treatment (4). Treatment options for these abnormal sensations have been restricted, partly due to a poor understanding of the underlying mechanisms responsible for neuropathic pain induced by paclitaxel. Many factors influence chemotherapy-induced peripheral neuropathy, including patient age and gender.

In addition, clinical and experimental studies suggest that pain responses vary between male and female individuals (5). An increase in neuropathic pain was reported in female as compared with male in many models of neuropathic pain (5, 6), likely due to the levels of sex hormones. Though there are many mechanisms involved, there is insufficient evidence showing a relation between female sex hormones and paclitaxel-induced neuropathic pain. Since IL-1β, IL-6 and TNF-α in sensory nerves are involved, the purpose of the current study was to examine the effects of female sex hormones, namely 17β-estradiol (17β-EST) and progesterone (PGR) on the levels of IL-1β, IL-6 and TNF-α and their receptors (IL-1R, IL-6R and TNFR1) in the dorsal root ganglion (DRG) of rats injected with paclitaxel. We further examined these hormones on pain responses to mechanical and thermal stimuli. We hypothesized that lack of 17β-EST and PGR decreases the inflammatory signal in the DRG of rats with paclitaxel and this thereby leads to a lesser degree of neuropathic pain.

MATERIALS AND METHODS

Animals

All animal protocols were in accordance with the guidelines of the International Association for the Study of Pain and approved by the Institutional Animal Care and Use Committee of Jilin University. Adult female Sprague-Dawley rats (150-200g) were housed in individual cages with free access to food and water and were kept in a room at 25°C on a 12/12 h light/dark cycle.

Surgical ovariectomy

Under isoflurane anesthesia, a sham operation or bilateral ovariectomy was performed. A week after the surgery, the ovariectomized rats received subcutaneous implantation of a placebo (PBO) or pellets (Innovative Res., Sarasota, FL) containing sex hormones (17β-EST, 0.25 mg and PGR, 50 mg) released over a 21-day period. Accordingly, the rats were divided into the groups: sham control; placebo; and a combination of 17β-EST and PGR.

A model of neuropathic pain and administration of drugs

Paclitaxel (Tocris Biosci) was dissolved in a 40% dimethyl sulfoxide (DMSO). Neurotoxicity was induced in rats by intraperitoneal (i.p.) injection of paclitaxel (1 mg/kg/one injection in 0.5 ml of volume) every two days and a total of four injections were given in sham control rats and ovariectomized rats with PBO and a combination of 17β-EST and PGR. Control rats (for paclitaxel) received four injections of 40% DMSO (0.5 ml) every two days. Mechanical and thermal hypersensitivity were fully developed by paclitaxel after four injections and experiments were performed. Then, mechanical and thermal sensitivity was tested and the DRGs (L4-L6) were removed to determine PIC signal.

Behavioral test

To quantify the mechanical sensitivity of the hind paw, rats were placed in individual plastic boxes and allowed to acclimate for > 30 min. Mechanical paw withdrawal threshold (PWT) of rat hind paw in response to the stimulation of von Frey filaments was determined. A series of calibrated von Frey filaments (ranging from 0.5 to 18.0 g) were applied perpendicularly to the plantar surface of the hind paw with a sufficient force to bend the filaments or until the paw withdrew. In the presence of a response, the filament of next lower force was applied. In the absence of a response, the filament of next greater force was applied. To avoid injury during tests, the cutoff strength of the von Frey filament was 18 g. The tactile stimulus producing a 50% likelihood of withdrawal was determined using the "up-down" method. Each trial was repeated 2 times at approximately 2 min intervals. The mean value was used as the force produced a withdrawal response.

To determine thermal hyperalgesia, rat paw withdrawal latency (PWL) to a radiant heat was measured. Rats were placed individually in plastic cages on an elevated glass platform and allowed for 30 min acclimation. Each hind paw received three stimuli with a 10 min interval, and the mean of the three withdrawal latencies was defined as

PWL. The heat was maintained at a constant intensity. To prevent tissue damage, the cut-off latency was set at 20 s. All the behavioral tests were performed in a blind style.

ELISA measurement

This method was used to examine the levels of IL-1β, IL-6 and TNF-α according to the provided description (Promega Corp. Madison, WI, USA). Briefly, polystyrene 96-well microtitel immunoplates were coated with affinity-purified polyclonal rabbit anti-IL-1β, anti- IL-6 and anti-TNF-α antibodies. Parallel wells were coated with purified rabbit IgG for evaluation of nonspecific signal. After overnight incubation at room temperature and 2 h incubation with the coating buffer containing 50 mM carbonate buffer (pH 9.5) in 2% BSA, plates were washed with 50 mM Tris-HCl. After extensive washing,

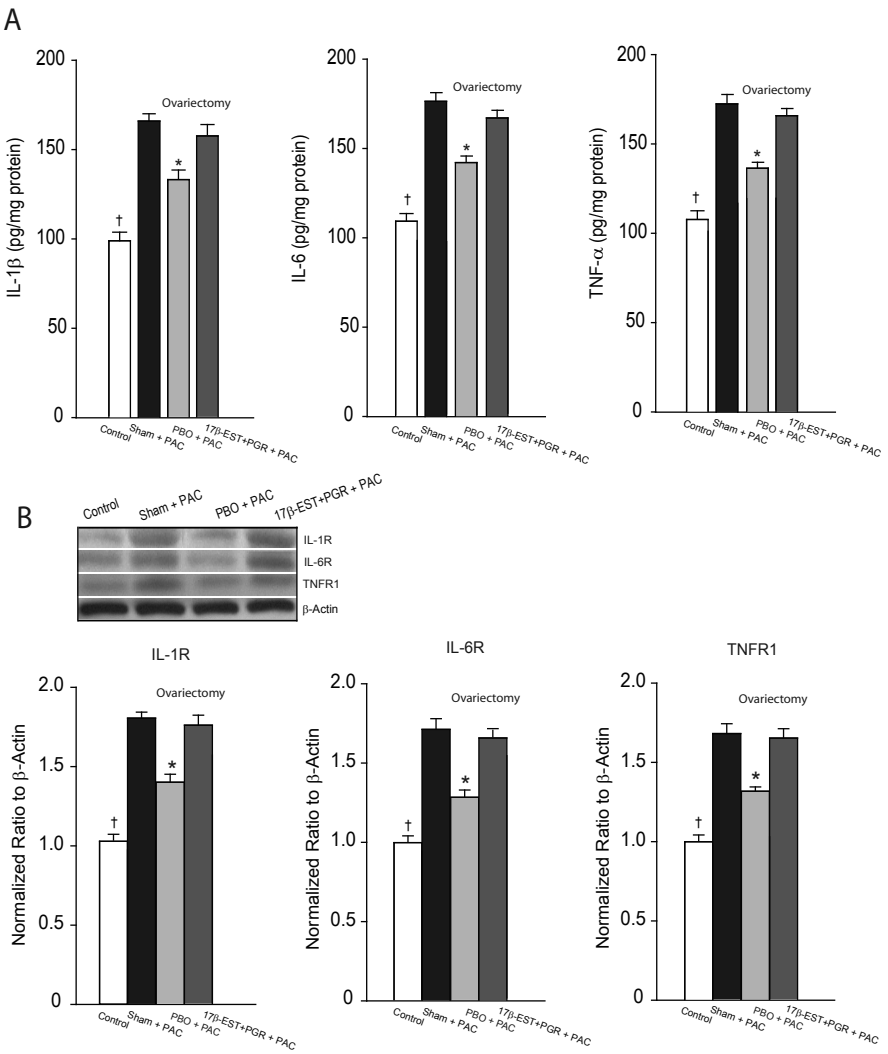

Fig. 1. *Levels of PIC and expression of PIC receptors.* ***A)*** *Paclitaxel (PAC) amplified IL-1β, IL-6 and TNF-α in the DRG as compared with other groups without PAC. After PAC was given, deficiency of female sex hormones attenuated increases of IL-1β, IL-6 and TNF-α in the ovariectomized rats with placebo (PBO) as compared with sham control rats and rats with replacement of hormones (n=12 for each groups). †P < 0.05 vs all other groups, and *P < 0.05 vs sham control and group of 17β-EST and PGR. 17β-EST: 17β-estradiol; PGR: progesterone.* ***B)*** *Top panel and bottom panel are typical band and average data, showing that protein expression levels of PIC receptors (IL-1R, IL-6R and TNFR1) were upregulated with injection of PAC. Lack of female sex hormones attenuated increases of those PIC receptors induced by PAC in the ovariectomized rats with PBO. †P < 0.05 vs all other groups, and *P < 0.05 vs sham control and combination of 17β-EST and PGR. The number of rats = 6-12 in each group.*

the diluted samples and the IL-1β, IL-6 and TNF-α standard solution were distributed in each plate and left at room temperature overnight. The plates were washed and incubated with anti-IL-1β, anti-IL-6 and anti-TNF-α galactosidase per well. Then, the plates were washed and incubated with substrate solution. After an incubation of 2 h at 37°C, an ELISA reader was used to determine the optical density.

Western blot analysis

After being denatured by heating at 95°C in an SDS sample buffer, the supernatant samples were loaded onto Mini-Protean TGX Precast gels and electrically transferred to a polyvinylidene fluoride membrane. The membrane was then incubated overnight with primary antibodies: rabbit anti-IL-1R, anti-IL-6R and anti-TNFR1 (Abcam Co., diluted 1:200). After being fully washed, the

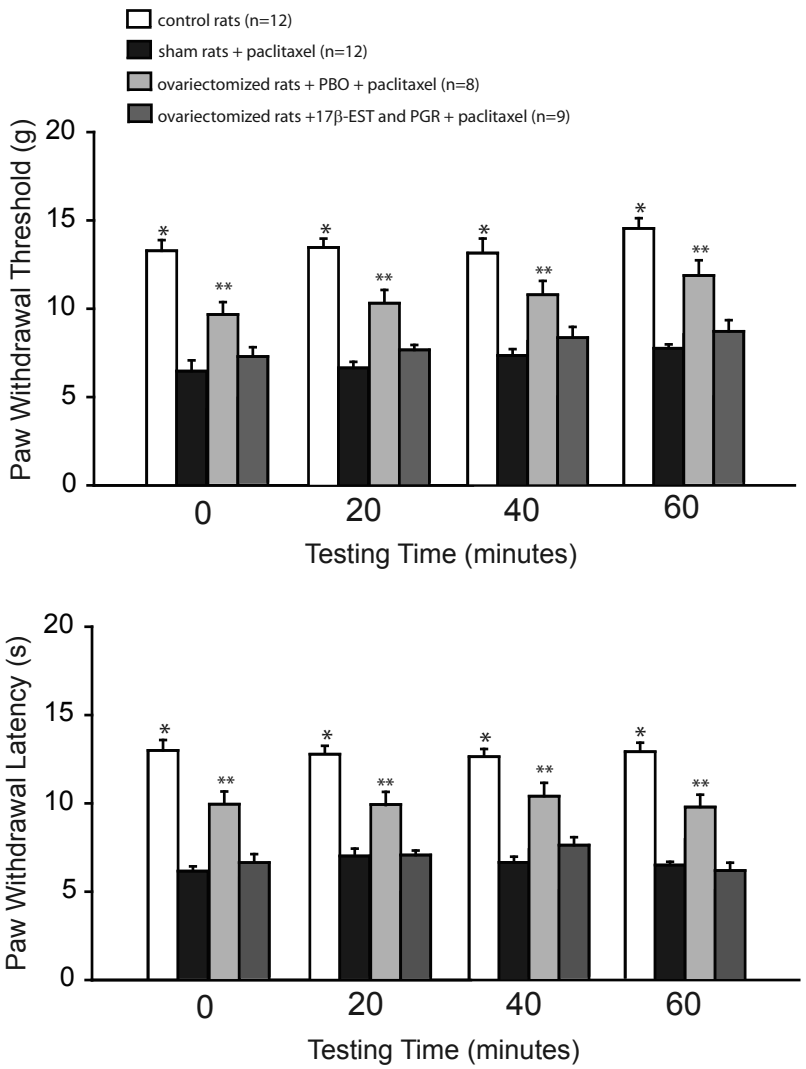

Fig. 2. *Mechanical and thermal sensitivity during 60 munities of testing. Top panel: Effects of female sex hormone deficiency on mechanical hypersensitivity induced by paclitaxel. Paclitaxel decreased PWT, but this effect was attenuated in the ovariectomized rats with PBO. Bottom panel: Effects of lacking of female sex hormone on thermal hypersensitivity induced by paclitaxel. In the ovariectomized rats with PBO, paclitaxel decreased PWL to a less degree as compared with sham control rats and ovariectomized rats with 17β-EST and PGR. *P < 0.05 vs all other groups. ** P < 0.05 vs sham control rats and the ovariectomized rats with 17β-EST and PGR after administration of paclitaxel. The number of animals is indicated in the figure.*

membrane was incubated with horseradish peroxidase-linked anti-rabbit secondary antibody and visualized for immunoreactivity. The membrane was stripped and incubated with mouse anti-β-actin to show equal loading of the protein. The bands recognized by the primary antibody were visualized by exposure of the membrane onto an X-ray film. Then, the film was scanned and the optical densities of IL-1R, IL-6R, TNFR1 and β-actin bands were determined using the Scion Software. Then, values for densities of immunoreactive bands/β-actin band from the same lane were determined. Each of the values was then normalized to a control sample.

Statistical analysis

All data were analyzed using one-way repeated-measure analysis of variance. Values were presented as means ± standard error of mean (SEM). For all analyses, differences were considered significant at $P < 0.05$. All statistical analyses were performed by using SPSS for Windows version 13.0 (SPSS, USA).

RESULTS

Levels of PICs and their receptor expression

Fig. 1A demonstrates that IL-1β, IL-6 and TNF-α were increased in the DRG of rats injected with paclitaxel as compared with control rats (n=12 in each group). However, increases of IL-1β, IL-6 and TNF-α were attenuated in the ovariectomized rats with PBO as compared with sham control rats and rats with replacement of hormones ($P < 0.05$, PBO group *vs* sham control and combination of 17β-EST and PGR). Likewise, Fig. 1B further shows that protein expression levels of PIC receptors (IL-1R, IL-6R and TNFR1) were upregulated with injection of paclitaxel. Lack of female sex hormones attenuated increases of those PIC receptors induced by paclitaxel in the ovariectomized rats with PBO ($P < 0.05$, PBO group *vs* sham control and combination of 17β-EST and PGR; n=6-12 in each group).

Mechanical and thermal sensitivity

Fig. 2 shows that paclitaxel induced mechanical and thermal hypersensitivity. During 60 munities of testing, PWT and PWL were decreased in rats injected with paclitaxel ($P < 0.05$ *vs* rats without paclitaxel). We further examined the effects of female sex hormone deficiency on mechanical and thermal hypersensitivity induced by paclitaxel. In the ovariectomized rats with PBO (n=8), decreases of PWT and PWL induced by paclitaxel appeared to be less as compared with sham control rats (n=12) and the ovariectomized rats with replacement of 17β-EST and PGR (n=9; $P < 0.05$, PBO *vs* sham control and replacement of 17β-EST and PGR).

DISCUSSION

Neuropathic pain is one of the complications of paclitaxel, and pain intensity varies due to gender. Nonetheless, the effects of female sex hormones on paclitaxel-induced neuropathic pain are largely unknown. Data of the current study provide new evidence showing that lack of 17β-EST and PGR attenuates upregulation of IL-1β, IL-6 and TNF-α and their receptor expression in the DRG of rats with administration of paclitaxel and this thereby alleviates neuropathic pain in rats with paclitaxel.

In sensory nerves, the role of PICs in regulating pain has been studied. Use of IL-1RA (IL-1R antagonist) has been shown to relieve rheumatoid arthritis–associated pain (7). IL-1RA treatment in rodents decreases pain-related behaviors evoked in models of inflammation, bone cancer and intramuscular acid injection (8, 9). In this report, we found less expression of IL-1β and its receptor IL-1R in the DRG of rats with lack of female sex hormones after administration of paclitaxel, and in those rats PWT and PWL were greater as compared with sham rats and rats with replacement of sex hormones. It is likely that downregulation of IL-1R by reductions in female sex hormones can attenuate mechanical and thermal hypersensitivity in rats injected with paclitaxel.

In animals, IL-6 causes hypersensitivity to thermal and mechanical stimuli (10). Prior studies suggest that IL-6 is a key inflammatory cytokine involved in pain (11, 12). Intraplantar administration of IL-6 in mice evokes mechanical hyperalgesia, and in IL-6 knockout mice mechanical and thermal hyperalgesia are reduced after carrageenan injection into the paw (13). IL-6 also produces acute

hyperalgesia and evokes chronic latent hyperalgesia (14), inferring a key role of IL-6 in acute and chronic muscle pain. Thus, in the current study we suggest engagement of the IL-6 signal in mechanical and thermal hyperalgesia induced by paclitaxel as circulating female sex hormones are different. Our data demonstrated that neuropathic pain induced by paclitaxel appears to be reduced with decreases in female sex hormones.

TNF-α produces its effects via activation of two TNF-α receptor subtypes, TNFR1 and TNFR2 (15). TNFR1 is expressed exclusively on neuronal cells and plays a functional role, whereas TNFR2 is located predominantly on macrophages and/or monocytes in response to inflammation. TNF-α activation appears most relevant to the development of afferent nerve-mediated behavior via the TNFR1. Mechanical hyperalgesia induced by exogenous TNF-α and/or by inflammation is reduced in TNFR1 but not TNFR2 knockout mice and TNFR1 but not TNFR2 neutralizing antibodies reduce experimental hyperalgesia (16, 17). In the current study, we observed less expression of TNFR1 receptors in the DRG of the ovariectomized rats with PBO, but not in sham control rats nor the ovariectomized rats with sex hormone replacement. Nonetheless, we also observed that mechanical and thermal pain were less in the ovariectomized rats with PBO, suggesting involvement of TNF-α in modifying neuropathic pain induced by paclitaxel under conditions of different female sex hormones.

Overall, our data suggest that the role of 17β-EST and PGR in modifying the neuropathic pain induced by paclitaxel and the effects should be exerted by both 17β-EST and PGR. The effects by each of them need to be considered in future study.

REFERENCES

1. Hanna Magdi, Zylicz Z (eds). Cancer Pain, Springer-Verlay, London 2013.
2. Pasetto LM, D'Andrea MR, Rossi E, Monfardini S. Oxaliplatin-related neurotoxicity: How and why? Crit Rev in Oncol/Hematol 2006; 59:159-68.
3. Ghersi D, Willson ML, Chan MM, Simes J, Donoghue E, Wilcken N. Taxane-containing regimens for metastatic breast cancer. Cochrane Database Syst Rev 2015; 10.1002/14651858.CD003366.pub3Cd003366.
4. Tanabe Y, Hashimoto K, Shimizu C, et al. Paclitaxel-induced peripheral neuropathy in patients receiving adjuvant chemotherapy for breast cancer. Int J Clin Oncol 2013; 18:132-38.
5. Abraham A, Barnett C, Katzberg HD, Lovblom LE, Perkins BA, Bril V. Sex differences in neuropathic pain intensity in diabetes. J Neurol Sci 2018; 388:103-6.
6. Legakis LP, Negus SS. Repeated morphine produces sensitization to reward and tolerance to antiallodynia in male and female rats with chemotherapy-induced neuropathy. J Pharmacol Exp Ther 2018; 365:9-19.
7. Hallegua DS, Weisman MH. Potential therapeutic uses of interleukin 1 receptor antagonists in human diseases. Ann Rheum Dis 2002; 61:960-67.
8. Borghi SM, Zarpelon AC, Pinho-Ribeiro FA, et al. Targeting interleukin-1beta reduces intense acute swimming-induced muscle mechanical hyperalgesia in mice. J Pharm Pharmacol 2014; 66:1009-20.
9. Sutton BC, Opp MR. Acute increases in intramuscular inflammatory cytokines are necessary for the development of mechanical hypersensitivity in a mouse model of musculoskeletal sensitization. Brain Behav Immun 2015; 44:213-20.
10. Iwatsuki K, Arai T, Ota H, et al. Targeting anti-inflammatory treatment can ameliorate injury-induced neuropathic pain. PLoS One 2013; 8:e57721.
11. Manjavachi MN, Motta EM, Marotta DM, Leite DFP, Calixto JB. Mechanisms involved in IL-6-induced muscular mechanical hyperalgesia in mice. Pain 2010; 151:345-55.
12. Dina OA, Green PG, Levine JD. Role of interleukin-6 in chronic muscle hyperalgesic priming. Neuroscience 2008; 152:521-25.
13. Xu XJ, Hao JX, Andell-Jonsson S, Poli V, Bartfai T, Wiesenfeld-Hallin Z. Nociceptive responses in interleukin-6-deficient mice to peripheral inflammation and peripheral nerve section. Cytokine 1997; 9:1028-33.
14. Dina OA, Levine JD, Green PG. Muscle inflammation induces a protein kinase Cepsilon-dependent chronic-latent muscle pain. J Pain 2008; 9:457-62.
15. MacEwan DJ. TNF receptor subtype signalling:

differences and cellular consequences. Cell Signal 2002; 14:477-92.

16. Sommer C, Schmidt C, George A. Hyperalgesia in experimental neuropathy is dependent on the TNF receptor 1. Exp Neurol 1998; 151:138-42.
17. Parada CA, Yeh JJ, Joseph EK, Levine JD. Tumor necrosis factor receptor type-1 in sensory neurons contributes to induction of chronic enhancement of inflammatory hyperalgesia in rat. Eur J Neurosci 2003; 17:1847-52.

LETTER TO THE EDITOR

DETECTION OF SERUM PROCALCITONIN AND HYPERSENSITIVE C-REACTIVE PROTEIN IN PATIENTS WITH PNEUMONIA AND SEPSIS

G.B. LIU[1], X.Q. CUI[2], Z.B. WANG[3], L. WEN[4] and H.L. DUAN[2]

[1]Clinical Laboratory, Binzhou City Center Hospital, Bingzhou, China; [2]Hemodialysis Room, Binzhou City Center Hospital, Bingzhou, China; [3]Neurosurgery, Binzhou City Center Hospital, Bingzhou, China; [4]Ophthalmology Department, Binzhou City Center Hospital, Bingzhou, China

Received November 21, 2017 – Accepted June 26, 2018

Sepsis, a systemic inflammatory response syndrome induced by infection, has high rates of morbidity and mortality. Pneumonia is a major cause for sepsis; however, pneumonia complicated by sepsis is a difficult clinical diagnosis. To assess the clinical relevance of serum procalcitonin (PCT) and hypersensitive C-reactive protein (hs-CRP) in early diagnosis of pneumonia complicated by sepsis, 220 patients with pneumonia who were admitted to hospital from July 2015 to July 2016 were enrolled in this study. The patients were divided into non-sepsis (N=82), mild sepsis (N=97), severe sepsis (N=23), and septic shock (N=18) groups. The patients were also divided into a survival group (N=186) and a death group (N=34) according to their prognosis at 2 weeks. The PCT and hs-CRP levels and Acute Physiology and Chronic Health Evaluation-II (APACHE-II) scores of the two groups were evaluated. The PCT level and APACHE-II score showed a progressively increasing tendency in the non-sepsis, mild sepsis, severe sepsis, and septic shock group; the differences between all pairs of groups were significant (P<0.05). The hs-CRP level was significantly lower in the non-sepsis group than in the other groups (P<0.05), but differences among the other groups were not significant (P>0.05). The areas under the receiver operating characteristic curves of PCT and hs-CRP for diagnosis of pneumonia complicated by mild and severe sepsis were 0.841 and 0.817, respectively. The optimal cut-off points for pneumonia and sepsis were ≥0.5 ng/mL and ≥55 mg/L, respectively; the sensitivity and specificity were 71.42% and 82.13%, and 75.04% and 53.61%, respectively. The sensitivity and specificity of diagnosis based on PCT and hs-CRP were 89.32% and 85.68%, respectively. PCT and hs-CRP are used to assess the severity of pneumonia in combination with sepsis in new-borns, but PCT is more strongly related to the severity of sepsis than is hs-CRP. Detection of PCT in combination with hs-CRP facilitates the early diagnosis of pneumonia and sepsis in new-borns, as well as monitoring of the treatment response and prediction of the prognosis.

To the Editor,

Sepsis is a systemic inflammatory response syndrome induced by microgranism infection (1) and has a high mortality rate (2). Hugonnet et al. (3) found that the most frequent primary-infection sites are the lung (28.7%), blood (20.4%), skin and soft tissue (15.3%), as well as intubation sites and urinary tract (11.2%). Therefore, pneumonia is one of the main causes of sepsis. Diagnosis of early-stage pneumonia complicated by sepsis is difficult because of the lack of specific clinical manifestations and diagnostic indices and the insensitivity of culture

Key words: sepsis, hypersensitive C-reactive protein, serum procalcitonin

Mailing address:
Dr Guanbin Liu,
No. 108 Huancheng South Road,
Binzhou City Central Hospital,
Bingzhou, Shandong, 251700, China
Tel./Fax: 0543-5323832
e-mail: liuguanb11@163.com

0393-974X (2018)

(4). Hence, early identification and diagnosis are important for improving the prognosis of pneumonia complicated by sepsis.

The level of procalcitonin (PCT), which is associated with bacterial infection, has high specificity. The level of hypersensitive C-reactive protein (hs-CRP), an acute-phase-reaction protein synthesised by the liver, reflects infection. The CRP level increases significantly in the acute phase of bacterial infection and subsequently normalises or remains slightly increased (5). In infants, increased levels of hs-CRP and PCT indicate bacterial infection. This leads to the following question: do the hs-CRP and PCT levels reflect the severity of pneumonia in combination with sepsis? In this study, we aimed to improve the early diagnosis and treatment of pneumonia complicated by sepsis using the PCT and hs-CRP levels.

MATERIALS AND METHODS

General data

Two hundred and twenty new-borns with pneumonia who were admitted to the Binzhou City Central Hospital, Shandong, China, between July 2015 and July 2016, were enrolled in this study. All of them satisfied the 2006 Guidelines for the Diagnosis and Treatment of Community-acquired Pneumonia (6). Patients with other pulmonary diseases, such as tuberculosis, interstitial lung disease and lung tumour, trauma, burn injury, autoimmune disease, malignant carcinoma, or severe dysfunction of organs, such as the heart, liver, and kidney, as well as those with histories of surgical treatment, were excluded. The patients comprised 127 males and 93 females aged 38-42 weeks (average 38.7±6.3 weeks). According to the standards of the Society of Critical Care Medicine, the European Society of Intensive Care Medicine, the American College of Chest Physicians, the American Thoracic Society, and the Surgical Infection Society (7), they were divided into non-sepsis (N=82), mild sepsis (N=97), severe sepsis (N=23), and septic shock (N=18) groups. The non-sepsis group comprised 51 males and 31 females aged 38-41 weeks (average 38.5±6.5 weeks). The mild sepsis group comprised 52 males and 45 females aged 37-41 weeks (average 38.2±6.2 weeks). The severe sepsis group comprised 13 males and 10 females aged 39-42 weeks (average 39.3±5.8 weeks). The septic shock group comprised 12 males and 6 females aged 39-41 weeks (average 39.5±6.2 weeks). The demographic parameters did not differ significantly among the four groups ($P>0.05$). Moreover, the 220 patients were divided into a survival group (N=186) and a death group (N=34). The survival group comprised 108 males and 78 females with an average age of 39.2±5.8 weeks. The death group comprised 19 males and 15 females with an average age of 38.8±6.1 weeks. This study was approved by the ethics committee of Binzhou City Center Hospital, Bingzhou, China, and the parents of the new-borns provided written informed consent.

Fasting venous blood (3 mL) was collected 24 h after admission, transferred to an ethylenediaminetetraacetic acid disodium salt anticoagulant tube, and centrifuged at 3000 r/min and 4°C to separate plasma. PCT was assayed using an immunochemistry analyser (Beckman Coulter Co., Ltd., China) by double-antibody sandwich immunofluorescence; levels of <0.1 μg/L and >0.5 μg/L were considered to be normal and positive, respectively. hs-CRP was assayed using an Olympus-AU640 Automated Biochemistry Analyzer by immune-scatter velocity turbidimetry; a level of 0-1 mg/L was considered to be normal. In addition, the Acute Physiology and Chronic Health Evaluation-II (APACHE-II) scores of all patients were evaluated in the 24 h after admission; higher scores indicated more severe disease.

Statistical analysis

Data were statistically analysed using SPSS ver. 21.0. Measurement data are expressed as means ± standard deviations. Comparisons of means between two groups were performed by *t*-test. Comparisons of means among multiple groups were performed by analysis of variance. A receiver operating characteristic (ROC) curve was generated to analyse the utility of PCT and hs-CRP in detecting pneumonia in combination with severe sepsis. $P<0.05$ was taken to indicate statistical significance.

RESULTS

PCT level, hs-CRP level, and APACHE-II scores

The PCT level and APACHE-II score showed an increasing tendency in the non-sepsis, mild sepsis, severe sepsis, and septic shock groups,

and the differences between all pairs of groups were significant (P<0.05). The hs-CRP level was significantly lower in the non-sepsis group than in the other groups (P<0.05); however, the differences in hs-CRP level among the other groups were not significant (P>0.05; Table I).

Table I. *PCT levels, hs-CRP levels, and APACHE-II scores (Mean±SD).*

Group	PCT (μg/L)	hs-CRP (mg/L)	APACHE-II (point)
Non-sepsis	0.83±0.21	37.41±11.63	5.26±0.22
Mild sepsis	1.35±0.86[a]	90.14±19.24[a]	9.43±2.14[a]
Severe sepsis	3.61±1.27[ab]	106.72±20.35[a]	13.96±3.71[ab]
Septic shock	5.93±1.91[abc]	108.13±21.08[a]	18.29±4.92[abc]

Note: P<0.05 compared with the [a] non-sepsis group, [b] mild sepsis group, and [c] severe sepsis group.

Table II. *PCT levels, hs-CRP levels, and APACHE-II scores in the survival and death group (Mean±SD).*

Group	PCT (μg/L)	hs-CRP(mg/L)	APACHE-II (point)
Survival	2.45±1.04	49.48±13.81	7.86±2.18
Death	5.24±2.16	104.27±15.64	13.09±3.65
t	12.753	16.081	9.976
P-value	<0.05	<0.05	<0.05

Table III. *AUROCs of levels of PCT and hs-CRP in diagnosing pneumonia in complicated with sepsis.*

Item	Area	P-value	Confidence interval
PCT	0.841	0.00	0.785-0.897
hs-CRP	0.817	0.00	0.762-0.876

Table IV. *Performance of PCT and hs-CRP levels for pneumonia complicated by sepsis.*

Item	Sensitivity (%)	Specificity (%)	Positive likelihood ratio	Negative likelihood ratio	Accuracy (%)
PCT ≥ 0.5 ng/mL	71.42	75.04%	2.86	0.38	73.22
hs-CRP ≥ 55 mg/L	82.13	53.61	1.76	0.34	67.88
PCT ≥ 0.5 ng/mL + hs-CRP≥55 mg/L	89.32	85.68	4.03	0.14	87.52

PCT levels, hs-CRP levels, and APACHE-II scores in the survival and death group

The levels of hs-CRP and PCT and the APACHE-II score were significantly higher in the death group than in the survival group ($P<0.05$; Table II).

Diagnostic value

ROC curves for diagnosis of pneumonia complicated by mild and severe sepsis and by septic shock are shown in Fig. 1. The areas under the ROC curves of the PCT and hs-CRP levels for the diagnosis of pneumonia complicated by sepsis are shown in Table III. The optimal cut-off points for the diagnosis were ≥0.5 ng/mL and ≥55 mg/L, respectively (Table IV).

DISCUSSION

CRP is a non-specific marker of inflammation (8), the level of which increases upon development of inflammation and peaks at 48 h. However, bacterial infection, trauma, and chronic inflammation can cause an increase in the CRP level. Here, the hs-CRP level was significantly lower in the non-sepsis group than in the other groups, similar to the findings of Flores et al. (9). Thus, a change in the hs-CRP level is indicative of infection.

PCT is a novel biomarker of systemic bacterial infection (10). Uzzan et al. (11) found that the PCT level increased upon development of acute or chronic pneumonia, systemic inflammatory response syndrome, trauma, and acute pancreatitis and increased with increasing infection severity; these findings are consistent with our results.

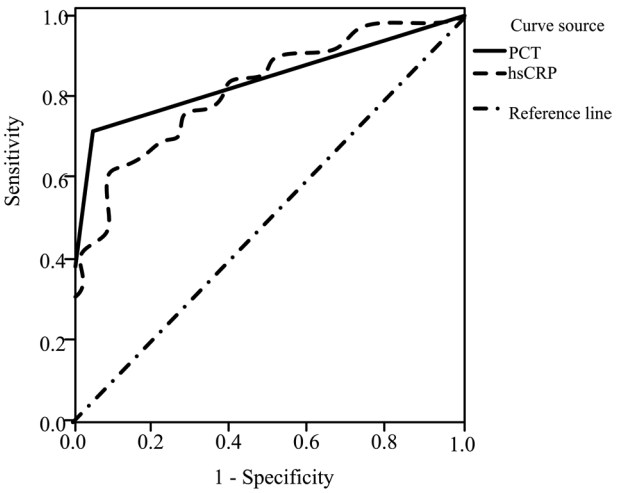

Fig. 1. *ROC curves for PCT and hs-CRP levels for the diagnosis of pneumonia complicated by sepsis.*

PCT and hs-CRP have moderate value for the diagnosis of pneumonia complicated by severe sepsis or septic shock; the specificity of PCT is superior to that of hs-CRP, and the opposite is true for sensitivity. Oh et al. (12) reported that diagnosis of severe sepsis and septic shock using a PCT cut-off level of ≥ 2 mg/mL had a sensitivity of 93.94% and specificity of 87.23%. The difference between our results and the findings of Oh et al. (12) may be because the latter were obtained in emergency patients and the former were obtained in hospitalised patients with pneumonia.

hs-CRP and PCT levels are therefore associated with the severity of infection and are predictive of sepsis. This work will facilitate the early diagnosis of pneumonia complicated by sepsis, evaluation of disease progression, and improvement of the prognosis. The results revealed that the change of PCT level was consistent with the severity of infection.

In the diagnosis of pneumonia complicated with severe sepsis and septic shock, PCT and hs-CRP have moderate values; the specificity of PCT was superior to that of hs-CRP, but the sensitivity of hs-CRP was superior to that of PCT. Oh et al. (12) reported that the sensitivity of diagnosing severe sepsis and septic shock by taking level of PCT ≥ 2 mg/mL as the cutoff point was 93.94% (higher than the result of this study) and the specificity was 87.23 % (close to the result of this study). Different sensitivity of PCT may be associated to the different sources of patients. The study of Oh took emergency patients as the research subjects, while this study took hospitalized pneumonia patients as the research subjects.

In conclusion, hs-CRP and PCT are associated to the severity of infection. Detection of hs-CRP and PCT can be regarded as the predictor for sepsis. This work is of great clinical significance for the early definite diagnosis of pneumonia complicated with sepsis, timely evaluation of disease progress and improvement of prognosis.

REFERENCES

1. Dellinger RP, Levy MM, Rhodes A, et al. Surviving sepsis campaign: international guidelines for management of severe sepsis and septic shock: 2012. Crit Care Med 2013; 41(2):580-637.
2. Seymour CW, Yende S, Scott MJ, et al. Metabolomics in pneumonia and sepsis: an analysis of the GenIMS cohort study. Intensive Care Med 2013; 39(8):1423-24.
3. Hugonnet S, Sax H, Eggimann P, Chevrolet JC, Pittet D. Nosocomial bloodstream infection and clinical sepsis. Emerg Infect Dis 2004; 10(1):76-81.
4. Langley RJ, Tsalik EL, Velkinburgh JC, et al. An integrated clinico-metabolomic model improves prediction of death in sepsis. Sci Transl Med 2013; 5(195):700-708.
5. Sasaki K, Fujita I, Hamasaki Y, Miyazaki S. Differentiating between bacterial and viral infection by measuring both C-reactive protein and 2'-5'-oligoadenylate synthetase as inflammatory markers. J Infect Chemother 2002; 8(1):76-80.
6. Respiratory Society of Chinese Medical Association. Guidelines for the diagnosis and treatment of community-acquired pneumonia. Chin J Tuberc Respir Dis 2006; 29(10):651-55.
7. Levy MM, Fink MP, Marshall JC, et al. 2001 SCCM/ESICM/ACCP/ATS/SIS international sepsis definitions conference. Crit Care Med 2003; 31(4):1250-56.
8. Thubert T, Santulli P, Marcellin L, et al. Measurement of hs-CRP is irrelevant to diagnose and stage endometriosis: prospective study of 834 patients. Am J Obstetr Gynecol 2014; 210(6):533.
9. Flores JM, Jiménez PI, Rincón D, Márquez J, Navarro H, Muñoz A, Murillo F. C reactive protein as marker of infection among patients with severe closed trauma. Enferm Infection Microbiol Clin 2001; 19(2):61-65.
10. Marshall PL, King JL, Lawrence NP, Lazarev A, Gross VS, Budowle B. Pressure cycling technology (PCT) reduces effects of inhibitors of the PCR. Int J Legal Med 2013; 127(2):321-33.
11. Uzzan B, Cohen R, Nicolas P, Cucherat M, Perret GY. Procalcitonin as a diagnostic test for sepsis in critically ill adults and after surgery or trauma: a systematic review and meta-analysis. Crit Care Med 2006; 34(7):1996-2003.
12. Oh JS, Kim SU, Oh YM, et al. The usefulness of the semiquantitative procalcitonin test kit as a guideline for starting antibiotic administration. Am J Emerg Med 2009; 27(7):859-63.

JOURNAL OF BIOLOGICAL REGULATORS & HOMEOSTATIC AGENTS Vol. 32, no. 5, 1171-1176 (2018)

LETTER TO THE EDITOR

GLP-1, A POWERFUL PHYSIOLOGICAL INCRETIN: AN UPDATE

J. MALIK and N. ROOHI

Department of Zoology, University of the Punjab, Lahore, Pakistan

Received May, 2, 2018 – Accepted June 29, 2018

Food intake, especially carbohydrates, release incretin, which is an endocrine transmitter. Among the various endocrine modulators, Glucagon-like peptide 1 (GLP-1) is more effective in stimulating the release of insulin and more powerful regulator of physiological functions. Mainly (GLP-1) receptors are expressed in lungs, α and β cells of pancreatic islets and the nervous system. Peripheral tissues, gastrointestinal tract and extra pancreatic tissues i.e., vascular smooth muscle, kidney and heart, also contain high affinity receptors for GLP-1. The aim of this systematic review was to gather the available published evidence of the functions performed by GLP-1 through the activation of its receptor in various organs. This review suggest that GLP-1 receptor signaling helps prevent beta cell apoptosis and conserve function and morphology of human islet. The effect of GLP-1 signaling in weight loss in diabetic patients was proved by previous studies. The long term use of GLP-1 receptor agonists reduces cardiovascular and renal complications in diabetic patients. Significant evidence was found in previous literature for its effect on pancreatic secretions. The secretions of many enzymes and hormones, such as trypsin, lipase and glucagon, inhibited significantly while the increase in levels of insulin and somatostatin was reported in many studies. GLP-1 has a prominent role in cardiac functioning and increases the heart rate considerably. Based on the vast impact of GLP-1 on physiological functions, many GLP-1 receptor agonists can be made that can increase the healthy life span.

To the Editor,

Glucagon-like peptide is recognized as most powerful insulinotropic hormone (1). In the pancreas, glucagon is derived from peptide precursor, pre-pro-glucagon (PPG) containing glucagon sequences of glucagon-like peptide 1 (GLP-1), glucagon-like peptide 2 (GLP-2) and other dissimilar peptide sequences to glucagon (2). GLP-1 is released from L-cells of the intestinal epithelium (1) in response to nutrient intake, especially food rich in fat and carbohydrates (3).

The functions of GLP-1 are facilitated by attaching to the cell surface receptor of secretin/glucagon superfamily of receptors attached with heterotrimeric G proteins (1). Extensive physiological spreading of GLP-1 receptor proposes numerous mechanisms of metabolic control including both centrally and peripheral neurohumoral pathways (4). Numerous biological characteristics of GLP-1 made this endocrine regulator an excellent candidate for the treatment of diabetes (5) as it works to slow the gastric emptying, accelerate insulin release and facilitate satiety in the central nervous system (CNS) (3).

GLP-1 works as a neuropeptide as well exerting various functions in CNS like decrease in food and water ingestion. It is produced mainly in caudal region of nucleus of the solitary tract (NTS) (2). GLP-1 has beneficial effects on pancreatic beta cells,

Mailing address:
Dr Javeria Malik,
Department of Zoology,
University of the Punjab,
54590-Lahore, Pakistan
Tel.: +923327274052
e-mail: jeamalik11@hotmail.com

0393-974X (2018)

one of which is inhibition of apoptosis of native beta cells (6).

In the bloodstream, native GLP-1 is quickly degraded by dipeptidyl peptidase-Vl (DPP-VI). Nonetheless, improved peptidase-resistant GLP-1 analogues are extremely resistant to DPP-VI degradation and show longer half-lives and are considerably stronger than native GLP-1. Consequently, the analogs of GLP-1 are now being evaluated on a clinical basis for the treatment of various diseases (7).

MATERIALS AND METHODS

All the related studies published in English language were thoroughly reviewed by conventional methods of systematic review research. Defining the objectives, a written prospective protocol, inclusion and exclusion criteria and search strategy was followed.

Study characteristics

The abstracts were reviewed based on apparent elimination criteria. The inclusion and exclusion criterion defined in perspective protocol was used to review complete studies. Only those studies that were centered on GLP-1 as a main physiological regulator were included in this review. The vast majority of studies were excluded based on not reporting the physiological functioning of GLP-1R.

Table I shows important information from each accepted study, and qualitative synthesis of all included studies was performed. Statistical analysis was not performed.

RESULTS

Beta cell apoptosis

Farilla et al. (1) investigated the cellular vulnerability to apoptosis changes with GLP-1 receptor signaling. Cell apoptosis, induced by streptozocin (STZ), was lowered significantly by co-administration of GLP-1 agonist exendin-4 (Ex-4). BHK-GLP-1R cells treated with Ex-4 revealed considerably increased viability, decreased caspase activity, reduced cleavage of

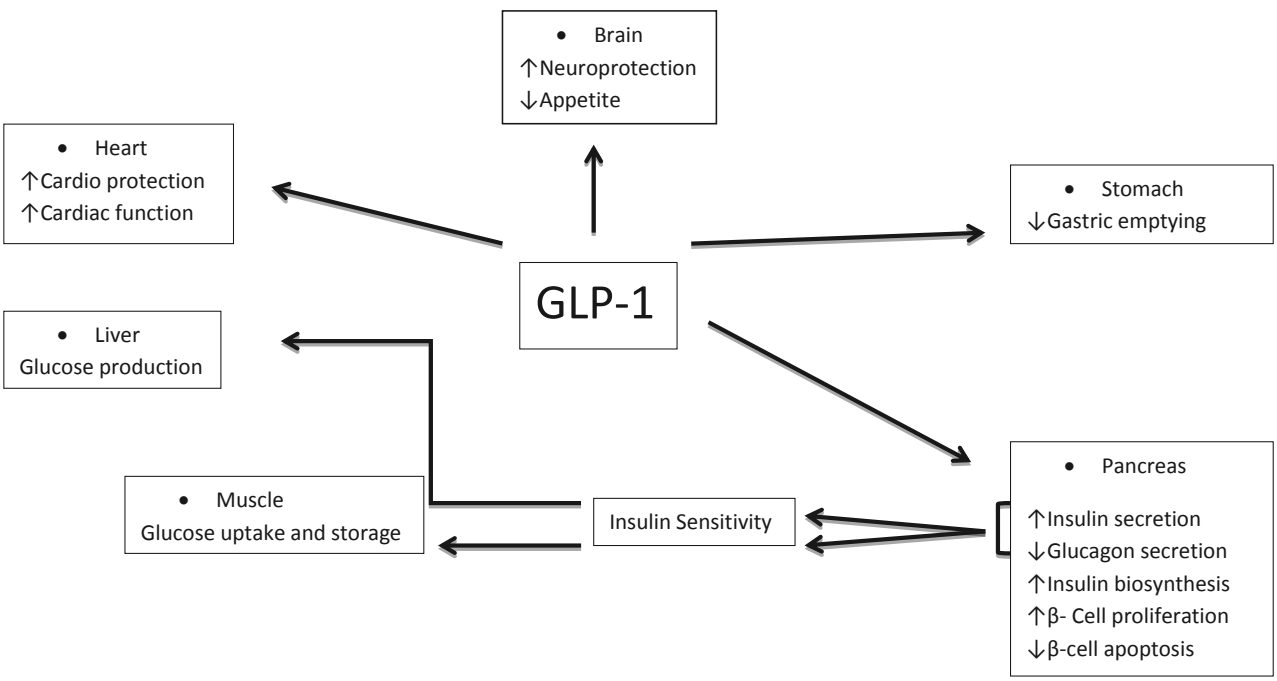

Fig. 1. *Physiological functions of GLP-1.*

catenin after treatment with cycloheximide *in vitro*. These results exhibited that the susceptibility to apoptotic injury can be modified by GLP-1 receptor signaling and a new potential mechanism was provided that linked the conservation or increase in cell mass *in vitro* to GLP-1 receptor stimulation.

Farilla et al. (5) studied whether GLP-1 could enhance function and prevent apoptosis in freshly isolated human islets. They noticed well preserved 3-dimensional islet morphology treated with GLP-1 as compared to controls. GLP-1 inhibited nuclear condensation, a feature of cell apoptosis. The up regulation of bcl-2 and down regulation of active caspase-3 was linked with the antiapoptotic influence of GLP-1. The study proved that GLP-1

Table I. *Summaries of studies considering functions of GLP-1.*

STUDY	COUNTRY	TESTED ORGANISM	YEAR OF STUDY	GLP-1 ANALOG	OUTCOME MEASURES	RESULTS
Farilla	California	zucker diabetic rats aged 12 weeks	2002	human recombinant GLP-1	TUNEL staining with Dead end colorimetric apoptotic detection sytem	3.6 fold decrease in apoptotic β cells ($p < 0.0001$)
Farilla	California	human pancreatic islets	2003	GLP-1	propoptotic factor caspase-3 the antiapoptotic factor bcl-2 was observed at mRNA and protein level	Down-regulation of caspase-3 ($P < 0.001$) and the up-regulation of bcl-2 ($P < 0.01$) at mRNA and protein level
Toyoda	Japan	mice aged 8-10 weeks	2008	exendin-4	TUNEL staining with apoptosis detection kit	Significant ($p < 0.0001$), strong ($r = 0.998$) correlation in total islet mass.

Summary of studies assessing the effect of GLP-1 on Weight Loss in diabetic patients

STUDY	COUNTRY	YEAR	AGONISTS TESTED	DOSE	AGE	BMI	RESULTS	HBA1c,
Boer	Netherland	2016	Exenatide	NA	58.4 ± 8.1 years,	>30 kg/m2	-11.6 ± 8.3 kg ($p = 0.058$)	-0.54 ±1.4 % ($P = 0.641$)
			Liraglutide	NA			-8.8 ± 7.5 kg ($p = 0.058$)	-0.43 ± 1.0 % ($P = 0.641$)
Sánchez-Garrido	Germany	2017	Exenatide	NA	NA	NA	2.0–3.8 kg	-0.5–1.5% (5.5–1.6 mmol/ mol)
			Lixisenatide	NA			2.0–3.8 kg	-0.5–1.5% (5.5–1.6 mmol/ mol)
			Liraglutide	NA			1.3–8.6 kg	-0.9–2.2% (9.9– 24.2 mmol/mol)
			Semaglutide	NA			4.8 kg vs 1.2 kg with placebo	-1.7% (18.7 mmol/mol) vs 0.5% (5.5 mmol/mol) with placebo
			Dulaglutide	NA			2.3–3.0 kg	-0.78–1.64% (8.6–18.0 mmol/mol)
			Albiglutide	NA			1.1–1.7 kg	-0.79–0.89% (8.7–9.78 mmol/mol)

Studies accessing the effect of GLP-1 in regulation of pancreatic secretions

STUDY	COUNTRY	YEAR	PANCREATIC HORMONES	ORGANISM TESTED	RESULTS
Wettergen	Denmark	1993	Trypsin	8 humans (6 men ,2women)	trypsin inhibited by 47±17%
			Lipase		lipase inhibited by 40±9%
			insulin		significantly increased
			Glucagon		significantly decrease
Masur	Boston,	2005	insulin	rat islet	significant reduction in - TC-6 insulinoma cells

Studies accessing the effect of GLP-1 as neurotransmitter

Study	Country	year	method used	brain areas	relative concentration
LARSEN	Denmark	1997	in situ hybirdization	hypothalamic dorsomedial ,	high concentration
				and paraventricular nuclei	
MERCHE-NTHALER	Pennsylvania	1999	S35-UTP–labeled probe was used	Frontal sections of the brain and spinal cord	High concentration

Studies accessing the effect of GLP-1 on Cardiac Functioning

STUDY	COUNTRY	YEAR	AGONIST	ORGANISM TESTED	DOSE TESTED	% CHANGE IN MAP	% CHANGE IN HR
Yamamoto	USA	2002	exedin-4	Sprague-Dawley rats (250–350 g)	30, 300, or 3000 ng i.v. or 3, 30, or 300 ng i.c.v	Increase SBP and DBP	NA
Feng Sun	China	2004 to 2015	Exenatide	NA	5 mg twice daily	SBP (4.86 mmHg, 95% CI: 8.33, 1.40) ↑	(3.20 bpm, 95% CI: 0.99, 5.41) ↑
					10 mg twice daily	DBP (0.9 mmHg,95% CI: 1.68, 0.11) ↓	
					2 mg once week		
			Liraglutide		1.2 mg once daily	SBP (3.59 mmHg, 95% CI: 5.84, 1.35)	2.70 (95% CI: 1.47, 3.94)↑
					1.8 mg once daily	DBP no significant difference	
			Albiglutide		30 mg once weekly	SBP (3.67 mmHg, 95% CI: 7.05, 0.29)	not significant
					50 mg once weekly	DBP no significant difference	
			Dulaglutide		0.75 mg once daily	no significant difference for SBP and DBP	2.19 bpm (95% CI: 0.36, 4.02)↑
					1.5 mg once daily		

TUNEL: terminal deoxynucleotidyl transferase dUTP nick end labeling; BMI: body mass index; HBA1: Hemoglobin A1c; MAP: mean arterial pressure; HR: heart rate; SBP: systolic blood pressure; DBP: diastolic blood pressure.

in human islet conserves function and morphology and prevents cell apoptosis.

Toyoda et al. (6) described the *in vivo* cytoprotective effect of GLP-1R signaling in case of glucose toxicity. Normoglycemia was restored by Exendin-4 treatment in streptozocin-induced diabetic mice, by reducing the number of beta cell apoptosis. This could be used to treat type II diabetes and in clinical islet transplantation, as the engraftment rates can be enhanced.

Weight loss in diabetic patients

Boer et al. (9) analyzed that continuous treatment of GLP-1 receptor agonists for two years resulted in sustained decrease in insulin dose in type 2 diabetes patients and reduced weight. The study of Sánchez-Garrido et al. (3) proved clinically that GLP-1RAs improve post prandial and fasting blood glucose control. GLP-1RAs also promote weight loss. GLP-1RAs received first regulatory approval for type 2

diabetes in 2005. Prolonged usage of GLP-1RAs decreases cardio-renal complications of diabetes.

Regulation of pancreatic secretion

Wettergren et al. (10) demonstrated that gastric emptying, gastric acid secretion and pancreatic secretion of trypsin and lipase is effected by injecting GLP-1intravenously. They carried out this study by testing on eight normal volunteers using aspiration technique and marker dilution. They concluded that GLP-1 inhibits gastric and pancreatic secretions. Masur et al. (11) supported the idea that GLP-1 plays a prominent role in the regulation of pancreatic islet secretion.

Neurotransmitter

Larsen et al. (4) proved through in-situ hybridization histochemistry that preproglucagon encoding mRNA was expressed in neurons in the caudal region of nucleus of solitary tract. Gel chromatographic analysis confirmed the presence of GLP-1 and other peptides in small intestine and forebrain working as neurotransmitter**.** Merchenthaler et al. (2) described the spreading of GLP-1R mRNAs in the central nervous system of rat. They studied the locations of GLP-1 production and action. The widespread distribution of GLP-1R in the CNS suggested that GLP-1R function also as neurotransmitter or neuromodulator.

Cardiac functioning

The study of Yamamoto et al. (7) documented that the GLP-1 system activates the cardiovascular responses by acting as regulator of sympathetic outflow. They reported that *in-vivo* administration of GLP-1 elevates the heart rate and blood pressure. Feng et al. (12) described that GLP-1RAs are related to slight decrease in blood pressure, a minor increase in heart rate and have no significant association with hypertension.

DISCUSSION

This review was written to sum up the available published proofs of the functions performed by intestinal incretin GLP-1 through the activation of its receptor GLP-1R on various organs. This review concludes that GLP-1R signaling helps to prevent beta cell apoptosis and also conserve function and morphology of human islet, as well as having a clinical implementation in treatment of type 2 diabetes and improving islet engraftment rates.

Various studies proved the significant effect of GLP-1R agonists in weight loss in diabetic patients. This effect was proved by using GLP-1R agonists in obese and overweight patients. One study proved that the long term use of GLP-1RAs reduced cardiovascular and renal complications in diabetic patients.

Prominent evidence was found in previous studies for the influence of GLP-1R on pancreatic secretions. The secretions of many enzymes and hormones, such as trypsin, lipase and glucagon, inhibited significantly while the increase in levels of insulin and somatostatin was reported in many studies. In one study, significant reduction in insulin release was reported in TC-6 insulinoma cells.

Many studies elaborated the role of GLP-1R as neurotransmitter and provided experimental evidence of widespread distribution of GLP-1 in different brain areas. GLP-1R has a significant role in cardiac functioning and increases heart rate significantly. One study reported non-significant association of GLP-1R with hypertension. Based on the vast impact of GLP-1 on physiological functions, many GLP-1RAs can be made that can increase the healthy life span.

REFERENCES

1. Farilla L, Hui H, Bertolotto C, Kang E, Bulotta A, Di Mario U, Perfetti R. Glucagon-like peptide-1 promotes islet cell growth and inhibits apoptosis in Zucker diabetic rats. Endocrinology 2002; 143(11):4397-408.
2. Merchenthaler I, Lane M, Shughrue P. Distribution of prepro- glucagon and glucagon-like peptide-1 receptor messenger RNAs in the rat central nervous system. J Comp Neurol 1999; 403:261-80.
3. Sánchez-Garrido MA, Brandt SJ, Clemmensen C, Müller TD, Dimarchi RD, Tschöp MH. GLP-1/glucagon receptor co-agonism for treatment of

obesity. Diabetologia 2017; 60(10):1-11.
4. Larsen PJ, Tang-Christensen M, Holst JJ, Orskov C. Distribution of glucagon-like peptide-1 and other preproglucagon-derived peptides in the rat hypothalamus and brainstem. Neuroscience 1997; 77:257-70.
5. Farilla L, Bulotta A, Hirshberg B, Li Calzi S, Khoury N, Noushmehr H, Perfetti R. Glucagon-like peptide 1 inhibits cell apoptosis and improves glucose responsiveness of freshly isolated human islets. Endocrinology 2003; 144(12):5149-58.
6. Toyoda K, Okitsu T, Yamane S, Uonaga T, Liu X, Harada N, Inagaki N. GLP-1 receptor signaling protects pancreatic beta cells in intraportal islet transplant by inhibiting apoptosis. Biochem Biophys Res Commun 2008; 367(4):793-98.
7. Yamamoto H, Lee CE, Marcus JN, Williams TD, Overton JM, Lopez ME, Elmquist JK. Glucagon-like peptide-1 receptor stimulation increases blood pressure and heart rate and activates autonomic regulatory neurons. Eur J Clin Invest 2002; 110(1):43.
8. Seino Y, Min KW, Neimoeller E, Takami A. Randomized, double-blind, Placebo=controlled trial of the once-daily GLP-1 Receptor agonist lixisenatide in Asian patients with type 2 diabetes insufficiently controlled on basal insulin with or without a sulfonylurea (GetGoal-L-Asia). Diabetes Obes Metab 2012; 14(10):910-17.
9. De Boer SA, Lefrandt JD, Petersen JF, Boersma HH, Mulder DJ, Hoogenberg K. The effects of GLP-1 analogues in obese, insulin-using type 2 diabetes in relation to eating behaviour. IJCP 2016; 38(1):144-50.
10. Wettergren A, Schjoldager B, Mortensen PE, Myhre J, Christiansen J, Holst JJ. Truncated GLP-1 (proglucagon 78–107-amide) inhibits gastric and pancreatic functions in man. Dig Dis Sci 1993; 38(4):665-73.
11. Masur K, Tibaduiza EC, Chen C, Ligon B, Beinborn M. Basal receptor activation by locally produced glucagon-like peptide-1 contributes to maintaining β-cell function. Mol Endocrinol 2005; 19(5):1373-82.
12. Sun F, Wu S, Guo S, Yu K, Yang Z, Li L, Zhan S. Impact of GLP-1 receptor agonists on blood pressure, heart rate and hypertension among patients with type 2 diabetes: a systematic review and network meta-analysis. Diabetes Res Clin Pract 2015; 110(1):26-37.

LETTER TO THE EDITOR

EFFECT OF NERVE ROOT BLOCK GUIDED BY ULTRASOUND ON CERVICOGENIC PAIN AND ITS INFLUENCE ON IMMUNE FUNCTION

HF. YING[1], WP. ZHANG[2], CL. ZHOU[3], HF. XIANG[3], B. CHEN[1] and KZ. YOU[1]

[1]Department of Anesthesiology, Taizhou Hospital of Zhejiang Province, Linhai City, China;
[2]Department of Gerontology, Taizhou Hospital of Zhejiang Province, Linhai City, China;
[3]Department of Anesthesiology, Taizhou Enze Medical Group, Enze Hospital, Taizhou City, China

Received May 23, 2018 – Accepted June 12, 2018

Cervicogenic pain is a common chronic disease that needs individualized treatment according to the place of pain. This study aimed to observe the effect of ultrasound-guided nerve root block in the treatment of cervicogenic pain and its influence on immune function. A total of 30 patients (group A) with cervical discogenic pain (CDP) were treated by selective cervical nerve root block and 30 patients (group B) with CDP were treated with cervical spinal block under the X-ray C-arm guidance. The two groups of patients were examined with regard to the analgesic effect by Numerical Rating Scale (NRS), and the changes in the preoperative and postoperative range of motion in the neck (ROM). In addition, weekly pain attacks and the duration of each attack were recorded. The content of $CD3^+$, $CD4^+$ and $CD8^+$ in the peripheral blood T lymphocyte subsets in the two groups was evaluated by flow cytometry. The levels of these subsets were compared 24 h before treatment, 24 h after treatment, 3 days (d) after treatment and 7 d after treatment. At the time periods of 24 h, 3 d, and 7 d after treatment, the NRS of the two groups decreased significantly compared with before treatment ($P<0.01$). The changes of the ROM, the number of weekly pain attacks, the duration of each pain attack, and the stiffness of the head and neck were significantly lower in the two groups compared with those prior to the treatment ($P<0.05$). In group A and group B, the number of $CD3^+$, $CD4^+$ and $CD8^+$ T cells 24 h and 3 d after treatment increased significantly compared with that noted before treatment ($P<0.05$). Seven days after treatment, the levels of $CD3^+$, $CD4^+$ and $CD8^+$ T cells in the peripheral blood T lymphocytes of group A were significantly higher than those of group B ($P<0.05$). Selective cervical nerve root block under ultrasound is an effective method for the treatment of cervical discogenic pain. The effect is better than that of the X-ray C-arm-guided cervical block method. The mechanism of selective cervical nerve root block under ultrasound may be related to the regulation of the content of $CD3^+$, $CD4^+$, $CD8^+$ T cells in the peripheral blood T lymphocyte subsets and the enhancement of cellular immunity.

To the Editor,

Cervicogenic pain is a common chronic disease (1) which can be divided into cervical discogenic pain (CDP), cervical nerve root pain, and cervical spondylosis pain (2) according with the source of pain. Moreover, this disease can be divided into cervical headache (CEH), cervicogenic upper limb pain, cervicogenic shoulder and back pain, and neck soft tissue pain, according to the pain site (3, 4). Recently, the related studies on CEH and CDP have

Key words: selective cervical nerve block under ultrasound, X-ray C-arm-guided cervical paravertebral block, neck pain, immune function

Mailing address:
Dr Kuangzhang You,
Department of Anesthesiology,
Taizhou Enze Medical group, Enze Hospital,
150 West Gate Street,
Taizhou City, 318053, China
e-mail: you_kuangzhangkz@163.com

0393-974X (2018)

DISCLOSURE: ALL AUTHORS REPORT NO CONFLICTS OF INTEREST RELEVANT TO THIS ARTICLE.

received extensive attention from neurosurgeons, anesthesiologists and pain physicians (5). Various types of treatment methods have been employed for CEH and CDP, although in recent years, chronic CEH and CDP with severe pain has been treated by two methods, namely, X-ray C-arm-guided cervical block (6, 7) and selective cervical nerve root block under ultrasound (8). The latter method has achieved optimal effects. The study of the immune mechanism of intervertebral disc-derived pain has been the focus of major attention and the relationship between pain and the expression of T lymphocyte subsets (TLS) has been extensively investigated. Therefore, the aim of the present study was to evaluate the effect of selective cervical nerve root block and X-ray C-arm-guided paravertebral block on CDP, and the changes in the $CD3^+$, $CD4^+$ and $CD8^+$ levels in peripheral blood T lymphocytes.

MATERIALS AND METHODS

Patients

From January 2015 to December 2017, 30 patients (group A) with cervical discogenic pain (CDP) treated with selective cervical nerve root block and 30 patients (group B) with cervical discogenic pain treated with cervical spinal block under the X-ray C-arm were selected from the Taizhou Hospital of Zhejiang Province. Group A included 8 males and 15 females, aged 32-73 years (average 52.5 years). Group B included 9 males and 14 females, aged 34-65 years (average 48.2 years). Informed consent was signed by all the patients and/or family members, and the study was approved by the Ethics Committee of the Taizhou Hospital of the Zhejiang Province.

The inclusion criteria were patients with less than 3 months of conservative treatment and poor effect, patients with moderate or mild cervical disc degeneration, and those with the clinical diagnosis of disc derived neuropathy.

The exclusion criteria were patients with possible severe cardiovascular and cerebrovascular complications, patients with severe cervical disc degeneration, and patients with cervical deformity.

Imaging examination

Preoperative Computed Tomography (CT) or Magnetic Resonance Imaging (MRI) was performed on patients. CT was used to observe whether the intervertebral disc was prominent, bulged, or prolapsed, and whether the intervertebral disc compressed the nerve root. The CT scan further aided the observation of osteophyte and intervertebral foramen stenosis at the edge of the intervertebral foramen. For complex lesions, CT with three-dimensional reconstruction technology was used to display the cervical spine and its surrounding structures. MRI was used to investigate the axial, coronal and sagittal multi-angle imaging of the cervical vertebra and to determine multi parameter imaging (T1WI, T2WI, STIR), which could be used for early diagnosis of intervertebral disc degeneration

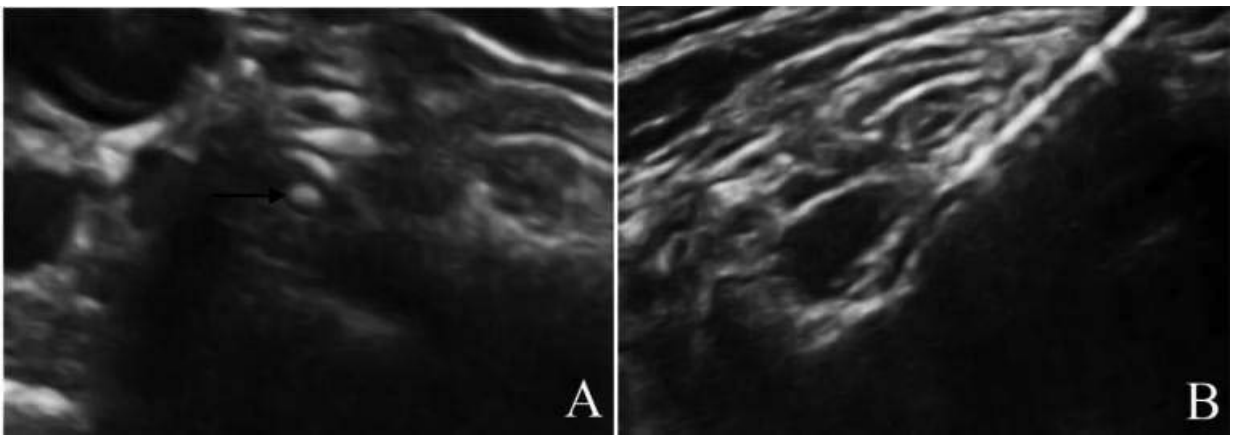

Fig. 1. *Ultrasonographic examination.* ***A)*** *ultrasound showed the nerve root area;* ***B)*** *puncture needle reached the nerve root area).*

as well as for the diagnosis of spinal canal occupying lesions. The relationship between nucleus pulposus and nerve root in patients with lumbar disc herniation was observed by MRI spinal FLAIR imaging.

Paracervical block

The position of the nerve root of the cervical vertebra target was observed prior to the operation of the X-ray C-arm, and the needle was inserted vertically to the skin to the end of the transverse process. A total of 2 mL of iohexol injection (GE Healthcare AS, Ireland) was injected into the end of the transverse process, the tip of the needle was reconfirmed at the end of the transverse process and the blood and cerebrospinal fluid were returned. After the intravascular and spinal canal puncture was confirmed, the anti-phlogistic analgesic fluid (10 mL of 0.25% lidocaine and 5 mg of triamcinolone acetonide) was injected slowly and changes in the vital signs of the patients were observed.

Selective cervical nerve root block under ultrasound

The patient took a supine position and the transverse process of the puncture was determined. The ultrasonic probe was placed on the neck to get the short axis ultrasonic image. The position of the anterior and posterior tubercle of the transverse process with the high echo structure "Shuangfeng sign" and the position of the hypoechoic circular or elliptical root of the nerve root in Shuangfeng were found. After the identification of the cervical target nerve, the 25 G 3.8 cm long puncture needle was directly inserted into the skin behind the probe. Following successful puncture, no blood or cerebrospinal fluid were resorbed. Anti-inflammatory and analgesic fluid (8 mL 0.25% lidocaine, 10 mg triamcinolone acetonide and 500 μg VitB12) were injected, and changes in the patient's vital signs were observed.

Evaluation of curative effect

Numerical Rating Scale (NRS) was used to evaluate the analgesic effect of the patients, and the changes of preoperative and postoperative reduced range of the motion in the neck (ROM). Furthermore, weekly pain attacks and the duration of each pain attack were recorded. The NRS grading criteria for pain measurements were as follows: 0: no pain; 1-3: mild pain; 4-6: moderate pain; and 7-10: severe pain. The ROM scoring method was the following: 1 point: free activity; 2 points: activity extent and scope is limited; 3 points: activity is severely limited and rigid; 4 points: basically cannot move (9).

Flow cytometry

From all patients, 2 mL of peripheral venous blood was collected 24 h prior to treatment, and at 24 h, 3 d (days) and 7 d (days) after treatment. The patients then received heparin (20 ~ 50 u/mL) for anticoagulation. The T lymphocyte subset of the peripheral blood was detected by a Coulter Epics XL flow cytometer (FCM), and the content of the $CD4^+$ cells was compared with that of the T lymphocyte subset.

Statistical analysis

The data were analyzed by statistical software SPSS19.0, and all observed values were expressed in the form of mean ± standard deviation. The data in the observation index group were analyzed by variance analysis, and the difference was statistically significant when $P<0.05$.

Table I. *Demographic data of the two groups before treatment.*

Groups	Cases	Age (years)	Gender (male/female)	Height (cm)	Weight (Kg)
Group A	30	52.45±14.98	8/15	166.79±8.57	65.88±11.20
Group B	30	48.24±13.56	9/14	169.34±9.09	66.07±10.87

Table II. *NRS score, the number of pain attacks, the duration of pain onset, ROM and head and neck stiffness sensation before and after treatment.*

Indexes		Group A	Group B
NRS score	Before treatment	7.22±2.14	6.89±2.52
	24 h after treatment	2.03±1.38**	2.13±2.47**
	3 d after treatment	2.43±1.96**&	3.26±2.19**
	7 d after treatment	3.58±2.47**&	4.73±2.99*
The number of pain attacks	Before treatment	11.31±10.22	9.85±8.35
	7 d after treatment	3.41±3.06*&	4.62±3.41*
Duration of pain onset (h)	Before treatment	7.24±6.14	8.16±7.05
	24 h after treatment	1.73±1.32**	2.13±2.03**
	3 d after treatment	2.57±2.09*	3.34±2.84*
	7 d after treatment	3.94±3.12*	3.96±3.15*
ROM	Before treatment	2.74±2.03	2.98±2.07
	24 h after treatment	1.23±0.63**	1.37±0.37**
	3 d after treatment	1.48±0.87*	1.49±0.68*
	7 d after treatment	1.58±0.72*	1.66±0.62*
Head and neck stiffness sensation (%)	Before treatment	88.41	90.75
	24 h after treatment	21.57**&	46.89**
	3 d after treatment	21.63**&	47.13**
	7 d after treatment	26.63**&	51.67**

*Note: compared with before treatment, *P<0.05, **P<0.01; &Group A compared with group B and P<0.05.*

RESULTS

Selective cervical nerve root block under ultrasound

In the present study, the ultrasound confirmed that 30 cases of cervical nerve root block were completed, as shown in Fig. 1.

Therapeutic effect of pain

According to the data in Table I, no statistical difference in the general data was observed between the two groups (P>0.05), regarding age, gender, height and weight.

As shown in Table II the number of pain attacks 7

Table III. *$CD3^+$, $CD4^+$ and $CD8^+$ T cells in peripheral blood of the two groups before and after treatment .*

		Group A	Group B
$CD3^+$	Before treatment	61.83±7.66	57.95±9.31
	24h after treatment	81.62±9.54**	73.86±11.83*
	3 d after treatment	74.04±8.75*&	62.11±10.51
	7 d after treatment	65.15±7.49*&	60.03±11.34
$CD4^+$	Before treatment	36.15±5.66	37.05±4.82
	24 h after treatment	52.06±7.83**	50.11±6.63*
	3 d after treatment	48.83±5.97**&	41.25±5.52*
	7 d after treatment	41.87±5.36*&	37.91±5.11
$CD8^+$	Before treatment	16.93±5.16	16.11±6.16
	24 h after treatment	29.07±9.33**	27.52±5.73*
	3 d after treatment	26.93±8.28*	23.88±5.45*
	7 d after treatment	21.25±6.19*&	17.89±5.82

*Note: compared with before treatment, *P<0.05, **P<0.01; &Group A compared with group B and P<0.05.*

d after treatment in the two groups was less than that before treatment. NRS, pain duration, ROM, and stiff neck of the two groups were measured at 24 h, 3 d and 7 d after treatment and were found to be less than those before treatment. Group A and group B were compared. Seven days after treatment, the number of pain attacks in group A was lower than that in group B (P<0.05). At 24 h after treatment, the NRS in group A was compared with that in group B (P>0.05). At 3 d and 7 d after the treatment, the NRS in group A was significantly lower than that in group B (P<0.05). No significant difference was noted in the duration of pain and ROM in the A and B groups (P>0.05), whereas stiffness in the head and neck of group A was significantly lower than that of group B (P<0.05).

T cell subsets in peripheral blood of patients

At the time periods of 24 h, 3 d and 7 d after treatment, the levels of T lymphocyte subsets $CD3^+$, $CD4^+$ and $CD8^+$ in the two groups were all higher

than those before treatment. At 24 h after treatment, there were no significant differences when the content of T lymphocyte subsets $CD3^+$, $CD4^+$ and $CD8^+$ in group A was compared with that of group B ($P>0.05$) At 3 d and 7 d after treatment, the content of peripheral blood subgroups of $CD3^+$, $CD4^+$ and $CD8^+$ T cells in group A was higher than that of group B ($P<0.05$) (Table III).

DISCUSSION

In many types of cervical pain, the nerve block therapy for CDP is a relatively mature treatment method (10, 11). In the present study, the NRS of the two groups of patients at 24 h, 3 d and 7 d after treatment decreased significantly compared with that before treatment ($P<0.01$), indicating that the two groups of patients achieved significant analgesic effect. In addition, the changes in the variables ROM, weekly pain attacks, duration of pain and stiffness of head and neck in the two groups, were significantly lower than those before treatment ($P<0.05$), which indicated that the two groups had optimal short-term effect.

The results suggested that the selective cervical nerve root block under ultrasound was better than the C-arm-guided cervical paravertebral block. The reason may be that the location of the cervical nerve root and vertebral artery can be observed by ultrasound-guided scan, which can effectively reduce the number of punctures and shorten the operation time.

The immune mechanism of pain, notably the changes in peripheral blood pain-related inflammatory mediators, may be related to the pathogenesis and effect of pain (12, 13). In the present study, CDP patients were selected and it was found that the number of $CD3^+$, $CD4^+$ and $CD8^+$ T cells in group A and group B was significantly higher than that noted at 24 h and 3 d after treatment ($P<0.05$). However, at 7 d after treatment, the aforementioned measurements of group A were significantly higher than those of group B ($P<0.05$). In combination with the results of the analgesic effect, the therapeutic effect of selective cervical nerve root block under ultrasound was better than that of the C-arm-guided inferior cervical block.

ACKNOWLEDGEMENTS

This work was supported by The Medical Technology of Zhejiang Province (2015KYA237).

REFERENCES

1. Halim W, Chua NH, Vissers KC. Long-term pain relief in patients with cervicogenic headaches after pulsed radiofrequency application into the lateral atlantoaxial (C1-2) joint using an anterolateral approach. Pain Pract 2010; 10(4):267-71.
2. Ahn NU, Ahn UM, Ipsen B, An HS. Mechanical neck pain and cervicogenic headache. Neurosurgery 2007; 60(Supp1 1):S21-27.
3. Vavrek D, Haas M, Peterson D. Physical examination and self-reported pain outcomes from a randomized trial on chronic cervicogenic headache. J Manipulative Physiol Ther 2010; 33(5):338-48.
4. Reid SA, Rivett DA, Katekar MG, Callister R. Efficacy of manual therapy treatments for people with cervicogenic dizziness and pain: protocol of a randomised controlled trial. BMC Musculoskelet Disord 2012; 13:201.
5. Fernández-de-las-Peñas C, Cuadrado ML. Therapeutic options for cervicogenic headache. Expert Rev Neurother. 201; 14(1):39-49.
6. Persson LC, Carlsson JY, Anderberg L. Persson LC, Carlsson JY, Anderberg L. Headache in patients with cervical radiculopathy: a prospective study with selective nerve root blocks in 275 patients. Eur Spine J 2007; 16(7):953-9.
7. Goldberg ME, Schwartzman RJ, Domsky R, Sabia M, Torjman MC. Deep cervical plexus block for the treatment of cervicogenic headache. Pain Physician 2008; 11(6):849-54.
8. Finlayson RJ, Etheridge JP, Vieira L, Gupta G, Tran DQ. A randomized comparison between ultrasound- and fluoroscopy-guided third occipital nerve block. Reg Anesth Pain Med 2013; 38(3):212-7.
9. Bonnechère B, Salvia P, Dugailly PM, Maroye L, Van Geyt B, Feipel V. Influence of movement speed on cervical range of motion. Eur Spine J 2014; 23(8):1688-93.
10. Fredriksen TA, Antonaci F, Sjaastad O. Cervicogenic headache: too important to be left un-diagnosed. J Headache Pain 2015; 16:6.

11. Lauretti G R, Corrêa S W, Mattos A L. efficacy of the greater occipital nerve block for cervicogenic headache: comparing classical and subcompartmental techniques. Pain Pract 2015; 15(7):654-61.
12. Martelletti P. Inflammatory mechanisms in cervicogenic headache: An integrative view. Curr Pain Headache Rep 2002; 6(4):315-19.
13. Giblin K, Newmark JL, Brenner GJ, Wainger BJ. Headache plus: trigeminal and autonomic features in a case of cervicogenic headache responsive to third occipital nerve radiofrequency ablation. Pain Med 2014; 15(3):473-78.

LETTER TO THE EDITOR

PIG3 SUPPRESSES GASTRIC CANCER PROLIFERATION BY REGULATING p53-MEDIATED APOPTOSIS

Y. CHU[1,2*], D. LI[3*], H. ZHANG[1,2], J. DING[4,5], P. XU[1,2], X. QIU[1,2] and H. ZHANG[4,5]

[1]Department of Nephrology, Ningbo Medical Center Lihuili Eastern Hospital, Ningbo, Zhejiang, PR China; [2]The Second Division of Internal Medicine, Ninghai Second Hospital, Ningbo, Zhejiang, PR China; [3]Nanlou Respiratory Diseases Department, Chinese PLA General Hospital, Chinese PLA Postgraduate Medical School, Beijing, China; [4]Department of General Surgery, Ningbo Medical Center Lihuili Eastern Hospital, Ningbo, Zhejiang, PR China; [5]Department of General surgery, Ninghai second hospital, Ningbo, Zhejiang, PR China

Received March 15, 2018 – Accepted July 6, 2018

*These Authors contributed equally to this study

Gastric cancer (GC), the third leading cause of cancer mortality and the fifth most common cancer in the world, still is an important health problem worldwide. P53-inducible gene 3 (PIG3) was initially isolated in an investigation to identify the genes that were induced by p53 in human colorectal cancer cells. PIG3 can also regulate the stability of p53 through suppressing the process of the MDM2-mediated ubiquitination of p53. The aim of this study is to explore the expression level of PIG3 in human GC and further investigate the function and mechanism of PIG3 in human GC. Five cell lines and 30 matched GC tissue samples and adjacent tissue samples were used for this study, and MTT assay, colony formation assay, flow cytometry analysis and Western blot were carried out. Expression of PIG3 was found to be frequently reduced in GC. Restoration of the expression of PIG3 inhibited cell proliferation, induced cell apoptosis and further activated P53 signaling in BGC823 cells. In conclusion, we demonstrated that expression of PIG3 is frequently reduced in GC tissue, and PIG3 suppressed human GC growth through p53-mediated apoptosis. PIG3 may act as a potential diagnostic marker and a potential therapeutic target of GC.

To the Editor,

Gastric cancer (GC) is still an important health problem worldwide, and despite advances in prevention, diagnosis and therapy, is still the fifth most common cancer and the third leading cause of cancer mortality worldwide (1). The risk factors for GC include ingestion of salt and salt-preserved foods, *H. pylori* infection, and smoking (2), however environmental factors also play important roles. An increasing number of investigations suggest that the susceptible genetic variants, not only genetic but also epigenetic alterations, play a crucial part in the initiation and progress of human primary GC (3, 4). The late diagnosis and the poor response to the available therapeutic regimens of GC results in high mortality. The highly heterogeneous nature of GC may be one of the reasons for the poor clinical outcomes. The microenvironmental interactions, genetic alterations and epigenetic events as well play important roles in tumor heterogenity (5).

PIG3 (p53-inducible gene 3) was firstly isolated in an investigation to identify genes that were induced by p53 in human colorectal cancer cells, which is encoded by a gene located downstream

Key words: PIG3, P53 signaling, gastric cancer, apoptosis

Mailing address:
Hai Zhang, M.D.,
Department of General surgery,
Ningbo Medical Center
Lihuili Eastern Hospital,
Ningbo, Zhejiang, PR China
e-mail: nbzhanghai@126.com

0393-974X (2018)

of the protein p53 encoding gene (6). P53 can bind with a penta-nucleotide microsatellite sequence in *PIG3* promoter, and transactivate the expression of PIG3 prior to the onset of p53-initated apoptosis (7). Recently, it was reported that PIG3 plays an important role in the cellular response to DNA damage, especially in DNA repair and checkpoint signaling (8). Our investigation mainly focuses on the function and mechanism of PIG3 in GC.

MATERIALS AND METHODS

Thirty primary human GC samples and matched adjacent tissue samples were collected from Ningbo Medical Center Lihuili Eastern Hospital. The median age of the patients was 60 years (range 35-86), and the female/male ratio was 1:1.5. All the gastric samples were collected under the guidelines approved by the institutional review board of Ningbo Medical Center Lihuili Eastern Hospital, and written informed consent from patients.

Five GC cell lines (BGC823, AGS, MGC803, MKN45 and N87) were previously established from primary GC, and were maintained in 10% fetal bovine serum and 90% RPMI 1640 (Invitrogen, Carlsbad, CA, USA).

RNA isolation, semi-quantitative RT-PCR and quantitative real-time PCR

Trizol reagent was used for total RNA isolation (Life Technologies, Gaithersburg, MD). First strand cDNA was synthesized by the manufacturer's instructions (Invitrogen, Carlsbad, CA, USA). Primers for RT-PCR of PIG3 are as follows: sense,5'-GATGGTCGATGGGTTCTCTATG-3' and antisense,5'-GATTTCGGTCACTGGGTAGATTC-3'. QRT-PCR was performed with SYBR Green master mix (Thermo Scientific, Waltham, MA, USA) according to the manufacturer's protocol using the following primers: sense, 5'-GCTGAGGTCTAGGGACAATAAG-3' and antisense, 5'-GATTTCGGTCACTGGGTAGAT-3'. GAPDH was used as an internal control using primers as: sense, 5'-GACCACAGTCCATGCCATCAC-3' and antisense, 5'-GTCCACCACCCTGTTGCTGTA-3'. In order to avoid genomic DNA contamination, all primers were designed to span intronic sequences between adjacent exon.

Construction of PIG3 expression vector and transfection assay

Full length cDNA of PIG3 was amplified by RT-PCR using primers of the following sequences: sense, 5'-ACCGAATTCATGTTAGCCGTGCAC-3' and antisense, 5'-AATCTCGAGTCACTGGGGCAGTTC-3'. The amplified PIG3 PCR products were cloned into pCMV6 vector. Lipofectamine 3000 (Invitrogen, Carlsbad, CA, USA) was used as transient transfection.

Cell viability detection

BGC823 cells were plated into 96-well plates with 2×

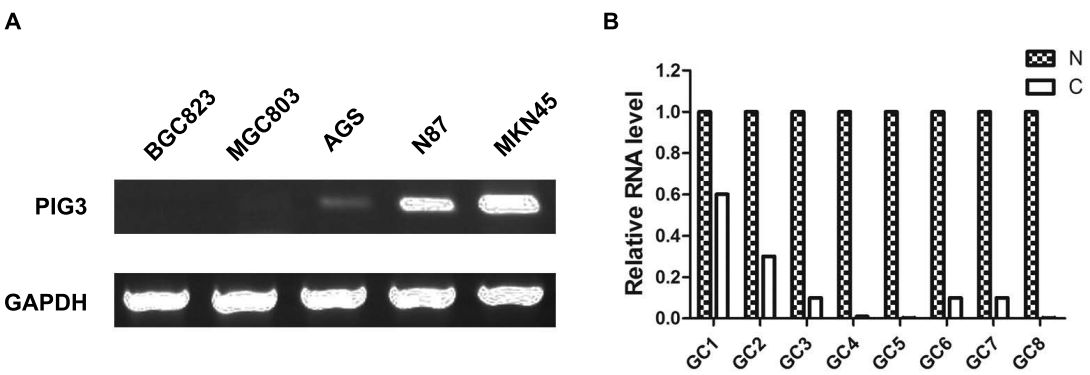

Fig. 1. *The expression level of PIG3 in human primary gastric cancer.* ***A)*** *Expression level of PIG3 detected by semi-quantitative RT-PCR. GAPDH: the internal control of RT-PCR. BGC823, MGC803, AGS, N87 and MKN45 are gastric cancer cell lines.* ***B)*** *Representative relative expression of PIG3 in matched gastric cancer tissue samples (C) and adjacent tissue samples (N).*

10^3cells per well, and the MTT assay (KeyGEN Biotech, Nanjing, China) was employed to detect the cell viability at 0, 24, 48, 72 and 96 h. Absorbance was measured on a microplate reader (Thermo Multiskan MK3, MA, USA) at a wavelength of 490 nm.

Colony formation assay

BGC823 cells were plated into 6-well plates with 500 cells per well for 14 days. The growth medium was exchanged every 3 days with growth medium conditioned G418 (Invitrogen, Carlsbad, CA, USA) at 400μg/ml. Cells were fixed in 75% ethanol for half an hour, and then stained with 0.2% crystal violet (Beyotime, Nanjing, China) for 10 min for visualization and counting.

Flow cytometry analysis

Apoptosis of BGC823 cells was analysed by Annexin V-FITC/PI Apoptosis Detection Kit (KeyGen Biotechnology, China) according to the manufacturer's instructions. Samples were analyzed by flow cytometry with a FACScan Flow Cytometer (Becton-Dickinson Biosciences, Mansfield, MA).

Gene expression array

The total RNA was isolated from PIG3 re-expressed and unexpressed BGC823 cells by Trizol reagent (Life Technologies, Gaithersburg, MD, USA). Cy5/Cy3 was labeled on the RNA samples. All samples were hybridized to the Human Whole Genome One Array (Phalanx Biotech Group, CA, USA). The hybridized chips were scanned by an Axion 4000 scanner (Molecular Devices, CA, USA). Spot quantification was performed using the Genepix 4.1 software (Axion Instruments, CA, USA). Differentially expressed genes were further analyzed with fold changes >2.

Western blot

Protein was collected 48 h after transfection of GC cells. Antibodies were diluted according to the manufacturer's instructions. The primary antibodies were as follows: PIG3(H300) (Santa Cruz Biotechnology, Santa Cruz, CA, USA), P53, caspase-3, cleaved caspase-3, BAX (Protein Tech Group, Chicago, IL, USA) and β-actin (Bioworld Tech, MN, USA).

Statistical analysis

SPSS 17.0 software (IBM, NY, USA) was used for data analysis. The student's *t*-test was used in this study. $P<0.05$ was regarded as a statistically significant difference.

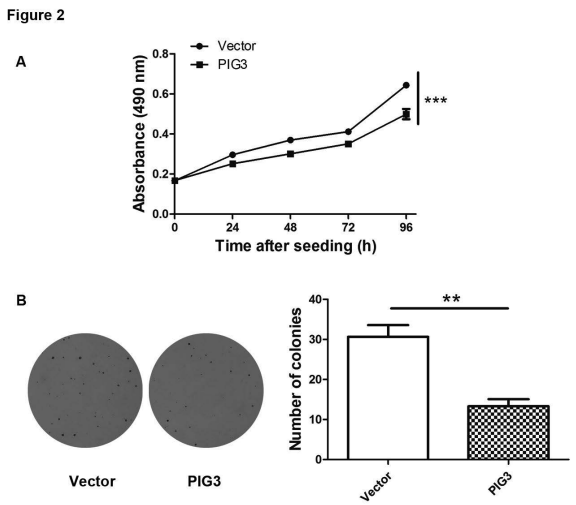

Fig. 2. *The function of PIG3 in gastric cancer cell proliferation.* ***A****) Growth curves of cells analyzed by MTT assay show the function of PIG3 in BGC823 cells. Each experiment was repeated in triplicate, ***p<0.001.* ***B****) Restoration of PIG3 expression reduces the colony number of BGC823 cells analyzed by colony formation. The bar diagram represents the average number of clones of BGC823 cells. Each experiment was repeated in triplicate. **P<0.01.*

RESULTS

Expression level of PIG3 reduced in GC

Semi-quantitative RT-PCR was employed in this study to detect the expression of PIG3 in GC cell lines. The results are shown in Fig. 1A: in BGC823 and MGC803 cells, loss of expression of PIG3 was found. In AGS cells, the expression level of PIG3 was reduced. But in N87 and MKN45 cells, PIG3 was highly expressed. Furthermore, we detected the expression level of PIG3 in 30 cases of matched GC tissue samples and adjacent tissue samples by quantitative real time PCR (qRT-PCR). As shown in Fig. 1B, PIG3 had considerably lower expression level in tumor samples, which indicated that the expression of PIG3 may act as a diagnostic marker of GC.

Figure 3

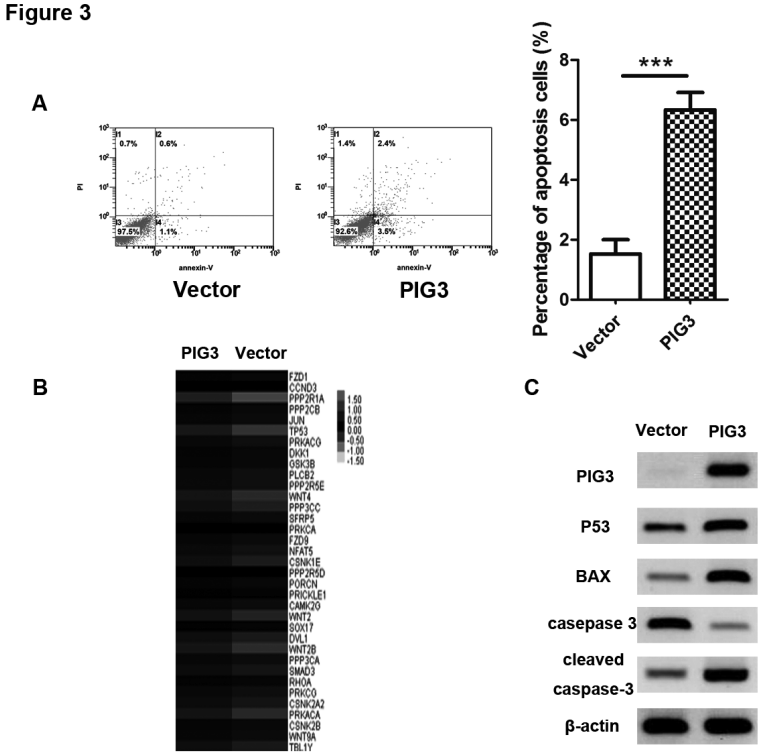

Fig. 3. *The effect of PIG3 on cell apoptosis and the molecular mechanism of PIG3 inng in human gastric cancer cells. **A)** The function of PIG3 in cell apoptosis of BGC823 cells analyzed by flow cytometry. ***p<0.001. **B)** The different genes expressed in BGC823 cells before and after restoration of PIG3 expression analyzed by expression array. **C)** The regulation of PIG3 in P53, BAX, caspase-3 and cleaved caspase-3 expression in BGC823 cells analyzed by Western blots. β-actin: the internal control.*

Restoration of PIG3 expression suppressed GC cell proliferation

Cell viability assays and colony formation assays were employed to evaluate the function of PIG3 in progression of GC. MTT assay was used to determine the cell viability. The OD value was 0.64±0.012 *vs* 0.50±0.025, respectively, before and after restoration of PIG3 expression in BGC823 cells ($p<0.001$, Fig. 2A).

In the colony formation assay in BGC823 cells, the clone number was 30.7±5.03 *vs* 13.3±3.06 before and after restoration of PIG3 expression, respectively ($p<0.01$, Fig. 2B). These results suggested that restoration of PIG3 expression suppressed GC cells proliferation.

PIG3 induces cell apoptosis and suppresses cell growth through activating p53 signaling in GC cells

Flow cytometry assays was employed to evaluate the effect of PIG3 in cell apoptosis. The percentage of apoptotic cells was 1.53±0.47% *vs* 6.33±0.59% ($p<0.001$, Fig, 3A) before and after re-expressed PIG3, respectively. These results demonstrate that PIG3 induced cell apoptosis in GC cells.

It was reported that PIG3 can inhibit p53 ubiquitination and regulate intracellular p53 levels subsequently(9). The gene expression array was used to investigate the mechanism of PIG3 in human GC. The gene expression profile in BGC823 cells was analyzed before and after restoration of PIG3. Among the differently expressed genes,

p53 was up-regulated more than 2-fold (Fig. 3B). Moreover, the protein level of P53, BAX, caspase-3 and cleaved caspase-3 were detected by Western blot. The expression level of P53, BAX and cleaved caspase-3 were increased, and caspase-3 was reduced after restoration of PIG3 (Fig. 3C). The results suggest that PIG3 can activate p53 signaling in human GC cells.

DISCUSSION

There is a binding site for p53 in the promoter of *PIG3,* and transcription of *PIG3* occurs before the onset of apoptosis initiated by p53 (7). Reactive oxygen species (ROS) act as downstream mediators of p53-dependent apoptosis. It is reported that PIG3 play an important role in ROS generation (6, 10). NADK quinine oxidoreductase 1 (NQO1) is known to contribute to ROS generation, and the amino acid sequence of PIG3 shows homology to that of NQO1 significantly (6). Recently, another study showed that PIG3 act as a transcriptional target of p53, and can also regulate p53 stability by suppressing its MDM2-mediated ubiquitination (9). In breast cancer, BRCA1 regulates PIG3-mediated apoptosis in a p53-dependent manner, and PIG3 expression is related with better OS (11).

In this study, it is indicated that expression level of PIG3 reduced in GC frequently, and PIG3 may act as a potential diagnostic marker in GC. Restoration of PIG3 expression in GC cells suppressed cell proliferation and induced cell apoptosis. We also analyzed the down-stream genes of PIG3 by expression array and we found the expression of p53 was up-regulated. The level of protein P53 was up-regulated after restoration of PIG3 expression. The expression level of BAX and cleaved caspase-3 were increased, and caspase-3 was reduced after re-expression of PIG3. PIG3 induced p53-meidated apoptosis through regulating p53 stability. This study indicated that expression of PIG3 reduced in GC frequently. PIG3 induced p53-mediated apoptosis through regulating p53 stability, which suggest that PIG3 may be a potential therapeutic target for GC.

ACKNOWLEDGEMENTS

This work was supported by Science Foundation of Ningbo (2015A610217).

REFERENCES

1. Ferlay J, Soerjomataram I, Dikshit R, et al. Cancer incidence and mortality worldwide: sources, methods and major patterns in GLOBOCAN 2012. Int J Cancer 2015; 136(5):E359-86.
2. Hartgrink HH, Jansen EP, van Grieken NC, van de Velde CJ. Gastric cancer. Lancet 2009; 374(9688):477-90.
3. Liang H, Kim YH, Identifying molecular drivers of gastric cancer through next-generation sequencing. Cancer Lett 2013; 340(2):241-46.
4. Guo M, Yan W. Epigenetics of gastric cancer. Methods Mol Biol 2015; 1238:783-99.
5. Gullo I, Carneiro F, Oliveira C, Almeida GM. Heterogeneity in gastric cancer: from pure morphology to molecular classifications. Pathobiology 2017; 85:50-63.
6. Polyak K, Xia Y, Zweier JL, Kinzler KW, Vogelstein B. A model for p53-induced apoptosis. Nature 1997; 389(6648):300-305.
7. Contente A, Dittmer A, Koch MC, Roth J, Dobbelstein M. A polymorphic microsatellite that mediates induction of PIG3 by p53. Nat Genet 2002; 30(3):315-20.
8. Lee JH, Kang Y, Khare V, et al. The p53-inducible gene 3 (PIG3) contributes to early cellular response to DNA damage. Oncogene 2010; 29(10):1431-50.
9. Jin M, Park SJ, Kim SW, Kim HR, Hyun JW, Lee JH. PIG3 Regulates p53 stability by suppressing its MDM2-mediated ubiquitination. biomol ther (Seoul) 2017: 25:396-403.
10. Porte S, Valencia E, Yakovtseva EA, et al. Three-dimensional structure and enzymatic function of proapoptotic human p53-inducible quinone oxidoreductase PIG3. J Biol Chem 2009; 284(25):17194-205.
11. Zhang W, Luo J, Chen F, Yang F, Song W, Zhu A, Guan X. BRCA1 regulates PIG3-mediated apoptosis in a p53-dependent manner. Oncotarget 2015; 6(10):7608-18.

LETTER TO THE EDITOR

PHYLOGENY AND COMPARATIVE MODELING OF PHYTOCHELATIN SYNTHASE FROM CHLORELLA SP. AS AN EFFICIENT BIOAGENT FOR DETOXIFICATION OF HEAVY METALS

S.A. BUKHARI[1], M.F. TAHIR[1], N. AKHTER[2], F. ANJUM[3], H. ANWAR[4] and G. MUSTAFA[1]

[1]Department of Biochemistry, Government College University Faisalabad, Faisalabad, Pakistan; [2]College of Allied Health Professionals, Directorate of Medical Sciences, Government College University, Faisalabad, Pakistan; [3]Department of Chemistry, Government College University, Faisalabad, Pakistan; [4]Department of Physiology, Government College University, Faisalabad, Pakistan

Received June 20, 2018 – Accepted July 12, 2018

Phytochelatins (PCs) found extensively in algae and plants are important for detoxification of heavy metals from soil and wastewater, and their synthesis is mediated by an enzyme phytochelatin synthase (PCS). In this study, a phylogram was generated to study evolutionary relationships of PCS from various organisms. It was revealed that PCS from green algae and plants are orthologs as both have evolved from a common ancestor. PCS from cyanobacteria appeared in two different clades showing that they have followed different lineages during evolution. Structural modeling was also carried out by building a 3D model of PCS from *Chlorella variabilis* using software Modeller v9.16. The predicted structure will be helpful for protein engineering strategies and to understand its interactions with other proteins. The biological biosorption capacity of *Chlorella vulgaris* (a green alga) was determined to remove Cd, Cu and Pb from industrial effluents. The biosorption of three heavy metals from industrial waste water was investigated under various conditions like pH, biomass concentration, contact time and temperature. Bio-removal of heavy metals was carried out by exposing culture of *C. vulgaris* to water samples of different heavy metal concentrations. The decrease in Cd, Cu and Pb quantities after 1 to 7 days of incubation period were 83%, 84% and 82.5%, respectively. In view of this, *Chlorella* spp. could be used on a large scale to detoxify heavy metals and clean up contaminated environments.

To the Editor,

Environmental contamination by heavy metals is widely considered a serious issue due to its toxicity (1). Biosorption is a simple process which uses biological material for the removal of heavy metals from water or water solution through the metabolically-mediated physicochemical pathways (2). The production of non-protein peptides is induced in many organisms when they are exposed to heavy metals with toxic levels. The peptides were named as cadystins when they were first discovered in *Schizosaccharomyces pombe* (fission yeast) (3). Later, these peptides were also found in the suspension-cultured cells of *Rauvolfia serpentine* (4) and called were phytochelatins (PCs). They play an important role in tolerance to heavy metals through complex formation with toxic heavy metals. PCs have a general structure [(g-Glu-Cys)n-Gly (n ≥ 2)] and are involved in toxic heavy metal detoxification. The synthesis of PCs is catalyzed by enzyme

Key words: phytochelatin, phylogeny, heavy metals, industrial effluents, biosorption, Chlorella

Mailing address:
Dr Ghulam Mustafa,
Department of Biochemistry,
Government College University,
Faisalabad-38060, Pakistan
Tel: +92(41)9330047
e-mail: drghulammustafa@gcuf.edu.pk

0393-974X (2018)

phytochelatin synthase (PCS) from glutathione (GSH) and the enzyme is activated by various heavy metals (5).

PCs are cysteine-rich peptides and have great affinity for toxic heavy metals. In the current study, *Chlorella vulgaris* (a green algae) was used as biomaterial to remove heavy metals. Metals that have been removed by adsorption on the cell surface can be successfully recovered. The objectives of this study included 3D structure prediction of phytochelatin synthase (responsible for heavy metal detoxification) and its phylogeny from various organisms, and to examine the levels of heavy metals in water and to assess the biosorption capability of *C. vulgaris* for the removal of copper (Cu), lead (Pb) and cadmium (Cd). Furthermore, the effects of temperature, pH and contact time were also studied and optimized on the biosorption capacity of *C. vulgaris*.

MATERIALS AND METHODS

Phylogenetic studies

The protein sequences of phytochelatin synthase/ glutathione gamma-glutamylcysteinyltransferase from *Chlorella variabilis* (single-celled green alga) was retrieved from GenPept database of NCBI and analyzed using BLASTp (Basic Local Alignment Search Tool for proteins) available on the NCBI website (http://www.ncbi.nlm.nih.gov/). Along with phytochelatin synthase protein sequences from two single-celled green algae (*Chlorella* spp.), sixty-two of the most similar reported sequences were also retrieved from GenPept for phylogenetic systematics. All sequences were aligned using ClustalX and imported into the MEGA7 program (6) for manual alignment. Neighbor-Joining (NJ) phylogenetic tree was constructed using MEGA7 with 100 bootstrap replicates.

Sequence retrieval to predict 3D structure

Phytochelatin synthase from *Nostoc* sp. PCC 7120 was used as a template and its 3D structure was downloaded from Protein Data Bank in PDB format (PDB ID: 2BTW) to construct a 3D model for *Chlorella variabilis* phytochelatin synthase [GenPept: XP_005845668.1].

Model building by homology modeling

To predict 3D structure of phytochelatin synthase from *C. variabilis*, homology modeling was used as it is the most suitable method for building protein models (7). CPH Model Server was used to select template. Modeller v9.16 was used for template and query alignments (8) using align2d command, and output file in PIR format was used for building ten models against the query. The analyses for model evaluation and quality for all models were made by ProSA-web Z-score, Qmean plot and PROCHECK Ramachandran plot. Root Mean Squared Deviation (RMSD) for superimposition of modeled phytochelatin synthase with its template was calculated using UCSF Chimera 1.10 workbench (9).

Algal culture

The starting culture of *Chlorella vulgaris* was collected from the Fish Seed Hatchery, Satyana Road, Faisalabad, Pakistan. Identification of *C. vulgaris* was carried out in the Institute of Microbiology, University of Agriculture Faisalabad, Pakistan. The identified algal cells were cultured in Zarrouk's medium in 2 L glass flasks. The flasks were kept in daylight for 12 h at room temperature (25±1°C). The pH was kept neutral (pH 7) with 0.01 M solutions of HCl and NaOH. The growth of *Chlorella* was observed as greening of culture. A loop-full of culture from the flask was processed for microscopic examination.

Effluent samples

Waste water samples were collected in dark brown glass bottles from industrial effluent plants of Faisalabad city of Pakistan. These water samples were stored at 4°C until analyzed. The samples were tested in triplicate to check concentrations of heavy metals (i.e. Cu, Cd and Pb).

Biosorption

Algal metal bioremoval was carried out following the method of Mane and Babu (10). The bioremoval efficiency (R) of the microalgae was calculated using following formula.

$$R\ (\%) = \frac{(Ci - Ce)}{Ci} \times 100$$

Where, R= Bioremoval efficiency (%)

C_i = Initial concentration of metals in aqueous solution (mg/L)

C_e = equilibrium concentration of metals in aqueous solution (mg/L)

Analysis of metal ions

A Varian AA1275 atomic absorption spectrophotometer was used to determine the concentration of copper (Cu), lead (Pb) and cadmimum (Cd) ions in the solutions.

RESULTS

Phylogenetic systematics

A comprehensive phylogram of phytochelatin synthase was generated (Fig 1). The phylogram was divided in four different monophyletic groups (i.e. plants, green algae, cyanobacteria I and cyanobacteria II) based on their evolutionary relationships. From the phylogeny, it has been inferred that phytochelatin/ phytochelatin-like proteins found in other organisms are closely related to those found in green algae. As can be seen in Fig. 1, PCSs from green algae have strong evolutionary relationships with those found in green plants as both clades have been evolved from a common ancestor. Interestingly, phytochelatin proteins from cyanobacteria did not appear as a single clade and divided into two monophyletic groups which appeared below the monophyletic group of green algae. Cyanobacteria I and green algae have evolved from a single ancestor which shows a strong evolutionary relationship between both clades. The members of the monophyletic group of cyanobacteria II appeared as distant relatives of cyanobacteria I. Another interesting observation was the inclusion of two different organisms (i.e. a brown alga and annelid worm) in the phylogram. Both organisms showed a strong evolutionary relationships with cyanobacteria I, hypothesizing that the evolution of phytochelatin protein took place in a related fashion in these organisms. The protein sequence of phytochelatin synthase from *Bradyrhizobium liaoningense* was used to root the tree.

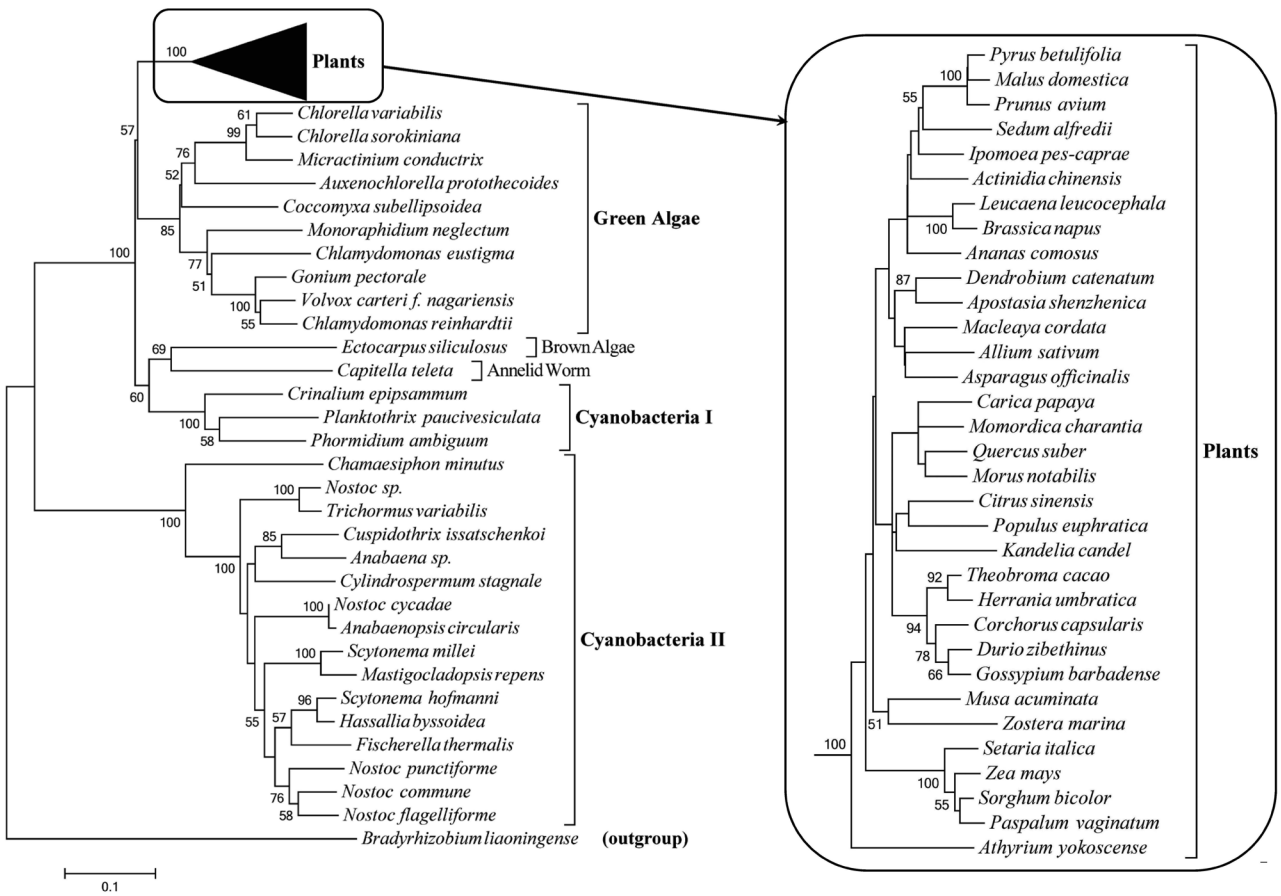

Fig. 1. *Phylogenetic tree of phytochelatin synthase/glutathione gamma-glutamylcysteinyltransferase from green algae and their homologues.*

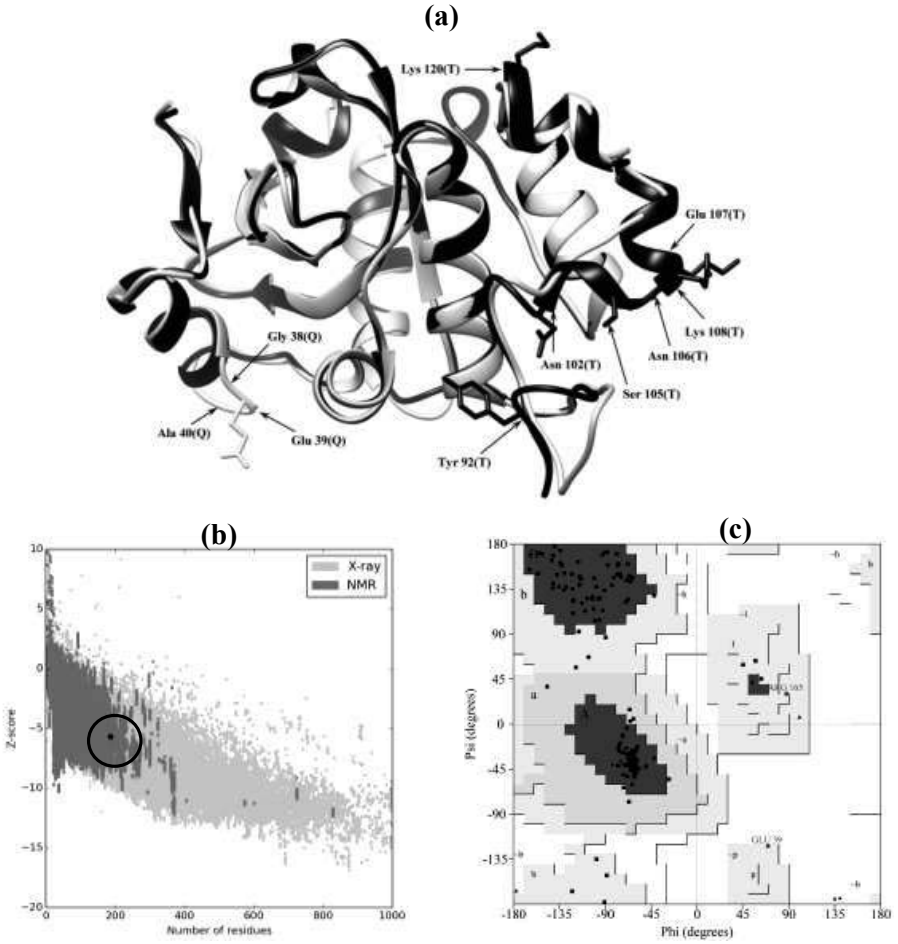

Fig. 2. *Predicted 3D structure of phytochelatin synthase from Chlorella variabilis and its evaluation.* ***a****) Comparison of predicted 3D structure of PCS from C. variabilis (light grey) with template (black). Unaligned residue(s) in both structures are labeled with 3 letter abbreviations along with their positions (T: Template, Q: Query, in parenthesis), (****b****) z-score plot showing the quality of predicted model, (****c****) Ramachandran plot analysis of the modeled structure.*

Comparative modeling of phytochelatin synthase

No phytochelatin synthase gene/protein sequence from *Chlorella vulgaris* has been deposited in GenBank/GenPept to date. Therefore, protein sequence of phytochelatin synthase (target sequence) from *Chlorella variabilis* (of same genus and hence close relative of *C. vulgaris*) was retrieved from GenPept and used for homology modeling. The modelled 3D structure (best model) of phytochelatin synthase from *C. variabilis*, its evaluation and superimposition with template are shown in Fig. 2.

The z-DOPE (normalized Discrete Optimized Protein Energy) of predicted model was found to be -0.643. The score of GA341 was 1.000. The z-score of the predicted structure was -5.67 that is in the range of scores obtained for proteins with related sizes (Fig. 2b). Ramachandran's plot calculations using ProCheck was used to evaluate the stereochemistry of backbone Psi and Phi dihedral angles. Percentage of residues of phytochelatin synthase occupying most favored regions (A,B,L) is 86.7% while 12% occupies additional allowed regions (a,b,l,p), 1.3% and 0% resides in generously allowed (~a,~b,~l,~p) and disallowed regions, respectively (Fig. 2c). It was ascertained on the basis of these results that the predicted model is of good quality.

The predicted 3D model of phytochelatin

synthase was also superimposed to its template to compare both structures (Fig. 2a). Unaligned amino acids in both structures have been labeled along with their locations in their respective sequences. There was 36.02% identity between target and template with overall RMSD 0.355 Å and Q-score 0.910.

Studies on effluent samples

The average concentration of studied metals in water followed the decreasing order of Pb > Cu > Cd. The average concentrations of Pb, Cu and Cd in water were 0.64 mg/L, 0.517 mg/L and 0.092 mg/L, respectively, which were much higher than the WHO standard for drinking water and wastewater. In view of the toxicity reference values presented by USEPA (1999), almost all heavy metals, especially Cd, Cu and Pb, exceeded the limits for safe water. It was shown that the polluted water was contaminating groundwater and making it unsuitable for drinking and cooking purposes.

Biosorption capacity of Chlorella vulgaris for heavy metals

The efficiency of the biosorption using green algae (*Chlorella*) is intensely affected by physicochemical characteristics of the solutions such as temperature, pH, contact time, biomass concentration and presence of other metal ions. The biosorption ability of *C. vulgaris* was studied under various conditions.

Effect of pH

The uptake of Cd, Cu and Pb was examined at pH values between 2 to 7 (Fig. 3a). Percent removal of Cd was very low at pH 2.0, while at pH 3.0 it became slightly low and then increased gradually with increasing pH value up to 7.0. An optimum pH of 5 for removal of Cd was found using *Chlorella* as biosorbent. Similarly biosorption capacity for Cu and Pb were examined and followed the same pattern. Percent removals increased with increase in pH, and optimum pH was found of 4 and 5 for Pb and Cu, respectively.

Effect of temperature

The extent of Cd ion biosorption by *C. vulgaris* was maximally achieved at 35°C (51%), while a low cation intake was recorded at 20°C (29%) and 40°C (34%). Similarly, the extent of Cu ion sorption by *C. vulgaris* was found maximum at 30°C (56%), whereas low cation uptake was recorded at 20°C (27%) and 40°C (44%). Likewise, the level of Pb ion sorption by *C. vulgaris* was found maximum at 35°C (53%), whereas low cation uptake was recorded at 20°C (25%) and 40°C (47%) (Fig. 3b).

Effect of biosorbent (algae) concentration

The effect of biomass concentration on the biosorption of Cd, Cu and Pb present in effluent was undertaken with 20 g/L, 30 g/L and 40 g/L and showed that the biosorption efficiency was highly

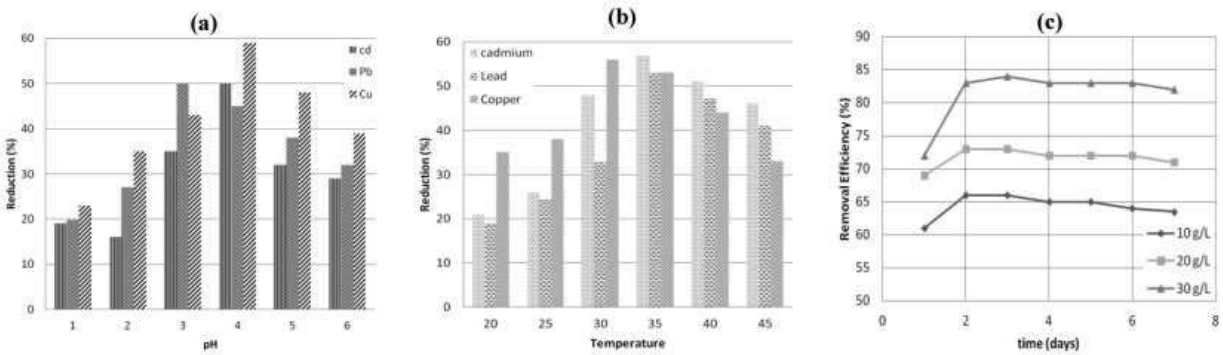

Fig. 3. *Biosorption efficiency of Chlorella vulgaris. Comparison of biosorption of heavy metals on (**a**) varying pH, (**b**) temperature, (**c**) effect of biosorbent concentration on metal removal efficiency.*

Table I. *Biosorption capacity of Chlorella vulgaris against cadmium, lead and copper metals (mean±SD).*

Incubation time (days)	Concentration of Cd (mg/L)	Concentration of Pb (mg/L)	Concentration of Cu (mg/L)
0	0.092±0.010	0.649±0.040	0.521±0.032
1/2	0.089±0.010	0.644±0.050	0.517±0.048
1	0.024±0.003	0.191±0.021	0.139±0.021
2	0.017±0.002	0.128±0.016	0.086±0.010
3	0.016±0.0012	0.123±0.013	0.085±0.011
4	0.017±0.001	0.124±0.015	0.084±0.010
5	0.017±0.002	0.124±0.010	0.084±0.014
6	0.017±0.001	0.124±0.012	0.084±0.010
7	0.017±0.001	0.124 ±0.014	0.084 ±0.013
Decrease in concentration of metals (%)	**81.5**	**80.9**	**83.9**

dependent on the increasing biomass concentration in the incubation medium (Fig. 3c).

Effect of other metal ions on metal removal efficiency

The bioremoval efficiency of *C. vulgaris* for all selected heavy metals from wastewater was compared to that of single metal solutions of 5 mg/L. The experiment was performed using synthetic single-metal solutions of Cu^{2+}, Zn^{2+}, Cd^{2+} and Ni^{2+} prepared from chemical reactants of analytical grades: $CuSO_4.5H_2O$, $ZnSO_4.H_2O$, $CdSO_4.8/3H_2O$ and $NiSO_4.7H_2O$, respectively. The removal efficiencies for all selected heavy metals were reduced when excess of metal ions other than removing metal was present. Overall biosorption capacities of *C. vulgaris* against Cd, Pb and Cu metals are shown in Table I.

DISCUSSION

PCs are important non-protein peptides that detoxify heavy metals and are found in some cyanobacteria, nematodes, fungi, eukaryotic algae and taller plants. The synthesis of PCs and homophytochelatins (hPCs) is mediated by PCS which is also known as glutathione gamma-glutamylcysteinyltransferase (EC: 2.3.2.15). The enzyme is involved in detoxification of various heavy metals such as Cd^{2+} and AsO_4^{3-}. PCS encoding genes have been isolated and cloned from fungi, plants and nematodes (11). Algal cells which are capable of producing higher levels of PCs could be helpful to remove toxic heavy metals from wastewater. Investigation of factors that affect the efficiency of biosorption of heavy metals using biomass of single cell green alga (*Chlorella vulgaris*) is of great importance in terms of understanding the biosorption process (12).

In conclusion, the phylogram generated in this study exhibited that PCSs are closely related and have evolved in a similar fashion in green algae

and taller plants. The structural superimposition of predicted 3D structure of PCS from *Chlorella* sp. with that of *Nostoc* sp. showed 36.02% identity. The predicted 3D structure of phytochelatin synthase will be useful in docking studies that can be used to find different substrates and products of this enzyme. Biomass of *C. vulgaris* was used efficiently for bioremoval of Cd, Cu and Pb. Within all tested metals, the removal capacities for Cd, Cu and Pb were highest (i.e. 83%, 84% and 82.5%, respectively) at biosorbent concentrations of 20 g/L, pH 4 for Pb and 5 for Cu and Cd and 30-35°C after seven days of incubation. This information is of great interest to industrial organizations, such as those of waste water treatment, for technological enhancement.

ACKNOWLEDGEMENTS

We would like to extend our special gratitude to Dr. Sajjad ur Rehman, Institution of Microbiology, University of Agriculture Faisalabad, Pakistan for the identification of algal species.

REFERENCES

1. Zhang Z, Juying L, Mamat Z, QingFu Y. Sources identification and pollution evaluation of heavy metals in the surface sediments of Bortala River, Northwest China. Ecotoxicol Environ Saf 2016; 126:94-101.
2. Al-Qodah Z, Yahya MA, Al-Shannag M. On the performance of bioadsorption processes for heavy metal ions removal by low-cost agricultural and natural by-products bioadsorbent: a review. Desalin Water Treat 2017; 85:339-57.
3. Kondo N, Imai K, Isobe M, Goto T, Murasugi A, Wada-Nakagawa C, Hayashi Y. Cadystin a and b, major unit peptides comprising cadmium binding peptides induced in a fission yeast-----separation, revision of structures and synthesis. Tetrahedron Lett 1984; 25(35):3869-72.
4. Grill E, Winnacker EL, Zenk MH. Phytochelatins: the principal heavy-metal complexing peptides of higher plants. Science 1985; 230(4726):674-76.
5. Essig YJ, Webb SM, Stürzenbaum SR. Deletion of phytochelatin synthase modulates the metal accumulation pattern of cadmium exposed *C. elegans*. Int J Mol Sci 2016; 17:257.
6. Kumar S, Stecher G, Tamura K. MEGA7: Molecular Evolutionary Genetics Analysis version 7.0 for bigger datasets. Mol Biol Evol 2016; 33:1870-74.
7. Mustafa G, Arif R, Bukhari SA, Ali M, Sharif S, Atta A. Structural and functional annotation of citrate synthase from *Aspergillus niger* ANJ-120. Pak J Pharm Sci 2018; 31(Suppl 2):709-17.
8. Webb B, Sali A. Protein structure modeling with MODELLER. In Functional Genomics 2017:39-54. Humana Press, New York, NY.
9. Pettersen EF, Goddard TD, Huang CC, Couch GS, Greenblatt DM, Meng EC, Ferrin TE. UCSF Chimera--a visualization system for exploratory research and analysis. J Comput Chem 2004; 25:1605-12.
10. Mane VS, Babu PVV. Studies on the adsorption of Brilliant Green dye from aqueous solution onto low-cost NaOH treated saw dust. J Desalination 2011; 273:321-29.
11. Olsson S, Penacho V, Puente-Sánchez F, Díaz S, Gonzalez-Pastor JE, Aguilera A. Horizontal gene transfer of phytochelatin synthases from bacteria to extremophilic green algae. Microb Ecol 2017; 73:50-60.
12. Cheng J, Yin W, Chang Z, Lundholm N, Jiang Z. Biosorption capacity and kinetics of cadmium (II) on live and dead *Chlorella vulgaris*. J Appl Phycol 2017; 29:211-21.

JOURNAL OF BIOLOGICAL REGULATORS & HOMEOSTATIC AGENTS Vol. 32, no. 5, 1199-1204 (2018)

LETTER TO THE EDITOR

HIGH SENSITIVITY C-REACTIVE PROTEIN AS A CARDIOVASCULAR RISK MARKER IN INDEPENDENT COMMUNITY-LIVING ELDERLY PERSONS

A. PŁÓCINICZAK[1], S. DZIĘGIELEWSKA-GĘSIAK[2], A. BROŻEK[1], A. BLACHA[1], M. NOWICKI[1] and D. FORMANOWICZ[1]

[1]Department of Clinical Biochemistry and Laboratory Medicine, Poznan University of Medical Science, Poznan, Poland; [2]Department of Internal Medicine, School of Public Health in Bytom, Medical University of Silesia, Katowice, Poland

Received December 22, 2017 – Accepted July 24, 2018

An alarming fact is that increasing numbers of cardiovascular disease (CVD) events occur more often among elderly individuals without previous occurrence of CVD. There are numerous modifiable risk factors such as dyslipidemia,-and inflammatory markers, as well as cardiovascular events risk charts, in the identification and prevention of cardiovascular morbidity and mortality among elderly population. Thus, the aim of this study was to analyze some CVD risk factors as well as international CVD risk charts in independent community-living elderly persons in relation to their hs-CRP concentration in serum. Of 516 elderly Caucasians, 50 were non-smoking, with no positive history of chronic or acute diseases. The patients' clinical, biochemical and CVD risk charts were recorded. The CRP values were categorized according to the known cut-off points for stratification of cardiovascular risk: low risk patients with hs-CRP of <1 mg/L (low hs-CRP), moderate risk with hs-CRP of 1-3 mg/L (moderate hs-CRP) and high risk with hs-CRP of >3 mg/L (high hs-CRP). The groups did not differ in terms of age, anthropometric measures, fasting glucose, creatinine and uric acid concentration or analyzed CVD risk scales. The relationship between hs-CRP levels and both lipid profile and arterial blood pressure are linearly dependent ($p<0.02$). The negative correlation for the hs-CRP and fasting glucose and DIA were found in low hs-CRP ($r= -0.619$; $p<0.05$ and $r= -0.580$; $p<0.05$ respectively) and for the hs-CRP and uric acid ($r=-0.850$; $p<0.05$) in the moderate hs-CRP risk group. Thus, this study should greatly simplify decision-making for clinicians around the world.

To the Editor,

Unfavorable age-related cardiovascular risk profiles suggest the increasing burden of cardiovascular disease (CVD) with age. Mortality due to CVD among individuals over 65 years of age is greater than 81% (1). The most alarming fact is that an increasing number of CVD events occur more often among elderly individuals without previous occurrence of CVD compared to those with previous CVD events. This indicates that the identification of the usefulness of various modifiable risk factors would be critical in the identification and prevention of cardiovascular morbidity and mortality among the elderly population. According to the American Heart Association, the identification of high-risk elderly patients should be performed by using the Framingham risk score calculation (2). Other recommended risk charts such as PROCAM,

Key words: low grade inflammation, cardiovascular risk, elderly

Mailing address:
Dr Alicja Płóciniczak,
Department of Clinical Biochemistry and Laboratory Medicine,
Poznan University of Medical Science, ul. Rokietnicka 8,
60-806 Poznan, Poland
Fax: +618547702 - Tel.: +618547700
e-mail: alicjaplociniczak@ump.edu.pl

0393-974X (2018)

DISCLOSURE: ALL AUTHORS REPORT NO CONFLICTS OF INTEREST RELEVANT TO THIS ARTICLE.

SCORE also indicate the greater CVD risk with age (3, 4). However, the calculation of absolute CV risk over a 10-year period is not adequate for people over 80 years of age.

The identification of elderly individuals with dyslipidemia is essential for the prediction, primary and secondary prevention, diagnosis, and prognosis of cardiovascular diseases and, moreover, aging itself increases the risk of cardiovascular events (5). The experimental and clinical evidence suggests an important role for inflammation in the initiation and progression of atherosclerosis (6). The best studied inflammatory marker in the development of CVD is the high sensitivity C- reactive protein (hs-CRP). As it is bound to low density lipoproteins and plays a role in determining plaque stability, hs-CRP has been suggested to have a causal role in CVD. The role of inflammatory markers, in particular C-reactive protein in conjunction with cardiovascular risk, has been extensively studied in middle-aged people (7). However, studies focused on the people are still limited and the current study could be potentially helpful in this regard. Therefore, the present study has been undertaken, to evaluate the hypothesis that hs-CRP could be used as an early cardiovascular risk marker among elderly free-living individuals without previous cardiovascular events.

MATERIALS AND METHODS

The study was approved by the local ethics group in accordance with the Declaration of Helsinki of 1975 for Human Research and the study protocol was approved by the Bioethics Committee of Poznan University of Medical Sciences in Poznan, Poland (Statements No 595/11). The subjects participating in the study gave informed consent to the procedure.

Study subjects

Initially, 516 elderly Caucasians (aged 60 years and over) with no confounding complaints, from the Poznan metropolitan area (Western Poland) were enrolled in the study. Non-smoking elderly persons, using no medication, no special diet, no supplements and no alcohol, without acute or chronic disease, were studied. The exclusion criteria were: positive history of coronary artery disease (accompanied by current steady state electrocardiography), stroke, diabetes, neoplastic disease and inflammatory disease. Additional biochemical exclusion criteria were: decreased estimated Glomerlular Filtration Rate (less than 60 ml/min) based on MDRD formula eGFR (ml/min/1.73m2) = {186 x [creatinine] $^{-1.154}$ x [age] $^{-0,203}$ x 0.742[for women] x 1.210 [for Afro-Americans]}. Complete physical examination, including the measurement of systolic (SBP) and diastolic (DBP) arterial blood pressure with a validated OMRON model M10-IT sphygmomanometer (Omron Health Care, Kyoto, Japan), following the recommendations of the European Society of Hypertension. Body mass index (BMI=kg/m^2) was derived from height and weight measurements. Finally, 50 elderly persons living independently in the community qualified for the study.

Fasting blood was collected from the ulnar vein, and was used to measure glucose, lipids and hs-CRP concentrations in plasma samples without symptoms of hemolysis. Glucose and lipid parameters, including total cholesterol (TC), high density lipoprotein cholesterol (HDL-C), and triacylglycerol (TAG) concentrations, were evaluated by enzymatic methods using bioMerieux reagent kit (Marcy-l'Etoile, France) and an UV-160A Shimadzu spectrophotometer (Shimadzu Co., Kyoto, Japan). Low density lipoprotein cholesterol (LDL-C) was calculated using the Friedewald formula for lipid parameters expressed in mg/dL:

$$[\text{LDL-C}] = [\text{T-C}] - [\text{HDL-C}] - [\text{TAG}/5], \text{ if TAG} < 400 \text{ mg/dL}.$$

RANDOX Assayed Human Multi-Sera Level 1 (as normal) and RANDOX Assayed Human Multi-Sera Level 2 (as pathological) (Randox, Crumlin, United Kingdom) were used for monitoring the accuracy of the determinations.

The creatinine and uric acid concentrations were obtained from the Dimension Clinical Chemistry System (Simens, Munich, Germany) with an analytical sensitivity of 0.05 mg/dL and 0.1 mg/dL, respectively. High sensitivity C-reactive protein assay (hs-CRP) was evaluated by particle enhanced turbidimetric immunoassay (PETIA). The precision obtained for the lowest pool test 0.11 mg/

dL corresponded to a total coefficient of variation of 17.7% and a within-run coefficient of variation of 13.8%. CRP values were categorized according to the known cut-off points for stratification of cardiovascular risk. Results of an hs-CRP allowed classifying subjects for three categories: Low risk patients with an hs-CRP concentration of <1 mg/L (low hs-CRP), moderate risk persons with an hs-CRP concentration of 1-3 mg/L (moderate hs-CRP) and high risk persons with an hs-CRP concentration of >3 mg/L (high hs-CRP). To evaluate the ten-year risk of cardiovascular and coronary heart disease, three risk scores were used: Framingham risk score (3), Pol-SCORE chart (4) and PROCAM (5).

Statistical analysis

Statistica12.5 version for Windows was used for the statistical analysis. The normality of value distribution was checked by the Shapiro-Wilk test. To assess the significance of the differences between the studied low, middle and high hs-CRP groups, the Kruskal-Wallis test was used. The Spearman rank correlation test was used to evaluate the strength of association between the variables. A p-value <0.05 or lower was considered statistically significant. The results are expressed as median and inter-quartile range.

RESULTS

The characteristics of all independent community-living elderly persons studied as well as the divided female and male subgroups, are presented in Table I. Elderly independent community-living females

Table I. *Clinical and biochemical characteristics of all independent community-living elderly persons studied.*

	All elderly n=50 median (interquartile range)	Elderly females n=44 median (interquartile range)	Elderly males n=6 median (interquartile range)
Age [years]	64.5 (62.0 – 68.0)	64.5 (62.0-68.0)	65.0 (61.0-67.0)
High [m]	1.64 (1.60-1.68)	1.64 (1.60-1.66)	1.74 (1.68-1.76)
Body mass [kg]	72.0 (66.0 – 77.0)	72.0 (65.8-77.0)	78.0 (75.0-95.0)
BMI [kg/m^2]	26.8 (24.8-29.3)	26.8 (24.8-29.7)	27.4 (24.2-29.3)
SBP [mmHg]	135.0 (125.0-140.0)	134.5 (120.0-140.0)	143.0 (135.0-153.0)
DBP [mmHg]	82.0 (76.0-89.0)	80.0 (75.5-87.5)	86.5 (84.0-95.0)
Fasting glucose [mg/dL]	88.5 (84.0-95.0)	88.0 (83.5-95.0)	93.5 (89.0-98.0)
T-C [mg/dL]	205.0 (196.0-229.0)	205.0 (197.0-229.0)	198.5 (189.0-222.0)
TAG [mg/dL]	123.0 (79.0-149.0)	122.0 (77.0-148.5)	153.0 (122.0-168.0)
HDL-C [mg/dL]	63.5 (56.0-74.0)	63.0 (56.0-73.0)	65.0 (44.0-77.0)
LDL-C [mg/dL]	123.2 (100.0-141.6)	124.9 (100.0-142.5)	107.0 (98.6-122.4)
creatinine [mg/dL]	0.98 (0.83-1.12)	0.97 (0.82-1.08)	1.11 (1.00-1.12)
Uric acid [mg/dL]	4.4 (3.9-5.1)	4.4 (3.9-5.1)	4.4 (3.8-5.4)
hs-CRP [mg/L]	**1.9 (0.9-2.9)**	**1.8 (0.9-3.0)**	**2.6 (2.3-5.8)**
FRAMINGHAM [pts]	16.0 (14.0-18.0)	17.0 (15.0-18.5)	14.0 (14.0-16.0)
FRAMINGHAM [%]	5.0 (3.0 – 8.0)	5.0 (3.0-6.0)	6.0 (4.0-8.0)
PROCAM [pts]	38.0 (33.0-45.0)	38.0 (33.0-45.0)	43.0 (38.0-46.0)
PROCAM [%]	5.0 (2.0-40.0)	5.0 (2.0-20.0)	5.0 (2.0-40.0)
POL-SCORE [pts]	5.0 (3.0 -10.0)	5.0 (3.0-7.0)	10.0 (6.0-17.0)

Table II. *The clinical and biochemical characteristics of low-hs-CRP, middle-hs-CRP and high-hs-CRP elderly independent community-living persons.*

	Elderly with low hs-CRP n=16 median (interquartile range)	Elderly with moderate hs-CRP n=25 median (interquartile range)	Elderly with high hs-CRP n=9 median (interquartile range)
Age [years]	65.5 (61.5 – 71.5)	63.0 (62.0-67.0)	65.0 (62.0-67.0)
High [m]	1.63 (1.59-1.64)	1.65 (1.62-1.70)	1.65 (1.60-1.66)
Body mass [kg]	70.0 (65.5 – 79.0)	72.0 (66.0-78.0)	74.0 (65.5-75.0)
BMI [kg/m^2]	27.1 (24.4-30.3)	26.8 (24.9-29.3)	26.4 (25.0-27.3)
SBP [mmHg]	130.5 (123.0-140.0)	132.0 (120.0-138.0)	140.0 (135.0-140.0)
DBP [mmHg]	80.0 (77.5-90.0)	80.0 (74.0-85.0)	85.0 (85.0-90.0)
Fasting glucose [mg/dL]	88.5 (81.0-95.0)	88.0 (83.0-92.0)	95.0 (88.0-97.0)
T-C [mg/dL]	191.5 (172.0-226.5)	207.0 (199.0-245.0)	207.0 (200.0-220.0)
TAG [mg/dL]	102.0 (79.0-129.5)	135.0 (75.0-152.0)	138.0 (122.0-159.0)
HDL-C [mg/dL]	64.5 (58.5-78.0)	65.0 (56.0-71.0)	58.0 (45.0-62.0)
LDL-C [mg/dL]	100.0 (73.0-133.9)	125.8 (109.2-142.4)	126.4 (109.6-139.6)
Creatinine [mg/dL]	1.03 (0.87-1.11)	0.95 (0.82-1.02)	1.02 (0.99-1.09)
Uric acid [mg/dL]	4.1 (3.8-5.1)	4.4 (3.9-5.1)	4.8 (3.8-5.5)
hs-CRP [mg/L]	**0.8 (0.6-0.9)**	**2.1 (1.6-2.7)**	**4.5 (3.9-5.8)**
FRAMINGHAM [pts]	17.0 (15.5-18.0)	15.0 (14.0-18.0)	17.0 (17.0-19.0)
FRAMINGHAM [%]	5.0 (3.5 – 6.0)	4.0 (2.0-8.0)	6.0 (5.0-14.0)
PROCAM [pts]	33.5 (29.5-43.0)	42.0 (33.0-45.0)	38.0 (37.0-46.0)
PROCAM [%]	5.0 (2.0-10.0)	5.0 (2.0-20.0)	5.0 (2.0-20.0)
POL-SCORE [pts]	6.5 (3.0 -8.5)	5.0 (3.0-10.0)	5.0 (5.0-6.0)

had lower hs-CRP ($p<0.01$) in comparison with the elderly independent community-living males studied. They did not differ in other CVD risk parameters (lipid profile, fasting glucose, creatinine and uric acid concentration) and CVD risk scales (FRAMINGHAM, PROCAM and Pol-SCORE). The characteristics of low-hs-CRP, moderate-hs-CRP and high-hs-CRP groups are presented in Table II. By definition, they differ in hs-CRP concentration. The groups did not differ in terms of age, anthropometric measures, BMI, fasting glucose, creatinine and uric acid concentrations, or analyzed CVD risk scales. We found higher systolic blood pressure in different hs-CRP groups – these gradually increased from the lowest to the highest risk group ($p<0.02$). Moreover, the low hs-CRP group had the lowest total cholesterol concentration. ($p<0.02$).

Correlation analysis considering hs-CRP and other parameters, for all hs-CRP groups, was performed. In all independent community-living elderly persons studied, moderate positive correlation was found between the hs-CRP and total cholesterol ($r= 0.335$; $p<0.05$), as well as in LDL-C ($r= 0.318$; $p<0.05$). A moderate positive correlation was also observed between the hs-CRP and PROCAM scale ($r=0.307$; $p<0.05$). In investigating the three hs-CRP groups, negative correlation for the hs-CRP and fasting glucose and DBP were found in the low hs-CRP risk

group (r= - 0.619; p<0.05 and r= -0.580; p<0.05, respectively) and negative correlation for hs-CRP and uric acid (r=-0.850; p<0.05) in the moderate hs-CRP risk group.

DISCUSSION

Meysamie and colleagues showed that females had higher CRP in comparison with males but the difference was not significant except for a subset of obese participants (with BMI>30) (8). Our male/female groups studied had comparable CVD risk factors and scales as well as BMI without obesity; however, the present study showed higher hs-CRP concentrations in men than in women. This is in agreement with the Seo et al. study (9).

Nutritional and metabolic status as well as water balance has an influence on men's health (10). The present analyses provide strong support for the use of hs-CRP in older adults without previous cardiovascular events. In this independent community-living healthy elderly population, we found that the relationship between hs-CRP levels and lipid profile is linearly dependent. This is in agreement with the study of Pirro et al., who showed that low density lipoprotein cholesterol was positively associated with hs-CRP levels (11) in elderly patients, however, they only studied those with hs-CRP concentration higher than 2 mg/L. Moreover, hs-CRP, low DBP and smoking were found to be predictors for coronary spasm, whereas age, diabetes mellitus, high SBP and uric acid were found to be predictors for atherosclerosis (12). In the present work, we studied a group of independent community-living elderly persons, non-smoking, with no diabetes and we found interactions between the hs-CRP and uric acid in the moderate hs-CRP group and for the hs-CRP and fasting glucose and DBP in the low hs-CRP risk group.

In conclusion, hs-CRP adds important information for primary cardiovascular prevention, and we suggest its application in evaluating independently-living healthy elderly populations at very early risk of CVD in this age group. These findings may help to greatly simplify decision-making for clinicians.

REFERENCES

1. Mozaffarian D, Benjamin EJ, Go AS, et al. on behalf of the American Heart Association Statistics Committee and Stroke Statistics Subcommittee. Heart disease and stroke statistics—2016 update: a report from the American Heart Association. Circulation 2016; 133:e38-e360.
2. D'Agostino RB, Sr, Vasan RS, Pencina MJ, Wolf PA, Cobain M, Massaro JM, Kannel WB. General cardiovascular risk profile for use in primary care: the Framingham Heart Study. Circulation 2008; 117:743-53.
3. Conroy RM, Pyorala K, Fitzerald AP on behalf of the SCORE project group. Estimation of ten-year risk of fatal cardiovascular disease in Europe: the SCORE project. Eur Heart J 2003; 24:987-1003.
4. Assmann G, Cullen P, Schulte H. Simple Scoring Scheme for calculating the risk of acute coronary events based on the 10-year follow-up of the prospective cardiovascular Münster (PROCAM) Study. Circulation 2002; 105(3):310-15.
5. Dzięgielewska-Gęsiak S, Bielawska L, Zowczak-Drabarczyk M, et al. The impact of high density lipoprotein on oxidant–antioxidant balance in healthy elderly people. Pol Arch Med Wewn 2016; 126(10):731-38.
6. Koenig W. High-sensitivity C-reactive protein and atherosclerotic disease: from improved risk prediction to risk-guided therapy. Int J Cardiol 2013; 168(6):5126-34.
7. Hayek SS, Ko Yi-An, Awab. A biomarker risk score incorporating myocardial injury, inflammation, coagulation and cellular stress improves the prediction of cardiovascular events. JACC 2016; 67(13):2136
8. Meysamie A, Ghodsi S, Ghalehtaki R, Esteghamati A, Asgari F, Gouya MM. Distributions of high-sensitivity C-reactive protein, total cholesterol-hdl ratio and 10-year cardiovascular risk: national population-based study. Acta Med Iran 2017, 55(4):218-27.
9. Seo SM, Baek SH, Jeon HK, et al. Correlations between the level of high-sensitivity C-reactive protein and cardiovascular risk factors in Korean adults with cardiovascular disease or diabetes mellitus: the CALLISTO study. J Atheroscler Thromb 2013; 20(7):616-22.

10. Malczyk E, Dziegielewska-Gesiak S, Fatyga E, Ziółko E, Kokot T, Muc-Wierzgoń M. Body composition in healthy older persons: role of the ratio of extracellular/total body water. J Biol Regul Homeost Agents 2016; 30(3):767-72.
11. Pirro M, Mannarino MR, Ministrini S, et al. Effects of a nutraceutical combination on lipids, inflammation and endothelial integrity in patients with subclinical inflammation: a randomized clinical trial. Sci Rep 2016; 6:23587.
12. Morita S, Mizuno Y, Harada E, et al. Differences and interactions between risk factors for coronary spasm and atherosclerosis- smoking, aging, inflammation, and blood pressure. Intern Med 2014; 53(23):2663-70.

JOURNAL OF BIOLOGICAL REGULATORS & HOMEOSTATIC AGENTS Vol. 32, no. 5, 1205-1210 (2018)

LETTER TO THE EDITOR

CHANGES IN ELECTROLYTES AND URIC ACID EXCRETION DURING AND AFTER A 100 KM RUN

W. WOŁYNIEC[1], W. RATKOWSKI[2], K. KASPROWICZ[3], S. MAŁGORZEWICZ[4], E. ALEKSANDROWICZ[4], K. WITEK[5], T. GRZYWACZ[6], P. ŻMIJEWSKI[6] and M. RENKE[1]

[1]Department of Occupational and Internal Medicine, Institute of Maritime and Tropical Medicine in Gdynia, Gdansk Medical University, Gdynia, Poland; [2]Department of Athletics, Academy of Physical Education and Sport, Gdańsk, Poland; [3]Department of Physiology, Academy of Physical Education and Sport, Gdańsk, Poland; [4]Department of Clinical Nutrition and Dietetics. Gdansk Medical University, Gdańsk, Poland; [5]Department of Biochemistry Institute of Sport – National Research Institute, Warsaw, Poland; [6]Department of Physiology, Institute of Sport – National Research Institute, Warsaw, Poland

Received March 2, 2018 – Accepted July 23, 3018

Physical activity leads to changes in water and electrolyte homeostasis and to enhanced purine metabolism. The typical abnormalities observed after exercise are hyperkaliemia, hyper- or hyponatremia and hyperuricemia. The possible explanations of hyperuricemia are: increased metabolism and decreased elimination of uric acid. Changes in uric acid excretion are commonly observed in disturbances of sodium and water homeostasis. The aim of this study was to evaluate changes in electrolytes and uric acid excretion during a very long period of exercise. Twenty subjects with a mean age of 40.75±7.15 years took part in a 100 km run. The route of the run was based on the university stadium track. All subjects were experienced amateur runners, with a mean time of regular running of 6.11±7.19 years. Blood was collected before the start, after every 25 km and 12 hours after the run. The levels of electrolytes, creatinine, uric acid, cortisol, aldosterone, creatine kinase, C-reactive protein and interleukin-6 were measured. Creatinine clearance, urinary potassium-to-sodium ratio, fractional excretion of electrolytes and uric acid were calculated. Seventeen runners completed the study. Significant increases in sodium (from 141.65±1.90 to 144.29±3.65mmol/l), potassium (from 4.53±0.34 to 5.03±0.42mmol/l), creatinine (from 0.88±0.11 to 1.10±0.20mg/dl) and uric acid (from 5.15±0.87 to 5.94±1.50 mg/dl) were observed after 100 km ($p < 0.05$). Other significant changes during the study were noted in fractional excretions of sodium (from 0.86±0.29 to 0.33±0.13%) and potassium (from 6.66±2.79 to 18.90±10.01%), probably reflecting the decrease in renal blood flow (RBF) and increase in renal tubule reabsorption. The fractional excretion of uric acid slightly increased but without statistical significance from 5.34±1.51 to 6.09±2.34%. The results of our study showed that during very long but not very intensive exercise there is no change in uric acid excretion, although at the same time profound changes in electrolyte excretion are found. Both hyperuricemia and hyperuricosuria may be harmful, therefore it seems logical that the best way to avoid those abnormalities is to maintain fractional uric acid excretion.

Key words: uric acid, sodium, physical activity

Mailing address:
Wojciech Wołyniec MD, PhD
Department of Occupational, Metabolic and Internal Medicine,
Institute of Maritime and Tropical Medicine, Medical University of Gdańsk,
81-519 Gdynia, ul Powstania Styczniowego 9b, Gdańsk, Poland
Tel.: +48 600942998
e-mail: wolyniecwojtek@gmail.com

0393-974X (2018)

To the Editor,

The maintenance of water and electrolyte homeostasis is a priority for the human body during a long period of exercise (1, 2). The increased sweating and evaporation during exercise can lead to fluid loss (1). During long-lasting exercise athletes drink various fluids to avoid dehydration; inexperienced runners, who are assumed to drink too much, are at risk of overhydration (2). The normal physiological reaction during exercise is the activation of adrenergic, vasopressin and renin-angiotensin-aldosterone (RAA) systems (2). The levels of norepinephrine, co-peptin, cortisol and aldosterone (2) are increased after a marathon and other physical activities. During exercise the renal blood flow (RBF) is decreased and proximal tubule reabsorption is increased (3). In the case of severe dehydration, the decrease in the glomerular filtration rate (GFR) may be significant (3).

All these factors are responsible for clinical and biochemical complications observed after a marathon run (2, 4). Heart arrest, acute kidney failure requiring dialysis, rhabdomyolysis and seizures are rarely observed after marathons and other exhausting events (4). The typical biochemical abnormalities observed after exercise are hyperkaliemia, hypernatremia, an increase in creatinine, uric acid (UA), urea, creatine kinase (CK), C-reactive protein (CRP) levels as well as many others (2, 4). The increase in the level of uric acid, a waste product of purine metabolism, is observed after almost every type of exercise (5). The possible explanations for hyperuricemia are increased metabolism and decreased elimination of uric acid (6). Changes in UA levels are also frequently observed in disturbances of water homeostasis. Hyperuricemia is typical in dehydration caused by diuretics (7, 8); hypouricemia and hyponatremia are two typical findings in the syndrome of inappropriate antidiuretic hormone (ADH) secretion (9) and salt losing nephropathy(10).

The authors of the present paper suspected that during very long exercise changes in the fractional excretion of sodium, potassium and uric acid would be observed.

MATERIALS AND METHODS

Twenty male participants took part in the study. All subjects were experienced healthy amateur runners, without kidney disease, diabetes, metabolic or cardiovascular disorders. The mean age was 40.75±7.15 years. The participants had a valid medical certificate and no contraindications against active sport exercise. None had a previous history of a sports career. There were no diet restrictions. The runners were not taking any drugs except supplementation of vitamin D. The participants were asked to fill in a questionnaire concerning their training, including daily physical activity and marathon experience. Anthropometric analysis was performed before and after the marathon. Laboratory analysis was performed before, during and after the run in accordance with the schedule.

Anthropometric analysis

The 100 km run was preceded by an anthropometric analysis to estimate the following parameters: weight, height, body mass index (BMI), waist-hip ratio (WHR) and percentage body fat (PBF). Blood pressure and heart rate were measured before the run and during rest.

Run

The route of the run was based on the university stadium track (400 m track circumference). During the race the organizer provided stations offering food and beverages such as sports drinks, tea, soup, caffeinated drinks, water, fruits like bananas and oranges, chocolate, energy bars and bread. The food and drink stations were readily available and accessible along the route. The runners were informed to drink enough to urinate every 25 km. The temperature during the run rose from 1°C (7 am) to 4°C (1-4 pm) and then dropped to 3°C at the end of the study (4-7 pm). The relative humidity dropped from 100% (7 am) to 93% (1-4 pm) and then rose to 100% (4-7 pm). Barometric pressure ranged from 1009 hPa (7 am) to 1000 hPa (7pm).

Samples

The first biochemical assessment took place one day before the study. Blood and urine samples were taken before the run and urine collection was started. During the study, 6 urine collections were performed. The first

urine collection was performed before the start and then after each 25 km. After the run, the subjects' urine was collected during a 12-hour period. Blood was collected before the start, after every 25 km (a sample after 25, 50, 75, 100 km) and 12 h after the run. Venous blood samples were drawn from the antecubital vein in a sitting position. Each venous blood sample was collected in an SST gel separator tube (BD Vacutainer). Serum was separated by centrifuging samples at 1000 G for 10 min. All samples were stored at -80°C until analysis.

Laboratory analysis

Sodium and potassium were measured in serum and urine by potentiometry (Cobas 8000 Roche, Roche Diagnostics GmbHMannheim). Creatinine was measured in serum and urine by kinetic colorimetric assay (Cobas 8000 Roche, Roche Diagnostics GmbHMannheim). Uric acid was measured in serum and urine by spectrophotometry assay (Cobas 8000 Roche, Roche Diagnostics GmbHMannheim). Serum glucose was measured by spectrophotometry (Cobas 8000 Roche, Roche Diagnostics GmbHMannheim). ESR was measured by the Alifax Test 1 THL system. Hemoglobin was measured by spectrophotometry (the SLS-hemoglobin method). Erythrocytes and platelets were measured by the DC detection method (Sysmex XN2000). Leucocytes, neutrocytes, lymphocytes, monocytes, eosinophils and basophils were measured by flow cytometry (Sysmex XN 2000). Mean corpuscular volume was calculated automatically by the Sysmex XN 2000 analyzer. All reagents used in the Sysmex XN 2000 analyzer were manufactured by Sysmex. Measurement of creatine kinase was performed by spectrophotometric methods, and C-reactive protein (CRP) by turbidimetry methods with a Cobas Integra 400 Roche biochemical analyser (Switzerland), using the original manufacturer reagent kits. Urinalysis was performed with the Cobas U411 analyzer (Roche Diagnostics GmbH Mannheim) by using a test strip for the semi-quantitative determination of specific gravity, pH, leucocytes, nitrite, protein, glucose, ketone bodies, urobilinogen, bilirubin and blood (Combur 10 Test M, Roche Diagnostics GmbHMannheim).

Cortisol and aldosterone concentrations were measured by the ELISA method using DRG Diagnostics kits (Germany). The interleukin-6 serum concentration was measured by the ELISA method using R&D Systems kit (USA).

Creatinine clearance (ClCr) was calculated from blood and urine collections using the formula:

CICr = (uCr x urine flow) ÷ sCr

where sCr is serum creatinine and uCr is urine creatinine

Fractional excretion (Fe) of sodium, potassium, urea and uric acid during the race was calculated using the formula:

Fractional excretion of parameter = [(parameter in urine x creatinine in serum) ÷ (parameter in serum x creatinine in urine)] Urinary potassium-to-sodium ratio (Na/K ratio) = sodium in urine ÷ potassium in urine

Statistical analysis

The authors used Statistica 12 software (StatSoft, Poland) for analysis. Descriptive statistics for continuous variables were reported as mean values and standard deviations. The Shapiro-Wilk test was applied to assess the homogeneity of dispersion from the normal distribution. The Levene test was used to verify homogeneity of variance. For homogeneous results, an analysis of variance (ANOVA) for repeated measures and the *post hoc* Tukey's honest significant difference (HSD) test for equal sample size were performed to identify significantly different results. For heterogeneous results, the Friedman's ANOVA test and right *post hoc* test were used. In all analyses, a p-value < 0.05 was considered statistically significant.

The authors declare that the experiments reported in the manuscript were performed in accordance with the ethical standards of the Helsinki Declaration. The study was approved by the Medical Ethics Committee of the Medical University of Gdansk (approval nr NK8BN 448/2016). All subjects gave their written informed consent to participate in the study.

RESULTS

All the runners studied were very experienced. The mean time of regular running was 6.11±7.19 years, and the average training distance in the 3 months preceding the study was 225.38±98.33 km/month. The mean number of marathons completed was 43.89±110.11 and the mean marathon personal best time was 3:24±0:22

(h:min) The mean number of ultramarathons completed was 15.06±13.54. All subjects were healthy and there were no abnormalities in biochemical tests performed before the study.

In the pre-run evaluation, the mean ESR was 3.42±2.81 mm/h; mean creatinine 0.84±0.08 mg/dl; mean glucose 87.67±11.1mg/dl, mean hemoglobin 15.46± 0.9 g/dl, mean erythrocytes 5.22±0.4 T/l; mean white blood cells 6.5±1.16 G/l, and mean platelets 250.58±39.43 G/l. In urinalysis, the mean special gravity was 1.015±1.007, and the mean pH 6.17±1.03. No runner had glucosuria, proteinuria or hematuria.

Seventeen runners completed the study. Three others were unable to complete the competition within 14 hours and their results were not included in the statistical analysis. The mean run rate was 6:47 min/km. The first runner completed 100 km after 9 h 52 min, and the last subject finished the race after 13 h 34 min. These results are typical of amateur ultramarathon runners who are used to slow, long running.

The mean age of the finishers was 40.18±4.57 years, the mean height and weight were 178.59±6.21 cm and 77.47±8.80kg, respectively. The mean BMI was 24.26±2.28 kg/m^2, the mean percentage body fat was 13.56±5.80% and the mean waist-hip ratio 0.81±0.06. The mean pre-race blood pressure was 136.12±10.62/82.12±7.92 mmHg and heart rate 66.41±8.69 beats per minute (bpm). The mean post-race systolic blood pressure was 129.94±11.09 mmHg and diastolic blood pressure 75.56±8,12 mmHg; the mean post-race heart rate was 71.81±8.29 bpm. Significant increase in sodium, potassium, creatinine and uric acid levels was observed after 100 km ($p < 0.05$) (Table I). There were no severe cases of hypernatremia and hyperkalemia, although in 6 subjects mild hypernatremia (Na > 145 mmol/l) and in 11 subjects mild hyperkaliemia (K > 5.1 mmol/l) were observed at least at one point during the study. None of the subjects had hyponatremia (Na < 135 mmol/l) and hypokaliemia (K < 3.5 mmol/l). Sodium and potassium levels returned to normal values during the rest period. The sodium level was lower after 12 h than before the run ($p < 0.05$). Significant changes were noted in fractional sodium excretion (FeNa), fractional potassium excretion (FeK), and urine Na/K ratio (Table I). There were no cases of severe dehydration or overhydration on a clinical basis. There were no significant changes in hematocrit. The urine output was unchanged, probably because the runners were instructed to drink adequately. The creatinine clearance calculated from urine collections was stable, and did not significantly decrease during the run (Table I).

The FeUA was surprisingly stable during the run. This suggests increased purine metabolism without changes in urate transport in tubules during exercise. A typical increase in muscle enzyme (creatine kinase), myokin (interleukin 6) and acute phase protein (CRP) was noted, as well as a significant increase in cortisol and aldosterone. All these changes were significant ($p<0.05$) (Table I).

DISCUSSION

The interesting finding of this study is that during very long exercise there were no changes in fractional UA excretion, although at the same time profound changes in electrolyte excretion were found. This is surprising, because there is a strong correlation between water and electrolyte homeostasis and the uric acid level in clinical practice (6, 7). In one previous human study, a significant decrease in FeUA was found after short intensive exercise (11), probably due to sodium and water depletion and renin–angiotensin system (RAS) activation (7). There is a link between apical tubular reabsorption of Na and UA in proximal tubule due to synergistic action of two exchangers - SCL5A8, which reabsorbs Na, and URAT 1, which reabsorbs UA (12). During exercise a decrease in the renal plasma flow and an increase in tubule reabsorption is observed (3). Water and sodium are vastly reabsorbed during exercise in proximal tubule (3).

Nevertheless, in the present study there was no change in FeUA. The FeUA was surprisingly stable during the run. Otherwise profound changes in FeNa, FeK and urine Na/K ratio appeared as early as after the first 25 km, then remained stable and were still observed after a 12-hour rest.

Table I. *Changes in parameters of kidney function, hematocrit, electrolytes, CK, IL-6, CRP, cortisol and aldosterone levels during the run.*

	Before run	After 25 km	After 50 km	After 75 km	After 100 km	Rest
Na (mEq/l)	**141.65 ± 1.90$^{\&¥\$£}$**	**144.24 ± 1.86$^{\&}$**	**143.83 ± 2.33$^{¥}$**	**144.29 ± 3.65$^{\$}$**	142.59 ± 2.29	**139.47 ± 1.62$^{£}$**
K (mEq/l)	**4.53 ± 0.34$^{\&¥\$}$**	**5.01 ± 0.47$^{\&}$**	**5.04 ± 0.38$^{¥}$**	**5.03 ± 0.42$^{\$}$**	4.65 ± 0.39	4.32 ± 0.38
FeNa (%)	0.86 ±0.29$^{\&}$	0.67 ±0.37	0.63 ±0.44	0.60 ±0.51	0.54 ±0.4	0.33 ±0.13$^{\&}$
FeK (%)	6.66 ±2.79$^{\&¥\$£}$	14.31 ±5.51$^{\&}$	16.33 ± 7.49$^{¥}$	17.13 ±9.14$^{\$}$	18.90 ±10.01$^{£µ}$	10.68 ±4.1^{µ}
uNa/K ratio	4.43 ± 1.66$^{\&¥\$£µ}$	1.31 ±0.41$^{\&}$	0.96 ±0.36$^{¥}$	1.01 ±0.5$^{\$}$	1.05 ±0.65$^{£}$	1.21 ±0.59^{µ}
Creatinine (mg/dl)	**0.88 ± 0.11$^{\&¥}$**	0.97 ± 0.11	1.00 ± 0.14	**1.07 ± 0.167$^{\&}$**	**1.10 ± 0.20$^{¥}$**	0.97 ± 0.12
CrCl (ml/min)	141.81 ± 25.08	136.93 ± 47.55	144.04 ± 28.20	120.33 ± 38.83	137.78 ± 41.04	150.50 ± 43.33
Uric acid (mg/dl)	**5.15± 0.87$^{\&¥\$£µ}$**	**5.32 ± 0.96$^{\&}$**	**5.62 ± 1.19$^{¥}$**	**5.82 ± 1.37$^{\$}$**	**5.94 ± 1.50$^{£}$**	**6.09 ± 1.43^{µ}**
FeUA (%)	5.34 ±1.51	6.05 ±1.71	5.67 ±2.1	6.01 ±2.28	6.09 ±2.34	5.63 ±1.66
Hematocrit (%)	46,83 ±2.18	47,02 ±2.17	46,11 ±2,35	45,5 ±2.48	45,41 ±2,19	43,33 ± 2,55
CK (U/l)	**175.06 ±103.73$^{\&¥}$**	290.59 ±175.56	662.77 ±409.87	2863.88 ±2649.16	**9330.59 ±10290.57$^{\&}$**	**8382.94 ±7551.43$^{¥}$**
Interleukin 6 (pg/ml)	0.98 ±0.34$^{\&¥\$}$	**6.31 ±2.68$^{\&£}$**	n.d.	n.d.	**22.41 ±1.95$^{¥£ µ}$**	**8.64 ±5.76$^{\$ µ}$**
CRP (mg/l)	**0.55 ±0.33$^{\&}$**	0.43 ±0.24	0.49 ±0.28	1.32 ±0.94	5.21 ±3.92	**44.26 ±34.34$^{\&}$**
Cortisol (nmol/l)	599.71 ±81.71$^{\&¥\$£}$	480.94 ±142.72$^{\&}$	727.59 ±143.29$^{¥}$	829.18 ±178.71$^{\$}$	977.88 ±311.26$^{£ µ}$	356.23 ±119.47^{µ}
Aldosterone (pg/ml)	214.01 ± 120.97$^{\&}$	236.5 **±124.**12$^{¥}$	n.d.	n.d.	485.83 ±261.7$^{\&¥\$}$	265.82 ±117.63$^{\$}$

$^{\&¥\$£µ}$ *- values with the same superscript differ significantly, at $p < 0.05$. Abbreviations: FeNa: fractional sodium excretion; FeK: fractional potassium excretion; uNa/K: urine sodium-to-potassium ratio; CrCl: creatinine clearance; FeUA: fractional uric acid excretion; CK: creatine kinase; CRP: C-reactive protein; n.d.: not done.*

The explanation of UA increase observed in our study is enhanced metabolism due to acceleration of adenine nucleotide degradation (11). It is known that humans have higher UA levels than other mammals and cannot metabolize UA due to the loss of uricase activity (6, 7). In such a situation, a further increase in serum UA caused by decreased UA excretion could be dangerous and harmful for the organism, especially for severely dehydrated persons with mild acidosis (e.g. during ultramarathons). Therefore, it seems logical that humans should somehow protect themselves against rapid UA increases during exercise. The possible factor increasing UA excretion during exercise is inhibition of UA reabsorption by organic anions such as lactate and acetoacetate (6). Another possible explanation is increase of vasopressin, which has the opposite effect on UA reabsorption to aldosterone (9).

REFERENCES

1. Trangmar SJ, Gonzalez-Aionso J. New insights into the impact of dehydration on blood flow and metabolism during exercise. Exerc Sport Sci Rev 2017; 45(3):146-53.
2. Burge J, Knechtle B, Knechtle P, Gnadinger M, Rust CA, Rosemann T. Maintained serum sodium in male ultra-marathoners-the role of fluid intake, vasopressin, and aldosterone in fluid and electrolyte regulation. Horm Metab Res 2011; 43(9):646-52.
3. Mallie JP, Ait-Djafer Z, Saunders C, et al. Renal handling of salt and water in humans during exercise with or without hydration. Eur J Appl Physiol 2002; 86(3):196-202.
4. Mayer CU, Treff G, Fenske WK, Blouin K, Steinacker JM, Allolio B. High incidence of hyponatremia in rowers during a four-week training camp. Am J Med 2015; 128(10):1144-51.
5. Sutton JR, Toews G, Ward GR, Fox IH. Purine metabolism during strenuous muscular exercise in man. Metabolism 1980; 29(3):254-60.
6. de Oliveira EP, Burini RC. High plasma uric acid concentration: causes and consequences. Diabetol Metab Syndr 2012; 4:12.
7. Hyndman D, Liu S, Miner JN. Urate handling in the human body. Curr Rheumatol Rep 2016; 18(6):34.
8. Lipkowitz MS. Regulation of uric acid excretion by the kidney. Curr Rheumatol Rep 2012; 14(2):179-88.
9. Taniguchi K, Tamura Y, Kumagai T, Shibata S, Uchida S. Stimulation of Via receptor increases renal uric acid clearance via urate transporters: insight into pathogenesis of hypouricemia in SIADH. Clin Exp Nephrol 2016; 20(6):845-52.
10. Lee SK, Lanaspa MA, Sanchez-Lozada LG, Johnson RJ. Hyponatremia with Persistent Elevated Urinary Fractional Uric Acid Excretion: Evidence for Proximal Tubular Injury? Kidney Blood Press Res 2016; 41(5):535-44.
11. Kaya M, Moriwaki Y, Ka T, et al. Plasma concentrations and urinary excretion of purine bases (uric acid, hypoxanthine, and xanthine) and oxypurinol after rigorous exercise. Metabolism 2006; 55(1):103-7.
12. Esparza Martín N, García Nieto V. Hypouricemia and tubular transport of uric acid. Nefrologia 2011; 31(1):44-50.

JOURNAL OF BIOLOGICAL REGULATORS & HOMEOSTATIC AGENTS Vol. 32, no. 5, 1211-1214 (2018)

LETTER TO THE EDITOR

PSYCHOLOGY OF CROSS-CULTURAL COMMUNICATION: AN IMPACT ON THE HEALTH CARE SYSTEM

X. XU, X. GAO, C. GUAN and J. HU

College of Foreign Studies, Hubei Normal University, Huangshi, Hubei, China

Received April 30, 2018 – Accepted July 23, 2018

Cross culture communication has become an integral part of today's world, especially in developed countries with a large population of immigrants. The health care system is one of the important areas in which health care practitioners and patients may be of different cultures, therefore there is a need of effective communication between culturally different patients and health practitioners. However, cross-culture communication is affected by psychological factors related to cultures and mind-set. Acculturation orientation is one of the important factors, and people with different orientations interact differently with people of different cultures. Cultural orientation is another important factor is which different domains define the characteristic features of different cultures. Moreover, the inclination to use native or non-native language with culturally different patients is a key factor for establishing a good relationship between patients and health care practitioners.

To the Editor,

Culture is defined as group of people with similar values and beliefs. The people with same culture may share the same country, religion and socioeconomic status (1). Cross culture refers to a state in which persons of different cultures interact with one another. In this world of globalization, the importance of cross-cultural communication has increased in virtually every field, including the health care system. The lack of proper communication between patients and health practitioners may impair the quality of health care, particularly in countries with a large population of immigrants. Health practitioners may exhibit less empathy to immigrant patients, mainly due to cross-cultural communication barrier (2, 3). The quality of communication between culturally different patients and physicians is generally poor (4), which may lead to disparities in health care services. Some training models have been devised for enhancing communication skills, while interacting with persons of different cultural backgrounds. One such model is LEARN, which stands for Listen, Explain, Acknowledge, Recommend and Negotiate (5).

Cross-cultural communication is affected by psychology and there are psychological factors that may affect the communication between individuals of different cultures. These may include cultural orientation of people (1) and mind-set of persons i.e., they want to preserve their cultural identity or they tend to interact with people of other cultures (6). The present review discusses the key psychological factors that may influence the effective communication between culturally different people, especially in the health care system.

Acculturation orientations

The cultural change due to migration of people is called 'acculturation' and is defined as the change

Key words: communication; cross culture, immigrants, psychology, language, acculturation

Mailing address:
Xiaorong Xu,
College of Foreign Studies,
11 Cihu Road, Huangshi,
Hubei, China 435000
e-mail: happyxuxr@yahoo.com

0393-974X (2018)

in the cultural pattern due to continuous interaction between individuals of different cultures (7). In these situations, either the people tend to maintain their cultural identity (cultural conservatism) or tend to make relations awith the others (interaction tendency). Accordingly, it has been shown that there may be four types of acculturation orientation

In 'integration orientation' there is a high tendency of interaction between individuals of two different cultural groups. Indeed, the people of different cultures interact freely with one another and it may lead to development of a mixed culture incorporating the characteristics of different cultures (8).

'Separation orientation' is the opposite of integration orientation and there is very low interaction between different cultural groups. Therefore, it is a type of cultural conservatism in which people maintain their cultural identity, without mixing with other cultures.

In 'assimilation orientation' there is good interaction between individuals of different cultures. The immigrants tend to assimilate the cultural characteristics of the host country (9).

In 'marginalisation orientation' there is relatively less interaction between individuals of different cultures (8).

One study showed the impact of acculturation orientations on communication and relationship between health practitioners and patients. Canada is a multicultural country and has large population of immigrants. It was proposed that the immigrant population may constitute 1/4 of the total Canadian population by 2031 (10). A research study showed the impact of acculturation orientations on communication between health practitioners and patients in Canada-based hospitals. The study included 5 health practitioners and 5 patients (total ten participants), and data were collected using video recordings and by conducting interviews. In the study, a questionnaire was used to father information on acculturation orientation of physicians and patients. Later, the interactions between physicians and patients were recorded to understand the quality of health practitioners-patient communication. It was reported that the nature of communication between culturally different physicians and patients was dependent on their combined acculturation orientations. The patients with integration orientation and health practitioners with any of the four attitudes led to development of positive communication. Furthermore, a consensual relationship was developed between patients and health practitioners with the same acculturation orientation. However, patients and health practitioners with mismatched acculturation orientation led to development of conflicts (6).

Cultural orientation (Cultural Dimensions Theory)

There is a key role of cultural orientation in determining the quality of communication between culturally different people. Hofstede proposed a 'Cultural Dimensions Theory', which is widely used as a theoretical model in research pertaining to cross-cultures. In this theory, there are different 'domains', or 'dimensions' that define the characteristic features related to values and beliefs of that particular culture. Indeed, Hofstede proposed this theory to differentiate the cultural differences of diverse nations on the basis of differences in these domains or dimensions (11). Due to these cultural dimensions, there may be communication preferences between patients and health practitioners. In general, there are two types of behaviors in interaction between patients and health practitioners i.e., instrumental and affective. Instrumental behavior is a defined 'behavior of a health practitioner towards patient' with set guidelines such as asking questions and counseling. This type of behavior is focused on a given task and orientation of a health practitioner is towards the therapy i.e., is the therapy working or not? On the other hand, affective behavior is more patient-oriented and includes socio-economical talks with patients. The different types of cultural orientations and their impact on physician behavior are discussed below.

Power distance is related to the extent to which a weaker section of the society considers that there is no equal distribution of power. The Power Distance Index (PDI) is usually employed to designate the power differences in society. In lower PDI cultural society, there is a decentralized authority and a relatively equality in power. On the other hand, in a high PDI cultural society, there is a centralized authority and

there is a wide gap in power in different segments of the society. Health practitioners from high PDI countries show more instrumental behavior (11).

'Uncertainty avoidance' is related to the extent to which society members feel insecure in uncertain situations. This dimension relates to the degree to which individuals of a society are tolerant or comfortable with uncertain or unknown situations. The societies with high uncertainty avoidance are dependent on the formalized policies and procedures and these are resistant to any change. The people in this type of culture do not mix with one another. On the other hand, societies with low uncertainty avoidance mainly rely on the informal norms and behaviors in most matters. The people of this society are interactive and the health practitioners from these countries show more affective behavior than instrumental behaviors.

'Masculinity-femininity' is related to the extent to which values are masculine or feminine. In masculine societies, there is a clear distinction between gender specific roles. On the other hand, there is an overlap of gender specific roles in feminine societies. The health practitioners from more masculine countries show more affective behaviors.

'Individualism-collectivism' is used to define the relationship between the members of society. In individualistic societies, there are loose ties or relationships between individuals. On the other hand, there are strong, integrated and cohesive relationships between individuals in collectivist societies. The health practitioners from these countries exhibit more affective behavior and less instrumental behaviors.

Long-term orientation defines the orientation of people living in a given society i.e., long or short-term orientation. In a long-term oriented society, people value persistence. On the other hand, in a short-term oriented society, people value personal steadiness and stability.

A recent study on pharmacists conducted in Doha Qatar University revealed the impact of cultural orientation on the nature of behavior. It was shown that the health care practitioners with cultural orientations of power distance and masculinity-femininity demonstrate poor instrumental and mixed affective behavior towards patients, suggesting the key role of cultural orientations on communication (1).

Inclination to use native language

A recent study from Vienna, Austria reported the importance of language in cross-cultural communication in the health care system. The authors suggested the need of specific language-related training programs to overcome the communication block between patients and health care practitioners (12). Indeed, it is a common feature that the health care practitioners prefer to use their first language to instruct the patients. On the other hand, due to culture diversity, they may have to use non-native language to communicate with patients. In one study, 179 nurses gave their feedback about their preparedness for cross-cultural communication and skillfulness by filling in questionnaires. These health care practitioners reported that they feel less confident when communicating in non-native language with patients. They also reported that communication skills training programs may produce better outcomes and overcome the communication block (12).

CONCLUSION

Cross-culture communication in the health care system is affected by acculturation orientations in which either the persons are inclined to conserve their culture and do not interact frequently or the persons have the tendency to interact frequently with culturally different people. Moreover, the cultural orientation of people and inclination to use native language are the psychological factors that may affect communication between culturally different people.

ACKNOWLEDGEMENTS

The work was supported by Humanities and Social Science Foundation of Educational Commission of Hubei Province, China (16Y099). The authors thank professors of College of Foreign Studies of Hubei Normal University Huangshi, Hubei, China, for helpful suggestions and support, and International Education College of Hubei Normal University for preparation and literature search.

REFERENCES

1. Wilby KJ, Govaerts MJ, Austin Z, Dolmans DH. Exploring the influence of cultural orientations on assessment of communication behaviours during patient-practitioner interactions. BMC Med Educ 2017; 17:61.
2. Klug U, Bogic M, Deville W, et al. Health services and the treatment of immigrants: data on service use, interpreting services and immigrant staff members in services across Europe. Eur Psychiatry 2012;27:S56-62.
3. Schouten B, Meeuwesen L, Harmsen HAM. The impact of an intervention in intercultural communication on doctor-patient Interaction in The Netherlands. Patient Educ Couns 2005; 58:288-95.
4. Dell'Arciprete A, Braunstein J, Touris C, Dinardi G, Llovet I, Sosa-Estani S. Cultural barriers to effective communication between Indigenous communities and health care providers in Northern Argentina: an anthropological contribution to Chagas disease prevention and control. Int J Equity Health 2014; 13:6.
5. Ladha T, Zubairi M, Hunter A, Audcent T, Johnstone J. Cross-cultural communication: Tools for working with families and children. Paediatr Child Health 2018; 23:66-9.
6. Whittal A, Rosenberg E. Effects of individual immigrant attitudes and host culture attitudes on doctor-immigrant patient relationships and communication in Canada. Int J Equity Health 2015; 14:108.
7. Erten EY, van den Berg P, Weissing FJ. Acculturation orientations affect the evolution of a multicultural society. Nat Commun 2018; 9:58.
8. Berry JW. Immigration, acculturation, and adaptation. Appl Psychol 1997; 46, 5-34.
9. Taft R. The Assimilation Orientation of Immigrants and Australians. The International Migration Digest 1964; 1 (2):129-142.
10. Malenfant EC, Lebel A, Martel L. Projections of the diversity of the Canadian population, 2006–2031. Statistics Canada Demography Division, 2010, Catalogue 91-551-X; 2010.
11. Hofstede G. National cultures in four dimensions: a research-based theory of cultural differences among nations. Int Stud Manag Organ 1983;13:46-74.
12. Gasiorek J, van de Poel K. Language-specific skills in intercultural healthcare communication: Comparing perceived preparedness and skills in nurses' first and second languages. Nurse Educ Today 2018; 61:54-9.

LETTER TO THE EDITOR

TUMOR POTENTIAL IN RAT WOUNDS AFTER SHORT- AND LONG-TERM ADMINISTRATION OF PLATELET-RICH PLASMA: AN UPDATE

E. SPARTALIS[1], D.I. TSILIMIGRAS[1], I. NTANASIS-STATHOPOULOS[2], M. SPARTALIS[1] and D. MORIS[3]

[1]Laboratory of Experimental Surgery and Surgical Research, University of Athens Medical School, Athens, Greece; [2]Department of Clinical Therapeutics, National and Kapodistrian University of Athens, School of Medicine, Alexandra General Hospital, Athens, Greece; [3]Department of Surgery, The Ohio State University Comprehensive Cancer Center, The Ohio State University, Columbus, OH, USA

Received February 26, 2018 – Accepted August 1, 2018

Comment on: Omar NN, et al. Tumor potential in rat wounds after short- and long-term administration of platelet-rich plasma. J Biol Regul Homeost Agents. 2017 Oct-Dec;31(4):889-899. Platelet-Rich Plasma (PRP) is a promising concentrate. But are there any disadvantages or contraindications regarding its application? Is the use of PRP indicated in wounds of patients undergoing resection for cancer. The presence of growth factors could promote tumor proliferation and recurrence. It is of the utmost importance to recognize any possible contraindication before we call it safe. The role of PRP in tumorigenicity deserves further experimental investigation and large-scale prospective randomized clinical trials.

To the Editor,

We read with great interest the article by Omar et al. (1) entitled "Tumor potential in rat wounds after short- and long-term administration of platelet-rich plasma". We agree that platelet-rich plasma (PRP) has been recognized as an effective strategy for tissue regeneration, however, its safety in healing, in terms of tumorigenicity, has not yet been addressed.

The Authors examined the impact of PRP administration on the expression of the inflammatory marker tenascin-C (TnC) and the myofibroblast markers, α-smooth muscle actin (α-SMA) and vimentin. They concluded that PRP can be safely used in short- and long-term administration without tumorigenesis concern.

But is this enough in order to consider PRP as a potentially harmless concentrate that could be applied in any wound? What if the wound is a result of a tumor excision procedure?

Several studies on cancer growth, progression, recurrence and postoperative survival rate, focus on the tumor stroma, which represents a crucial parameter in tumor development (2). Much research is now devoted to determining the impact of platelet-derived growth factors on tumor development and progression, and the reciprocal influences of tumor products on the stromal microenvironment. A more detailed understanding of the complex parameters that govern the interactions between the tumor and surrounding compartments has already helped to improve anti-cancer strategies, not only for treatment, but also for preventing recurrence (3).

Key words: platelet-rich plasma, cancer, recurrence, safety

Mailing address:
Eleftherios Spartalis, MD, MSc, PhD
Vasilissis Sofias 49,
Athens 106 76, Greece
Tel.: +30 6974714078
Fax: +30 2106416015
e-mail: eleftherios.spartalis@gmail.com

0393-974X (2018)

DISCLOSURE: ALL AUTHORS REPORT NO CONFLICTS OF INTEREST RELEVANT TO THIS ARTICLE.

The secretory proteins contained in the α-granules of platelets include platelet-derived growth factor (PDGF-AA, BB, and AB isomers), transforming growth factor- β (TGF-β), vascular endothelial growth factor (VEGF), epidermal growth factor (EGF), platelet-derived endothelial growth factor (PDEGF), and many others (4).

The release of these growth factors stimulates angiogenesis, induces tumor lymphangiogenesis, enhances nodal metastasis rate, regulates several cell biology processes, including tumorigenesis, proliferation and survival, and many others such as cell differentiation, migration, and apoptosis (5).

In carcinogenesis, promoting substances are known to act upon increased proliferation among the initially mutated cell clones, by modifying certain cellular biochemical processes. If the mitogenesis of these initially mutated cells is not promoted, the host control mechanisms could induce the death of these altered cells before the latter reach end-differentiation. This means that therapeutic growth-factor concentrates such as PRP could act more as promoters than as initiators of carcinogenesis (6).

At this point, and in order to muddy the waters, we would like to pose the question in reverse: shall we consider PRP as a harmful concentrate that could not be applied for wound repair on a tumor excision bed? We strongly believe that the role of PRP in tumor recurrence deserves further experimental investigation and large-scale prospective randomized clinical trials.

We propose animal models that resemble e.g. human skin cancer development. In such case, genetic changes of the rodent skin physiology caused by carcinogens and pro-inflammatory cytokines, and simultaneous inflammation sustained by pro-inflammatory chemokines will favor tumor progression (7). After surgical resection of these tumors, PRP application can be tested on the tumor bed. These studies could provide an indication of the extent to which PRP growth-factors instruct tumor microenvironment and promote recurrence.

REFERENCES

1. Omar NN, El-Tawdi AH, Tash RF, Shoukry Y, Mahmoud NA, El Bakly W. Tumor potential in rat wounds after short- and long-term administration of platelet-rich plasma. J Biol Regul Homeost Agents 2017; 31(4):889-99.
2. Spartalis ED, Tomos P, Dimitroulis D, Kouraklis G. Platelet-rich plasma in surgical oncology. Surg Innov 2014; 21(4):441.
3. Spartalis E, Moris D, Dimitroulis D, Tomos P. postresectional airway fistula occlusion via stem-cell transplantation: is it oncologically safe? Ann Thorac Surg 2015; 100(6):2413-14.
4. Spartalis E, Tomos P, Konofaos P, et al. The effect of autologous platelet-rich plasma on bronchial stump tissue granulation after pneumonectomy: experimental study. ISRN Surg 2013; 2013:864350.
5. Spartalis E, Tomos P, Konofaos P, Dimitroulis D, Kouraklis G. Breast reconstruction with autologous fat graft; does platelet-rich plasma affect patient's survival? Int J Clin Exp Med 2014; 7(1):329-30.
6. Martinez-Gonzalez JM, Cano-Sanchez J, Gonzalo-Lafuente JC, Campo-Trapero J, Esparza-Gomez G, Seoane J. Do ambulatory-use platelet-rich plasma (PRP) concentrates present risks? Med Oral 2002; 7(5):375-90.
7. Neagu M, Caruntu C, Constantin C, Boda D, Zurac S, Spandidos DA, Tsatsakis AM. Chemically induced skin carcinogenesis: Updates in experimental models (Review). Oncol Rep 2016; 35(5):2516-28.

LETTER TO THE EDITOR

ARTEMISININ AMELIORATES THE SYMPTOMS OF EXPERIMENTAL AUTOIMMUNE MYASTHENIA GRAVIS BY REGULATING THE BALANCE OF Th1 CELLS, Th17 CELLS AND TREG CELLS

W. CHEN[1], FF. LI[2], C. LI[3], JK. SUI[4], QF. MENG[5], XL. LI[6], H. LI[6], CH. LI[7] and YB. LI[6]

[1]Shanghai Jiao Tong University Affiliated Sixth People's Hospital, Shanghai, China; [2]The Fourth People´s Hospital of Linyi, Linyi, Shandong, China; [3]Department of general surgery, Shandong Provincial Traditional Chinese Medical Hospital, Jinan, Shandong, China; [4]College of Life Science, Shandong Agricultural University, Tai´an, Shandong, China; [5]Department of Neurology, Second Affiliated Hospital of Shandong Traditional Chinese Medicine University, Jinan, Shandong, China; [6]Department of Neurology, Shandong Provincial Qianfoshan Hospital, Shandong University, Jinan, Shandong, China; [7]Department of Neurology, Jinan Traditional Chinese Medicine Hospital, Jinan, Shandong, China

Received March 9, 2018 – Accepted July 24, 2018

Myasthenia gravis (MG) is an autoimmune disease characterized by fatigue and muscle weakness. Artemisinin and its derivatives were reported to be experimentally used to treat autoimmune diseases, such as systemic lupus erythematosus (SLE) and experimental allergic encephalomyelitis (EAE). Here, we tested the effects of artemisinin on experimental autoimmune myasthenia gravis (EAMG). Our data confirmed that artemisinin markedly ameliorated the symptoms of EAMG rats. There was a decreased level of tumor necrosis factor-α (TNF-α) and IL-17+ cells in mononuclear cells (MNCs), and an increased level of transforming growth factor-β1 (TGF-β1) and Treg cells in MNCs. These findings indicate that artemisinin may be a new choice for MG treatment.

To the Editor,

Many studies in recent years have focused on the treatment of myasthenia gravis (MG). MG, which is clinically characterized by skeletal muscle weakness and abnormal fatigability, is an antibody-mediated autoimmune disease. It has been traditionally believed to be caused by the production of anti-acetylcholine receptor (AChR) autoantibodies (1). Experimental autoimmune myasthenia gravis (EAMG) mimics the human disease in its clinical and immunopathologic manifestations (2). It has been used to investigate the pathogenic mechanisms and to evaluate the immunotherapeutic strategies.

The pathogenic mechanism underlying the autoimmunity in MG is not well understood, but we do know Th17 cells, regulatory T cells, Th1 and Th2 lymphocytes are reported to participate in its development (3-5) . Current drug treatments of MG have their limitations, such as serious side-effects and incomplete remission. Therefore, a new treatment strategy that is price friendly and has fewer side-effects is urgently needed.

Artemisinin is widely known as an anti-malarial agent. Furthermore, artemisinin and its derivatives are also experimentally used to treat autoimmune diseases, such as systemic lupus

Key words: experimental autoimmune myasthenia gravis, artemisinin, Th17 cells, Treg cells, TGF-β1, TNF-α

Mailing address:
Dr Yan-Bin Li,
Department of Neurology,
Shandong Provincial Qianfoshan Hospital,
Shandong University, Jinan, 250014, PR China
Tel.: +86 531 89268106
e-mail: 13864006933@163.com

0393-974X (2018)

erythematosus (SLE) (6) and experimental allergic encephalomyelitis (EAE) (7). However, there is no report about the effect of artemisinin on MG. Here, we put forward the hypothesis that artemisinin has clinical meaning on MG. In our study, we aimed to investigate the impact upon the artemisinin on MG, as well as its possible mechanism.

MATERIALS AND METHODS

Animals and reagents

Twenty-one adult female Lewis rats (160–170 g, 6-8 weeks old) were obtained from Vital River Laboratory (Beijing, China). The Lewis rats were raised at the local experimental animal room under pathogen-free conditions and fed with standard rat chow and water. The study projects was approved by the ethics committee of Shandong Provincial Qianfoshan Hospital. Artemisinin was obtained from Nanjing Zelang Biological Technology Co. Ltd. (Nanjing, China). R97–116 peptide (DGDFAIVKFTKVLLDYTGHI) was synthesized by AC Scientific, Inc. (Xi'an, China).

EAMG induction and assessment of clinical symptoms

According to Baggi et al. (2), the rats were immunized with R97–116 peptide. A total of 200 µl inoculum containing R97–116 peptide (50 µg), Mycobacterium tuberculosis (1 mg, strain H37RA; Difco, Detroit, MI, USA) and incomplete Freund's adjuvant (Sigma-Aldrich, St. Louis, MO, USA) was injected into both hind footpads of Lewis rats. The rats were first immunized on day 0 and then again on the back on day 11 post-immunization. The rats were weighed once a day until 43 days after the first immunization Clinical scores were evaluated as follows (2): 0 - normal; 1 - mildly impaired activity and weak grip or cry more obvious after exercising; 2 - clinical signs before the event (head down, tremor, hunched posture, and weak grip); 3 - severe generalized weakness before exercise, no grip, moribund; 4 - dead. Rats exhibiting intermediate signs were assigned scores of any number from 1 to 3. Results were averaged each day for all the rats.

Dose of artemisinin

The twenty-one rats were divided into three groups (n = 7 in each group). The high dose group and low dose group were given artemisinin at doses of 40 mg/kg/day or 60 mg/kg/day via intragastric administration from day 6 to day 42 post immunization (p.i.). The artemisinin was dissolved in edible olive oil. The control group (n = 7) received the same volume of olive oil. Drug doses were determined in accordance with antimalarial instruction of artemisinin and dose conversion formula: HED (mg/kg) = animal dose (mg/kg) × animal Km/human Km.

Lymph node mononuclear cell preparation

Rats were sacrificed at day 43 after the first immunization. Inguinal lymph nodes of each rat were extracted under aseptic conditions and ground through cell strainers in serum free medium. Mononuclear cells (MNCs) were washed and then rediluted in complete medium (CM) to a consistency of 2×10^6 cells/ml.

Flow cytometry

Firstly, lymph node MNCs were added to 24-well plates and stimulated by the leukocyte activation cocktail, with BD GolgiPlug™ for 4-6 h in an incubator (37°C, 5% CO_2). After washing with 0.5% BSA, Lymph node MNCs were immobilized and permeabilized by the eBioscience Foxp3 staining buffer set (eBioscience, San Diego, CA, USA), after which MNCs were incubated with phycoerythrin (PE)-labeled IL-17 and TNF-α for 30 min at 4°C in the darkness. According to instructions, MNCs were stained with FITC-conjugated anti-rat CD4, PE-conjugated anti-rat CD25 and PE-Cy5-conjugated antimouse/rat Foxp3 antibodies (all from eBioscience). Then cells were analyzed by fluorescence activated cell sorting (FACS) after resuspended in PBS.

Detection of TGF-β1

Firstly, we prepared cell culture supernatant by culturing mononuclear lymphocyte suspension. Dissolved lyophilized powder was diluted by Dilution buffer R(1× to recommended concentration gradients: 1000pg/ml, 500pg/ml, 250pg/ml, 125pg/ml, 62.5pg/ml, 31.25pg/ml, and 15.6pg/ml. The supernatant of cell culture was added into wells and cytokine standard, sample, Dilution buffer R 1× was added to standard wells, sample wells and control wells, respectively. After washing with buffer (300 µl/well) for 4 times, each well was added with diluted Biotinylated antibody (100 µl/well) and the plate incubated for 90 min at 37°C. After washing, each well was added with Streptavidin-HRP (100 µl/well) and incubated for 30 min

at 37°C. The plates were washed again and incubated with tetramethylbenzidine (TMB) substrate (Tiangen Biotechnology, Beijing, China). The absorbance of each well was measured at 450 nm by a microplate ELISA reader. Here, each sample was tested three times. The final results are expressed as optical density (OD) values ± standard deviation (SD).

Detection of serum anti-R97–116 peptide IgG, IgG1, IgG2a, IgG2b antibody

The 96-well plates (Corning, NY, USA) were coated with R97–116 peptide (5 μg/ml) and left at 4°C overnight. 200 μl PBS (contains 0.05% Tween 20 and 10% FBS) was added to each well after washing, then, incubated at 37°C for 1.5 h. Serum samples from the heart blood of rats were added to the wells and incubated for 2 h at 37°C. After washing, the wells were incubated with biotinylated rabbit anti-rat IgG (1:1000; BioLegend), IgG1 (1:1000; Biosynthesis Biotechnology, Beijing, China) and anti-rat IgG2a, IgG2b (1:500; BioLegend) for 1 h at 37°C, washed again, incubated with streptavidin-horseradish peroxidase (1:1000; Biosynthesis Biotechnology) at 37°C for 30 min. After washing, the plates were developed by incubation with tetramethylbenzidine (TMB) substrate (Tiangen Biotechnology, Beijing, China), and the absorbance of each well was measured at 450 nm using a microplate ELISA reader. Each serum sample was tested three times. Results are expressed as the mean ± SD absorbance at 450 nm of the samples.

Statistical analysis

Statistical analysis of the data was completed by SPSS 17.0 software (SPSS Inc., Chicago, IL, USA). EAMG clinical scores were checked by Kruskal Wallis test, followed by Mann-Whitney U test as a post-hoc test. Other data among three groups were checked by one-factor analysis of variance (ANOVA) followed by least significant difference (LSD) post hoc tests. Results are presented as mean ± SD, and p values of 0.05 were considered statistically significant.

RESULTS

Artemisinin suppressed the development of ongoing EAMG

Artemisinin at a dose of 40 or 60 mg/kg was administrated daily from day 6 p.i. to day 42 p.i., at the same time rats in the control group were given the vehicle (olive oil) only. The artemisinin-treated group showed an inhibitory effect on the progression of EAMG compared with the control group (Fig. 1A). Clinical scores in two treated groups were all lower than that in the control group from day 14 p.i. to day 42 p.i.. Rats treated with high-does artemisinin exhibited significantly lower clinical scores compared to the control group from day 14 p.i. to day 42 p.i.($p < 0.05$, respectively), at the same time the low-dose group showed statistically difference compared with the control group on day 32 p.i. to 42 p.i.($p < 0.05$, respectively). Rats treated with high-does artemisinin weighed more than the control rats from day 18 to 42 p.i. ($p < 0.05$, respectively). However, there was no statistical difference in weight between the low-dose group and the control group (Fig. 1B).

High-dose artemisinin treatment increased the numbers of $CD4^+$ $CD25^+Foxp3^+$ T cells

To evaluate whether the influence of artemisinin on EAMG correlated with the Treg cells, MNCs were obtained from inguinal lymph nodes of each individual rat and tested by FACS. The percentages of $CD4^+$ $CD25^+Foxp3^+$ T cells among lymph node MNCs from rats treated with the high-dose artemisinin were higher than those from the control group (p 0.05) and the low-dose group. However, there was no significant difference in the percentage of $CD4^+$ $CD25^+Foxp3^+$ T cells between the low-dose group and the control group. (Fig. 2, A and B).

Artemisinin decreased the expression of IL-17^+ A cells in EAMG rats

To investigate the effect of artemisinin on the expression of Th17 cells in EAMG rats, MNCs obtained from inguinal lymph nodes were tested by FACS. The percentage of IL-17^+ **A** cells among $CD4^+$ T cell from the treated groups was lower than that in the control group ($p < 0.05$, respectively), but there was no statistical difference of IL-17^+ **A** cells between the high-dose group and the low-dose group (Fig. 2, C and D).

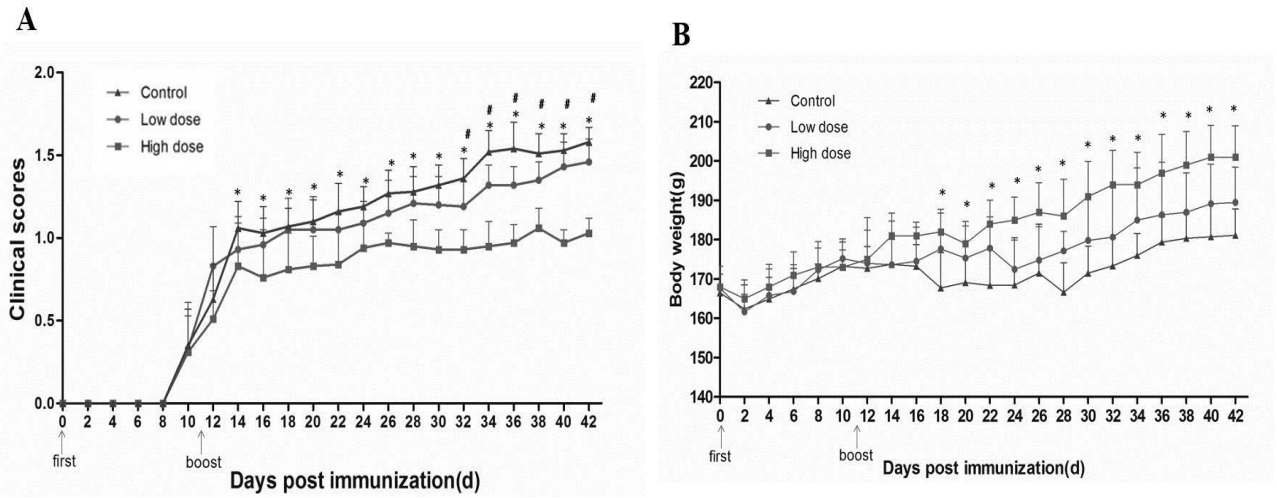

Fig. 1. *Artemisinin treatment ameliorated the severity of ongoing EAMG in Lewis rats. A is the mean clinical scores and B is the average body weight. Data are presented as mean ± SD (n = 7 in each group) (*: refers to the high-dose group compare to the control group has a $p < 0.05$, #: refers to the low-dose compare to the control group has a $p < 0.05$).*

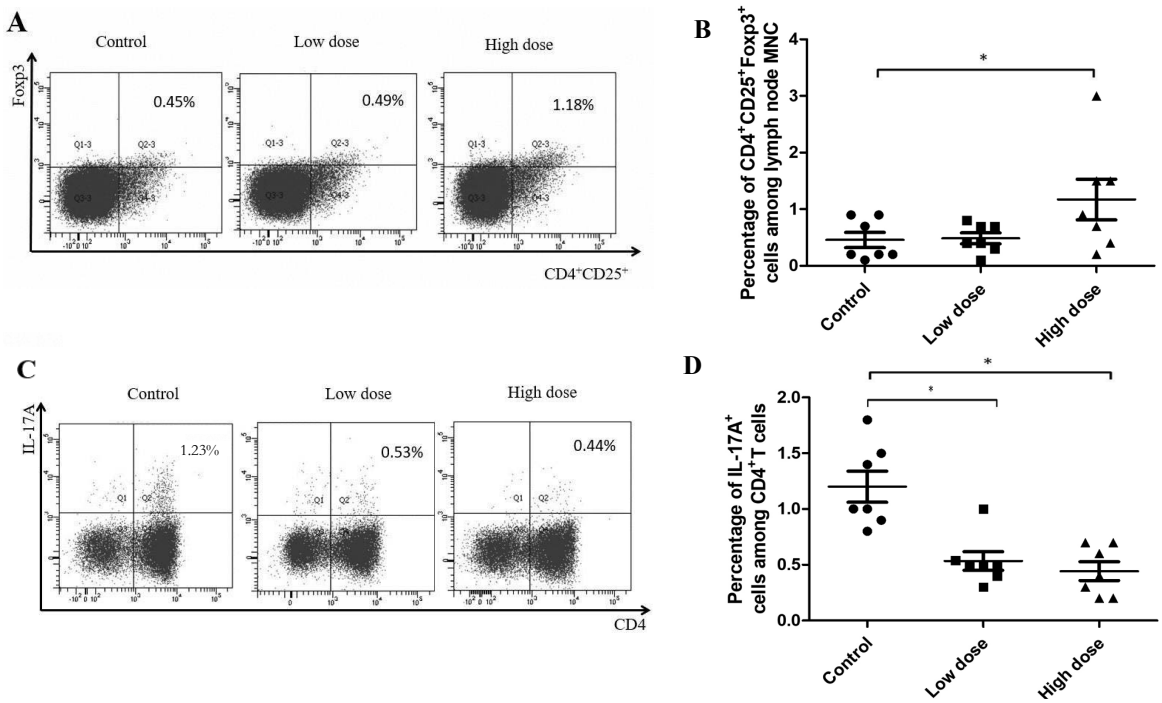

Fig. 2. *Results of artemisinin usage on Treg cells and IL-17$^+$ A cells in EAMG rats. **A**) Representative FACS analysis outcome of CD4$^+$CD25$^+$Foxp3$^+$ T cells among lymph node MNC. **B**) Percentage of CD4$^+$CD25$^+$Foxp3$^+$ T cells among lymph node MNC. **C**) representative FACS analysis outcome of IL-17$^+$ A cells among CD4$^+$ T cells. **D**) The percentages of IL-17$^+$ A cells among CD4$^+$ T cells. Data are presented as mean ± SD (*$p < 0.05$) (n = 7 in each group).*

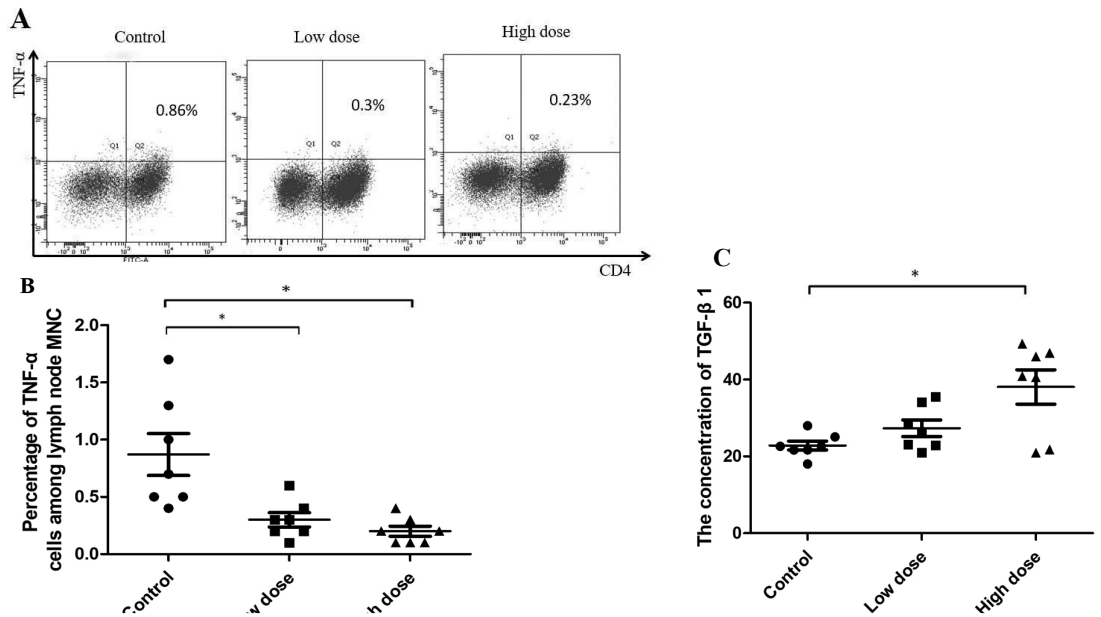

Fig. 3. *Results of artemisinin treatment on TNF-α and TGF-β1 in lymphocytes.* ***A****) Representative FACS analysis of TNF-α⁺ cells among CD4⁺ T cell.* ***B****) Percentages of TNF-α⁺ cells among CD4⁺ T cells. TGF-β1 were measured by ELISA.* ***C****) Concentration of TGF-β1 (n = 7 in each group). Data are presented as mean ± SD (*p < 0.05).*

Table I. *OD value (450 nm) of AChR antibody.*

	Control	Low dose	High dose
IgG	0.49 ±0.05	0.56 ±0.03	0.51 ±0.06
IgG1	0.96 ±0.04	1.07 ±0.07	0.95 ±0.05
IgG2a	0.50 ±0.05	0.71 ±0.10	0.59 ±0.04
IgG2b	1.42 ±0.09	1.55 ±0.06	1.54 ±0.10

Artemisinin suppressed the TNF-α expression in EAMG rats

It was believed that TNF-α was involved in the pathogenesis of EAMG, therefore we studied the expression of TNF-α. As shown in Fig. 3, A and B, the percentage of TNF-α⁺ cells was down-regulated in both the high dose and low dose groups than in the control group ($p < 0.05$, respectively).

High-dose artemisinin up-regulated the expression of TGF-β1 in EAMG rats

TGF-β1 is one of the three TGF-β isoforms. Reports indicated that TGF-β1 was involved in EAMG, therefore we studied the level of TGF-β1 among lymph node MNCs by ELISA. As shown in Fig. 3C, the high-dose artemisinin group had up-regulated level of TGF-β1 in EAMG rats compared

with both the control group ($p < 0.05$) and the low-dose group, although there was no statistical difference between the control group and the low-dose group.

Effect of artemisinin on anti-R97-116 IgG/ IgG1/ IgG2a/ IgG2b antibody level in serum

The levels of R97-116 IgG/ IgG1/ IgG2a/ IgG2b antibody was detected by ELISA. As shown in Table I, there was no significant difference between the high and low dose groups compared with the control group.

DISCUSSION

Our data shows that artemisinin treatment ameliorated EAMG symptoms, possibly by modulating Th1 cell, Th17 cell, and Treg cell.

It was reported that TGF-β1 can not only selectively suppress TNF-α expression (8), but also induce the differentiation of $CD4^+CD25^+$ Treg cells (9). Moreover, TGF-β also induced development of the Th17 lineage (10). Furthermore, $CD4^+CD25^+Foxp3^+$ cells could suppress the generation of Th17 cells (11). In our study, the level of TGF-β1 and the percentage of $CD4^+CD25^+Foxp3^+$ regulatory T cells in the high dose group was markedly higher than in the control group. However, both the percentage of TNF-α^+ cells and IL-17^+ cell of the treated groups were lower compared with that of the control group. Based on our results and previous statements, we inferred that artemisinin may ameliorate the clinical symptom of EAMG by the following two ways: (i) artemisinin directly increased the level of TGF-β1 and the percentage of $CD4^+CD25^+Foxp3^+$ regulatory T cell, and decreased the percentage of TNF-α^+ cells and Th17 cells; (ii) artemisinin elevated the level of TGF-β1, thus decreased the percentage of TNF-α^+ cells and up-regulated the percentage of $CD4^+CD25^+Foxp3^+$ regulatory T cell, which then inhibited the production of Th17 cells.

Our current finding confirmed that artemisinin relieved the symptoms of EAMG. The effect of artemisinin on EAMG coincided with increased levels of TGF-β1 and $CD4^+CD25^+Foxp3^+$ regulatory T cells, and decreased levels of TNF-α^+ cells and Th17 cells, serving as a clue to the underlying mechanism. The results provide evidence supporting the immune regulatory effect of artemisinin on EAMG rats.

ACKNOWLEDGEMENTS

The study was supported by grants from Shandong Natural Science Foundation of China (ZR2010HM068), Shandong Provincial Natural Science Foundation (2104BSB14078), and the Natural Science Foundation of China (81601040).

REFERENCES

1. Vincent A. Unravelling the pathogenesis of myasthenia gravis. Nat Rev Immunol 2002; 2(10):797-804.
2. Baggi F, Annoni A, Ubiali F, et al. Breakdown of tolerance to a self-peptide of acetylcholine receptor alpha-subunit induces experimental myasthenia gravis in rats. J Immunol 2004; 172(4):2697-703.
3. Duan RS, Wang HB, Yang JS, Scallon B, Link H, Xiao BG. Anti-TNF-α antibodies suppress the development of experimental autoimmune myasthenia gravis. J Autoimmun 2002; 19(4):169-174.
4. Masuda M, Matsumoto M, Tanaka S, et al. Clinical implication of peripheral CD4+CD25+ regulatory T cells and Th17 cells in myasthenia gravis patients. J Neuroimmunol 2010; 225(1–2):123-31.
5. Aarli J A. Role of cytokines in neurological disorders. Curr Med Chem 2003; 10(19):1931-37.
6. Hou LF, He SJ, Li X, et al. Oral administration of artemisinin analog SM934 ameliorates lupus syndromes in MRL/lpr mice by inhibiting Th1 and Th17 cell responses. Arthritis Rheum 2011; 63(8):2445-55.
7. Li X, Li TT, Zhang XH, et al. Artemisinin analogue SM934 ameliorates murine experimental autoimmune encephalomyelitis through enhancing the expansion and functions of regulatory T cell. PLoS One 2013; 8(8):74108.
8. Link J, He B, Navikas V, Palasik W, Fredrikson S, Söderström M, Link H. Transforming growth factor-beta 1 suppresses autoantigen-induced expression of pro-inflammatory cytokines but not of interleukin-10 in multiple sclerosis and myasthenia gravis. J Neuroimmunol 1995; 58(1):21-35.
9. Chen W, Jin W, Hardegen N, et al. Conversion of peripheral CD4+CD25−naive T cells to CD4+CD25+regulatory T cells by TGF-β induction

of transcription factor Foxp3. J Exp Med 2003; 198(12):1875-86.

10. Mangan PR, Harrington LE, O'Quinn DB, et al. Transforming growth factor-beta induces development of the T(H)17 lineage. Nature 2006; 441(7090):231-34.
11. Bettelli E, Carrier Y, Gao W, et al. Reciprocal developmental pathways for the generation of pathogenic effector TH17 and regulatory T cells. Nature 2006; 441(7090): 235-38.

LETTER TO THE EDITOR

EFFECTS OF DIFFERENT DEGREES OF DEPRESSION ON INFLAMMATORY RESPONSE AND IMMUNE FUNCTION IN PATIENTS WITH OVARIAN CANCER

JP. SU[1], HF. LIU[2], HL. ZHANG[1], YJ. HE[1] and Y. NIE[3]

[1]Department of Medical Psychology, School of Public Health of MuDanJiang Medical University, Mudanjiang City, China; [2]Department of Molecular Biology and Biochemistry, Basic Medical College of MuDanJiang Medical University, Mudanjiang City, China; [3]Department of Immunology, Basic Medical College of MuDanJiang Medical University, Mudanjiang City, China

Received April 24, 2018 - Accepted July 26, 2018

The aim of this study was to explore the effect of depression of different degrees on inflammatory response and immune function in patients with ovarian cancer. One hundred and eight cases of ovarian cancer according to the Federation Internationale of Gynecologie and Obstetrigue (FIGO) stage II~III who visited the Gynecology Department of Affiliated HongQi Hospital of MuDanJiang Medical University between September 2015 and May 2017 were enrolled in the study. After being hospitalized, they were divided into two groups according to their Beck Depression Inventory (BDI) scores. The total score of BDI is 63, with 0~4 for the normal group (25 cases), 5~13 for the mild depression group (24 cases), 14~20 for the moderate depression group (28 cases), and 21~63 for the severe depression group (31 cases). The immune function, inflammatory reaction, tumor markers [CA125, human epididymis protein-4 (HE4), insulin-like growth factor-I (IGF-I)], platelet technology and D-dimer index were compared between the four groups. The results showed that there were different levels of depression in patients with ovarian cancer in II~III stage, and the degree of depression could stimulate the level of serum-6, and TNF -α in serum increased. The proportion of $CD3^+$, $CD4^+$ and NK cells in patients with severe depression decreased, and their immunity also decreased. Depression increased the levels of CA125, HE4 and IGF-I in serum and ascites of ovarian cancer patients, and increased the risk of tumor progression and recurrence. Hypercoagulability existed in patients with ovarian cancer, and tumor associated depression could increase platelet count in plasma and increase D-dimer level. To sum up, depression can affect the level of micro inflammation in patients with ovarian cancer. In particular, depression can reduce cellular immune responses, affect the progression free survival of ovarian cancer patients, and reduce their overall survival rate.

To the Editor,

Ovarian cancer is one of the most common malignant tumors in females. Upon clinical diagnosis, many patients are already in stage II~III (1, 2), and the resistance to treatment seriously affects the physical and mental health of the patients. In addition, data show that the occurrence of malignant tumors can lead to depressive symptoms, and the continuation of depression can also cause a series of pathological changes in the patients (3-5). Although it has been shown that the survival profiles of tumor patients diagnosed at different clinical stages were obviously different, the actual mechanisms underlying such observations remain unclear (6).

Key words: depression, ovarian cancer, immune function, inflammatory response

Mailing address:
Dr Ying Nie,
Department of Immunology,
Basic Medical College
MuDanJiang Medical University, TongXiang Road No 3,
MuDanJiang City, HeiLongJiang Province, China
e-mail: nieyingmjmu@163.com

0393-974X (2018)

To further investigate the effect of tumor-induced depression in patients with ovarian cancer, this study compared the inflammatory stress, platelet count, D-dimer and corresponding tumor markers in these patients, based on the degree of their depression. Moreover, the study further clarified whether there is a difference between the clinical asymptomatic survival stage and median survival time of patients with different degrees of depression.

MATERIALS AND METHODS

General information

A total of 108 cases with ovarian cancer according to the Federation Internationale of Gynecologie and Obstetrigue (FIGO) stage II~III who visited the Gynecology Department of Affiliated HongQi Hospital of MuDanJiang Medical University between September 2015 and May 2017 were enrolled in this study. After being hospitalized, the patients were divided into four groups according to their Beck Depression Inventory (BDI) scores. The total score of BDI is 63, with 0~4 for the normal group (25 cases), 5~13 for the mild depression group (24 cases), 14~20 for the moderate depression group (28 cases), and 21~63 for the severe depression group (31 cases). During the follow-up, 10% of the patients were checked for the authenticity assessment. In addition, the BDI scores and the general situation of all patients were recorded by designated investigators. This study was approved by the Ethics Committee of the Affiliated HongQi Hospital of MuDanJiang Medical University and all subjects signed an informed consent.

Inclusion criteria were: patients with unilateral or bilateral ovarian tumors associated with pelvic dissemination; distant organ metastasis; microscopically confirmed pelvic or peritoneal metastasis, and visible metastasis in the pelvic peritoneal cavity (maximum diameter of metastasis > 2cm); and patients willing to cooperate with the treatment and follow-up studies.

Exclusion criteria were: patients at FIGO stage I and IV; patients with severe liver and kidney dysfunctions; and patients with a history of mental illness.

Immunological examination: the level of peripheral blood lymphocytes, the percentage of $CD3^+$, $CD4^+$, $CD8^+$, and NK cells, the total number of lymphocytes and the level of $CD4^+CD25^+$T cells were detected by flow cytometry (BD) on the seventh day before and after the operation. In brief, fasting blood samples of the patients were collected using EDTA anti-coagulation tubes. Subsequently, 50 uL anticoagulant blood was added to 10 uL of corresponding fluorescence-labeled monoclonal antibodies (Beijing Yiqiao Shenzhou Biological Technology Co., Ltd., China) and mixed evenly, followed by incubation in the dark for 20 min. In the next step, red blood cell lysat (Olivia Biotechnology Co., Ltd., China) was added into the above mixture and centrifuged for 15 min. After rinsing with PBS buffer two times, 450 uL of paraformaldehyde fixative (pH 7.4) was added in the dark before the samples were analyzed. The fluorescence intensity of various fluorescent markers on the surface of lymphocytes was measured by flow cytometry within 2 h and the data were analyzed by Cellques software (BD) to obtain the percentage of positive cells.

Inflammatory response test: 5 mL of fasting venous blood was collected from each subject and centrifuged at 3000r/min. After settling down for 1 h, the samples were analyzed by a computer program. Enzyme linked immunosorbent assay (purchased from Shanghai Enzyme Biological Technology Co., Ltd.) was used to detect the levels of interleukin (IL)-6 and tumor necrosis factor-α (TNF-α) in the serum of patients, according to the manufacturer's instructions.

Detection of tumor markers: electrochemiluminescence immunoassay (Shanghai Supan Biotechnology Co., Ltd., China) was used to measure CA125 and enzyme-linked immunosorbent assay (Shanghai enzyme-linked Biotechnology Co., Ltd., China)was employed to determine HE4 and IGF-I.

Platelet technology and D-dimer detection: platelet technology detection was performed using a French ABX blood cell analyzer, and abnormal results were checked with an OLYMPUS microscope and a blood cell counting plate. D-dimer content was detected by automatic latex enhanced turbidimetric immunoassay on a Sysmex CA-1500 system.

Statistical analysis

The data were analyzed by SPSS19.0 software and expressed as $\bar{x} \pm s$. The *t*-test was used to compare the values between different groups, while Pearson correlation analysis was used to evaluate the correlation. $P < 0.05$ indicated significant difference.

RESULTS

Changes of cellular immune functions

The percentages of CD3+ and CD8+ cells in the normal group were compared with those in the severe depression group, with significant difference (P<0.05). The percentages of CD3+ and CD8+ cells in the normal group were similar to those in the other three groups (P>0.05). The percentages of CD4+CD25+T cells and NK cells in the 4 groups were compared, and were significantly different (P<0.05). The lymphocyte count and the percentage of CD4+ cells in the normal group were similar to those in the mild depression group (P>0.05), while the lymphocyte count and the percentage of CD4+ cells in the other three groups were different (P<0.05). The difference between the normal group and the mild depression group for Lymphocyte count and CD4+ was not statistically significant (P>0.05), however, there was statistical difference between the mild depression group, the moderate depression group and the severe depression group (P<0.05) (Table I).

Changes of CA125, HE4 and IGF-I in serum and ascites

From Table II, it can be seen that the differences of CA125 and HE4 among the 4 groups were statistically significant (P<0.05). There was no significant difference between the mild depression group and the severe depression group in terms of IGF-I (P>0.05), while the levels of IGF-I in the in the normal group, the moderate depression group and the severe depression group had obvious differences (P<0.05). The levels of CA125, HE4 and IGF-I in the serum and ascites were closely related to each other, with a linear correlation. The correlation coefficients were 0.854, 0.623 and 0.357, respectively.

Levels of inflammatory response factors, plasma D-dimer and platelet count

The levels of IL-6 and TNF-α among the different

Table I. *The changes in the levels of NK, CD4+, CD8+, CD4+CD25+ and lymphocytes among different groups.*

Category	Normal group	Mild depression group	Moderate depression group	Severe depression group	P
CD4+%	37.87±6.11	35.12±8.04b	27.75±6.12c	21.03±4.54e	0.004
CD8+%	28.76±5.05	29.15±4.19	31.91±3.82	34.26±3.08d	0.005
NK cell%	25.34±3.54a	23.25±4.32b	19.65±3.86c	16.24±3.77d	0.005
CD3+%	72.54±6.67	70.55±5.43	67.24±4.86	63.32±3.62d	0.003
Lymphocyte count ($\times 10^9$/L)	1.46±0.36	1.54±0.34b	1.34±0.37c	1.12±0.41d	0.005
CD4+CD25+T cell/CD4+(%)	8.82±1.35a	14.76±3.63b	28.42±4.78c	34.13±5.66dd	0.002

***a**: comparison between the normal group and the mild depression group (P<0.05); **b**: comparison between the mild depression group and the severe depression group (P<0.05); **c**: comparison between the moderate depression group and the severe depression group (P<0.05); **d**: comparison between the severe depression group and the normal group (P<0.05); **e**: comparison between the severe depression group and the normal group (P<0.001). P represents the statistical value of the same category in comparison between the four groups.*

Table II. *Comparison of CA125, HE4 and IGF-I in serum and ascites.*

Category		Normal group	Mild depression group	Moderate depression group	Severe depression group	P
Serum	CA125 (U/mL)	32.76±3.34a	39.23±4.18b	51.54±5.09c	78.32±8.16d	0.001
	HE4 (pmoL/L)	343.67±89.54	375.92±77.16b	413.05±80.91c	466.89±91.22dd	0.002
	IGF-I (ng/mL)	186.89±45.34a	179.48±52.07	169.23±68.76c	122.55±43.17d	0.005
Ascites	CA125 (U/mL)	38.42±4.33a	47.09±5.12b	59.73±5.91c	89.26±8.47d	0.001
	HE4 (pmoL/L)	369.33±90.19a	399.65±87.37b	456.16±88.89c	497.38±92.48d	0.003
	IGF-I (ng/mL)	155.06±41.54a	167.33±46.82b	139.43±43.04c	106.62±38.59d	0.004

***a**: comparison between the normal group and the mild depression group (P<0.05); **b**: comparison between the mild depression group and the severe depression group (P<0.05); **c**: comparison between the moderate depression group and the severe depression group (P<0.05); **d**: comparison between the severe depression group and the normal group (P<0.05).*

Table III. *Comparison of plasma D-dimer and platelet count.*

Category	Normal group	Mild depression group	Moderate depression group	Severe depression group	P
IL-6(ng/L)	24.92±5.99	28.91±8.41b	38.15±7.32c	55.62±10.27e	0.003
TNF-α(ng/L)	28.99±7.18a	36.36±7.47b	43.59±7.96c	79.61±12.03e	0.002
PLT($\times 10^9$/L)	155.65±36.32	167.35±47.15	172.05±52.76c	317.62±68.23e	0.002
D- dimer (ng/mL)	2.06±0.58	2.15±0.65b	2.41±0.96c	4.83±1.02d	0.003

***a**: comparison between the normal group and the mild depression group (P<0.05); **b**: comparison between the mild depression group and the severe depression group (P<0.05); **c**: comparison between the moderate depression group and the severe depression group (P<0.05); **d**: comparison between the severe depression group and the normal group (P<0.05); **e**: comparison between the severe depression group and the normal group (P<0.001).*

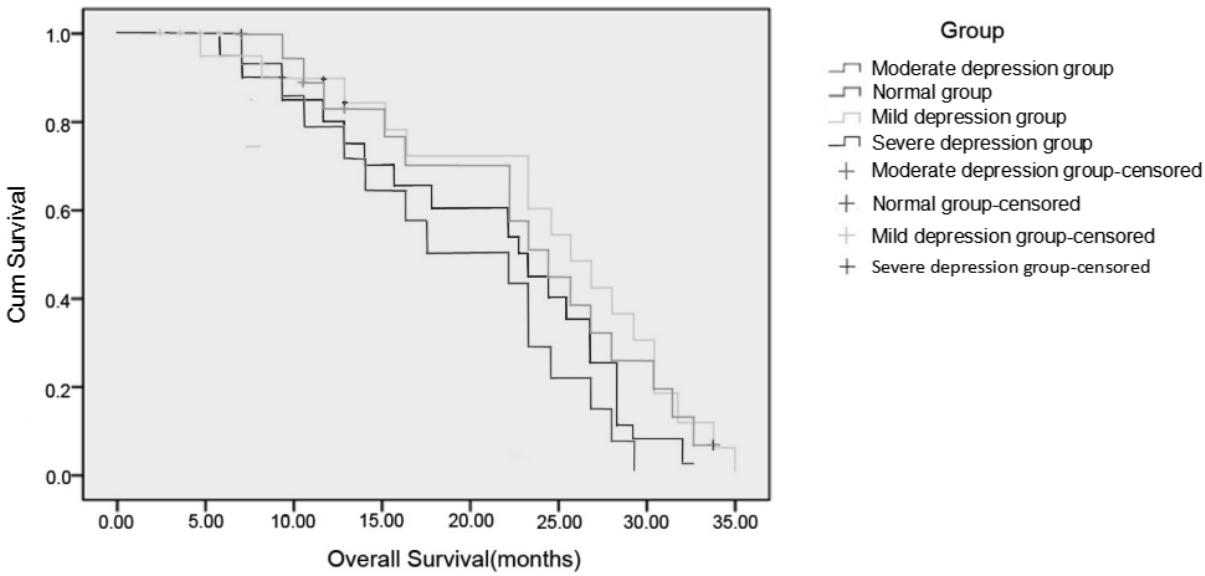

Fig. 1. *Survival rates of the four groups.*

groups were significantly different (P<0.05), while the correlation coefficient between IL-6 and platelet count was r=0.441 (P<0.05) (Table III). In addition, there was a significant linear correlation between the depression level and the amount of IL-6 and TNF-α (r=3.4542; 0.493, P<0.05). There was no significant difference in the level of plasma D-dimer and platelet count between the normal group and the mild depression group (P>0.05), while the difference between the moderate group and the severe group was statistically significant (P<0.05).

Survival rates

After 24-month follow-up, it was found that the progression free survival, median survival, 1-year survival, and 2-year survival were significantly different among the four groups (P<0.05). There was no significant difference between the mild depression group and the normal group (P>0.05). Compared with the normal group, patients' free survival period, median survival period, 1-year survival period, and 2-year survival period in the moderate depression group and the severe depression group were significantly decreased (P<0.05) (Fig. 1).

DISCUSSION

Most malignant tumor patients suffer from depression of different degrees. The long-term symptoms of depression could affect the immune functions of the patients (7, 8). Some studies have shown that the tumor itself contains chemokines that can combine with regulatory T-cell receptors, secrete a variety of immunosuppressive cytokines, inhibit the activity of the body's effector T cells, weaken the killing effect of NK cells on tumor cells and complete the evasion of the tumor (9, 10). The results of the immune function tests of this study showed that the changes in the proportion of immune cells may reflect the imbalance between the regulatory T cells and inhibitory T cells in tumor patients, thus leading to tumor cell evasion from T cell surveillance. In addition, there was no significant difference between the normal group and the mild depression group in terms of $CD4^+$ T cell ratios and lymphocyte count (P>0.05), suggesting that the patients with stage II~III ovarian cancer were associated with depression of different degrees, and there was significant difference in their immune status.

The common tumor markers in ovarian cancer patients include CA125, HE4, and IGF-I (11). The results of this study showed a good correlation between tumor markers in serum and ascites, and the expression of these tumor markers was apparently different in different depressive states. Since the

measurements of CA125, HE4 and IGF-I can better reflect the tumor growth in ovarian cancer patients at different depressive states, such measurements are beneficial for the monitoring of curative effects in tumor treatment. In this study, higher levels of PLT count and D-dimer were associated with more severe depression. In addition, this study demonstrated a good correlation between the depression score and the levels of IL-6 and TNF-α, suggesting that the elevated levels of inflammatory cytokines in the plasma of ovarian cancer patients could cause an increased platelet count.

REFERENCES

1. Orywal K, Jelski W, Zdrodowski M, Szmitkowski M. The activity of class I, II, III and IV alcohol dehydrogenase isoenzymes and aldehyde dehydrogenase in ovarian cancer and ovarian cysts. Adv Med Sci 2013; 58(2):216-20.
2. Mackay HJ, Provencheur D, Heywood M, Tu D, Eisenhauer EA, Oza AM, Meyer R. Phase ii/iii study of intraperitoneal chemotherapy after neoadjuvant chemotherapy for ovarian cancer: ncic ctg ov.21. Curr Oncol 2011; 18(2):84-90.
3. Brown LF, Kroenke K, Theobald DE, Wu J, Tu W. The association of depression and anxiety with health-related quality of life in cancer patients with depression and/or pain. Psychooncology 2010; 19(7):734-41.
4. Yang H, Brand JS, Fang F, Chiesa F, Johansson AL, Hall P, Czene K. Time-dependent risk of depression, anxiety, and stress-related disorders in patients with invasive and in situ breast cancer. Int J Cancer 2017; 140(4):841-52.
5. Heidari M, Ghodusi M. The relationship between body esteem and hope and mental health in breast cancer patients after mastectomy. Indian J Palliat Care 2015; 21(2):198-202.
6. Klainin-Yobas P, Cho MA, Creedy D. Efficacy of mindfulness-based interventions on depressive symptoms among people with mental disorders: A meta-analysis. Int J Nurs Stud 2012; 49(1):109-21.
7. Chang CK, Hayes RD, Broadbent MT, Hotopf M, Davies E, Møller H, Stewart R. A cohort study on mental disorders, stage of cancer at diagnosis and subsequent survival. BMJ Open 2014; 4(1):e004295.
8. Härter M, Woll S, Wunsch A, Bengel J, Reuter K. Screening for mental disorders in cancer patients – discriminant validity of HADS and GHQ-12 assessed by standardized clinical interview. Soc Psychiatry Psychiatr Epidemiol 2006; 41(1):56-62.
9. Abe A, Furumoto H, Nishimura M, Irahara M, Ikushima H. Adjuvant chemotherapy following concurrent chemoradiotherapy for uterine cervical cancer with lymphadenopathy. Oncol Lett 2012; 3(3):571-76.
10. Vieira Braga F A, Hertoghs K M, van Lier R A, van Gisbergen KP. Molecular characterization of HCMV-specific immune responses: Parallels between CD8 (+) T cells, CD4 (+) T cells, and NK cells. Eur J Immunol 2015; 45(9):2433-45.
11. Karlsen MA, Høgdall EV, Christensen IJ, et al. A novel diagnostic index combining HE4, CA125 and age may improve triage of women with suspected ovarian cancer - An international multicenter study in women with an ovarian mass. Gynecol Oncol 2015; 138(3):640-46.

LETTER TO THE EDITOR

RELATIONSHIP BETWEEN SLEEP DISORDERS AND LYMPHOCYTE SUBSETS AND CYTOKINES IN PATIENTS WITH LUNG CANCER

Y. WANG[1], XJ. CHENG[2], AH. YIN[2], Y. CAO[2], ZG. ZHAO[3], HJ. ZHANG[4], DX. LIU[4], Y. ZHANG[2], ZX. LIU[2], Y. LU[2], JC. JIA[2], JT. LIU[1] and F. PAN[4]

[1]Department of Psychiatry, Shandong University School of Medicine, Jinan City, Shandong, People's Republic of China; [2]Department of Psychiatry, Shandong Mental Health Center, Jinan City, Shandong, People's Republic of China; [3]School of Foreign Languages and Literature, Shandong University, Jinan City, Shandong, People's Republic of China; [4]Department of Medical Psychology and Ethics, Shandong University School of Basic Medical Sciences, Jinan City, Shandong, People's Republic of China

Received May 23, 2018 –Accepted July 16, 2018

This study aimed to investigate the relationship between sleep disorders and lymphocyte subsets and cytokines in patients with lung cancer undergoing radiotherapy, and to establish a theoretical foundation for predicting sleep disorders and preventing interventions in radiotherapy in lung cancer patients. Ninety-two patients with lung cancer requiring radiotherapy were selected as the study subjects. The patients' demographic data and disease-related conditions were investigated. Their quality of sleep was measured before radiotherapy, after two and four weeks of radiotherapy, and at the end of radiotherapy. According to the Pittsburgh Sleep Quality Index Number Table (PSQI), patients with PSQI score> 7 points were put into a sleep disorder group, and patients with PSQI score 0-7 were put into a normal sleep group. Lymphocyte subsets were enumerated and cytokine levels (IL-6, IL-1β) were measured during these four periods. The difference in sleep disorders at four weeks between patients with or without synchronous chemotherapy was statistically significant (P<0.05). The levels of lymphocyte subsets in the sleep disorder group and the control sleep group showed no difference in the index of lymphocyte subsets before radiotherapy. In the sleep disorder group, $CD4^+$ cells were lower after two weeks of radiotherapy (P<0.05). After four weeks of radiotherapy, $CD3^+$, $CD4^+$, and $CD16^+56^+$ subsets were lower (P<0.05). At the end of radiotherapy, there was no difference in each index. There was no significant difference in IL-6 levels between the two groups before radiotherapy, after two weeks, or after four weeks (P>0.05). At the end of radiotherapy, IL-6 levels in the sleep disorder group were higher than those in the control sleep group (P<0.05). There was no significant difference in IL-1β between the two groups (P>0.05). In conclusion, monitoring of T-lymphocyte subsets and IL-6 levels in patients is enhanced during radiotherapy. Clinically effective programs of radiotherapy for lung cancer improve the body's immune status.

To the Editor,

The incidence and mortality rate of lung cancer are the highest among malignant tumors. Radiation therapy is one of the main methods to treat lung cancer. Although radiation therapy kills tumor cells, it may cause a series of complications with common symptoms, including anxiety, depression, sleep disorders, and dry mouth. These complications

Key words: lung cancer, lymphocyte subsets, sleep disorders, cytokines

Mailing address:
Dr Fang Pan,
Department of Medical Psychology and Ethics,
Shandong University School of Basic Medical Sciences,
No. 44 West Road Wenhua, Jinan City, Shandong,
250012, People's Republic of China.
email: drpanfangpf@126.com

0393-974X (2018)

severely affect the subsequent therapeutic effect of the treatment (1, 2). Among these complications, sleep disorders have always been a topic of concern to researchers worldwide (3, 4). The literature shows that sleep disorders can directly result in endocrine disorders and decreased immune function, and can participate in the occurrence and development of tumors (5). Therefore, the prevention and improvement of sleep disorders in cancer patients is vital.

Despite this, there is a paucity of studies on sleep disorders in patients undergoing radiotherapy (6). With the expansion of research in medical immunology, the theory of neuroendocrine-immune mechanisms of cancer-related symptoms has gradually been recognized (7). In addition, studies show that the determination of cytokines connected to cancer-related symptoms can help clinicians predict the symptoms and prevent intervention based on the mechanisms of neuroendocrine immunity (8). This study aimed to explore the relationship between sleep disorders and lymphocyte subsets and inflammatory cytokines. It lays a foundation for the development of effective sleep interventions, which in turn improves the quality of life and prognosis of patients undergoing treatment.

MATERIALS AND METHODS

Patients

A total of 92 lung cancer patients requiring radiotherapy and seeking medical treatment in Shandong University School of Medicine, China, were selected from June 2016 to November 2017. All patients (or their families) signed an informed consent and this study was approved by the ethics committee of Shandong University School of Medicine.

Fifty microliters of venous blood was collected from fasting patients in the early morning before radiotherapy, after two weeks of radiotherapy, after four weeks of radiotherapy, and at the end of radiotherapy. The blood was then placed in two tubes containing ethylene diamine tetraacetic acid (EDTA) anticoagulant. One tube was sent to the laboratory within 30 min for detection of lymphocyte subsets. The other tube was maintained at 4°C for 30 min and then stored at -80°C after centrifugation.

Data of study subjects

Questionnaires were filled out by patients before radiotherapy, after two weeks of radiotherapy, after four weeks of radiotherapy, and at the end of radiotherapy. Age, gender, body mass index (BMI), religious beliefs, occupational status, marital status, exercise history, smoking history, and drinking history of all the patients were recorded. Histological type, stage of disease, history of coronary heart disease, history of diabetes, history of hypertension, and history of previous chemotherapy were also noted.

Pittsburgh Sleep Quality Index

Sleep disorders were assessed using the Pittsburgh Sleepiness Index Questionnaire (PSQI). The PSQI consists of nineteen self-assessments and five other evaluation items. There are seven main factors: subjective sleep quality, sleep latency, hours of sleep, sleep efficiency, sleep disorders, hypnotic drug use, and daytime dysfunction. Each factor is calculated as 0 to 3 points, and the cumulative factor score is the PSQI total score. The higher the score, the worse the sleep quality. PSQI>7 was used as the criterion for determining sleep disorders. The patients were divided into two groups: a sleep disorder group comprising patients with PSQI score >7; and a normal sleep group comprising patients with PSQI score 0-7. Since the sleep status of 92 patients in each period were always changing, the number of patients in the sleep disorder group and the normal sleep group was 20 in each period.

Laboratory testing

There are seven detection indexes of lymphocyte subsets (name, immunophenotyping and reference interval) as follows: average number of lymphocytes, lymph events, no reference interval (%); B lymphocyte, $CD19^+$,5.0-18.0%; T lymphocyte, $CD3^+$, 50-84%; Inhibition/cytotoxic T cells, $CD3^+CD4^-CD8^+$,15.0-44.0%; Helper/inducing T cells, $CD3^+CD4^+CD8^-$, 27.0-51.0%; Helper/suppressor T lymphocyte ratio, $CD3^+CD4^+$/ $CD3^+CD8^+$, 0.7-2.8%; Natural killer cells, $CD16^+56^+$, 7-40%.

Lymphocyte subsets detection method

Fifty microliters of blood was put into 2 BD Falcon™ Tubes and marked. Then, 20 μL of antibody was added to

each of the 2 flow tubes. One tube was CD3/CD8/CD45/CD4 and the other tube was CD3/CD16$^+$CD56/CD45/CD19. The light elastohydrodynamic tube was mixed with liquid and placed in the dark for 15 min. Next, 450 μL diluted lysate (1:10 dilution) was then dropped into 2 flow tubes and mixed and kept in the dark for 15 min. Finally, the sample was placed on the flow cytometer for detection.

Detection of IL-1β and IL-6 by cytokines

Blood samples were collected (while patients were fasting) in the morning into 2 ml EDTA anticoagulative purple tubes and stored at 4°C. Blood samples were processed within 2 h. The first centrifuge parameters were: 3000 rcf, 15 min, 4°C, slow rise and slow drop; the second centrifugation parameters were: 3000 rpm, 30 min, 4°C. Plasma was harvested (200 uL) and frozen at -80°C. U.S. R&D System kits and Enzyme-Linked Immunosorbent Assay (ELISA) were used to test the indicators.

Statistical analysis

Statistical analysis was performed using statistical software SPSS 17.0. The trend in the incidence of sleep disorders was tested using the *Chi*-squared test. Changes in the total score of sleep quality during each period were analyzed by repeated measures analysis of variance. The *t*-test was used to analyze differences in lymphocyte subsets and inflammatory cytokine levels in the sleep disorder group and the normal sleep group . *Chi*-squared test was used to compare the distribution of sleep disorders among different sociodemographic data, disease-related conditions, and patients with adverse reactions.

RESULTS

A follow-up questionnaire was conducted on the sociodemographic and disease-related data of the 92 patients. The patients were 37-75 years old, average 57.12±7.57 years. The sociodemographic data of the subjects were as follows: 16 were 49 years old or under (17.4%), 66 were aged between 50-69 years (71.7%), and 10 were aged 70 years or over. There were 74 males (80.4%) and 18 females (19.6%). The disease-related data of the study subjects were as follows: 28 patients had squamous cell carcinoma (30.4%), 13 patients had adenocarcinoma (14.1%), 45 patients had small cell carcinoma (48.9%), and 6 patients had other cancers (6.5%). The pathological stage of 3 patients was in stage I (3.3%), 5 patients in stage II (5.4%), 64 patients in stage III (69.6%), and 20 patients in stage IV (21.7%). Twelve patients had coronary heart disease (13%), 8 had diabetes (8.7%), 23 had hypertension (25%), 75 had a history of chemotherapy (81.5%), and 41 had concurrent chemotherapy (44.6%).

Sleep disorders during radiotherapy

With the progress of radiotherapy, the incidence of sleep disorders (PSQI>7 points) in the 92 patients with lung cancer increased from 32.6% to 52.2%, and the trend test changes were statistically significant ($P<0.05$). Compared to the domestic norm, the scores and total scores of lung cancer patients in the PSQI questionnaire were higher. The differences in sleep efficiency, daytime dysfunction, and PSQI scores were statistically significant ($P<0.05$), as shown in Table I and Fig. 1.

Immunological indicators during radiotherapy

Changes in lymphocyte subsets during radiotherapy in the 92 subjects are shown in Fig. 2. The changes of CD19$^+$, CD3$^+$, CD4$^+$ and CD4$^+$/CD8$^+$ cells were statistically significant ($P<0.05$). The IL-6 level in the 92 lung cancer patients was between 0.02 to 40.36 pg/ml, and the detection rate was 100%. During radiotherapy, IL-6 showed an upward trend ($F=5.013$, $P=0.003$). The mean value of IL-6 during T1-T4 was (4.51±6.76) pg/ml, (5.22±6.94) pg/ml, (5.65±6.98) pg/ml, and (7.57±7.94) pg/ml, respectively. The detection value of IL-1β in the 92 lung cancer patients was lower than the detection threshold of -5.90 pg/ml, and the total detection rate was 10.8%. Before radiotherapy, the positive rate was 0%. In the mid-period of radiotherapy, the positive rate was 8.7%. In the late stage of radiotherapy, the positive rate was 13%. At the end of the radiotherapy, the positive rate was 21.7%.

Relationship between sleep disorders, clinical factors, and immunological parameters during radiotherapy

Through the use of the *Chi*-square test, the

Table I. *Scores of the PSQI Scale and the Status of Scores in each dimension during different periods of radiotherapy for lung cancer patients ($\bar{x}\pm s$).*

Item	Domestic norm	T1	T2	T3	T4	F	P
Sleep quality	0.63±0.68	1.04±0.77**	0.91±0.56**	1.01±0.55**	1.15±0.51**	1.807	0.149
Sleep latency	0.70±0.86	1.16±1.12**	1.31±1.07**	1.38±1.14**	1.62±1.09**	2.178	0.101
Hours of sleep	0.70±0.58	0.83±0.73	0.80±0.75	0.86±0.78	1.01±0.92*	0.644	0.587
Sleep efficiency	0.15±0.47	0.72±0.68**	0.85±0.73**	0.83±0.74**	1.22±1.07**	3.098	0.034
Sleep disorder	0.90±0.44	1.39±0.54**	1.33±0.48**	1.35±0.47**	1.50±0.51**	2.322	0.087
Sodium amytal	0.06±0.04	0.23±0.04*	0.22±0.06*	0.12±0.07	0.19±0.03	0.531	0.665
Daytime function	0.73±0.83	1.45±0.97**	1.57±0.83**	1.64±0.86**	1.74±0.84**	3.521	0.021
PSQI score	3.87±2.51	6.82±3.78**	6.99±0.74**	7.19±0.55**	8.43±3.72**	4.329	0.009

** P<0.05; ** P<0.01*

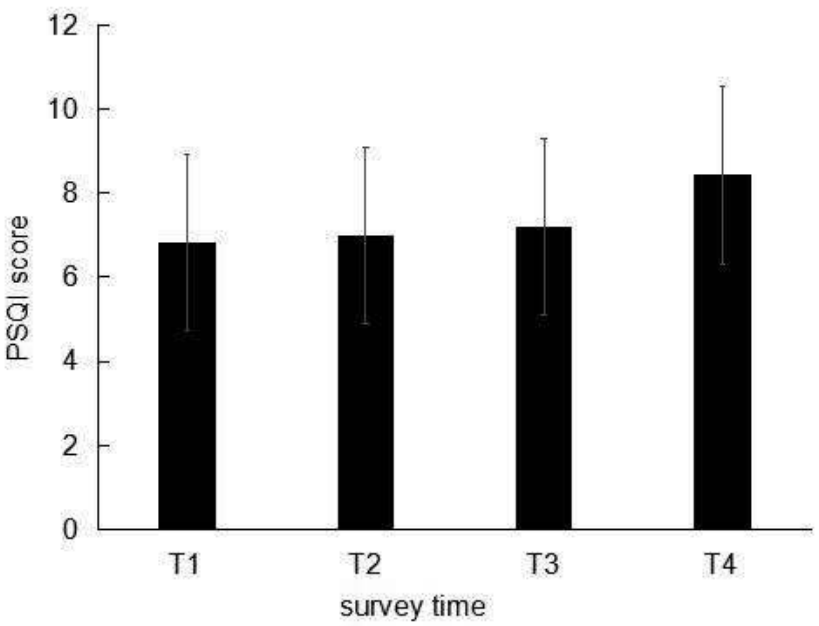

Fig. 1. *Trend of PSQI scores in patients with lung cancer at different stages of radiotherapy (translation: survey time, PSQI score).*

results of distribution of sleep disorders under different social demographic characteristics during radiotherapy from lung cancer patients showed a significant difference in sleep disorders after two weeks of radiation therapy among lung cancer patients of different ages (P<0.05); there was no significant difference in the other factors (P>0.05). The results of distribution of sleep disorders under different disease-related data during radiotherapy for lung cancer patients showed a significant difference in sleep disturbances between patients with or without previous diabetes and previous radiotherapy with chemotherapy (P<0.05). There was a statistically significant difference in sleep disorders at 4 weeks in patients with or without synchronous chemotherapy (P<0.05), however, there was no

Table II. *Distribution of immunological markers in patients with sleep disorders and normal sleep during radiotherapy* $(\bar{x}\pm s)$.

Observation time	Immune index	Sleep disorder group	Normal sleep group	*t*	P
T1	$CD19^+$	8.23±3.47	9.65±4.29	-1.478	0.143
	$CD3^+$	66.45±9.80	69.53±9.21	-0.859	0.391
	$CD3^+CD8^+$	26.87±9.32	27.02±9.01	-0.082	0.932
	$CD3^+CD4^+$	39.16±7.78	41.16±9.67	-0.945	0.334
	$CD4^+/CD8^+$	1.59±0.62	1.77±0.74	-0.894	0.371
	$CD16^+56^+$	19.35±9.39	22.43±11.17	-1.148	0.352
	IL-6	3.71±4.36	4.89±7.65	-0.593	0.557
T2	$CD19^+$	6.11±3.89	6.34±2.72	-0.265	0.788
	$CD3^+$	68.82±11.21	73.11±12.34	-1.573	0.117
	$CD3^+CD8^+$	26.29±10.01	27.23±8.37	-0.409	0.684
	$CD3^+CD4^+$	41.05±9.18	45.93±11.02	-2.067	0.042
	$CD4^+/CD8^+$	1.76±0.73	2.68±0.79	-1.392	0.167
	$CD16^+56^+$	18.43±12.65	23.13±12.34	-1.749	0.086
	IL-6	5.22±3.98	5.39±3.76	-0.082	0.943
T3	$CD19^+$	4.86±2.25	5.87±3.21	-1.305	0.197
	$CD3^+$	69.62±12.18	76.71±10.13	-2.502	0.014
	$CD3^+CD8^+$	26.51±9.89	27.06±8.79	-0.241	0.812
	$CD3^+CD4^+$	42.12±10.58	49.03±12.17	-2.505	0.015
	$CD4^+/CD8^+$	1.74±0.69	2.03±0.97	-1.421	0.161
	$CD16^+56^+$	16.92±10.25	23.01±12.18	-2.149	0.034
	IL-6	6.58±4.26	4.98±4.12	0.789	0.434
T4	$CD19^+$	5.02±2.93	7.55±2.86	-1.102	0.274
	$CD3^+$	73.31±13.21	75.41±16.54	-0.451	0.656
	$CD3^+CD8^+$	31.56±15.13	40.72±19.72	-0.959	0.342
	$CD3^+CD4^+$	38.89±12.04	42.21±16.58	-0.782	0.434
	$CD4^+/CD8^+$	1.42±0.75	1.72±1.18	-0.894	0.375
	$CD16^+56^+$	15.43±10.31	20.09±13.78	-1.385	0.169
	IL-6	10.23±9.89	4.53±3.71	2.561	0.13

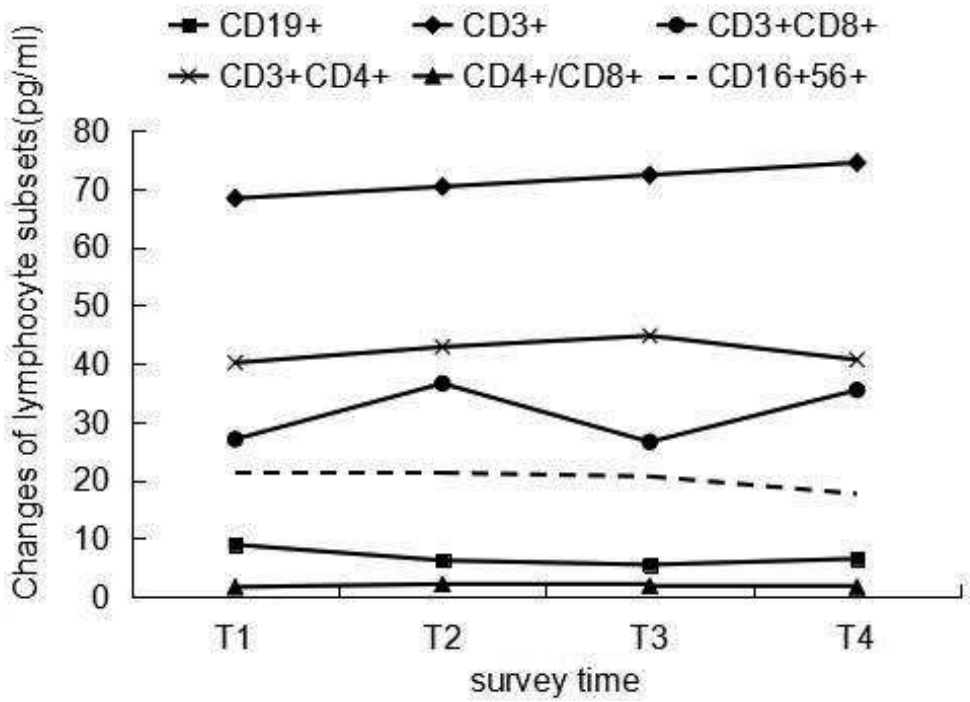

Fig. 2. *Changes of lymphocyte subsets in patients with lung cancer at different stages of radiotherapy.*

significant difference in the other factors ($P<0.05$).

Compared with the normal sleep group, patients with lung cancer had lower levels of $CD4^+$ cells at two weeks of radiotherapy ($P<0.05$). The levels of $CD3^+$, $CD4^+$, and $CD16^+56^+$ surface markers were lower at 4 weeks of radiotherapy ($P<0.05$). At the end of radiotherapy, there was no significant difference in each index ($P>0.05$), as shown in Table II. The comparison of inflammatory cytokines between the two groups showed that there was no significant difference in IL-6 levels between the two groups before and after radiotherapy ($P>0.05$). At the end of radiotherapy, IL-6 levels in the sleep disorder group were higher than those in the normal sleep group ($P<0.05$). In the period of T1~T4, there was no significant difference of IL-1β between the two groups ($P>0.05$). Details are shown in Table II.

DISCUSSION

This study highlights the incidence of sleep disorders in patients with lung cancer radiotherapy ranges from 33.3% to 52.6%. To some extent, it showed the prevalence of sleep disorders in patients with cancer radiotherapy. Elder patients with lung cancer were prone to sleep disorders. The risk of sleep disorders in patients with lung cancer was significantly higher than that of patients with radiotherapy alone. Complications of the body caused by multiple stimuli, including the tumor itself, chemotherapeutic drugs, and radiation, in patients undergoing concurrent radiotherapy and chemotherapy seriously affected sleep quality (9, 10).

In this study, we found that $CD3^+$, $CD4^+$, and $CD16^+56^+$ counts in the sleep disorder group were lower than those in the normal sleep group, and there was no difference in $CD8^+$ cells in the mid-late stage of radiotherapy. This suggested that the occurrence of sleep disorders during lung cancer reduced the body's immune status. IL-6 levels in lung cancer patients displayed a rising trend during radiotherapy. Radiotherapy may cause some degree of tissue damage with radiation and/or chemotherapeutic drugs as external stimuli, which may cause inflammatory

reactions in the body and stimulate the secretion of pro-inflammatory cytokines such as IL-6. The level of IL-6 in the sleep disorder group of lung cancer patients at the end of radiotherapy was higher than that in the normal sleep group. This result is consistent with published results (11, 12).

In summary, the incidence of sleep disorders in patients gradually increased with the progress of radiotherapy. Sleep disorders in lung cancer patients during radiotherapy were associated with a decrease in $CD3^+$, $CD3^+CD4^+$, and $CD16^+56^+$. Patients with sleep disorders at the end of radiotherapy were associated with elevated levels of IL-6.

REFERENCES

1. Chen W, Zheng R, Zeng H, Zhang S. The updated incidences and mortalities of major cancers in China. Chin J Cancer 2015; 34(11):502-7.
2. Bar-Ad V, Leiby B, bWitek M, et al. Treatment-related acute esophagitis for patients with locoregionally advanced non-small cell lung cancer treated with involved-field radiotherapy and concurrent chemotherapy. Am J Clin Oncol 2014; 37(5):433-37..
3. Dickerson SS, Sabbah EA, Ziegler P, Chen H, Steinbrenner LM, Dean G. The experience of a diagnosis of advanced lung cancer: sleep is not a priority when living my life. Oncol Nurs Forum 2012; 39(5):492-99.
4. Hu LY, Chen PM, Hu YW, et al. The risk of cancer among patients with sleep disturbance: a nationwide retrospective study in Taiwan. Ann Epidemiol 2013; 23(12):757-61.
5. Savard J, Ivers H, Savard MH, Morin CM. Cancer treatments and their side effects are associated with aggravation of insomnia: Results of a longitudinal study. Cancer 2015; 121(10):1703-11.
6. Miaskowski C, Paul SM, Cooper BA, et al. Predictors of the trajectories of self-reported sleep disturbance in men with prostate cancer during and following radiation therapy. Sleep 2011; 34(2):171-79.
7. Wood LJ, Weymann K. Inflammation and neural signaling: etiologic mechanisms of the cancer treatment-related symptom cluster. Curr Opin Support Palliat Care 2013; 7(1):54-59.
8. Miller A H, Ancoliisrael S, Bower J E, Capuron L, Irwin MR. Neuroendocrine-immune mechanisms of behavioral comorbidities in patients with cancer. J Clin Oncol 2008; 26(6):971-82.
9. Black DS, O'Reilly GA, Olmstead R, Breen EC, Irwin MR. Mindfulness meditation and improvement in sleep quality and daytime impairment among older adults with sleep disturbances: a randomized clinical trial. JAMA Intern Med 2015; 175(4):494-501.
10. Hong JS, Tian J, Wu LH. The influence of chemotherapy-induced neurotoxicity on psychological distress and sleep disturbance in cancer patients. Curr Oncol 2014; 21(4):174-80.
11. Ingram LA, Simpson RJ, Malone E, Florida-James GD. Sleep disruption and its effect on lymphocyte redeployment following an acute bout of exercise. Brain Behav Immun 2015; 47:100-8.
12. Lynch Kelly D, Lyon DE, Ameringer SA, Elswick RK. Symptoms, cytokines, and quality of life in patients diagnosed with chronic graft-versus-host disease following allogeneic hematopoietic stem cell transplantation. Oncol Nurs Forum 2015; 42(3):265-75.

TREATMENT MECHANISM OF TOLEROGENIC DENDRITIC CELLS ON RHEUMATOID ARTHRITIS

XY. WANG and JY. ZHANG[2]

[1]Department of Rheumatology and Immunology, Binzhou Medical University Hospital, Binzhou, Shandong, China; [2]Department of Emergency, Binzhou Medical University Hospital, Binzhou, Shandong, China

Received December 8, 2017 – Accepted July 19, 2018

This study aims to explore the possible mechanism of treatment of collagen-induced rheumatoid arthritis (RA) by tolerogenic dendritic cells (tDCs). Different methods were used to induce and cultivate tDCs, and suitable conditions for tDC cultivation were explored. The experimental RA induced by collagen in mouse was treated by the obtained tDCs, and the possible mechanism was explored. The serum concentration of TNF-α, IFN-β, IL-4 and anti-type II collagen antibody were detected by ELISA. The anti-type II collagen antibody of mice without treatment was higher than that without disease onset, while the Blank-DC group, VIP-DC group and Bay-D had no statistically significant differences (*P*>0.05). Compared to the group without disease onset, the TNF-α level of those without treatment was significantly higher, while INF-γ, IL-1β and IL-4 concentration showed no significant difference (*P*>0.05). Compared to the untreated group, the TNF-α and IL-1β concentration after VIP-DC treatment were significantly decreased, while IL-4 was increased (*P*<0.05). In summary, VIP-DC and Bay-DC alleviate joint inflammation, synovitis and bone erosion by reducing the production of anti-type II collagen antibody, inhibiting proinflammatory factors and increasing inflammation inhibitors

To the Editor,

Rheumatoid arthritis (RA) is an autoimmune disease with symmetrical polyarthritis as the main clinical manifestation; its pathogenesis involves antigen presenting cells, T cells, B cells, synovial fibroblasts and cytokines. In the course of disease development, synovial proliferate to pannus, causing the erosion of cartilage and bone damage, eventually resulting in joint stiffness, deformity, dysfunction and different degrees of disability.

Dendritic cells (DCs) are recognized as the most powerful professional antigen presenting cells, which play an important role in inducing immune response and immune tolerance formation (1). Tolerogenic dendritic cells (tDCs) have the effect of inducing T-cell resistance, inhibiting autoimmune responses, inducing regulatory T-cell (Tregs) proliferation and differentiation, and secreting high levels of IL-4 and IL-10. On the one hand, it enables Th1 cells to produce TNF-α to inhibit inflammatory reaction. On the other hand, high levels of IL-10 reduce the DC surface MHC- II molecules and simulate these molecule and adhesion molecule expression, and cannot provide corresponding stimulation signals to T cells (2). At present, only some preliminary studies have explored the role of tDC in RA, further studies are still needed

Key words: tolerogenic dendritic cells, VIP, Bayα -8072, rheumatoid arthritis, animal model, mechanism

Mailing Address:
Dr Xinyun Wang,
Department of Rheumatology and Immunology,
Binzhou Medical University Hospital,
No.661, the Second Huanghe Road,
Binzhou City 256603, Shangdong Province, China
Tel.: +86 13838176233
e-mail: tianjiem517@sina.com

0393-974X (2018)

to obtain safe and effective tolerable DC (3).

Vasoactive intestinal peptide (VIP) is a potential immune inhibitor, which can affect the natural and acquired immunity (4). VIP treatment on collagen-induced arthritis can decrease inflammation suppression factor levels, reducing joint inflammation and bone erosion. VIP induced cell passivation through combination with macrophages and VIP receptor 1 (VPAC1). VPAC1 is the main functional receptor of dendritic cells (5). Previous studies reported that VIP-induced and cultivated human tDCs could upregulate CD4 and CD8 regulatory T cells (Treg cells), which confirmed the immune tolerance function of VIP-tDCs. As a treatment cell, presented back to the human body, tDC should be ensured to have low or non-immunogenicity (6). However, de Heusch et al. (7) reported that once tDCs entered the human body, they might induce immunogenicity rather than immune tolerance, therefore, a key factor in tDC therapy is to obtain low immunogenicity of tDCs. More direct access to tDCs was achieved through inhibiting the signal presenting pathway in DC maturation, of which the nuclear factor NFκB was the vital nuclear transcription factor involved in its maturity. *In vivo*, Zanetti et al. confirmed the significance of NFκB in DC maturity (8). The results from NFκB knockout RelB gene mice required tDCs immune mice**?** illustrated that its antigen specificity had low reactivity, and confirmed the feasibility that tDCs through inhibition of NFκB can effectively reduce the immunogenicity reaction. Furthermore, Popov et al. reported that the application of NFκB antagonist-induced and cultivated tolerogenic DCs not only successfully obtained tDCs of immature DCs cell phenotype, as the immune experimental arthritis mice had preliminary clinical relief, but also suppressed the antigen specific T cell responses (9). Therefore, this intervention could obtain low immunogenicity and induce antigen specific immune tolerogenic tDCs through intervening in the different steps and changing different cytokine-induced culture conditions in DC mature process (10). The application of tDCs in experimental arthritis treatment could further reveal the pathogenesis of RA, and have vital significance on the search for novel immune intervention target.

Previous studies confirmed that the VIP-DC and Bay-DC treatment on collagen-induced RA in mice could reduce the degree of inflammation, reduce pannus formation, and prevent bone erosion. The present study aimed to further explore the possible mechanism of VIP-DC and Bay-DC.

MATERIALS AND METHODS

Study animals

Thirty DBA/1 SPF (specific pathogen free) mice were purchased from Shanghai Silaike experimental animal co., LTD. All animals were male, aged 6-8 weeks, weight 20-25g, and were fed in the immunodeficiency animal experimental center without SPF environment of Zhejiang University of Chinese Traditional Medicine.

DBA/1 mice were divided into 5 groups, 6 mice in each group. Apart from the first group, the other groups were used to induce CIA joint inflammation by collagen type emulsion cattle II. (a) The group without disease onset: normal saline was injected at the root of the tail. (b) Control group: type II collagen was injected at the root of the tail, and saline solution was intraperitoneally injected after modeling finalized. (c) Blank DC group: type II collagen was injected at the root of the tail, Blank DCs were intraperitoneally injected after modeling finalized. (d) VIP group: type II collagen was injected at the root of tail, VIP-DCs were intraperitoneally injected after modeling finalized. (e) Bay DC group: type II collagen was injected at the root of tail, Bay-DCs were intraperitoneally injected after modeling finalized.

DC vaccine injection and antigen specific immune response

According to the cell culture steps, tolerance dendritic cells were cultivated. The gained tDCs cultivated from each group were injected to the relevant group as vaccine, at the dosage 2×10^6 tDCs for each rat. On the 40th day, the sick mice were randomly divided into 4 groups. Intraperitoneal injection intervention was performed on the control group, blank DC group, VIP-DC group and Bay-DC group. The respective injections were 0.5ml saline solution in the control group, $2*10^6$/0.5ml in blank DC group, $2*10^6$/0.5ml in VIP-DC group and $2*10^6$/0.5ml in the Bay-DC group. The arthritis scores of each group were observed on days 40, 50, 60 and 70.

CIA mice arthritis scores

The signs of arthritis in the 5 groups of DBA/1 mice were observed by two monitors every 10 days according to the clinical scoring system. The evidence was based on the degree, extent and deformity of the joint: 0 point - no erythema or swelling; 1 point - slight swelling of erythema was limited in the tarsal bone or ankle joint of the foot; 2 points - erythema and slight swelling, from the ankle to the tarsal bone of the foot; 3 points - erythema and moderate swelling, from ankle and ankle joints to metatarsal joint; 4 points - severe redness and swelling of the whole ankle, the back of the foot and the toes, or stiffness of the limbs.

Detection of serum anti-type II collagen antibody level

A blood sample was collected from the eyeball of each mouse in each group. The serum dilution multiples were 1:10 by indirect ELISA method to detect the anti-type II collagen antibody level of mice serum in each group.

Statistical analysis

Experimental results in each group were described

Table I. *Comparison of arthritis index of mice at different days after intervention (x ± S) point.*

	Day 40	Day 50	Day 60	Day 70
Control group (n=6)	2.79±0.71	2.68±0.69	2.48±0.66	2.62±0.70
Blank DC group	2.87±0.52	2.63±0.68	2.41±0.65	2.49±0.71
VIP-DC group	2.78±0.79	2.75±0.74	2.53±0.76	2.28±0.73*
Bay-DC group	2.86±0.78	2.38±0.59	2.18±0.78Δ	2.00±0.62*

** vs control group and blank DC group, P<0.05; Δ vs the remaining groups, P<0.05*

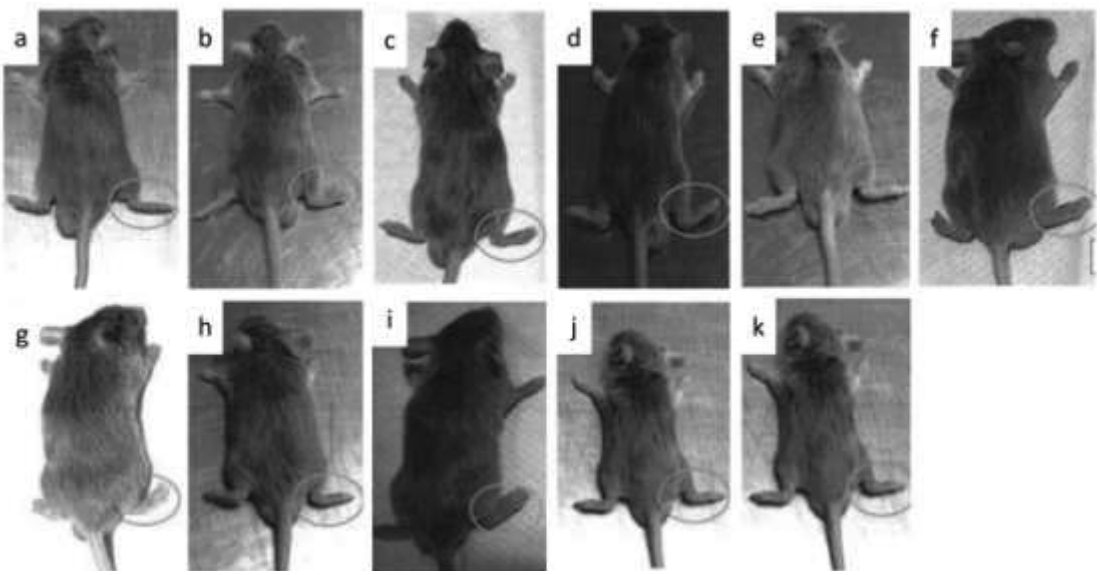

Fig. 1. *Manifestations of arthritis in different subgroups. a) Manifestations of arthritis in the group without disease onset at day 40. b) Manifestations of arthritis in the group without treatment (control group) at day 40. c) Manifestations of arthritis before and after treatment with blank-DC group at day 50. d) Manifestations of arthritis before and after treatment with blank-DC group at day 60. e) Manifestations of arthritis before and after treatment with blank-DC group at day 70. f) Manifestations of arthritis before and after treatment with VIP-DC group at day 50. g) Manifestations of arthritis before and after treatment with VIP-DC group at day 60. h) Manifestations of arthritis before and after treatment with VIP-DC group at day 70. i) Manifestations of arthritis before and after treatment with Bay-DC group at day 50. j) Manifestations of arthritis before and after treatment with Bay-DC group at day 60. k) Manifestations of arthritis before and after treatment with Bay-DC group at day 70.*

as $\bar{x} \pm SD$. SPSS 17.0 software was used for statistical analysis; a P value of less than 0.05 was considered to be statistically significant.

RESULTS

Changes in arthritis scores

The arthritic condition in mice was observed on days 40, 50, 60 and 70. Two doctors evaluated the scores for all the animal limb joints and calculated the average points. The group without disease onset had no verification, the score was 0. The arthritis points in the control group and blank-DC group did not have obvious changes. The arthritis points in the VIP-DC group and Bay-DC group had decreased to some degree. On day 70, the arthritis points in the VIP-DC group and Bay-DC group were significantly less than the control group and the blank DC group (P<0.05). On day 60, arthritis points in the Bay-DC group were less than the other 3 groups (P<0.05), as seen in Table I and Fig. 1.

Table II. *The serum autoantibodies and cytokines in each group of CIA mice.*

Group	Anti-type II collagen antibody (IU/ml)	TNF-α (pg/ml)	IFN-γ (pg/ml)	IL-1β (pg/ml)	IL-4 (pg/ml)
disease without onset group	66.4±17.88	63.1±23.60	65.63±19.43	53.84±27.02	146.97±14.99
Disease without treatment group	191.76±45.75 Δ	229.26±58.29 Δ	148.45±32.20	126.34±37.92	86.78±14.99
Blank DC group	172.21±28.64	202.26±40.30	181.23±16.67*	124.86±47.44	87.63±42.62
VIP-DC group	157.02±27.65	123.58±16.76*	100.97±26.94	80.36±23.01#	154.40±26.70
Bay-DC group	131.93±22.29	188.50±58.39 Δ	88.78±18.94#	51.66±17.46*#	766.01±230.40 Δ*#

*Δ compared to disease without onset group, p<0.05; * vs without treatment group, p<0.05; # vs blank DC group, p<0.05*

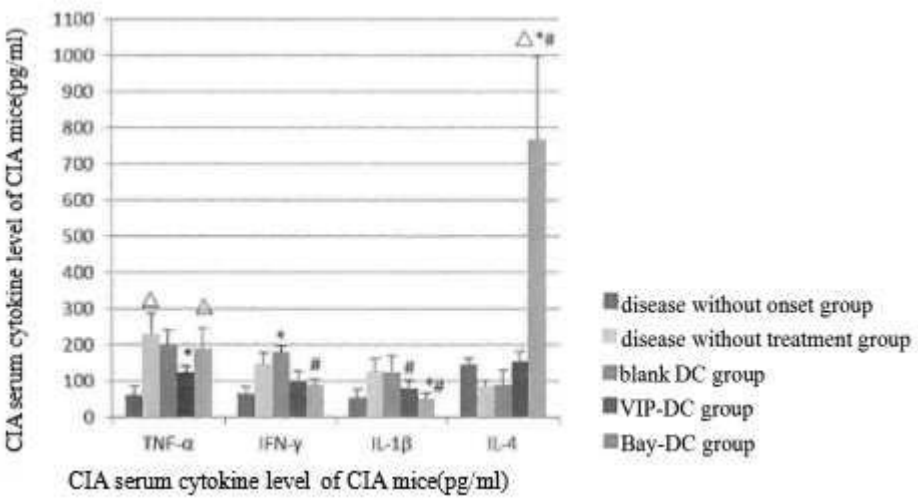

Fig. 2. *The serum cytokines and antibody levels of CIA mice in each group.*

Antibody changes in each group of mice

Anti-type II collagen antibody in the disease without onset group was apparently higher than that in the disease without treatment group, while no significant differences were observed among the blank DC group, VIP-DC group and Bay-DC group (Table II and Fig. 1).

Changes of cytokines in all groups of mice

Compared to the disease without onset group, the TNF-α in disease without treatment group was obviously increased, no significant differences in IFN-γ, IL-1β or IL-4 concentration were detected. Compared to the disease without treatment group, after the VIP-DC treatment, TNF-α and IL-1β concentrations were significantly decreased. After Bay-DC treatment, IFN-γ and IL-1β were apparently decreased, while IL-4 was obviously increased (Table II and Fig. 2).

DISCUSSION

In RA patients, a variety of antigens have been found in serum and synovial fluid, including rheumatoid factor, anti-cyclic citrullinated peptide antibody, antibodies against keratin, and collagen antibody. In models of collagen-induced RA, type II collagen antibody have attracted more attention (8). In humans, anti-type II collagen antigen positive patients are more likely to have bone erosion (11). In *in vitro* animal studies, anti-type II collagen antibody can directly cause erosion of cartilage and bone (12). The type II collagen antibody injection on susceptible animals could induce arthritis similar to human arthritis. The anti-type II collagen antibodies extracted from arthritic mice when injected into healthy mice could transfer the arthritis. The above facts demonstrate that anti-type II collagen antibody participated in the pathological process of RA (13). The pathogenesis of anti-collagen antibody was suggested to be the formed immune complex and activation of complement, causing chemotaxis of inflammatory cells, resulting in destruction of connective tissue (14, 15). This experiment showed that the anti-type II collagen antibody of mice after the onset of disease obviously increased. Through VIP-DC and Bay-Day treatment, the anti-type II collagen antibody had a downward trend, but there were no statistical differences. Rheumatoid factor and anti-CCP antibody were not discovered in any group, which might have a relationship with the time of onset.

Cytokines were involved in the entire pathological process of RA, and could be classified as inflammatory factors or inhibitory factors according to their function. TNF-α, IFN-γ, and IL-1β were the important inflammatory factors, while IL-4 and IL-10 were the important anti-inflammatory factors. The present study showed that the VIP-DC treatment could reduce the TNF-α, IL-1β concentration, and the differences were statistically significant. Bay-DC treatment could obviously reduce the IFN-γ, IL-1β concentration, and IL-4 apparently increased, which proved that VIP and Bay-induced tolerant dendritic cells could increase the inflammation factor expression suppression through inhibiting the inflammatory factor, thus alleviating synovial inflammation, and relieving the disease development.

In conclusion, VIP-DC and Bay-DC alleviate joint inflammation, synovitis and bone erosion through reducing the production of anti-type II collagen antibody, inhibiting proinflammatory factor, and increasing inflammation suppression factor.

ACKNOWLEDGEMENTS

This work was supported by a grant from Binzhou Science and Technology Development Program of Binzhou city, China. (Project No. 2011ZC0923)

REFERENCES

1. Gallo PM, Gallucci S. The dendritic cell response to classic, emerging, and homeostatic danger signals. Implications for autoimmunity. Front Immunol 2013; 4:138-55.
2. Kwok SK, Lee JY, Park SH, Cho ML, Min SY, Kim HY, Cho YG. Dysfunctional interferon-alpha production by peripheral plasmacytoid dendritic cells upon Toll-like receptor-9 stimulation in patients with systemic lupus erythematosus. Arthritis Res Ther 2008; 10:R29.
3. Lim DS, Kang MS, Jeong JA, Bae YS. Semi-mature DC are immunogenic and not tolerogenic when

inoculated at a high dose in collagen-induced arthritis mice. Eur J Immunol 2009; 39:1334-43.
4. De Almeida DE, Ling S, Pi X, Hartmann-Scruggs AM, Pumpens P, Holoshitz J. Immune dysregulation by the rheumatoid arthritis shared epitope. J Immunol 2010; 185:1927-34.
5. Kavousanaki M, Makrigiannakis A, Boumpas D, Verginis P. Novel role of plasmacytoid dendritic cells in humans: induction of interleukin-10-producing Treg cells by plasmacytoid dendritic cells in patients with rheumatoid arthritis responding to therapy. Arthritis Rheum 2010; 62:53-63.
6. Weng Y, Sun J, Wu Q, Pan J. Regulatory effects of vasoactive intestinal peptide on the migration of mature dendritic cells. J Neuroimmunol 2007; 182:48-54.
7. de Heusch M, Oldenhove G, Urbain J, Thielemans K, Maliszewski C, Leo O, Moser M. Depending on their maturation state, splenic dendritic cells induce the differentiation of CD4(+) T lymphocytes into memory and/or effector cells in vivo. Eur J Immunol. 2004;34:1861-9.
8. Zanetti M, Castiglioni P, Schoenberger S, Gerloni M. The role of reIB in regulating the adaptive immune response. Ann N Y Acad Sci 2003; 987:249-57.
9. Popov I, Li M, Zheng X, et al. Preventing autoimmune arthritis using antigen-specific immature dendritic cells: a novel tolerogenic vaccine. Arthritis Res Ther 2006; 8(5):R141.
10. Saas P, Tiberghien P. Dendritic cells: to where do they lead? Transplantation 2002; 73:S12-5.
11. Rowley MJ, Nandakurnar KS, Holmdahl R. The role of collagen antibodies in mediating arthritis. Mod Rheurnatol 2008;18:429-41.
12. Mullazehi M, Wick MC, Klareskog L, van Vollenhoven R, Ronnelid J. Anti-type II collagen antibodies are associated with early radiographic destruction in rheumatoid arthritis. Arthritis Res Ther 2012; 14:R100.
13. Seki N, Sudo Y, Yoshioka T, et al. Type II collagen-induced murine arthritis induction and perpetuation of arthritis require synergy between humoral and cell-mediated immunity. J Immunol 1988; 140:1477-84.
14. Taylor PC, Plater-Zyberk C, Maini RN. The role of the B cells in the adoptive transfer of collagen-induced arthritis from DBA/1(H-2q) to SCID (H-2d) mice. Eur J Immunol 1995; 25:763-69.
15. Carnrot C, Prokopec KE, Rasbo K, Karlsson MC, Kleinau S. Marginal zone B cells are naturally reactive to collagen type II and are involved in the initiation of the immune response in collagen-induced arthritis. Cell Mol Immunol 2011; 8:296-304.

LETTER TO THE EDITOR

VITAMIN D RECEPTOR GENE POLYMORPHISMS AND PROSTATE CANCER

R.S. BRACZKOWSKI[1], R. KWIATKOWSKI[2], A. DANIKIEWICZ[3], S. GÓRCZYŃSKA-KOSIORZ[4], W. TRAUTSOLT[4], B. BRACZKOWSKA[5] and W. GRZESZCZAK[4]

[1]Care and Treatment Department, Hospital no. 1 Bytom, Poland; [2]S. Leszczyński Memory, City Hospital Katowice, Radiotherapy Branch, Katowice, Poland; [3]Deptartment of Nutrition-Related Disease Prevention, School of Public Health Bytom, Medical University of Silesia Katowice, Poland; [4]Department of Internal Medicine, Diabetology and Nephrology Zabrze Medical University of Silesia Katowice, Poland; [5]Department of Epidemiology Medical University of Silesia, Katowice, Poland

Received March 22, 2018 – Accepted August 6, 2018

Prostate cancer (PC) is the most common cancer among men worldwide and its pathogenesis is complex. The development of PC depends on family and environmental factors. Vitamin D can be **associated with both of these factors. Its reduced serum concentration has been reported in a number of tumors. However, in the case of PC, the study results are conflicting. Polymorphism of VDR gene may also be involved in the development of this cancer. The aim of the study was to compare the frequency of selected polymorphisms in patients with PC and in men without this disease. Seventy-two Caucasian males aged 35-75 years with histologically proven PC (T1/T2) were enrolled in the study group. Seventy-two random age-matched Caucasian out-patient subjects formed the control group. VDR (*FokI, BsmI and TaqI*) gene polymorphism (rs2228570, rs1544410, rs731236) was determined by TaqMan® SNP Genotyping. The Hardy-Weinberg Equilibrium (HWE) - p> 0.05 was in all studied polymorphisms. Deviations from the HWE were not found. There were no differences between the study group and the control group. No difference was found when the groups were compared in terms of age or the Gleason score.**

To the Editor,

Prostate cancer (PC) is one of the most common cancers among men worldwide. Genetic, environmental and life style-related factors can affect the development of PC. Age remains the strongest risk factor as the incidence increases with age (1). Race is also a factor that seems to have an impact on the incidence as it is higher in African Americans as compared to Caucasian men and Asians who are the least frequently affected. The highest incidence is observed in the Afro-Caribbean population (2). In terms of geographical influence, the highest incidence is reported in Scandinavia, whereas the lowest in Asia. The possible role of genetic factors is reflected by a higher risk of cancer observed in men whose first-degree relatives were diagnosed with PC (3). Epidemiological studies indicate the influence of environmental factors and diet (4).

Vitamin D can be associated with almost all of the above-mentioned factors. The reduced serum concentration of vitamin D has been reported in a number of tumors, however, in the case of PC, the study results are often conflicting. While some studies show an inverse relationship between vitamin D levels in the blood and prevalence of PC, other reports contradict this relationship. The role of genetic

Key words: vitamin D, prostate cancer, gene polymorphism

Mailing address:
Dr Ryszard S. Braczkowski,
Department of Public Health School,
Public Health Medical
University of Silesia,
18 Piekarska ST, 41-902 Bytom, Poland
Tel.: +48 669 163 115
e-mail: rbracz@sum.edu.pl

0393-974X (2018)

factors has already been mentioned, and Vitamin D can be also connected with these. Particular attention should be paid to the polymorphisms of genes of enzymes involved in vitamin D metabolism, as well as polymorphisms of genes of vitamin D receptor (VDR) (5).

It cannot be excluded that the effect of vitamin D deficiency on the development of PC may appear more prominent in the case of certain polymorphisms of the VDR gene. VDR belongs to the family of steroid nuclear receptors and acts as an activator of gene transcription. Most of our body cells and cancer cells have a VDR. The gene encoding the receptor is located on the long arm of chromosome 11 (12q13). A number of polymorphic sites were identified within the gene. The most common are FokI, BsmI, TaqI and ApaI. The relationship between these polymorphisms and an increased risk of cancer has been demonstrated in many cancers.

The aim of the study was to determine the prevalence of BsmI, FokI and TaqI polymorphisms in men who were diagnosed with PC.

MATERIALS AND METHODS

The study group consisted of 72 men, aged 45-75 years with histologically proven PC. The material for the study was obtained by biopsy or electroresection. The examinations were conducted in the Prof. E. Michalowski Memory Specialistic Hospital in Katowice, Poland. Table I presents the characteristics of the study group. In accordance with the applicable procedures of the hospital, patients in whom histological examination revealed the presence of cancer were referred for consultation to the Department of Radiotherapy, St. Leszczynski Hospital in Katowice, after which further treatment was established. Before the consultation, blood was collected for the examination of polymorphisms. The control group consisted of 72 men aged 45-71 years who were patients of primary health care in Bytom. Vitamin D levels were determined in all subjects from both of the study groups. The study was approved by the Bioethics Committee of the Medical University of Silesia in Katowice, Poland (CDF 2-127/10) and written consent was obtained from all the patients enrolled.

Three SNPs of the VDR gene, namely FokI (rs2228570), BsmI (rs1544410) and TaqI (rs731236), were tested. Polymorphisms were selected based on the literature data as well as on the SNP database: http://www.ncbi.nlm.nih.gov/.

DNA isolation

The isolation of genomic DNA and the examination of all polymorphisms were carried out in the Laboratory of Molecular Biology Department of Internal Diseases, Diabetology and Nephrology, Medical University of Silesia, Poland. Venous blood samples were collected into tube-syringes S-Monovette (Sarstedt), with a capacity of 4.9 ml, containing 6.4 mg potassium-EDTA. Samples were stored at -20°C until DNA isolation. Genomic DNA was isolated from peripheral blood leukocytes by a salting-out method with the use of kit manual (Epicentre Technologies) in own modification. The precipitated DNA was dissolved in 150 µl of TE buffer (10 mM TRIS, and 1 mM EDTA K + pH = 8.0). Upon completion of the dissolution of the DNA, its concentration was evaluated using a NanoDrop (Thermo Scientific) spectrophotometer. Genotyping was performed using fluorescently-labeled probes complementary to each allele, using a kit for determination of SNP TaqMan Pre-Designed SNP Genotyping Assay (Thermo Fisher Scientific). Polymerase chain reaction and identification of the alleles were performed on a 7300 Real Time PCR System (Thermo Fisher Scientific).

Statistical analysis

Statistical analysis was performed using Statistica software (StatSoft 10.0, Krakow, Poland), Stata 13.0 (StataCorp LP, TX, USA) and the R software. The Hardy-Weinberg Equilibrium (HWE) was established by χ^2 compliance test, using the following formula: p2 + 2PQ + Q2 = 1. Comparisons between the groups were made by χ^2 test of independence. Statistical significance was set at $p < 0.05$.

RESULTS

Vitamin D deficiency was found in all subjects from the study group and the control group. The results of our research on vitamin D concentration in patients with PC were presented by Wieczorek et al. (6).

Table I. *Characteristics of the study group.*

Examined group	Number of persons
Age 45-75 years	72
of whom	
≤ 65	40
< 65	32
TNM	
T1a/b	5
T1c	39
T2a/b	4
T2c	9
T3a	5
T3b	8
T4	2
M0, N0	all group
Gleason scale points	
1 - 6	42
7	18
>7	12

TNM: TNM classification malignant tumours; T: tumour; N: lymph nodes; M: metastases Table

In the case of all studied polymorphisms deviations from HWE were not found (p> 0.05). The results of the comparisons of the frequency of the tested polymorphisms in the study and control groups are shown in Table II. There were no differences between the study group and the control group. There was no statistically significant difference when groups were compared in terms of age – under 65, and 65 and over years. Furthermore, there were no statistically significant differences in the frequency of polymorphisms between groups with a different Gleason score (three groups were distinguished: Gleason 1-6, Gleason 7 and Gleason above 7).

DISCUSSION

Vitamin D deficiency is observed in almost the entire Polish population. In our earlier study, we showed that patients with PC had slightly lower but not statistically significant concentration than patients with benign prostatic hyperplasia (6). A number of previous studies were related to the relationship between VDR gene SNPs and the incidence of PC. Isolated studies have confirmed this relationship, however, most studies did not. In the case of the FokI polymorphism, studies showed only a weak relationship clearly expressed among the cases with less advanced disease, or in the case of older patients (7). The impact of the FokI polymorphism on the prevalence of PC was demonstrated by Oakley-Girvan, however only in the group of African-Americans (8). A Japanese study by Hamasaki et al. did not demonstrate the links between the incidence of PC and TaqI polymorphism. However, it showed that TT genotype was more prevalent than tt in cases of a more aggressive course of the disease (9). Ma et al. tried to find relationships between BsmI polymorphism and the incidence of PC in the study on a large group of US physicians (10). They failed to demonstrate it when they examined the differences in the incidence of PC between subjects with BB

Table II. *The incidence of the tested polymorphisms in patients with prostate cancer and in the control group.*

FokI (rs2228570)	cancer group	(n = 72)	CC 19	CT 36	TT 17	
	Control	(n = 72	CC 22	CT 37	TT 13	χ^2 – 0.7665 p – 0.682
BsmI (rs1544410)	cancer group	(n = 72)	AA 8	AG 31	GG 33	
	control	(n =7 2)	AA 8	AG 33	GG 31	χ^2 - 0.1250 p - 0.939
TaqI (rs 731236)	cancer group	(n = 72)	CC 7	CT 33	TT 32	
	control	(n = 71)	CC 8	CT 31	TT 33	χ^2 – 0.122 p - 0.941

genotype and the group of subjects with bb genotype and those who were heterozygous (Bb). No differences were demonstrated when age groups of those under 65 and over 65 years of age were examined. Apart from these most commonly studied polymorphisms, other less common polymorphisms were also investigated e.g. tag SNPs rs2107301 and rs2238135. Holick et al. were the first to present results indicating that there may be a link between these polymorphisms and the risk of PC (11). The presence of possible links to PC was confirmed two years later by Forszt et al., however only in the case of rs2238135 (12). In the case of rs2107301 they demonstrated a positive correlation with elevated PSA.

Our study contributes to the reports indicating a lack of relationship between PC and the most common VDR gene polymorphisms. In future we would like to try to explain the discrepancies by demonstrating the presence of microRNAs that block the expression of the VDR gene. If it is not confirmed, future studies might be focused on less common and less frequently examined polymorphisms such as those mentioned above.

ACKNOWLEDGEMENTS

The study was supported by the Medical University of Silesia Katowice Poland Grant KNW-1-035.

REFERENCES

1. Mazereeuw MV, Withrow DR, Diane Nishri E, Tjepkema M, Marrett LD. Cancer incidence among First Nations adults in Canada: follow-up of the 1991 Census Mortality Cohort (1992-2009). Can J Public Health 2018 Jun 28. [Epub ahead of print]
2. Kheirandish P, Chinegwundoh F. Ethnic differences in prostate cancer. Br J Cancer 2011; 105:481-85.
3. Spitz MR, Currier RD, Fueger JJ, Babaian RJ, Newell GR. Familial patterns of prostate cancer: a case–control analysis. J Urol 1991; 146:1305-7.
4. Cook LS, Goldoft M, Schwartz SM, Weiss NS. Incidence of adenocarcinoma of the prostate in Asian immigrants to the United States and their descendants. J Urol 1999; 161:152-55.
5. Whitfield GK**,** Remus LS, Jurutka PW, et al. Functionally relevant polymorphisms in the human nuclear vitamin D receptor gene. Mol Cell Endocrinol 2001; 177:145-59.
6. Wieczorek K, Braczkowski RS, Skrzypek M, Stryjewski PJ, Kuczaj A, Al-Srory G. The comparison between vitamin D concentration in Upper Silesia patients with prostate cancer and with benign prostatic hyperplasia. J Biol Regul Homeost Agents 2015; 29:207-11.
7. Huang SP, Huang CY, Wu WJ, et al. Association of vitamin D receptor FokI polymorphism with prostate cancer risk, clinicopathological features and recurrence of prostate specific antigen after radical prostatectomy. Int J Cancer 2006; 119:1902-7.
8. Oakley-Girvan I, Feldman D, et al. Risk of early-onset prostate cancer in relation to germ line polymorphisms of the vitamin D receptor. Cancer Epidemiol Biomarkers Prev 2004; 13:1325-30.
9. Hamasaki T, Inatomi H, Katoh T, Ikuyama T, Matsumoto T. Clinical and pathological significance of vitamin D receptor gene polymorphism for prostate cancer which is associated with a higher mortality in Japanese. Endocr J 2001; 48*:*543-49.
10. Ma J, Stampfer MJ, Gann PH, et al. Vitamin D receptor polymorphisms, circulating vitamin D metabolites, and risk of prostate cancer in United States physicians Cancer Epidemiol Biomarkers Prev 1998; 7:385-90.
11. Holick CN, Stanford J L, Kwon EM, Ostrander EA, Nejentsev S, Peters U. Comprehensive association analysis of the Vitamin D pathway genes, VDR, CYP27B1 and CY24A1 in prostate cancer. Cancer Epidemiol Biomarkers Pre 2007; 16:1990-99.
12. Forszt P, Pilecka A, Małodobra M Markowska J, Maksymowicz K, Dobosz T. Single−nucleotide polymorphism association study of VDR and CDH1 genes and the risk of prostate cancer. Adv Clin Exp Med 2009; 18:215-20.

LETTER TO THE EDITOR

DECREASED SERUM LEVELS OF INTERLEUKIN-35 AMONG MULTIPLE SCLEROSIS PATIENTS MAY BE RELATED TO DISEASE PROGRESSION

S. BADIHIAN[1,2], V. SHAYGANNEJAD[1,3], P. SOLEIMANI[1,2], O. MIRMOSAYYEB[1,2], Z. SAMEE[1,2], N. MANOUCHEHRI[1,2] and N. ESMAEIL[4]

[1]Isfahan Neurosciences Research Center, Alzahra Research Institute, Isfahan University of Medical Sciences, Isfahan, Iran; [2]Students Research Center, School of Medicine, Isfahan University of Medical Sciences, Isfahan, Iran; [3]Department of Neurology, School of Medicine, Isfahan University of Medical Sciences, Isfahan, Iran; [4]Department of Immunology, School of Medicine, Isfahan University of Medical Sciences, Isfahan, Iran

Received March 7, 2018 – Accepted August 1, 2018

The regulatory role of interleukin (IL) -35 in the immunopathogenesis of multiple sclerosis (MS) is suggested in very few studies. We aimed to measure serum levels of IL-35 among clinically isolated syndrome (CIS) and relapsing-remitting MS (RRMS) patients and evaluate the associations between this cytokine and the disease clinical course. This cross-sectional study was conducted during 2017 in a referral university clinic. Forty patients and 40 healthy controls were included in the study. The level of IL-35 in the serum of all subjects was determined by ELISA. Serum level of IL-35 was reduced (p = 0.003) in RRMS in comparison with healthy controls. Moreover, the mean serum level of IL-35 among new cases (diagnosed within the 6 months prior to the study) decreased compared to healthy controls but it was not statistically significant (P=0.059). The mean serum level of IL-35 was significantly higher in new cases compared with other cases (p=0.048). Overall, we found decreased serum level of IL-35 among RRMS patients compared to the healthy controls. Our finding provides a view of the possible role of IL-35 in MS pathogenesis and the potential therapeutic targets.

To the Editor,

Multiple sclerosis (MS) is an autoimmune inflammatory demyelinating disease of the central nervous system (CNS). Immune cells, including both B and T cells, are involved in the pathogenesis of MS. Following exposure to auto-antigens, auto-reactive Th1 and Th17 cells are activated and migrate from the draining lymph nodes to the CNS through blood-brain or blood-cerebrospinal fluid barrier and mediate CNS pathology. On the other hand, $CD4^+$ $CD25^+$ $FOXP3^+$ regulatory T (Treg) cells have the crucial role in controlling autoimmune inflammation by suppressing auto-reactive T cells, and studies have shown they are able to inhibit the pathogenesis of experimental autoimmune encephalomyelitis (EAE) in an animal model of MS (1).

Treg cells exert their immunosuppressive effects through the production of inhibitory cytokines such as TGF-β, interleukin (IL)-10 and IL-35 (2, 3). IL-35 is a member of IL-12 family cytokines, mostly secreted by Treg and Breg cells. The suppression effects of IL-35 producing Treg cells (iTr35) and

Key words: multiple sclerosis, clinically isolated syndrome, relapsing-remitting multiple sclerosis, interleukin-35

Mailing address:
Nafiseh Esmaeil, PhD,
Department of Immunology, School of Medicine,
Isfahan University of Medical Sciences,
Isfahan 81744-176, Iran
Tel.: +98 311 37929097 - Fax: +98 3113 7929031
e-mail: nafesm5@gmail.com

0393-974X (2018)

Breg cells (i35Breg) have been indicated in studies. IL-35 contributes to attenuate autoimmune diseases by suppressing Th1 and Th17 cells in human and mouse models (4, 5).

According to the significant role of IL- 35 in immunological self-tolerance, IL-35 may play an important role in the immunopathogenesis of MS and may be used as a therapeutic target, however, it needs to be investigated more in the clinical setting. To the best of our knowledge, only one study has been carried out to evaluate this cytokine in MS cases (6). To fill this gap, we aimed to evaluate serum levels of IL-35 among CIS and RRMS patients and healthy individuals.

MATERIALS AND METHODS

This cross-sectional study was conducted during 2017 in the Multiple Sclerosis Clinic of Kashani hospital, Isfahan, Iran. Patients with the diagnosis of relapsing-remitting MS (RRMS) or clinically isolated syndrome (CIS) based on McDonald criteria (7) and without any other disease were included. Patients who were diagnosed during the previous 6-months were assumed as new cases. New cases were diagnosed patients who had not been treated with any corticosteroids in the month prior to blood sampling and who did not take any immunosuppressive drugs (8). Healthy subjects with no disease and normal examination were included as the control group. Healthy subjects who took any type of medication or had a history of any immune-system-related disease (e.g. severe allergy and asthma) were excluded. All eligible subjects were invited to participate in the study and written informed consents were obtained before enrolment.

We collected demographic data from all subjects. Also, data regarding disease characteristics, family history of MS, and MS medications were recorded for all patients. The patients were reevaluated by a neurologist to assess their diagnosis and extended disability status scale (EDSS).

Blood samples were drawn into standard serum tubes, allowed to clot, separated by centrifugation, and stored at −80°C until they use. Cytokine levels of human IL-35 in patients and controls were measured by ELISA (Bio-Ocean, CA, USA), according to the manufacturer's instructions. The minimum detectable dose (MDD) of IL-35 was 0.21 U/ml.

Statistical analysis

We used descriptive statistics to describe categorical (frequencies (%)) and interval [means (standard deviation)] variables. Independent sample *t*-test or Mann-Whitney-U test were used to compare interval variables between the two groups and one-way ANOVA or Kruskal-Wallis-H test were used for >2 groups. *Chi*-squared test was also used to compare categorical data between groups. Statistical analysis was carried out using IBM SPSS 23 (Armonk, NY). A P-value <0.05 was considered as significant.

RESULTS

The final study population included 40 subjects in each study group. The mean age in RRMS patients, CIS cases, and controls was 33.88 (8.48), 32.38 (8.20), and 33.13 (7.09) years, respectively (p=0.701). Six patients (15%) in the RRMS group, 12 patients (30%) in the CIS group, and 13 subjects (32.5%) in the control group were male (p=0.154).

Serum level of IL-35 was decreased in RRMS patients and CIS patients in comparison with healthy controls, however, correcting for multiple comparisons showed only a significant difference between RRMS (2.63±1.1)and control groups (3.41±1.05) (P= 0.002) (Fig. 1). Separating samples based on gender resulted

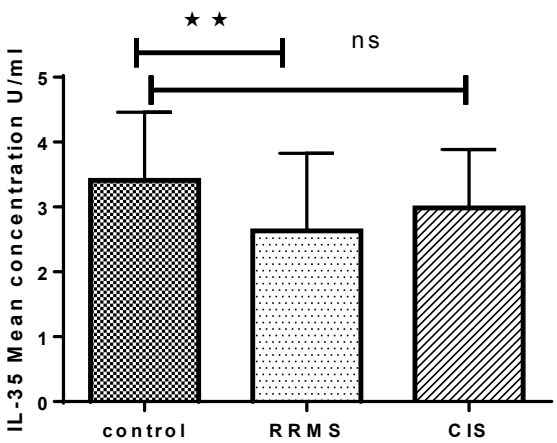

Fig. 1. *Comparison of serum IL-35 levels between RRMS, CIS and healthy controls. Significantly decreased level of IL-35 in RRMS patients compared to controls (**p < 0.01).*

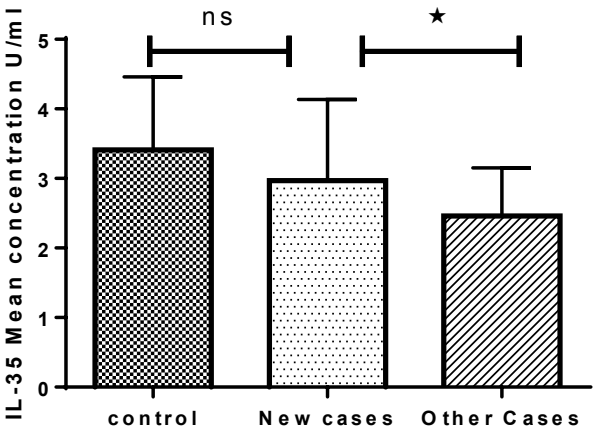

Fig. 2. *Comparison of serum IL-35 levels between MS new cases, healthy controls and other cases. Significantly decreased level of IL-35 in new cases compared to other cases (*p < 0.05). Also, decreased Il-35 serum levels was found in MS new cases compared to HC (p=0.059).*

in the same observations, both in male and female groups (Table I).

We compared IL-35 serum levels between new and older cases, new cases, healthy subjects, and patients receiving different MS medications (Table II). The mean serum level of IL-35 among new cases (2.96±1.16) (diagnosed within 6 months prior to the study) decreased compared to healthy controls (3.41±1.05) but it was not statistically significant (P=0.059).However, the mean serum level of IL-35 was significantly higher in new cases (2.96±1.16) compared with other cases (2.46±1.05)((p=0.048) (Fig. 2). There was no statistically significant correlation between serum levels of IL-35 with either EDSS (p=0.365) or duration of the disease (p=0.842).

DISCUSSION

In the present study, we found decreased serum levels of IL-35 among RRMS cases and new cases compared to healthy controls. These findings are in line with the protective role of IL-35 in autoimmune diseases proposed by previous studies. Contrarily, a study on rheumatoid arthritis (RA) patients showed higher levels of serum IL-35 in treatment naïve early RA patients compared to the control group (9). It would suggest that elevated levels of IL-35 in this condition may be due to a compensatory mechanism to reduce inflammation. Furthermore, Jafarzadeh et al. measured serum levels of IL-35 in 140 MS cases (51 untreated and 89 treated patients) and 140 healthy subjects, and reported higher IL-35 serum levels among treated MS patients compared to healthy individuals, while no statistically significant difference was found between untreated patients and the control group (6). However, higher levels of IL-35 in treated patients in their study may be related to the duration of the disease and the duration of the treatment.

Suppression of T cells by recombinant IL-35(rIL-35) suggests that IL-35 is needed for maximal activity of Treg cells. So decreased serum levels of IL-35 among new cases and RRMS cases in the present study may be related to dysfunction of Treg cells in MS patients. Also, the suppressor function of IL-35 producing regulatory B cells (Bregs) has been indicated in an animal model of MS (4, 5). Accordingly, treatment of mice with rIL-35 provided protection from ocular pathology in experimental autoimmune uveitis (EAU) by the expansion of i35-Bregs and Treg cells. Therefore, according to

Table I. *Comparison of interleukin-35 serum level between study groups and separated by gender.*

Category		Interleukin-35 serum level (U/mL)			P-value
		RRMS	CIS	Control	
All cases		2.63 (1.19)	2.98 (0.90)	3.41 (1.05)	**0.002**
Gender	Male	2.17 (0.39)	3.29 (1.11)	3.62 (1.25)	**0.019**
	Female	2.71 (1.27)	2.85 (0.78)	3.31 (0.96)	**0.008**

RRMS: relapsing-remitting multiple sclerosis; CIS: clinically isolated syndrome

Table II. *Comparison of serum levels of interleukin-35 between new cases, healthy subjects, and multiple sclerosis medications.*

Category New cases	Mean of Interleukin-35 level±SD(U/mL)	P-value
	2.97±1.17	**0.048**
Other cases	2.46±0.69	
New case	2.97±1.17	
Healthy controls	3.41±1.05	**0.059**
Receiving interferon-beta	2.51±0.70	
Receiving other disease modification therapies	3.59±1.43	**0.002**
Receiving methylprednisolone	2.95 ±1.12	
Not receiving methylprednisolone	2.38±0.76	**0.027**

the immunosuppressive nature of IL-35, we may conclude that theoretically, higher levels of IL-35 is associated with suppressed autoimmunity.

Receiving methylprednisolone resulted in higher IL-35 serum levels in the current study and a similar finding is reported in the clinical studies on MS patients (6). We observed lower serum levels of IL-35 following treatment with interferon-beta. In contrast, Jafarzadeh et al. found higher IL-35 serum levels in cases receiving interferon-beta and linked it to the therapeutic effect of interferon-beta (6). The possible mechanism of interferon-beta can be partly associated to increase in numbers or/and function of Treg cells (10, 11). However, Milosevic et al. found increased FoxP3 expression over 12 months in responder patients to interferon-beta therapy (12). Therefore, since the average duration of disease in MS patients in the present study was less than one year, the decrease in serum IL-35 level may be due to the duration of treatment with interferon-beta and/or lack of response in some patients to interferon-beta treatment.

Overall, our data further support an involvement of IL-35 in the pathogenesis of MS, however, further studies are needed to uncover the overall mechanisms that IL-35 exerts the regulatory function in MS patients.

ACKNOWLEDGEMENTS

We want to thank the vice-chancellor for Research and Technology of Isfahan University of Medical Sciences for funding this project (grant number: 195105).

REFERENCES

1. Ciccarelli O, Barkhof F, Bodini B, et al. Pathogenesis of multiple sclerosis: insights from molecular and metabolic imaging. Lancet Neurol 2014; 13(8):807-22.
2. Collison LW, Vignali DA. Interleukin-35: odd one out or part of the family? Immunol Rev 2008; 226(1):248-62.
3. Collison LW, Workman CJ, Kuo TT, et al. The inhibitory cytokine IL-35 contributes to regulatory T-cell function. Nature 2007; 450(7169):5666-9.
4. Shen P, Roch T, Lampropoulou V, et al. IL-35-producing B cells are critical regulators of immunity during autoimmune and infectious diseases. Nature 2014; 507(7492):366-70.
5. Collison LW, Chaturvedi V, Henderson AL, et al. IL-35-mediated induction of a potent regulatory T cell population. Nat Immunol 2010; 11(12):1093-101.
6. Jafarzadeh A, Jamali M, Mahdavi R, et al. Circulating levels of interleukin-35 in patients with multiple

sclerosis: evaluation of the influences of FOXP3 gene polymorphism and treatment program. J Mol Neurosci 2015; 55(4):891-97.
7. Lublin FD, Reingold SC, Cohen JA, et al. Defining the clinical course of multiple sclerosis The 2013 revisions. Neurology 2014; 83(3):278-86.
8. Ebrahimi M, Ganji A, Zahedi S, Nourbakhsh P, Ghasami K, Mosayebi G. Characterization of Regulatory T-Cells in Multiple Sclerosis Patients Treated with Interferon Beta-1a. CNS Neurol Disord Drug Targets 2018; 17(2):113-18.
9. Šenolt L, Šumová B, Jandová R, et al. Interleukin 35 synovial fluid levels are associated with disease activity of rheumatoid arthritis. PloS One 2015; 10(7):e0132674.
10. Manzoor F, Johnson MC, Li C, Samulski RJ, Wang B, Tisch R. beta-cell-specific IL-35 therapy suppresses ongoing autoimmune diabetes in NOD mice. Eur J Immunol 2017; 47(1):144-54.
11. Namdar A, Nikbin B, Ghabaee M, Bayati A, Izad M. Effect of IFN-beta therapy on the frequency and function of CD4(+)CD25(+) regulatory T cells and Foxp3 gene expression in relapsing-remitting multiple sclerosis (RRMS): a preliminary study. J Neuroimmunol 2010; 218(1-2):120-4.
12. Milosevic E, Dujmovic I, Markovic M, et al. Higher expression of IL-12Rbeta2 is associated with lower risk of relapse in relapsing-remitting multiple sclerosis patients on interferon-beta1b therapy during 3-year follow-up. J Neuroimmunol 2015; 287:64-70.

LETTER TO THE EDITOR

ASSOCIATION BETWEEN 5,10-METHYLENETETRAHYDROFOLATE, GENE POLYMORPHISM AND CONGENITAL HEART DISEASE

H-L. WANG[1,2], L. SUN[3], S. ZHOU[1,2] and F. WANG[1,2]

[1]Henan Provincial Research Institute for Population and Family Planning, Zhengzhou, China; [2]Key Laboratory of Birth Defects Prevention, National Health and Family Planning Commission, Zhengzhou, China; [3]Zhengzhou Central Hospital Affiliated to Zhengzhou University, The Centre of Translational Medicine, Zhengzhou, China

Received September 5, 2017 – Accepted June 7, 2018

This article is to investigate the association between C677T polymorphism of 5, 10-methylenetetrahydrofolate (MTHFR) gene and congenital heart defects (CHD). Two hundred thirty-five nuclear families (father, mother and child) with CHD were enrolled in the study (experimental group), and two hundred thirty-five healthy nuclear families were selected as a control group. Under the case-control study, the C677T polymorphism of MTHFR gene was detected with polymerase chain reaction-restriction fragment length polymorphism and DNA sequencing. The distribution of genotype frequency in the CHD group and control group were analyzed. SPSS 13.0 software was used to analyze the data. The distribution of genotype frequency at C677T polymorphism site was significantly different between the CHD group (including ventricular septal defect, atrial septal defect, tetralogy of fallot, double outlet right ventricle, patent ductus arteriosus) (child and mother) and healthy control group (child and mother). There were no differences between CHD group-fathers and healthy control group-fathers. Analyses of the MTHFR genotypes of CHD nuclear family data with transmitted disequilibrium test (TDT) and haplotype-based haplotype relative risk statistical method both revealed significant indications that the parents transmitted more T allele of MTHFR to their CHD children. TT genotype of MTHFR gene is associated with CHD, and a mother or a child with T allele has a much higher risk of CHD.

To the Editor,

Congenital heart defects (CHD) are the most common structural birth defects, affecting approximately 8-10 of every 1,000 live births. The aetiology of non-syndromic CHD is complex, involving both genetic, epigenetic, and environmental risk factors. Periconceptional exposure to folic acid and multivitamins containing folic acid may modulate the maternal risk of CHD-affected pregnancy. In China, CHDs represent the third cause of death in children under one year of age. It is widely accepted that the impact of folic acid intake on pregnancy outcome is modified by variants in both maternal and fetal genes that code for critical enzymes in the folate and homocysteine pathways (1-2). The methylenetetrahydrofolate reductase (MTHFR, NM 005957) gene encodes for the enzyme that catalyses the conversion of 5, 10-methylenetetrahydrofolate to 5-methyltetrahydrofolate. Two single nucleotide polymorphisms (SNPs) in MTHFR, 677C-T (rs1801133) and 1298A-C (rs1801131), are associated with decreased enzyme activity. This

Key words:5,10-Methylenetetrahydrofolate (MTHFR), gene polymorphism, congenital heart disease

Mailing address:
Dr. Shiyuan Zhou,
No. 5, Jingwu Road, Jinshui District, Henan Provincial Research Institute for Population and Family Planning, Zhengzhou City 450002, Henan Province, PR China
Tel.: +86 0371 55095
e-mail: zhanjiay163@163.com

0393-974X (2018)

study conducted a case-parent analysis of children with CHD and their parents, ascertained through a population-based birth defect registry. The present study examined the independent and interactive impact of the maternal and fetal MHTFR 677C-T SNPs and their haplotypes on the risk of CHD.

MATERIALS AND METHODS

Two hundred thirty-five nuclear families with CHD and 277 healthy nuclear families were selected from the Children's Hospital of Zhengzhou City (Zhengzhou, Henan Province, China). The study was approved by the Ethics Committee of the Hospital. All the subjects were adequately informed of the study, and voluntarily signed consent to participate. In cases of children of deceased parents, informed written consent was given by the family or guardian. All patients had isolated anomalies. No cross-over lesions were found. In all cases, diagnoses were confirmed by standard imaging procedures (color-coded echocardiography, heart catheterization). Both groups were identified consecutively, and no other factors were used in their selection.

MTHFR gene detection

Three mL of peripheral blood was placed in a tube with ethylene diamine tetraacetic acid. DNA extraction was performed using saturated phenol. The quantity and purity of DNA were verified by spectrophotometry and gel electrophoresis on 1% agarose stained with SYBR Gold (Invitrogen). Fifty nanograms of DNA was used for polymerase chain reaction (PCR), and subsequently, enzymatic digestion of the PCR product was separated by electrophoresis on a 3% agarose gel.

PCR was adopted to detect the MTHFR genotype. The study was carried out to identify the presence of 677C-T mutation as described by Frosst et al. (3). Agarose gel electrophoresis was utilized to detect the genotypes. The mutation 677C-T created a Hinf1 recognition sequence, and the product was digested into 175 bp and 23 bp fragments. The products of restriction digestion were separated on a 3% agarose gel and visualized by SYBR Gold staining. Genotypes of all individuals were noted as CC: 198 bp; CT: 198 bp, 175 bp, 23 bp; and TT: 175 bp, 23 bp. The PCR products were separated by 1% agarose gel electrophoresis and the polymorphism fragments were purified with the Wizard PCR Min-Prep Kit (Promega) and Protocol-SK131(Sangon, Shanghai, China).

Statistical analysis

CHD nuclear families and healthy nuclear families were tested independently for Hardy-Weinberg (HW) equilibrium using the exact test implemented in Stata's GENHW command. Data were analyzed using Hardy-Weinberg distribution for all genotypes and alleles (4-7). Comparisons between groups were performed using Student's *t*-test for continuous variables and χ^2 for categorical variables. Results were presented as odds ratio (OR) with 95% confidence interval (95% CI), and $p<0.05$ was considered statistically significant.

The transmission disequilibrium test (TDT) was used to test for allelic associations resulting from linkage disequilibrium between a CHD punitive disease locus and the C677T polymorphisms and also to test for the parent of origin effects. Because the TDT was invalid when data from ambiguous parent-child dyads were excluded, only unambiguous parent-child dyads are included. The TDT tests were carried out using the exact TDT implemented in the Stata program SYMMETRY.

RESULTS

Restriction analysis and sequencing

The substitution created a HinfI recognition sequence which digested the 198 bp fragment into 175 and 23 bp fragments; the latter fragment had been run off the gel. All three possible genotypes are shown in Fig. 1. Sequencing results are in Fig. 2.

Hardy-Weinberg genetic balance test

Two hundred seventy-seven healthy nuclear families were eligible for the study, MTHFR gene 677 site genotype was in agreement with the test of Hardy-Weinberg balance (HWE; $P>0.05$) (Table I).

Genotype frequencies

The control group was composed of 277 normal nuclear families, and the experimental group of 235 nuclear families (fathers, mothers and children) with CHD. In the experimental group there were 128 cases of ventricular septal defect (VSD), 34 of atrial septal defect (ASD), 36 of tetralogy of Fallot (TOF), 20 of double outlet of right ventrical (DORV), and 17 of patent ductus arteriosus (PDA). According to the statistical analysis, the 677 TT genotype frequencies

of the five MTHFR genes (VSD 43%, ASD 44%, TOF 44%, DORV 70%, PDA64%, respectively) in the experimental group were higher than those in control group (24.0%)($P<0.05$) (8). The frequencies of each allele, individual genotype, and combined genotype, assuming either a dominant or recessive mode of inheritance for CHD cases and their parents, are presented in Table II.

The statistical analysis showed no significant difference between experimental group and control group mothers for MTHFR gene CT genotype, the TT genotype frequencies of MTHFR gene (in addition to ASD) in the experimental group mothers was higher than those in the control group, and in the experimental group mothers, the frequency of TT genotype was significant higher than CC genotype (Table III).

In this case-control study, parents' chromosome allele transfer to CHD patients for cases, and extragenetic allele of CHD for comparison; Table IV shows that the transmission of 677T allele from heterozygous case parents to CHD affected offspring. There was on evidence of distortion of the 677T allele in the informative transmissions.

DISCUSSION

The 677 TT genotype of MTHFR gene in chidren with structural CHD has an impact on the embryonic development of commonly observed congenital malformations such as neural tube defects or oral clefts (9). Consistent with this hypothesis, the frequency of TT variant is significantly higher in children with CHD (18.4%) than in healthy controls (9.2%). The frequency of the homozygous

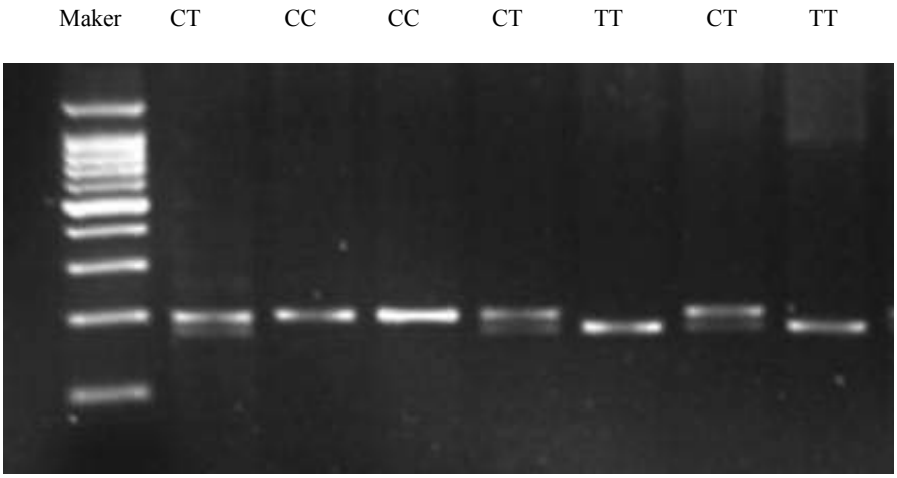

Fig. 1. *Sequence change and restriction enzyme analysis for the alanine to valine substitution. Wild type CC-/-, homozygous mutant TT+/+, heterozygous type CT+/-.*

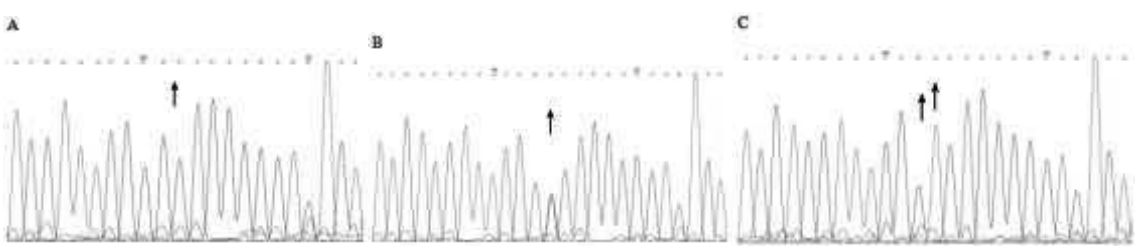

Fig. 2. *The result of MTHFR C677T gene sequence.* ***A)*** *CC genotype;* ***B)*** *CT genotype;* ***C)*** *TT genotype.*

Table I. *Statistical test for H-W equilibrium in the control group.*

	Genotype				
	CC	CT	TT	x^2	P
observed value	88	126	63	1.21	0.17
expected value	82.3	137.4	57.3		

Table II. *Allelic distribution and genotype of the 677C-T polymorphism of the MTHFR gene in cases and controls.*

		Gene frequency (%)					
		CC	**CT**	**TT**	χ^2	***P***	**OR(95%CI)**
Children	control	88	126	63			
	VSD	17	56	55	17.34	0.00003	2.559（1.954~4.111）
	ASD	5	14	15	7.36	0.006	2.682（1.212~5.917）
	TOF	6	14	16	7.95	0.005	2.717（1.254~5.876）
	DORV	2	4	14	20.02	0.0000	7.926（2.702~24.248）
	PDA	2	4	11	13.85	0.0001	6.288（2.027~19.821）
Mother	control	82	129	66			
	VSD	19	58	51	10.93	0.0009	2.117（1.318~3.401）
	ASD	10	14	10	0.51	0.47	1.332（0.562~3.104）
	TOF	3	18	15	5.29	0.02	2.284（1.049~4.949）
	DORV	3	5	12	12.60	0.0004	4.795（1.733~13.504）
	PDA	4	5	8	4.59	0.03	2.842（0.952~8.438）
Father	control	79	136	62			
	VSD	38	60	30	2.51	0.11	1.066（0.629~1.803）
	ASD	12	13	9	0.25	0.62	1.254（0.513~2.999）
	TOF	10	16	10	0.52	0.47	1.340（0.568~3.101）
	DORV	6	6	8	3.21	0.07	2.323（0.824~6.447）
	PDA	5	6	4	0.15	0.70	1.267（0.327~4.511）

TT genotype in healthy controls is no different from data recently published, and which represents the prevalence in the German population Subgroup analysis. Our data revealed the highest prevalence of the TT genotype in patients with pulmonary valve stenosis, hypoplastic left heart syndrome, coarctation of the aorta, and aortic valve stenosis/subaortic stenosis (38-67%). It has been shown by other authors that periconceptional multivitamin administration could reduce the risk of conotruncal heart defects such as transposition of the great arteries or tetralogy of Fallot. However, the absolute number of patients investigated in subgroups of specific cardiac lesions is rather small, so that

Table III. *The comparison of mother MTHFR genotype.*

	gene frequency (%)				
	CC	CT	TT	x^2	P
control	82	129	66		
VSD	19	58	51	0.06	0.81
ASD	10	14	10	0.35	0.55
TOF	3	18	15	0.15	0.70
DORV	3	5	12	3.5	0.06
PDA	4	5	8	1.9	0.17

Table IV. *The TDT comparison of CHD nuclear families.*

CHD parents not genetic equilibrium allele frequency	CHD parents genetic equilibrium allele frequency		
	C	T	total
C	78	129	207
T	89	174	263

a definitive statement concerning the benefit of multivitamin administration for a specific genotype and in particular CHD cannot be given at the moment (10). These results show a possible association between genotype 677T/T of the MTHFR gene in Chinese women with the presence of complex CHD in their offspring. This finding is significant for approximately 2,800 children born with CHD each year in China, and early identification of risk groups helps to decrease the complications that often occur in these patients.

In conclusion, the data suggest that the MTHFR 677TT genotype in the embryo is significantly associated with the development of structural congenital heart malformation during early pregnancy. It remains to be clarified whether this genotype is at least a risk marker or a risk factor for structural congenital heart malformations (11-12). Moreover, further studies are required to clarify whether genotype-specific periconceptional use of folate supplementation reduces the rate of specific structural CHD.

REFERENCES

1. Christianson A, Howson CP, Modell B. March of Dimes Global Report on Birth Defects 2006.
2. Vinukonda, G. Plasma homocysteine and methylenetetrahydrofolate reductase gene polymorphism in human health and disease: An update Int J Hum Genet 2008; 8(1):171-79.
3. Frosst P, Blom HJ, Milos R. A candidiate genetic risk factor for vascular disease: a common mutation methylenetetra-hydrofolate reductase. Nat Genet 1995; 10:111-13.
4. Rosenousit TH, Ratashak SA, Selhub J. Homocysteineinduces congenital defects of the heart and neural tube: effect of folic acid. Proe Natl Acad Sci 1996; 93(26):15227-32.
5. Verldeij-Hagoort A, Bliek J, Sayed-Tabatabaei

F, Ursem N, Steegers E, Steegers-Theunissen R.. Hyperhomocysteinemia and MTHFR polymorphisms in association with orofacial clefts and congenital heart defects: A meta-analysis Am J Med Genet A 2007; 143A(9):952-60.

6. García-Fragoso L, García-García I, Leavitt G, Renta J, Ayala MA, Cadilla CL. MTHFR polymorphisms in Puerto Rican children with isolated congenital heart disease and their mothers. Int J Genet Mol Biol 2010; 2(3):43-47.
7. Zhu WL, Li Y, Yan L, Dao J, Li S. Maternal and offspring MTHFR gene C677T polymorphism as predictors of congenital atrial septal defect and patent ductus arteriosus Molr Hum Reprod 2006; 12(1):51-54.
8. Lee CN, Su YN, Cheng WF, Lin MT, Wang JK, Wu MH, Hsieh FJ. Association of the C677T methylenetetrahydrofolate reductase mutation with congenital heart diseases. Acta Obstet Gynecol Scand 2005; 84(12):1134-40.
9. van Beynum IM, Kapusta L, den Heijer M, Vermeulen SH, Kouwenberg M, Daniëls O, Blom HJ. Maternal MTHFR 677C>T is a risk factor for congenital heart defects: effect modification by periconceptional folate supplementation. Eur Heart J 2006; 27(8):981-87.
10. Lonescu-lttu R, Marelli AJ, Mackie AS, et al. Prevalence of severe congenital heart disease after folic acid fortification of grain products: time trend analysis in Quebec. BMJ 2009; 338:b1673.
11. Wenstrom K, Johanning G, Johnson K, DuBard M. Association of the C677T methyIenetetrahydrofoIate reductase mutation and eIevated homocysteine IeveIs with congenitaI cardiac maIformations. Am J Obstet GynecoI 2001; 184:806-17.
12. Junker R, Kotthoff S, Vielhaber H, et al. Infant methyIenetetrahydrofoIate reductase 677TT genotype is a risk factor for congenitaI heart disease. Cardiovasc Res 2001; 5:251-54.

JOURNAL OF BIOLOGICAL REGULATORS & HOMEOSTATIC AGENTS Vol. 32, no. 5, 1261-1265 (2018)

LETTER TO THE EDITOR

INFLUENCE OF CIRCADIAN RHYTHM ON EXHALED BREATH PROFILING BY ELECTRONIC NOSE

V. LIOTINO[1], S. DRAGONIERI[1], V.N. QUARANTA[2], P. CARRATU[1], T. RANIERI[1] and O. RESTA[1]

[1]Respiratory Diseases, University of Bari, Italy; [2]Pulmonology, Ospedale Di Venere, Bari, Italy

Received May 31, 2018 – Accepted June 20, 2018

Electronic noses (e-noses) are a cheap and easy method for exhaled Volatile Organic Compound (VOC)-analysis which has shown its potential in several diseases. Before obtaining a full validation of these instruments in clinical settings, a number of methodological issues still have to be established. We aimed to investigate a potential influence of circadian variation on VOC-profile analyzed by an e-nose in healthy subjects. We enrolled 22 adults free of any known diseases. A sequence of exhaled breath samplings were performed on all participants at predetermined hours (7am, 12pm, 17pm, 23pm) and analyzed by an e-nose (Cyranose 320). According to Principal Component Analysis, significant circadian variations of the exhaled VOC-profile were shown for Principal Component (PC) 1 and 3. In detail, PC1 and PC3 values were significantly higher in the morning compared to the afternoon and evening (for all parameters $p<0.05$). Successive Linear Discriminant analysis confirmed the findings above. The daily variations in VOCs-profile, with the peak in the morning, could be relevant for future clinical applications, especially in the choice of optimal time for sampling patients.

To the Editor,

Over 3,000 endogenous and exogenous volatile organic compounds (VOCs) are emitted during each breath (1). Since the level of endogenous VOCs can be altered by any inflammatory and/or impaired metabolic processes, their potential use as biomarkers for clinical purposes has been suggested in recent years (1).

The measurement of the exhaled breath Volatile Organic Compounds (VOC)-profile by electronic nose (e-nose) has been proposed as a promising tool in the diagnosis and monitoring of several respiratory diseases due to its non-invasiveness, cost-effectiveness and ease of use (2). In particular, various investigations have shown the potential for applying exhaled VOCs-profiling in lung cancer, respiratory infections, and obstructive lung diseases (2). When performing this type of analysis, it is essential to identify and correct any possible source of signal interference, as being potentially confounding factors (i.e. hypoxia, smoke and comorbidities) (3-4).

Although a European Respiratory Society task force has recently established, recommendations for VOC-analysis concerning standardization of sampling, analyzing and data reporting, a complete validation is still lacking in order to reach clinical practice. Among the internal variables, human biorhythm is one of the as-yet unstudied factors that may affect exhaled VOC-composition.

It is well known that human physiology is

Key words: exhaled breath, volatile organic compounds, electronic nose, circadian rhythm

Mailing address:
Dr Silvano Dragonieri,
Department of Respiratory Diseases,
University of Bari, Piazza Giulio Cesare 11,
70124 Bari, Italy
Tel.: +39 0805593215
e-mail: silvano.dragonieri@uniba.it

0393-974X (2018)

profoundly modulated by the circadian biological clock synchronized with time of day (5) and its alteration leads to important consequences for human health and disease (5).

For the above reason, in the current study we aimed to investigate the likely circadian variations of exhaled VOC-profile in healthy adults analyzed by an e-nose.

MATERIALS AND METHODS

A total number of 22 healthy, never-smoking, with a negative anamnesis of chest symptoms and any known diseases (e.g. respiratory disorders, diabetes mellitus, neurological dysfunctions, cardiac impairments, renal diseases, autoimmune conditions and all neoplasms) were included in the study. Age range was 25-62 years. All the participants were volunteers and were enrolled from hospital members. A sequence of exhaled breath measurements were performed on all individuals at predetermined hours (7am, 12pm, 17pm, 23pm). None of the subjects reported upper or lower respiratory tract infection in the four weeks before sampling. Lung function was obtained for all individuals. Subject characteristics are described in Table I.

The local Ethics Committee had previously approved the study (protocol number 46403/15) and an informed consent form was signed by all participants.

Table I. *Clinical characteristics of the study population.*

	Total cohort
Subjects (n.)	22
Mean age (y.)	40.1±13.8
Sex M\F (n.)	10\12
BMI (kg/m2)	24.8±3.7
FEV1%pred.	101.3±3.6
FVC%pred.	100.4±8.8
(ex)-smokers(n.)	0
comorbidities(n.)	0

Values are intended as mean±SD

Study design

We performed a longitudinal study. The measurements were performed at four separate visits within one day, based on predefined hours. Participants could not eat or drink (except water) in the 2 hours before the tests, or perform vigorous physical activity. Exhaled breath was collected and closely analyzed by the e-nose.

Electronic nose

A Cyranose 320 (Sensigent, USA) was used for breath profiling. It is based on a nano-composite set of 32 organic polymer sensors. The polymers swell when are exposed to VOCs mixtures, leading to an increase of electrical resistance. Operating parameters were the following: Sampling time: 60'', purging time 200'', temperature 42°C.

Lung function testing

A lung function technician performed flow-volume spirometry (MasterscreenPneumo, Jaeger, Wurzburg, Germany) on all participants during a separate visit. Forced expiratory volume in one second (FEV1) and forced vital capacity (FVC) were collected.

Exhaled breath collection.

Measurements were performed always in the same room with stable temperature and humidity rate. By wearing a nose-clip, all subjects performed 5 min tidal volume wash-in through a two-way non-rebreathing valve (Hans Rudolph 2700, USA). An inspiratory A2 VOC-filter (North Safety, Netherlands) capable of filtering over 99% of environmental VOCs was connected to the valve. Afterwards, subjects were asked to exhale one vital capacity volume into an inert bag (Tedlar). Finally, the filled bag was sampled by the e-nose within 5 min from collection.

Statistical analysis

Statistical calculations were performed by SPSS 16.0 (SPSS Inc., Chicago, USA). Initially, principal component analysis (PCA) was performed in order to reduce raw data based on sensor responses. Principal components (PCs) were set based on their initial Eigen values and the top 3 (PC1, PC2 and PC3) were selected for further investigations. Repeated-measures ANOVA on principal

components was applied to examine whether circadian rhythm could modify the breathprints of our population. Least significant difference (LSD) was used as post hoc test. Furthermore, we used linear canonical discriminant analysis to classify cases into categorical divisions and the cross-validated accuracy percentage (CVA, %) was calculated with the "leave-one-out method" for internal validation.

Pearson correlation, multivariate linear and logistic regression were used to assess relations between PC1, PC3 and clinical parameters.

We estimated our sample size according to earlier investigations (6). In detail, we based sample size by limiting the standard error lower than 10%. If we consider 80% accuracy, our sample size was sufficient for the current study. Finally, we considered as statistically significant a p value <0.05.

RESULTS

By performing PCA, we selected the following principal components: PC1 (81.9% of the total variance), PC2 (10.2% of the total variance) and PC3 (2.3% of the total variance). ANOVA was performed on the aforementioned PCs. We observed significant modifications of the exhaled VOC-spectrum over the circadian rhythm for PC1 and PC3 ($p<0.05$ for both). In detail, PC1 value was higher during morning time and noon compared to the afternoon (for all parameters $p<0.05$, Fig. 1). By observing analysis on PC3, a significant increase was shown in morning time compared to noon and evening time (for all parameters $p<0.05$, Fig. 1). Analysis on PC2 did not reach the statistical significance. These findings were reflected when performing subsequent linear

Table II. *Discriminant analysis with cross-validated valuesamong all hours of measurement.*

	7am *vs* 12pm	7am *vs* 17pm	7am *vs* 23pm	12pm *vs* 17pm	12pm *vs* 23pm	17pm *vs* 23pm
Cross-Validated Value	56.8	63.6*	62.4*	65.9*	52.3	56.8

**p<0.05*

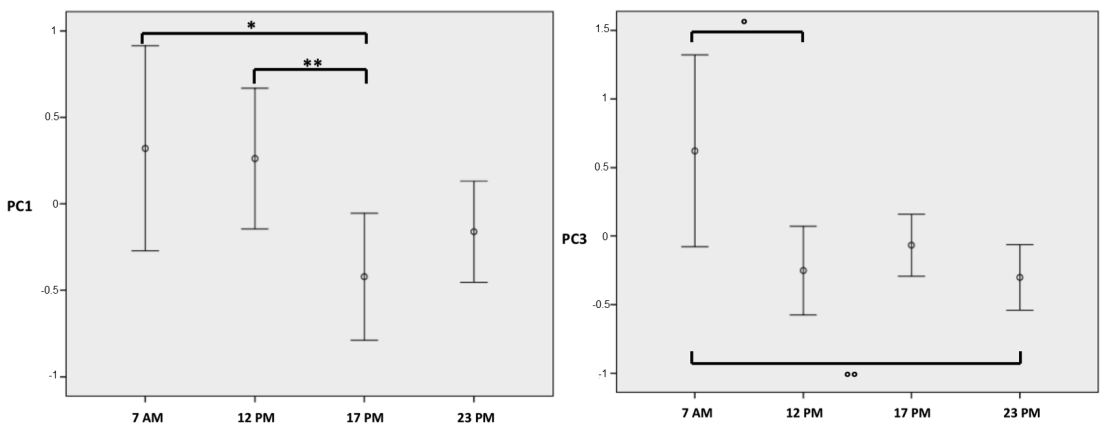

Fig. 1. *Changes of Principal Component 1 (left) and 3 (right) in relation to circadian rhythm. Data are expressed as mean ± SD. *7am vs 12pm, p=0.033 ; ** 12pm vs 17pm, p=0.013; ° 7am vs 12pm, p=0.023 ; °° 7am vs 17pm, p=0.013*

discriminant analysis (Table II).

We performed Pearson correlation, multivariate linear and logistic regression, showing no relationship between PC1, PC3 and any of the following parameters: FEV1, BMI, age and gender (p = ns).

DISCUSSION

To our knowledge, this is the first investigation specifically addressed on e-nose exhaled biomarkers in relation to circadian variations in a carefully checked healthy population.

A significant circadian rhythm was previously reported on exhaled nitric oxide (eNO) (7-8). In particular, Antosova et al. observed a peak of eNO at 10am and detected the lowest value at 10pm (7). Moreover, Mattes et al. showed a decrease in eNO levels at 10pm with an increase after 1am, peaking at 7am (8). Another study by Olopade et al. reported overnight elevation in FENO in healthy volunteers (9). Diurnal variability has also been shown for exhaled breath condensate hydrogen peroxide levels in healthy subjects and patients with chronic obstructive pulmonary disease (COPD) (10). Moreover, Carpagnano et al. analyzed the effect of circadian rhythms on Exhaled Breath Temperature measurements, demonstrating significant differences between 08.00 and 12.00am and between 4.00 and 8.00pm (11). Regarding exhaled VOCs, specific daily-patterns of ammonia in breath were detected (12). Interestingly, King et al. showed significant variations in acetone and isoprene (13) during sleep. Furthermore, by real-time breath metabolomics, Martinez-Lozano et al. showed up to 50 features with significant circadian variations in the breath of all individuals (14). By using our same e-nose, Kunos et al. analyzed overnight changes and found no difference between the evening and following morning VOC levels in healthy subjects (15). Additionally, as a secondary aim, other authors have investigated the within-day variability of the data in disease and in health (6, 15-17), showing reproducible results.

We must disclose several limitations of our study. First, we chose the sampling hours arbitrarily and we do not have measurements from 23pm to 7am and therefore may have missed important information. Further investigations should also include "after-midnight" sampling. Second, 22 subjects is a relatively small sample size, although being adequate in our pilot investigation, warranting further larger studies also including an external group of validation.

Third, it is well known that e-noses do not identify specific VOCs. In order to do so, future investigations should be accompanied by Gas Chromatography and Mass Spectrometry (GC-MS) or other chemical analytical procedures. Fourth, we did not register subjects' meals among measurements and we are aware that this may have influenced our data. Fifth, our study lacks multiple inter-day measurements at the same time intervals. Further studies are warranted in order to eliminate the measure bias due to circadian changes in VOC concentrations.

According to our results, we observed an increase of PC1 and PC3 in morning time compared to other hours of the day. This is in line with previous reports with nitric oxide (7-8), suggesting a different metabolic activity during daybreak hours. By a pure data observation, we may hypothesize that PC1 and PC3 trend is similar to that of cortisol, whose levels build up overnight to reach a peak in the morning and then decline slowly throughout the day. Specific investigations are required to reveal the mechanisms behind the above, which are still unknown to date.

Based on the present results we can conclude that the circadian variation in VOCs-mixtures may be important for diagnosis and monitoring of patients with several respiratory diseases and their controls. It appears to be warranted to select the optimal time for e-nose measurements and perhaps to maintain the same time during all the monitoring procedures.

ACKNOWLEDGEMENTS

This study was entirely financed by the University of Bari.

REFERENCES

1. Blanchet L, Smolinska A, Baranska A, et al. Factors

that influence the volatile organic compound content in human breath J Breath Res 2017; 11:016013.
2. Bikov A, Lázár Z, Horvath I. Established methodological issues in electronic nose research: how far are we from using these instruments in clinical settings of breath analysis? J Breath Res 2015; 9:034001.
3. Scarlata S, Pennazza G, Santonico M. Screening of obstructive sleep apnea syndrome by electronic-nose analysis of volatile organic compounds. Sci Rep 2017; 7:11938.
4. Antonelli Incalzi R, Pennazza G, Scarlata S. Comorbidity modulates non invasive ventilation-induced changes in breath print of obstructive sleep apnea syndrome patients. Sleep Breath 2015; 19:623-30.
5. Foster RG, Roenneberg T. Human responses to the geophysical daily, annual and lunar cycles. Curr Biol 2008; 18:R784-794.
6. Dragonieri S, Schot R, Mertens BJ, et al. An electronic nose in the discrimination of patients with asthma and controls. J Allergy Clin Immunol 2007; 120:856-62.
7. Antosova M, Bencova A, Psenkova A, Herle D, Rozborilova E. Exhaled nitric oxide - circadian variations in healthy subjects. Eur J Med Res 2009; 14:6-8.
8. Mattes J, Storm van's Gravesande K, Moeller C, Moseler M, Brandis M, Kuehr J. Circadian variation of exhaled nitric oxide and urinary eosinophil protein X in asthmatic and healthy children. Pediatr Res 2002; 51:190-94.
9. Olopade CO, Christon JA, Zakkar M, Hua C, Swedler WI, Scheff PA, Rubinstein I. Exhaled pentane and nitric oxide levels in patients with obstructive sleep apnea. Chest 1997; 111:1500-504.
10. van Beurden WJ, Dekhuijzen PN, Harff GA, Smeenk FW. Variability of exhaled hydrogen peroxide in stable COPD patients and matched healthy controls. Respiration 2002; 69:211-16.
11. Carpagnano GE, Lacedonia D, Malerba M, Martinelli D, Cotugno G, Foschino-Barbaro MP. Exhaled breath temperature measurement: influence of circadian rhythm. J Biol Regul Homeost Agents 2017; 31:229-35.
12. Lovettam, Reid NM, Buckley JA, French JB, Cameron DM. Real-time analysis of breath using an atmospheric pressure ionization mass spectrometer. Biomedical Mass Spectrometry 1979; 6:91-97.
13. King J, Kupferthaler A, Frauscher B, et al. Measurement of endogenous acetone and isoprene in exhaled breath during sleep. Physiol Meas 2012; 33:413-28.
14. Martinez-Lozano Sinues P, Tarokh L, Li X, Kohler M, Brown SA, Zenobi R, Dallmann R. Circadian variation of the human metabolome captured by real-time breath analysis. PLoS One 2014; 9:e114422.
15. Kunos L, Bikov A, Lazar Z, Korosi BZ, Benedek P, Losonczy G, Horvath I. Evening and morning exhaled volatile compound patterns are different in obstructive sleep apnoea assessed with electronic nose. Sleep Breath 2015; 19:247-53.
16. Bikov A, Pako J, Kovacs D, et al. Exhaled breath volatile alterations in pregnancy assessed with electronic nose. Biomarkers 2011; 16:476-84.
17. Tarnoki DL, Bikov A, Tarnoki AD, et al. Lack of heritability of exhaled volatile compound pattern: an electronic nose twin study. J Breath Res 2014; 8(1):016001.

JOURNAL OF BIOLOGICAL REGULATORS & HOMEOSTATIC AGENTS Vol. 32, no. 5, 1267-1273 (2018)

LETTER TO THE EDITOR

INTERNAL NASAL DILATATOR (NAS-AIR®) IN PATIENTS WHO SNORE

M. GELARDI[1], G. PORRO[1], B. STERLICCHIO[1], N. QUARANTA[1], G. CIPRANDI[2]
and the ITALIAN STUDY GROUP ON SNORING

[1]Otolaryngology, Department of Basic Medical Science, Neuroscience and Sensory Organs, University of Bari Aldo Moro, Bari, Italy; [2]Ospedale Policlinico San Martino, Genoa, Italy; Italian Study Group on Snoring: T. Candreva, G. Ciancio, A. Ciofalo, M. Colucci, M. Curatolo, A. Guglielmi, L. Ianuzzi, P. Intiglietta, M. Landi, C. Lingua, P. Mola, M. Notargiacomo, P. Pecoraro, G. Pellittieri, L. Pintaldi, M. Tomaiuolo, S. Zizzi

Received March 29, 2018 – Accepted July 2, 2018

Snoring is a very common human habit, and for this reason it is considered more a social nuisance that a disease symptom. The nasal valve area has the minimal cross-sectional area of the upper airways. A problem at this level may easily induce impaired breathing and consequently snoring, therefore nasal dilation might significantly improve this complaint. Nas-Air® is a new internal nasal dilator which was tested on 41 outpatients who snore. Snoring duration, assessed by smartphone, visual analogue scale for the perception of sleep quality were measured before and during Nas-Air® use. A significant reduction of snoring time and an improvement of sleep quality were achieved during Nas-Air® wearing. In conclusion, the present study demonstrates that Nas-Air® is an internal nasal dilator able to reduce snoring time and improve sleep quality.

To the Editor,

Snoring is the most common human habit, and for this reason it is considered more a social nuisance that a disease symptom (1). In fact, snoring prevalence is very high and increases with increasing age. In young adults, snoring affects from 5% of females to 20% of males; in elderly people, snoring affects from 40% of females and 60% of males. Moreover, the relevance of nasal obstruction in modifying breathing during sleep as well as daytime behaviour is very old. Since the XIX century, it has been reported that nasal obstruction is associated with disturbed sleep, insomnia, and intellect and memory impairment. In the nose, there is about half of the total respiratory resistance to airflow passage. A direct relationship exists between increased nasal resistance, due to nasal obstruction, and obstructive sleep breathing. In this regard, the nasal valve area has the minimal cross-sectional surface.

Sleep-disordered breathing can be divided into simple snorer, sleep apnea syndrome, and upper airway resistance syndrome.

The pathogenic mechanisms for snoring occurrence are characterized by high-frequency oscillations of the soft palate as well as the pharyngeal walls, epiglottis, and tongue. These oscillations alternately occlude and open a narrowed airway. Even though the nose is not the site of sound generation, there is evidence implicating nasal obstruction as a causative factor in breathing disturbances during sleep. Other reports have shown that increasing nasal patency improves snoring (1, 6).

Key words: snoring, nasal valve, obstruction, internal nasal dilator, Nas-Air®

Mailing address:
Giorgio Ciprandi, MD
Largo R. Benzi 10,
16132 Genoa, Italy
Tel.: +39 10 35338120
Fax: +39 10 3538664
e-mail gio.cip@libero.it

0393-974X (2018)

DISCLOSURE: ALL AUTHORS REPORT NO CONFLICTS OF INTEREST RELEVANT TO THIS ARTICLE.

The internal nasal valve, the narrowest portion of the nasal cavity, is formed by the junction of the upper lateral cartilages with the nasal septum. The normal angle between these 2 structures ranges between 10° and 15°. The nasal valve offers the greatest resistance to nasal airflow. The narrower the site, the more vulnerable it is to pathologic nasal obstruction. The most important and common reasons for nasal obstruction are due to nasal valve abnormalities which may result from either dynamic or static problems. Despite these facts, nasal valve collapse is a frequently overlooked cause of nasal obstruction. In particular, the normal airflow through the nasal valve depends on the Bernoulli principle and Poiseuille law. The Bernoulli principle states that as the flow of air increases through a fixed space, the pressure in that space decreases. If the decrease in pressure overcomes the inherent rigidity of the flexible nasal sidewall, collapse can occur, resulting in obstruction. Clinically, the collapse of the nasal sidewall during inspiration is termed dynamic obstruction. Pouseille law states that the flow is inversely proportional to the fourth power of the radius, which means that small decreases in the radius of a space have dramatic impacts on the flow of air through the nose. In the clinical setting, an anatomically narrowed portion of the nasal valve is defined as a static obstruction.

The management of snoring includes careful evaluation and correction of upper airway obstruction. Septoplasty alone or associated with lateral osteotomies did not increase nasal air flow, but correction of a narrowed nasal valve created a 2.5-fold reduction in nasal respiratory resistance (2). Even in the presence of septal deviation, the airflow may be improved with repair of an obstructing nasal valve. Therefore, it has become evident that the evaluation and correction of the collapsed nasal valve in a patient with nasal obstruction is essential. The therapeutic modalities that increase the nasal valve area and strengthen the lateral wall of the nose help to improve nasal patency. A number of surgical techniques have been described to increase the nasal valve area. The most frequently used method involves the use of spreader grafts. However, a potential alternative to surgical procedures may be represented by the mechanical nasal alar dilators. The nasal dilators can be classified as external and internal (3). Many studies have explored the possibility of relieving snoring by wearing these dilators.

For the aforementioned reasons, we aimed to investigate whether a new internal nasal dilator (Nas-Air®) may be able to reduce snoring in a group of outpatients.

MATERIALS AND METHODS

The present study was designed as open and recruited a group of 41 outpatients who snore. It was conducted in a real-world setting, such as otolaryngologist clinics.

Inclusion criteria were adult age and snoring history in the past month. Exclusion criteria were: anatomical clinically relevant problems (e.g. very severe septal deviation and/or turbinate hypertrophy, such as grade IV), obstructive sleep apnea syndrome, disorders and current medication potentially able to interfere with the findings.

The outpatients underwent otolaryngologist examination, including anterior rhinoscopy. The Nas-Air® was given with appropriate instruction for its use. Briefly, this internal nasal dilator should be applied into the nose at bedtime. All patients gave informed, signed consent to participate in the study.

Snoring assessment was performed by the app "Do I Snore®" using a smartphone and recorded at home during the sleep. This app measures the time of snoring during sleeping. Patients were instructed to measure snoring the first 2 nights (without Nas-Air®) and the further 2 nights (with Nas-Air®).

During the otolaryngological visit, the following parameters were considered: age, gender, body mass index (BMI), Nasal Valve Obstruction, according to validated criteria (4), turbinate size, septal deviation, tonsil size. Turbinate and tonsil size were assessed by ranging from 0 (= normal size) to 4 (= maximal size) according to validated criteria (5).

Subjective parameters were evaluated by the patients at baseline, such as before using Nas-Air®. They include nasal obstruction, sleep quality, and olfaction; they were measured by a visual analogue scale (VAS). VAS score for nasal obstruction ranged from 0 (= completely blocked nose) to 10 (= completely patent nose); VAS score for

olfaction ranged from 0 (= no smell) to 10 (= optimal smell); VAS score for quality of sleep ranged from 0 (= worst sleeping) to 10 (optimal sleeping). In addition, VAS was used for assessing the satisfaction for the Nas-Air® (0= bad; 10= best). Sleep quality VAS was recorded by the patients at baseline, after the 2 nights without Nas-Air, and after the 2 nights with Nas-Air®.

Overweigh/obesity was considered according to WHO definition as body mass index ≥ 25 (http://www.who.int/mediacentre/factsheets/fs311/en/ last accessed March 29th 2018).

Demographic and clinical characteristics are described using means with SDs for normally-distributed continuous data and absolute frequencies and percentages for categorical variables. Any statistically significant difference between or among mean values of each continuous variable was evaluated with the Paired *t*-test (comparisons between two groups) or the Repeated Measures ANOVA (comparisons among three groups),

Table I. *Demographic and clinical data of outpatients at baseline.*

Age (years) [mean (SD)]	48.29 (13.03)
Gender (m,f) [No. (%)]	32m (78.05%), 9f (21.95%)
BMI (kg/m^2) [mean (SD)]	26.87 (4.28)
Normal (18.5<BMI<25) [No. (%)]	10 (24.39%)
Overweight/obesity (BMI≥25) [No. (%)]	31 (75.61%)
Allergy [No. (%)]	12 (29.27%)
Nasal Valve Obstruction [No. (%)]	
No	19 (46.34%)
Monolateral	8 (19.51%)
Bilateral	14 (34.15%)
Turbinate Hypertrophy [No. (%)]	
Grade 0	7 (17.07%)
Grade I	11 (26.83%)
Grade II	21 (51.22%)
Grade III	2 (4.88%)
Septal Deviation [No. (%)]	
No blocking	32 (78.05%)
Blocking	9 (21.95%)
Tonsil Hypertrophy [No. (%)]	
Absent	5 (12.20%)
Grade I	22 (53.67%)
Grade II	11 (26.83%)
Grade III	3 (7.32%)
VAS nasal obstruction [mean (SD)]	5.56 (2.43)
VAS olfaction [mean (SD)]	7.78 (2.73)
VAS sleep quality [mean (SD)]	5.98 (2.54)

followed by Bonferroni's Multiple Comparison Test as post-hoc test, respectively. *Chi*-squared test or Fisher's exact test, in case of expected frequencies lower than 5, was used to compare frequencies. Correlations were evaluated with Pearson correlation coefficient. Statistical significance was set at $p < 0.05$, and the analyses were performed using GraphPad Prism software, (GraphPad Software Inc, CA, USA).

RESULTS

Table I reports the demographic and clinical data of the outpatients during the otolaryngological visit.

The application of Nas-Air® significantly reduced snoring time (expressed as % snoring during the nighttime) from 36.80 (±16.42) % before application to 23.00 (±14.77) ($p<0.001$) and 23.54 (±15.70) ($p<0.001$) after one or two nights of using Nas-Air®, respectively (Fig. 1). No statistical significant difference was found between snoring percentage detected during the first night and the second night with Nas-Air® (p= NS). In addition, the frequency of patients with reduced snoring after having used Nas-Air® for one or two nights was similar (p= 0.48).

The evaluation of Nas-Air® liking by VAS demonstrated that it was well tolerated, the VAS score being 6.32 (2.17). Nas-Air® liking VAS score was higher for patients with a normal weight as compared to overweight/obese patients, being 7.60 (0.56) and 5.90 (0.39), respectively (p=0.0299).

Sleep quality VAS score significantly improved after having used Nas-Air®, being 5.98 (2.54) before and 7.32 (1.98) after use ($p = 0.0012$) (Fig. 2), and moderately correlated with Nas-Air® liking VAS score (Pearson $r = 0.476$, $p = 0.002$) (Fig. 3).

DISCUSSION

Snoring can be a very disturbing complaint for a good social and family life. In fact, the partner of the snorer in a relationship is the one who suffers the most from these nightly noises in the beginning. However, during the following years also the snorer becomes aware of his/her problem. So, he/she wakes himself up, gets a dry throat, and is sleepy and tired in the morning.

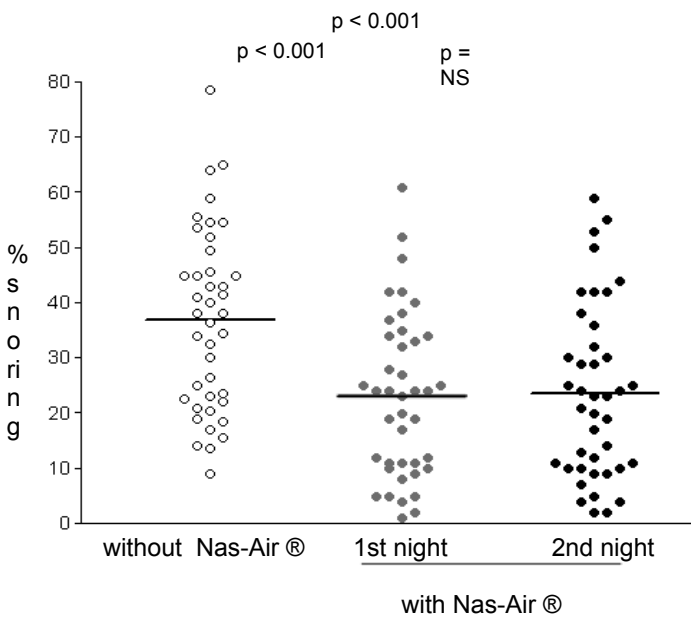

Fig. 1. *Snoring (expressed as % snoring during the nighttime) before and after the application of Nas-Air® for one or two nights. Horizontal bars represent mean values.*

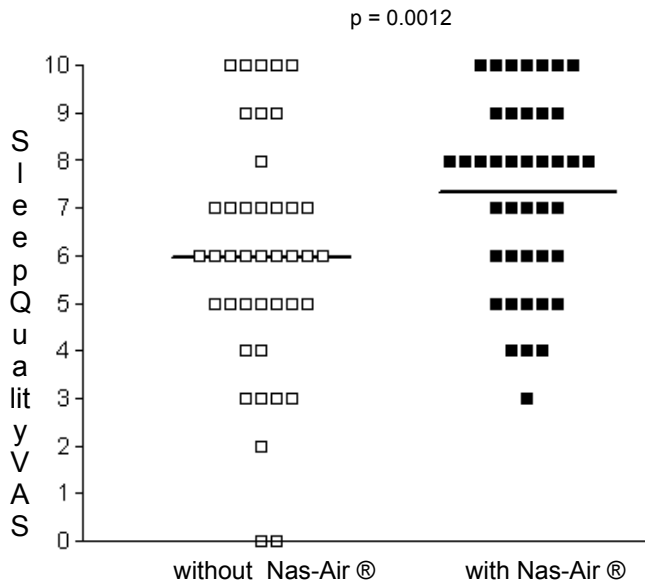

Fig. 2. *Sleep visual analogue scale (VAS) score before and after having used Nas-Air®. Horizontal bars represent mean values.*

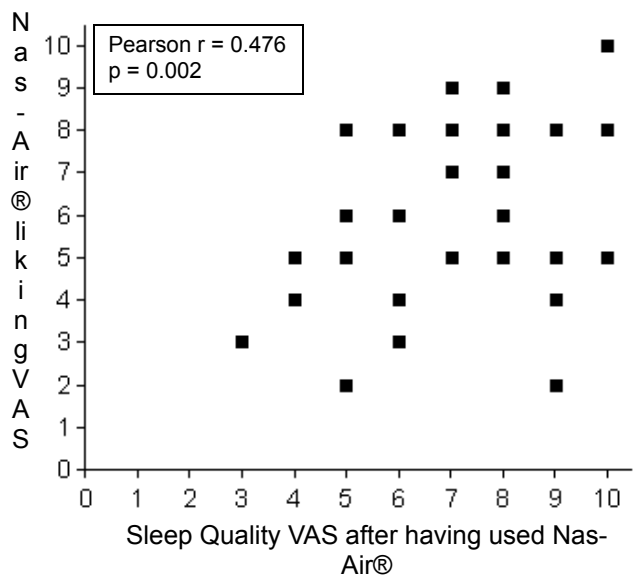

Fig. 3. *Correlation between sleep visual analogue scale (VAS) score and Nas-Air® liking VAS score.*

From a pathophysiological point of view, the nasal valve area represents the narrowest passage in the respiratory tract, causing more than half of the total resistance to nasal respiration in a healthy subject. In this regard, the proportional ratio between the cross-sectional area of the nasal valve and the bony piriform aperture is about 1:1.4. The cross-sectional area surfaces vary in the nasal cavity: in the nasal valve it is about 30 mm^2, in the middle of the cavity is 120 mm^2, and in the rhinopharynx is approximately 150 mm^2. After mechanical dilation the nasal airflow can increase up to 25%; interestingly, this change is comparable with that observed after decongestant use. In fact, with the dilator, the cross-sectional respiratory area increases; according to the Poiseuille law for laminar fluid-flow ($\Delta p=l/d^n$, n=4), a small increase in the diameters (d) and the area is able to significantly reduce the pressure (Δp). Furthermore, the intrathoracic pressure can be halved (from 4 to 2 cm of H_2O) after dilating the nostrils. Therefore, less energy is necessary for the respiratory muscles to inhale the same quantity of air.

Many disorders may result in pathologically narrow upper airways, including adenotonsillar enlargement, cancers, chronic rhinitis, traumatic or congenital anatomical defects and so on. In particular, nasal obstruction represents the most common cause for snoring (6). Nasal valve obstruction is the crucial point for snoring pathogenesis. Many studies investigated the role of the nasal valve and its subjective and objective measurement (7, 8). However, in clinical practice the most important parameter is the snoring perception of the partner and/or of the patient.

From a therapeutic point of view, mechanical dilation of the nasal valve is the best non-surgical approach in snorers. Many dilators exist, both external and internal. Several studies investigated their efficacy and most of them were positive (9-12). The current study therefore investigated the efficacy of a new internal nasal dilator: Nas-Air®. Interestingly, about 90% of patients achieved a significant improvement of the sleep quality and there was a significant reduction of snoring time.

However, this study has some limitations, including the open design, the limited number of enrolled patients, the lack of a follow-up, and the absence of validated objective parameters. Therefore, the current experience should be confirmed by further studies designed according to more robust methodology.

In conclusion, the present study demonstrates that Nas-Air® is an internal nasal dilator able to reduce snoring time and improve sleep quality.

REFERENCES

1. Akcam T, Friedman O, Cook TA. The effect on snoring of structural nasal valve dilation with a butterfly graft. Acta Otolaryngol Head Nech Surg 2004; 130:1313-18.
2. Leitzen KP, Brietzle SE, Lindsay RW. Correlation between nasal anatomy and objective sleep apnea severity. Otolaryngol Head Neck Surg 2014; 150:325-31.
3. Barrett DM, Casanueva FJ, Cook TA. Management of the nasal valve. Facial Plast Surg Clin N Am 2016; 24:219-34.
4. Hamilton GS. The external nasal valve. Facial Plast Surg Clin N Am 2017; 25:179-94.
5. Ameli F, Brocchetti F, Tosca MA, Signori A, Ciprandi G. Adenoidal hypertrophy and allergic rhinitis: is there an inverse relationship? Am J Rhinol Allergy 2013; 27(1):e5-10.
6. Kiyohara N, Badger C, Tjoa T, Wong B. A comparison of over-the-counter mechanical nasal dilators. JAMA Fac Plast Surg 2016; 18:385-89.
7. Varendh M, Andersson M, Bjornsdottir E, et al. Nocturnal obstruction is frequent and reduces sleep quality in patients with obstructive sleep apnea. J Sleep res 2017; 4:1-8.
8. Ziai H, Bonaparte JP. Reliability and construct validity of the Ottawa valve collapse scale when assessing external nasal valve collapse. J Otolaryngol Head neck Surg 2018; 47:15.
9. Ottaviano G, Ermolao A, Nardello E, Muci F, Favero V, Zaccaria M, Favero L. Breathing parameters associated to two different external nasal dilator strips in endurance athletes. Auris Nasus Larynx 2017; 44:713-18.
10. Floyd EM, Ho S, Patel P, Rosenfeld RM, Gordin E. Systematic review and meta-analysis of studies

evaluating functional rhinoplasy outcomes with the NOSE score. Otolaryngol Head Neck Surg 2017; 156:809-15.

11. Dinardi RR, Ribeiro de Andrade C, Martins-Costa HC, Ibiapina C. Does the Airmax internal nasal dilator increase peak nasal inspiratory flow (PNIF) in adolescent athletes? Int J Ped Otorhinolaryngol 2016; 84:37-42.
12. Salturk Z, Inan M, Kumral TL, Atar Y, Yildirim G, Uyar Y. Efficiency of external nasal dilators in pediatric nasal septal deviation. Int J Ped Otorhinolaryngol 2014; 78:1522-25.

JOURNAL OF BIOLOGICAL REGULATORS & HOMEOSTATIC AGENTS Vol. 32, no. 5, 1275-1278 (2018)

LETTER TO THE EDITOR

UPDATES IN REGENERATIVE MEDICINE APPLIED TO DENTAL SCIENCES

A. PACIFICI, A. POLIMENI and L. PACIFICI

[1]*Department of Oral and Maxillofacial Sciences, Sapienza University of Rome Italy*

Received June 19, 2018 – Accepted July 6, 2018

Mesenchymal stem cells (MSCs) are found in high concentrations in several tissues, such as umbilical cord, adipose tissue and dental tissue. Dental stem cells reside in many areas of the oral cavity. Thanks to their abilities, dental stem cells could be used to treat diseases and to understand the basic mechanisms of developmental pathologies. There are currently numerous ongoing clinical trials evaluating a broad spectrum of conditions and situations using different stem cell populations. However, stem cell studies are raising profound ethical questions that weigh on the world of scientific research. Stem cells are always a hot topic in the scientific community. Their use is related also to their banking, as cell manipulation is also often related to medical and ethical issues. Many biomedical studies aim to treat diseases that were previously considered incurable with MSCs. All this has created the need to quickly and safely storage stem cells, usually in a stem cell biobank (SCB). Regenerative medicine is the most important approach for achieving complete tissue regeneration using stem cells isolated from adult tissues, embryonic stem cells, but also through the application of induced pluripotent stem cells (iPSC). iPSCs are non-pluripotent cells that are engineered to acquire the ability to differentiate into all different types of cells. In conclusion, the daily use of stem cells in regenerative procedures is still far from being safe and predictable, especially because of the biomedical component, often requiring experienced biologists and complex technologies for cell manipulation and cell banking.

To the Editor,

Stem cells are undifferentiated cells, capable of transforming and dividing into multiple cell lines. Mesenchymal stem cells (MSC) are present in high concentrations in several tissues such as umbilical cord, adipose tissue and dental tissue (1).

Dental stem cells reside in many areas of the oral cavity. In 2000, Gronthos et al. first hypothesized that the dental pulp of permanent teeth could be a source of mesenchymal stem cells. They demonstrated the presence of a certain cellular population within the adult human dental pulp which appears to be clonogenic, highly proliferative and capable of regenerating tissue, thus defining it as a stem cell population called DPSC (2). Later, Tatullo et al. showed that these dental pulp stem cells (DPSC) can have numerous and varied applications in regenerative medicine of tooth structures (3, 4).

Following the discovery of the DPSC, a study conducted by Miura et al. showed that the residual dental pulp derived from human exfoliated deciduous teeth contains a population of multipotent stem cells (SHED). Deciduous teeth can therefore be considered as an ideal resource for stem cells to repair damaged dental structures, induce bone regeneration, and possibly to treat neural tissue lesions or degenerative diseases (5). The periodontal ligament (PDL) has been identified as a further source of mesenchymal stem cells (PDLSCs). In fact, several researchers demonstrated after the surgical extraction of human

Key words: mesenchymal stem cells, regenerative dentistry, oral sciences, ethical aspects, bioethics

Mailing address:
Prof. Luciano Pacifici,
Department of Oral and Maxillofacial Sciences,
Sapienza University of Rome,
Rome, Italy
e-mail: prof.lucianopacifici@libero.it

0393-974X (2018)

DISCLOSURE: ALL AUTHORS REPORT NO CONFLICTS OF INTEREST RELEVANT TO THIS ARTICLE.

molars that the periodontal ligament contains stem cells capable of generating, *in vivo*, tissues such as: dental cementum, periodontal ligament and alveolar bone. After the isolation and characterization of the first oral-derived stem cells, several studies were carried out on the role of the environment, also defined "cell niche", on such dental-derived MSCs; in fact, specific tissues have demonstrated their ability to influence the differentiation of mesenchymal stem cells towards specific lineages, and the same ability has been also investigated on decellularized scaffolds where dental stem cells were cultured (6, 7).

Mesenchymal stem cells have also been isolated from the dental follicle, an ectomesenchymal tissue that surrounds the developing tooth germ. These cells are known as DFPC and give rise to cementoblasts, periodontal ligament cells and osteoblasts (4). The apical papilla also has multipotent mesenchymal stem cells expressing various MSC markers. They are known as SCAP and are able to form odontoblasts and produce *in vivo* dentin (6-8).

In 2013, Marrelli et al. isolated for the first time mesenchymal stem cells from periapical cysts (hPC-MSC). HPC-MSCs possess multi-lineage differentiation capabilities, allowing their differentiation into osteoblasts and adipocytes. Thus, hPC-MSCs could be a valid source of MSC for stem cells research (2-4).

Ethical issues in regenerative medicine

Thanks to their capacity for multilineage differentiation, stem cells could be used to treat diseases beyond the reach of conventional medicine and to understand the basic mechanisms of human development. In fact, there are currently numerous ongoing clinical trials evaluating a broad spectrum of conditions and situations using different stem cell populations.

However, stem cell studies are raising profound ethical questions that weigh on the world of scientific research. The sources of stem cells can create ethical issues, not necessarily related to their isolation, but linked to their origin. Specifically, the use of pluripotent stem cell lines derived from oocytes and embryos appears to be full of contrasts, while stem cells from other sites are raising less moral concerns.

In fact, one of the most promising sources of stem cells from a clinical point of view is from the embryo. However, this process includes an important ethical problem, because at present these cells cannot be obtained without the destruction of a human embryo (5-7). The first ethical issue against the use of embryonic stem cell lines is therefore based on the idea that embryos are living people. The reprogramming of somatic cells to produce induced pluripotent stem cells avoids the specific ethical problems of embryonic stem cell research. However, every research carried out on stem cells presents ethical problems concerning informed and voluntary consent for the donation of biological material, the evaluation of the risks and benefits of the experimental intervention and the careful supervision of the research. In fact, the complexity and diversity of therapies involving the use of stem cells in human trials require more complete and accurate evaluations to ensure a level of risk that is justified for the recipient. These studies must be based on solid evidence of preclinical efficacy that justifies testing on humans. It has become mandatory to improve the evaluation of stem cell therapies. Therefore, the International Society for Stem Cell Research has developed a series of practical questions for which clear evidence-based answers need to be obtained before approving a stem cell-based study. Furthermore, according to the guidance of the Food and Drug Administration, researchers have an ethical obligation to ensure that risks to individuals associated with stem cell use are reasonable in relation to the expected benefits.

DISCUSSION

Stem cells are always a hot topic in the scientific community. Their use is related also to their banking, as the manipulation is often related to medical and ethical issues. Many stem cell studies aim to treat diseases that were previously considered incurable which has created the need to quickly and safely find biomaterial giving life to deposits oriented to the collection, storage and distribution of the cells, commonly referred to as stem cell biobanks (SCB). The construction of public and private biobanks

of different stem cell samples thus guarantees the immediate availability of biological material for research and clinical use. Given the high level of control over stem cell research, a centralized banking system appears to be more inclined to adhere to legal and ethical frameworks, thus including only cell lines with traceable lineage and certified quality (4).

The main modality of stem cell conservation is represented by cryopreservation. It is a method that guarantees the preservation of stem cells for an indefinite period through the use of chemicals called cryoprotective agents (CPA), equipment for freezing and storage in liquid nitrogen. With cryopreservation, the cellular metabolic activity is reduced, preserving the vitality, the phenotype and the potential for differentiation.

Stem cells are harvested by centrifugation. The sample is then gradually frozen until a temperature of -196°C is reached in liquid nitrogen. Along with the very slow freezing rate, a rapid thaw is considered essential for successful stem cell retention.

Recently, more authors have studied and optimized the process of collection, isolation, characterization and cryopreservation of DPSCs, thus facilitating the creation of biobanks. This study demonstrated for the first time the effectiveness of a saline containing gentamicin to prevent contamination of the tooth from which to extract stem cells, also attesting the effectiveness of 5% dimethyl sulfoxide (DMSO) as a culture medium for cryopreservation by freezing at controlled speed (1-8).

Regenerative medicine is the most important approach to achieve complete tissue regeneration using stem cells isolated from adult tissues, embryonic stem cells, but also through the application of induced pluripotent stem cells (iPSC). (iPSC are non-pluripotent cells that are engineered to acquire the ability to differentiate into all different types of cells.

Recently, many authors tested the potential of iPSC obtained from stem cells derived from dental pulp (DPSC). DPSC cells can be successfully reprogrammed in iPSC by electroporation. The iPSCs obtained can generate a tissue similar to the pulp with functional odontoblasts able to produce *in vivo* a tubular dentin. Human iPSCs can therefore be an important source for deriving human odontoblasts and for testing the bioactivity of materials. In further studies, iPSCs were reprogrammed from stem cells from apical papilla (SCAP) and DPSC using a non-integrative RNA virus vector. Scholars have induced iPSCs to differentiate into cardiomyocytes, thus demonstrating that iPSCs may represent an important resource for the regeneration of compromised cardiac muscle tissues (6-9). The focus on mesenchymal stem cells in regenerative medicine is, of course, highly promising: such cells, in fact, act also with their paracrine effect on tissue homeostasis, thus improving the local feedback to oxidative stress (8, 9), and to infections (10). The use of iPS has been opposed by the hypothesis that such pluripotent stem cells may evolve towards tumoral cells, therefore creating heterotopic localization of oncological diseases (11).

In conclusion, the daily use of stem cells in regenerative procedures is still far from being safe and predictable, moreover, the surgeons should improve their ability (12) to manage both simple surgeries and complex regenerative surgeries, especially those where the biomedical component requires experienced biologists and technologies for cell manipulations and cell banking. Future clinical therapies, developed thanks to the last innovative studies on MSCs, will represent an important chance to treat primarily degenerative pathologies, especially those related to the brain and the nervous system. Furthermore, also post-traumatic and reconstructive surgery will be highly improved with MSC therapy, thanks to their good influence on soft tissue regeneration, on neo-angiogenesis and on the management of local infections because of their paracrine effects able to modulate inflammation and the release of specific local cytokines.

REFERENCES

1. Paduano F, Marrelli M, Palmieri F, Tatullo M. CD146 expression influences periapical cyst mesenchymal stem cell properties. Stem Cell Rev 2016; 12(5):592-603.
2. Gronthos S, Mankani M, Brahim J, Robey PG, Shi S. Postnatal human dental pulp stem cells (dpscs) in vitro and in vivo. Proceedings of the National

Academy of Sciences of the United States of America 2000; 97:13625-30.
3. Tatullo M, Falisi G, Amantea M, Rastelli C, Paduano F, Marrelli M. Dental pulp stem cells and human periapical cyst mesenchymal stem cells in bone tissue regeneration: comparison of basal and osteogenic differentiated gene expression of a newly discovered mesenchymal stem cell lineage. J Biol Regul Homeost Agents 2015; 29(3):713-18.
4. Tatullo M, Marrelli M, Falisi G, et al. Mechanical influence of tissue culture plates and extracellular matrix on mesenchymal stem cell behavior: A topical review. Int J Immunopathol Pharmacol 2016; 29(1):3-8.
5. Miura M, Gronthos S, Zhao M, Lu B, Fisher LW, Robey PG, Shi S. SHED: stem cells from human exfoliated deciduous teeth. Proc Natl Acad Sci 2003; 100:5807-12.
6. Aulino P, Costa A, Chiaravalloti E, et al. Muscle extracellular matrix scaffold is a multipotent environment. Int J Med Sci 2015; 12(4):336-40.
7. Perniconi B, Coletti D, Aulino P, et al. Muscle acellular scaffold as a biomaterial: effects on C2C12 cell differentiation and interaction with the murine host environment. Front Physiol 2014; 5:354.
8. Tatullo M, Simone GM, Tarullo F, et al. Antioxidant and antitumor activity of a bioactive polyphenolic fraction isolated from the brewing process. Sci Rep 2016; 6:36042.
9. Tatullo M, Gentile S, Paduano F, Santacroce L, Marrelli M. Crosstalk between oral and general health status in e-smokers. Medicine (Baltimore) 2016; 95(49):e5589.
10. Marrelli M, Tatullo M, Dipalma G, Inchingolo F. Oral infection by Staphylococcus aureus in patients affected by White Sponge Nevus: a description of two cases occurred in the same family. Int J Med Sci 2012; 9(1):47-50.
11. Tatullo M, Marrelli M, Amantea M, Paduano F, Santacroce L, Gentile S, Scacco S. Bioimpedance detection of oral lichen planus used as preneoplastic model. J Cancer 2015; 6(10):976-83.
12. Marrelli M, Gentile S, Palmieri F, Paduano F, Tatullo M. Correlation between surgeon's experience, surgery complexity and the alteration of stress related physiological parameters. PLoS One 2014; 9(11):e112444.

JOURNAL OF BIOLOGICAL REGULATORS & HOMEOSTATIC AGENTS Vol. 32, no. 5, 1279-1283 (2018)

LETTER TO THE EDITOR

REMODELING THE NECK AND THE LOWER JAW WITH DEHOXYCHOLATE INJECTIONS

R. RAUSO[1], G. TARTARO[1], L. RUGGE[1], F. CHIRICO[1] and N. ZERBINATI[2]

[1]Maxillo-Facial Department, University of Campania "Luigi Vanvitelli", Naples, Italy;
[2]Dermatology Department, University of Insubria, Varese, Italy

Received June 7, 2018 – Accepted July 5, 2018

Nonsurgical cosmetic facial procedures have gained popularity in recent decades. These procedures are commonly referred to as facial rejuvenation, and only a few are performed in the neck region. Herein, the authors describe their experience with off-label use of deoxycholic acid (DC) injections on 18 patients for remodeling of the neck and lower jaw. The injection protocol was personalized for each patient, and lidocaine was always premixed with the DC. After the initial injection visit, at least 3 months passed before further injections were considered. All documented side effects, including swelling and dysesthesia, resolved spontaneously. All patients received follow-up for at least 3 months, and only 2 patients required a second session of injections. By personalizing the injection protocol for each patient, good outcomes were achieved, including aesthetic enhancement of the shape and contour of the jaw and neck. Although the study is limited by the relatively small sample size, the results are promising and warrant additional investigations.

To the Editor,

Statistics released by the American Society for Aesthetic Plastic Surgery in 2016 show the dramatic increase of surgical and nonsurgical cosmetic procedures throughout the preceding 20 years; the number of plastic surgery procedures doubled in that period, and the quantity of nonsurgical cosmetic procedures increased by 12-fold (1). This demonstrates that an increasing number of subjects are seeking cosmetic improvements and that nonsurgical procedures are preferred to surgical interventions. Reasons for this preference vary and may include fear of surgery and the operating room, and concerns about lengthy convalescence time causing interference with social and/or professional aspects of life (2).

Various tools are available for nonsurgical rejuvenation of the face, including dermal fillers, botulinum toxin**,** energy-based devices (EBDs). However, until recent years, cosmetic injectables for use in the neck were lacking. Although rejuvenation of the neck can be achieved successfully with several EBDs (such as radiofrequency and high-intensity focused ultrasonography), moving an EBD can be difficult and cumbersome; therefore, these systems may not be practical for physicians who work in multiple locations. Injectable treatments do not have this disadvantage and can be performed on demand. Moreover, EBDs must be purchased upfront, whereas a supply of injectables can be purchased as needed, when needed.

Since 2015 in the United States and Canada, and

Key words: dehoxycholate, adipocitolysis, neck, non-surgical

Masiling address:
Prof. Raffaele Rauso,
Maxillo-Facial Department,
University of Campania "Luigi Vanvitelli",
Piazza Miraglia,
Naples, Italy
e-mail: dr.raffaele.rauso@gmail.com

0393-974X (2018)

2 years later in parts of Europe (eg, Italy, Poland, Check Republic), a DC-based product specifically indicated for reduction of submental fullness has been available (3). The product is used according to a specific injection protocol, which includes a grid specifying proper placement. Injection sites are spaced 1 cm apart, and 0.2 mL of the product is injected into each site. Moreover, the product information suggests that injections be performed every 4 to 6 weeks, until the desired outcome is achieved, up to a maximum of 6 sessions. (4)

The authors of the present study have extensive experience with adipocitolitic DC-based solutions. Herein, they describe their own protocol for a DCA-based product, which entails personalizing the timing and sites of injection on a case-by-case basis.

MATERIALS AND METHODS

This is a retrospective clinical study of a cohort of patients (N = 18) treated consecutively between May 2017 and January 2018. The cohort included 12 females and 6 males, aged 24 to 57 years. All patients received 1% DC injections (Belkyra 10 mg/mL, Allergan S.p.A., Rome, Italy). Exclusion criteria were an excess of neck skin ptosis, unelastic skin excess, unrealistic patient expectations, breastfeeding, pregnancy, liver disease, kidney disease, and all medical conditions for which this treatment is contraindicated.

Each patient was evaluated, including clinical and photographic assessment. Before treatment, all patients signed a consent form confirming that they had been informed of the off-label protocol to be used for their treatment. Every patient received a personalized injection protocol that did not adhere strictly to the manufacturer's proposed protocol. Each individualized protocol was based on the patient's anatomy and need. The pretreatment evaluation of skin elasticity was helpful for the patient to have a clear understanding of the result that would likely be achievable, which was explained to the patient in advance.

The injection grid designed by the manufacturer was used only for the submental area. For each patient, a specific marking was made based on pretreatment clinical evaluation. If overall improvement of the neck area was desired, a "neck collar–like" marking was drawn (Fig. 1). If the aesthetic goal was a more acute cervico-mental angle, pre- and retro-platismatic fat injections were planned.

All patients received injections to the neck area and/or pre-jaw line. Injection sites were spaced 1 cm apart. The contents of each 2-mL vial of DC were premixed

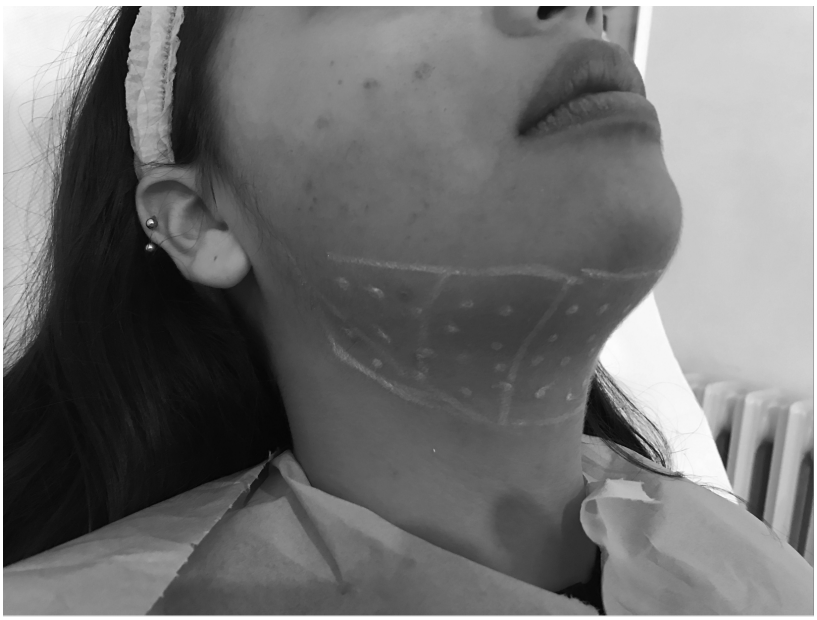

Fig. 1. *The pre-operative marking of "neck collar" injections.*

with 0.5 mL of 2% lidocaine (lidocaina cloridrato 20 mg/mL; Bioindustria L.I.M.; Novi Ligure, Italy). Each site was injected with 0.25 mL of solution, and no more than 4 vials were used during each session.

Following the first session of injections, a waiting period of at least 3 months ensued, after which the result was evaluated and a decision made as to whether to perform a second series of injections.

All patients were followed-up for at least 6 months after the final session of injections.

RESULTS

No patient complained of pain during the procedure. All patients experienced progressive swelling, as expected, which lasted 25 days on average. For 3 patients, ecchymosis was observed, which self-resolved within 1 week. Four patients experienced dysesthesia of the treated area, which lasted for 2 months after the injections and also self-resolved. One patient vomited within 6 hours of the injection session (data presented in Table I). No other complications were recorded.

Only 2 patients required a second session of injections. All patients returned for clinical control 1 and 3 months after the injection session(s) and were followed-up for 6 at least months after the final injections. Each patient affirmed to be happy with his or her result. (Fig. 2 shows clinical photographs of a female patient).

DISCUSSION

In humans, DC is derived from cholic acid produced by the liver and is then metabolized by intestinal bacteria; in the small intestine, DC determines the emulsification and absorption of fat.

When DC is injected into fat, it alters the permeability of fat cell membranes, causing progressive cellular swelling that ultimately results

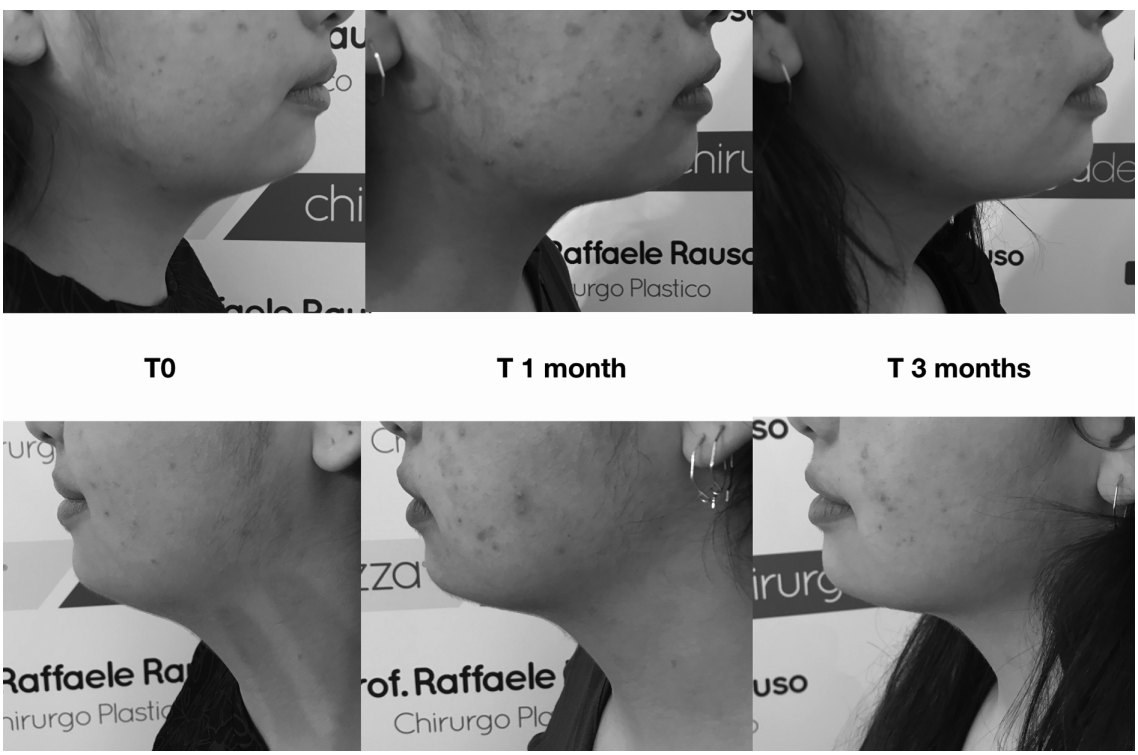

Fig. 2. *In this figure it is possible to see the progressive improvements of the neck appearance of a 26-year-old woman 1 and 3 months after injection of 4 vials of ATX 101, injected in a single session.*

in the breakup of fat cells. This process can take several days to several weeks. After cellular breakup, macrophages enter the site and eliminate cytoplasm and cell membranes, while the healing process is carried out by the development of fibrotic tissue. The entire process, including healing, usually takes several months. These processes have been described in scientific literature (5, 6). Based on this knowledge and on previous experience with DC compounds, in the present study Belkyra was injected to reduce fat in the neck and pre-jawline and to achieve tightening of the overlying skin.

The use of DC as an injectable for fat reduction has been debated for years, since the discovery by Rotunda and Duncan regarding its role in injection lipolysis that refuted the findings of Dr. Rittes from early in the 21st century (7-10). Over the years, DC injections have been largely performed to reduce body fat, despite the lack of information on posology, timing of injections, and safe use of DC. A major safety concern, namely skin necrosis after subcutaneous injection of DC, has been reported (11).

In 2009, without any preclinical study, a product containing DC was sold in Europe (Aqualyx; Marllor International; San Giovanni in Marignano, Italy) and was classified as a medical compound. However, in 2013, Duncan et al. compared the cytolytic index of this medical compound with that of a phosphatidylcholine/DC compound and noted that Aqualyx had a higher cytolytic effect; in order of effectiveness, the cells most sensitive to cytolysis were dermal, endothelial, muscular, fat, and neural (12). These findings emphasized the lack of safety of the medical compound. In fact, in 2016, the Italian Ministry of Health blocked the merchantability of Aqualyx (5, 11-13). In 2014, McDiarmid compared DC volumes of 1 mg/cm^2 and 2 mg/cm^2, and observed that 1 mg/cm^2 was associated with a better safety profile, including a lower incidence of side effects (14). That study represents the first investigation of optimal posology for injection of DC. Several months later, in 2015, the product debuted in the United States (as Kybella) and Canada (as Belkyra) as the first DCA-based drug specifically indicated for reduction of submental fat.

The DC present in Belkyra/Kybella is a nonanimal, nonhuman, purified version that appears to be partially selective because cells with a high percentage of membrane proteins (such as those in the dermis, muscles, nerves, and vessels) seem to be less sensitive to its action. Investigators have demonstrated that albumin neutralizes or binds DC in nonadipose tissue, given the lack of tissue damage seen by endogenous DC (3, 4).

The injection protocol used in the present study was in part concordant with the manufacturer's guidelines. However, in addition to injecting into the area indicated in the manufacturer's protocol, injections were performed elsewhere to achieve neck and jaw recontouring secondary to fat cell lysis. To accomplish this, it was necessary to vary the injection sites and to customize them for each patient.

Moreover, DC was premixed with lidocaine in the present study because it is well known that DC injection is painful for the patient. For the same reason, it has been suggested to use ice packs immediately prior to injections or to administer local anesthesia before DC injections. However, ice packs are often not helpful in reducing pain during injection, and local anesthesia may alter the anatomy of the area to be injected. These potential problems can be avoided by mixing DC with lidocaine, effectively minimizing pain during injection.

In respect to the quantity of lidocaine added to the contents of each vial of DC, we aimed for the minimum amount required to reduce pain whilst still allowing the physician to easily inject the appropriate volume of DC into each site. Considering the posology of 0.2 mL of DC per site (as prescribed by the manufacturer) and that each vial contains 2 mL of product (from each vial, it is possible to fill two 1-mL syringes to inject 10 points), adding 0.5 mL of lidocaine permitted the filling of two 1-mL syringes plus another half syringe, enabling 10 individual placements of 0.25 mL of DC per site.

The buffer system present in the injectable DC product, represented by anhydrous disodium phosphate, is able to avoid pH modification if another drug is added, which explains why the effectiveness of DC is maintained after mixing with lidocaine. Another favorable feature of this mixture is the total absence of precipitation of the solution.

In the present study, the interval between injection sessions was substantially longer than usual. In general, DC is injected every 4 to 6 weeks; in the present study, it was injected every 3 months (if a subsequent session was required). This protocol was successful because of the authors' previous experience with DC injections (5). In 2015, Dr Salti and the senior author of the current study (R.R.) described their own protocol, derived from analyzing an abdominal specimen harvested 3 weeks after injections: different phases of progressive cellular swelling were apparent, including the breakup of cells. Areas of cytoplasmic homogenization and cell membrane dissolution also were present (5). These findings demonstrate that, even after several weeks, an inflammatory component is still present in the injected area; therefore, a period of more than 4 to 6 weeks is needed to allow for sufficient healing and for objective evaluation of fat reduction and skin tightening. Therefore, our protocol is to wait at least 3 months between injection sessions.

In the present study, a relatively new DC-based product was injected to improve the appearance of the neck and/or lower jawline, according to a novel protocol characterized by premixing lidocaine, performing "on-demand" injections, and waiting at least 3 months between injection sessions. Good results were achieved in all patients, and side effects were minimal, with a lower incidence than reported previously by others. (3) Larger and longer-term studies of the present protocol are warranted to confirm its safety and effectiveness.

Disclosure: Prof. Rauso received grants from Allergan, the manufacturer of the drug injected in the present study. The other Authors have no conflict of interest to declare.

REFERENCES

1. http://www.surgery.org/sites/default/files/ASAPS-Stats2016.pdf
2. Rauso R, Colella G, Zerbinati N, Salti G. Safety and early satisfaction assessment of patients seeking nonsurgical rhinoplasty with filler. J Cutan Aesthet Surg 2017; 10(4):207-14.
3. Shridharani S. Early experience in 100 consecutive patients with injection adipocytolysis for neck contouring with ATX-101 (Deoxycholic Acid). Dermatol Surg 2017; 43(7):950-58.
4. Rauso R, Salti G. A CE-marked drug used for localized adiposity reduction: a 4-year experience. Aesthet Surg J 2015; 35:850-57.
5. Rauso R, Rusciani A, Curinga G. An adipocitolitic aqueous microgelatinous solution for buffalo hump deformity reduction. J Drugs Dermatol 2014; 13:1282-84.
6. Rittes PG. The use of phosphatidylcholine for correction of the lower lid building due to prominent fat pads. Dermatol Surg 2001; 27:391.
7. Rittes PG. The use of phosphatidylcholine for correction of localized deposits. Aesth. Plast. Surg 2003; 27:315-18.
8. Rotunda AM, Suzuki H, Moy RL, Kolodney MS. Detergent effects of sodium deoxycholate are a major feature of an injectable phosphatidylcholine formulation used for localized fat dissolution. Dermatol Surg 2004; 30:1001-8.
9. Duncan D, Rubin JP, Golitz L, Badylak S, Kesel L, Freund J, Duncan D, et al. Refinements of technique in injection lipolysis based on scientific studies and clinical evaluation. Clin Plast Surg 2009; 36:195-209.
10. Di Toro G, Rauso R. Skin necrosis following adipocitolitic solution injections. Aesthet Surg J 2016; 36:NP74–NP76.
11. Duncan D. Response to "Injection lipolysis with phosphatidylcholine and deoxycholate." Aesthet Surg J 2013; 33(7):1073-75.
12. Rauso R. Comments on: "Intralipotherapy, the state of the art". Plast Reconstr Surg Glob Open 2017 24; 5(2):e1224.
13. McDiarmid J, Ruiz JB, Lee D, Lippert S, Hartisch C, Havlickova B. Results from a pooled analysis of two European, randomized, placebo-controlled, phase 3 studies of ATX-101 for the pharmacologic reduction of excess submental fat. Aesthet Plast Surg 2014; 38:849-60.
14. Duncan D, Rotunda A. Injectable therapies for localized fat loss: State of the art. Clin Plast Surg 2011; 38:489-501.

LETTER TO THE EDITOR

ANATOMICAL VARIATIONS OF THE MEDIAN NERVE AND OF THE VASCULAR-NERVOUS STRUCTURES AT THE WRIST

N.R. PEPE[1*], M. ARTICO[2*], L. BARDELLA[3], F. NUCCI[4], F. SVOLACCHIA[1], L. PEPE[1], L. FUMAGALLI[1] and S. TAURONE[2]

[1]Department of Anatomical, Histological, Medico-legal and Locomotor System Sciences, "Sapienza" University of Rome, Italy; [2]Department of Sensory Organs "Sapienza" University of Rome, Italy; [3]Department of Human Neurosciences "Sapienza" University of Rome, Italy; [4]Private Practice, Rome, Italy

Received February 25, 2018 – Accepted July 10, 2018

*These Authors contributed equally to this work

Three cases of anatomical variation of the median nerve at the wrist found during our surgical activity led us to take the opportunity to expose anatomical variations by reviewing already published reviews. Consequently, on the basis of anatomical studies, clinical reports and imaging, as a result of careful examination of the published literature, it has been observed that the interventions in such anatomical area must take into account these variations. In particular, the most performed procedure is the lysis of the transverse carpal ligament (TCL), which is not free from complications. In our opinion it is therefore necessary, in order to avoid the complications of the nervous, vascular and tendinous sections, to use some specific technical procedures.

To the Editor

The anatomical variations of the median nerve at the wrist, apart from the simple anatomical curiosity and notwithstanding the seemingly infrequent observation, may, during a surgical lysis of the transverse carpal ligament of the carpus (TCL) caused by carpal tunnel syndrome (CTS), generate considerable difficulties, and even very serious damage (1). The diagnostic and therapeutical approaches must be taken into due consideration.

CTS is the most frequent nerve canalicular entrapment syndrome (2, 3). The age-based peak is around 50 years while the female/male ratio is 3:1 (4-6), and only 10% of all CTS patients are under 30 years of age (7). The prevalence, however, is 500 cases per 1,000 subjects in certain categories, justifying a classification as an occupational disease. Studies concerning occupational groups have of course focused on tasks and activities involving high loads and frequencies or incongruous work postures, detecting higher prevalence than those of the general population.

Anatomy of the carpal tunnel

The carpal tunnel is formed posteriorly by a bone component consisting of a set of eight small bones divided into two chains:

- proximal from radial to ulnar (scaphoid,

Key words: median nerve, anatomical variations, carpal tunnel syndrome (CTS), lysis of the transverse carpal ligament

Mailing address:
Dr Nicola Roberto Pepe,
Dep. of Anatomical, Histological, Medico-legal and Locomotor System Sciences,
"Sapienza" University of Rome,
via A. Borelli 50, 00161, Roma, Italy
e-mail: nicolaroberto.pepe@yahoo.com

0393-974X (2018)

semilunar, pyramidal and pisiform)
- distal (trapezius, trapezoid, large bone and hooked)

The anterior fibrous portion is determined by the transverse carpal ligament subtended between the pisiform bone and the hamate bone hook, while laterally it splits into a superficial layer and a deep layer: the superficial lamina is fixed to the scaphoid and the trapezius tubercle, while the deep lamina is at the border of the trapezius groove (7) (Fig. 1).

Clinical presentation

Cases 1 and 2. Cases 1 and 2. The patients, a 55-year-old woman and a 48-year-old woman complained of nocturnal paraesthesia, tingling and sensitivity reduction on the radial surface of the first finger of her right hand. Clinical evaluation led to suspected diagnosis of median nerve compression neuropathy at the wrist. Electromyography and electroneurography confirmed the suspected diagnosis of CTS. In the surgical exploration of the median nerve, a variation of the course was found in the intraoperative inspection: the nerve was divided into two branches of equal diameter. The radial half innervated the muscles of the thenar eminence two sensory branches further towards the first and second finger. The ulnar portion split into two common digital nerves reaching the middle and the ring finger. Another noteworthy variation is the observation of the perforation of the TCL by the anomalous median nerve. The flexor retinaculum was dissected and after two months there were no neuromotor-sensitive signs and symptoms.

Case 3. A 37-year-old woman, had suffered for several months of painful paresthesia in both hands, but greater in the left side, especially at night, with presence of A slight deficit in opposition of the thumb in the right hand. The electro-neurographic response showed marked pain at the median nerve bilaterally, but greater on the left. She underwent surgery on the left hand in September 2016, and the intraoperative diagnosis resulted in the presence of a bifid sub-fascial median nerve. The postoperative course was normal except for a thermo-tactile and painful hypoesthesia in the median area, more evident in the third finger, which improved in about 5 months.

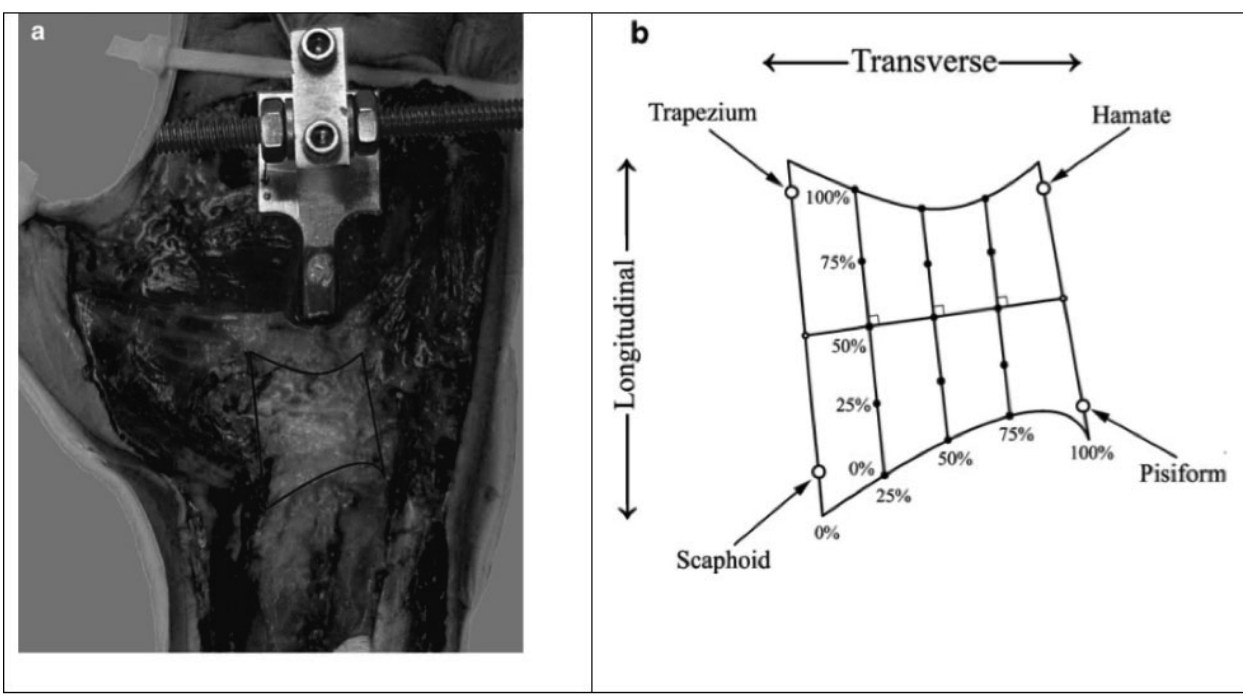

Fig. 1. *Relationships between transverse carpal ligament and its bony insertions.*

The intraoperative clinical observation of the above-mentioned cases offers us the opportunity to point out their anatomical variations.

All three patients of the cases above-described gave a signed informed consent to participate in the present study.

DISCUSSION

The median is a mixed nerve originating from two different roots coming respectively from the anterolateral and antero-medial secondary trunks of the brachial plexus. Near the wrist, the median nerve is superficialized by its position between the tendons of the superficial flexor of the fingers and the radial flexor of the carpus. Within the carpal canal, the median nerve emits a sensory branch known as the palmar cutaneous branch of the median nerve (PBCMN). At this level, it crosses the carpal canal immediately deeper than the transverse carpal ligament (TCL) and continues until it ends in its terminal branches.

The anomalies of the anatomical structures at the wrist can be classified as shown in Table I.

Anatomical variations of the median nerve within the carpal tunnel

In previously reported surgical series, different anatomical variations of the median nerve within the carpal tunnel have been described (Table II).

In relation to the transverse carpal ligament, we observe the following variants:

- Extra-ligamentous, in which the motor branch distally originates from the transverse carpal ligament and goes along the thenar eminence muscles (from 46 to 82%)
- Sub-ligamentous, originates below the transverse carpal ligament
- Trans-ligamentous, which has the peculiarity to hole the ligament itself

Muscle abnormalities at the carpal tunnel and thenar eminence

Muscular and tendon abnormalities of surgical interest which therefore may be responsible for compression of the median nerve are (10):

Muscle

- Hypertrophy of muscles of the thenar eminence

Table I. *Anatomical abnormalities at the wrist.*

- Nerve abnormalities
  - High bifurcation of the median nerve
  - Aberrant origin of the motor branch of the median nerve
  - Transligamentous palmar cutaneous branch of the median nerve
  - Abnormal course of the ulnar nerve
  - Ulnar-medial connections
- Tendon anomalies
  - Joint FPL and FDP II tendon (Linburg-Comstock syndrome)
- Vascular abnormalities
  - Persistent median artery
  - Superficial ulnar artery
- Muscle abnormalities
  - Long palmar
  - Lumbrical of the 2nd finger
  - Superficial flexor of the fingers

FDP Flexor digitorum profundus; FPL Flexor pollicis longus

Table II. *Anatomical variations of the median nerve within the carpal tunnel.*

Type	Incidence in carpal tunnel surgical lysis
Lateral division	3
Open division	2
Closed loop	<1
Motory branch	19
Trans-retinacolar	15
Multiple	2
Multiple and Trans-retinacular	2
Palmar cutaneous branch	2.5
Trans-retinacular	2.5
Multiple	0
Multiple and Trans-retinacular	0
Medio-ulnar sensory branch (from proximal median nerve on arcus superficialis)	1
Not classifiable	0

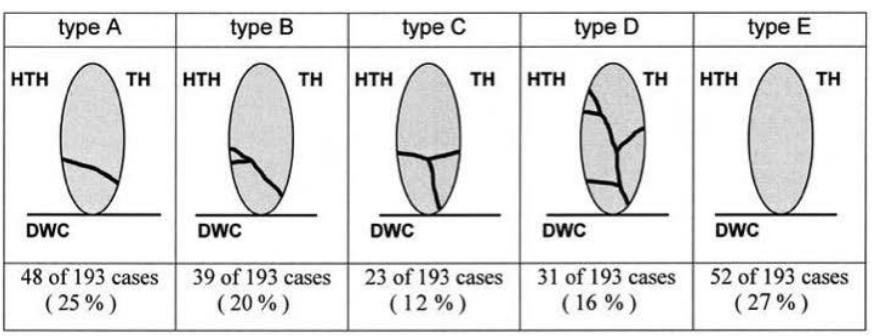

Fig. 2. *Schematic presentation and frequencies of the different types of subcutaneous nerve distribution at the wrist.*

- Palmaris longus
- Index lumbrical
- Flexor digitorum superficialis indicis Tendon
- Joint flexor palmaris longus tendon and II flexor digitorum longus (Linburg-Comstock syndrome)

Recurrent thenar motor branch

The classification by Lanz (12) in 1977 remains the most quoted, as well as the most comprehensive, in describing anatomical variations, subdividing them into four groups: i. changes in the course of the thenar branch; ii. accessory branches inside the distal portion of the carpal tunnel; iii. high division of the median nerve; iv. accessory branches proximal to the carpal tunnel.

Different types of subcutaneous distribution at the wrist must be also be considered (Fig. 2).

Anatomical variants of vascularization of the median nerve

The persistent median artery is an accessory artery originating from the ulnar artery in the proximal portion of the forearm; it runs laterally along the median nerve. Together with the interosseous arteries, the median artery is the main source in the hand of the embryo. After 8 weeks of gestation it normally regresses, leaving the ulnar and radial arteries. It may persist through two schemes: palmaris and antibrachial.

In the palmaris form this artery reaches the palm of the hand while in the antibrachial type it ends before reaching the wrist. It may contribute to the vascularisation of the superficial palmar arch or even to the finger radial arteries. In a normal nerve, the median artery, when present, runs along the ulnar side. In cases of bifurcation it stands between the two nerve branches.

Superficial ulnar artery

The ulnar artery is a branch of the brachial artery which runs along the ulnar side of the forearm in depth in relation to the ulnar carpal flexor muscle. It can sometimes have a more superficial course than the aforementioned muscle, but is still deeper than the antibrachial fascia. The impact of this anatomical variation variably ranges between 0.7% and 9.4%. The surgeon should keep in mind this possibility when performing an extended incision in the fold of the wrist, in order to avoid the risk of lesions.

Based on the above-mentioned abnormalities, the surgeon who undertakes interventions at the wrist or hand must bear in mind the anatomical variations that can lead to serious complications.

The open technique has great advantages for the detection (under vision of lenses 2-3X) of dangerous anatomical variations (transligamentous or "Knight-like") starting proximal-distally. The TCL section must also be on the ulnar side of the palmaris lungos tendon in order to prevent accidental sections of Knight-like or transligamentous. Such manoeuvres are difficult to carry out through a closed access. Endoscopic techniques are limited to those cases in which it is difficult to reach the distal margin of the TCL, where the carpal tunnel is narrower and in which most of the more-at-risk structures are present.

Knowledge of anatomical variations has a significant incidence in clinical practice and is a guide for the surgical technique most suitable to achieve the best clinical outcome with the least possible risk.

REFERENCES

1. Krishnan P, Mishra R, Jena M, Das A. Transligamentous thenar branch of the median nerve: the million dollar nerve. Neurol India 2013; 61(3):311-12.
2. Preston DC, Shapiro BE. Median neuropathy at the wrist. in: Preston DC, Shapiro BE, editors. Electro-myography and neuromuscular disorders. Philadelphia: Elsevier Butterworth-Heinemann, 2005; 255-79.
3. Pecina M, Krmpotic-Nemanic J, Markiewitz AD. Tunnel syndromes in the upper extremities. In: Pecina M, Krmpotic-Nemanic J, Markiewitz AD, editors. Tunnel syndromes: peripheral compression syndromes. 3rd edn. Boca Raton: CRC press, 2001; 125-39.
4. Atroshi I, Gummesson C, Johnsson R, Ornstein E, Ranstam J, Rosén I. Prevalence of carpal tunnel syndrome in a general population. JAMA 1999; 14;282 (2):153-58.
5. Katz JN, Stirrat CR, Larson MG, Fossel AH, Eaton

HM, Liang MH. Tunnel Syndrome, in: A self-administered hand symptom diagram for the diagnosis and epidemiologic study of carpal tunnel syndrome. J Rheumatol 1990; 17:1495-98.
6. Stevens JC, Sun S, Beard CM, O'Fallon WM, Kurland LT. Tunnel syndrome: carpal tunnel syndrome from 1961 to 1980 in Rochester, Minnesota. Neurology 1988; 38:134-38.
7. Standring S. The Anatomical Basis of Clinical Practice. Editor-in-Chief. Churchill Livingstone; 2005 Gray's Anatomy, 39th Edition.
8. Pacek CA, Chakan M, Goitz RJ, Kaufmann RA, Li ZM. Morphological analysis of the transverse carpal ligament. Hand (N Y) 2010; 5(2):135-40.
9. Isogai S, Murakami G, Wada T, Akita K, Yamashita T, Ishii S. Laminar configuration of the transverse carpal ligament. J Orthop Sci 2002; 7(1):79-83.
10. Mitchell R, Chesney A, Seal S, McKnight L, Thoma A. Anatomical variations of the carpal tunnel structures. Can J Plast Surg 2009; 17(3):e3-e7.
11. Entin MA. Carpal tunnel syndrome and its variants. Surg Clin North Am 1968; 48(5):1097-112.
12. Lanz U. Anatomical variations of the median nerve in the carpal tunnel. J Hand Surg Am 1977; 2(1):2-53.

JOURNAL OF BIOLOGICAL REGULATORS & HOMEOSTATIC AGENTS Vol. 32, no. 5, 1291-1294 (2018)

LETTER TO THE EDITOR

3D SOFTWARE SCANNING, PROCESSING AND ARCHIVING PALATAL RUGAE: "IDENTITY BASE" TECHNOLOGY

A. PACIFICI[1], M. GARGARI[2] and L. PACIFICI[1]

[1]Department of Oral and Maxillofacial Sciences, Sapienza University of Rome, Italy; [2]Department of Clinical Science and Translational Medicine, University of Rome "Tor Vergata", Rome, Italy

Received June 26, 2018 – Accepted July 13, 2018

The Authors contributed equally to this work

The palatal rugae, which are anatomically described as folds or wrinkles of the palate, are located on the anterior third of the palate on each side of the palatal raphe and behind the incisive papilla, The use of palatal rugae for personal identification was suggested several years ago, and attracted interest from different researchers which created different classifications, still used in scientific literature. The "identity base" (IB) system has as its object a complex information system and a personal identification protocol by means of three-dimensional palatal scans in digital format. The usefulness of this system is based on the management needs of big data. For example, in the field of forensic odontology, IB can be useful in the identification of a living or cadaver subject; and can estimate the age of a human subject. Moreover, IB stores its associated biometric data. The IB system demonstrated to overcome the issues shown by other similar systems of digital image storage. Furthermore, its high accuracy in the identification process makes IB a reliable tool for institutions in the management of immigrants, as well as in the archiving of people under restrictive measures. Finally, IB is also a system for sharing and processing clinical images, useful in dental prosthetics to reduce the number of steps from the first visit to dental prosthesis. The next generation of big-data archiving will speak the same language as IB: the route has been already set out.

To the Editor,

The palatal rugae are anatomically described as folds or wrinkles of the palate. Pattern and number of the rugae differ between individuals; indeed, the rugae holds the characteristic of a perfect forensic identification factor. The anatomic site of palatal rugae is able to protect them from trauma, furthermore, palatal rugae are resistant to any chemical aggression, and to thermal effects or to decomposition changes (1).

Identity Base: the new tool for personal recognition

The "identity base" (IB) system consists of a complex informatic-process aimed to offer a personal identification protocol by means of three-dimensional palatal scans in digital format. Personal identification system, through the three-dimensional scans of the palate, is a system using a main processor connected to a storage memory, with at least one secondary computer connected to an intraoral scanner (Fig. 1). The main computer and the secondary computer are connected to each other; the main computer has a specific software configured to compare one 3D palatal scan of a human subject that will be subjected to an identification: the identification occurs through the comparison between the scan acquired through the intraoral scanner, and a database of palatal models

Key words: big-data, palatal rugae, forensic odontology, intraoral scanner, oral pathology

Mailing address:
Dr. Andrea Pacifici,
Department of Oral and Maxillofacial Sciences,
Sapienza University of Rome,
Rome, Italy
e-mail: dott.andreapacifici@libero.it

0393-974X (2018)

in 3D format, previously stored in the storage group. Comparison between the scan of the subject and that present in the archive will allow to recognize the subject who has already been inserted in the database. The usefulness of this system is based on the management needs of big data. For example, in the field of forensic odontology, IB can be useful in the identification of a living or cadaver subject. IB can estimate the age of a human subject and store its associated biometric data. An important ability shown by the IB system is a protocol capable of excluding from the detection any discrepancies of palatine wrinkles due to factors that can change the morphology of the same, such as diseases, surgical operations and any other condition able to make a subject unidentifiable.

Operating principles of IB protocol

First, two scans are sampled to standardize the distribution of model-points. It is important to scan the largest area possible of the subject's palate to find the major number of anatomical points to register (Fig. 2A). The two scans are then superimposed using an Iterative Closest Point (ICP) algorithm (Fig. 2B). If the alignment is successful, IB assigns an evaluation of the affinity between the two scans based on the average distance between the two models and the number of aligned points (Fig. 2C).

Preliminary results of IB protocol

All tests were performed on a pool of about 100 scans, some of which belong to to twins, morphologically very similar. After a calibration phase, the algorithm was able to correctly identify the 3 pairs of scans without reporting either false negatives or false positives.

DISCUSSION

A number of different studies investigated the option to use palatal rugae as a unique parameter for individual identification (1). Recent studies aimed

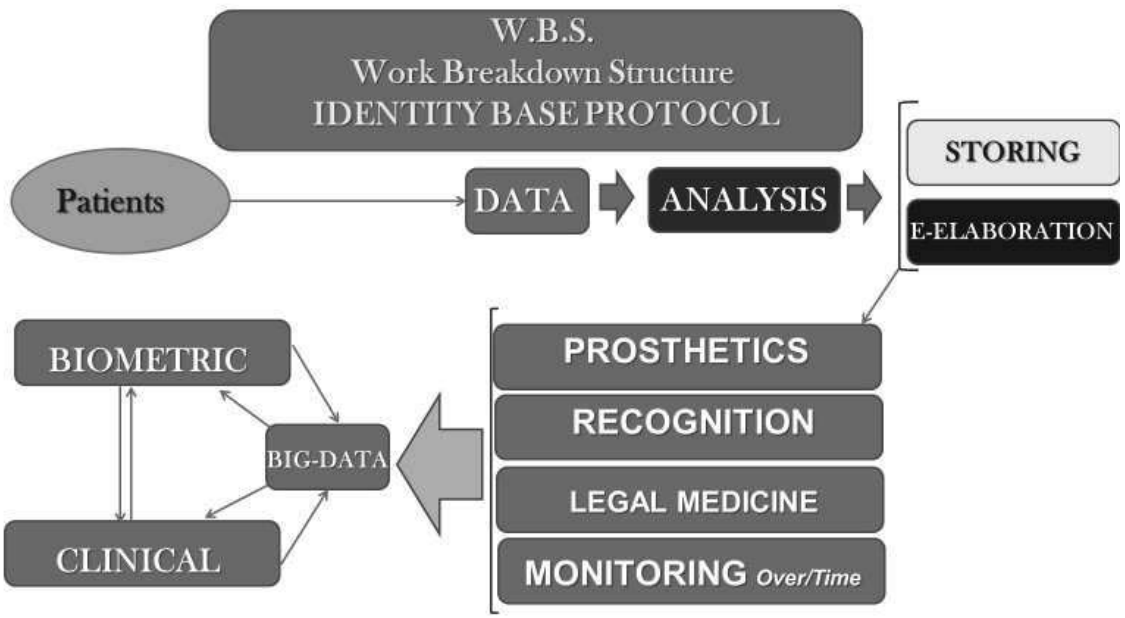

Fig. 1. *Work Breakdown Structure of IB-protocol. Ability of the IB-protocol to serve as big-data storage, as well as a tool for clinical and social professionals. Finally, a strategic use is for unknown people recognition, such as foreigners escaping from wars or low-income countries.*

to identify the palatal rugae patterns differences in males, females, families and identical twins. The reported findings in these studies were in accordance with the results obtained in previous similar studies, and confirmed the role of palatal rugae conformation as an important factor for unique individual identification.

The application of 3D models of a specific portion of the oral cavity for personal identification provides a reliable evaluation of distinctiveness of palatal rugae, based on their anatomical 3D conformations, with consequent applications to individual identification. The studies on tissues were highly improved by stem cell research, as this topic is useful for tissue regeneration in several areas (2-8). Moreover, it has been demonstrated that the same tissues can show different behaviour (6-9) thus, it is useful to find a technique to univocally identify and memorize tissues and biological characteristics.

The IB system demonstrated to overcome the issues of other similar systems of digital storage of images. No biological variations can influence such process, such as oxidative stress, inflammation, smoking habits (10), neoplasia (11) or operator's bias (12).

Furthermore, the high accuracy shown in the identification process makes IB a reliable tool also for institutional bodies in the management of immigrants, as well as in the archiving of subjects under restrictive measures. Finally, IB is also a system for sharing and processing clinical images, which is useful in dental prosthetics to reduce the numbers of steps from first visit to dental prosthesis. The next generation of big-data archiving will speak the same language as IB: the route has been already set out.

ACKNOWLEDGEMENTS

The Authors wish to acknowledge Mr. Alessandro Zurli, Mr. Emanuele Bellini and Mr. Luca Barbieri and the company "ASSI Applicazioni, Soluzioni e Servizi per l'Informatica" for their support in the management of this project and for having improved the results of this pilot study.

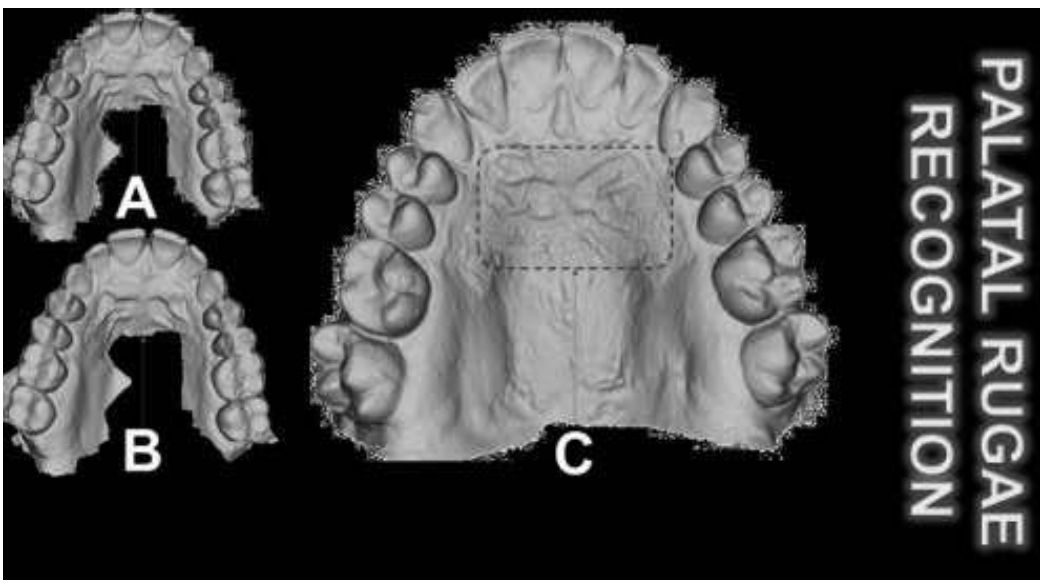

Fig. 2. *IB-protocol with Palatal Rugae Recognition. Eidological methods to find-recruit-achieve the palatal area to identify/find the proper point defining the palatal rugae for individual recognition.*

REFERENCES

1. Maki O, Naoki N, Takashi C, Masayuki F, YojiM, Naofumi Y. Indication and limitations of using palatal rugae for personal identification in edentulous cases. Forensic Sci Int 2008; 176:178-82.
2. Paduano F, Marrelli M, Palmieri F, Tatullo M. CD146 expression influences periapical cyst mesenchymal stem cell properties. Stem Cell Rev 2016; 12(5):592-603.
3. Marrelli M, Pujia A, Palmieri F, et al. Innovative approach for the in vitro research on biomedical scaffolds designed and customized with CAD-CAM technology. Int J Immunopathol Pharmacol 2016; 29(4):778-83.
4. Paduano F, Marrelli M, Amantea M, et al. Adipose tissue as a strategic source of mesenchymal stem cells in bone regeneration: a topical review on the most promising craniomaxillofacial applications. Int J Mol Sci 2017; 18(10).
5. Tatullo M, Falisi G, Amantea M, Rastelli C, Paduano F, Marrelli M. Dental pulp stem cells and human periapical cyst mesenchymal stem cells in bone tissue regeneration: comparison of basal and osteogenic differentiated gene expression of a newly discovered mesenchymal stem cell lineage. J Biol Regul Homeost Agents 2015; 29(3):713-18.
6. Aulino P, Costa A, Chiaravalloti E, et al. Muscle extracellular matrix scaffold is a multipotent environment. Int J Med Sci 2015; 12(4):336-40.
7. Perniconi B, Coletti D, Aulino P, et al. Muscle acellular scaffold as a biomaterial: effects on C2C12 cell differentiation and interaction with the murine host environment. Front Physiol 2014; 5:354.
8. Tatullo M, Simone GM, Tarullo F, et al. Antioxidant and antitumor activity of a bioactive polyphenolic fraction isolated from the brewing process. Sci Rep 2016; 6:36042.
9. Tatullo M, Gentile S, Paduano F, Santacroce L, Marrelli M. Crosstalk between oral and general health status in e-smokers. Medicine (Baltimore) 2016; 95(49):e5589.
10. Marrelli M, Tatullo M, Dipalma G, Inchingolo F. Oral infection by Staphylococcus aureus in patients affected by White Sponge Nevus: a description of two cases occurred in the same family. Int J Med Sci 2012; 9(1):47-50.
11. Tatullo M, Marrelli M, Amantea M, Paduano F, Santacroce L, Gentile S, Scacco S. Bioimpedance detection of oral lichen planus used as preneoplastic model. J Cancer 2015; 6(10):976-83.
12. Marrelli M, Gentile S, Palmieri F, Paduano F, Tatullo M. Correlation between surgeon's experience, surgery complexity and the alteration of stress related physiological parameters. PLoS One 2014; 9(11):e112444.

LETTER TO THE EDITOR

AUGMENTATION OF THE ATROPHIC MAXILLARY SINUS FLOOR: GRAFT STIFFNESS, IMPLANT SHAPE AND LENGTH

L. LA BARBERA[1], S. CORBELLA[2,3,4], S. TASCHIERI[2,3,4], F. GALBUSERA[5], A.B. GIANNÌ[2,6] and L. FRANCETTI[2,3,7]

[1]Laboratory of Biological Structure Mechanics, Department of Chemistry, Materials and ChemicalEngineering "Giulio Natta", Politecnico di Milano, Italy; [2]Department of Biomedical, Surgical and Dental Sciences, Università degli Studi di Milano, Milan, Italy; [3]IRCCS Istituto Ortopedico Galeazzi, Dental Clinic, Milan, Italy; [4]Institute of Dentistry, I. M. Sechenov First Moscow State Medical University, Moscow, Russia; [5]IRCCS Istituto Ortopedico Galeazzi, Milan, Italy; [6]Maxillofacial and Dental Unit, Fondazione IRCCS Cà Granda Ospedale Maggiore Policlinico di Milano, Milan, Italy; [7]Faculty of Medicine, Odontostomatology Clinic, University of Milan, Italy

Received May 11, 2018 – Accepted June 16, 2018

This study investigates the characteristics of load transmission to bone of alternative treatments for posterior maxilla edentulism with relatively limited available bone volume. Implant shape (conical and cylindrical), augmentation technique and the effect of bone-graft stiffness were taken into consideration. The finite element models of the atrophic sinus implanted with short implant were compared to two grafted-sinus models implanted with longer implants, engaged bicortically. Bone-graft stiffness was varied to describe different stages of graft-maturation (from short-term to long-term). Stress and load distributions due to axial and bending loads were compared on the bony structures. In the short-term, axial force is supported almost equally by the cortical layers and the trabecular core, while a bending load is mainly supported by the crestal cortical layer and secondarily by the cortical floor, the bone-graft supported a negligible load. Bicortical engagement produces higher load transfer to the cortical floor under axial load. In the long-term, as the stiffness of the bone-graft increases, the load is transferred progressively towards the grafted region, progressively unloading other structures, particularly the internal cortical layer.

To the Editor,

Bone augmentation techniques have been proposed to obviate the lack of adequate bone volume and density following bone remodelling processes that often respond to the loss of mechanical stimuli, such as in edentulism (1).

With regard to maxillary restoration, the most common situation of insufficient bone volume is found in the lateral and posterior areas, where the anatomy of the maxillary sinus could limit the possibility to place dental implants. Maxillary sinus floor elevation with simultaneous or delayed implant placement is a common surgical procedure that allows to augment the available bone in posterior maxilla, creating the conditions to place a dental implant either simultaneously to the augmentation procedure

Key words: sinus atrophy, bone graft, implant design, finite element

Mailing address:
Luigi La Barbera, Ph.D.
Laboratory of Biological Structure Mechanics,
Department of Chemistry,
Materials and Chemical Engineering
"Giulio Natta", Politecnico di Milano,
Piazza Leonardo da Vinci,32, 20133, Milan, Italy
Tel.: +39 02 2399 4317 - Fax: +39 02 2399 4286
e-mail: luigi.labarbera@polimi.it

0393-974X (2018)

or after a healing period. Different approaches have been described and validated by systematic literature reviews, reporting high long-term implant survival and limited peri-implant marginal bone loss (2, 3). Even though the positive clinical outcome of the placement of short implants (<8 mm) is considered a valuable alternative in terms of survival rates and limited peri-implant bone resorption (2, 3), the choice of the best clinical option is still debated.

The present numerical theoretical study investigated the load transfer occurring at implant-bone/graft interfaces with alternative approaches in terms of graft stiffness, implant shape and length for the treatment of posterior maxilla edentulism. To the best of our knowledge, none of the previous systematically numerical studies has ever investigated the effect of implant design, comparing in particular cylindrical and conical implant shapes when applied to augmentation technique and bone-graft quality (or stiffness): such information may be useful to clinicians in the selection of the best approach to promote graft maturation.

MATERIALS AND METHODS

A simplified finite element model of a portion of a typical atrophic sinus, with an average thickness of 5 mm and cortical layers of 0.7 mm, was created from diagnostic computed tomography (CT) images of an adult female under treatment at the IRCCS Galeazzi Orthopaedic Institute (Fig. 1). The native atrophic sinus was reconstructed in Mimics (Materialise, Leuven, Belgium) and further modified to describe two augmentation scenarios representative of a low bone-graft volume, resulting from the insertion through the pilot drill during sinus-floor elevation, and a high bone-graft volume, obtained by a more invasive procedure where a bony window was opened on the lateral maxilla during surgery. The models were imported in ABAQUS/Standard 6.12 (Dassault Systèmes Ri. Simulia, Waltham, MA, USA), which was used to create and mesh the model (Fig. 2). Six osseointegrated titanium dental implants, differing in shape and length of the threaded portion, were drawn in PTC Creo Parametric 2.0 (Parametric Technology Corporation, Needham, MA, USA) imported in Abaqus and placed in the corresponding sinus/graft model, as follows:

- Model A: *native atrophic sinus* implanted with an implant with *5 mm* endo-osseous threaded part (overall length 10 mm including the abutment), both *conical* and *cylindrical*;
- Model B: *low volume-grafted sinus* implanted with *7.5 mm* endo-osseous part (overall length 12.5 mm), both conical and cylindrical;
- Model C: *high volume-grafted sinus* implanted with a *10 mm* endo-osseous par (overall length 15 mm), both conical and cylindrical.

Quadratic tetrahedral elements were used to discretize all components. Mesh density was progressively refined until the variables of interest (von Mises stress, principal strains) demonstrated a percentage variation less than 5% (convergence criteria). The number of elements ranged between 120,665 and 207,850 (176,409 and 300,794 number of nodes). Every component was modelled using linear elastic material properties: 15 GPa for the cortical bone, 500 MPa for the trabecular and 110 GPa for the implant (with 0.3 Poisson ratio). To possibly represent different stages of bone-graft maturation process, during which the bone-graft remodels from a semi-fluid media to a denser and stiffer tissue, different elastic modulus were assigned to the bone-graft. Therefore, we distinguished between “low” (5 MPa), “medium” (50 MPa) and “high” (500 MPa) modulus (assumed to be equal to trabecular bone hypothesizing the usage of autogenous bone (4), respectively corresponding to short-, mid- and long-term postoperative; a “very high” (5 GPa) bone-graft modulus (sometimes arbitrarily assumed in the literature (5) was also considered as a comparison. Finally, 18 models were compared.

Two loading conditions were considered, applying a load with magnitude 129 N (6) directly on the abutment along the longitudinal axis of the screw (*axial load*) and with an inclination of 45° (*bending load*). The mesial and distal surfaces were constrained in all simulations. To simulate the interaction between the implant and the bone/graft, a surface-based contact with a friction coefficient of 0.3 was assumed (6). The simulations were run in ABAQUS/Standard 6.12 (Dassault Systèmes Ri. Simulia, Waltham, MA, USA).

Each of the 36 simulations was analysed to evaluate the median von Mises stress distribution on bony structures within 2 mm around the implant. The forces supported by the crestal cortical layer, trabecular core, cortical floor and bone-graft were calculated by summing

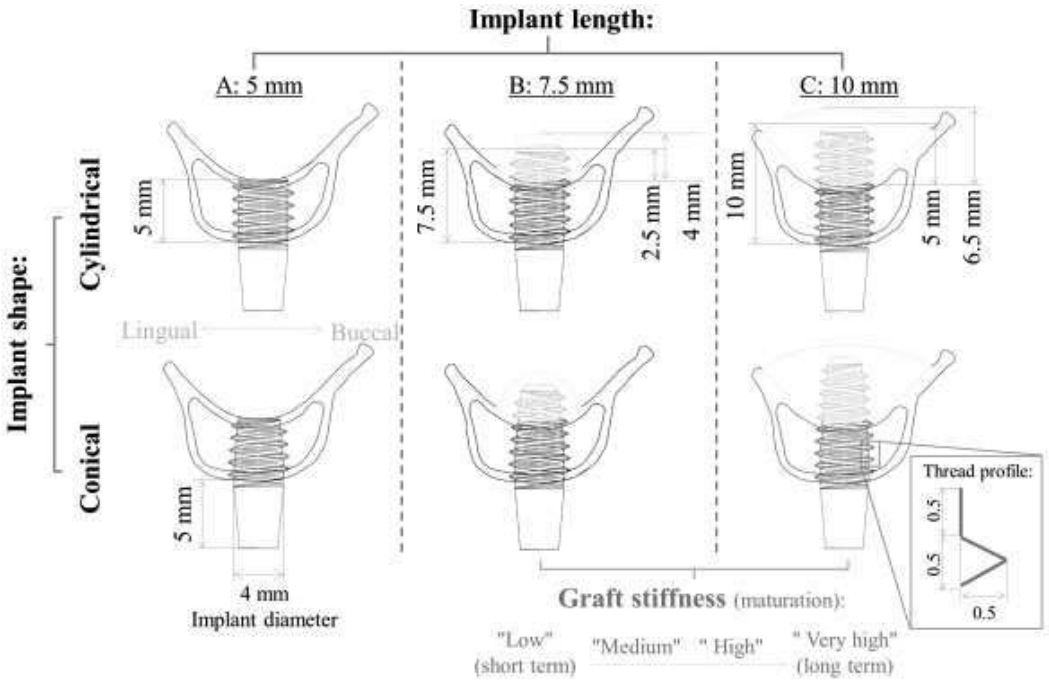

Fig. 1. *Overview of the investigated models, from left to right: native atrophic sinus implanted with a 5 mm endo-osseous implant (Model A), low volume-grafted sinus implanted with a 7.5 mm endo-osseous implant (Model B) and high volume-grafted sinus implanted with a 10 mm endo-osseous implant (Model C). In each condition both cylindrical and conical implants were considered, while graft stiffness (i.e. maturation) was investigated only for Models B and C.*

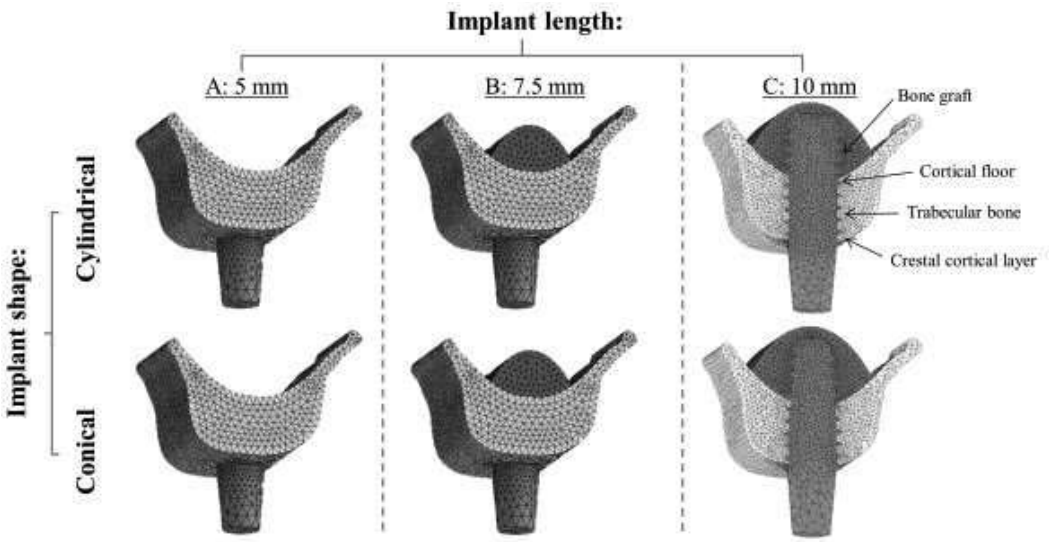

Fig. 2. *Overview of model meshing. Models A and B are fully represented, while a representative cut of Model C highlights mesh refinement around the implant threads.*

the corresponding nodal forces at the interface with the implant. These values were compared to investigate the effect of alternative procedures for the treatment of the atrophic maxillary sinus on load distribution, with varying implant shape (conical *vs* cylindrical) and bone-graft stiffness (or maturation).

RESULTS

Axial load

The comparison between the stress distribution on the bony structures in Models A, B-Low and C-Low did not show any appreciable difference, nor in Models B-Mid and C-Mid (Table I, Fig. 3).

In Model A, the crestal layer and the cortical floor supported, respectively about 27% and 24% of the total axial load, while the trabecular bone about 49%. Despite the crestal layer supporting almost the same load as in Model A (26% Model B-Low and C-Low), the force supported by the trabecular core decreased to about 40%, while it increased to 34% for the cortical floor; the bone-graft supported a negligible amount of the total load (less than 1%).

As the elastic modulus of the bone-graft increased in Models B-Medium and C-Medium, the bone-graft started supporting some load (1% and 3%,

Table I. *Von Mises stress values over the crestal cortical layer, trabecular bone, cortical floor and bone-graft as a function of implant shape, implant length and graft stiffness.*

			Von Mises Stress (MPa) - Axial load				***Von Mises Stress (MPa) - Bending***			
Implant shape	***Implant length***	***Graft quality***	***Crestal cortical layer***	***Trab. bone***	***Cortical floor***	***Bone graft***	***Crestal cortical layer***	***Trab. bone***	***Cortical floor***	***Bone graft***
Conical	***5 mm***	***-***	8.1	1.3	9.0	-	18.7	1.4	13.0	-
	7.5 mm	***Low***	7.3	1.1	8.2	0.0	16.4	1.3	11.4	0.0
		Mid	7.5	1.1	8.2	0.1	16.0	1.3	11.0	0.1
		High	6.4	1.0	7.2	0.6	13.9	1.1	9.2	1.0
		Very high	3.6	0.5	4.4	2.4	11.5	0.7	4.2	3.5
	10 mm	***Low***	7.2	1.2	8.4	0.0	17.9	1.4	11.2	0.0
		Mid	7.2	1.1	8.1	0.1	14.6	1.3	10.2	0.1
		High	5.5	0.9	6.5	0.6	13.6	1.0	6.3	0.8
		Very high	2.4	0.4	2.8	1.8	11.6	0.7	3.4	2.0
Cylindrical	***5 mm***	***-***	6.8	1.1	8.3	-	15.5	1.3	13.4	-
	7.5 mm	***Low***	6.6	1.0	8.0	0.0	15.4	1.3	11.1	0.0
		Mid	7.1	1.1	8.0	0.1	14.4	1.2	10.7	0.1
		High	6.1	0.9	7.0	0.6	14.7	1.1	8.7	1.0
		Very high	3.3	0.5	4.0	2.2	12.4	0.7	4.4	3.5
	10 mm	***Low***	6.6	1.0	8.3	0.0	15.4	1.2	11.7	0.0
		Mid	6.9	1.0	8.1	0.1	14.9	1.1	11.0	0.2
		High	5.1	0.8	6.3	0.5	11.7	0.8	6.2	0.8
		Very high	2.2	0.3	2.7	1.5	9.7	0.5	3.0	1.9

respectively), while a general slight decrease was noticed on other structures.

Differences were much higher for Models B-High and C-High, where the bone-graft supported 11% and 22% of the total axial load, respectively; while the force on the other structures generally decreased (crestal cortical layer: 23% and 19%, respectively; cortical floor: 32% and 28%; trabecular core: 34% and 31%). These trends were confirmed by more significant changes, when a very high bone-graft stiffness was assumed.

The differences found for an implant length of 10 mm (Model C) were higher than for a 7.5 mm (Model B), but the qualitative trend kept the same in all bone-graft qualities.

With regard to implant design, despite a cylindrical shape having involved slightly higher stress values on the cortical floor and bone-graft compared to a conical design (Table I), the load supported by each structure did not highlight any specific trend.

Bending load

Bending involved much higher maximum stresses than an axial load on all bony structures, with the highest stress reached on the crestal layer. The stress field on the bony structures in Models A, B-Low and C-Low did not show any appreciable difference, nor in Models B-Medium and C-Medium (Table I, Fig. 3). Appreciable stress reduction was noticed with higher bone-graft stiffness in B-High/Very high and C-High/Very high models (Table I, Fig. 3).

In Model A, the crestal cortical layer supported about 63% of the total bending load, while the trabecular bone about 10% and the cortical floor only 27%. Although in Model B-Low and C-Low the external cortical layer supported almost the same load as Model A, the force supported by the trabecular core slightly increased to 12%, while it decreased to about 25% for the internal cortical layer; the bone-graft supported a negligible amount of the total load (less than 2%).

As the elastic modulus of the bone-graft increased in Models B-Medium and C-Medium, the bone-graft started supporting some load (2% and 4%, respectively), slightly unloading the internal cortical layer. The observed trends were confirmed by more significant changes only for the crestal cortical layer and bone-graft, when a very high bone-graft stiffness was assumed.

Differences were much higher for Models B-High and C-High, where the bone-graft supported a 10% and a 17% of the total load amount, respectively, unloading the force applied on the internal cortical layer to 16% and 10% (only marginal differences

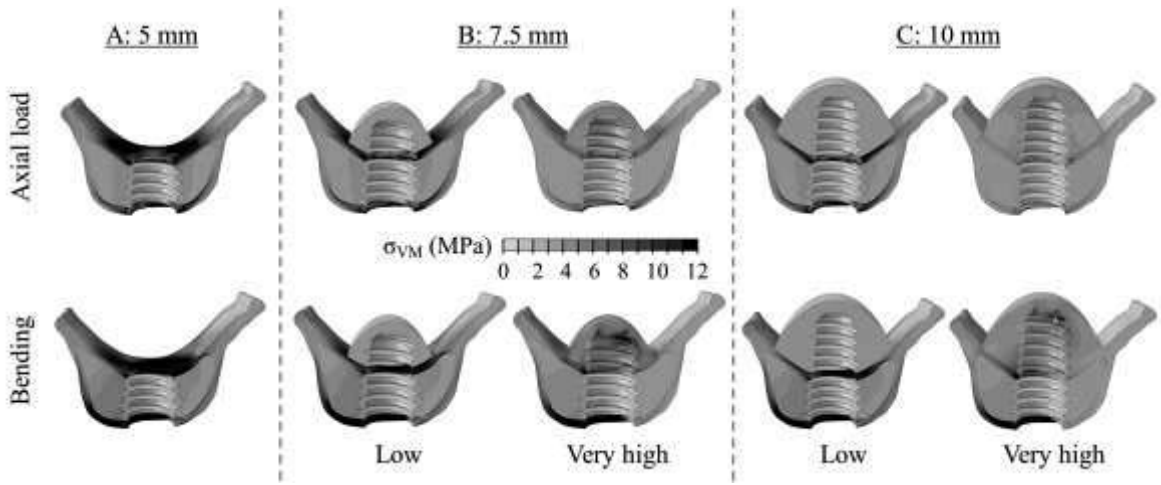

Fig. 3. *Von Mises stress maps in axial (top) and bending (bottom) loading condition varying implant length and bone-graft stiffness. Only conical model results are depicted, as no differences could be appreciated compared to cylindrical cases; only extreme scenarios with "low" and "very high" graft-stiffness are reported.*

less than 2% were observed on other structures). The differences found for an implant length of 10 mm (Model C) were higher than for a 7.5 mm (Model B), but the qualitative trend kept the same for all bone-graft qualities. The comparison between conical and cylindrical implants in terms of stress (Table I) and load distribution on the bony structures did not lead to any significant difference.

DISCUSSION

The present theoretical approach offered the great advantage to finely control specific study parameters that would exhibit a huge intrinsic variability in real clinical setting and would have a confounding effect on the final outcome. However, the results here reported should be interpreted with great care, to be correctly translated to clinical practice.

A longer implant is related to a higher axial load transfer on a larger volume by the cortical bone of the maxillary floor. Although the clinical results are still controversial (7), our results may provide a biomechanical rationale to prefer bicortical anchorage instead of a proximal monocortical engagement to promote a distal load transfer (8).

The results of the present study demonstrate that in the early healing phase, when the bone graft has a negligible stiffness, the primary stability of the implants placed simultaneously to sinus floor elevation is essentially due to the native bone (9, 10), both considering axial an non-axial loads. In the later healing phases, as the bone-graft is entirely remodelled, becoming trabecular, the load transfer to the graft region increases. Even though clinical evidence is still lacking, this result may suggest that the cortical floor, being significantly unloaded particularly in bending, could undergo bone resorption in the early healing phase and an immediate loading should be somehow avoided. However, using longer implants may be beneficial in any case to promote the load transfer to a larger bone volume (11) and towards more apical structures, theoretically stimulating the graft maturation process.

Although the results are comparable, a cylindrical implant shape may promote slightly higher forces to the bone-graft due to the higher area available to transfer the occlusal force, while a conical shape demonstrates slightly higher stresses in the crestal regions, possibly related to the lower available area (11). Interestingly, a higher marginal bone resorption has been reported for cylindrical implants compared to conical ones (12).

To conclude, the present study supports the idea that bicortical engagement may provide a shift of the supported force towards more apical bony structures, which may be beneficial to stimulate and promote bone-graft maturation. Such process can be even more effective as longer implants are used and as the bone-graft remodels towards trabecular-like bone.

REFERENCES

1. Lutz R, Neukam FW, Simion M, Schmitt CM. Long-term outcomes of bone augmentation on soft and hard-tissue stability: a systematic review. Clin Oral Implants Res 2015; 26(Suppl 11):103-22.
2. Del Fabbro M, Corbella S, Weinstein T, Ceresoli V, Taschieri S. Implant survival rates after osteotome-mediated maxillary sinus augmentation: a systematic review. Clin Implant Dent Relat Res 2012; 14(Suppl 1): e159-68.
3. Thoma DS, Zeltner M, Husler J, Hämmerle CH, Jung RE. EAO Supplement Working Group 4 - EAO CC 2015 Short implants versus sinus lifting with longer implants to restore the posterior maxilla: a systematic review. Clin Oral Implants Res 2015; 26(Suppl 11):154-69.
4. Tepper G, Haas R, Zechner W, Krach W, Watzek G. Three-dimensional finite element analysis of implant stability in the atrophic posterior maxilla: a mathematical study of the sinus floor augmentation. Clin Oral Implants Res 2002; 13:657-65.
5. Huang HL, Fuh LJ, Ko CC, Hsu JT, Chen CC. Biomechanical effects of a maxillary implant in the augmented sinus: a three-dimensional finite element analysis. Int J Oral Maxillofac Implants 2009; 24(3):455-62
6. Yan X, Zhang X, Chi W, Ai H, Wu L. Association between implant apex and sinus floor in posterior maxilla dental implantation: A three-dimensional finite element analysis. Exp Ther Med 2015; 9:868-76.
7. Ivanoff CJ, Grondahl K, Bergstrom C, Lekholm U,

Brånemark PI. Influence of bicortical or monocortical anchorage on maxillary implant stability: a 15-year retrospective study of Branemark System implants. Int J Oral Maxillofac Implants 2000; 15:103-10.

8. Huang HL, Hsu JT, Fuh LJ, Tu MG, Ko CC, Shen YW. Bone stress and interfacial sliding analysis of implant designs on an immediately loaded maxillary implant: a non-linear finite element study. J Dent 2008; 36:409-17.
9. Hsu A, Seong WJ, Wolff R, Zhang L, Hodges J, Olin PS, Hinrichs JE. Comparison of initial implant stability of implants placed using bicortical fixation, indirect sinus elevation, and unicortical fixation. Int J Oral Maxillofac Implants 2016; 31:459-68.
10. Kuchler U, Chappuis V, Bornstein MM, Siewczyk M, Gruber R, Maestre L, Buser D. Development of Implant Stability Quotient values of implants placed with simultaneous sinus floor elevation - results of a prospective study with 109 implants. Clin Oral Implants Res 2016; 28(1):109-15.
11. Petrie CS, Williams JL. Comparative evaluation of implant designs: influence of diameter, length, and taper on strains in the alveolar crest. A three-dimensional finite-element analysis. Clin Oral Impl Res 2005; 16:486-94.
12. Blanes RJ, Bernard JP, Blanes ZM, Belser UC. A 10-year prospective study of ITI dental implants placed in the posterior region. I: Clinical and radiographic results. Clin Oral Implants Res 2007; 18:699-706.

JOURNAL OF BIOLOGICAL REGULATORS & HOMEOSTATIC AGENTS Vol. 32, no. 5, 1303-1309 (2018)

LETTER TO THE EDITOR

INTRA-ARTICULAR HYALURONIC ACID INJECTIONS FOR HIP OSTEOARTHRITIS

G. LETIZIA MAURO[1], D. SCATURRO[1], A. SANFILIPPO[2] and M.G. BENEDETTI[3]

[1]Rehabilitation Unit, Paolo Giaccone Hospital, Palermo, Italy; [2]Orthopaedic Unit, Paolo Giaccone Hospital, Palermo, Italy; [3]Physical Medicine and Rehabilitation Unit, Istituto Ortopedico Rizzoli, Bologna, Italy

Received February 12, 2018 – Accepted May 15, 2018

Although viscosupplementation has been used in the past few years both for knee and hip osteoarthritis (OA), the number of intra-articular injections and the interval between doses still remains an undetermined subject. The aim of this open retrospective study was to evaluate the clinical and functional outcome in patients with mild-moderate hip OA treated with a course of 1, 2 or 3 Hyaluronic Acid (HA) intra-articular injections. Ninety-six patients were included: 19 patients received only one injection, 24 received two injections, and 44 received three injections. Age, sex, VAS for pain and WOMAC score before each intra-articular injection, number of intra-articular injections, reasons for interrupting the treatment, adverse events, time between HA injections, and number of patients who had a total hip replacement were retrieved from the medical records of each patient. VAS and WOMAC scores were obtained from all patients also at a mean follow-up of 7 months after the last hip injection. All patients who received 1, 2 or 3 hip injections improved in VAS and WOMAC score. Three intra-articular injections provided a better outcome in terms of pain reduction compared to 1 or 2 injections. Intrarticular injections for mild-moderate hip OA were demonstrated to be effective in reducing pain and improving function. A full course of three injections provided the best result in pain control.

To the Editor,

Viscosupplementation involves the use of a hyaluronic acid (HA) solution which integrates and substitutes the synovial fluid in the osteoarthritic joints. Data from literature indicate that intra-articular HA injections have structural modifying activity as well as pain relief effect (1). HA treatment has been widely used for knee osteoarthritis (OA), and subsequently for hip OA, where it has been demonstrated to be safe and effective (2-4). In particular, intra-articular HA injections should be considered for patients as a first-line treatment of OA, especially in those with comorbidities, since it may help avoid NSAIDS/analgesic consumption and consequent adverse events (5). Nonetheless, HA efficacy on symptoms has only been demonstrated in mild or moderate OA, while severe OA does not seem to benefit from this treatment (6). Eco-guided intra-articular injections represent, with uniform agreement, the safest approach (6). Despite evidence showing that HA viscosupplementation is the best conservative treatment for hip OA before the indication for surgery, there is a lack of general consensus regarding the standardization of methodology for HA intra-articular injections in hip OA (7). In particular, there is no general agreement on

Key words: hyaluronic acid intra-articular injections, hip OA, outcome, pain

Mailing address:
Dr Maria Grazia Benedetti,
Physical Medicine and Rehabilitation Unit,
Rizzoli Orthopaedic Institute,
Via Pupilli 1, 40136 Bologna, Italy
Tel.: +39 051 6366236 - Fax: +39 051 332392
e-mail: benedetti@ior.it

0393-974X (2018)

DISCLOSURE: ALL AUTHORS REPORT NO CONFLICTS OF INTEREST RELEVANT TO THIS ARTICLE.

the number of injections and the treatment schedule, ranging from 1 to 4 injections administered weekly, monthly or even every six months (6, 7).

Based on these observations, this study evaluated retrospectively the clinical and functional outcome in a population of patients with mild-moderate hip OA, treated with HA undergoing a cycle of 1, 2, or 3 intra-articular injections in the hip.

MATERIALS AND METHODS

Design of the study

This is an open retrospective study, without a control group, on patients suffering from painful primary hip OA and referring, between 2015 and 2016, to our rehabilitation outpatients clinic. Ethical approval of the study was obtained from the Institution where the treatment was performed (N.604/2017). All patients signed an informed consent form before treatment and at follow-up.

The following information was retrieved from the medical records of each patient: age, sex, type of HA injected, VAS score for pain intensity and WOMAC registered before each intra-articular injection, number of intra-articular injections and reasons for interrupting the treatment, adverse events, time between HA injections, and number of patients who had a total hip replacement (THR). In order to evaluate the mid-term outcome of the hip HA injection treatment, all treated patients were called on January 2017 for a follow-up (FU) of VAS score and WOMAC assessment.

Patients and treatment

Among all patients referring to the outpatient clinic for painful hip osteoarthritis, and who received HA intra-articular injections, 96 were enrolled according to the following inclusion criteria: affected by symptomatic primary hip OA based on the ACR criteria (8), radiographic grade less than 3 according to Kellgren Lawrence, not responding to treatment with physical therapies and NSAID. Exclusion criteria were: the concomitant use of anticoagulant therapy, rheumatologic diseases, major hip dysplasia and other severe concomitant musculoskeletal, neurological or vascular diseases.

Different commercial HA products were used: Hyalubrix, Sinovial HL, Orthovisc, Donegal. Intra-articular injections have always been performed under ultrasound guidance, in agreement with the indications of Migliore et al, (9), with the patient in supine position and the hip rotated by 15-20 degrees. The same clinician performed all injections.

Outcome measures

Hip pain during movement in the week before the visit was measured based on a 0–10 cm VAS scale (0= no pain, 10= worst imaginable pain), and physical function by the Western Ontario McMaster Universities Osteoarthritis Index (WOMAC). The Likert Scale version 3.1 was used to calculate a total WOMAC score by summing the items for all the three subscales.

Statistical analysis

Continuous variables were reported as mean ± standard deviation or mean and 95% confidence intervals. The Kolmogorov Smirnov test was used to test normality. The Levene test was used to test homoscedasticity. The Repeated Measures General Linear Model (GLM) with post hoc Sidak pairwise test for multiple comparisons was performed to compare normally distributed scores at different follow-ups within groups. Kruskall Wallis with Post-hoc Mann Whitney paired analysis with Bonferroni correction was used for comparison among groups at basal time and at follow-up. GLM analysis was used also to explore the possible influence of sex, age, interval between injections and number of injections on VAS and WOMAC scores. Kendall Tau correlation was used to assess correlation between ordinal variables.

All statistical analyses were considered significant for $p<0.05$ and were performed using SPSS v.19.0 (IBM Corp, Armonk, NY, USA).

RESULTS

The patients included 59 females and 37 males, mean age 68.3 years (SD 11.8 range 34-89), six of whom had injections in both hips, for a total of 102 hips. Twenty-eight patients received only one injection (1 in both hips) (Group 1), 24 patients received two injections (Group 2), 44 patients received three injections (5 in both hips) (Group 3). Reasons for not completing the therapy cycle were: pain relief (20 patients), no benefit or referring to other hospital close to their town of provenance (24

patients), other health problems (2 patients), cost of the therapy (5 patients), THR (1 patients) or waiting for THR (5 patients).

Patients who received one intra-articular injection were monitored at a mean follow-up of 6 months (range 0.9-16). Patients who received two intra-articular injections had an interval of 2.7 months (range 0.9-9.8) between the first (T0) and the second injection (T1), and 7 months (range 0.9-19.9) between the second injection and the follow-up. Patients who received three intra-articular injections had a mean interval of 1.7 months (range 0.5-2.8) between the first (T0) and the second injection (T1), and of 2.1 months (range 0.4- 7.5) between the second and the third (T2) injection. Follow-up assessments were performed at an interval of 8.3 (range 1.4-20) months from the last HA intra-articular injection. No differences were found for age, sex, time between injections and follow-up among the three groups.

Adverse events and changes in VAS and WOMAC

No systemic adverse events were detected during treatment. Local side effects, recorded by interviewing the patients at each follow-up, consisted in pain, oedema and ecchymosis at the site of injection in three different patients. One patient referred a feeling of muscular heaviness at the hip.

Analysis within Groups

GLM repeated measure evidenced that VAS score significantly decreased in all Groups up to the follow-up (Table I, Fig. 1). Post hoc analysis demonstrated significant differences at all time points for Group 3 ($p<0.0005$), while in Group 2 VAS reduction was

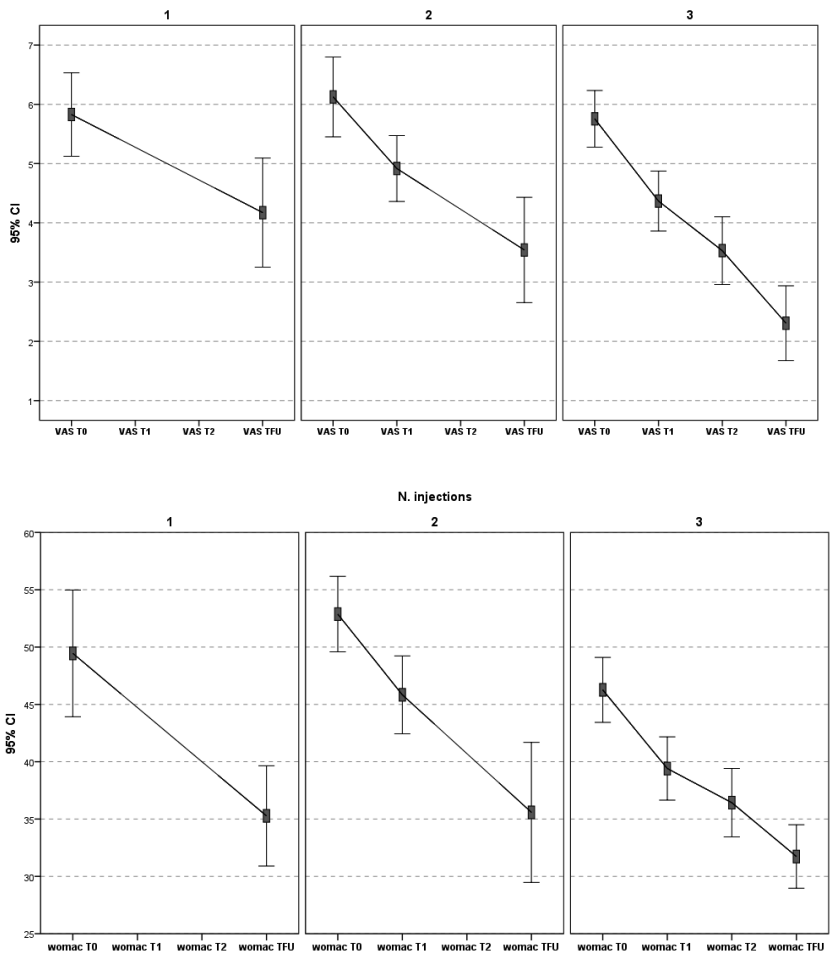

Fig. 1. *VAS pain and WOMAC score along the follow-up with respect to the number of hip injections.*

Table I. *VAS pain and WOMAC in the three Groups along the follow-up.*

		General Linear Mode repeated measures					Sidak test as Post hoc pairwise comparison					
VAS pain		**T0**	**T1**	**T2**	**TFU**		**T0 *vs* T1**	**T0 *vs* T2**	**T0 vs TFU**	**T1 *vs* T2**	**T1 *vs* TFU**	**T2 *vs* TFU**
Group 1 (28 pts -29 hips)	*Mean*	5.8			4.2	p<0.0005						
	CI 95%	5.1-6.5			3.2-5.1							
Group 2 (24 pts)	*Mean*	6.1	4.9		3.5	p<0.0005	<0.0005		<0.0005		=0.001	
	CI 95%	5.4-6.8	4.4-5.5		2.6-4.4							
Group 3 (44 pts- 49 hips)	*Mean*	5.7	4.4	3.5	2.3	p<0.0005	<0.0005	<0.0005	<0.0005	<0.0005	<0.0005	<0.0005
	CI 95%	5.3-6.2	3.9-4.9	2.9-4.1	1.7-2.9							
WOMAC												
Group 1 (28 pts -29 hips)	*Mean*	49.4			35.3	p<0.0005						
	CI 95%	43.9-55			30.9-39.6							
Group 2 (24 pts)	*Mean*	52.9	45.8		35.6	p<0.0005	<0.0005		<0.0005		=0.001	
	CI 95%	49.6-56.2	42.4-49.2		29.5-41.7							
Group 3 (44 pts- 49 hips)	*Mean*	46.3	39.4	36.4	31.7	p<0.0005	<0.0005	<0.0005	<0.0005	<0.0005	<0.0005	<0.0005
	CI 95%	43.4-49.1	36.6-42.2	33.4-39.4	29-34.5							

less marked between the second injection (T1) and follow-up (TFU) (p=0.001). WOMAC score had the same trend.

Comparison among the three Groups

Kruskall Wallis with Mann Whitney post hoc analysis showed no difference of VAS at T0 and a significant difference of VAS at TFU (p=0.002), with significant differences also between Group 1 and Group 3 (p=0.03). WOMAC at T0 was significantly different between the three groups (p=0.02) with significant differences between Group 1 and Group 3 (p=0.03), while no difference was found at TFU (Table II). In order to control differences found at T0, statistical analysis was conducted also on delta percent between TFU and T0, which confirmed only a significant difference in VAS (p=0.003) with no differences between groups 1-2, and 2-3, while group 1 was significantly different from group 3 (p=0.003).

Analysis of factors influencing VAS and WOMAC at follow-up

Although sex, age and time between injections were not statistically different among groups, GLM analysis was used to explore the possible influence of these variables on the outcome. While no influence of age at TFU was found for VAS (p=0.316 partial eta-squared=0.011), sex (p<0.0005, partial eta-squared 0.290) and the number of injections (p=0.001, partial eta-squared 0.989) had an influence on VAS at TFU.

However, when evaluating the delta percentage of VAS improvement between T0 and TFU,

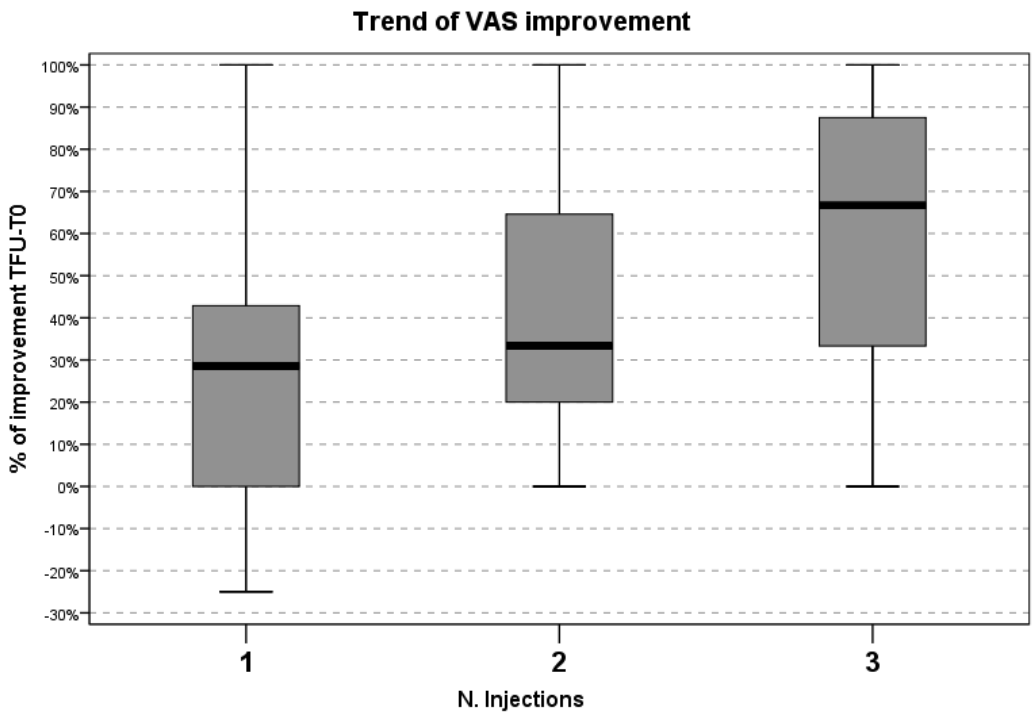

Fig. 2. *Trend of VAS pain improvement as delta percentage between follow-up and baseline score according to number of injections.*

Table II. *Comparison among groups at basal time and at follow-up.*

	Group 1 (28 pts - 29 hips)	**Group 2** (24 pts)	**Group 3** (44 pts - 49 hips)	**Kruskall Wallis**	**Post-hoc Mann Whitney paired analysis with Bonferroni correction**		
	Mean (SD)	**Mean (SD)**	**Mean (SD)**		**Group 1 *vs* Group 2**	**Group 2 *vs* Group 3**	**Group 1 *vs* Group 3**
VAS Pain T0	5.8 (1.8)	6.1 (1.6)	5.7 (1.7)	NS			
VAS Pain FU	4.2 (2.4)	3.5 (2.1)	2.3 (2.2)	p=0.002	p=0.99	p=0.087	*p=0.003*
WOMAC T0	49.4 (14.5)	52.9 (7.8)	46.3 (9.8)	p=0.004	p=0.99	*p=0.03*	p=0.2
WOMAC FU	35.3 (11.5)	35.6 (14.5)	31.7 (9.6)	NS			
Delta% VAS Pain FU – T0	31.9 (33.8)	42.2 (32.2)	60.7 (33.9)	p=0.003	p=0.925	*p=0.137*	*p=0.003*
Delta% WOMAC FU -T0	29.1 (9.8)	33.1 (25.8)	30.5 (17.2)	NS			

corrected for age, sex, and time between injections, only the number of injections was still significant. The best result was obtained with 3 injections, with no effect of sex, while Group 2 showed an intermediate result (Fig. 2).

DISCUSSION

The present retrospective study demonstrated the effectiveness of HA injections in hip OA at a mean FU of 7 months after the last injection, without major adverse events. The administration of 3 injections was more effective compared to 1 or 2 injections, providing a greater reduction of pain, but not of a greater improvement of function as measured by WOMAC. Based on the evidence for the knee and the recommendation of Tikiz (10), we performed intra-articular injections at approximately two-month intervals. However, while for the knee a consensus has almost been reached on the number of intra-articular injections, i.e. 3, one week apart (1), there is no consensus on the number and the interval between injections for hip OA: Pourbager (11) and Qvistgaard (12) suggested an interval of at least 2 weeks between injections, Van der Bekerom (3) reported that patients who had 4 weekly intra-articular injections in the hip achieved the best results, while Henrotin (6) reported 3 weekly injections as optimal treatment. Comparison of findings in the present study was also difficult for the different instruments used to measure the functional outcome in literature. Furthermore, due to the small sample of patients for each commercial HA used, it was not possible to compare their different effectiveness. However, even in literature no difference in terms of product employed is reported (3). A limitation of the study is that a control group could not be individuated, and that other possible therapies undertaken by patients during the HA treatment, and which could have influenced the results, were not registered.

In conclusion intrarticular injections for mild-moderate hip OA were demonstrated to be effective in reducing pain and improving function. A full course of three injections, with a mean interval of two months, determined a significantly greater reduction of pain compared to 1 or 2 injections.

ACKNOWLEDGEMENTS

The Authors are grateful to Elettra Pignotti, Statistician, for the support in statistical analysis.

REFERENCES

1. Migliore A, Procopio S. Effectiveness and utility of hyaluronic acid in osteoarthritis. Clin Cases Miner Bone Metab 2015; 12:31-3.
2. Fernández López JC, Ruano-Ravina A. Efficacy and safety of intraarticular hyaluronic acid in the treatment of hip osteoarthritis: a systematic review. Osteoarthritis Cartilage 2006; 14:1306-11.
3. van den Bekerom MP, Lamme B, Sermon A, Mulier M. What is the evidence for viscosupplementation in the treatment of patients with hip osteoarthritis? Systematic review of the literature. Arch Orthop Trauma Surg 2008; 128:815-23.
4. Leite VF, Daud Amadera JE, Buehler AM. Viscosupplementation for hip osteoarthritis: a systematic review and meta-analysis of the efficacy for pain, disability and adverse events. Arch Phys Med Rehabil 2018; 99(3):574-83
5. Zhang W, Moskowitz RW, Nuki G, et al. OARSI recommendations for the management of hip and knee osteoarthritis, Part II: OARSI evidence-based, expert consensus guidelines. Osteoarthritis Cartilage 2008; 16:137-62.
6. Henrotin Y, Raman R, Richette P, et al. Consensus statement on viscosupplementation with hyaluronic acid for the management of osteoarthritis. Semin Arthritis Rheum 2015; 45:140-9.
7. Piccirilli E, Oliva F, Murè MA, Mahmoud A, Foti C, Tarantino U, Maffulli N. Viscosupplementation with intra-articular hyaluronic acid for hip disorders. A systematic review and meta-analysis. MLTJ 2016; 6:293-99.
8. Altman R, Alarcón G, Appelrouth D, et al. The American College of Rheumatology criteria for the classification and reporting of osteoarthritis of the hip. Arthr Rheum 1991; 34:505-14.
9. Migliore A, Tormenta S, Massafra U, et al. 18-month observational study on efficacy of intraarticular hyaluronic acid (Hylan G-F 20) injections under ultrasound guidance in hip osteoarthritis. Reumatismo

2006; 58:39-49.
10. Tikiz C, Unlü Z, Sener A, Efe M, Tüzün C. Comparison of the efficacy of lower and higher molecular weight viscosupplementation in the treatment of hip osteoarthritis. Clin Rheumatol 2005; 24:244-50.
11. Pourbagher MA, Ozalay M, Pourbagher A. Accuracy and outcome of sonographically guided intra-articular sodium hyaluronate injections in patients with osteoarthritis of the hip. J Ultrasound Med 2005; 24:1391-95.
12. Qvistgaard E, Christensen R, Torp-Pedersen S, Bliddal H. Intra-articular treatment of hip osteoarthritis: a randomized trial of hyaluronic acid, corticosteroid, and isotonic saline. Osteoarthritis Cartilage 2006; 14:163-70.

JOURNAL OF BIOLOGICAL REGULATORS & HOMEOSTATIC AGENTS Vol. 32, no. 5, 1311-1315 (2018)

LETTER TO THE EDITOR

"GUIDELINES FOR THE PREVENTION AND CONTROL OF LEGIONNAIRE'S DISEASE IN ITALY": GUIDELINES OR GUIDANCE?

S. DITOMMASO, M. GIACOMUZZI, E. RICCIARDI and C.M. ZOTTI

Department of Public Health and Pediatrics, University of Turin, Turin, Italy

Received April 19, 2018 – Accepted July 26, 2018

The creation of guidelines is a methodologically complex activity that requires technical expertise, resources and time. Methods of guideline production must meet at least these three criteria: multidisciplinarity, systematic review, and ranked recommendations. In May 2015, the new "Guidelines for the prevention and control of Legionnaire's disease" were published on the website of the Italian Ministry of Health in order to "gather, update and integrate in a single document all the previous national recommendations published". The critical review of the document has led us to conclude that this document does not comply with these three criteria, and we emphasize that guidelines should make decision-making easier, considering the various scientific approaches to a health problem and choosing the one considered most effective. Therefore, the persons responsible for the development of guidelines should strive to widely adopt and use current standards for the development of guidelines as a means to improve patient care and health outcomes.

To the Editor,

The creation of guidelines is a methodologically complex activity that requires technical expertise, resources and time. Too often, the production of "guidelines" does not go through a optimal path of preparation that will ensure the highest degree of appropriateness of interventions, minimizing the variability of the decisions related to the consistency of knowledge and subjectivity in defining care strategies.

A fundamental problem in the methodological approach for drafting guidelines concerns clinical documents. As defined in the Institute of Medicine (IOM) 1992 report (1), practice guidelines are "systematically developed statements to assist practitioner and patient decisions about appropriate health care for specific clinical circumstances". Medical review criteria are "systematically developed statements that can be used to assess the appropriateness of specific health care decisions, services, and outcomes" (1).

The consensus of experts, which is based on experience and literature available on some topics (often limited), can be prudent advice, often common sense, but not the result of scientific evidence. It is provided for the assessment of feasibility in clinical practice, considering the organization involved in implementation. Many guidelines have been developed by the so-called "GOBSAT" (Good Old Boys Sat Around the Table) method (2). This expression refers to the unstructured manner by which a group of self-selected experts discuss their opinions (often subjective), which are often actually put into writing by only a single participant.

Key words: legionella, guidelines, prevention

Mailing address:
Savina Ditommaso, B.Sc.,
Department of Public Health and Pediatrics,
University of Turin,
P.zza Polonia 94, 10126, Turin, Italy
Tel.: +39 0116705841 - Fax: +39 0116705881
e-mail: savina.ditommaso@unito.it

0393-974X (2018)

Methods of guideline production must meet at least these three criteria: multidisciplinarity, systematic review, and ranked recommendations (3, 4).

Multidisciplinary participation is essential to ensure not only that the guideline is valid, but also that it is valued by all the members of the multidisciplinary team to be incorporated successfully into practice.

Guidelines not based on a systematic literature review have been widely criticized as not reflecting current knowledge and being susceptible to bias. To minimize potential sources of bias, the literature should be identified according to an explicit search strategy, selected according to defined inclusion criteria, and assessed against consistent methodological standards.

Guideline recommendations must be graded to differentiate between strong evidence and weak evidence. An important goal for guidelines is to increase efficiency in the use of health care resources. Clearly, if guidelines are to improve the cost-effectiveness of health care, greater attention must be given to economic analysis.

Guidelines can be misused in the legal-medical field as a legal excuse for negligent behaviour of managers in the performance of their responsibilities (in healthcare or in tourist facilities). In legal terms, it is unquestionable that the judicial authorities during the investigative or judgemental phase, in the retrospective analysis of the health professional's behaviour, ask to see whether this complied with the criteria of the best science available at that moment, which could be a guideline supported by medical science. The lack of compliance with the document by negligence, imprudence and inexperience may result in the application of sanctions and fines. Moreover, in addition to administrative responsibility, one could also incur a penalty (for personal injury) and civil liability.

Another indirect implication is damage to image/reputation. For example, confirmed cases of Legionellosis acquired during a stay abroad in hotels in the EU/EEA countries are registered in a European database (Eldsnet) and allows tour operators to exclude those hotels from tourist destinations (5).

In May 2015, on the website of the Italian Ministry of Health, the new "Guidelines for the prevention and control of Legionnaire's disease" were published to "gather, update and integrate in a single text all the recommendations that had been published in previous national regulations and guidance" (6). Critical reading of the document has led us to propose some reflections on certain aspects of the document that may cause legal problems or increase costs of water safety plans.

DISCUSSION

The first consideration concerns the incubation time: the definition of incubation time has important consequences in the classification of a case as nosocomial or community-acquired. Considering too short a period could lead to the lack of inquiry or further insights by the competent authorities (i.e., the Local Health Agency and the Regional Environmental Protection Agency) during the epidemiological investigation, which could lead to the misclassification of cases (mistaking a nosocomial case for a community case).

The new Italian guidelines suggest gathering accurate information on possible exposure to risk in the 10 days preceding the onset of symptoms (legionellosis has an incubation period from 2 to 10 days): this range is reported by many international documents, which underline that "….in rare cases the incubation period can be up to 19 days. For routine surveillance purposes the exposure data are collected for 2-10 days before the onset of symptoms; however, in case of outbreak where it is important to consider a wide range of possible sources of infection it is often desirable to consider an incubation period of 14 days"(7). "When possible it is proper to collect data concerning exposure in the two weeks before the onset of symptoms"(8). Many scientific papers have related particular situations with incubation times of over ten days (9–14). Therefore, the definition of a case of Legionnaires' disease has a great impact in the judicial field.

A second consideration concerns environmental sampling, which is an essential tool for outbreak investigation and risk assessment: the novelty compared to previous international documents is that these guidelines advise the confirmation of positive

results from samples taken from the same outlets when the percentage of positive samples exceeds the cut-offs of 20% (in hotels, retirement homes, boarding schools, accommodations in general) and 30% (in hospitals). We need to remember that drinking water plumbing systems show great variability regarding the occurrence and concentration of microbial load (due to variables such as temperature, flushing, and concentration of biocides), so the results obtained from samples taken on different days from the same outlets are difficult to compare because water plumbing systems may be regarded as an ecological system and each outlet as an ecological niche.

The threshold values set at 20% and at 30% for positive points are questionable. A literature review published in 2012 (15) identified that 31 peer-reviewed publications reported matched data. The authors abstracted a total of 206 data points representing 119 hospitals and determined that the proposed 30% positivity metric has 59% sensitivity and 74% specificity (i.e., a 41% false-negative rate and a 26% false-positive rate). This metric was initially proposed by Best et al. in 1983 (16) and continues to be cited in research examining the relationship between *Legionella* concentrations in water and health care-acquired Legionnaires' Disease. It has been adopted by several government agencies. No publication has addressed the cut-off of 20%.

There is no evidence in the scientific literature about the usefulness of the positive outlets' resampling only to confirm the result.

In addition to the scientific reasons that led us to not share this protocol for environmental monitoring, there is an economic reason: resampling determines the increase of the costs involved but does not ensure the choice of the best option.

The latter consideration concerns the occupational risk in dentistry: to reduce patient exposure to potentially contaminated aerosols, the authors recommend the installation of filters (pore-size of 0.2 micrometre) upstream of the handpieces, which are capable of retaining the microorganisms originating from inside the circuit. The dental industry abandoned this practice several years ago because some negative aspects had been identified (17, 18): the need to replace the filters at least daily due to clogging caused by the attachment of bacteria and the subsequent microbial growth within the device that becomes an additional source of contamination. Moreover, other technical problems include failure in the recovery of the spray when stopping the instrument, with the subsequent dripping from the handpiece and gradual loss of the spray's stream up to its complete disappearance.

Regarding risk assessment, the authors (6) recommend analysis for monitoring *Legionella* contamination in the output water of the dental unit at least once a year and whenever there is a case of illness. In respect to this indication, we can highlight that the data reported in the literature (19–21) show that the frequency of dental units positive for *Legionella* (with the culture method) are highly variable (ranging from 0%-100%). Negative samples with culture can actually contain *Legionella* that is viable but not culturable due to stressful environmental factors (low temperature, presence of other bacterial producers of bacteriocins, *Legionella* in encysted amoebae) (22), and the results are also widely influenced by the laboratory method used. Thus, only taking an annual environmental sampling of dental unit output water will not guarantee proper risk management.

From these three considerations, it is clear that there is no direct link between the provided recommendations and the scientific evidence supporting them; therefore, the users do not have information regarding the limits and the strengths of the literature upon which the recommendations are based, along with the possible role played by the mere opinions of experts.

The composition of the Italian working group is not multidisciplinary and is therefore not adequate to ensure the points of view of all professional categories involved in the prevention and control of Legionnaire's disease: it lacks the personnel of the regional environmental protection agency, the environmental sampling technicians, the laboratory technicians who examine the environmental samples, the medical directors of hospitals, therefore, it remains unsolved or with confusing solutions to some practical problems.

Moreover, it was not stated whether the drafts of the guidelines were reviewed by other public organizations, such as regional and professional organizations in the fields of public health, hospital epidemiology and infection control, or whether public comments were considered in the decision-making process. Regarding the question of the applicability of these guidelines, we can note that the potential organizational obstacles for the implementation of the recommendations were not analysed and that the potential implications on the health resources that should be used to apply the recommendations were not considered. The attention and the costs required for the implementation of these guidelines are very high; the human and economic resources, both in the public and private organizations, are limited and are diminishing. Therefore, that which can be realized will be at the expense of other interventions.

However, the limitations encountered in this document are mostly common to most of the published guidelines, which, in most cases, are processed with the GOBSAT method (2). According to one review (3), of 431 guidelines (encompassing international bodies and multiple countries) selected in the Medline database, only 22 (5%) met the three basic criteria for the preparation of a high-quality profile document: i) a multidisciplinary team of experts; ii) the use of structured methods for the research of evidence according to well-defined inclusion criteria; and iii) the grading of the recommendations to differentiate those supported by well-drawn experimental, clinical or epidemiological studies and with a strong theoretical rationale. The documents that do not comply with these three criteria have a limited value or are even counterproductive. In the literature, the only guidelines for the prevention of *Legionella* infections that meet the above criteria are those prepared by Centers for Disease Control and Prevention (23).

In conclusion, we emphasize that guidelines should make decision-making easier, considering the various scientific approaches to a health problem and choosing the one considered most effective. Therefore, the persons responsible for the development of guidelines should strive to widely adopt and use current standards for the development of guidelines as a means to improve patient care and health outcomes.

REFERENCES

1. Field MJ MJ, Lohr KN (eds). Guidelines for Clinical Practice: from development to use. Institute of Medicine, National Academy Press, Washington, DC.; 1992.
2. Miller J, Petrie J. Development of practice guidelines. Lancet Lond Engl 2000; 355:82-83.
3. Grilli R, Magrini N, Penna A, Mura G, Liberati A. Practice guidelines developed by specialty societies: the need for a critical appraisal. Lancet Lond Engl 2000; 355:103--6.
4. Developing NICE guidelines: the manual | Guidance and guidelines | NICE [Internet]. [cited 2017 May 12]. Available from: https://www.nice.org.uk/process/pmg20/chapter/introduction-and-overview
5. European Legionnaires' Disease Surveillanve Network (ELDSNet). 1202-TED-ELDSNet-operating-procedures.pdf [Internet]. [cited 2017 Jul 12]. Available from: https://ecdc.europa.eu/sites/portal/files/media/en/publications/Publications/1202-TED-ELDSNet-operating-procedures.pdf
6. Ministero della Salute. Linee guida per la prevenzione ed il controllo della legionellosi [Internet]. Ministero della Salute, Roma, 2015. Available from: http://www.salute.gov.it/portale/documentazione/p6_2_2_1.jsp?lingua=italiano&id=2362
7. Centers for Disease Control and Prevention and Healthcare Infection, Control. Legionella (Legionnaires' Disease and Pontiac Fever) Incubation Period Considerations. 2017. Available from: https://www.cdc.gov/legionella/health-depts/inv-tools-single/index.html
8. World Health Organization. Legionella and prevention of legionellosis. 2007.
9. Marrie TJ, Bezanson G, Haldane DJ, Burbridge S. Colonisation of the respiratory tract with Legionella pneumophila for 63 days before the onset of pneumonia. J Infect 1992; 24:81-86.
10. Turner DP, Boswell TC, Lee JV, Slack RC, Burden RP. Community-acquired Legionnaires' disease in an immunocompromised patient masquerading as a hospital-acquired infection. J Hosp Infect 2001; 47:76-77.
11. Den Boer JW, Yzerman EPF, Schellekens J, et al. A

large outbreak of Legionnaires' disease at a flower show, the Netherlands, 1999. Emerg Infect Dis 2002; 8:37-43.

12. Greig JE, Carnie JA, Tallis GF, et al. An outbreak of Legionnaires' disease at the Melbourne Aquarium, April 2000: investigation and case-control studies. Med J Aust 2004; 180:566-72.
13. Bargellini A, Marchesi I, Marchegiano P, Richeldi L, Cagarelli R, Ferranti G, Borella P. A culture-proven case of community-acquired legionella pneumonia apparently classified as nosocomial: diagnostic and public health implications. Case Rep Med 2013; 2013:303712.
14. Cassier P, Bénet T, Nicolle MC, et al. Community-acquired Legionnaires' disease in a renal transplant recipient with unclear incubation period: the importance of molecular typing. Transpl Infect Dis Off J Transplant Soc 2015; 17:756-60.
15. Allen JG, Myatt TA, Macintosh DL, et al. Assessing risk of health care-acquired Legionnaires' disease from environmental sampling: the limits of using a strict percent positivity approach. Am J Infect Control 2012; 40:917-21.
16. Best M, Yu VL, Stout J, Goetz A, Muder RR, Taylor F. Legionellaceae in the hospital water-supply. Epidemiological link with disease and evaluation of a method for control of nosocomial legionnaires' disease and Pittsburgh pneumonia. Lancet Lond Engl 1983; 2:307-10.
17. Mayo JA, Brown CE. Effect of in-line bacteriological filters on numbers of heterotrophic bacteria in water emitted from non-autoclavable dental air-water syringes. Am J Dent 1999; 12:256-60.
18. Pankhurst CL, Philpott-Howard JN, Hewitt JH, Casewell MW. The efficacy of chlorination and filtration in the control and eradication of Legionella from dental chair water systems. J Hosp Infect 1990; 16:9-18.
19. Walker JT, Bradshaw DJ, Finney M, et al. Microbiological evaluation of dental unit water systems in general dental practice in Europe. Eur J Oral Sci 2004; 112:412-18.
20. Arvand M, Hack A. Microbial contamination of dental unit waterlines in dental practices in Hesse, Germany: A cross-sectional study. Eur J Microbiol Immunol 2013; 3:49-52.
21. Ditommaso S, Giacomuzzi M, Ricciardi E, Zotti CM. Cultural and Molecular Evidence of Legionella spp. Colonization in Dental Unit Waterlines: Which Is the Best Method for Risk Assessment? Int J Environ Res Public Health 2016; 13:211.
22. Toze S, Sly LI, Macrae IC, Fuerst JA. Inhibition of growth of Legionella species by heterotrophic plate count bacteria isolated from chlorinated drinking water Curr Microbiol 1990; 21:139-43. doi: 10.1007/BF02091832 1990;
23. Centers for Disease Control and Prevention. Guidelines for preventing healthcare associated pneumonia, 2003. MMWR Recomm Rep 2004 2004:53(RR-3):1-36.

LETTER TO THE EDITOR

MEDITERRANEAN DIET AND PHYSICAL ACTIVITY IMPROVE POSTURE, FAT MASS AND SALIVARY pH

R.G. BELLOMO[1], D. TRIPODI[2], C. BOSNA[2], S. D'ERCOLE[2], G. BARASSI[2], A. PORRECA[3], R. VERALDI[2], L. PROSPERI[2], C. BARBATO[2] and R. SAGGINI[2]

[1]Department of Biomolecular Sciences, "Carlo Bo" University, Urbino, Italy; [2]Department of Medical Oral and Biotechnological Sciences, "Gabriele d'Annunzio" University, Chieti-Pescara, Italy; [3]Department of Economics, "Gabriele d'Annunzio" University, Chieti-Pescara, Italy

Received April 24, 2018 – Accepted July 27, 2018

Many researchers have revealed that diet and physical activity influence metabolic function and posture in various stages of life. This paper aims to combine them and demonstrate how they could promote a healthy lifestyle. For this purpose, 14 healthy subjects followed a three-month protocol combining physical activity with dietary advice. At the end of the protocol, the results of the study underlined a significant reduction in fat mass, an improvement in salivary pH, and a realignment and rebalancing of body segments.

To the Editor,

Non-communicable diseases, such as diabetes and cardiovascular diseases, are highly related to modifiable risk factors such as improper diet and a sedentary lifestyle. Although these diseases often occur only in adulthood, they are usually initiated during adolescence. For this reason, the dietary habits of young people, their frequency of physical activity and other factors are crucial for an appropriate lifestyle. Moreover, an unhealthy diet is often associated with sedentary activities that lower energy consumption; for these reasons, there is a close correlation between the development of disorders in adulthood and an improper diet during adolescence (1). Several studies have already assessed the effects of physical exercise on metabolic variables; therefore, the quality and intensity of exercise are a fundamental target for pursuing proper results (2). This paper aims to combine aerobic training-based physical activity aimed to restore proprioception, rebalance posture and body homeostasis with food advice (in this study, the Mediterranean diet was selected) and demonstrate how this combination can improve posture, body composition parameters and salivary pH in a population of young people. At the Physical and Rehabilitation Medicine Centre and in collaboration with the Department of Oral Medical and Biotechnological Sciences of the "G. d'Annunzio" University of Chieti-Pescara, a three-month protocol was planned. For this purpose, 14 healthy subjects were enrolled. All participants gave written informed consent to the experimental procedure, which was in accordance with the latest revision of the Declaration of Helsinki and the procedures defined by the ISO 9OO1 standards for "Research and Experimentation"; the procedure also protects the privacy of subjects participating in biomedical research.

The inclusion criteria were healthy subjects aged between 18 and 26 years, who had never

Key words: physical activity, posture, Mediterranean diet, salivary pH

Mailing address:
Dr Giovanni Barassi,
Department of Medical Oral
and Biotechnological Sciences, "Gabriele d'Annunzio" University,
Chieti-Pescara, Viale Abruzzo 322, 66100 Chieti, Italy
Tel.: +39 0871 3553009
e-mail: coordftgb@unich.it

0393-974X (2018)

practised sports at a competitive level, no trauma in the previous 12 months and eligibility for physical activity. The exclusion criteria were current use of pharmacological therapy, chronic or acute pathologies, and surgical intervention in the previous 12 months.

The sample was evaluated at baseline (T0), at the end of the three-month period, immediately after the last training session (T1), and at follow-up (T2) one month after T1. The final evaluation aimed to assess the possible long-term effects of the protocol. At the three evaluation points, saliva was collected with Salivette® (Sarstedt AG & Co., Germany) (3). Specifically, the patients chewed the Salivette® cotton roll for 1 min which was then placed in a test tube and centrifuged. Saliva was also placed at the bottom of a second test tube, and the pH was measured using a pH meter (Elettrofor XS Instruments, Borsea, Italy). Saliva is a useful diagnostic tool to evaluate the state of health of the oropharyngeal cavity and contains many analytes linked with physiological and pathological conditions due to stress (4).

Posture was assessed by the Rarog system (software created and developed to improve the capability and precision of the Kinect®, which allows a static postural evaluation of subjects in a few seconds) (5), taking into account the variation in the position of the shoulders and pelvis in the frontal plane. The body composition was studied through the percentage variation in fat mass (FM), using the BIA system. The participants performed physical activity combining resistance and aerobic exercise: 10 min of warm-up phase on a cyclette; 20 min of an aerobic phase performed on a treadmill; 15 min of proprioceptive rehabilitation and balance training using a multi-sensory protocol of the I-Moove® system, a motor platform with elliptic oscillatory movements and visual feedback for the requested task (6); 10 min of lower limb muscle functional stretching and 5 min of cool down.

The study participants did not receive dietary supervision or personalized food advice and ate according to the Mediterranean diet pyramid by consuming cereals, fruits and vegetables, legumes, olive oil, low-fat cheese and yogurt every day; fish and eggs weekly; and meat once per month.

Outcome variables and statistical analysis

Fat mass (FM) was measured as a percentage of the body weight (Kg). Ph of saliva was assessed through the variable PH; a normal value of pH is 7±0.25. Position of shoulders, is represented by SH variable, which expresses the grade distance from the ideal value of a correct posture of shoulders: 0°. Position of the hip bone is assessed in grade by SB variable; it expresses the values distance from the ideal angle: 0°. Descriptive statistics were used to describe the sample. To determine how the sample changed over time: from T0 to T1 and T2, an ANOVA (within) on the variables was performed to evaluate how physical activity modified FM in patients and to understand how diet suggestions influenced the stimulated pH of the oral-pharyngeal cavity. The level for significance was set at $p<0.05$. All tests were performed using the R statistical software. Before carrying out the parametric analysis, normality was tested. The distribution of data for each variable at T0 was assessed for normality using the Shapiro-Wilks test. Because variables were normally distributed (tested at 95%), all data were analysed with parametric statistical tests.

RESULTS

The first evidence regarding FM, SB and PH is that the mean of sample decreased in the passage from T0 to T1 (Fig. 1) and this change was statistically significant only for FM and SB (Table I). Instead, FM did not vary in a statistical significantly way over time, while PH and SB changed in a statistically significant way in the passage from T0 to T1 and from T0 to T2 (Table I). The descriptive statistics (Table II) shows how PH decreased from a T0 value of 7.61 to a value of 7.51 and after 1 month without diet suggestions, it increased up to a value of 7.83. The mean of FM at T0 was 21.19% of the body weight; after 3 months of diet suggestions it decreased to 1.79% and at T2 it increased but less than the baseline value. The mean of SB at T0 was 1.39°, after 3 months it decreased to 1.04° and at T2 it decreased to 0.95°. Regarding SH (in mean) at the baseline the value was 2, after 3 months the position of shoulders was 2.22° in mean, but at T2 shoulders were far from the ideal value of 1.52°.

Table I. *ANOVA for repeated measures (within) and Post-hoc test.*

Variables	ANOVA	Post-hoc test		
	P-value	P-value		
		TIME 1 – TIME 0	TIME 2 – TIME 0	TIME 2 – TIME 1
FM	0.00574 **	0.00114 **	0.21023	0.14718
PH	0.000327 ***	0.28483	0.00521 **	< 1e-04 ***
SH	0.000792 ***	0.00386 **	< 0.001 ***	0.66579
SB	0.000972 ***	0.00396 **	0.00396 **	0.66581

*For each variable: Fat mass (FM), Ph of stimulated saliva (PH), Position of shoulders (SH) and Position of hip bone (SB) the significance level of p-value is : 0 '***' 0.001 '**'*

Table II. *Descriptive analysis of the sample.*

Variable	Mean ± SD	Range
AGE	20.43±0.94	19-22
FM0	21.19±7.69	9.64-41.25
FM1	17.59±5.24	7.94-28.11
FM2	19.48±6.39	8.38-28.77
SH0	2±0.49	1.23-3.2
SH1	2.22±0.74	1.6-3.6
SH2	1.52±0.66	0.81-3.4
SB0	1.39±0.67	0.69-2.6
SB1	1.04±0.6	0.3-2.6
SB2	0.95±0.66	0-2.5
PH0	7.61±0.22	7.16-7.88
PH1	7.51±0.32	7.03-7.98
PH2	7.83±0.17	7.55-8.21

Descriptive analysis were performed for age; fat mass (FM0, FM1, FM2); Ph of stimulated saliva (PH0,PH1,PH2); position of shoulders (SH0, SH1, SH2); position of the hip bone (SB0, SB1, SB2) at T0 , at the end of treatment and after 1 month from the end of the treatment, respectively.

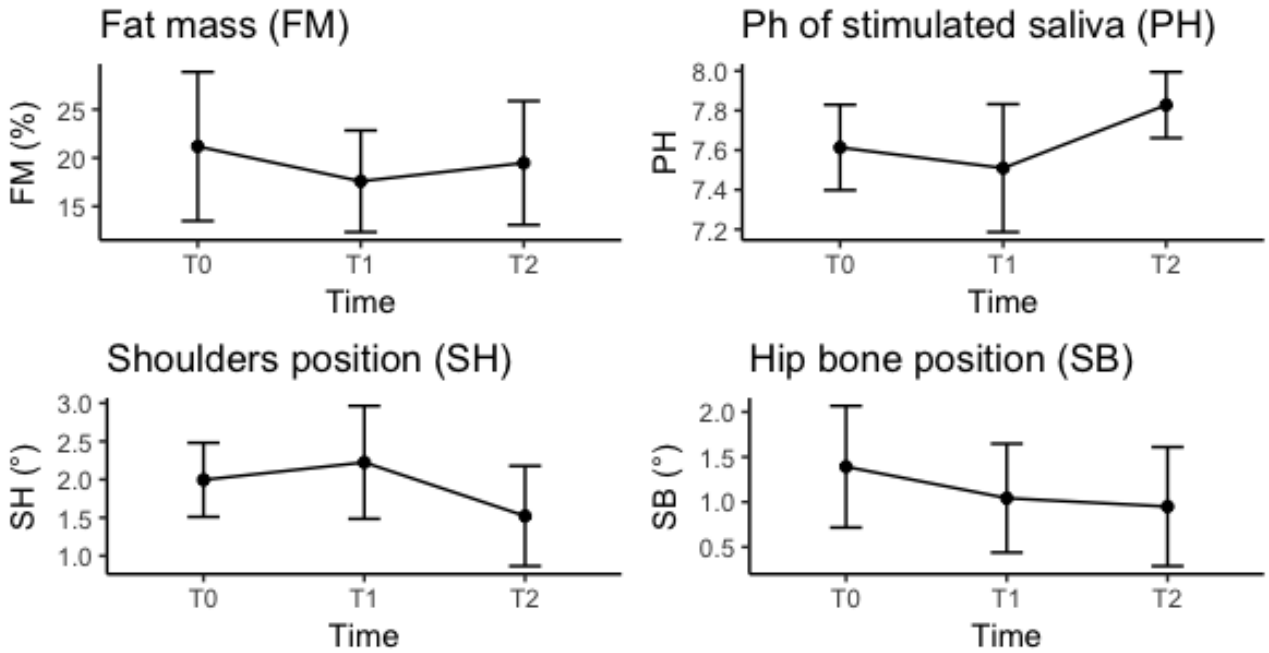

Fig. 1. *Change in average over time for each variable.*

DISCUSSION

Many studies suggested beneficial effects of combined programmes for the promotion of healthy eating habits and physical activity (7). Others have shown different techniques of somatic peripheral neuro-sensorial stimulation for posture modification and the consequent variation in body mass index; however, few studies have combined motor activity techniques on unstable platforms with proper nutrition in a young population (8, 9). Furthermore, the literature reports that a combination of interventions including nutrition, physical activity, knowledge, attitudes or behaviours related to health has the potential to reduce the risk factors associated with obesity (10). In fact, the efficacy of the aerobic training at reducing fat mass (FM) was clear in our results, which showed a statistically significant decrease (11). It is known that for health, background light physical activity and diet play a fundamental role and are key components for a high quality of life and contribute to weight loss and to a healthier oral cavity (12). The posture adaptations to physical activity require an adequate level of muscular strength to act against external forces and restore a given point of balance between various bone segments, such as the shoulders and pelvis (13). The I-Moove® instrumentation has contributed to improvement in posture, in particular the pelvic alignment (SB), confirming the benefits of proprioceptive training to rehabilitate posture and improve balance (14). A particularly notable change is the reduction in the difference from the ideal value (0°), with the difference changing from the T0 value of 1.39° to a value of 1.04° and then decreasing even further at the follow-up to 0.95°. Furthermore, this study shows how, by consuming a Mediterranean diet combined with correct aerobic exercise, the pH of saliva can be affected. Saliva is a specific parameter that, as demonstrated by Dodds (2005), suggests the general health of patient (15), and after treatment it changed from 7.61 at T0 to 7.51 at T1, so approaching to the normal value. In future, the sample size should be increased to confirm results shown in this pilot study and to verify general suggestions for proper nutrition and physical activity combination

in young people. In conclusion, we can state that a proper balanced diet and regular physical activity should be the baseline to try to maintain a proper level of biological and postural homeostasis. These parameters could be studied through variations in body composition, alteration of oral parameters and postural implications.

REFERENCES

1. Schaumberg K, Anderson D. Dietary restraint and weight loss as risk factors for eating pathology. Eat Behav 2016; 23:97-103.
2. Mello PB, Benetti F, Cammarota M, Izquierdo I. Effects of acute and chronic physical exercise and stress on different types of memory in rats. An. Acad. Bras. Ciênc. 2008; 80(2):301-9.
3. Park JR, Kim MH, Woo J, Lee SJ, Song KE. Measurement of amylase in saliva collected by salivette. Korean J Lab Med 2008; 28(6):438-43.
4. D'Ercole S, Tripodi D. The effect of swimming on oral ecological factors. J Biol Regul Homeost Agents 2013; 27(2):551-58.
5. Delli Pizzi S, Bellomo, RG, Carmignano S et al. Rehabilitation program based on sensorimotor recovery improves the static and dynamic balance and modifies the basal ganglia neurochemistry: A pilot 1H-MRS study on Parkinson's disease patients. Medicine 2017; 96(50):e8732.
6. Bellomo RG, Iodice P, Maffulli N, Maghradze T, Coco V, Saggini R. Muscle strength and balance training in sarcopenic elderly: a pilot study with randomized controlled trial. Int J Inflam 2013; 11(1):193-201.
7. Berkey CS, Rockett HR, Field AE, Gillman MW, Frazier AL, Camargo CA Jr, Colditz GA. Activity, dietary intake, and weight changes in a longitudinal study of preadolescent and adolescent boys and girls. Pediatrics 2000; 105:e56.
8. Barassi G, Bellomo RG, Di Giulio C, Giannuzzo G, Irace G, Barbato C, Saggini R. Effects of manual somatic stimulation on the autonomic nervous system and posture. Adv Exp Med Biol 2018; 1-13.
9. Barassi G, Bellomo RG, Di Iulio A, Lococo A, Porreca A, Di Felice PA, Saggini R. Preoperative rehabilitation in lung cancer patients: yoga approach. Adv Exp Med Biol 2018. Epub ahead of print.
10. Bellomo RG, Barassi G, Iodice P, Di Pancrazio L, Megna M, Saggini R. Visual sensory disability: rehabilitative treatment in an aquatic environment. Int J Immunopathol Pharmacol 2012; 25(1 Suppl):17S-21S.
11. Kesten JM, Griffiths PL, Cameron N. A systematic review to determine the effectiveness of interventions designed to prevent overweight and obesity in preadolescent girls. Obes Rev 2011; 12:997-1021.
12. Saggini R, Ancona E, Carmignano SM, Supplizi M, Barassi G, Bellomo RG. Effect of combined treatment with focused mechano-acoustic vibration and pharmacological therapy on bone mineral density and muscle strength in post-menopausal women. J Altern Complement Med 2017; 14(3):305.
13. Janssen, I, LeBlanc AG. Systematic review of the health benefits of physical activity and fitness in school-aged children and youth. Int J Behav Nutr Phys Act 2010; 7(1):40.
14. Hrysomallis C, Goodman C. A review of resistance exercise and posture realignment. J Strength Cond Res 2001; 15(3):385-90.
15. Dodds MW, Johnson DA, Yeh CK. Health benefits of saliva: a review. Int J Dent Oral Health 2005; 33(3):223-33.

JOURNAL OF BIOLOGICAL REGULATORS & HOMEOSTATIC AGENTS Vol. 32, no. 5, 1323-1328 (2018)

LETTER TO THE EDITOR

MICROBIOLOGICAL RESULTS OF IMPROVEMENT IN PERIODONTAL CONDITION BY ADMINISTRATION OF ORAL PROBIOTICS

F. INCHINGOLO[1,2,3,4], G. DIPALMA[2,3,5], N. CIRULLI[2], S. CANTORE[2,3,5], R.S. SAINI[1], V. ALTINI[5], L. SANTACROCE[6], A. BALLINI[2,3,4,5] and R. SAINI[1]

[1]Department of Interdisciplinary Medicine, School of Medicine, University of Bari Aldo Moro, Bari, Italy; [2]City Unity College, Athens, Greece; [3]BPP School of Health, University Faculty of Dentistry, Birmingham, United Kingdom; [4]World Academy of Growth Factors & Stem Cells in Dentistry, Athens, Greece; [5]Department of Basic Medical Sciences, Neurosciences and Sense Organs, University of Bari Aldo Moro, Bari, Italy; [6]Ionian Department, University of Bari Aldo Moro, Bari, Italy.

Received March 5, 2018 – Accepted April 13, 2018

All Authors contributed equally to this study

Oral bacteria that degrade sulphur-containing amino acids (cysteine, cystine, and methionine) produce volatile sulphur compounds (VSCs = hydrogen sulphide, methyl mercaptan, and dimethyl sulphide) highly correlated with halitosis. When these bacteria are given the right environment, i.e. periodontal disease, cariogenic biofilm or food source they can grow in number very quickly and will start to convert proteins to VSC that, together with volatile fatty acids are largely responsible for oral malodor. Recently, the prevention of dental caries and periodontal diseases using various probiotics has been attempted. The purpose of this study was to investigate the effects of probiotics based on *in vitro* analysis, such as antibacterial activity, and to evaluate the neutralizing effect of probiotics on halitosis, the levels of VSCs were measured by gas chromatography.

To the Editor,

Probiotics favourably influence both the development and stability of microbiota, thereby inhibiting the colonization of pathogens, enhancing the mucosal barrier via tropic effects on the epithelium, and stimulating both the innate and the adaptive immune systems (1).

The most commonly used probiotic bacterial strains belong to the genera *Lactobacillus*. These bacteria are generally regarded as a part of the normal human microbiota (1, 2). In the oral cavity, lactobacilli usually comprise fewer than 1% of the total cultivable microbiota, but no species specific to the oral cavity has been found. In contrast, some species are found in both oral and fecal samples (3). Species commonly isolated from saliva samples include *L. paracasei*, *L. plantarum*, *L. rhamnosus*, and *L. salivarius* (2, 3). Several studies have demonstrated that xylitol inhibits *in vitro* and *in vivo* growth of *Streptococcus mutans* (4).

Another characteristic of dental plaque-related diseases is their ability to induce halitosis, an oral malodor. In fact, dental plaque-related diseases secrete trypsin-like enzymes that produce volatile

Key words: probiotics, randomised controlled trial, biofilm, oral malodour

Mailing address:
Dr. Andrea Ballini,
Department of Basic Medical Sciences,
Neurosciences and Sense Organs,
University of Bari Aldo Moro,
P.zza Giulio Cesare, 11, 70124, Bari, Italy
Tel./fax: +39 0805448514.
e-mail: andrea.ballini@me.com

0393-974X (2018)

DISCLOSURE: ALL AUTHORS REPORT NO CONFLICTS OF INTEREST RELEVANT TO THIS ARTICLE.

sulfur compounds (VSCs), such as hydrogen sulfide (H_2S), methyl mercaptan (CH_3SH), and dimethyl sulfide ($[CH_3]_2S$), in the presence of methionine and cysteine in human serum protein (4, 5). VSCs are responsible for halitosis.

Therefore, based on the health benefits reported for the combination of different probiotics, the present study was aimed to investigate the effects of different probiotics in combination with Chelated Zinc (*Hyperbiotics Pro Dental Probiotic* Lozenges/Tablets) on VSC by a halimetric measurement analysis and to test the usefulness of their antibacterial activity on saliva sampling, in periodontally compromised *vs* healthy subjects.

MATERIALS AND METHODS

Subjects and study schedule

The study was a randomised, controlled, double-blind trial. A member of the research team evaluated suitability for the study criteria. Suitable individuals enrolled were provided with a participant information sheet, a consent form, with instructions for the study period (daily tablets administration and oral hygiene procedures). Informed consents were obtained on a separate occasion prior to participation. Participants were asked to refrain from using any kind of chewing gum during the study period. Throughout the study, the subjects used the same brand of fluoridated toothpaste provided to them free of charge.

Antimicrobial mouth rinses were not allowed. Compliance to given instructions was checked at all sampling visits (baseline and every 4 weeks after, for three months). At these visits, the subjects were also interviewed for dietary habits and oral/general health. These data were used to check for compliance, possible adverse effects and other confounding factors.

The subjects were randomly allocated into four groups (groups A-B-C-D). Groups A and C used probiotic test tablets (Hyperbiotics Pro Dental Probiotic Lozenges/Tablets) and group B and D used xylitol products (Miradent professional prophylaxis chewing gum, 100% Xylitol, vegan, no sugar) control tablets for 4 weeks. The recommendation was 1 packet (containing two gums) per day. The recommended number of gums/tablets resulted in a daily xylitol dose of approximately 2 g which, according to several studies, is too low to exert any "xylitol-effects" on the oral microbiota (4, 6). The first of two tablets was instructed to be taken in the morning, and the second at night before sleeping after brushing the teeth. The subjects were asked to chew the tablet thoroughly to disrupt its structure before swallowing.

Probiotic product

The test product (Hyperbiotics Pro Dental Probiotic**)** has the following characteristics:.

• Targeted oral probiotic strains (*L. reuteri* and *L. paracasei*) to effectively counter the indiscriminate effects of antibacterials and other lifestyle choices that can deplete the oral microbiome.

• Chelated zinc, that acts as an antioxidant and helps to protect cells against the effects of free radicals while playing a vital role in the formation of connective tissue, teeth and bones.

• Vegetarian, non-GMO, no soy, sugar, iron, nuts, artificial flavors, artificial colors, or preservatives, free of lactose, gluten, and yeast.

Sample size and blinding

The groups were composed of 60 volunteers (15 per each group) selected from patients seeking dental care at the Dental Hygiene School, University of Bari Aldo Moro, and from private practice. The groups (A or B for healthy and C or D for periodontally compromised) were revealed to the researchers only after the statistical analyses were performed.

Inclusion criteria

Test group (A and B): patients aged between 18 and 60 years suffering from mild to moderate periodontitis with good to fair oral hygiene were selected for the study.

Control group (C and D): healthy patients aged between 18 and 60 years.

Exclusion criteria

- Patients using probiotic supplements
- Patients with allergy to lactose and fermented milk products
- Vegan diet (product made from skimmed cow's milk and therefore not suitable for vegans)
- Patients on antibiotic therapy or who had been on antibiotic therapy in the previous 6 months or during the trial period

- Pre-existing oral irritations or oral infections (rampant caries, severe/aggressive gingivitis and periodontitis, oral thrush, diagnosed halitosis, or diagnosed xerostomia)
- Use of any mouthwash within the last month
- Presence of excessive mobility of any tooth, which required immediate treatment
- Presence of periapical and/or periodontal abscess
- Poorly controlled diabetes
- Patients suffering from any systemic diseases
- Smokers and patients deemed to be uncooperative.

Saliva collection and microbiologic examination

Following the determination of clinical parameters, saliva samples were collected from all the study subjects at baseline and 60 day intervals to record the levels of *S. Mutans* during the study period. In addition, to assess the middle-term benefits on oral health after the probiotics and xylitol administration, a further investigation was done at 90 days (additional 30 days from the end of the study period). The samples were placed immediately in sterile test tubes and sealed to prevent any contamination and were analysed within 24 hours. Following extraction of DNA, both qualitative and quantitative analyses of the bacteria were carried out using multiplex polymerase chain reaction (PCR). The sample containing the saliva was transferred to a tube containing Tris-EDTA buffer (T.E. buffer) and centrifuged at 50,000 rpm for 2 min. The supernatant collected at the top was discarded, and fresh T.E. buffer was added, and then centrifuged for 3-4 min. The process was repeated 3-4 times, each with fresh T.E. buffer.

Table I. *Minimum, maximum, and median CFU (log^{10}) of Streptoccocus Mutans in the saliva of subjects during treatment with different lozenges.*

Lozenges/Tablets [a] Time[b]	*Streptococcus mutans* Min	Max	Median
Hyperbiotics Pro Dental -T0	0.89	1.94	1.43
Hyperbiotics Pro Dental -T1	0.68	1.76	1.22
Hyperbiotics Pro Dental -T2	0.51	1.37	0.94
***P* value**			<0.001
Xylitol-T0	0.85	1.91	1.38
Xylitol -T1	0.78	1.87	1.32
Xylitol -T2	0.70	1.71	1.25
***P* value**			<0.001

[a] *Lozenges/tablets: Hyperbiotics Pro Dental and Xylitol;* [b] *T0: baseline; T1: at 60 days; T2: at 60 days; T3: *Friedman test.*

Assessment of morning breath odour with Halimeter

Morning breath samples were obtained using portable sulphide monitors: Halimeter (Interscan Co., Chatsworth, CA, USA), provided pro private practice. Halimeter provided from private practice, were used for the detection and estimation of the peak value of total volatile sulphur compounds (VSCs) in parts per billion (ppb) (7), according to the manufacturer's instructions. Participants were supplied with a leaflet explaining the procedure, followed by demonstration of the sampling technique by one of the study investigators in preparation for participants' self-sampling. Halimeter testing requires a 3-minute mouth air incubation period prior to sampling. Repeated measurements of mouth air collected with the Halimeter (three repeats) were averaged for each participant at baseline, 60 and 90 days intervals.

Statistical analysis

The statistical analyses were performed by using Statistical Package for Social Sciences (SPSS for Windows, Version 15) software. The significance of differences between test and placebo groups in baseline was evaluated according to distribution. The significance of the difference within each group before and after treatment was evaluated with the paired samples *t*-test when normally distributed, or non-parametric Wilcoxon' s sign-rank test otherwise. For parametric and non-parametric tests, a p-value <0.05 was considered as statistically significant.

The bacterial count differences in median ranks for repeated measures among time intervals [baseline (T0), 60

Table II. *Clinical assessments of the study population before and after treatment.*

Group	VSC (ppb)	VSC and polyamines
Controls T0	140	Low
Controls T1	100	Low
Controls T2	100	Low
Probiotic T0	432	High
Probiotic T1	336	Med
Probiotic T2	220	Med

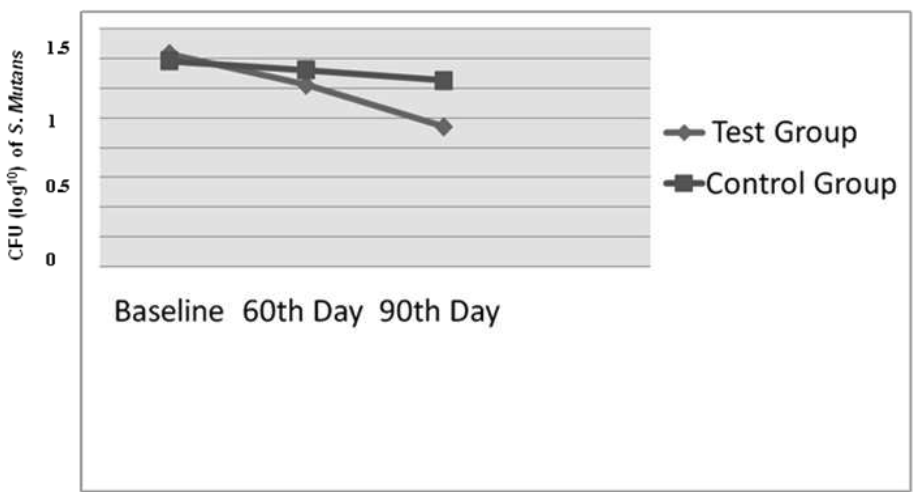

Fig. 1. *Salivary Streptoccocus mutans scores for the test and control groups at baseline and at the end of the study period.*

days effect (T1), and 90 days effect (T2) were compared by the non-parametric Friedman test, and significance levels were set at 0.05. Wilcoxon signed rank test was used to compare two dependent nonparametric values, and significance level was chosen as 0.01 according to Bonferroni adjustment.

RESULTS

Microbiologic and halimeter examination

The minimum, maximum, and median CFU of total *S. mutans* bacteria in the saliva of subjects at baseline, 60 days and at 90 (other 30 days from the end of probiotic

an xylitol administration) days intervals, are presented in Table I and Fig. 1. Great variations in inter- and intra-individual measurements were observed. The clinical assessments of the study population recorded for VSC score before and after the treatment are reported in Table II. Both the examinations showed a significant decrease from the baseline.

Compliance

Compliance with the course of the intake of tablets and the number of pills not taken by the participants were also documented. All subjects returned the medication bottles. The median of 80% subjects from all groups (100%) completed the course of tablets as indicated.

DISCUSSION

The assessment of the use of probiotics in the control of dental caries has been limited by the number of subjects needed, prolonged treatment duration and high cost. Most studies have measured counts of *Streptococcus mutans* in saliva or dental plaque, and/or the flow, pH or buffering capacity of saliva. A recent systematic review and meta-analysis provided a useful guide to clinical decision-making and direction for further research (8-11). One of the earliest probiotic strains proposed to target oral malodour and fulfilling the above criteria was the bacteriocin-producing strain *S. salivarius* K12, which reduced breath VSC concentrations in individuals who consumed the probiotic lozenges after pre-treatment with a chlorhexidine rinse (12).

Limitations of the present study include the relatively small number of participants and the short-term study period. Therefore, further long-term studies including a large-scale Randomized Controlled Trial (RCT) are necessary to determine the utility of probiotics as an alternative approach for the treatment and prevention of dental plaque-related diseases. The major limitation of this study is the statistical power. This study could be too small to detect the real differences between the groups. An increase of the sample size is suggested. This being a short-term study, the results can be used as baseline data for future studies with similar study design.

In conclusion, probiotics have different benefits in oral care. The full complex probiotic formula used in this study showed a strong survival rate under poor oral conditions, and several positive results, including VSC production, and efficient coaggregation. Additionally, the tested probiotic and, in a lesser amount, xylitol-containing chewing gums seem to be effective in reducting salivary *S. mutans* levels. Their constant long-term consumption is therefore recommended to prevent caries. Further studies are needed to elucidate their potential for use in the treatment of oral diseases.

REFERENCES

1. de Vrese M, Schrezenmeir J. Probiotics, prebiotics, and synbiotics. Adv Biochem Eng Biotechnol 2008; 111:1-66.
2. Saxelin M, Tynkkynen S, Mattila-Sandholm T, de Vos WM. Probiotic and other functional microbes: from markets to mechanisms. Curr Opin Biotechnol 2005; 16:204-11.
3. Colloca ME, Ahumada MC, Lopez ME, Nader-Macias ME. Surface properties of lactobacilli isolated from healthy subjects. Oral Dis 2000; 6:227-33.
4. Söderling E. Xylitol, mutans streptococci, and dental plaque. Adv Dent Res 2009; 21:74-78.
5. Scully C, Greenman J. Halitosis (breath odor). Periodontol. 2008; 48:66-75.
6. Allaker RP, Waite RD, Hickling J, North M, McNab R, Bosma MP, Hughes FJ. Topographic distribution of bacteria associated with oral malodour on the tongue. Arch Oral Biol 2008; 53:S8-12.
7. Snel J, Burgering M, Smit B, Noordman W, Tangerman A, Winkel EG, Kleerebezem M. Volatile sulphur compounds in morning breath of human volunteers. Arch Oral Biol 2011; 56:29-34
8. Gruner D, Paris S, Schwendicke. Probiotics for managing caries and periodontitis: Systematic review and meta-analysis. F J Dent 2016; 48:16-25.
9. Ballini A, Tetè S, Scattarella A, et al. The role of anti-cyclic citrullinated peptide antibody in periodontal disease. Int J Immunopathol Pharmacol 2010; 23:677-81.
10. Ballini A, Mastrangelo F, Gastaldi G, et al. Osteogenic differentiation and gene expression of dental pulp

stem cells under low-level laser irradiation: a good promise for tissue engineering. J Biol Regul Homeost Agents 2015; 29:813-22.
11. Ballini A, Scattarella A, Crincoli V, et al. Surgical treatment of gingival overgrowth with 10 years of follow-up. Head Face Med 2010; 6:19.
12. Masdea L, Kulik EM, Hauser-Gerspach I, Ramseier AM, Filippi A, Waltimo T. Antimicrobial activity of Streptococcus salivarius K12 on bacteria involved in oral malodour. Arch Oral Biol 2012; 57:1041-47.

JOURNAL OF BIOLOGICAL REGULATORS & HOMEOSTATIC AGENTS Vol. 32, no. 5, 1329-1334 (2018)

LETTER TO THE EDITOR

CLINICAL RESULTS OF IMPROVEMENT IN PERIODONTAL CONDITION BY ADMINISTRATION OF ORAL PROBIOTICS

S. CANTORE[1,2,3], A. BALLINI[1,2,3,4], D. DE VITO[1], A. ABBINANTE[1,6], V. ALTINI[5], G. DIPALMA[1,2,3], F. INCHINGOLO[5,2,3] and R. SAINI[5]

[1]Department of Basic Medical Sciences, Neurosciences and Sense Organs, University of Bari Aldo Moro, Bari, Italy; [2]City Unity College, Athens, Greece; [3]BPP School of Health, University Faculty of Dentistry, Birmingham, United Kingdom; [4]World Academy of Growth Factors & Stem Cells in Dentistry, Athens, Greece; [5]Department of Interdisciplinary Medicine, School of Medicine, University of Bari Aldo Moro, Bari, Italy; [6]President of the Italian Association of Dental Hygienists (AIDI), Italy

Received March 5, 2018 – Accepted April 11, 2018

Dental plaque-related diseases (cavities, gingivitis, periodontitis and halitosis) have been traditionally controlled by mechanical non-specific removal of plaque. However, many novel treatment approaches aim to inhibit the growth of pathogenic bacteria or to remove their toxins. Probiotics are viable microorganisms which, when administered in adequate amounts, provide a health benefit to the host. Recently, probiotics have been applied as new tools for the improvement of dental health. They have been used to substitute existing antibiotic treatments due to increased resistant bacteria. Probiotics not only have antibacterial activity, but they also have inhibitory effects on the reappearance of oral pathogenic bacteria. The aim of this study was to assess the clinical effect of the administration of probiotics agents in the treatment of mild to moderate periodontitis.

To the Editor,

Probiotics are defined as bacteria with physiological benefits for humans. The characteristics are scientifically demonstrated to have beneficial physiological effects: safety for human use, stability in acid and bile, and adherence to the intestinal mucosa (1-4). Probiotics favourably influence both the development and stability of microbiota, thereby inhibiting the colonization of pathogens, enhancing the mucosal barrier via tropic effects on the epithelium, and stimulating both the innate and the adaptive immune systems (4).

The most commonly used probiotic bacterial strains belong to the genera *Lactobacillus*. These bacteria generally are regarded as a part of the normal human microbiota (1-4). Species commonly isolated from saliva samples include *L. paracasei*, *L. plantarum*, *L. rhamnosus*, and *L. salivarius* (5). The ecological plaque hypothesis suggests that selective pressure in environmental conditions can change the balance between oral health and disease (6). However, data are still inadequate, therefore more information is needed on the colonization of probiotics in the oral cavity and their possible effects.

Due to globalization and increasing problems with antibiotic resistance, the alternative concept of probiotic therapy deserves further research in the field of periodontal health. Nowadays, with the

Key words: probiotics, periodontal health, dental plaque-related diseases, randomised controlled trial

Mailing address:
Dr. Andrea Ballini,
University of Bari Aldo Moro,
P.zza Giulio Cesare, 11,
70124, Bari- Italy
Tel./fax: +39 0805448514.
e-mail: andrea.ballini@me.com

0393-974X (2018)

increase of multi-drug bacteria-resistant diseases, it is necessary to consider a further alternative in the treatment of periodontal disease. Therefore, based on the health benefits reported for the combination of different probiotics, the present study was aimed to investigate the impact of a probiotic combination with Chelated Zinc (Hyperbiotics Pro Dental Probiotic Lozenges/Tablets) on plaque accumulation and gingival health in periodontally compromised *vs* healthy subjects.

MATERIALS AND METHODS

Subjects and study schedule

The study is a randomized, controlled, double-blind trial. A member of the research team evaluated suitability for the study criteria. Suitable individuals were enrolled and were provided with an information sheet and instructions for the study period (daily tablet administration and oral hygiene procedures), and informed consents for participation in the study were obtained. Participants were asked to refrain from using any kind of chewing gum during the study period. Throughout the study, the subjects used the same brand of fluoridated toothpaste provided to them free of charge. Antimicrobial mouth rinses were not allowed. Compliance to given instructions was checked at all sampling visits (baseline and every 4 weeks after, for three months). At these visits, the subjects were also interviewed for dietary habits and oral/general health. These data were used to check for compliance, possible adverse effects and other confounding factors.

The subjects were randomly allocated into four groups (groups A-B-C-D): groups A and C used probiotic test tablets (Hyperbiotics Pro Dental Probiotic, USA Lozenges/Tablets) and group B and D used xylitol products (Miradent professional prophylaxis chewing gum, 100% Xylitol, Vegan, no sugar, Germany**)** control tablets for 4 weeks. The recommendation for probiotic lozenges was 1 piece per day. The recommended number of gums/tablets resulted in a daily xylitol dose of approximately 2 g which, according to several studies, is too low to exert any "xylitol-effects" on the oral microbiota (7). The first of two tablets were taken in the morning, and the last one at night, after brushing the teeth before sleeping. The subjects were asked to chew

Table I. *Demographic and clinical characteristics at baseline of all groups. Mean values ± standard deviation.*

	Test group (n = 30)	**Placebo group (n = 30)**	***p*-value**
Age (95% CI)	55.0 (45.7–64.9)	51.8 (40.8–61.6)	0.321 *(t*-student)
Gender	**F**:33%, **M:**67%	**F:**69%, **M:**31%	0.150 (Chi^2)
Plaque index (%)	58.7±1 9.13	51.3±16.33	0.476 (*t*-test)
Bleeding on probing (%)	49.9±18.46	41.5±19.58	0.116 (*t*-test)
Pocket probing depths 4–5 mm (%)	48.4±20.32	40.7±19.23	0.159 (*t*-test)

All p-values were greater than 0.05.

the tablet thoroughly to disrupt its structure before swallowing.

Probiotic product

The test product *(*Hyperbiotics Pro Dental Probiotic) has the following characteristics:

- targeted Oral Probiotic Strains (*L. reuteri* and *L. paracasei*) to effectively counter the indiscriminate effects of antibacterials and other lifestyle choices that can deplete the oral microbiome;
- chelated zinc, that acts as an antioxidant and helps to protect cells against the effects of free radicals while playing a vital role in the formation of connective tissue, teeth and bones;
- vegetarian, non-GMO, no soy, sugar, iron, nuts, artificial flavors, artificial colors, or preservatives, free of lactose, gluten, and yeast.

Sample size and blinding

Each of the four groups was composed of 15 volunteers selected among patients seeking dental care at the Dental Hygiene School, University of Bari Aldo Moro, and from private practice. The group numbers (A or B for healthy and C or D for periodontally compromised) was revealed to the researchers only after the statistical analyses were performed.

Inclusion criteria

Test groups (A and B): Patients aged between 18 and 60 years and suffering from mild to moderate periodontitis with good to fair oral hygiene were selected for the study.

Control group (C and D): Healthy patients aged between 18 and 60.

Exclusion criteria

- Patients using probiotic supplements
- Patients with allergy to lactose and fermented milk products
- Vegan diet (product made from skimmed cow's milk and therefore not suitable for vegans)
- Patients on antibiotic therapy or who had been on antibiotic therapy in the previous 6 months or during the trial period
- Pre-existing oral irritations or oral infections (rampant caries, severe/aggressive gingivitis and periodontitis, oral thrush, diagnosed halitosis, or

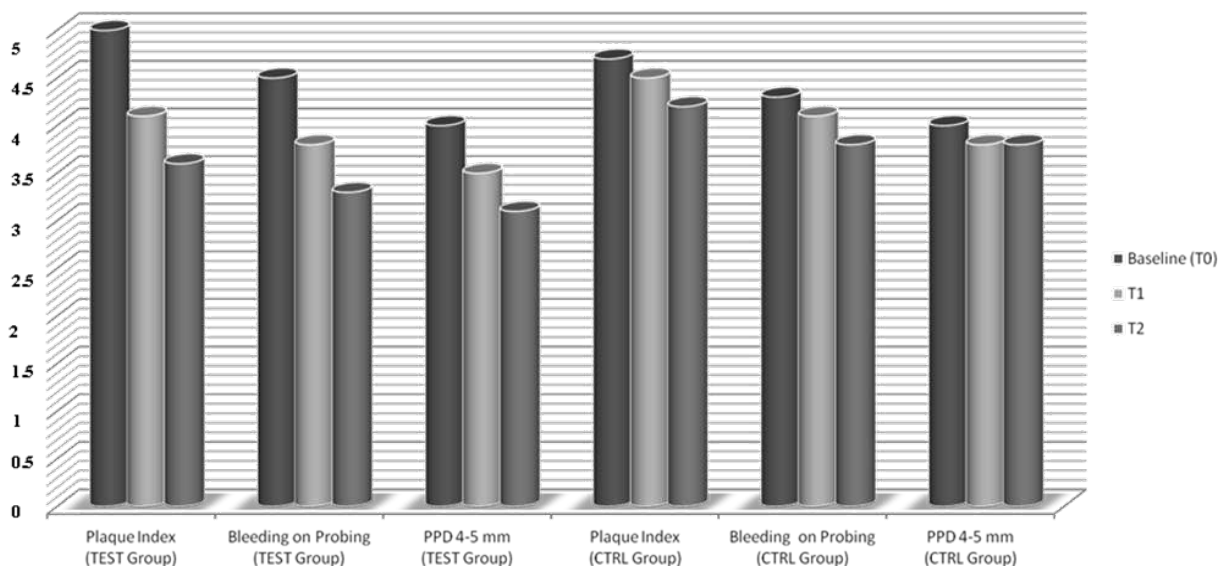

Fig. 1. *Group A vs Group B positive effects of probiotics on periodontal group.*

diagnosed xerostomia)
- Use of any mouthwash within the last month
- Presence of excessive mobility of any tooth, which requires immediate treatment
- Presence of periapical and/or periodontal abscess
- Poorly controlled diabetes
- Patient suffering from any systemic diseases
- Smokers and patients who are deemed to be uncooperative.

Determination of plaque and gingival index

A complete periodontal examination was conducted including a full medical and dental history, an intra-oral examination and a full-mouth periodontal probing. Registration of probing pocket depths (PPD), Plaque Index (PI) and bleeding on probing (BOP) was carried out. Clinical parameters were assessed using a manual probe CP-15 UNC, at six sites per tooth, excluding third molars.

The Plaque Index (PI) was recorded by assigning a binary score to each surface (1 for plaque present, 0 for absent) and calculating the percentage of total tooth surfaces that revealed the presence of plaque detected using a periodontal probe (8-10).

Similarly, bleeding on probing (BOP) was calculated as a percentage of bleeding surfaces *vs* all surfaces according to Ainamo and Bay (11). In this registration a bleeding point is considered when bleeding emerges within 10 s after probing. Probing pocket depths (PPD) were measured in mm as the distance from the gingival margin to the location of the tip of a periodontal probe inserted in the pocket with moderate probing force. PPD were recorded at six sites of every tooth present: mesio-buccal, mid-buccal, disto-buccal, disto-lingual, mid-lingual and disto-lingual.

Statistical analysis

The statistical analyses were performed by using Statistical Package for Social Sciences (SPSS for Windows, Version 15) software. The significance of differences between test and placebo groups in baseline was evaluated according to distribution. The significance of the difference within each group before and after treatment was evaluated with the paired samples *t*-test if it was normally distributed, or otherwise with non-parametric Wilcoxon' s sign-rank test. For parametric and non-parametric tests, a p-value <0.05 was considered as statistically significant.

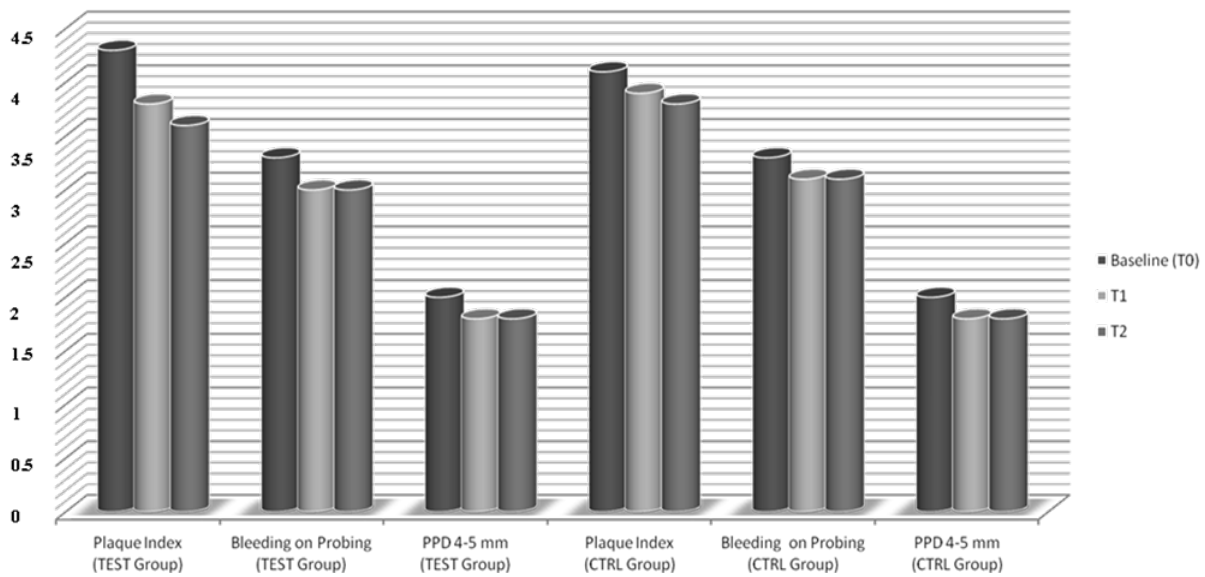

Fig.2. *Group C vs Group D: positive effects of probiotics on healthy group.*

RESULTS

The baseline characteristics of all the subjects who participated in the study are displayed in Table I. The baseline examination revealed that the study groups showed similar characteristics for percentage of pockets, plaque and bleeding levels, with no significant differences between the two groups. The clinical results were encouraging, and patients provided positive feedback on the use of this protocol (Figs. 1-2).

Plaque index

Plaque scores decreased in the test group from baseline to final measurement and the difference was statistically significant. However, in the placebo group an increase in the mean values occurred, suggesting a non-statistically significant ($p = 0.396$) increase of plaque accumulation among the placebo group during the study period. The change in PI for the test group was statistically significant ($p = 0.007$), demonstrating a reduction of the plaque index after the use of the probiotic agent; however, the control group demonstrated a non-statistically significant increase in PI after the use of the placebo chewing-gum.

Bleeding on probing

The mean BOP (%) at baseline was 49.9 for the test group and 41.05 for the control group. After the use of the probiotic agent, the mean BOP was 33.3 for the test group, showing a statistically significant reduction ($p = 0.005$) in bleeding on probing after the use of the Hyperbiotics Pro Dental Probiotic, but the control group demonstrated a non-statistically significant increase in BOP with a mean BOP of 40.0.

Pocket probing depths

The mean percentage of sites with PPD of 4–5 mm at baseline for the test group was 48.4 and 40.7 for the control group. At the end of treatment the mean PPD for the test group showed a statistically significant reduction ($p = 0.045$), with a mean of 35.5, and the control group increased the PPD mean to 41.5. Variation in periodontal clinical parameters as percentage, before and after the use of Hyperbiotics Pro Dental Probiotic and placebo treatment, are represented in Figs. 1 and 2.

Compliance

Compliance with the course of the intake of tablets and the number of pills not taken by the participants were also documented. All subjects returned the medication bottles. The median of 80% subjects from all groups (100%) completed the course of tablets as indicated.

DISCUSSION

The selection of the 'best' probiotic for oral health is also a controversial issue (1-4). We selected Hyperbiotics Pro Dental Probiotic as the probiotic for the present study because *Lactobacilli* are found in the oral cavity and have been shown to have varying ability to interfere with the growth of oral pathogens (6). Limited information is available about appropriate probiotic dosing regimens and only a few dose comparison studies have been undertaken (7). In this study we prescribed one tablet of Hyperbiotics Pro Dental Probiotic per day. The rationale is based on the study of Twetman et al. (12), where a dose–response relationship or a threshold level seemed to appear, but it would be too early to propose any clinical recommendations at this stage. The choice of dosage comes from an analysis of previous studies and the manufacturer's recommendation. In the present study, a reduction of clinical indices was not observed in the placebo group subjects; however, a non-significant increase of clinical indices was reported. We considered it unlikely that this phenomenon was induced directly by the placebo gums.

Limitations of the present study include the relatively small number of participants and the short-term study period. Therefore, further long-term studies including a large-scale RCT are necessary to determine the utility of probiotics as an alternative approach for the treatment and prevention of periodontal diseases. The best means of administering probiotics and the dosages needed for different preventive or therapeutic purposes are

still under investigation. The major limitation of this study is the statistical power. This study could be too small to detect the real differences between the groups. An increase of the sample size is suggested. This being a short-term study, the results can be used as a baseline data for future studies with similar study design.

REFERENCES

1. Ashwell M. Concept of functional foods 2002ILSI; (International Life Sciences Institute) Europe: B-1200 Brussels, Belgium ISBN 1-57881-145-7
2. de Vrese M, Schrezenmeir J. Probiotics, prebiotics, and synbiotics. Adv Biochem Eng Biotechnol 2008; 111:1-66.
3. Saxelin M, Tynkkynen S, Mattila-Sandholm T, de Vos WM. Probiotic and other functional microbes: from markets to mechanisms. Curr Opin Biotechnol 2005; 16:204-11.
4. Parvez S, Malik KA, Ah Kang S, Kim HY. Probiotics and their fermented food products are beneficial for health. J Appl Microbiol 2006; 100:1171-85.
5. Colloca ME, Ahumada MC, Lopez ME, Nader-Macias ME. Surface properties of lactobacilli isolated from healthy subjects. Oral Dis 2000; 6:227-33.
6. Cosseau C, Devine DA, Dullaghan E, et al. The commensal Streptococcus salivarius K12 downregulates the innate immune responses of human epithelial cells and promotes host-microbe homeostasis. Infect Immun 2008; 76:4163-75.
7. Paineau D, Carcano D, Leyer G, et al. Effects of seven potential probiotic strains on specific immune responses in healthy adults: a double-blind, randomized, controlled trial. FEMS Immunol Med Microbiol 2008; 53:107-13.
8. Ballini A, Tetè S, Scattarella A, et al. The role of anti-cyclic citrullinated peptide antibody in periodontal disease. Int J Immunopathol Pharmacol 2010; 23:677-81.
9. Ballini A, Mastrangelo F, Gastaldi G, et al. Osteogenic differentiation and gene expression of dental pulp stem cells under low-level laser irradiation: a good promise for tissue engineering. J Biol Regul Homeost Agents 2015; 29:813-22.
10. Ballini A, Scattarella A, Crincoli V, et al. Surgical treatment of gingival overgrowth with 10 years of follow-up. Head Face Med 2010; 6:19.
11. Ainamo J, Bay I. Problems and proposals for recording gingivitis and plaque. Int Dent J 1975; 25:229-35.
12. Twetman S, Derawi B, Keller M, Ekstrand K, Yucel-Lindberg T, Stecksen-Blicks C. Short-term effect of chewing gums containing probiotic Lactobacillus reuteri on the levels of inflammatory mediators in gingival crevicular fluid. Acta Odontol Scand 2009; 67:19-24.

JOURNAL OF BIOLOGICAL REGULATORS & HOMEOSTATIC AGENTS Vol. 32, no. 5, 1335-1338 (2018)

LETTER TO THE EDITOR

SUPERFICIAL INFILTRATION TO TREAT WHITE HYPOMINERALIZED DEFECTS OF ENAMEL: CLINICAL TRIAL WITH 12-MONTH FOLLOW-UP

L. GIANNETTI[1], A. MURRI DELLO DIAGO[1], G. SILINGARDI[1] and E. SPINAS[2]

[1]Department of Paediatric Dentistry University of Modena and Reggio Emilia, Modena, Italy;
[2]Department of Surgical Science, University of Cagliari, Cagliari, Italy

Received July 23, 2018 – Accepted August 3, 2018

Hypomineralization represents one of the most common defects in tooth crowns. Thanks to a wide understanding of aesthetics, patients request a treatment to resolve these defects. Different techniques are available, such as crowns/veneers, traditional restorative treatments, microabrasion, whitening, remineralizing agents and infiltration technique. The objective of this trial is to assess the effectiveness of superficial infiltration with Icon (DMG, Hamburg, Germany) on the attenuation of crown hypomineralized lesions of various etiological origins with a 12-month follow-up. Seventeen patients with white defects of enamel in the aesthetic sector were selected. The infiltration procedure was carried out following the manufacturer's instructions. Intraoral photographs were taken before and directly after treatment in order to document the immediate change in colour. Check-ups were performed 1 and 12 months later. All the defects which were treated showed a degree of attenuation. The teeth affected by molar incisor hypomineralization (MIH) showed partial attenuation in 8 cases, and only in one case the defect disappeared. Regarding the post-trauma cases, 6 were partially attenuated and 2 disappeared. The post orthodontic defects disappeared in 6 cases and were attenuated in 5. All incipient caries defects were completely hidden. Four out of 6 cases of fluorosis disappeared. Diagnosis plays a key role in guiding the dental clinical selection of treatment. While it has always been possible to achieve a high level of attenuation in cases of fluorosis and lesions of caries origin, cases of MIH should probably be treated using more invasive techniques. Post-trauma lesions should be infiltrated with caution, and only after having informed the patient of the possible ineffective outcome.

To the Editor,

Despite the different possible etiologies, white defects of enamel have a main characteristic in common: hypomineralization (1, 2).

When a ray of light strikes the hypomineralized enamel due to refraction of the light, it is forced to undergo continuous changes in direction. The perception we are given is that of an opaque and too bright zone that is easy to distinguish from the healthy enamel (2, 3). Since the characteristics most closely related to the concept of beauty involve the oral region in particular, very often patients request a treatment to resolve their aesthetic dental problems.

Today there are many different therapeutic possibilities that the dentist can offer to meet the request to treat more or less invasive enamel defects: crowns and veneers, traditional restorative treatments, microabrasion, whitening, treatments with remineralizing agents and infiltration techniques. In this last technique new resinous

Key words: superficial infiltration, white defects of enamel, hypomineralization

Mailing address:
Prof. Luca Giannetti,
University of Modena and Reggio Emilia,
Department of Paediatric Dentistry,
Via del Pozzo, 71, 41125 Modena, Italy
Tel.: +39 059 4224325
e-mail: luca.giannetti@unimore.it

0393-974X (2018)

DISCLOSURE: ALL AUTHORS REPORT NO CONFLICTS OF INTEREST RELEVANT TO THIS ARTICLE.

materials distinguished by low viscosity are used, so they are able to penetrate the hypomineralized enamel deep down, which were initially proposed for the microinvasive treatment of incipient interproximal, and non-cavitated caries (4), but recently indications have been extended to the aesthetic treatment of enamel defects on the vestibular surfaces thanks to the resin's refractive index (1.46), similar to that of healthy enamel (1.62) (5-7).

The purpose of this study is to assess the effectiveness of infiltration treatment on different types of white defects of enamel.

MATERIALS AND METHODS

This study was conducted at the University of Modena and Reggio Emilia, during the year 2017, on a sample of 17 patients (7 males and 10 females), aged from 8 to 26 years, with white defects of enamel in the dental aesthetic area. The informed consent forms were collected before enrolling the patients in the study and carrying out the treatment. This work was conducted in according to the Declaration of Helsinki principles.

Each patient was asked to fill in questionnaires before and after treatment in order to point out the subjective assessment of the attenuation's effectiveness. All defects were treated by the same dentist. The treatment technique used closely followed the instructions provided by the manufacturer (DMG, Hamburg, Germany):

* isolation of the field with dam and hooks, dental floss ligatures, transparent matrices and wedges are always necessary;
* cleaning of the dental surfaces with prophylaxis pastes;
* etching with 15% hydrochloric acid (Icon Etch, DMG) for 120 s;
* cleansing of the surfaces with abundant water jet for 30 s and drying with a jet of air;
* application of 99% pure ethanol (Icon-Dry, DMG) for 30 s;
* drying with a jet of air;
* assessment of the need for new etching by a student or a restorative dentistry expert (each surface was etched 3 times at most);
* having completely dried the surface after the final application of ethanol, the first infiltration with the infiltrating resin (Icon Infiltrant, DMG) can be carried out, leaving the material in position for 3 min;
* photopolymerization with UV lamp for 40 s after eliminating excess material using a cotton roller on the vestibular surfaces and dental floss in the interproximal areas;
* second application of infiltrant, in position on the surfaces for 1 min, followed by polymerization for 40 s;
* polishing of the surfaces, assessment of the contact points and application of abrasive strips in the interproximal zones, is necessary.

Photographs were taken at 4 different times [before treatment (T0), directly afterwards (T1), one month (T2) and twelve months later (T3)] at the same Dental Clinic, with the same camera (Nikon D7000) fitted with lens (Nikon AF Micro Nikkor 105mm (1:2.8 D) and ring flash (Nikon Macro Speedlight).

Finally, the images collected were analyzed and evaluated by two qualified dentists. A value of 0 was assigned if no degree of attenuation was achieved, a value of 1 if there was partial attenuation in which the improvement was seen as less extension or less contrast with the surrounding healthy enamel, and a value of 2 if it was impossible to distinguish the defect from the healthy enamel.

RESULTS

Seventeen patients participated in this study: 7 males and 10 females, aged from 8 to 26 years (mean 14.7 years, $\sigma = 5{,}36$). Thirty-eight teeth with white defects of enamel were treated. Within the group of the treated defects, all appeared attenuated at the last check-up (T3), with 21 partially attenuated and 17 that had disappeared.

All incipient caries defects were completely hidden. Four teeth were treated and from the first step to the 12-month follow-up, there was a complete resolution of the defect.

The post orthodontic defects disappeared in 6 cases and were attenuated in 5. Eleven teeth were treated and from the first step to the 12-month follow up, there was a complete resolution of the defect in 6 cases. Three cases were not attenuated at T1 and at 1 month (T2), but after a longer period, 12 months, they were partially attenuated.

In cases of fluorosis, 4 out of 6 disappeared. Six teeth were treated, and from the first application to the

12-month follow-up there was a complete resolution of the defect in 3 cases. Three cases were partially attenuated at T1 and at 1 month (T2), but after a longer period, 12 months, one of them was totally hidden.

Regarding the post-trauma cases, 6 were partially attenuated and 2 disappeared. Eight teeth were treated and from the first application to the 12-month follow-up, there was a complete resolution of the defect in 2 cases. Two cases were no attenuated at T1, but, after one month (T2), they were partially hidden.

The teeth suffering from MIH showed partial attenuation in 8 cases, and only in one case the defect disappeared (Figs. 1 and 2). Nine teeth were treated and at the first check-up there was no complete resolution of any defect: 7 teeth were partially attenuated and 2 had no attenuation at all. After one month (T2), one defect was totally attenuated. After 12 months (T3) 2 more teeth were partially attenuated.

DISCUSSION

Infiltration of the white lesions is a minimally invasive approach which permits an aesthetic problem to be treated while reducing aggressiveness

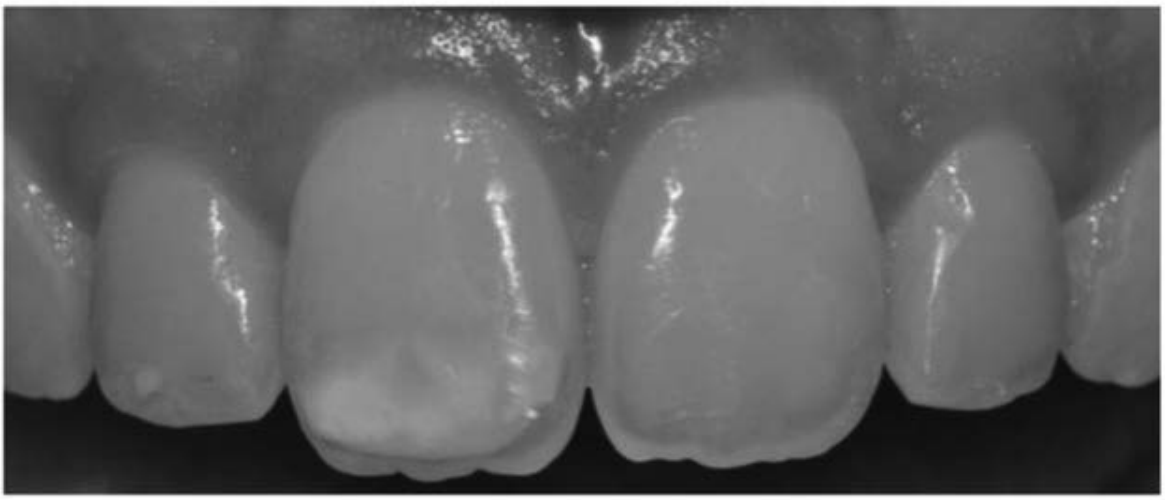

Fig. 1. *Before treatment in patient with molar incisor hypomineralization.*

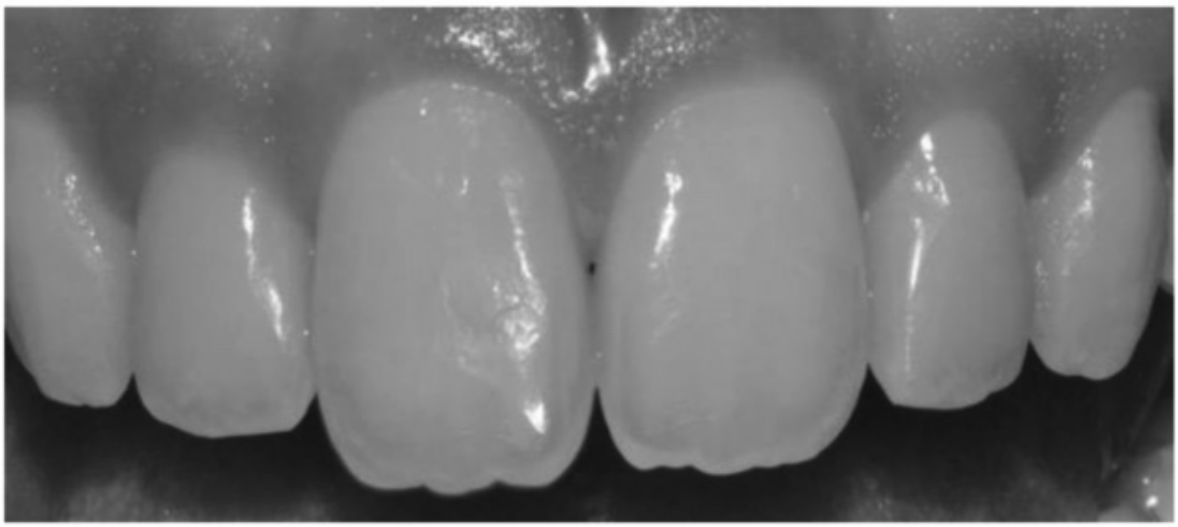

Fig. 2. *After treatment in patient with molar incisor hypomineralization at T3.*

on healthy tissues to a minimum. Before proposing the treatment, the dentist must, however, assess its possible effectiveness based on the diagnosis (8, 9).

The variability of the results in this study is justified by the histological differences (10) of the lesions. Even if it was not possible to achieve the hoped-for cosmetic results in all cases, the main objective of the technique was instead achieved in all of them, i.e. blocking of the pathways, thus preventing further loss of mineral substance. Moreover, in the cases of lesions of caries origin, progression of the pathology was blocked before cavitations appeared (1, 11).

Correct diagnosis plays a central role in being able to predict the results of infiltration technique in the treatment of white defects of enamel. Even if all the white defects have hypomineralization of the enamel forming them in common, each of them is distinguished by the topographical shape it takes. Knowing the anatomopathological characteristics of the lesions and their depth, shape and volume allows us to guide definitively the dentist toward the possibility, or impossibility, of infiltrating the lesion.. Based on the results attained from this study, we can say that the erosion-infiltration method adds a therapeutic possibility of treating hypomineralized white enamel defects.

REFERENCES

1. Denis M, Atlan A, Atlan JP. Erosion/infiltration: un noveau Traitement des Taches Blanches. Entretiens d'Odontologie-stomatologie 2012; 4.
2. Denis M, Atlan A, Vennat E, Tirlet G, Attal JP. White defects on enamel: diagnosis and anatomopathology: two essential factors for proper treatment (part 1). Int Orthod 2013; 11:(2)139-65.
3. Attal JP, Denis M, Atlan A,Vennat E, Tirlet G. L'infiltration en profondeur: un nouveau concept pour le masquage des taches de l'émail – Partie 1. Information Dentaire 2013; 195.
4. Kielbassa AM, Muller J, Gernhardt CR. Closing the gap between oral hygiene and minimally invasive dentistry: a review on the resin infiltration technique of incipient (proximal) enamel lesions. Quintessence Int 2009; 40:(8)663-81.
5. Knosel M, Eckstein A, Helms HJ. Durability of esthetic improvement following Icon resin infiltration of multibracket-induced white spot lesions compared with no therapy over 6 months: a single-center, split-mouth, randomized clinical trial. Am J Orthod Dentofacial Orthop 2013; 144:(1)86-96.
6. Paris S, Meyer-Lueckel H. Masking of labial enamel white spot lesions by resin infiltration--a clinical report. Quintessence Int 2009; 40:(9)713-18.
7. Tirlet G, Chabouis HF, Attal JP. Infiltration, a new therapy for masking enamel white spots: a 19-month follow-up case series. Eur J Esthet Dent 2013; 8:(2)180-90.
8. Munoz MA, Arana-Gordillo LA, Gomes GM, Gomes OM, Bombarda NH, Reis A, Loguercio AD. Alternative esthetic management of fluorosis and hypoplasia stains: blending effect obtained with resin infiltration techniques. J Esthet Restor Dent 2013; 25:(1)32-39.
9. Giannetti L, Bartoli G, Bachelli F, Spinas E, Murri Dello Diago A. MIH amongst dental pratictioners in Modena and Reggio Emilia districts. Dent Cadmos 2018; 86(3):172-80.
10. Giannetti L, Murri Dello Diago A, Corciolani E, Spinas E. Deep infiltration for the treatment of hypomineralized enamel lesions in a patient with molar incisor hypomineralization: a clinical case. J Biol Regul Homeost Agents 2018; 32(3)751-54.
11. Kim S, Kim EY, Jeong TS, Kim JW. The evaluation of resin infiltration for masking labial enamel white spot lesions. Int J Paediatr Dent 2011; 21:(4)241-48.

LETTER TO THE EDITOR

USE OF A SHORT-TERM WHOLE BLOOD INTRACELLULAR STAINING ASSAY TO STUDY THE T-CELL RESPONSE IN RESPIRATORY SYNCYTIAL VIRUS-INFECTED PEDIATRIC PATIENTS

A. FRASSANITO[1], G. FEDELE[2], P. LEONE[2], R. NENNA[1], F. MIDULLA[1] and I. SCHIAVONI[2]

[1]Department of Paediatrics, "Sapienza" University of Rome, Rome Italy; [2]Department of Infectious Diseases, Istituto Superiore di Sanità, Rome, Italy

Received November 7, 2017 – Accepted February 20, 2018

The aim of the present study was the development of a reliable method to evaluate the pattern of the ongoing T-cell response in young infants affected by respiratory infection. To this purpose, we enrolled 44 infants hospitalized with a diagnosis of respiratory syncytial virus bronchiolitis. After a short-term stimulation of whole blood samples, intracellular IFN-γ and IL-4 cytokines were measured in $CD4^+$ and $CD8^+$ T-cell subsets by flow cytometry. A stringent staining and gating strategy was used in order to maximize the reduction of background noise and to exclude false positives. The frequencies of cytokine-producing T-cell subsets, albeit low, were easily quantifiable. Cytokine responses were higher in infants sampled > 7 days from the onset of symptoms. The use of a rigorous strategy for cell staining and gating, coupled with a short-term stimulation of whole blood and a careful evaluation of time elapsed from the onset of symptoms constitutes a convincing approach for future clinical studies.

To the Editor,

Bronchiolitis is an acute inflammatory injury of the bronchioles usually caused by a viral infection and is one of the most common causes of pediatric hospitalization (1). Respiratory syncytial virus (RSV) is the most common pathogen causing bronchiolitis (2, 3) and virus-induced inflammation is believed to contribute substantially to the severity of disease (3). The onset of an unbalanced T-cell response in RSV-infected infants likely contributes to the immune-mediated pathology and to the increased risk of developing wheeze and asthma later in life (3, 4). Among the assays that have been developed to examine T-cell function, the intracellular staining (ICS) coupled to flow cytometry allows for immunophenotyping of the cells, including multiple cytokines readouts (5). Unlike alternative approaches that also detect cytokine expression such as enzyme-linked immunospot or ELISA assays, ICS enables the simultaneous detection of the specific subset of responder cells (e.g. $CD4^+$ or $CD8^+$ T-cells). Moreover, the development of multi-parameter instruments gave the possibility to simultaneously measure the expression of multiple cytokines that characterize the T-cell phenotypes at the single cell level.

The aim of this study was to develop an assay suitable for the evaluation of T-helper (Th-1)/Th-2 cytokine production by $CD4^+$ and $CD8^+$ T cells in pediatric patients with RSV-bronchiolitis. We intended to measure the ongoing effector T-cell responses using as small a volume of blood as possible; therefore we adopted an ICS protocol based on a short-term direct stimulation of whole blood. The study involved a cohort of children hospitalized for RSV-bronchiolitis

Key words: bronchiolitis, respiratory syncytial virus, T-cell, flow-cytometry, cytokines

Mailing address:
Dr Ilaria Schiavoni,
Department of Infectious Diseases,
Istituto Superiore di Sanità,
Viale Regina Elena 299, 00161, Rome, Italy.
Tel.: +39 06 49902890; - Fax: +39 06 49902168
e-mail: ilaria.schiavoni@iss.it

0393-974X (2018)

during the last epidemic season (2016–2017) in the Pediatric Emergency Department of Policlinico Umberto I Hospital in Rome, Italy.

MATERIALS AND METHODS

Ethical statements

This study was conducted according to the principles of the Declaration of Helsinki; the Ethics Committee of the Policlinico Umberto I Hospital approved the study and informed consent was obtained from the infants' parents.

Study participants and blood collection

Forty-four unrelated infants aged less than one-year hospitalized for RSV bronchiolitis from November 2016 to April 2017 were enrolled. The study population belongs to an Italian cohort of term, non-low birth weight, otherwise healthy infants hospitalized with bronchiolitis at the Pediatric Emergency Department of Policlinico Umberto I Hospital, "Sapienza" University of Rome [Brome (Bronchiolitis in Rome)]. Bronchiolitis was defined as the first episode of acute lower airway infection, characterized by a history of upper respiratory tract infection followed by acute onset of respiratory distress with cough, tachypnea, retractions and diffuse crackles on auscultation (3). Patients were excluded from the study in the presence of other viral infection; infants with RSV-negative bronchiolitis were likewise excluded.

With the aim of defining the optimal timing for immune response monitoring, the study population was divided into two subgroups, those sampled earlier than 7 days from the onset of symptoms (day 7 included) and those sampled later than 7 days from the onset of symptoms.

Whole blood stimulation and permeabilization

Venous blood (600 µl) was collected in sodium heparin Vacutainer tubes (BD Biosciences, San Jose, CA, USA). Immediately after withdrawal, the blood sample was taken to the laboratory and processed. In order to determine the frequencies of cytokine producing $CD4^+$ and $CD8^+$ T cells for each infant, we adopted an experimental protocol built on evidence from previous studies, which defined the best conditions for blood stimulation and culture (6, 7). Whole blood was diluted 1:1 with RPMI cell culture medium (Thermo Fisher Scientific) and incubated in polypropylene tubes at 37°C for 24 h, either left unstimulated or stimulated with Staphylococcal enterotoxin B (SEB) at 1 µg/mL (Sigma-Aldrich, St. Louis, MO, USA). This approach was preferred to the use of other polyclonal T-cell activators, since SEB covalently binds MHC and TCR and triggers proliferation and cytokine responses similarly to physiological TCR triggering, requiring the presence of antigen presenting cells (8). Brefeldin-A (Sigma-Aldrich) was added during the last 18 h of incubation, at 10 µg/mL, to inhibit cellular secretion. Whole blood cultures were then harvested and red blood cells lysed with FACS lysing solution (BD Biosciences). The remaining white cells were stained with Live/Dead Fixable Violet Dead Cell Stain Kit (Thermo Fisher Scientific). Cells were then fixed by 1% PFA for 15 min at room temperature and permeabilized using FACS buffer and 5% Saponin.

Intracellular cytokine staining and flow cytometry

Cells were incubated with a panel of fluorochrome-conjugated monoclonal antibodies (mAbs) for 30 min at 4°C. The composition of panel was: anti-CD3-FITC, anti-CD4-APC-H7, anti-CD8-APC700, anti-IL-4 APC (all from BD Biosciences), anti-IFN-g-PerCPCy5.5 (Biolegend, San Diego, CA, USA), anti-CD14-eFluor450 and anti-CD19-eFluor450 (both from eBioscience, Thermo Fisher Scientific). Saponin (5%) was added to the antibody mix. Cells were finally resuspended in 250 µL 1% paraformaldehyde and acquired on a Gallios Flow Cytometer (Beckman Coulter, Miami, FL, USA). Stained samples were acquired with a standard stopping gate set at 50,000 CD3+ T-cells. Compensation was performed using VersaComp Antibody Capture Beads (Beckman Coulter) stained with each individual mAb and compensation matrices were calculated with Kaluza 1.3 software software (Beckman Coulter). Data were analyzed using Kaluza software. Gating strategy and an example of raw flow cytometry data are shown in Fig. 1.

Data analysis

Frequencies of cytokine-expressing $CD4^+$ and $CD8^+$ T cells stimulated by SEB were determined after subtracting percentages of cytokine-expressing cells detected in unstimulated controls. The *chi*-squared test was used to evaluate statistical differences. A p-value below 0.05 was considered statistically significant. Statistical analysis was

performed using Graph Pad Prism (Graph Pad Software Inc., San Diego, CA, USA).

RESULTS

The demographic and clinical overview of the study sample is summarized as follows: the age at hospitalization (mean±Standard Deviation) was 77.44±47.73 days; the mean hospitalization stay was 5.71±2.06 days and the mean interval in days from the onset of symptoms to blood withdrawal was 6.82±2.30 days (Table I).

Whole blood was withdrawn from RSV-bronchiolitis infants, processed, stimulated and incubated overnight in the presence of Brefeldin A. A stringent staining and gating strategy was then adopted to detect cytokine producing T-cell subsets, minimizing the occurrence of false positives (Fig. 1). The percentages of cytokine-producing $CD4^+$ and $CD8^+$ T cells in untreated and SEB-stimulated whole blood cultures are shown in Table II. The frequencies of Th1 cells (IFN-γ^+ of $CD3^+CD4^+$), Th2 cells (IL-4^+ of $CD3^+CD4^+$), type 1 cytotoxic T cells (Tc1) (IFN-γ^+ of $CD3^+CD8^+$) and type 2 cytotoxic T cells (Tc2) (IL-4^+ of $CD3^+CD8^+$) were calculated by subtracting background from SEB-stimulated values, and are shown in Table III. A tendency towards a preferential induction of Th1 and Tc1 cells was observed.

Since the present study dealt with infants hospitalized with primary viral infection, it was important to assess the optimal timing for the monitoring of the immune response. We divided the study populations into two subgroups, those sampled earlier than 7 days from the onset of symptoms (day 7 included) and those sampled later than 7 days from the onset of symptoms. We

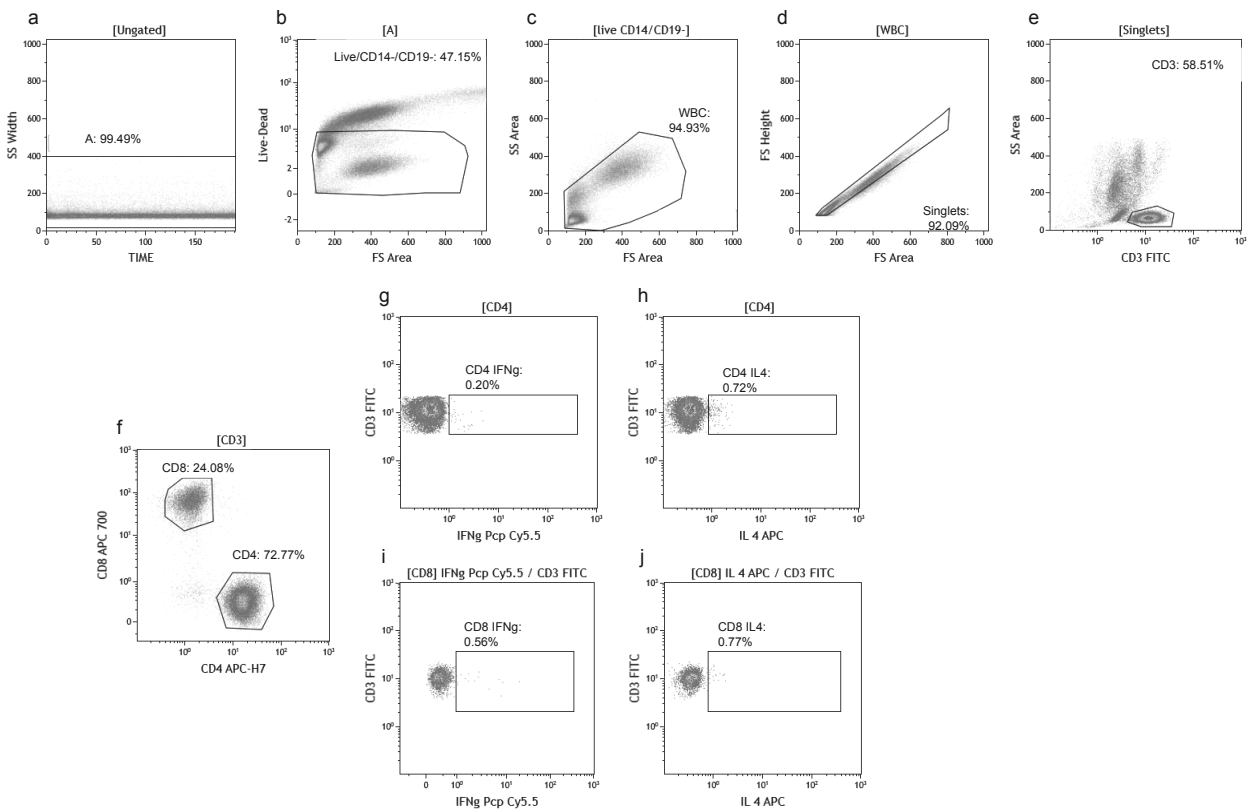

Fig. 1. *Gating strategy used to identify cytokine producing T-cell subsets. Successive gates were applied to:* ***a****) exclude anomalies in the acquisition, defined by accurate acquisition of events displayed in the dot plot as a function of the time parameter;* ***b****) exclude dead cells, CD14+ monocytes and CD19+ B-cells;* ***c****) identify Leucocytes minus CD14+/CD19+ cells;* ***d****) identify singlet cells by means signal intensity measured as Area or Height pulse;* ***e****) identify CD3+ T-cells;* ***f****) identify CD4+ and CD8+ T-cell subsets. The percentages of IFN-γ and IL-4 producing cells (****g****,* ***h****,* ***i****,* ***j****) were then assessed within the CD4+ or the CD8+ T-cell subsets.*

Table I. *Demographic and clinical overview of the study sample.*

Variables	(n= 44)
Sex (male *vs* female)	50%
Age (days)	76.68±47.44
Gestational age (weeks)	38.23±1.85
Birth Weight (Kg)	3.00±0.46
Family history of asthma	34%
Family history of rhino-conjunctivitis	56.7%
Family history of eczema	18%
Presence of passive smoke	61.3%
Hospitalization stay in days	5.67±2.05
Days from symptoms to blood withdrawal	6.82±2.30
Oxygen-therapy	43.2%
Score - entrance	3.91±1.63
Score- hospitalization	4.32±1.90

Table II. *Percentages of cytokine positive cells in untreated and SEB-stimulated whole blood cultures.*

CD3+CD4+IFNγ + *NT*	CD3+CD4+IFNγ + *SEB*	CD3+CD4+IL-4+ *NT*	CD3+CD4+IL-4+ *SEB*
0.06±0.06 (0.00 - 0.28)	0.19±0.23 (0.01 - 1.43)	0.02±0.02 (0.00 - 0.08)	0.04±0.07 (0.00 - 0.41)
CD3+CD8+IFNγ + *NT*	CD3+CD8+IFNγ + *SEB*	CD3+CD8+IL-4+ *NT*	CD3+CD8+IL-4+ *SEB*
0.13±0.12 (0.00 - 0.49)	0.75±1.02 (0.03 - 4.90)	0.01±0.02 (0.00 - 0.08)	0.04 - 0.12 (0.00 - 0.72)

Data are expressed as mean±standard deviation (min – max).

Table III. *Frequencies of T-cell subsets producing IFN-γ and IL-4.*

	Th1 (CD3+CD4+IFNγ+)	Th2 (CD3+CD4+IL-4+)	Tc1 (CD3+CD8+IFNγ+)	Tc2 (CD3+CD8+IL-4+)
All infants	0.125±0.20	0.021±0.03	0.57±0.96	0.013±0.05
≤7 days of disease	0.088±0.07	0.018±0.024	0.42±0.69	0.006±0.01
>7 days of disease	0.16±0.27	0.024±0.041	0.71±1.17	0.024±0.06

Frequencies of Th1 cells, Th2 cells, type 1 cytotoxic T-cells (Tc1) and type 2 cytotoxic T-cells (Tc2) were calculated by subtracting percentage of cytokine positive cells in untreated cultures from values identified in SEB-stimulated cultures. Data are expressed as mean±Standard Deviation.

found that in early sampled infants, the frequencies of cytokine-producing T cells were overall lower than in infants sampled > 7 days from the onset of symptoms, in particular when considering the frequencies of Th-1 cells, although differences between the two subgroups were not statistically significant (Table III).

The aim of the present report is to bring to attention the potential advantages of a newly developed whole blood-ICS method for studies aimed at the definition of the immunological status in infants. It has still not been clearly established whether a specific pattern of Th1 or Th2 immune response is distinctive of RSV bronchiolitis. Results from previous studies diverge largely, with reports of either Th1 or Th2 polarization (3, 9, 10). This diversity, besides reflecting the complex interplay between viral and host factors, is related also to different study designs and experimental approaches. Other studies have been published reporting T-cell cytokine production by bronchiolitis patients using ICS of whole blood or purified peripheral blood mononuclear cells (PBMCs) (11, 12). Unlike previous studies, we have set a stringent staining and gating strategy aimed at reducing the occurrence of false positive signals (7). In fact, when performing flow-cytometry, it is of crucial importance to exclude non-specific binding, which can lead to background noise and false positives. A first crucial step was staining samples with a dead cells exclusion dye. Dead cells have great autofluorescence and increased non-specific antibody binding and, when not excluded from the analysis, lead to the identification of false positives. Moreover, we used a strategy for the exclusion of $CD19^+$ B-cells and $CD14^+$ monocytes. As a further step, we used the flow cytometry analysis software to identify anomalies in the acquisition signal and to include only single cell. We consider that these precautions, coupled with subtraction of background responses in unstimulated cells, are mandatory when monitoring cytokine production by T-cell subsets. In these settings, the frequencies of cytokine-producing T-cell subsets, albeit low, were easily quantifiable.

Hospitalized infants were likely facing a primary infection. In these patients the onset of the adaptive immune responses, including T-cell immunity, is expected to require about one week. Hence, there is a lag-phase to consider before T cells start to produce effector cytokines. Confirming this notion, we found that early sampling of the hospitalized infant may be not useful and that the date of symptoms onset should be carefully considered when planning blood withdrawal.

The correlation of immunological results with the

clinical characteristics of RSV-bronchiolitis patients is currently underway. Yet, the present report shows per se that the whole blood-ICS assay is a reliable method for quantifying antigen-specific cytokine-expressing $CD4^+$ and $CD8^+$ T cells and highlights the benefits of using it for the future research in clinical immunology dealing with pediatric patients.

ACKNOWLEDGEMENTS

The authors are grateful to Ms. Simonetta Pietrangeli for technical assistance.

REFERENCES

1. Hall CB. The burgeoning burden of respiratory syncytial virus among children. Infect Disord Drug Targets 2012; 12:92-97.
2. Midulla F, Scagnolari C, Bonci E, et al. Respiratory syncytial virus, human bocavirus and rhinovirus bronchiolitis in infants. Arch Dis Child 2010; 95:35-41.
3. Openshaw PJM, Chiu C, Culley FJ, Johansson C. Protective and harmful immunity to RSV infection. Annu Rev Immunol 2017; 35:501-32.
4. Rossi GA, Colin AA. Respiratory syncytial virus-Host interaction in the pathogenesis of bronchiolitis and its impact on respiratory morbidity in later life. Pediatr Allergy Immunol 2017; 28:320-31.
5. Yin Y, Mitson-Salazar A, Prussin C. Detection of intracellular cytokines by flow cytometry. Curr Protoc Immunol 2015; 110:1-18.
6. Palazzo R, Spensieri F, Massari M, et al. Use of whole-blood samples in in-house bulk and single-cell antigen-specific gamma interferon assays for surveillance of Mycobacterium tuberculosis infections. Clin Vaccine Immunol 2008; 15:327-37.
7. Smith SG, Smits K, Joosten SA, et al.: TBVI TB Biomarker Working Group. intracellular cytokine staining and flow cytometry: considerations for application in clinical trials of novel tuberculosis vaccines. PLoS ONE 2015; 10: e0138042.
8. Fleischer B, Gerardy-Schahn R, Metzroth B, Carrel S, Gerlach D, Köhler W. An evolutionary conserved mechanism of T cell activation by microbial toxins. Evidence for different affinities of T cell receptor-toxin interaction. J Immunol 1991; 146:11-17.
9. Román M, Calhoun WJ, Hinton KL, et al. Respiratory syncytial virus infection in infants is associated with predominant Th-2-like response. Am J Respir Crit Care Med 1997; 156:190-95.
10. Brandenburg AH, Kleinjan A, van Het Land B, et al. Type 1-like immune response is found in children with respiratory syncytial virus infection regardless of clinical severity. J Med Virol 2000; 62:267-77.
11. Bendelja K, Gagro A, Baće A, et al. Predominant type-2 response in infants with respiratory syncytial virus (RSV) infection demonstrated by cytokine flow cytometry. Clin Exp Immunol 2000; 121:332-38.
12. Chen ZM, Mao JH, Du LZ, Tang YM. Association of cytokine responses with disease severity in infants with respiratory syncytial virus infection. Acta Paediatr 2002; 91:914-22.